



**Performance Assessment for the
Area 5 Radioactive Waste Management Site
at the Nevada Test Site, Nye County, Nevada
(Rev. 2.1)**

Prepared by

**G. J. Shott, L. E. Barker, S. E. Rawlinson,
M. J. Sully, and B. A. Moore**

Prepared for

**the U.S. Department of Energy
Nevada Operations Office
under Contract Number
DE-AC08-96NV11718**

January 1998



**Performance Assessment for the
Area 5 Radioactive Waste Management Site
at the Nevada Test Site, Nye County, Nevada
(Rev. 2.1)**

Prepared by

**G. J. Shott¹, L. E. Barker¹, S. E. Rawlinson¹,
M. J. Sully¹, and B. A. Moore²**

Prepared for

**the U.S. Department of Energy
Nevada Operations Office
under Contract Number
DE-AC08-96NV11718**

January 1998

¹Bechtel Nevada

²U.S. Department of Energy, Nevada Operations Office

EXECUTIVE SUMMARY

This report documents the methods and results of a performance assessment conducted for the Area 5 Radioactive Waste Management Site (RWMS) at the Nevada Test Site (NTS). The Department of Energy (DOE) has established policies and guidelines for the disposal of radioactive waste in DOE Order 5820.2A, *Radioactive Waste Management* (DOE, 1988a), which requires that each disposal site prepare and maintain a site-specific performance assessment. A performance assessment is a systematic analysis of the potential risks posed by a waste management system to the public and to the environment and a comparison of those risks to established performance objectives. The performance objectives contained in DOE Order 5820.2A are:

1. Protect public health and safety in accordance with standards specified in applicable Environmental Health (EH) Orders and DOE Orders.
2. Assure that external exposure to the waste and concentrations of radioactive material which may be released into surface water, groundwater, soil, plants, and animals results in an effective dose equivalent that does not exceed 25 mrem yr⁻¹ to any member of the public. Releases to the atmosphere shall meet the requirements of 40 Code of Federal Regulations (CFR) 61. Reasonable effort shall be made to maintain releases of radioactivity in effluents to the general environment as low as reasonably achievable (ALARA).
3. Assure that the committed effective dose equivalents received by individuals who inadvertently may intrude into the facility after the loss of institutional control (100 years) will not exceed 100 mrem yr⁻¹ for continuous exposure or 500 mrem for a single acute exposure.
4. Protect groundwater resources consistent with federal, state, and local requirements.

The purpose of this assessment is to provide reasonable assurance of compliance with the performance objectives for a period of 10,000 years after closure.

FACILITY DESCRIPTION

The NTS is a 3,500 km² (1,351 mi²) DOE facility in southern Nye County, Nevada, approximately 105 km (65 mi) north of Las Vegas. The NTS was used as the continental nuclear weapons testing site from 1951 to 1992. The Area 5 RWMS is a low-level radioactive waste management site located within Frenchman Flat, in the southeastern corner of the NTS. The closest permanent settlement to the RWMS is Indian Springs, 42 km (26 mi) to the southeast.

The Area 5 RWMS lies within a biogeographical region transitional between the Mojave Desert and the Great Basin Desert. The site is surrounded by desert shrub communities

characterized by low, but variable productivity and standing biomass. The climate is

The arid nature of the site also affects potential land use. The land surrounding the NTS remains mostly uninhabited because of limited water resources and government ownership. The population density of the surrounding counties is only 0.5 persons km^{-2} , much less than the 28 persons km^{-2} reported for the continental United States. Agriculture in Nevada is limited by the arid climate, infertile soils, and mountainous topography. Only 2.1 percent of the total land area in southern Nevada is used for agriculture. Production of livestock is the most common agricultural activity, accounting for approximately 90 percent of the land in farms. No economically significant mineral resources are known to exist within the vicinity of the Area 5 RWMS. Future development of Frenchman Flat appears unlikely assuming current land use patterns continue.

Disposal of low-level radioactive waste (LLW) began at the Area 5 RWMS in 1961. Initially, only waste generated on the NTS was disposed. In 1978, operations were expanded to include disposal of waste from off-site generators. From 1983 to 1989, high-specific activity waste was disposed in deep augered shafts known as Greater Confinement Disposal (GCD). Mixed waste (MW) was disposed in a single unlined pit from 1987 to 1990. As of 1996, the site was open and accepting LLW from DOE generators around the nation.

This performance assessment is limited to wastes disposed from the inception of DOE Order 5820.2A on September 26, 1988, to the estimated date of closure. Since 1988, the Area 5 RWMS has disposed of LLW and MW in shallow unlined trenches and pits. As of the end of Fiscal Year (FY) 1993, these disposals were estimated to amount to 1×10^5 Ci of long-lived activity in 4.7×10^4 m^3 of waste. High-specific activity waste containing 4×10^3 Ci of activity has been disposed in a single GCD borehole during this same period.

LONG-TERM SITE PERFORMANCE

The performance assessment has evaluated the release of radionuclides from the intact and subsided site and from releases caused by inadvertent human intrusion. Exposing members of the general public to releases from the intact and subsided site has been evaluated for three pathway scenarios. Three intruder scenarios have been evaluated. Intruder scenarios are hypothetical events evaluated to set conservative waste concentration limits.

Base Case Release and Pathway Scenarios for the General Public

Three exposure scenarios for the general public were evaluated. Two scenarios were selected to represent current land use patterns in southern Nevada. The first scenario, the transient occupancy scenario, assumes that members of the general public visit the site for recreational or commercial activities, but do not permanently reside near the site. The second scenario, the open rangeland scenario, assumes that a ranch has been established at the nearest available site with water and that range-fed cattle have access to the closed disposal site. A third, much less probable scenario, assumes that a ranch has been established at the RWMS boundary. This scenario, referred to as the resident farmer scenario, represents an extreme bounding estimate of site performance.

The dose to the general public under the assumptions of the transient occupancy scenario was estimated for a screened list of nonvolatile radionuclides at 100 years, 10,000 years, and at the time of the maximum dose. In the first 10,000 years after closure, the total effective dose equivalent (TEDE) from all nonvolatile radionuclides would be less than 0.6 mrem yr^{-1} to a person spending up to 2,000 hours per year at the Area 5 RWMS. The dose is mostly due to external exposure from the short-lived progeny of ^{226}Ra and inhalation of ^{238}U . Because estimated doses are linear in time of occupancy, it is possible to estimate the dose per hour spent at the site. Individuals visiting the site 10,000 years after closure are expected to receive a TEDE of approximately $3 \times 10^{-4} \text{ mrem}$ for each hour spent at the site.

The release of volatile radionuclides was evaluated separately. These calculations were done under the extremely conservative assumption that gaseous radionuclides were released at a maximum rate, based on diffusion in the air-filled pores and diluted into a 2-m (7-ft) atmospheric mixing zone. The TEDE from ^3H , ^{14}C , and ^{85}Kr combined was less than $0.01 \text{ mrem yr}^{-1}$ at 100 years. Doses from volatile and nonvolatile radionuclides released through the atmospheric pathway summed to 0.2 mrem yr^{-1} at 10,000 years.

Doses were evaluated under the assumptions of the open rangeland scenario for two off-site locations with water resources, Indian Springs and Cane Springs. The maximum TEDE within the 10,000-year compliance interval was less than 0.2 mrem yr^{-1} and occurred at 10,000 years. The doses at the two off-site locations are approximately equal because most of the dose is attributable to ingestion of beef and milk produced at the Area 5 RWMS. Approximately 85 percent of the dose at 10,000 years is attributable to the ingestion of ^{238}U , ^{234}U , and ^{210}Pb and its short-lived progeny in milk.

Volatile radionuclides were again evaluated separately. Volatile radionuclides were assumed to be released from the site by diffusion and advected through the atmosphere to the off-site location. The TEDE from exposure to volatile radionuclides was less than $3 \times 10^{-4} \text{ mrem yr}^{-1}$. The TEDE from exposure to volatile and nonvolatile radionuclides released through the atmospheric pathway was less than $4 \times 10^{-4} \text{ mrem yr}^{-1}$.

A resident farmer located 100 m (330 ft) from the site boundary was estimated to receive a TEDE from all pathways of 4 mrem yr^{-1} at 10,000 years. The pathways in decreasing order of significance were external irradiation (51 percent), inhalation (21 percent), plant ingestion (18 percent), milk ingestion (4 percent), soil ingestion (4 percent), and beef ingestion (0.6 percent). The maximum dose from the release of volatile radionuclides occurred at closure and was attributable to the release of volatile ^3H . The dose from ^3H at closure, 6 mrem yr^{-1} , decreases to $0.03 \text{ mrem yr}^{-1}$ by the end of active institutional control at 100 years.

The radon flux was estimated for two inventories, the average inventory disposed by shallow land burial and the estimated inventory for Pit 6. Pit 6 is expected to receive thorium wastes that have the potential to generate ^{222}Rn as ^{230}Th decays. The thorium is destined for a deeper or lower cell. Routine low-level waste will be disposed in the upper cell.

The flux of ^{222}Rn released from the disposal site was assumed to be directly proportional to the activity concentration of ^{226}Ra in the buried wastes. For the shallow land burial inventory, the activity concentration of ^{226}Ra will increase very slowly over the next 10,000 years, not reaching a peak for several million years. The predicted flux remains below the performance objective of $20 \text{ pCi m}^{-2} \text{ s}^{-1}$ throughout the 10,000-year compliance interval. The flux exceeds the performance objective in approximately 30,000 years and reaches a peak of $156 \text{ pCi m}^{-2} \text{ s}^{-1}$ in 3.5×10^6 years.

The ^{226}Ra inventory in the lower cell of Pit 6 will increase and reach a maximum within 10,000 years. The activity concentration in the upper cell was assumed to be equal to the average shallow land burial activity concentration. The increased depth of burial of the thorium waste effectively attenuates the radon flux. Consequently, the Pit 6 radon flux is predicted to be the same as for the shallow land burial inventory.

Results for the base case release and pathway scenarios evaluated to estimate doses to members of the general public are summarized in Table 1.

Table 1 Maximum Performance Assessment Results Within 10,000 Years for Members of the General Public Exposed to Releases From the Intact Site Under the Transient Occupancy and Open Rangeland Scenario

Performance Objective	Performance Assessment Result
25 mrem yr ⁻¹ From All Pathways	0.6 mrem yr ⁻¹
10 mrem yr ⁻¹ from Airborne Emissions Excluding Radon	0.2 mrem yr ⁻¹
Average Annual ^{222}Rn Flux Less Than $20 \text{ pCi m}^{-2} \text{ s}^{-1}$	6 pCi m ⁻² s ⁻¹
Protect Groundwater Resources	Zero Release to Aquifer in 10,000 Years

A sensitivity analysis of the release of nonvolatile radionuclides showed that estimates of performance were most sensitive to the biological release rate coefficients K_{b1} and K_{r1} , which account for transport from the waste to surface soil by burrowing animals and plant uptake. A sensitivity analysis of waste inventory found that performance was most sensitive to the inventory of ^{234}U and ^{238}U . A sensitivity analysis of radon transport showed that waste porosity was the most sensitive parameter. Uncertainty analyses indicate that there is reasonable assurance of compliance with the performance objectives. Health detriment costs, estimated as part of an ALARA analysis, are low compared to the cost of engineered barriers. Therefore, installation of any additional engineered barriers at the Area 5 RWMS is unlikely to be cost effective.

Subsided Case Release and Pathway Scenarios for the General Public

Under the subsided case release scenario, the trenches at the Area 5 RWMS were assumed to undergo subsidence at the end of active institutional control, 100 years after closure.

Subsidence was assumed to cause the formation of cracks in the cap that would persist for 1,000 years. The slumping of cap soil into gaps between waste packages and into subsidence depressions was assumed to reduce cap thickness at 100 years. Decreased cap thickness was

assumed to lead to increased plant rooting in buried waste. Subsidence depressions were assumed to collect water, causing enhanced infiltration. Plant productivity was assumed to increase with increasing infiltration.

Subsidence was found to have three notable effects. First, cap thinning allowed plant roots to access a greater fraction of the disposed inventory and lead to a greater release of nuclides with high plant-soil concentration factors such as ^{14}C . This effect had only minor consequences, however, because of the low concentration of bioavailable elements in the Area 5 RWMS inventory. Subsidence caused the all-pathways TEDE, excluding the groundwater pathway, for the transient occupancy and resident farmer scenarios to increase approximately 30 to 50 percent at 10,000 years. The greater ^{14}C release caused the TEDE for the open rangeland scenario to increase to 0.3 mrem yr^{-1} at 10,000 years.

Second, cracks and fissures in the cap increased the release of some volatile radionuclides. The timing of cracking, however, ameliorated the effects. By the onset of cracking at 100 years, volatile ^3H releases have declined because of radioactive decay. The release of ^{14}C and ^{85}Kr was unaffected by subsidence because the base case assumes that the entire inventory is released in one year. The TEDE from release of gaseous radionuclides was unchanged by subsidence. Overall, increases in the dose from the atmospheric pathway were negligible. Cracking approximately doubled the release of ^{222}Rn during the first 1,000 years after closure. The ^{222}Rn flux limit was not exceeded for the subsided release scenario during the compliance period. Cracks are expected to fill naturally by erosion and collapse by the time ^{222}Rn flux becomes significant, after 10,000 years.

The third important effect was the potential to initiate a groundwater pathway if large amounts of run-on were assumed to pond in subsidence depressions and infiltrate. The estimated concentration of radionuclides transported to the uppermost aquifer was found to meet all state of Nevada drinking water standards. Transport of radionuclides to the aquifer may increase the all-pathways dose for the resident farmer. However, the all pathways TEDE

Table 2 Maximum Performance Assessment Results Within 10,000 Years for Members of the General Public Exposed to Releases From the Subsidized Site Under the Transient Occupancy and Open Rangeland Scenario

Performance Objective	Performance Assessment Result
25 mrem yr ⁻¹ From All Pathways	0.8 mrem yr ⁻¹
10 mrem yr ⁻¹ From Airborne Emissions Excluding Radon	0.2 mrem yr ⁻¹
Average Annual ²²² Rn Flux Less Than 20 pCi m ⁻² s ⁻¹	10 pCi m ⁻² s ⁻¹
Protect Groundwater Resources ²²⁶ Ra + ²²⁸ Ra < 5 pCi L ⁻¹ Gross Alpha < 15 pCi L ⁻¹ Dose from Man-made Beta-Gamma Emitters < 4 mrem yr ⁻¹	0.3 pCi L ⁻¹ 9 pCi L ⁻¹ 1 mrem yr ⁻¹

Intruder Scenarios

Intruder scenarios are hypothetical events analyzed to set activity concentration limits for wastes suitable for disposal in the near surface. Three intruder analyses, one acute and two chronic scenarios, were analyzed. They were the drilling scenario (acute), the intruder-agriculture scenario (chronic), and postdrilling scenario (chronic).

The drilling scenario is a short-term exposure scenario, where an intruder is exposed to contaminated drill cuttings while drilling a water well at the site. An inadvertent intruder drilling through a shallow land burial trench or pit is estimated to receive a TEDE of 0.14 mrem at 100 years and 0.17 mrem at 10,000 years. The maximum TEDE occurs at 3.5×10^6 years and is approximately 1.0 mrem.

The intruder-agriculture scenario is a chronic exposure scenario where an intruder is assumed to reside on a contaminated zone created during the excavation of a basement. The intruder is assumed to produce fruit, vegetables, meat, and milk within the contaminated zone. Twenty-five percent of the intruder's diet is assumed to be produced on site within the contaminated zone.

The TEDE received by an intruder under the assumptions of the intruder-agriculture scenario at 100 years was estimated to be 84 mrem yr⁻¹. Inhalation and external irradiation are the most important pathways, contributing 81 percent of the dose. Ingestion doses from agricultural pathways were only a few percent of the total dose throughout the analysis interval. By 10,000 years, the estimated TEDE increases to 157 mrem yr⁻¹ as the activity concentration of progeny of ²³⁸U and ²³⁵U increases. The increasing dose is attributable largely to external irradiation from ²²⁶Ra and its short-lived progeny. Reasonable assurance of compliance with

the performance objective can be obtained by increasing the thickness of the closure cap from

Table 3 Performance Assessment Results for Intruder Scenarios. Results are based on current waste management practices or assumed inventories.

Performance Objective	Performance Assessment Result	
	Shallow Land Burial	Pit 6 (PO6U)
Acute Scenario: 500 mrem yr ⁻¹ Drilling	0.2 mrem yr ⁻¹	22 mrem yr ⁻¹
Chronic Scenario: 100 mrem yr ⁻¹ Agriculture Postdrilling	157 mrem yr ⁻¹ 0.7 mrem yr ⁻¹	NA 177 mrem yr ⁻¹

NA - Scenario not applicable.

This Page Intentionally Left Blank

CONTENTS

EXECUTIVE SUMMARY	i
1.0 INTRODUCTION	1-1
1.1 Purpose and Scope	1-1
1.2 Overview of the NTS and the Area 5 RWMS	1-3
1.3 Performance Objectives	1-4
1.3.1 DOE Order 5820.2A, Radioactive Waste Management	1-4
1.3.2 DOE Order 5400.5, Radiation Protection of the Public and Environment	1-6
1.3.3 40 CFR 61, National Emission Standards for Hazardous Air Pollutants	1-7
1.3.4 40 CFR 141, National Interim Primary Drinking Water Regulations	1-7
1.3.5 Performance Objective Summary	1-10
1.4 Performance Assessment Method	1-11
2.0 FACILITY DESCRIPTION	2-1
2.1 Geography	2-1
2.1.1 DOE Operations	2-1
2.2 Meteorology	2-4
2.2.1 Climatic Setting	2-4
2.2.2 Precipitation	2-4
2.2.3 Temperature	2-8
2.2.4 Evaporation	2-8
2.2.5 Wind	2-8
2.3 Geology	2-9
2.3.1 Regional Geology	2-9
2.3.2 Geology of Frenchman Flat and the Area 5 RWMS	2-9
2.3.2.1 Structural Features	2-13
2.3.2.2 Potential for Seismic Activity	2-14
2.3.2.3 Evidence of Volcanism	2-15
2.3.2.4 Local Stratigraphy	2-17

CONTENTS

2.4	Hydrology	2-22
2.4.1	Regional Hydrology of the NTS	2-22
2.4.1.1	Surface Hydrology	2-22
2.4.1.2	Subsurface Hydrology	2-23
2.4.2	Hydrology of the Area 5 RWMS	2-37
2.4.2.1	Surface Hydrology	2-37

CONTENTS

3.0	ANALYSIS OF PERFORMANCE	3-1
3.1	Scenario Development and Selection	3-1
3.1.1	Release Scenarios	3-2
3.1.1.1	Analysis of Hydrologic Processes Potentially Affecting Release of Radionuclides	3-4
3.1.1.2	Summary of Hydrologic Processes and Their Effects on Release and Transport of Radionuclides from the Intact Disposal Site	3-7

CONTENTS

3.2.2.8	Conceptual Model for Release of Nonvolatile Radionuclides	3-59
3.2.2.9	Infiltration Conceptual Model for Subsided Case	3-61
3.2.2.10	Saturated-Zone-Flow and Capture-Zone Analysis	3-63
3.2.3	Pathway Scenario Assumptions and Conceptual Models	3-70
3.2.3.1	Transient Occupation Scenario	3-70
3.2.3.2	Open Rangeland Scenario	3-74
3.2.3.3	Radionuclide Screening	3-79
3.2.3.4	Full Pathway Analysis for the Open Rangeland Scenario ..	3-81
3.2.3.5	Resident Farmer Scenario	3-83
3.2.3.6	Summary of Pathway Conceptual Models	3-84
3.3	Intruder Conceptual Models and Assumptions	3-84
3.3.1	Acute Intruder Scenarios	3-87
3.3.1.1	Conceptual Models and Assumptions for the Acute Drilling Scenario	3-87
3.3.2	Chronic Intruder Scenarios	3-93
3.3.2.1	Conceptual Model and Assumptions for the Intruder-Agriculture Scenario	3-93
3.3.2.2	Conceptual Model and Assumptions for the Postdrilling Scenario	3-101
3.4	Computer Software	3-103
3.4.1	TIME-ZERO Computer Code	3-103
3.4.2	The CASCADR9 Computer Code	3-106
3.4.3	The RESRAD Computer Code	3-107
3.4.4	The CAP88-PC Computer Code	3-108
3.4.5	Radioactive Decay Computer Codes	3-109
3.4.6	The ODIRE Computer Code	3-109
3.5	Quality Assurance	3-109
3.5.1	Site Characterization and Monitoring Quality Assurance	3-110
3.5.2	Software Quality Assurance	3-110

CONTENTS

4.0	RESULTS OF ANALYSIS	4-1
4.1	Analysis Results For Members of the General Public	4-1
4.1.1	All-Pathways Analysis – Base Case Release Scenario	4-1
4.1.1.1	Results for the Transient Occupancy Scenario	4-2
4.1.1.2	Results for the Open Rangeland Scenario	4-4
4.1.1.3	Results for the Resident Farmer Scenario	4-6
4.1.2	All-Pathways Analysis – Subsided Case Release Scenario	4-8
4.1.2.1	Results for the Pathway Scenarios	4-9
4.1.3	Atmospheric Pathway – Base Case Release Scenario	4-11
4.1.3.1	Results for the Transient Occupancy Scenario	4-11
4.1.3.2	Results for the Open Rangeland Scenario	4-11
4.1.3.3	Results for the Resident Farmer Scenario	4-12
4.1.4	Atmospheric Pathway – Subsided Release Case	4-12
4.1.5	Radon Flux from Shallow Land Burial Trenches and Pits	4-13
4.1.6	Estimated Radon Flux from Pit 6 (P06U)	4-14
4.1.7	Protection of Groundwater Resources	4-16
4.2	Analysis Results for Intruder Scenarios	4-18

CONTENTS

4.3.3	Radon Flux Sensitivity and Uncertainty Analysis	4-48
4.4	Interpretation of Analysis Results	4-51
4.4.1	Interpretation of Doses to Members of the General Public	4-51
4.4.2	Interpretation of Radon Flux Results	4-53
4.4.3	Interpretation of Doses to Inadvertent Intruders	4-54

CONTENTS

Table 2	Maximum Performance Assessment Results Within 10,000 Years for Members of the General Public Exposed to Releases From the Subsidized Site Under the Transient Occupancy and Open Rangeland Scenario	vii
Table 3	Performance Assessment Results for Intruder Scenarios	ix
Table 1.1	Time Periods for Analysis	1-2
Table 1.2	Average Annual Concentrations Assumed to Produce a Total Body or Organ Dose of 4 mrem yr ⁻¹	1-8
Table 1.3	Concentrations of Man-Made Beta Particle and Photon Emitters in Drinking Water Assumed to Cause a Dose Equivalent of 4 mrem yr ⁻¹ to the Total Body or Any Organ at Equilibrium or After 50 Years of Intake	1-9
Table 1.4	Summary of Adopted Performance Objectives for the Period of Active Institutional Control	1-10
Table 1.5	Summary of Adopted Performance Objectives for the Postinstitutional Control Period	1-11
Table 1.6	Summary of Adopted Performance Objectives for Inadvertent Intruders ...	1-11
Table 2.1	Monthly Precipitation (cm) for the Period from January 1963 to December 1993 at Frenchman Flat (Well 5B)	2-7
Table 2.2	Summary of the Mean Particle Size Fraction in the Alluvium as Sampled From the Science Trench Boreholes	2-22
Table 2.3	Compilation of Regional Hydrologic Character for Water-Bearing Strata Observed at the NTS	2-26
Table 2.4	Summary of Pilot Well Drilling Log and Lithology Information	2-40
Table 2.5	Summary of Water Content Data From the Pilot Wells and Science Trench Borehole Studies	2-45
Table 2.6	Mean Water Quality Parameters for UE5PW-1, UE5PW-2, and UE5PW-3 for 1993	2-78
Table 2.7	Total Land Area and Farm Land in Southern Nevada for 1987	2-85
Table 2.8	Cropland in Nevada and Southern Nevada by Use and Crop Grown for 1987	2-86
Table 2.9	Irrigated Land and Irrigated Land by Use in Nevada and Southern Nevada for 1987	2-87
Table 2.10	Livestock Numbers in Nevada and Southern Nevada in 1987	2-87
Table 2.11	AUM ha ⁻¹ for Various Floral Communities on the NTS	2-89
Table 2.12	Aboveground Living Dry-Weight Biomass of NTS Plant Communities as Reported By Various Investigators for Frenchman Flat <i>Larrea</i> Communities	2-94
Table 2.13	Population Density of Rodents and Rabbits in <i>Larrea</i> Communities Near the Area 5 RWMS	2-97
Table 2.14	Estimated Surface Soil Radionuclide Inventory for Area 5 as of January 1, 1990, Excluding the Area 5 RWMS	2-100

CONTENTS

Table 3.1	Features, Events, and Processes Considered in the Development of the Release Scenarios	2-143
Table 3.2	Pathways Included in the Transient Occupation, Open Rangeland, and the Resident Farmer Scenario	2-146
Table 3.3	Summary of All-Pathways Modeling Cases Selected for Analysis	3-2
Table 3.4	Summary of Intruder Modeling Cases Selected For Analysis	3-9
Table 3.5	Serial Radioactive Decay Chains Present in the Area 5 Inventory	3-13
Table 3.6	Radionuclide Half-Lives, Branching Fractions, and Equilibrium Factors Used in the Performance Assessment	3-14
Table 3.7	Estimated Activity and Activity Concentration of Wastes Projected to be Disposed by Shallow Land Burial at the Area 5 RWMS from FY 1989 to FY 2028	3-17
Table 3.8	Preliminary Estimate of the Inventory of Thorium Waste That Could Be Disposed in the Lower Cell of Pit 6 (P06U)	3-18
Table 3.9	Parameter Values Assumed for the Universal Soil Loss Equation	3-21
Table 3.10	Assumed Integrity Life of Containers	3-25
Table 3.11	Bulk Densities of All Waste Containers in Selected Years	3-30
Table 3.12	Descriptions of Typical Waste From Three Largest Generators	3-32

CONTENTS

Table 4.3	Estimated All-Pathways TEDE from Nonvolatile Radionuclides at 10,000 Years and at the Time of the Maximum Dose for a Resident Farmer Located 100 m (330 ft) From the Area 5 RWMS	4-3
Table 4.4	Maximum Concentration of Long-lived Nuclides Expected to Reach the Aquifer in 10,000 Years Under the Subsided Case Release Scenario With Infiltration of Run-On	4-5
Table 4.5	Comparison of All-Pathway TEDE From Nonvolatile Radionuclides Under the Base Case Release and Subsided Case Release Scenario	4-7
Table 4.6	Maximum CEDE to a Resident Farmer at 100 m From Ingestion of 2 L day ⁻¹ of Groundwater	4-9
Table 4.7	Estimated Maximum TEDE for Volatile Radionuclides (excluding radon)	4-10
Table 4.8	Estimated TEDE for Exposure of a Resident Farmer to Volatile Radionuclides at the 100-m Buffer Boundary	4-10
Table 4.9	Estimated Radon Flux From Shallow Land Burial Trenches and Pits	4-11
Table 4.10	Estimated Total ²²² Rn Flux From Pit 6 (P06U)	4-12
Table 4.11	Estimated Total Radium Activity Concentrations at the Time of the Peak Uranium Concentration and at 10,000 Years	4-13
Table 4.12	Maximum Gross Alpha Activity at the Well Head, Excluding Background Radioactivity, Uranium, and Radon	4-15
Table 4.13	Soil Activity Concentrations and TEDE for the Acute Drilling Scenario With the Shallow Land Burial Inventory	4-17
Table 4.14	Soil Activity Concentrations and TEDE for the Acute Drilling Scenario for Pit 6 (P06U) at 100 Years	4-17
Table 4.15	Soil Activity Concentrations and TEDE for the Acute Drilling Scenario for Pit 6 (P06U) at 10,000 Years	4-20
Table 4.16	Soil Activity Concentrations and TEDE for the Intruder-Agriculture Scenario With the Shallow Land Burial Inventory	4-23
Table 4.17	Soil Activity Concentrations and TEDE for the Postdrilling Scenario With the Shallow Land Burial Inventory	4-25
Table 4.18	Soil Activity Concentrations and TEDE for the Postdrilling Scenario for Pit 6 (P06U) at 100 Years	4-27
Table 4.19	Soil Activity Concentrations and TEDE for the Postdrilling Scenario for Pit 6 (P06U) at 10,000 Years	4-31
Table 4.20	Estimated Radon-222 Dose Results for Intruders Residing Over a Shallow Land Burial Trench	4-34
Table 4.21	Results of the Sensitivity Analysis for ²²⁶ Ra in the Base-Case Release Model	4-36
Table 4.22	Results of Sensitivity Analysis for Nonvolatile ¹⁴ C in the Base Case Release Model	4-38
Table 4.23	Dose Conversion Factors for the Transient Occupancy Scenario (Cases [1] and [2])	4-39

CONTENTS

Table 4.24	Dose Conversion Factors for the Open Rangeland Scenario (Cases [3] and [4])	4-40
Table 4.25	Descriptive Statistics for Monte Carlo Uncertainty Analysis of Waste Activity Concentration	4-41
Table 4.26	Rank Correlations under Cases (1) and (2)	4-42
Table 4.27	Rank Correlations Under Case (3) and Case (4)	4-44
Table 4.28	Uncertainty Cases and Results for the Radon K-Factors for Shallow Land Burial	4-47
Table 4.29	Uncertainty Cases and Results for Radon K-Factors for Pit 6 (P06U)	4-48
Table 4.30	Radon Flux Results for Bounding Uncertainty Cases	4-49
Table 5.1	Maximum Performance Assessment Results for Members of the General Public in the Transient Occupancy and Open Rangeland Scenarios	4-50
Table 5.2	Performance Assessment Results for Intruder Scenarios	4-50

List of Figures

Figure 2.1	Location of the NTS-NAFR Complex Within the State of Nevada	2-2
Figure 2.2	Location of the Area 5 RWMS and Major Operational Areas on the NTS ...	2-3
Figure 2.3	Location of the Area 5 RWMS in Frenchman Flat	2-5
Figure 2.4	Monthly Mean Precipitation at the NTS From 1957 to 1964	2-6
Figure 2.5	Annual Wind Rose for Well 5B in Frenchman Flat for 1983 through 1993	2-10
Figure 2.6	Surficial Geology of the Frenchman Flat Basin in the Vicinity of the Area 5 RWMS	2-11
Figure 2.7	Map Showing the Major Structural Features of the Frenchman Flat Basin in the Vicinity of the Area 5 RWMS	2-12
Figure 2.8	Post-Caldera Basalt of the Nevada Test Site Region	2-16
Figure 2.9	Gravity Interpretation of the Elevation of the Top Surface of the Carbonate Section Underlying Frenchman Flat	2-18
Figure 2.10	Depth Profile for the Grain-Size Distribution (Unified Soil Classification System) in the Three Pilot Wells	2-21
Figure 2.11	Hydrogeology of the NTS in Cross Sections, With Regional Geology and a Groundwater Path Overlay	2-24
Figure 2.12	Cross-Sections Through Frenchman Flat to the Amargosa Desert Showing the Regional Groundwater Flow Pattern and Relationship Between Interbasin and Intrabasin Flow	2-32
Figure 2.13	General Groundwater Flow Directions in the NTS Area	2-34
Figure 2.14	Mean Cation and Anion Concentrations in Groundwater Found at the NTS and Trilinear Diagram Analysis Showing the Three Dominant Chemical Facies	2-35
Figure 2.15	100-Year Flood Zone Delineation Map at the Area 5 RWMS	2-39

CONTENTS

Figure 2.16	Cross-Section Showing Interpreted Hydrogeology for Frenchman Flat	2-41
Figure 2.17	Map Showing the Pilot Wells in Relation to the RWMS With Geologic Cross-Section Interpreted From Core and Drill Cuttings	2-42
Figure 2.18	Water Content Profile Beneath the Area 5 RWMS Based on the Pilot Well Data	2-44
Figure 2.19	Variation of Water Potential With Depth for the Pilot Wells and Science Trench Boreholes	2-47
Figure 2.20	Variation of Water Potential With Depth for Pilot Well 1 (UE5PW-1)	2-48
Figure 2.21	Variation of Water Potential With Depth for Pilot Well 2 (UE5PW-2)	2-49
Figure 2.22	Variation of Water Potential With Depth for Pilot Well 3 (UE5PW-3)	2-50
Figure 2.23	Variation of Water Potential With Depth for Borehole AP-1	2-51
Figure 2.24	Variation of Water Potential With Depth for Borehole AP-2	2-52
Figure 2.25	Variation of Water Potential With Depth for Borehole RP-1	2-53
Figure 2.26	Variation of Water Potential With Depth for Borehole RP-2	2-54
Figure 2.27	Saturated Hydraulic Conductivity Profiles for the Pilot Wells and Science Trench Boreholes Surrounding the Area 5 RWMS	2-56
Figure 2.28	Composite Moisture Retention Curves From Core Samples for Pilot Wells UE5PW-1, UE5PW-2, and UE5PW-3	2-58
Figure 2.29	Fitted Unsaturated Hydraulic Conductivity Functions From Core Samples in Pilot Wells UE5PW-1, UE5PW-2, and UE5PW-3	2-60
Figure 2.30	Comparison of Measured and Model Water Retention Relations for North Area 5 Lysimeter	2-61
Figure 2.31	Comparison of Measured and Model Water Retention Relations for South Area 5 Lysimeter	2-61
Figure 2.32	Depth Profiles of Dry Chloride Concentrations for Core Samples From the Pilot Wells and Science Trench Boreholes	2-63
Figure 2.33	Depth Profiles of $\delta^{18}\text{O}$ and δD in Core Samples From the Pilot Wells and Science Trench Boreholes	2-67
Figure 2.34	Comparison of Stable Isotopes Measured From Core Samples of the Pilot Wells to the Global Meteoric Water Line (MWL)	2-68
Figure 2.35	Population of Counties in Nevada Based on 1990 Census Estimates	2-82
Figure 2.36	Major Vegetation Types of the NTS	2-92
Figure 2.37	Map of the Low-Level Waste Management Unit (LLWMU)	2-102
Figure 2.38	Waste Management Units Within the Area 5 RWMS	2-105
Figure 2.39	Schematic of a GCD Cell	2-110
Figure 2.40	General Atomics Waste Stream Profile for FY 1989 through FY 1993 . . .	2-123
Figure 2.41	Inhalation Toxicology Research Institute Waste Stream Profile for FY 1989through FY 1993	2-124
Figure 2.42	Lawrence Livermore National Laboratory Waste Stream Profile for FY 1989through FY 1993	2-125
Figure 2.43	Pantex Waste Stream Profile for FY 1989 through FY 1993	2-126
Figure 2.44	Rocky Flats Plant Waste Stream Profile for FY 1989 through FY 1993 . . .	2-127

CONTENTS

Figure 2.45	Aberdeen Proving Grounds Waste Stream Profile for FY 1989 through FY 1993	2-128
Figure 2.46	Fernald Environmental Restoration Management Company Waste Stream Profile for FY 1989 through FY 1993	2-129
Figure 2.47	Sandia National Laboratories Waste Stream Profile for FY 1989 through FY 1993	2-130
Figure 2.48	Rocketdyne Waste Stream Profile for FY 1989 through FY 1993	2-131
Figure 2.49	Mound Waste Stream Profile for FY 1989 through FY 1993	2-132
Figure 3.1	Conceptual Model of Shallow Land Burial Pits and Trenches	3-26
Figure 3.2	Conceptual Model of Pit 6 (P06U) and Placement of Thorium Waste	3-27
Figure 3.3	Table of Expected Subsidence	3-37
Figure 3.4	Conceptual Model of Radionuclide Release	3-40
Figure 3.5	Conceptual Model of Root Uptake	3-51
Figure 3.6	Conceptual Model of Burrowing Animal Transport	3-55
Figure 3.7	Saturation Versus Depth	3-63
Figure 3.8	Recharge of the Uppermost Aquifer Over Time After Four Consecutive 1.07-m-Deep Ponding Events in a Subsidence Feature	3-65
Figure 3.9	Pathways Leading to Exposure of Members of the Public in the Base Case Release Scenario and the Transient Occupancy Scenario	3-71
Figure 3.10	Pathways Leading to Exposure of Members of the Public in the Base Case Release Scenario and the Open Rangeland Pathway Scenario	3-76
Figure 3.11	Pathways Leading to Exposure of a Hypothetical Intruder in the Intruder-Agriculture Scenario	3-95
Figure 3.12	Pathways Leading to the Exposure of a Hypothetical Intruder in the Postdrilling Scenario	3-102
Figure 4.1	Estimated Surface Soil Concentration for the Base Case and Subsided Case	4-2
Figure 4.2	All-Pathways TEDE for Nonvolatile Radionuclides Released Under the Base Case and Subsided Case Scenarios	4-4
Figure 4.4	Estimated ²²² Rn Flux From Pit 6 (P06U) for the Base Case and Subsided Case Release Scenarios	4-16
Figure 4.5	Cumulative Distribution Function of Monte Carlo Realizations of TEDE Under Case (1)	4-45
Figure 4.6	Cumulative Distribution Function of Monte Carlo Realizations of TEDE Under Case (2)	4-45
Figure 4.8	Cumulative Distribution Function of Monte Carlo Realizations of TEDE Under Case (4)	4-46
Figure 4.7	Cumulative Distribution Function of Monte Carlo Realizations of TEDE Under Case (3)	4-46

This Page Intentionally Left Blank

ACRONYMS

ALARA	As Low as Reasonably Achievable
ANSI	American National Standards Institute
ASME	American Society of Mechanical Engineers
AUM	Animal Unit Month
CEDE	Committed Effective Dose Equivalent
CFR	Code of Federal Regulations
D&D	Decontamination and Decommissioning
DOC	U.S. Department of Commerce
DOE	U.S. Department of Energy
DOE/NV	U.S. Department of Energy/Nevada Operations Office
EH	Environmental Health
EPA	U.S. Environmental Protection Agency
FEMA	Federal Emergency Management Agency
FEMP	Fernald Environmental Management Project
FY	Fiscal Year
GCD	Greater Confinement Disposal
GCDT	Greater Confinement Disposal Test
GMX	Gadgets, Mechanics, and Explosives
HAZMAT	Hazardous Materials
HQ	Headquarters (U.S. DOE)
ICRP	International Commission on Radiological Protection
LGFSTF	Liquified Gaseous Fuels Spill Test Facility (now known as HAZMAT Spill Center)
LLNL	Lawrence Livermore National Laboratory
LLW	Low-Level Waste
LLWIS	Low-Level Waste Information System
LLWMU	Low-Level Waste Management Unit
LMWL	Local Meteoric Water Line
MFP	Mixed Fission Products
MW	Mixed Waste
MWU	Mixed Waste Disposal Unit

ACRONYMS

MWL	Meteoric Water Line
MWSP	Mixed Waste Storage Pad
NAFR	Nellis Air Force Range
NCRP	National Council on Radiation Protection
NESHAP	National Emission Standards for Hazardous Air Pollutants
NRC	Nuclear Regulatory Commission
NTS	Nevada Test Site
NV	U.S. DOE/Nevada Operations Office
ppb	parts per billion
RCRA	Resource Conservation and Recovery Act
REEC _o	Reynolds Electrical & Engineering Co., Inc.
RSN	Raytheon Services Nevada
RWMS	Radioactive Waste Management Site
SMOW	Standard Mean Ocean Water
TEDE	Total Effective Dose Equivalent
TRU	Transuranic
TTR	Tonopah Test Range
USLE	Universal Soil Loss Equation

1.0 INTRODUCTION

The Nevada Test Site (NTS) is a U.S. Department of Energy (DOE) proving ground for defense-related technologies. It is located in the sparsely populated portion of southern Nye County, Nevada. The southern boundary of the NTS is approximately 105 km (65 mi) northwest of Las Vegas.

Two permanent radioactive waste management sites (RWMSs) have been established on the NTS. The Area 5 RWMS was established in 1961 for the disposal of low-level waste (LLW) generated on the NTS. In 1978, the role of the Area 5 RWMS was expanded to include disposal of LLW from off-site DOE generators and classified LLW from U.S. government agencies. The Area 3 RWMS was established in 1979 for the consolidation and disposal of atmospheric testing debris. The Area 3 RWMS currently accepts LLW in bulk containers from on-site and off-site generators. The two sites, approximately 27 km (17 mi) apart, are considered separate disposal sites for the purpose of performance assessment. This report is limited to the performance of the Area 5 RWMS.

1.1 Purpose and Scope

This report documents the method and results of a performance assessment conducted for the Area 5 RWMS. In DOE Order 5820.2A, *Radioactive Waste Management* (DOE, 1988a), which requires that each disposal site prepare and maintain a site-specific performance assessment, the DOE has established policies and guidelines for the disposal of radioactive waste. A performance assessment is a systematic analysis of potential risks posed by waste management systems to the public and to the environment, and the comparison of those risks to the established performance objectives. The current revision of the report, Revision 2.1, incorporates comments on Revision 2.0 received from the DOE Peer Review Panel.

A performance assessment is conducted by modeling the transport of radionuclides from the disposal site to the accessible environment and determining the dose to human populations. Natural environmental processes and inadvertent human intrusion into disposal cells are considered potential transport mechanisms in the analysis. The risks posed by the disposal site are assessed by comparing the predicted radiation doses to humans with the dose limits contained in the performance objectives established in DOE Order 5820.2A. Performance assessment involves the prediction, through modeling, of the future behavior of complex environmental systems and human populations. Predicting the outcome of future events based on current or historical conditions is an uncertain task.

Performance assessments are intended to be documents that are reviewed and revised as necessary. This assessment is based on the best information available at the time of preparation. Additional analyses may be required if significant changes occur in waste management practices, the disposal site inventory, the conceptual understanding of how the waste disposal system functions, or the discovery of new information concerning natural processes.

The scope of the performance assessment has been limited in four specific areas: the waste inventory, the time period for compliance assessment, waste types and constituents, and waste management practices. The scope has been limited in these areas based on the requirements and policies of DOE Order 5820.2A and DOE guidance on performance assessment (Case and Otis, 1988; Dodge *et al.* 1991; Wood *et al.* 1994).

The performance assessment considers wastes disposed in Area 5 from 1988, when current DOE waste management orders were issued, to the estimated date of closure. The Area 5 RWMS began accepting wastes from off-site generators in 1978. Assuming a 50-year operational lifetime beginning in 1978, the closure date becomes 2028. Because the analysis has been limited to disposals occurring after 1988, the operational period evaluated becomes 40 years.

DOE Order 5820.2A does not specify an explicit period for compliance assessment. Existing federal regulations governing disposal of radioactive wastes have set compliance periods ranging from 1,000 to 10,000 years, depending on the waste type and transport pathway. This performance assessment evaluates compliance with the performance objectives for a period of 10,000 years. However, the performance of the undisturbed disposal site has been assessed for the period beginning with the start of the active institutional control period and

ending when the maximum dose is predicted. In some instances, these analyses have been performed beyond 10,000 years. These analyses are provided to give the reader an indication of how doses are increasing or decreasing at the end of the 10,000-year compliance interval. Estimates of site performance at such great times in the future are uncertain. The time

trenches, and by burial in 36-m- (118-ft)-deep augered shafts known as Greater Confinement Disposal (GCD) boreholes. This performance assessment considers wastes disposed in both units.

Classes of wastes disposed in Area 5 include low-level radioactive wastes, mixed wastes (MWs), greater-than-Class-C wastes, and TRU wastes. Only low-level radioactive and mixed wastes have been disposed since 1988. Therefore, analyses have been limited to these two classes of waste. The assessment has been limited to toxicological and radiological hazards presented by the radioactive waste constituents.

1.2 Overview of the NTS and the Area 5 RWMS

The land within the boundary of the NTS was first used for defense purposes in 1941, when the area was incorporated into the Las Vegas Army Air Field. In 1951, Frenchman Flat and Yucca Flat were transferred to the Atomic Energy Commission, a predecessor of the DOE, for use as the primary continental nuclear weapons testing site. The NTS was selected as a nuclear weapons testing site because large tracts of government-owned land were available and the land immediately surrounding the site had some of the lowest population densities in the United States. Jackass Flats was added to the site in 1958 as part of the Nuclear Rocket Development Station (Beatley, 1976). In 1964, Pahute Mesa was added for underground nuclear weapons testing (Beatley, 1976). In its current configuration, the NTS encompasses 3,500 km² (1,351 mi²), an area larger than that of the state of Rhode Island. It is surrounded and further isolated on the north, east, and west by the Nellis Air Force Range (NAFR) and the Tonopah Test Range (TTR). Both are restricted areas controlled by the Air Force. The entire complex, including the surrounding Air Force-controlled land, encompasses 14,200 km² (5,483 mi²).

In addition to serving as a site for both above- and belowground nuclear weapons tests, the

humidities result in high evaporation rates. Approximately 240 m (790 ft) of dry unconsolidated alluvial sediments from the surrounding mountain ranges lie between the site and the uppermost aquifer. Recent hydrogeologic characterization studies suggest that recharge through the alluvial sediments is not occurring under the current climatic conditions. The arid climate, low or nonexistent recharge, and great distances to the water table make radionuclide transport through the vadose zone to the aquifer unlikely under the current climatic conditions.

Radionuclide transport through terrestrial and atmospheric pathways is insignificant under the current institutional controls because of the integrity of the disposal site and the remote location. The nearest off-site residents are in Indian Springs, Nevada (population 1,500), 42 km (26 mi) to the southeast. The arid climate, infertile soils, and lack of known mineral resources limit the potential future uses of the site. Land uses in the region include grazing, small-scale irrigation-based agriculture, mining, and recreational activities. Frenchman Flat is not an attractive site for any of these uses under current economic conditions.

1.3 Performance Objectives

Low-level radioactive waste disposal performance objectives establish the limits of risk acceptable for the permanent disposal of radioactive wastes. A performance assessment must identify each performance objective and conduct the appropriate analyses to assess compliance with the objective.

Radiation protection standards and recommendations have used a variety of dosimetric quantities. The biological risks of exposure to ionizing radiation are believed or assumed to

1.3.1 DOE Order 5820.2A, Radioactive Waste Management

Performance objectives for the management of LLW are contained in DOE Order 5820.2A. The performance objectives are:

1. Protect public health and safety in accordance with standards specified in applicable Environmental Health (EH) Orders and DOE Orders.
2. Assure that external exposure to the waste and concentrations of radioactive material which may be released into surface water, groundwater, soil, plants, and animals result in an effective dose equivalent that does not exceed 25 mrem yr^{-1} to any member of the public. Releases to the atmosphere shall meet the requirements of 40 Code of Federal Regulations (CFR) 61. Reasonable effort shall be made to maintain releases of radioactivity in effluents to the general environment as low as reasonably achievable (ALARA).
3. Assure that the CEDEs received by individuals who inadvertently may intrude into the facility after the loss of institutional control (100 years) will not exceed 100 mrem-yr for

If these considerations are not applicable, compliance should be based on criteria contained in the site-specific groundwater management plan and consistent with any formal land use plan. There are no applicable federal, state, or local regulatory requirements for groundwater protection at the Area 5 RWMS. There are no formal agreements with the state of Nevada or local officials applicable to groundwater protection. The groundwater protection policy of DOE/NV was developed to guide underground nuclear weapons testing and does not specifically address waste disposal. The DOE/NV groundwater protection policy is to prevent pollutants from reaching the groundwater (DOE/NV, 1993b).

The state of Nevada has promulgated standards for public drinking water supplies in Nevada Administrative Code 445. Characterization data for the uppermost aquifer indicates that the aquifer is a potential source of drinking water and preserving it as such is a conservative groundwater protection policy. Therefore, the adopted performance objective is that the uppermost aquifer is maintained to meet the state of Nevada drinking water standard. This standard includes by reference the maximum contaminant levels (MCLs) for radionuclides in the *National Primary Drinking Water Regulations* (40 CFR 141.15 and 141.16).

1.3.2 DOE Order 5400.5, Radiation Protection of the Public and Environment

DOE Order 5400.5 sets radiation protection standards for the public and environment. Standards applicable to LLW disposal are set for all DOE exposure modes, airborne emissions, and the drinking water pathway. Standards covering management and storage of spent nuclear fuel, high-level, and TRU wastes (paragraph c) are not applicable to LLW disposal. The applicable standards in DOE Order 5400.5 are:

- a. DOE Public Dose Limit—all exposure modes, all DOE sources of radiation. The exposure of members of the public to radiation sources as a consequence of all routine DOE activities shall not cause, in a year, an effective dose equivalent greater than 100 mrem. The dose limits also apply to doses to individuals who are exposed to radiation or contamination by radionuclides at properties subsequent to remedial activities and release of the property.
- b. Airborne Emissions Only—all DOE sources of radionuclides. To the extent

community drinking water standards of 40 CFR 141. The liquid effluents from DOE activities shall not cause private or public drinking water systems downstream of the facility discharge to exceed the drinking water radiological limits in 40 CFR 141.

The above requirements establish several performance objectives that must be considered in addition to those contained in DOE Order 5820.2A. Paragraph (a) of DOE Order 5400.5 sets a dose limit of 100 mrem yr⁻¹ for all DOE exposures. Radionuclides attributable to NTS activities were not detected in the off-site monitoring network during 1992, the most recent year that nuclear testing was conducted (DOE/NV, 1993a). Off-site doses from NTS atmospheric emissions were estimated to be 0.01 mrem in the 1992 NESHAP compliance report (Reynolds Electrical & Engineering Co., Inc. [REEC], 1992). These data indicate that doses from NTS operations are currently negligible. Doses received by persons residing on the NTS after loss of institutional control are more difficult to predict. It has been assumed that all DOE exposures from the NTS, excluding LLW, will amount to less than 75 mrem yr⁻¹. Therefore, the full 25 mrem yr⁻¹ allowable for LLW disposal can be used as the performance objective. Paragraph (d) specifically requires that drinking water supplies impacted by DOE activities meet 40 CFR 141. As noted above, this standard has been adopted for the drinking water pathway.

1.3.3 40 CFR 61, National Emission Standards for Hazardous Air Pollutants

DOE Order 5820.2A requires that airborne emissions meet the requirements of 40 CFR 61. Subpart H applies to emission of all radionuclides, other than radon, from DOE facilities. This standard limits radionuclide emissions to levels that would cause any member of the

1.3.4 40 CFR 141, National Interim Primary Drinking Water Regulations

Drinking water supplies operated by the DOE or impacted by DOE effluents are to meet the radiological standards of the Safe Drinking Water Act (SDWA), 40 CFR 141. The relevant standards in 40 CFR 141 are:

- Standard 1 §141.15(a) – Combined ^{226}Ra and ^{228}Ra - 5 pCi L⁻¹.
- Standard 2 §141.15(b) – Gross alpha particle activity (including ^{226}Ra , but excluding radon and uranium) – 15 pCi L⁻¹.
- Standard 3 §141.16(a) – The average annual concentration of beta particle and photon radioactivity from man-made radionuclides in drinking water shall not produce an annual dose equivalent to the total body or any internal organ greater than 4 mrem yr⁻¹.
- Standard 4 §141.16(b) – Except for radionuclides listed in Table 1.2, the concentration of man-made radionuclides causing 4 mrem yr⁻¹ total body or organ dose equivalents shall be calculated on a basis of a 2 L day⁻¹ drinking-water intake using the 168-hour data listed in “Maximum Permissible Body Burdens and Maximum Permissible Concentrations of Radionuclides in Air or Water for Occupational Exposure” (NBS Handbook 69), as amended August 1963, U.S. Department of Commerce (DOC). If two or more radionuclides are present, the sum of their annual dose equivalent to the total body or to any organ shall not exceed 4 mrem yr⁻¹.

Table 1.2 Average Annual Concentrations Assumed to Produce a Total Body or Organ Dose of 4 mrem yr⁻¹

Radionuclide	Critical Organ	pCi L ⁻¹
^3H	Total body	20,000
^{90}Sr	Bone marrow	8

The standard described above was designed for a comparison with laboratory measurements rather than model results. Therefore, several assumptions must be made. Standard 1 (§141.15[a]) is adopted with the assumption that laboratory measurements are equivalent to the transformation rate of ^{226}Ra and ^{228}Ra . Standard 2 (§141.15[b]) is adopted assuming that gross alpha as measured in a laboratory sample is equivalent to the total alpha particle emission rate excluding ^{238}U , ^{234}U , ^{222}Rn , ^{218}Po , ^{214}Po , ^{235}U , ^{219}Rn , ^{215}Po , ^{211}Bi , ^{211}Po , ^{220}Rn , ^{216}Po , ^{212}Bi , and ^{212}Po . Uranium is excluded based on the standard. Radon and its short-lived progeny are excluded, because it is unlikely that they will be present in laboratory samples prepared using standard methods. Standard §141.16(a) and §141.16(b) are adopted without modifications or assumptions. The 168-hour maximum permissible concentration (MPC)

values are the concentrations which if consumed at a continuous rate of 2.2 L day^{-1} will cause the maximum permissible dose in a year to the critical organ when equilibrium is reached or after 50 years of continuous intake if equilibrium is not reached. For beta-gamma emitters in water, the maximum permissible doses are 5 rem for the total body, blood-forming organs, and gonads; 29 rem for bone-seeking elements; 30 rem for the thyroid; and 15 rem for all other organs. The drinking-water limits (DWL) were obtained from

$$DWL (\text{pCi L}^{-1}) = 1E9 \text{ MPC}_{w-168\text{hr}} \frac{0.004 \text{ rem}}{H_L} \frac{2.2 \text{ L d}^{-1}}{2.0 \text{ L d}^{-1}} \quad (1.1)$$

where:

$\text{MPC}_{w-168\text{hr}}$ = the 168-hr maximum permissible concentration for water, $\mu\text{Ci ml}^{-1}$; and
 H_L = the maximum permissible dose equivalent for the appropriate critical organ, rem.

When a MPC is not listed in NBS Handbook 69 for a specific radionuclide, the limit for unlisted beta emitters with half-lives greater than two hours will be adopted. The concentration of long-lived beta-gamma emitting radionuclides yielding a dose equivalent of 4 mrem yr^{-1} to the whole body or any organ based on the 168-hour MPC are listed in Table 1.3. The limits for ^3H and ^{90}Sr are those listed in Table 1.2. The definition of man-made beta particle and photon-emitting radionuclide included in 40 CFR 141.1 is adopted. This definition excludes the beta-gamma emitting progeny of ^{232}Th , ^{238}U , and ^{235}U . Compliance with standards §141.16(a) and §141.16(b) will be demonstrated by performing a sum of the fractions calculation using the concentrations in Table 1.3.

Table 1.3 Concentrations of Man-Made Beta Particle and Photon Emitters in Drinking Water Assumed to Cause a Dose Equivalent of 4 mrem yr^{-1} to the Total Body or Any Organ at Equilibrium or After 50 Years of Intake

Radionuclide	Critical Organ	Conc. Limit (pCi L^{-1})	Radionuclide	Critical Organ	Conc. Limit (pCi L^{-1})
^3H	Total Body	20,000	^{126}Sn		30
^{14}C	Fat	2,000	^{129}I	Thyroid	1
^{36}Cl	Total Body	700	^{135}Cs	Total Body	900
^{60}Co	GI (LLI)	100	^{137}Cs	Total Body	200
^{59}Ni	Bone	300	^{133}Ba		30

Table 1.3 (continued)

Radionuclide	Critical Organ	Conc. Limit (pCi L ⁻¹)	Radionuclide	Critical Organ	Conc. Limit (pCi L ⁻¹)
⁶³ Ni	Bone	50	¹⁵¹ Sm	GI (LLI)	1,000
⁹⁰ Sr	Bone	8	¹⁵² Eu	GI (LLI)	200
⁹³ Zr	GI (LLI)	2,000	¹⁵⁴ Eu	GI (LLI)	60
⁹⁹ Tc	GI (LLI) [†]	900	²⁰⁷ Pb	GI (LLI)	200
¹⁰⁷ Pd		30	²⁴¹ Pu		2,000

[†]GI (LLI) - Gastrointestinal tract, lower large intestine.

Uranium is an important nuclide in the Area 5 RWMS inventory. Uranium is not included in the current standard. A MCL of 20 µg L⁻¹ has been proposed for uranium (EPA, 1991). Because this MCL is not currently enforceable, comparison with this proposed MCL will be provided for informational purposes only.

1.3.5 Performance Objective Summary

The previous sections have identified all the applicable performance objectives. Simplifying conservative assumptions have been made to minimize the number of performance objectives. The adopted performance objectives for each time interval are summarized in Tables 1.4 through 1.6.

Table 1.4 Summary of Adopted Performance Objectives for the Period of Active Institutional Control

Compliance Interval	Pathway	Compliance Point	Performance Objective
Period of Active Institutional Control	All Pathways (excluding airborne emissions)	Indian Springs, NV	25 mrem yr ⁻¹
	Air Emissions (excluding radon)	Indian Springs, NV	10 mrem yr ⁻¹
	Air Emissions (radon only)	Waste Cell Cap	20 pCi m ⁻² s ⁻¹
	Groundwater	Uppermost Alluvial Aquifer	²²⁶ Ra + ²²⁸ Ra < 5 pCi L ⁻¹ Gross Alpha < 15 pCi L ⁻¹ 4 mrem yr ⁻¹ man-made beta-gamma emitters

Table 1.5 Summary of Adopted Performance Objectives for the Postinstitutional Control Period

Compliance Interval	Pathway	Compliance Point	Performance Objective
Postinstitutional Control	All Pathways (excluding airborne emissions)	Cane Springs and Indian Springs, NV	25 mrem yr ⁻¹
	Air Emissions (excluding radon)	Cane Springs and Indian Springs, NV	10 mrem yr ⁻¹
	Air Emissions (radon only)	Waste Cell Cap	20 pCi m ⁻² s ⁻¹
	Groundwater	Uppermost Alluvial Aquifer	²²⁶ Ra + ²²⁸ Ra < 5 pCi L ⁻¹ Gross Alpha < 15 pCi L ⁻¹ 4 mrem yr ⁻¹ man-made beta-gamma emitters

Table 1.6 Summary of Adopted Performance Objectives for Inadvertent Intruders

Compliance Interval	Pathway	Exposure Mode	Performance Objective
Postinstitutional Control	All Pathways	Acute (<5 years) Chronic (> 5 years)	500 mrem 100 mrem yr ⁻¹

1.4 Performance Assessment Method

The method employed for the preparation of the performance assessment follows a logical sequence of steps as described by Case and Otis (1988). Performance assessment is an iterative process that proceeds sequentially from site characterization to conceptual model development, to outcome modeling and back to site characterization for the next cycle. The iteration or cycle follows the method of Revision 1 of the performance assessment (Magnuson *et al.*, 1992), but differs in the greater use of site-specific data for scenario development, modeling, and developing a refined conceptual model of the vadose zone.

The initial step in performance assessment is to set the scope of the analyses and identify the performance objectives. These activities have been documented in Chapter 1. The next step is to document relevant site characterization data from the RWMS. This assessment describes and evaluates additional site characterization data as directed by the DOE Peer Review Panel. Site characterization data has been documented in Chapter 2.

Chapter 2 also discusses the site inventory. The inventory used in this assessment has been limited to wastes disposed since implementation of DOE Order 5820.2A. Raw inventory data obtained from the site database records have been critically evaluated and revised. However, the inventory data still contain significant uncertainties. A specific inventory has been analyzed to assure that there is a reasonable probability that past disposals can meet the performance objectives. Continuing assurance of compliance with 5820.2A will be provided by developing radiological waste acceptance criteria based on this assessment and applying these limits to future disposals.

Chapter 3 describes the analyses conducted to assess compliance with the performance objectives. Performance analysis begins with developing and selecting scenarios for evaluation. Several deterministic site-specific scenarios have been developed. A scenario is defined here as a description of all the features, events, and processes influencing the waste disposal system performance. Each scenario consists of several scenario modules that have a corresponding conceptual model and mathematical model. Scenarios are developed by preparing a comprehensive list of features, events, and processes. This list is then screened to remove processes or events that will not influence performance, are deemed physically improbable for the NTS, are extremely rare or improbable events, or are outside the scope of

2.0 FACILITY DESCRIPTION

2.1 Geography

The NTS is located in southern Nevada, approximately 105 km (65 mi) northwest of Las Vegas (Figure 2.1). Approximately 3,500 km² (1,350 mi²) of land is encompassed by the current site boundary. The combined area of the NTS and the surrounding Air Force-controlled land, referred to as the NTS-NAFR complex, is approximately 14,200 km² (5,480 mi²). The NTS-NAFR complex is isolated further by U.S. Department of Interior-controlled land that surrounds much of the complex. Counties falling within an 80-km (50-mi) radius of the Area 5 RWMS include portions of Nye, Lincoln, and Clark Counties in Nevada; and Inyo County, California.

Las Vegas is the largest major metropolitan area near the NTS. Other population centers surrounding the NTS-NAFR complex and their distances from the Area 5 RWMS are: Indian Springs (42 km [26 mi]), Lathrop Wells (52 km [32 mi]), Pahrump (80 km [50 mi]), Beatty (82 km [51 mi]), Alamo (96 km [60 mi]), Goldfield (165 km [103 mi]), Warm Springs (177 km [110 mi]), and Tonopah (195 km [121 mi]). The permanent settlement closest to the RWMS is Indian Springs.

Mercury, a restricted access government facility that houses NTS administrative and support facilities, is located at the southeastern corner of the NTS. The Area 5 RWMS is located approximately 22 km (14 mi) north of Mercury, within the physiographic boundaries of Frenchman Flat. Frenchman Flat is an alluvium-filled closed basin in the southeast corner of the NTS (Figure 2.2). Frenchman Flat playa, a dry lake bed at the physiographic low of the

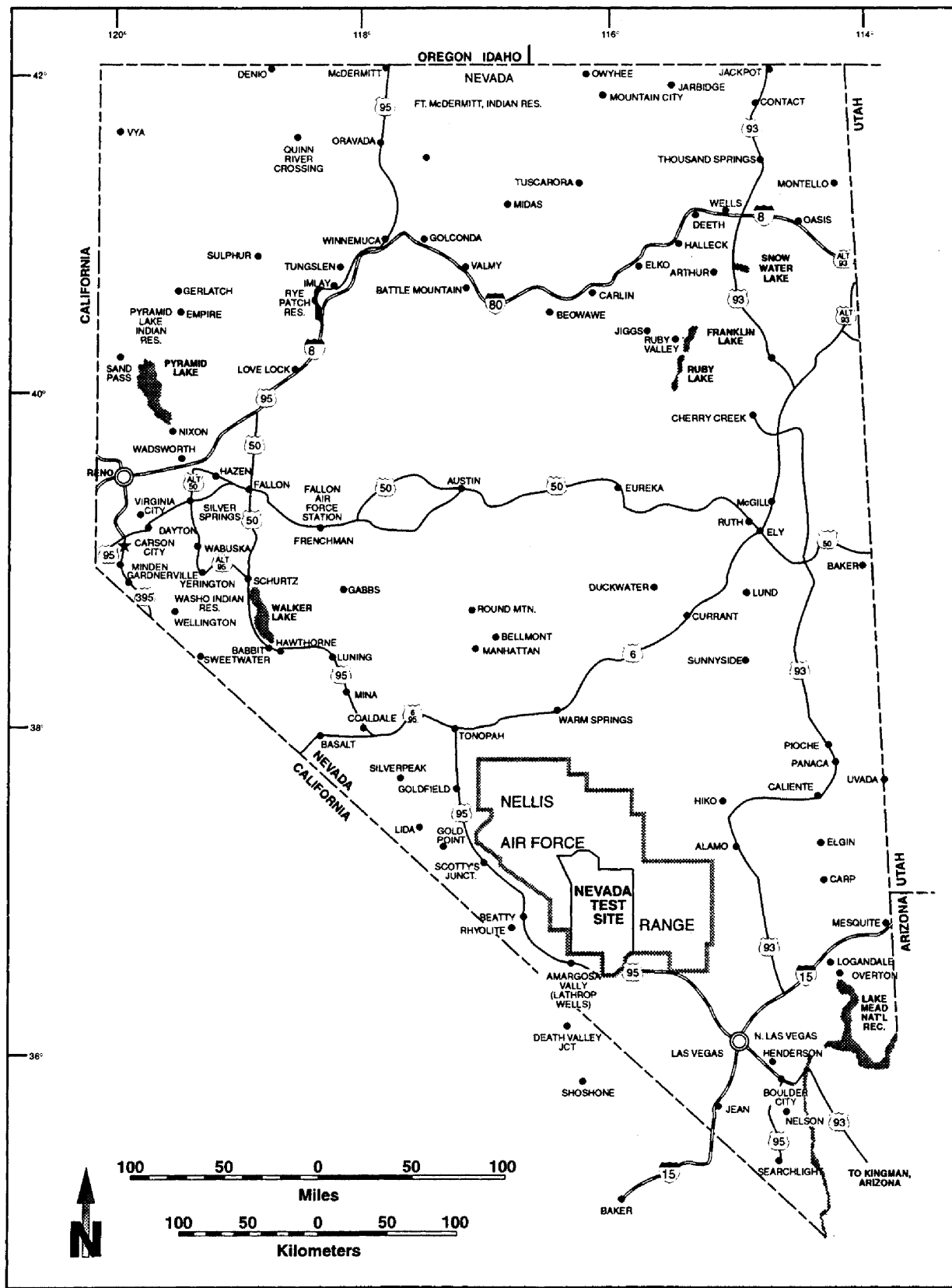


Figure 2.1 Location of the NTS-NAFR Complex Within the State of Nevada

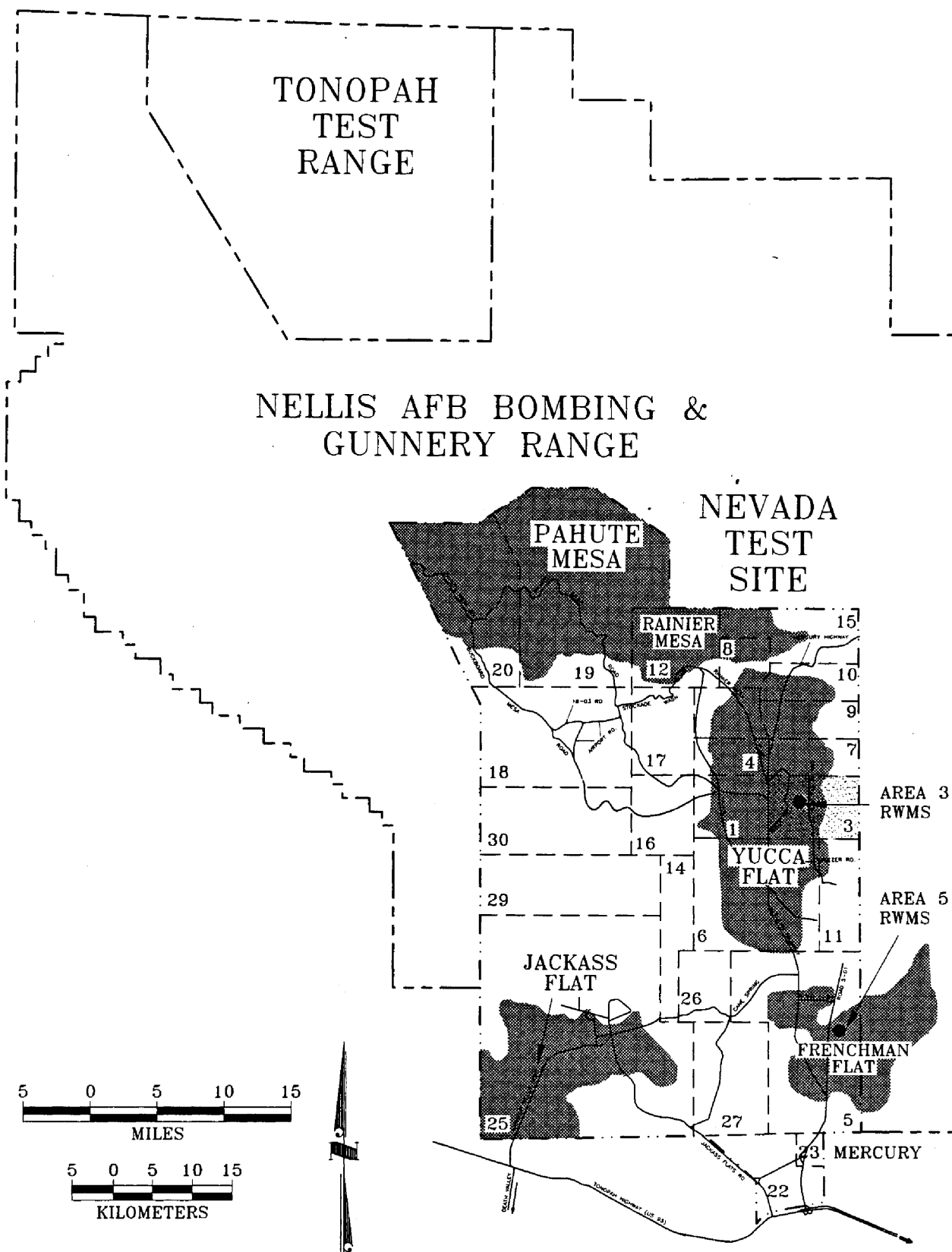
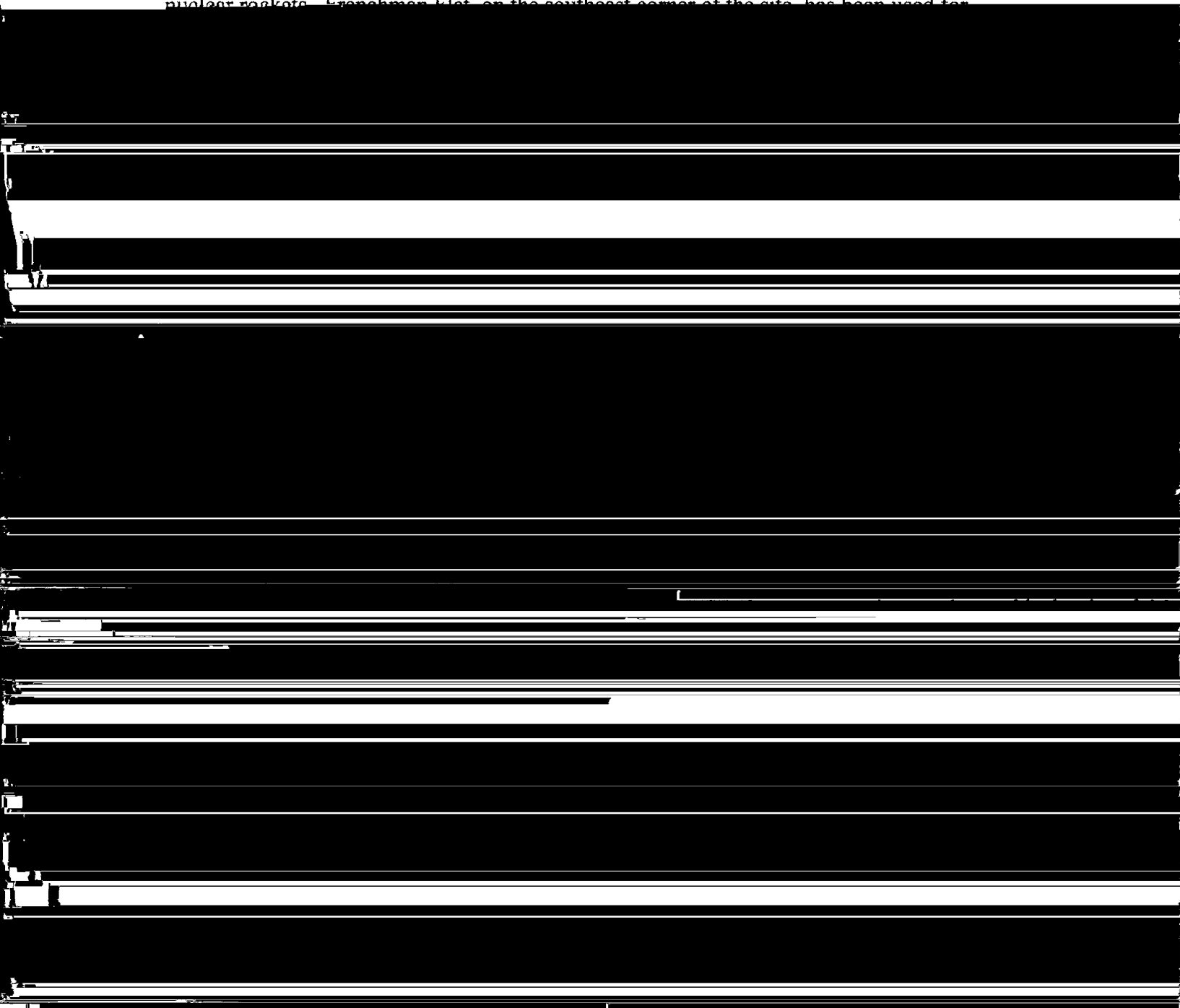
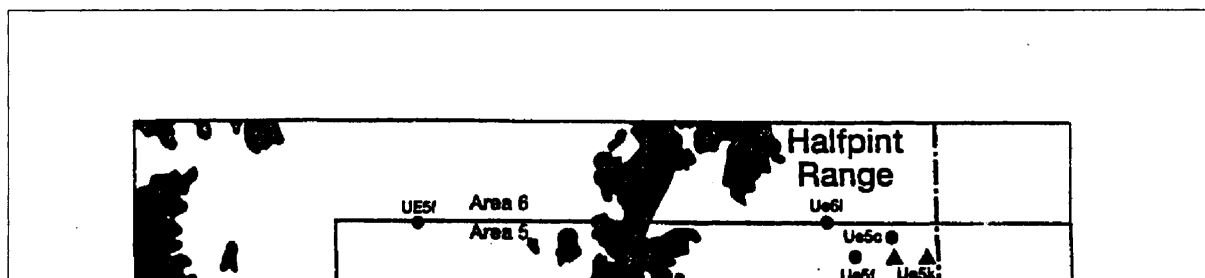


Figure 2.2 Location of the Area 5 RWMS and Major Operational Areas on the NTS

on the northwest region of the NTS, have been used for underground nuclear tests. The Jackass Flats area in the southwest corner of the site has been previously used for testing of nuclear rockets. Frenchman Flat, on the southeast corner of the site, has been used for



The other major facilities within Frenchman Flat are the Hazardous Materials (HAZMAT) Spill Center (formerly the Liquified Gaseous Fuels Spill Test Facility [LGFSTF]), located to the south on the playa, and the Device Assembly Facility (DAF), located approximately



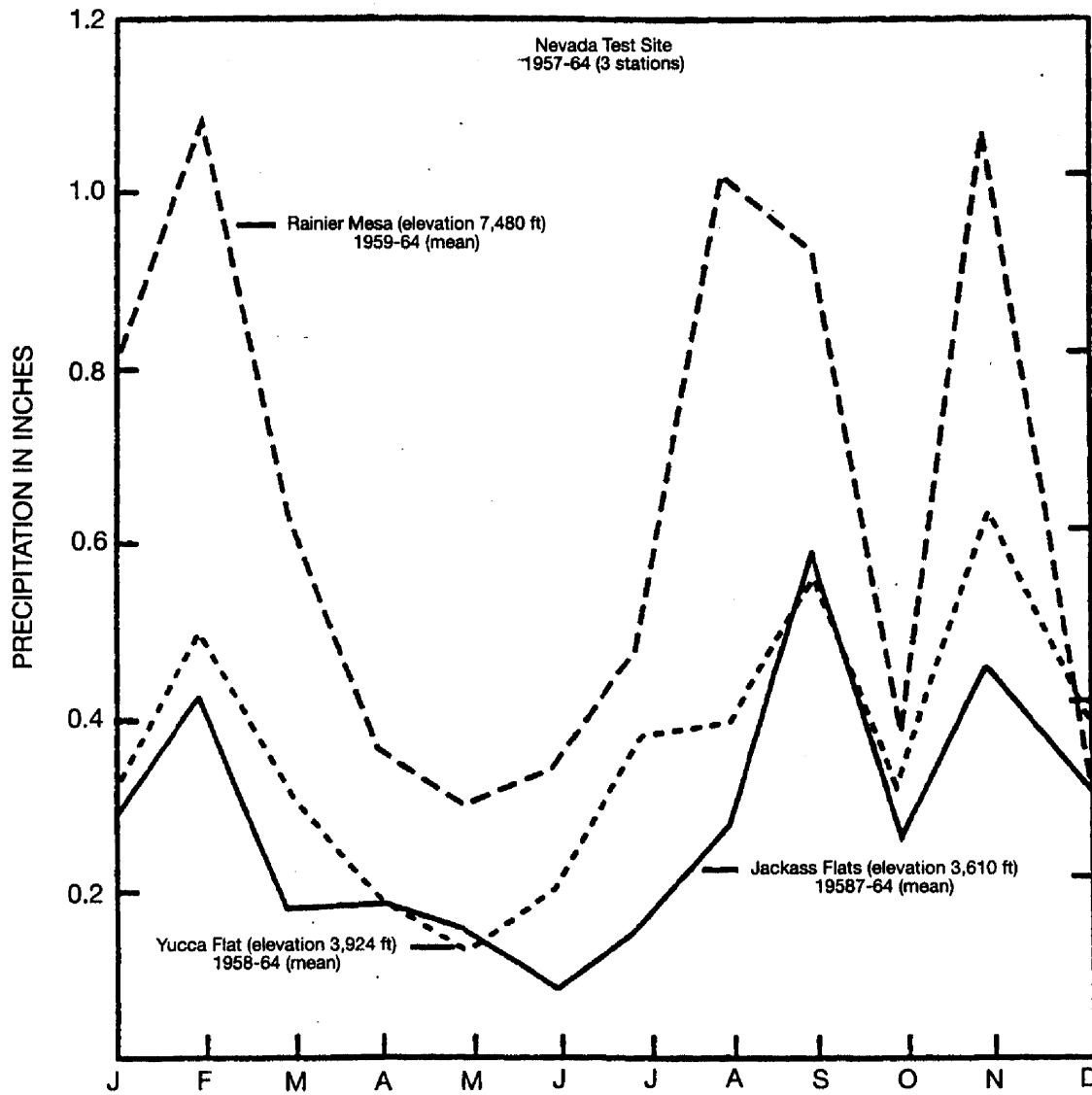


Figure 2.4 Monthly Mean Precipitation at the NTS From 1957 to 1964 (Winograd and Thordarson, 1975)

Table 2.1 Monthly Precipitation (cm) for the Period from January 1963 to December 1993 at Frenchman Flat (Well 5B).

Performance Assessment

YR	JAN	FEB	MAR	APR	MAY	JUN	JUL	AUG	SEP	OCT	NOV	DEC	YEAR
63	0.076	1.803	0.381	0.356	0.610	0.660	—	0.889	5.486	0.508	1.676	0.051	12.496
64	0.356	—	0.838	1.270	0.229	0.686	0.305	1.676	—	0.178	0.356	—	5.894
65	0.457	—	0.991	4.216	0.533	0.686	0.762	1.829	0.025	0.025	3.531	5.791	18.846
66	0.305	0.787	0.178	0.178	0.406	0.076	1.448	0.025	0.533	—	0.025	1.676	5.637
67	2.413	—	0.635	1.803	0.381	0.559	0.635	0.787	1.803	—	2.896	0.584	12.496
68	0.229	1.245	0.076	0.559	—	0.432	2.184	0.102	—	0.711	0.356	0.203	6.097
69	4.623	7.087	1.118	0.279	0.406	2.235	0.559	—	1.016	1.041	0.533	0.076	18.973
70	—	2.540	0.711	0.762	—	0.051	0.178	1.372	—	—	1.626	0.737	7.977

Area 5 Radioactive Waste

Rainfall varies markedly with the seasons as well as with elevation. The majority of rain falls during two seasons, with a larger peak in the winter and a smaller one occurring during the summer months. This bi-modal precipitation pattern results from two distinctive global weather patterns that develop during the summer and winter (*Figure 2.4*). During the summer, the lower Great Basin experiences frequent intrusions of warm moist tropical air, due to the formation of a high-pressure ridge located over the southern United States and northern Mexico. It has been widely accepted that the clockwise rotation of the air mass brings warm moist air up from the Gulf of Mexico to create a "summer monsoon season," characterized by local high-intensity thunderstorm activity of relatively short duration (Bryson and Lowry, 1955; Green and Sellers, 1964; Jurwitz, 1953; French, 1985). Additional investigation by Hales (1974) reveals that much of this summer moisture may be credited to moisture driven up from the Pacific Ocean by way of the Gulf of California. Precipitation during the winter months is governed by the formation of a high-pressure ridge in the Pacific and an accompanying low-pressure cell in the Gulf of Alaska, known as the Aleutian low. This combination often forces cold, wet air masses from the Pacific Northwest over the Great Basin and Rocky Mountains.

Although these storms are often longer in duration and less intense than their summer counterparts, they account for most of the annual moisture at the NTS. Snowfall is frequently observed at elevations greater than approximately 1,675 m (5,495 ft), but is rarely observed at the RWMS.

2.2.3 Temperature

NTS air temperatures vary highly with the seasons. Average daily temperatures range from 2°C (35°F) in January to 24°C (75°F) in August. Large daily fluctuations are common, especially on the playas and valley floors. Typical daily temperature ranges for the Area 5 RWMS run from -3° to 12°C (27° to 54°F) in January, and from 17° to 36°C (63° to 97°F) in July (Magnuson *et al.*, 1992).

2.2.4 Evaporation

Due to the exposure of the ground surface to high levels of incident solar radiation and wind

(3) localized small-scale convection currents due to nearby topography and terrain (Quiring, 1968). Northern winds tend to dominate in the winter and southern winds in the summer. Localized differential heating of the land surface during the day, coupled with a topographic trend toward greater elevation in the northern section of the NTS, result in southern winds flowing upslope during the day and northern winds moving downslope at night.

Wind speeds tend to be greater in the spring than in the fall. Because surface vegetation is sparse in the area, surface wind speed is categorized as calm only 2 percent of the time. Figure 2.5 summarizes the annual wind rose at Frenchman Flat for the years 1983 through 1993.

2.3 Geology

2.3.1 Regional Geology

The geology of the NTS consists of a thick section (more than 10,600 m [34,780 ft]) of Paleozoic and older sedimentary rocks, locally intrusive Cretaceous granitic rocks, a variable assemblage of Miocene volcanic rocks, and locally thick deposits of postvolcanic sands and gravels that fill the present-day valleys (Frizzell and Shulters, 1990). Figure 2.6 is a generalized geologic map of the NTS. More detailed stratigraphic information is available from recently updated maps of the NTS (Frizzell and Shulters, 1990). A summary of the general stratigraphy beneath the NTS, including lithologies and mode of emplacement, appears in Appendix B.

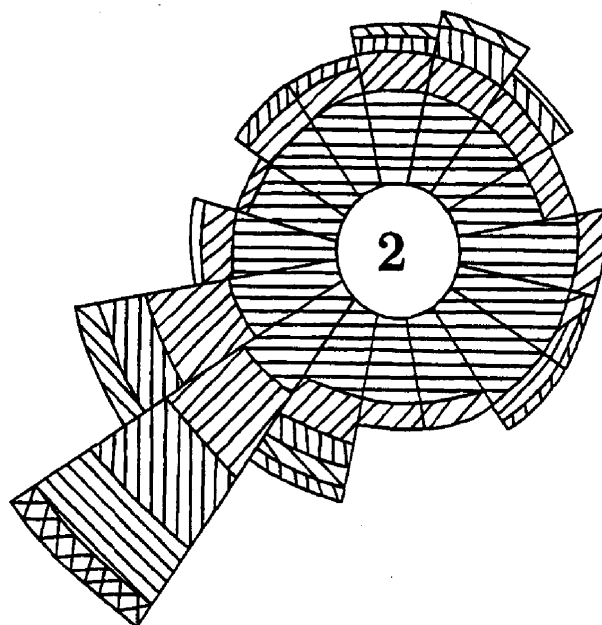
The NTS and surrounding areas are in the southern part of the Great Basin, the northernmost subprovince of the Basin and Range Physiographic Province (Figure 2.7). The Basin and Range Province is generally characterized by more or less regularly spaced, generally north-south trending mountain ranges separated by alluvial basins that were formed by faulting. The Great Basin subprovince is an internally drained basin; i.e., precipitation that falls over the basin has no outlet to the Pacific Ocean.

The topography of the eastern and southern NTS is typical of the Great Basin, with numerous north-south trending mountain ranges and intervening alluvial basins. In the northwest portion of the NTS, the physiography is dominated by the volcanic highlands of the Pahute and Rainier Mesas. There are three primary valleys on the NTS: Yucca Flat, Frenchman Flat, and Jackass Flats. Both Yucca and Frenchman Flats are topographically closed, with playas in the lowest portion of each basin. Jackass Flats is topographically open, with drainage via Fortymile Wash off the NTS.

2.3.2 Geology of Frenchman Flat and the Area 5 RWMS

Frenchman Flat is an intermontane basin typical of basin-and-range structure. The alluvium- and tuff-filled valley is rimmed mainly by Proterozoic and Paleozoic sedimentary rocks and

WIND ROSE WELL 5B (W5B) ANNUAL 1983-93



PERCENT CALMS IN CENTER

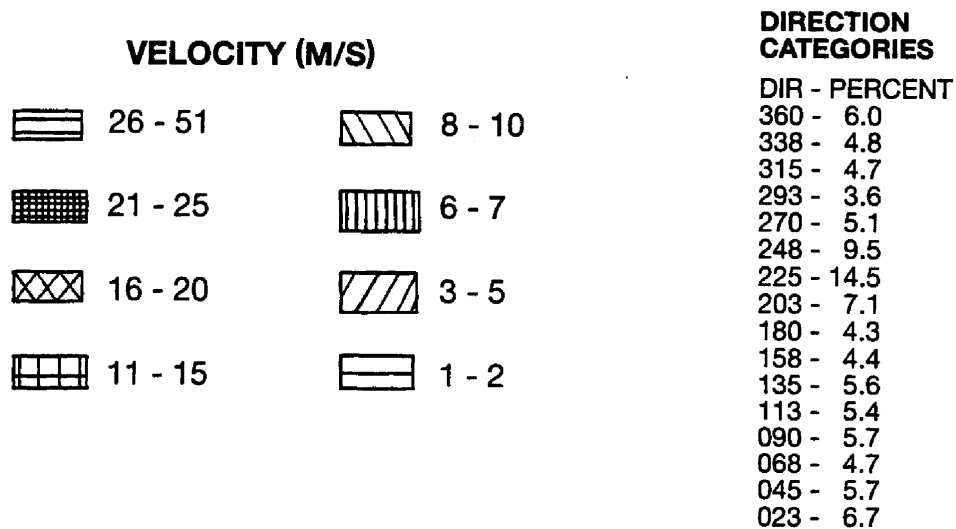
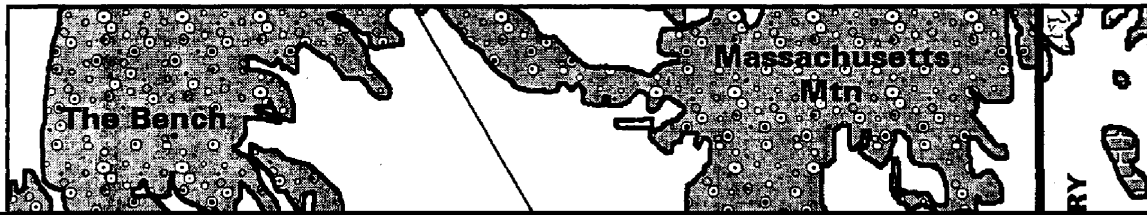
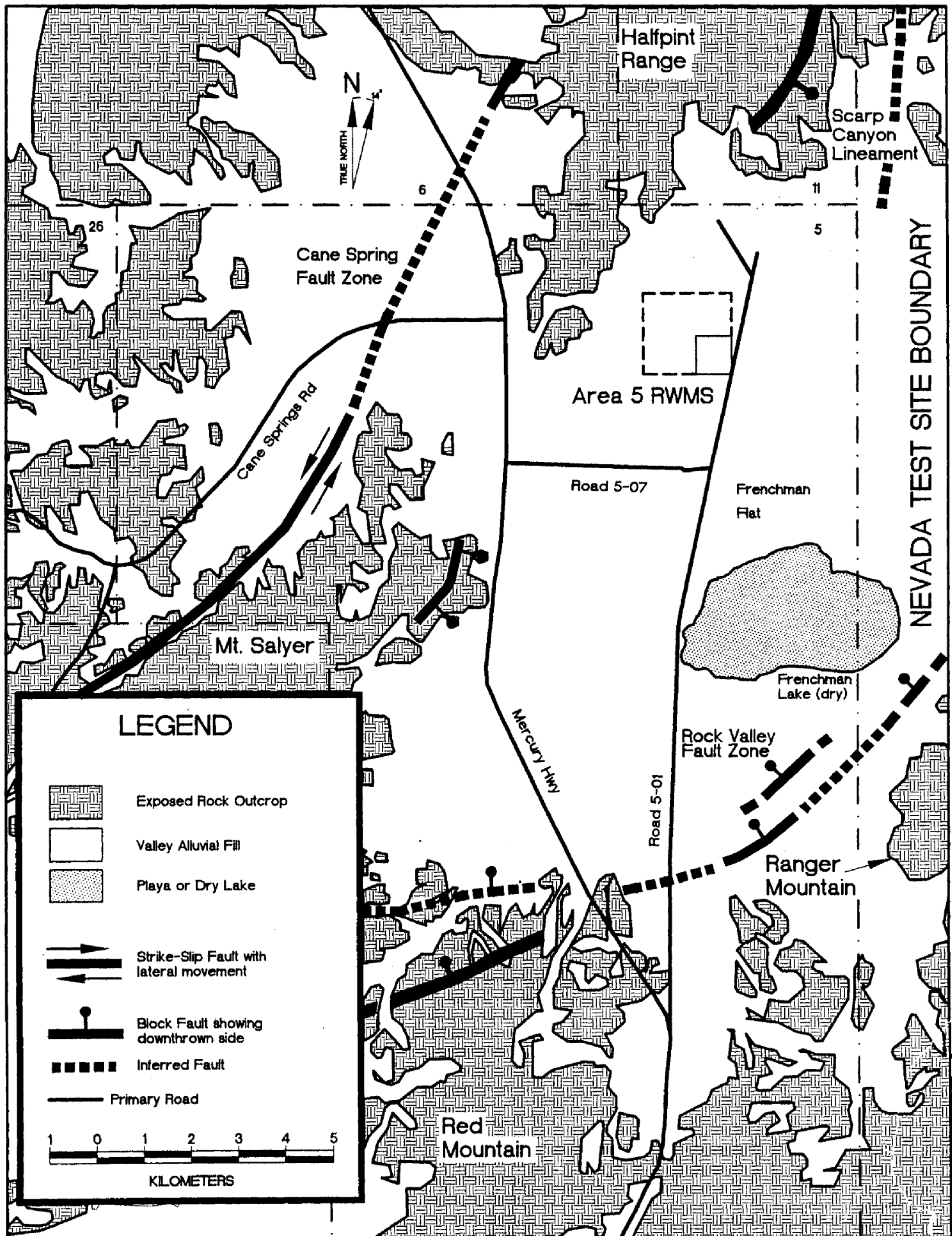


Figure 2.5 Annual Wind Rose for Well 5B in Frenchman Flat for 1983 through 1993





Cenozoic volcanic rocks. Frenchman Flat is bounded by the Halfpint Range to the north, the Ranger Mountains and the Buried Hills to the east-southeast, Mount Salyer to the west, and Mercury Ridge and Red Mountain to the south (*Figure 2.7*). It ranges in elevation from approximately 1,600 m (5,250 ft) above mean sea level in the surrounding mountain ranges to 940 m (3,080 ft) at Frenchman Flat Lake, a playa lake at the lowest point of the basin. The basin drains a 1,200 km² (460 mi²) watershed.

Proterozoic and Paleozoic rocks are generally extensive and occur under Frenchman Flat as basement rocks. In the lowlands areas of the basin, the basement rock units are overlain with alluvium, volcanic, and Tertiary sedimentary rocks. The infilling alluvium is 910 m (3,000 ft) deep at its maximum thickness. On the alluvial fans, the alluvium comprises interbedded gravel, sand, and silt with varying degrees of cementation. These coarse-grained deposits grade to the predominantly clayey silt deposits of the playa. Limited areas of wind-blown sand and silt are also present in portions of the lowland areas.

To the northwest and southeast, thrust faults have repeated sections of the Paleozoic and Precambrian rocks, and low-angle gravity faulting has created isolated blocks of the Paleozoic rocks out of stratigraphic order. Today, most prominent structures are related to basin-and-range extensional faulting that is younger than the volcanic rocks. In southern Frenchman Flat, fault strikes are mostly east-northeast with a significant strike-slip component of displacement. In northern Frenchman Flat, fault strikes are north-northeast with dominantly dip-slip normal faults.

Outflow sheets of ash-flow tuffs from the volcanic centers west and northwest of the basin occurred during the Tertiary Period. The youngest sediments of the valley are sand and gravel, derived from the volcanic and sedimentary rocks in the surrounding highlands.

2.3.2.1 Structural Features

Carr (1974) outlined the early structural development of the northern portion of Frenchman Flat. The early structural development is attributed to movement along several major fault systems associated with the initiation of Basin and Range tectonics. These systems include the Cane Spring Fault and the Rock Valley Fault Systems (*Figure 2.7*). Later, during the early and middle Tertiary, the valley continued to widen as ash-flow and ash-fall tuffs were deposited. The Cane Spring Fault plays an active role in the continuing development of the basin (Carr, 1974), although the rate of basin subsidence is unknown (Raytheon Services Nevada [RSN], 1991a).

The RWMS lies between two northeast-trending Tertiary fault zones: (1) the Cane Spring Fault, a left-lateral strike-slip fault 6.4 km (4.0 mi) to the west-northwest of the RWMS; and (2) the Rock Valley Fault zone, a strike-slip fault with a minor dip-slip component 8.9 km (5.5 mi) south of the RWMS.

A number of lineaments are apparent within the northern portion of Frenchman Flat (Miller *et al.*, 1993). However, no surface-cutting or Holocene faults have been identified within 914 m (3,000 ft) of the RWMS, indicating that the RWMS is in compliance with surface-fault-related criteria set forth by the Resource Conservation Recovery Act (RCRA) under 40 CFR 264.18.

Activities used to identify and evaluate any potential surface-cutting faults include:

(1) detailed mapping of waste disposal trenches and pits at the RWMS, (2) video logging of one of the GCD boreholes, (3) lineament map preparation and associated field investigation, (4) trench excavation and mapping, (5) subsurface evaluation of previously drilled boreholes, and (6) large-scale (1:6,000) air photo analysis and mapping of surficial deposits. Based on these activities, the only lineament confirmed to be fault-related and associated with surficial deposits is located 3.5 km (2.2 mi) northwest of the RWMS in the longitudinal valley of the Massachusetts Mountains. The faulting is believed to be late Tertiary to early Quaternary in age, based on bed attitudes and faulting of conglomeritic alluvium presumably of this age (Snyder *et al.*, 1993).

2.3.2.2 *Potential for Seismic Activity*

Rogers *et al.* (1977), Campbell (1980), Battis (1978), and Hannon and McKague (1975) have conducted seismic hazard studies of the NTS. They agree that the predicted maximum magnitude for an earthquake ranges from 5.8 to 7.0, with peak accelerations of 0.7 to 0.9 g. The estimated return period for the largest amplitude earthquakes expected (5.8 to 7.0) ranges from 12,700 to 15,000 years. These data suggest that there is the potential for a large earthquake somewhere within the NTS during the next 10,000 to 15,000 years.

The probability of the occurrence of at least one earthquake greater than 6.8 on the Richter scale is estimated in Appendix B. These calculations suggest there is about a 54 percent chance of one or more earthquakes greater than 6.8 in the next 10,000 years.

In August 1971, an earthquake of magnitude 4.3 occurred along the Cane Spring fault zone approximately 7.2 km (4.5 mi) northwest of the RWMS. An earthquake of 4.5 magnitude occurred in February 1972 along the Rock Valley fault system, approximately 7.2 km

2.3.2.3 *Evidence of Volcanism*

Studies of the NTS region are ongoing to assess the volcanic hazard at Yucca Mountain located approximately 45 km (28 mi) west of the RWMS. This information has been summarized with respect to applicability to the RWMS by RSN (1994). Volcanic centers nearest the RWMS include the Wahmonie-Salyer Center of intermediate rhyodacite to dacite composition, approximately 20 km (12 mi) to the west-southwest, and the Southern Nye County basalt ring dike in the Halfpint Range, located approximately 10 km (6 mi) to the northeast of the RWMS (Figure 2.8).

Several late Cenozoic, silicic (rhyolitic) caldera complexes occur in an eastward-trending belt between 37 degrees and 38 degrees north latitude (Stewart, 1980). A part of this belt, which includes the mesas of the NTS, has been termed the southwestern Nevada volcanic field (Byers, 1989). The Stonewall Caldera is the youngest (7.5 million years ago [Ma]) major silicic center in the area. Silicic volcanism is characterized by large-volume explosive

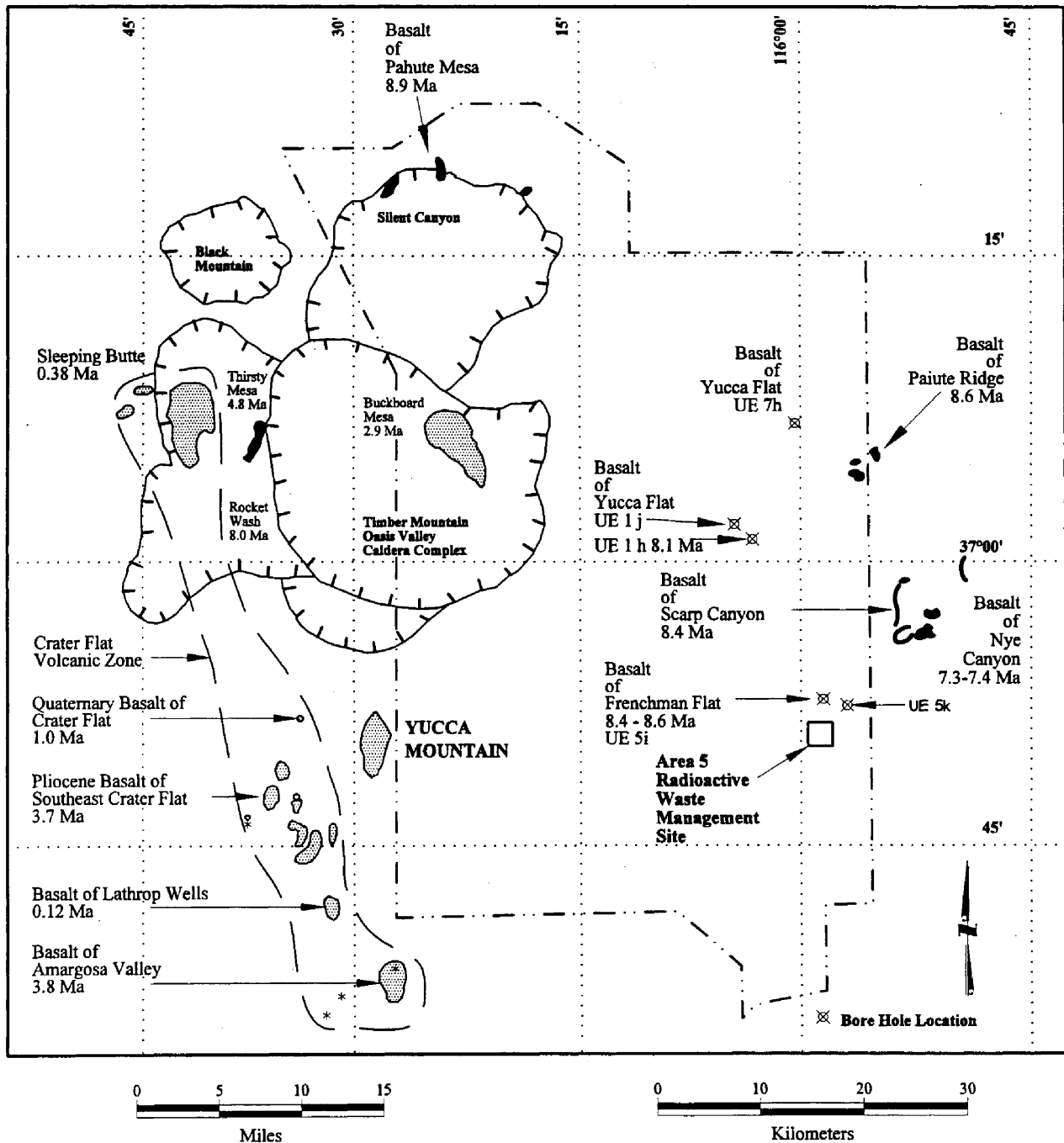


Figure 2.8

Post-Caldera Basalt of the Nevada Test Site Region. Shaded areas are the Older Post-Caldera Basalt. Stippled areas are the Younger Post-Caldera Basalt. Asterisks mark aeromagnetic anomalies identified as potential buried basalt centers or intrusions. Ages estimated in millions of years (modified from Crowe [1990]).

2.3.2.4 Local Stratigraphy

The stratigraphy of rock units from the surface to the lower carbonate units directly beneath Frenchman Flat is known to a reasonable degree based on both surface and subsurface investigations. These include numerous borehole descriptions collected to support underground testing, published well logs collected near the Area 5 RWMS (RSN, 1991b), core cuttings from the Pilot Wells (REECo, 1993b), investigations of surficial geology (RSN, 1991a; Frizzell and Shulters, 1990), Controlled Source Audiofrequency Magneto Telluric surveys (Zonge Engineering, 1990), and gravity data (Miller and Healey, 1965).

SUBSURFACE OBSERVATIONS

The Area 5 RWMS is built upon alluvium derived in part from the Tertiary volcanic rock exposed in the nearby Massachusetts Mountains and the Halfpint Range, as well as carbonates, quartzites, and other sedimentary rocks from the Nye Canyon area (Snyder *et al.*, 1994a). The thickness of the alluvium varies from zero at the edges of the basin to approximately 910 m (3,000 ft) in the center just north of the Frenchman Flat playa. The alluvial sediments are estimated to be Middle Miocene to Quaternary in age. The alluvium is estimated to be between 360 and 460 m (1,180 and 1,510 ft) thick directly beneath the Area 5 RWMS.

Beneath the alluvium lies a layer of interbedded Tertiary ash-flow and ash-fall tuff, estimated to be over 550 m (1,800 ft) thick. Well log data suggest that these units are predominantly Timber Mountain ash-flow tuff and tuff of the Wahmonie Formation (RSN, 1991b). More recently, site characterization studies (REECo, 1993b) identified lithologies, similar to the Ammonia Tanks Tuff of the Timber Mountain Group, 180 m (590 ft) beneath the surface in Pilot Well UE5PW-3, which is located approximately 1.8 km (1.1 mi) to the northwest of the

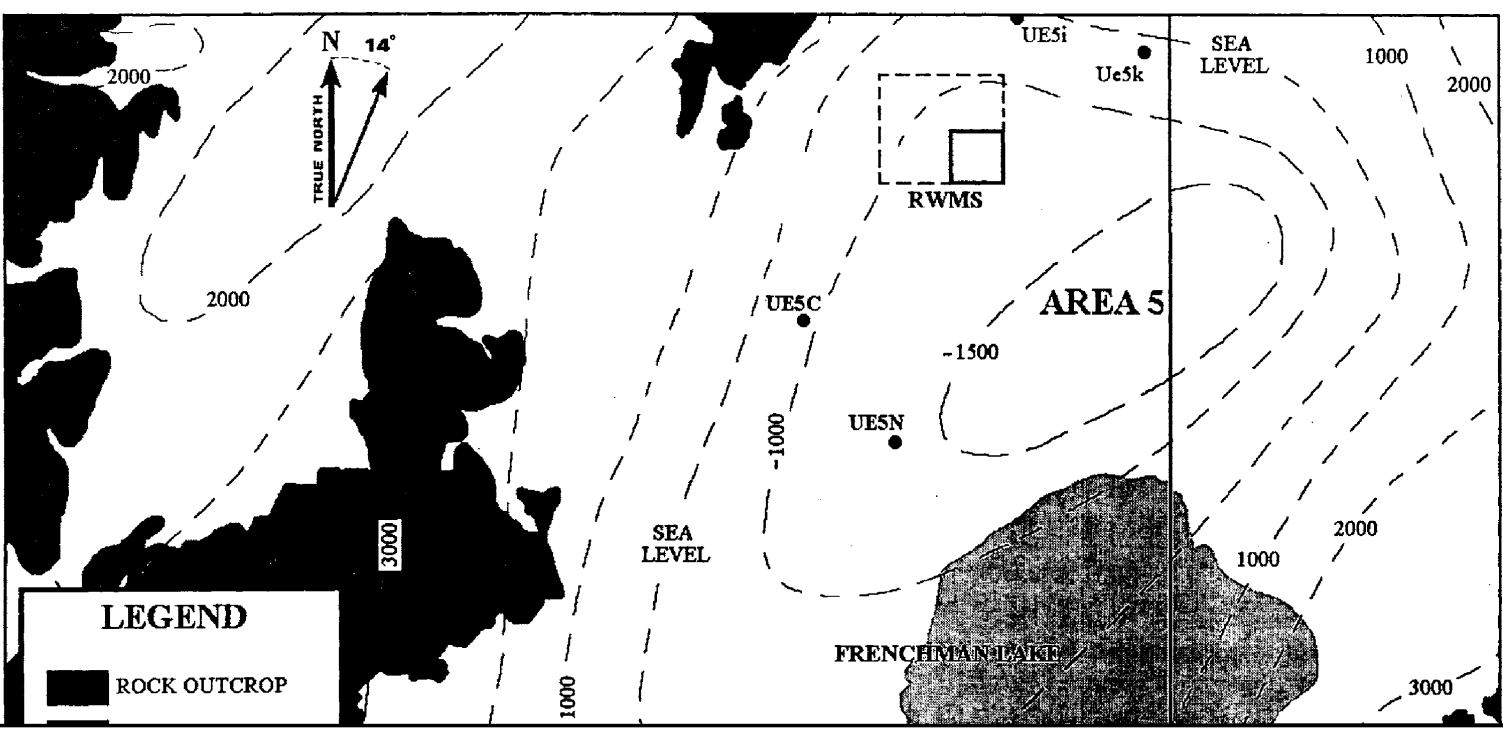


Figure 2.9 Gravity Interpretation of the Elevation of the T Underlying Frenchman Flat (adapted from Mill

thousand meters southeast of the RWMS. The gravity data suggest that the upper surface of the carbonate is approximately $1,340 \pm 150$ m ($4,395 \pm 490$ ft) below the surface at the Area 5 RWMS.

NEAR-SURFACE OBSERVATIONS OF ALLUVIAL SEDIMENTS

The near-surface stratigraphy of alluvial sediments has been studied in detail to a depth of approximately 11 m (36 ft) (RSN, 1991a; Snyder *et al.*, 1993). The near-surface structure displays features expected for lower-middle to distal alluvial fan deposition, including sheet-flood, stream channel, and debris flows. A grain-size analysis reveals alternating sequences of fine- and coarse-grained sediments, with occasional lenses of very coarse stream channel deposits (RSN, 1991a). All of the deposits are unconsolidated and were caused by water-

identification of caliche or variably cemented carbonate layers which, with their extremely low porosities and hydraulic conductivities, can greatly hinder the movement of water within the soil. Inorganic carbon concentrations were less than 1 percent by weight and nearly constant throughout the entire thickness of sampled alluvium (REECo, 1993b,c). Only a small increase was found in a 3-m (10-ft) interval from 167.6 to 170.7 m (550 to 560 ft) below the surface in Pilot Well UE5PW-2. This increase was accompanied by elevated levels of chloride, bromide, and sulfate as well. This isolated occurrence may indicate some degree of carbonate cementation at depth. However, any calcium carbonate accumulation at depth is expected to be discontinuous, as it is in the shallow subsurface, and it does not have a significant impact on groundwater flow. Organic carbon concentrations were generally an order of magnitude smaller than those of inorganic carbon.

PARTICLE SIZE ANALYSIS

Particle size distribution can influence the hydraulic conductivity of porous media and reflects the uniformity of an aquifer material. Particle size analysis by both the wet and dry sieve methods were performed on drill cuttings and core samples from all three Pilot Wells (REECo, 1993b) (Figure 2.10). The particle size analysis was limited to material less than the size of the core diameter (e.g., cobbles or boulders larger than approximately 0.09 m [0.3 ft] are not recovered in core samples).

Interpretation of the vertical distribution of gravel, sand, and fines within the three Pilot Wells varies according to hydrologic or geologic perspective. Although the sediment contains variable assemblages of grain sizes, and is therefore considered geologically heterogeneous, the variability does not significantly effect groundwater flow; thus, it is considered hydrologically homogeneous. UE5PW-1 displays a general fining upward sequence until approximately 40 m (130 ft) below the surface, where a coarsening upward

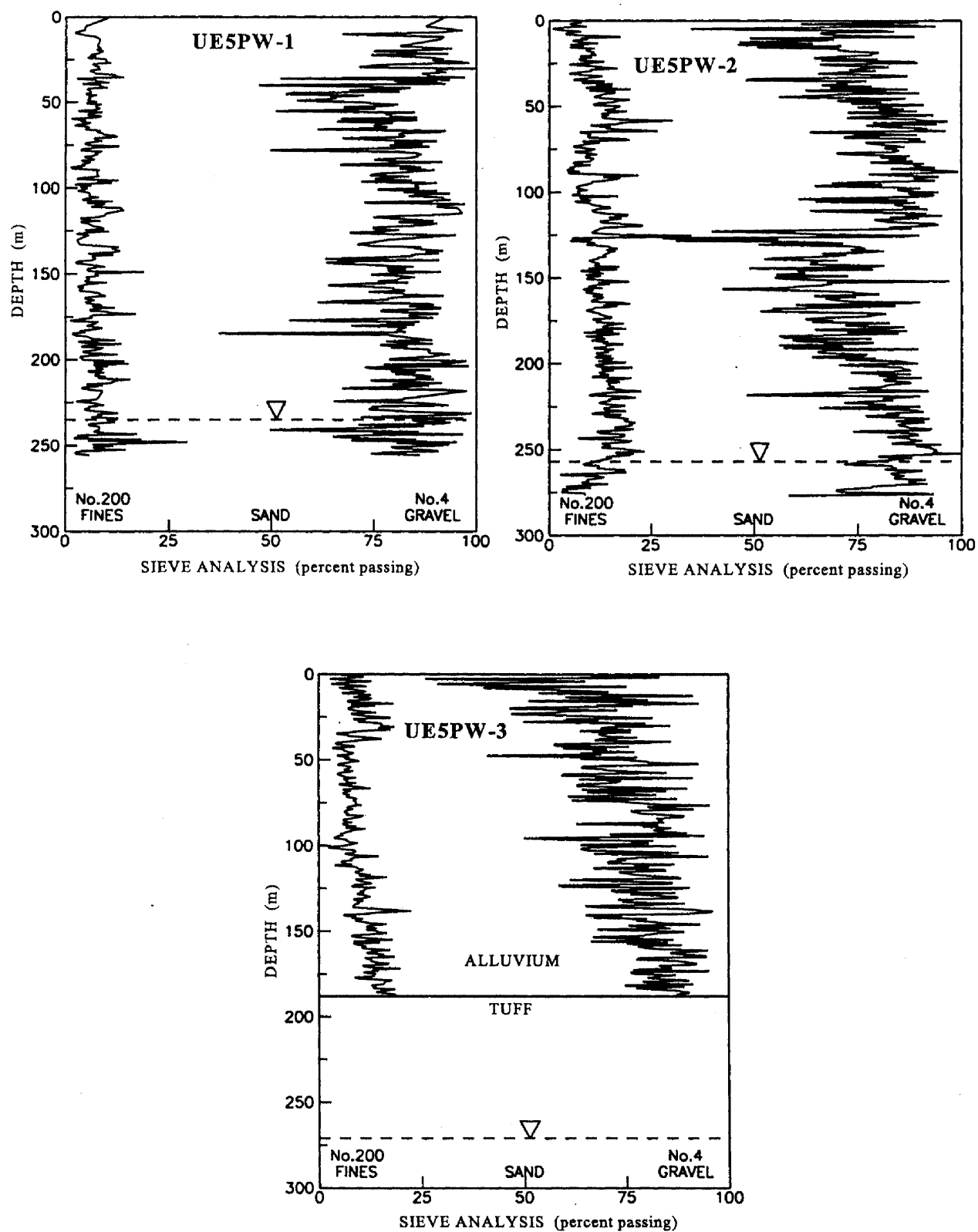


Figure 2.10 Depth Profile for the Grain-Size Distribution (Unified Soil Classification System) in the Three Pilot Wells (REEC, 1992b)

Table 2.2 Summary of the Mean Particle Size Fraction in the Alluvium as Sampled From the Science Trench Boreholes

PARTICLE SIZE FRACTION OF ALLUVIUM [†]										
Borehole Number	Mean Percent Passing Indicated Sieve Size									
	Gravel			Sands						Fines
	3/4	3/8	4	6	10	16	40	70	140	200
UE5ST-1	95.8	91.0	85.4	80.2	73.9	67.5	50.7	30.3	12.2	7.8
UE5ST-2A	98.6	94.3	86.8	81.9	75.5	68.4	51.7	32.8	13.4	8.5
UE5ST-2	96.0	91.1	84.4	79.2	72.8	66.5	51.1	32.4	13.3	8.5
UE5ST-4	94.1	89.6	84.5	80.2	74.9	69.2	54.3	35.2	15.1	9.6
UE5ST-5	98.5	96.0	88.7	84.8	80.5	74.3	53.7	32.1	14.2	10.2
UE5ST-6	94.6	88.2	82.4	78.0	73.2	67.3	50.1	29.9	12.5	8.1
UE5ST-7	94.5	89.1	83.3	78.0	72.4	66.1	47.8	29.6	9.9	5.0
Gross Mean	96.0	91.3	85.1	80.3	74.7	68.5	51.3	31.8	12.9	8.4

[†] Measured from 2,100 samples, Science Trench Borehole Project - REECo (1993c).

2.4 Hydrology

2.4.1 Regional Hydrology of the NTS

A majority of the potential radionuclide migration and exposure pathways identified by Shippers (1989) and Shippers and Harlan (1989) contain surface or groundwater as an important link (Kozak *et al.*, 1989). Therefore, it is crucial to understand and characterize the occurrence and movement of surface and groundwater near any waste facility.

2.4.1.1 Surface Hydrology

The arid climate of the NTS limits the occurrence of surface water in lower-elevation valleys to ephemeral washes created by precipitation runoff. Rainfall events that are intense enough to produce surface runoff are very few, typically originating in the higher elevations or mountain ranges as discrete, episodic events in the winter or summer. Recharge onto the valley floors is generally assumed insignificant because very few precipitation events result in enough moisture to produce runoff into the basins below (Dettinger, 1989). When large

events do occur, the ensuing runoff quickly seeps into the alluvial fan material, often within 1,000 m (3,280 ft) after entry into the valleys (Winograd and Thordarson, 1975). The presence of dry lakes or playas is evidence for past accumulation of runoff in the bottom of the valleys. Occasionally, water is observed to accumulate on the playa, but does not persist longer than a few days or weeks, probably due to a combination of evaporation and infiltration.

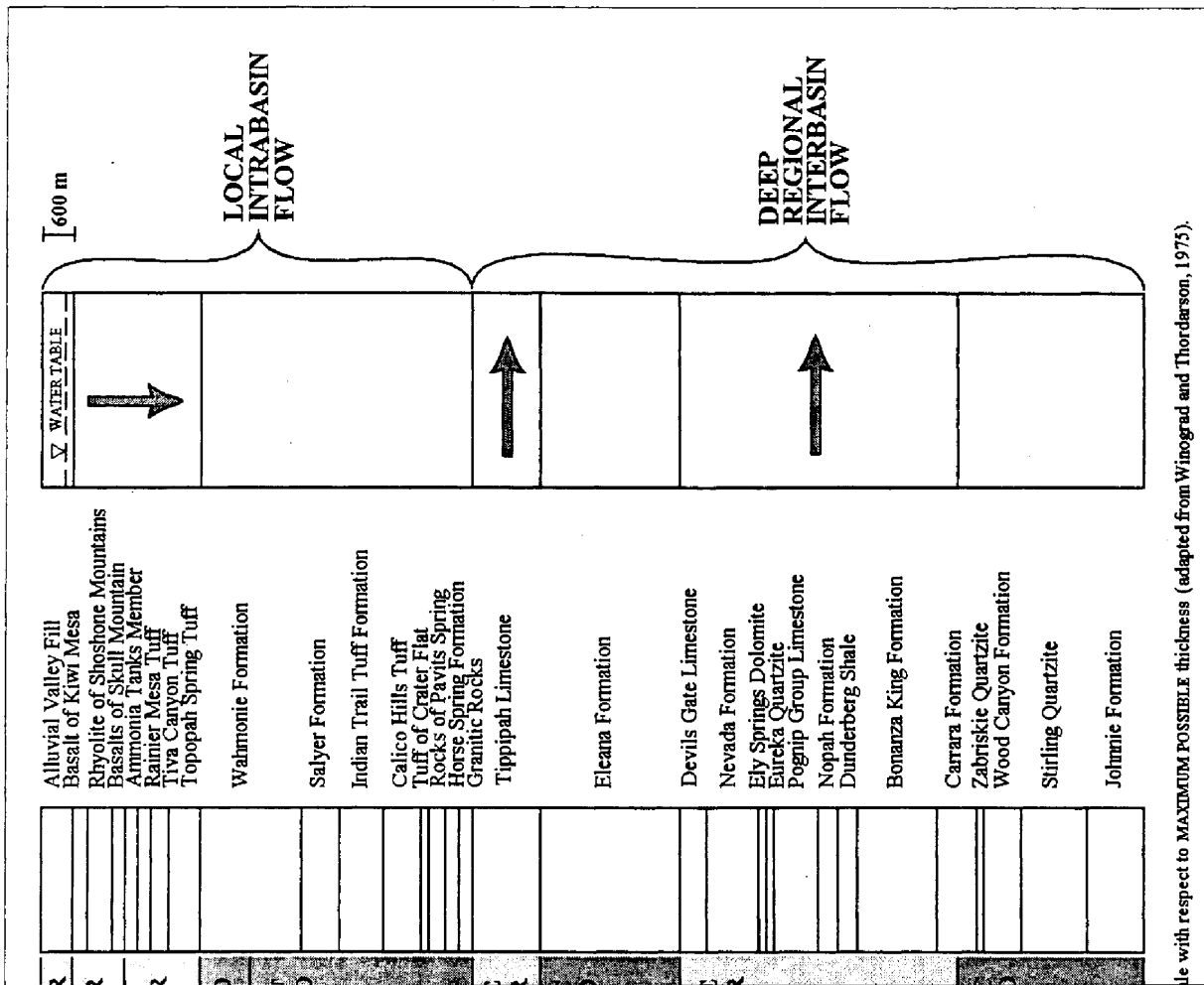
2.4.1.2 *Subsurface Hydrology*

Subsurface hydrology at the NTS can be divided into regions of saturated and unsaturated flow. Unsaturated flow addresses water flow and movement from the land surface down to the water table, where the interstices or fractures of the geologic media are completely filled with water. There is usually an inverse relationship between the thickness of an unsaturated zone and the amount of precipitation available on the surface. This relationship holds over the low-elevation valleys of the NTS, where annual rainfall is low and the unsaturated zone is thick. Winograd and Thordarson (1975) found that the depth to saturation (excluding perched water) varies from 200 to 600 m (656 to 1,968 ft) below the valley floors.

Beneath the unsaturated zone and the water table lies the region of saturated flow. Recharge from above and from horizontal movement within the saturated region is a function of the proximity of the aquifer to the surface and the lithology of the overlying rock units.

THE SATURATED FLOW REGION

Distribution and Character of Principal Aquifers and Aquitards



Scale with respect to MAXIMUM POSSIBLE thickness (adapted from Winograd and Thordarson, 1975).

outcrops on the mesa are buried beneath 1,000 m (3,280 ft) or more of alluvium in Yucca Flat and Jackass Flats. Further south and east, in the vicinity of Frenchman Flat, tuff is completely absent on the ridges near Mercury, where erosion and faulting have exposed the Paleozoic carbonate rocks.

The deepest saturated flow region occurs in the lower carbonate aquifer. Although other stratigraphic units play some role within the saturated flow region at various locations within the NTS, the lower carbonate aquifer provides the primary drainage for a large number of interconnected basins. This drainage occurs by horizontal movement of water through primary interstices and fractures in response to a largely horizontal hydraulic gradient at depth. The carbonate aquifer is generally confined above by either the upper clastic or tuff aquitard, except where it occurs near the surface in outcrops, such as in the ridges near Mercury. The aquifer is replenished primarily through horizontal flow from adjoining valleys and limited vertical flow from overlying strata. In general, regional saturated flow is primarily horizontal within this carbonate aquifer, which is overlain by a thick zone of unsaturated media of varying lithologies.

Figure 2.11 shows the four primary lithologies controlling the movement and occurrence of groundwater at the NTS: valley-fill alluvium, tuff, clastic rocks, and carbonate rocks. The ability of each rock to store and transmit water is a function of the available primary interstitial porosity and secondary openings, joints, and fractures. In general, alluvium, welded tuffs, and carbonates form aquifers, whereas the tuffs and clastic rocks tend to form aquitards that retard water movement.

Winograd and Thordarson (1975) have described suites of rock facies and lithologies which exhibit similar hydrologic character. These hydrologic units are presented below from the bottom to the top, oldest to the youngest. Interstitial porosities and hydraulic conductivities of these units are summarized in Table 2.3.

Lower-Clastic Aquitard

The lower-clastic aquitard consists of four formations (Burchfiel, 1964): the Zabriskie, Wood Canyon, Stirling, and Johnnie formations. These units are predominantly composed of quartzite and shale-siltstone layers with a total thickness estimated at over 3,000 m (9,842 ft). The lower-clastic aquitard, located predominantly within the saturated zone, forms the basal-confining unit above Precambrian bedrock throughout the study area. Although the aquitard is highly fractured, secondary porosity is generally absent in the subsurface because of extensive sealing by quartz, calcite, and mica-chlorite ingrowths. The unit as a whole has a very low effective porosity and overall permeability and is believed to form an effective barrier against downward groundwater movement from the overlying units. Ultimately, the unit probably influences the distribution of deep saturated ancestral drainage and discharge throughout the region.

Table 2.3 Compilation of Regional Hydrologic Character for Water-Bearing Strata Observed at the NTS (adapted from Winograd and Thordarson, 1975)

REGIONAL POROSITY AND PERMEABILITY					
Water-Bearing Unit	Total Interstitial Porosity (%)		Sat. Hydraulic Conductivity [†] (m day ⁻¹)		Relative Hydraulic Conductivity [‡]
	Range	Mean	Range	Mean	
Valley-Fill Aquifer	16-42	31	0.19 -2.0	1.2	moderate-high
Lava-Flow Aquifer	—	—	—	10.3	high
Welded-Tuff Aquifer	3-48	—	3.8-5.1	—	moderate
Lava-Flow Aquitard	5.7-14.1	—	—	—	low
Tuff Aquitard	19.8-48.3	37.7	—	0.006	low
Upper Carbonate Aquifer	—	—	—	—	moderate
Upper Clastic Aquitard	2.0-18.3	7.6	—	—	low
Lower Carbonate Aquifer	0.4-12.4	5.4	0.061-2.9	0.75	moderate
Lower Clastic Aquitard	0.2-10	3.8	—	0.006	low

[†]Calculated from transmissivities derived from drawdown curves in pump tests by Winograd and Thordarson (1975).

[‡]From hydraulic conductivity table for various classes of geologic materials after Bureau of Reclamation (1977).

Total interstitial porosities of 43 cores from the lower clastic aquitard were found to range

forms a transition zone to the clastic rocks just described, to the highly permeable Devils Gate limestone. The carbonate unit primarily lies deep within the saturated zone at the bottom of the stratigraphic column beneath practically all the basins including Yucca Flat, Jackass Flats, and Frenchman Flat. Winograd and Thordarson (1975) also noted that, due to thrust faulting, low-angle, normal faulting, and the existence of the extensive caldera complex to the northwest of the NTS, the carbonate aquifer underlying most of the NTS may not be hydraulically continuous with the same units to the northwest (if, indeed, they do exist beneath the calderas).

The lower-carbonate aquifer is unsaturated only where it outcrops as topographical highs, such as in the Halfpint Range, Ranger Mountains, and ridges near Mercury in the east and southeast portions of the NTS (*Figure 2.6*). Although the lower-carbonate aquifer has experienced the same degree of deformation, fracturing, and brecciation as the underlying lower clastic rocks, the fractures and joints have not experienced the same degree of cementation and thus are much more permeable to groundwater flow.

The average intercrystalline matrix porosity of the carbonates is very low. It has been estimated from core samples by Winograd and Thordarson (1975) at 5.4 percent, with a range from 0.4 to 12.4 percent. Winograd and Thordarson also determined the transmissivity from drawdown pumping tests of six wells, from which the saturated hydraulic conductivity can be derived. These values range from 0.061 to 2.9 m day⁻¹, with a median of 0.75 m day⁻¹ (median is reported rather than mean, because hydraulic conductivity was found to be lognormally distributed, and median values are more physically representative than means for lognormally distributed data). This represents a moderate degree of conductivity, according to tables from the Bureau of Reclamation (1977).

According to core logs, the degree of fracture fill and permeability is highly variable on a local scale. For example, Moore (1963) found a two order of magnitude difference in yield within a 200-m (656-ft) section of the Pogonip Group during a pump test. It has been suggested by Winograd and Thordarson (1975) that the wide variation in transmissivity could be the result of structural differences within the aquifer rather than changes in bulk lithology. This is because the observed variation occurred in five wells known to tap the aquifer in the upper brecciated plate of a low-angle thrust fault. Despite these local variations, there is evidence that the fracture transmissivity of the lower-carbonate aquifer as a whole may be homogeneous, even though it exhibits local heterogeneities. Winograd and Thordarson (1975) showed semilog time drawdown curves for various wells, where the second limb exhibited a constant slope, resembling curves for a grossly homogeneous aquifer. This conclusion is supported by model studies of Warren and Price (1961) and Parsons (1966).

The lower-carbonate aquifer plays a very active role in the deep regional saturated hydrologic region because of its great thickness, hydrologic characteristics, and extensive areal coverage. There are three sources of recharge for the aquifer: (1) precipitation at high elevations where

Cenozoic hydrologic units, and (3) lateral underflow into the aquifer from outside the immediate region. Downward leakage from overlying hydrologic units is considered secondary to the other sources of recharge and has been estimated to be 1 to 5 percent of total recharge (Winograd and Thordarson, 1975).

Upper-Clastic Aquitard

The upper-clastic aquitard consists of the entire thickness of the Eleana Formation and the Chainman Shale. Because of its limited extent, the aquitard is hydrologically important only beneath the western portion of Yucca Flat and northern Jackass Flats, where it is fully saturated and is more than 1,000 m (3,280 ft) thick. In this location, it hydraulically connects the upper- and lower-carbonate aquifers; elsewhere within the NTS, it has either been completely eroded or occurs far above the regional water table (Winograd and Thordarson, 1975).

The total interstitial porosity ranges from 2.0 to 18.3 percent, with an average of 7.6 percent.

~~Similar to the lower-clastic aquitard, it is believed to exhibit little to no fracture permeability.~~

In general, the strata exhibit matrices extensively altered to clay and zeolite minerals, resulting in a very low permeability. Although jointing occurs, water-bearing fractures are poorly connected, unconnected, or filled with alteration minerals (Winograd and Thordarson, 1975). Thordarson (1965) concluded that the unit should be classified as a fractured aquitard with high interstitial porosity but low permeability, and that regional groundwater movement is probably controlled by interstitial permeability rather than fracture permeability. Winograd and Thordarson (1975) measured the interstitial porosity of 72 cores from Yucca Flat and found a range from 19.8 to 48.3 percent, with a mean of 37.7 percent. They also suggested a transmissivity from bailing, swabbing, and injection tests of nine wells from which a gross saturated hydraulic conductivity can be approximated. This value, calculated at 0.004 to 0.008 m day⁻¹ based on a 304.8-m (1,000-ft) penetration, represents a relatively low value for conductivity according to tables from the Bureau of Reclamation (1977).

The tuff aquitard is unsaturated in topographical highs (e.g., the ridges surrounding Frenchman Flat, Mount Salyer, and Red Mountain) and exhibits great thickness. Beneath structural lows, such as Frenchman Flat, it is estimated to be in excess of 1,370 m (4,495 ft) thick beneath the alluvium. Because of its relatively large areal extent and thickness, it may

As the name implies, the tuff units comprising the aquifer have experienced varying degrees of welding and compaction, causing a great variation in both porosity and permeability. These zones, which are densely welded, have less than 5 percent porosity, while the non-welded basal or top portions of individual units may show porosities in excess of 50 percent (Winograd and Thordarson, 1975). Along with welding, the units exhibit a fair degree of columnar jointing and foliation in response to cooling stresses. Thus, although interstitial permeability is small due to welding, overall permeability is moderate because of jointing and fracturing. Core samples of the Topopah Spring, Tiva Canyon, and Rainier Mesa Tuffs show interstitial porosities ranging from 3 to 48 percent (Winograd and Thordarson, 1975). Saturated hydraulic conductivities calculated from drawdown curves of three pumping wells in the Topopah member in southern Yucca Flat yielded moderate values, ranging from 3.8 to 5.1 m day⁻¹.

Lava-Flow Aquifer

The lava-flow tuff aquifer is extremely limited in extent and composed primarily of three
formations restricted to the vicinity of Indian Flats. The permeability and porosity of this

into the valley-fill aquifer is severely hindered by the extreme conditions of high potential evapotranspiration and low rainfall experienced on the valley floors. Under the current climatic regime, recharge from the surface is generally considered nonexistent (REECo, 1993a,b; and Dettinger, 1989).

GROUNDWATER MOVEMENT

Winograd and Thordarson (1975) classified groundwater movement within the NTS into three categories: (1) movement of perched water, (2) intrabasin movement, and (3) interbasin movement. The first two categories describe localized groundwater movement within individual basins, while the third is concerned with deep, regional flow beneath and through basins.

Occurrence and Movement of Perched Water

Perched water consists of groundwater that has been separated from the underlying zone of saturation by unsaturated conditions, temporarily forming an inverted water table (Freeze and Cherry, 1979). At the NTS, perched groundwater forms principally within the aquitards in the foothills and ridges flanking the basins (namely, the tuff and lava-flow aquitard) as water travels to the regional water table below. The relatively low permeability of the units, compared to those units surrounding them, accounts for the existence of perched water, as drainage of water from overlying units is retarded from reaching the water table. Movement from localized perched water is downward. Thordarson (1965) showed that the occurrence of perched groundwater is erratic rather than widespread. Perched water is not known to occur beneath Yucca Flat, Jackass Flats, or Frenchman Flat.

Intrabasin Groundwater Movement

The movement of water from the Cenozoic aquifers and aquitards (Figure 2.12) to the underlying Paleozoic units is called intrabasin flow. It is believed that water stored within the Cenozoic aquifers eventually drains into the underlying Paleozoic units.

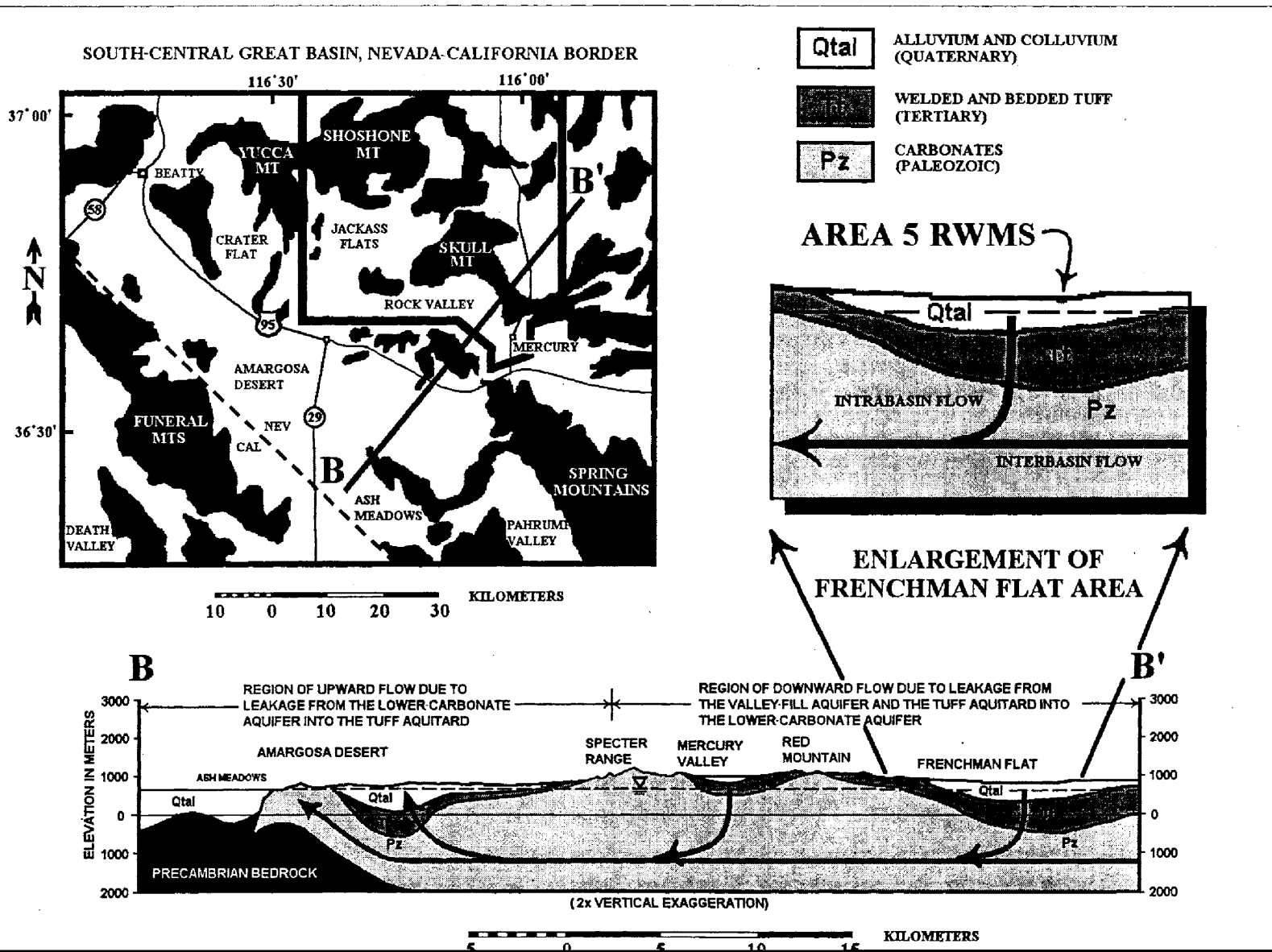


Figure 2.12

Cross-Sections Through Frenchman Flat to the Amargosa Desert Showing the Region of Groundwater Flow Pattern and Relationship Between Interbasin and Intrabasin Flow (adapted from Winograd and Thordarson, 1975)

flow within the lower-carbonate aquifer, confined by the lower-clastic aquitard on the bottom, and either the upper-clastic aquitard or tuff aquitard above. It is believed that the lower-carbonate aquifer and the lower-clastic aquifer are hydraulically connected throughout most, if not all, of the NTS (Winograd and Thordarson, 1975). As a result, groundwater flows laterally beneath both mountain ridges and basins with little regard for the overlying topography. This is what is known as interbasin flow.

Figure 2.12 illustrates the interbasinal-flow concept in the saturated zone. Section B-B' through Frenchman Flat shows the regional horizontal flow beneath the RWMS in the lower-carbonate aquifer. Recharge to the lower aquifer is provided by slow downward leakage from the tuff aquitard, welded-tuff aquifer, and valley-fill aquifer, and from horizontal movement within the aquifer.

In the NTS, lateral groundwater movement integrates several smaller intermontane valleys into a single basin, referred to as the Ash Meadows groundwater basin (Winograd and Thordarson, 1975; Rush, 1970). This interbasin flow is responsible for the discharge observed at Ash Meadows in the Amargosa Desert, 30 km (18.6 mi) south of the NTS. This discharge occurs through evapotranspiration, underflow, and the more than 30 springs which strike roughly along a common line. Hydraulic potential and groundwater chemistry data

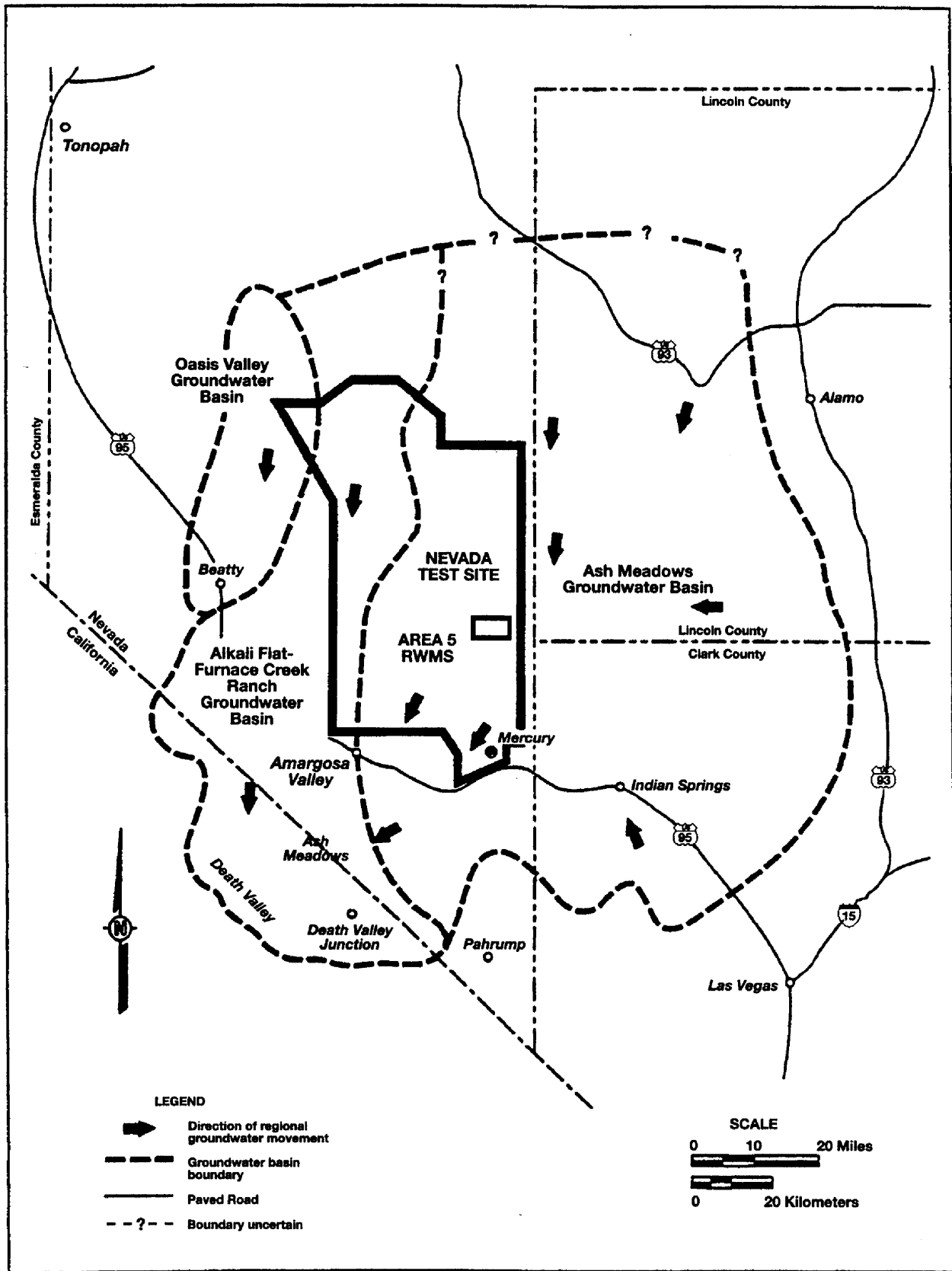
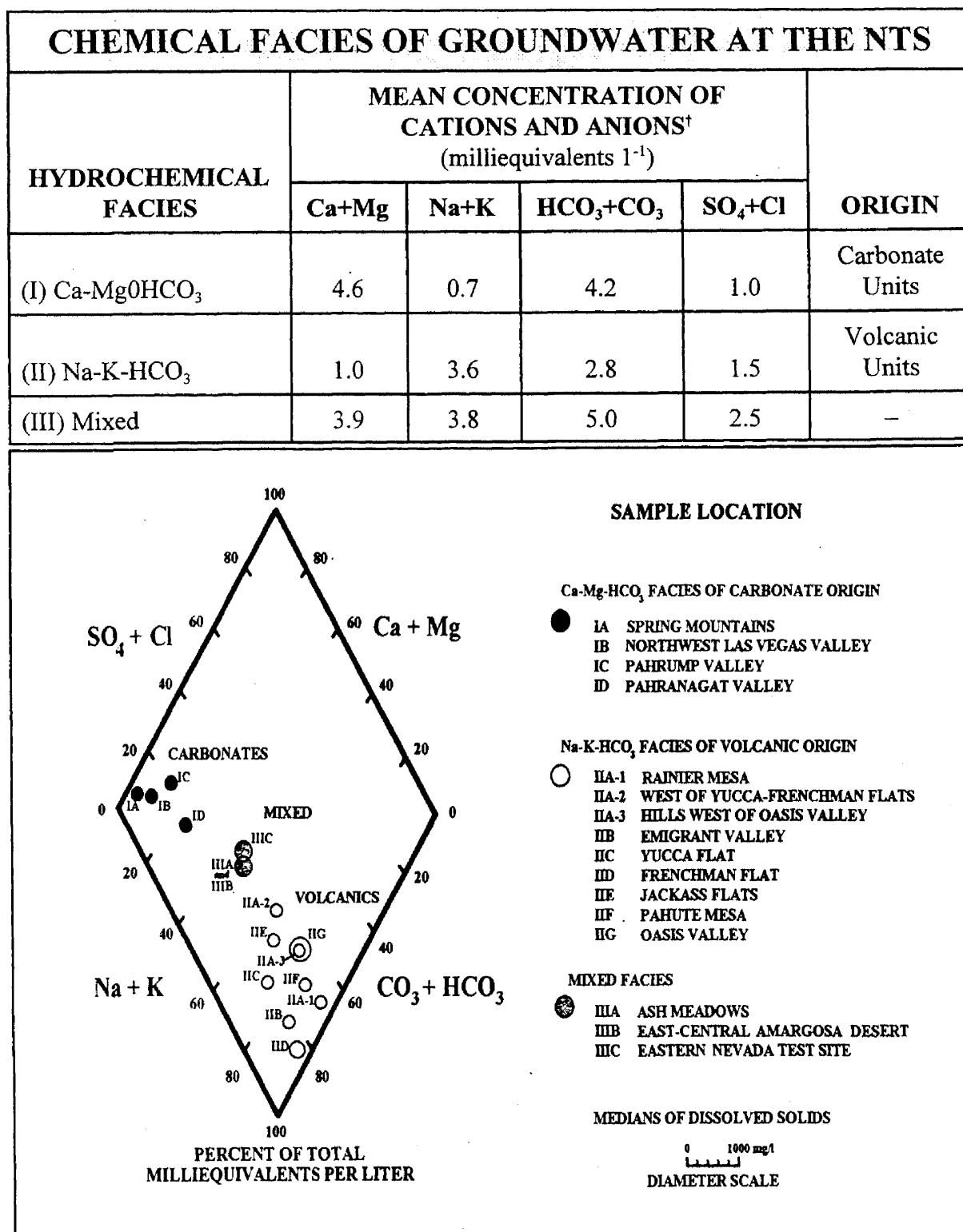


Figure 2.13 General Groundwater Flow Directions in the NTS Area (from Wadell, 1982)



[†]Mean values calculated from the average values of each cation and anion for individual valleys within each facies (adapted from Winograd and Thordarson [1975, Table 8]).

Figure 2.14 Mean Cation and Anion Concentrations in Groundwater Found at the NTS and Trilinear Diagram Analysis Showing the Three Dominant Chemical Facies

The Na-K-HCO₃ facies (II) is found within the lava-flow aquifer and tuff-aquitard units. The primary source of sodium comes from the alteration of rhyolitic glass containing sodic plagioclase feldspar (NaAlSi₃O₈), and from ion exchange with zeolites (Lipman, 1965; Hoover, 1968; and Hem, 1985), which are all major components of the volcanic units at the NTS. The facies also is seen in portions of the valley-fill aquifer, where a major portion of the alluvial-fill material has been derived from the erosion of volcanic units. The Ca-Mg-HCO₃ composition (I) is found within the Paleozoic carbonate units, such as the lower-carbonate aquifer and in the valley-fill aquifers that are composed of carbonate detritus. Most of the calcium and magnesium present is from the dissolution of limestone and dolomite (CaCO₃ and CaMg(CO₃)₂) mineralization in the unit as it conducts flow. Water of the mixed facies (III) contains portions of both the Na-K and Ca-Mg ions groups. Schoff and Moore (1964) noted that this type of water dominates in the lower carbonate, which is between the Amargosa Desert to the south and the eastern border of the NTS.

The Ca-Mg-HCO₃ facies (I) is of major importance in mapping the movement of deep interbasin groundwater flow within the Ash Meadows basin. Schoff and Moore (1964) observed that water in the Ash Meadows discharge area exhibited a chemistry similar to what would occur if water from the volcanic rocks in the valley basins (II) were mixed with water from the deep, carbonate aquifer (I), and suggested that groundwater within the NTS is moving southwestward toward Ash Meadows. Winograd and Thordarson (1975) offered further evidence for this conclusion by showing the water chemistry in the area surrounding

2.4.2 Hydrology of the Area 5 RWMS

This section describes the hydrology of the Area 5 RWMS. Its emphasis is on the vadose zone and the uppermost aquifer, or valley-fill aquifer, because these are the most relevant to the performance of the RWMS.

2.4.2.1 Surface Hydrology

The arid climate of Frenchman Flat limits the occurrence and movement of water on the surface. There is no permanent surface water within Frenchman Flat, except for small man-made impoundments. The alluvial fans of Frenchman Flat are incised with numerous dry desert washes that drain to the playa. Runoff from storm events occurs intermittently in these washes and may occasionally accumulate on the playa. As will be described in subsequent sections, water movement in the vadose zone at the Area 5 RWMS is predominantly vertical; therefore, the flow of surface water is not viewed as an important transport mechanism at the Area 5 RWMS. However, flooding and erosion caused by runoff in ephemeral channels do remain as potential issues in site performance.

EROSION IN EPHEMERAL CHANNELS OVER GEOLOGIC TIME

The Area 5 RWMS lies on three coalescing alluvial fan systems: the Scarp Canyon and Nye Canyon fan piedmont from the northeast, the southern Halfpint Range and Massachusetts Mountains fan from the north and northwest, and the Barren Wash fan from the west (Snyder *et al.*, 1995). Typical of alluvial fans in an arid climate, the channels on the surfaces of these alluvial fan systems are ephemeral; that is, they convey flow only in direct response to runoff-generating storms.

Snyder *et al.* (1995) evaluated the potential of erosion to expose buried waste at the Area 5 RWMS within the next 10,000 years. They did their evaluation using data collected from previous geomorphic surface mapping and trench and pit-wall mapping within and near the Area 5 RWMS (Snyder *et al.*, 1993, 1994). Snyder *et al.* (1995) found that the age of the surfaces at the Area 5 RWMS ranged from late Pleistocene (oldest) to late Holocene (youngest), with a predominant surface age from the middle Holocene to late Pleistocene. Late Holocene surfaces are present in the small active channels. In addition, net aggradation has likely occurred at the Area 5 RWMS since at least middle Pleistocene, but evidence of local channel incision and aggradation is present. The maximum depth of a channel incision found near the Area 5 RWMS is less than 1.5 m (5 ft), with most incisions less than 0.8 m (2.6 ft) deep. Furthermore, they stated that erosion caused by geomorphic processes is unlikely to reach a depth of 2 m (6.6 ft) at the Area 5 RWMS within the next 10,000 years. Because of the scarcity of rainfall and the physiographic nature of the RWMS, all available data indicates that channeling to 2.4 m (7.9 ft), the depth of buried waste, is possible but extremely unlikely.

NEAR-TERM FLOODING POTENTIAL AT THE AREA 5 RWMS

In addition to geomorphic studies, a flood assessment was completed to find whether the Area 5 RWMS lies within a 100-year flood hazard area (Schmeltzer *et al.*, 1993). This assessment determines the flood hazard assuming no significant changes in current climatic and hydrologic conditions. Over geologic time (e.g., 10,000 years), climatic and hydrologic conditions could change.

The flood assessment used Federal Emergency Management Agency (FEMA) accepted methods as stipulated in 40 CFR 270.14. Schmeltzer *et al.* (1993) identified three watersheds that could contribute flooding toward the Area 5 RWMS. These were the Barren Wash, Massachusetts Mountain/Halfpint Range, and Scarp Canyon watersheds. The total drainage area of these three watersheds is approximately 360 km² (139 mi²). The flood assessment included the Scarp Canyon watershed because the active part of the Scarp Canyon alluvial fan is located within 2 km (1.2 mi) of the Area 5 RWMS. The Nye Canyon watershed, as identified in Snyder *et al.* (1995), was excluded because it no longer drains toward the Area 5 RWMS.

A 100-year flood hazard map was delineated using the flood assessment results (Figure 2.15). This map shows that only the southwest corner of the Area 5 RWMS lies within a 100-year flood hazard area, which is defined by FEMA as an area with a 0.01 probability that a flood with a depth of flow greater than 0.3 m (1 ft) can occur in any given year. The southwest corner was impacted by two flood hazards: alluvial fan flooding on the Barren Wash alluvial fan and shallow concentrated flow draining from the Massachusetts Mountains.

The Barren Wash alluvial fan receives flow from the 210-km² (81-mi²) Barren Wash watershed. As indicated in Figure 2.15, the Area 5 RWMS is located on the lower eastern edge of the 100-year flood hazard area of the Barren Wash alluvial fan and is in a zone designated with a flow depth of 0.3 m (1 ft) and a flow velocity of 0.9 m s⁻¹. One major assumption in the FEMA methodology to evaluate alluvial fan hazards is that flood flow from the apex (e.g., the point where the flow becomes unpredictable) is just as likely to create a new path as it is to follow an existing channel. This means that the probability of a channel passing through any given point on a contour is uniform. Therefore, the 0.3-m (1-ft) depth and 0.9-m s⁻¹ designation can be described as the 0.01 probability in any given year that a channel with a depth of 0.3 m (1 ft) or greater and velocities of 0.9 m s⁻¹ or greater can occur within this zone.

The second flood hazard area is a result of flow draining from the Massachusetts Mountains and funneling into a shallow, wide channel that crosses the southwest corner of the Area 5 RWMS (Figure 2.15). The average 100-year depth and width of the shallow concentrated flow were approximately 0.6 m (2 ft) and 75 m (246 ft), respectively. The drainage area contributing to this flood hazard is approximately 16 km² (6.1 mi²).

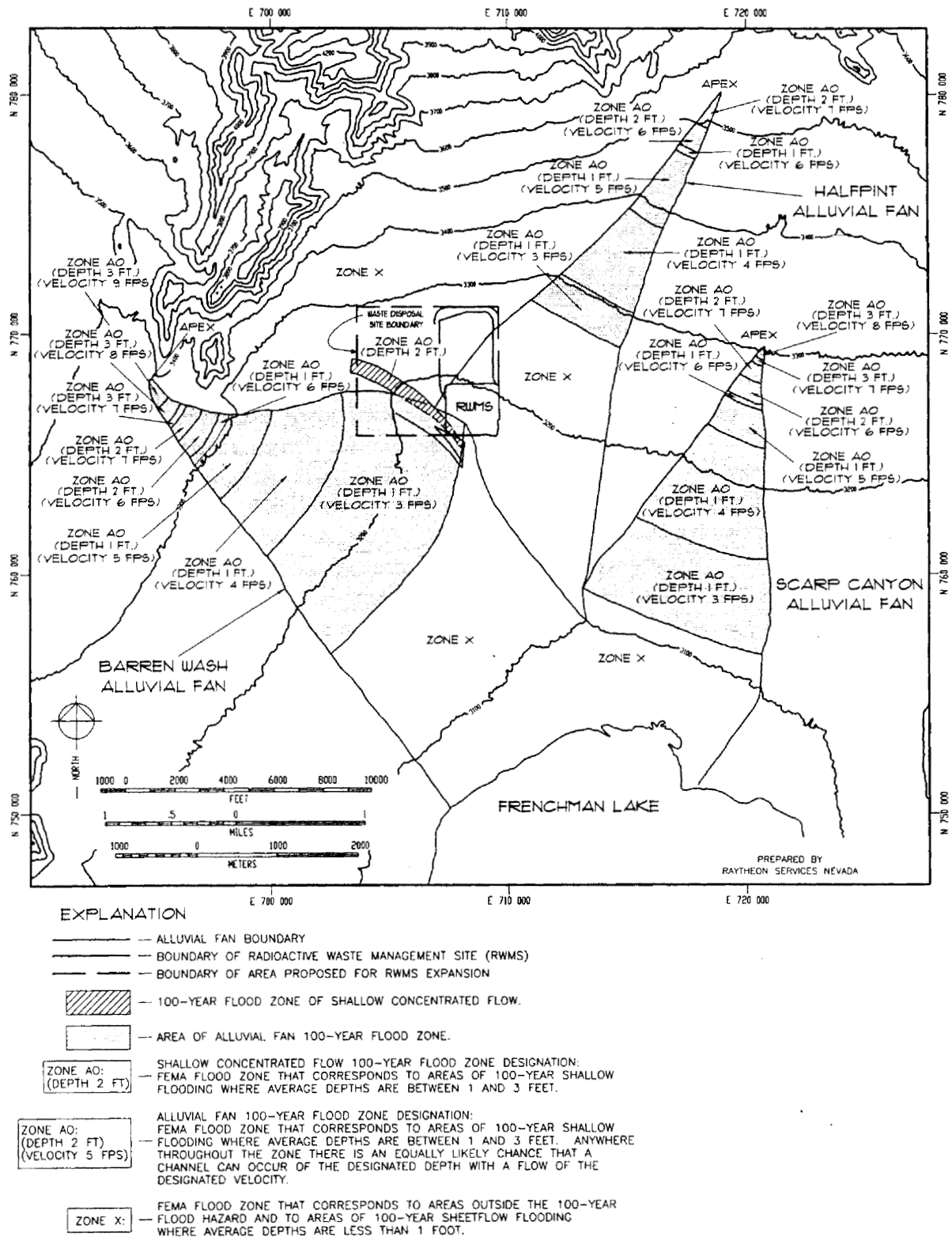


Figure 2.15 100-Year Flood Zone Delineation Map at the Area 5 RWMS (from Miller *et al.*, 1994)

Sheetflow from the 38-km² (14.6-mi²) Massachusetts/Halfpint watershed also could affect the Area 5 RWMS. However, flooding as sheetflow was not delineated as a 100-year flood hazard because 100-year depths of sheetflow average less than 0.3 m (1 ft) (*Figure 2.15*). This flood assessment also determined that a 100-year flood within the 105-km² (40.5-mi²) Scarp Canyon watershed will not impact the Area 5 RWMS. The western edge of the 100-year flood hazard on the Scarp Canyon alluvial fan is about 1.2 km (.74 mi) east of the Area 5 RWMS.

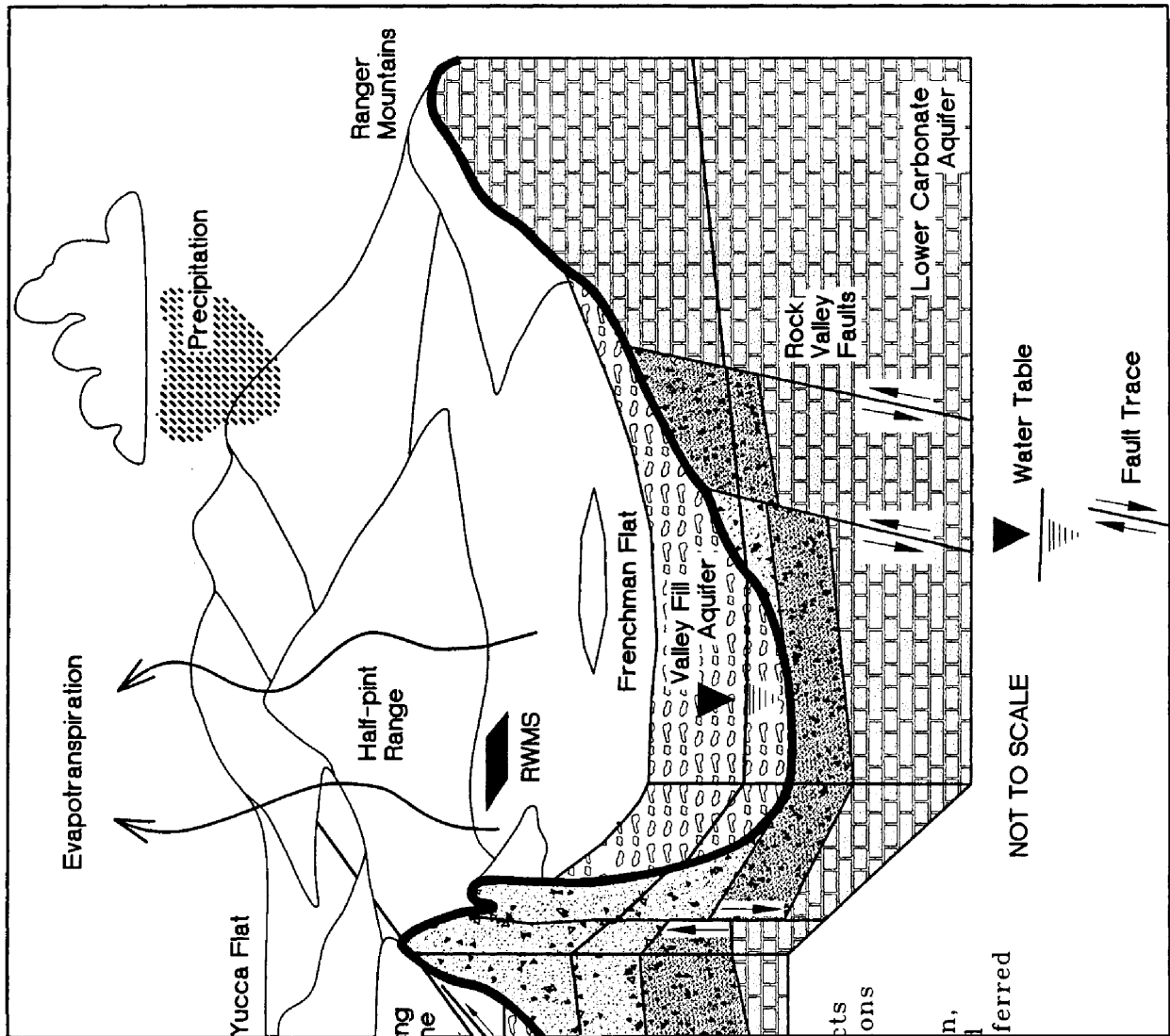
2.4.2.2 Subsurface Hydrology

An idealized conceptual model for the hydrogeologic cross-section of Frenchman Flat and surrounding mountain ridges has been developed based on work done by Case *et al.* (1984), Winograd and Thordarson (1975), Frizzell and Shulters (1990), RSN (1991a,b), and REECo (1993b) (*Figure 2.16*). The cross-section shown in the figure depicts stratigraphic and structural relations on a gross scale. Downward projection and possible intersections of the faults and bedding contacts with the water table in the subsurface remain uncertain and are highly interpretive. In spite of the uncertainties, several conclusions can be made. Well cuttings and drill logs from Pilot Wells UE5PW-1, UE5PW-2, and UE5PW-3 (*Figure 2.17* and *Table 2.4*) indicate that a thick section of unsaturated alluvium (vadose zone) lies below the RWMS. The minimum thickness of the vadose zone beneath the Area 5 RWMS is 236 m (774 ft). The top of the water table lies within the alluvial unit, except to the north as observed in Pilot Well 3 (UE5PW-3 [*Figure 2.17*]), and more than half of the alluvium is unsaturated directly beneath the RWMS. Winograd and Thordarson (1975) defined the saturated portion of alluvium as the valley-fill aquifer.

Table 2.4 Summary of Pilot Well Drilling Log and Lithology Information (from REECo, 1993b)

Borehole Number	Total Borehole Depth (m)	Lithology	Depth to Water (m)	Water Table Elevation [†] (m)
UE5PW-1	255.7	0 - 256 m alluvium	235.7	733.6
UE5PW-2	280.3	0 - 280 m alluvium	256.5	733.3
UE5PW-3	291.1	0 - 188 m alluvium 188 - 280 m welded tuff 280 - 291 m bedded tuff	271.7	733.5

† - from mean sea level datum



UE5PW-3

Figure 2.17

The 360- to 460-m- (1,184- to 1,509-ft)-thick alluvial unit is assumed to be underlain by approximately 550 m (1,804 ft) of tuff, which serves as an aquitard. Welded tuff (Ammonia Tanks member of the Timber Mountain Tuff) also was found 180 m (590.5 ft) beneath the surface in Pilot Well UE5PW-3 (*Figure 2.17*).

Welded tuff was not found to the depth penetrated in Pilot Wells UE5PW-1 and UE5PW-2; thus, the extent of the welded-tuff unit beneath the RWMS is unknown. Beneath the tuff aquitard lies the lower-carbonate aquifer which lies above the Precambrian bedrock. The thickness of the carbonate aquifer beneath the RWMS or within the basin is unknown.

PROPERTIES OF THE VADOSE ZONE

The vadose zone beneath the Area 5 RWMS is the primary barrier between the site and the uppermost aquifer. Four investigations have described the physical, chemical, and hydrologic properties of the vadose zone at the Area 5 RWMS. Spatial variation in properties up to a depth of 9 m (29.5 ft) have been investigated in existing excavations (pits and trenches) at the RWMS (REECo, 1993e). The properties of core and cuttings samples of the near-surface vadose zone up to a depth of 37 m (121 ft) have been reported for nine Science Trench Boreholes (REECo, 1993c) and four additional Science Boreholes (Blout *et al.*, 1995). The properties of core and cutting samples of the deep vadose zone up to 291 m (955 ft) deep have been described during the Pilot Well study (REECo, 1993b). The location of these wells and trenches is shown in *Figure 2.17*.

Water Content

Water-content values for the alluvium and tuff beneath the Area 5 RWMS have been determined for more than 1,000 samples from both drill cuttings and core samples from the Pilot Wells and Science Trench Boreholes (*Figure 2.18* and *Table 2.5*) (REECo, 1993b,c). All samples were collected using dry drilling techniques. A comparison of the volumetric water content profiles from the wells and boreholes indicates that the water content throughout the unsaturated zone is remarkably low, with an overall average of 8.72 percent by volume (5.39 percent by mass). Because the average porosity for the alluvium has been established at about 31 percent, these data show that only 25 percent of the total void space is filled with fluid.

Trends in water content are observed with depth. In the near surface (5 to 10 m [16.4 to 32.8 ft] depth), volumetric water contents as low as 1 to 3 percent are observed (REECo, 1993b,c; Blout *et al.*, 1995; Levitt *et al.*, 1996). Under these conditions, a discontinuous water phase may develop, leading to reduced rates of water movement. The evolution of the air-water interfaces in a drying porous medium was addressed by Gardner and Chatelain (1947) who described conceptually the formation in dry soil of a discontinuous water phase restricted to capillary wedges at the contact points of the solid phase. Connecting films no more than a molecule thick are suggested by Bear (1972):

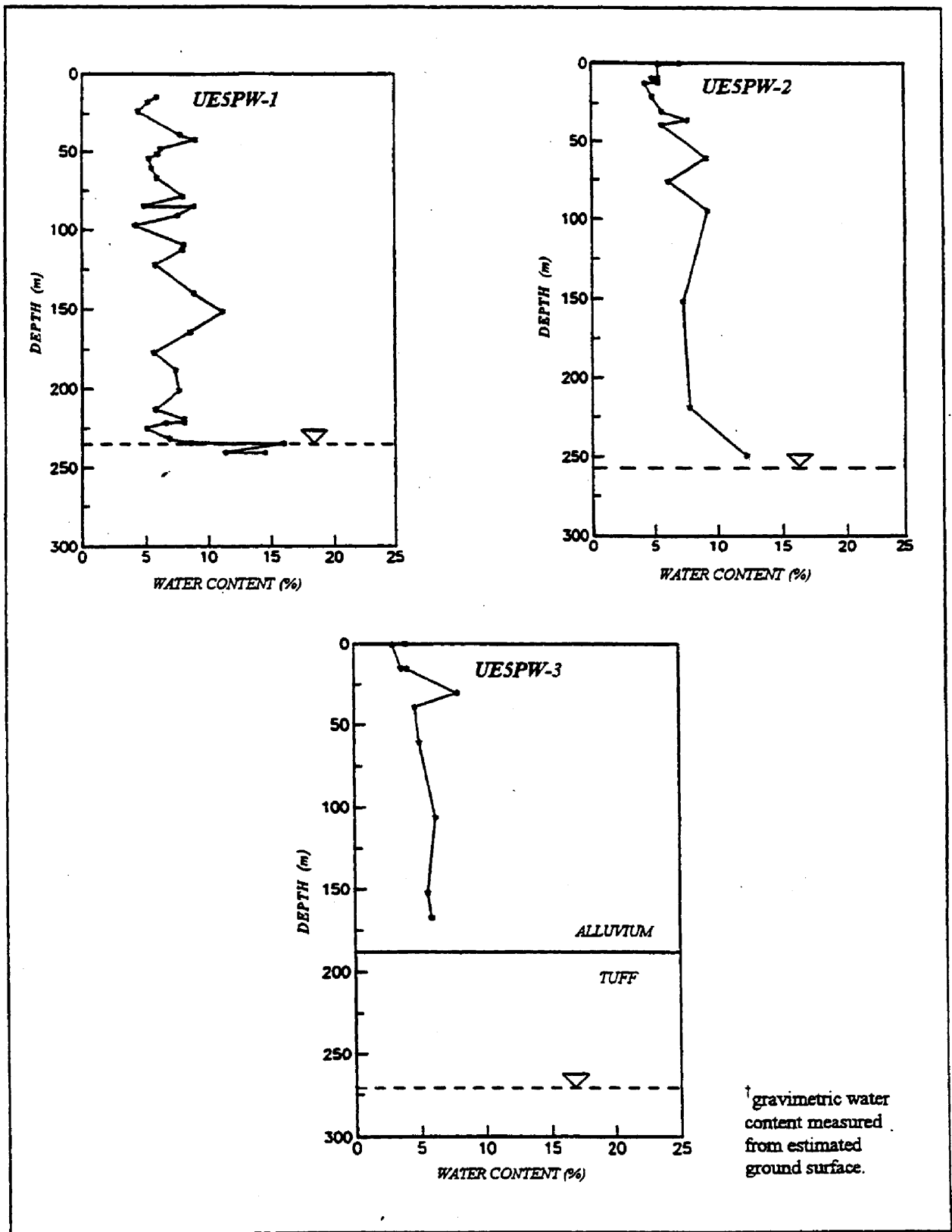


Figure 2.18 Water Content Profile Beneath the Area 5 RWMS Based on the Pilot Well Data (REECo, 1993b)

Table 2.5 Summary of Water Content Data From the Pilot Wells and Science Trench Borehole Studies (REECo, 1993b,c)

VADOSE ZONE WATER CONTENT (θ)					
Borehole or Well Number	Gravimetric Water Content			Number of Samples [†]	Standard Deviation
	Min.	Max.	Mean		
UE5PW-1	2.6	13.9	6.6	138	2.0
UE5PW-2	2.0	12.2	6.6	58	2.2
UE5PW-3	2.5	8.4	4.9	50	1.4
UE5ST-1	1.9	9.2	5.2	155	1.4
UE5ST-2a	2.9	7.4	4.8	99	0.9
UE5ST-2	2.4	21.4	5.7	193	2.1
UE5ST-3	—	—	—	—	—
UE5ST-4a	3.3	7.3	5.4	12	1.1
UE5ST-4	1.2	12.1	5.4	174	1.5
UE5ST-5	2.1	7.4	3.7	46	0.9
UE5ST-6	1.3	11.6	5.0	80	1.7
UE5ST-7	1.9	10.8	3.7	47	1.8
Overall Mean Water Content [†] 5.39 % (wt.) 8.72 % (vol.)					

[†] Total of 1,052 samples.

At very low water saturation . . . water forms rings called pendular rings around the grain contact points. At this low water saturation the rings are isolated and do not form a continuous water phase, except for a very thin film of nearly molecular thickness on the grain's surfaces. Practically no pressure can be transmitted from one ring to the next within the water phase.

Scheidegger (1974) also notes that there is no possibility of flow in the pendular phase which occurs in the form of pendular bodies throughout the porous medium. Similarly, Hillel (1980) writes,

In coarse-textured soils, water sometimes remains almost entirely in capillary wedges at the contact points of the particles, thus forming separate and discontinuous pockets of water. In aggregated soils, too, the large interaggregate

spaces which confer high conductivity at saturation become (when emptied) barriers to liquid flow from one aggregate to its neighbors.

The low-volumetric water contents observed in the near surface suggest the presence of a discontinuous water phase. Low water contents will impede the flow of liquid by reducing the hydraulic conductivity.

Water Potential

The water potential gradient is of prime importance in determining the magnitude and direction of movement of liquid water in dry soils. Depth profiles of water potential for each of the Pilot Wells and Science Trench Boreholes were determined from both core samples and drill cuttings by REECo (1993b,c) and are shown in Figure 2.19. The figures show consistently high negative values of potential (indicating very dry conditions) within the upper 35 m (115 ft) of alluvium within all profiles. The data gathered from the Science Trench Boreholes (*Figure 2.19*) show the strongest positive upward gradient is within the upper 9 m (29.5 ft) of alluvium.

Because convective flow is driven by a gradient in total potential, static zones or regions of

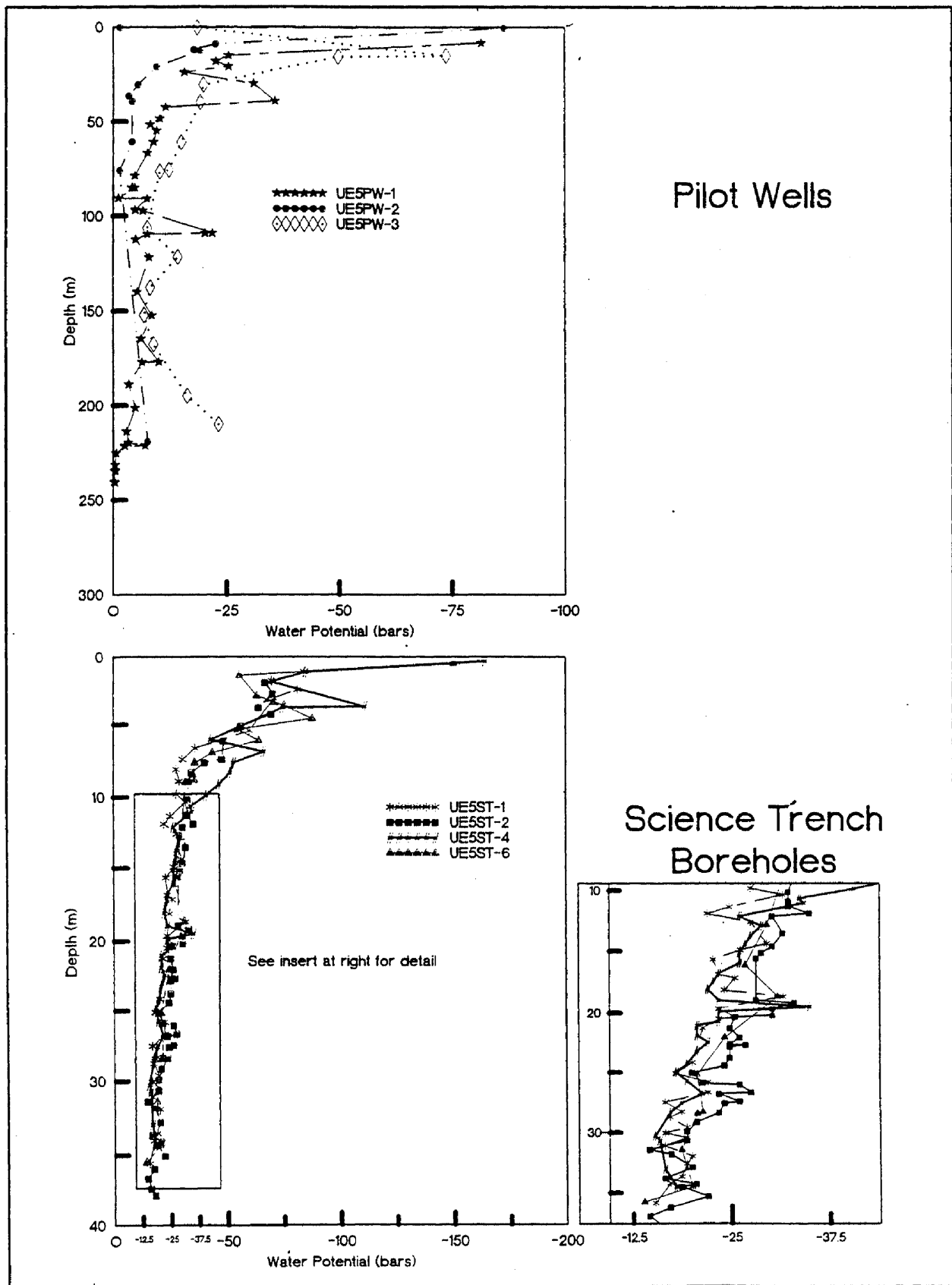


Figure 2.19 Variation of Water Potential With Depth for the Pilot Wells and Science Trench Boreholes (REECo, 1993b,c)

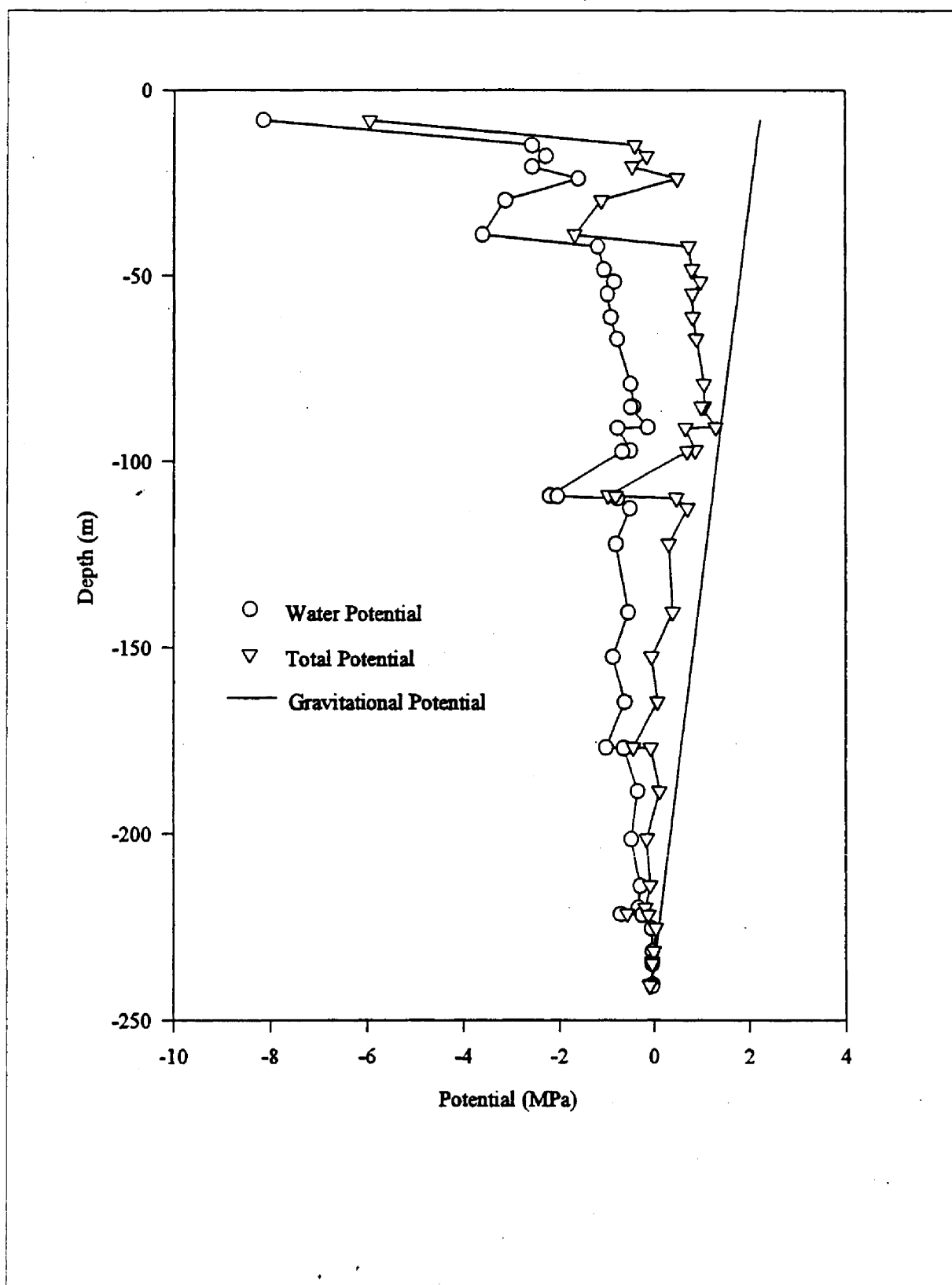
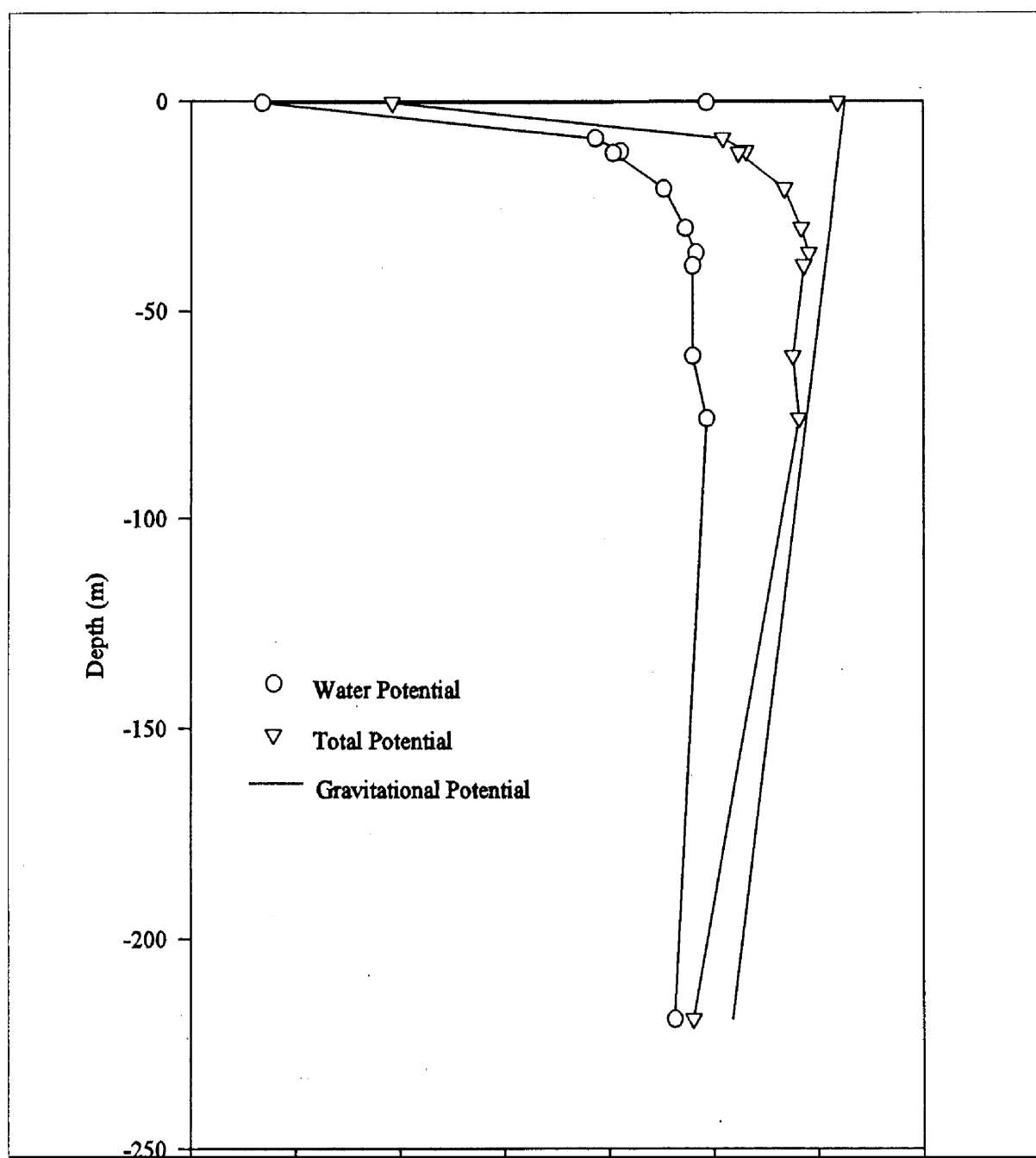


Figure 2.20 Variation of Water Potential With Depth for Pilot Well 1 (UESPW-1)



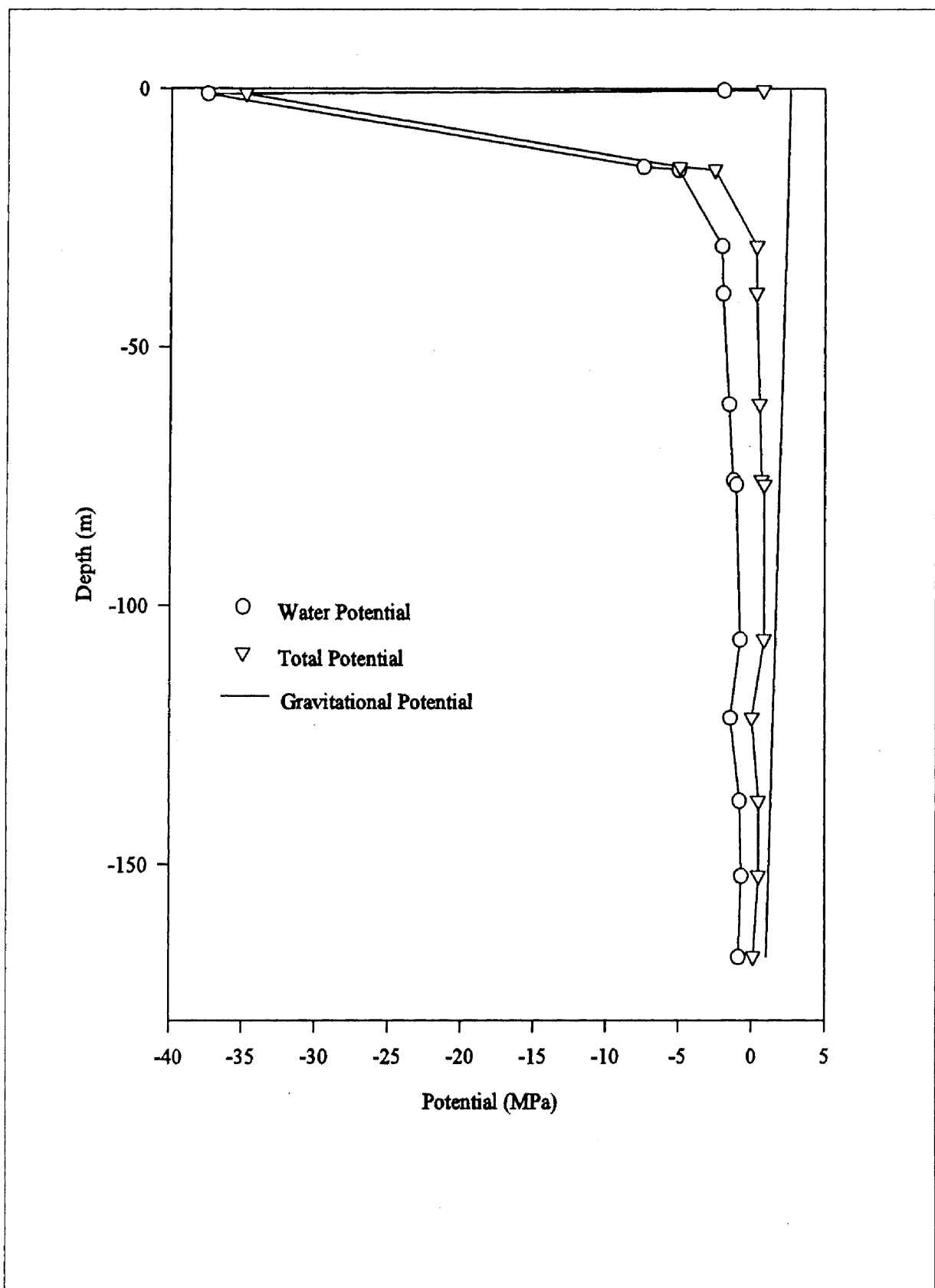


Figure 2.22 Variation of Water Potential With Depth for Pilot Well 3 (UE5PW-3)

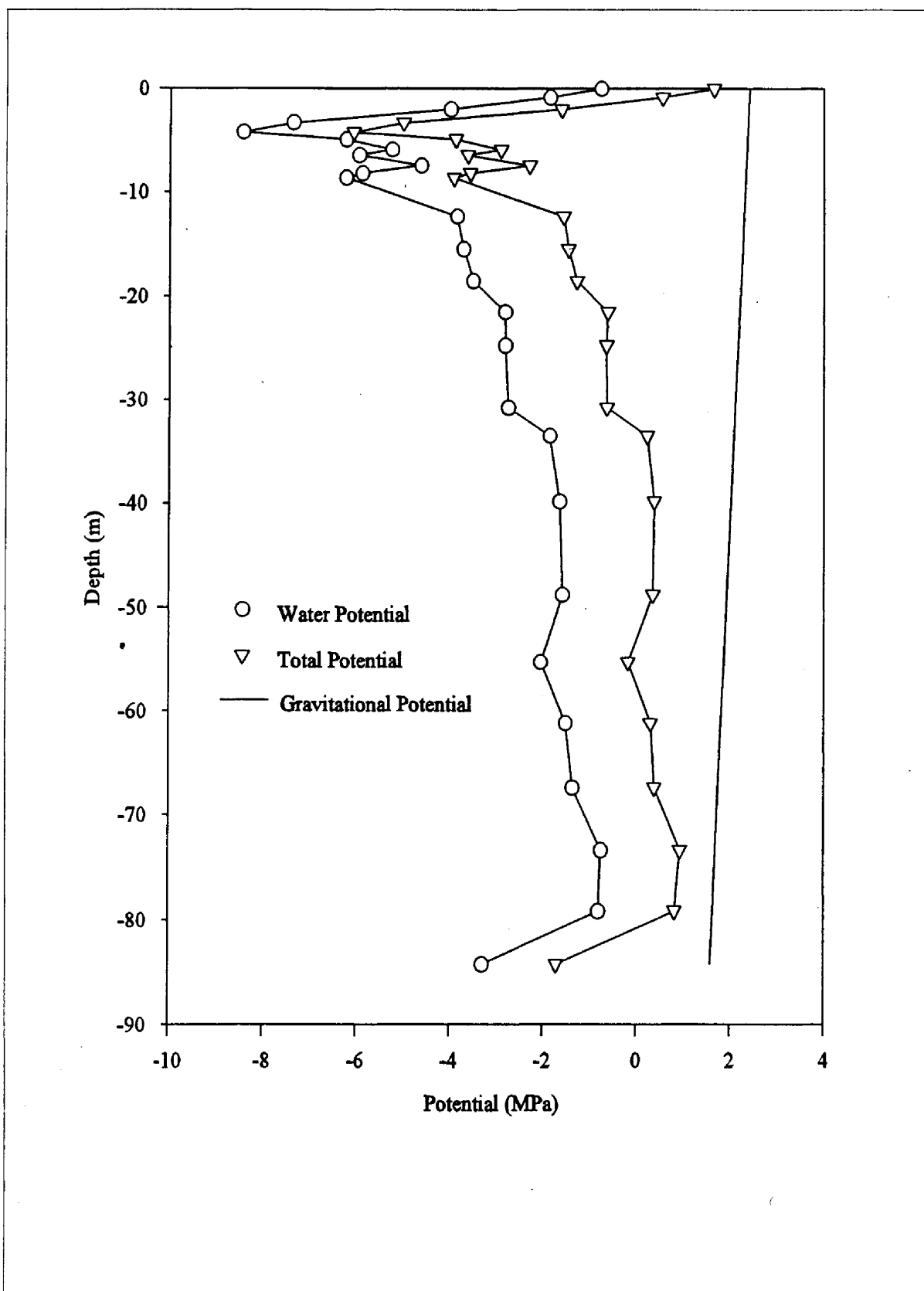


Figure 2.23 Variation of Water Potential With Depth for Borehole AP-1

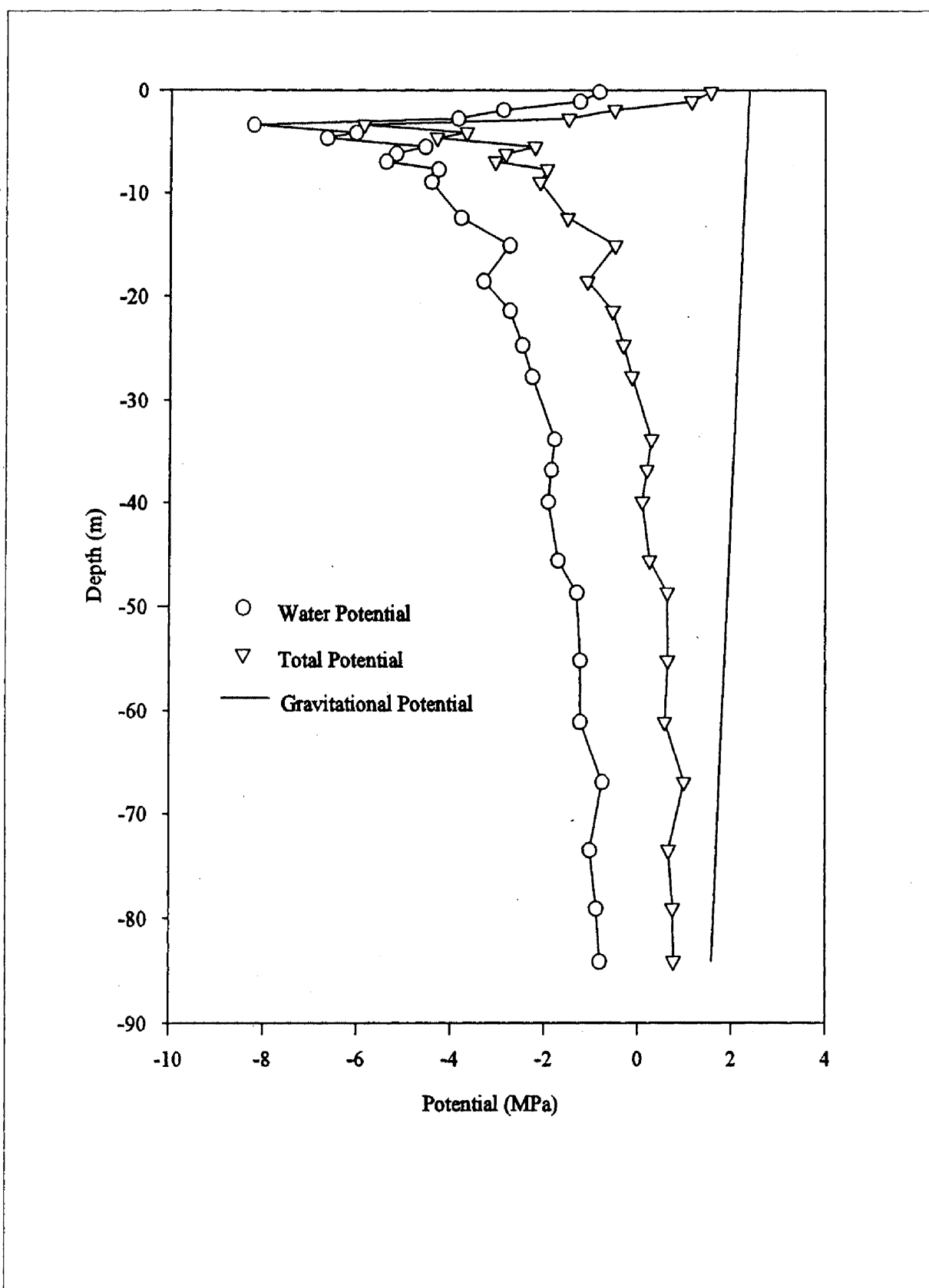


Figure 2.24 Variation of Water Potential With Depth for Borehole AP-2

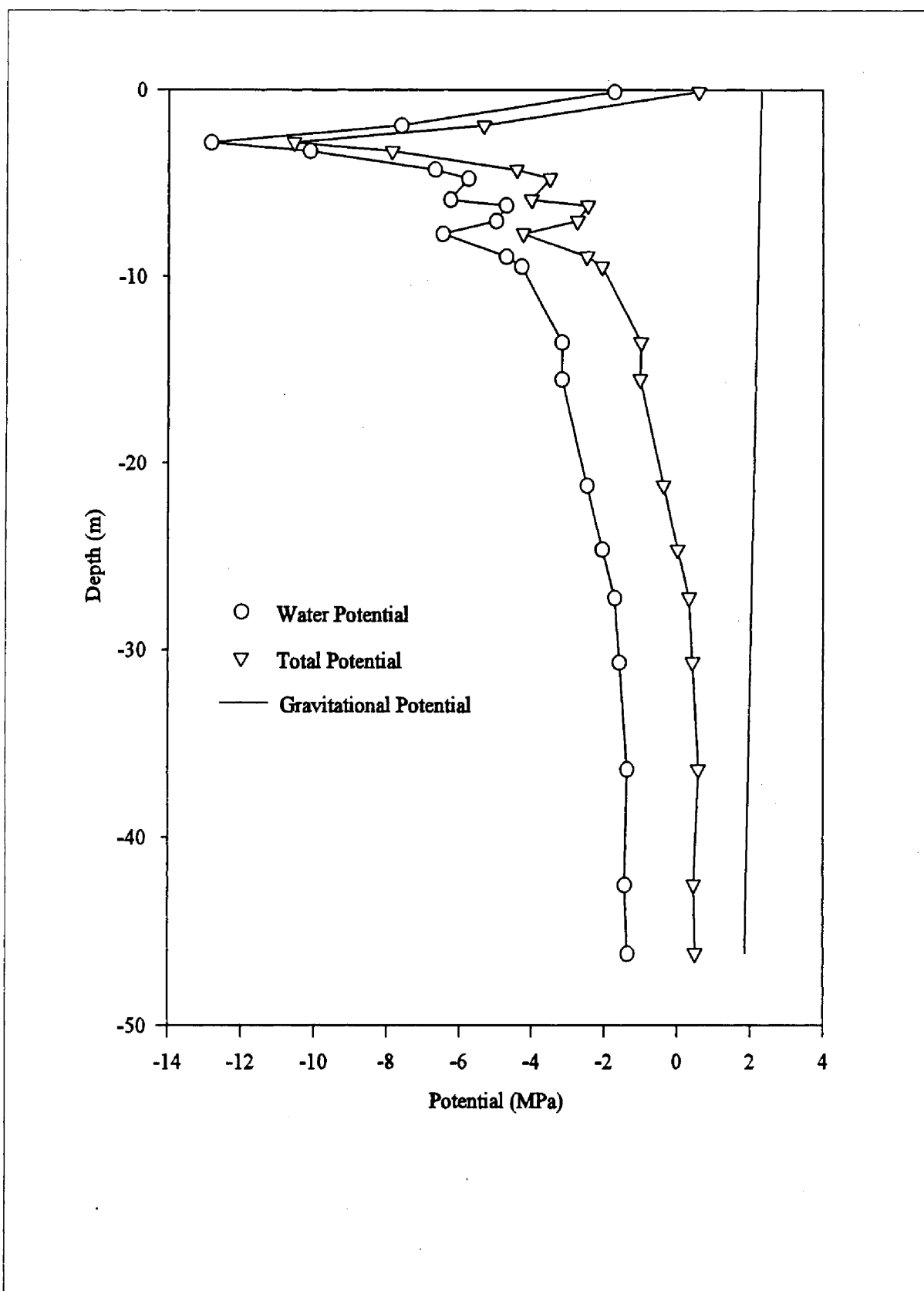


Figure 2.25 Variation of Water Potential With Depth for Borehole RP-1

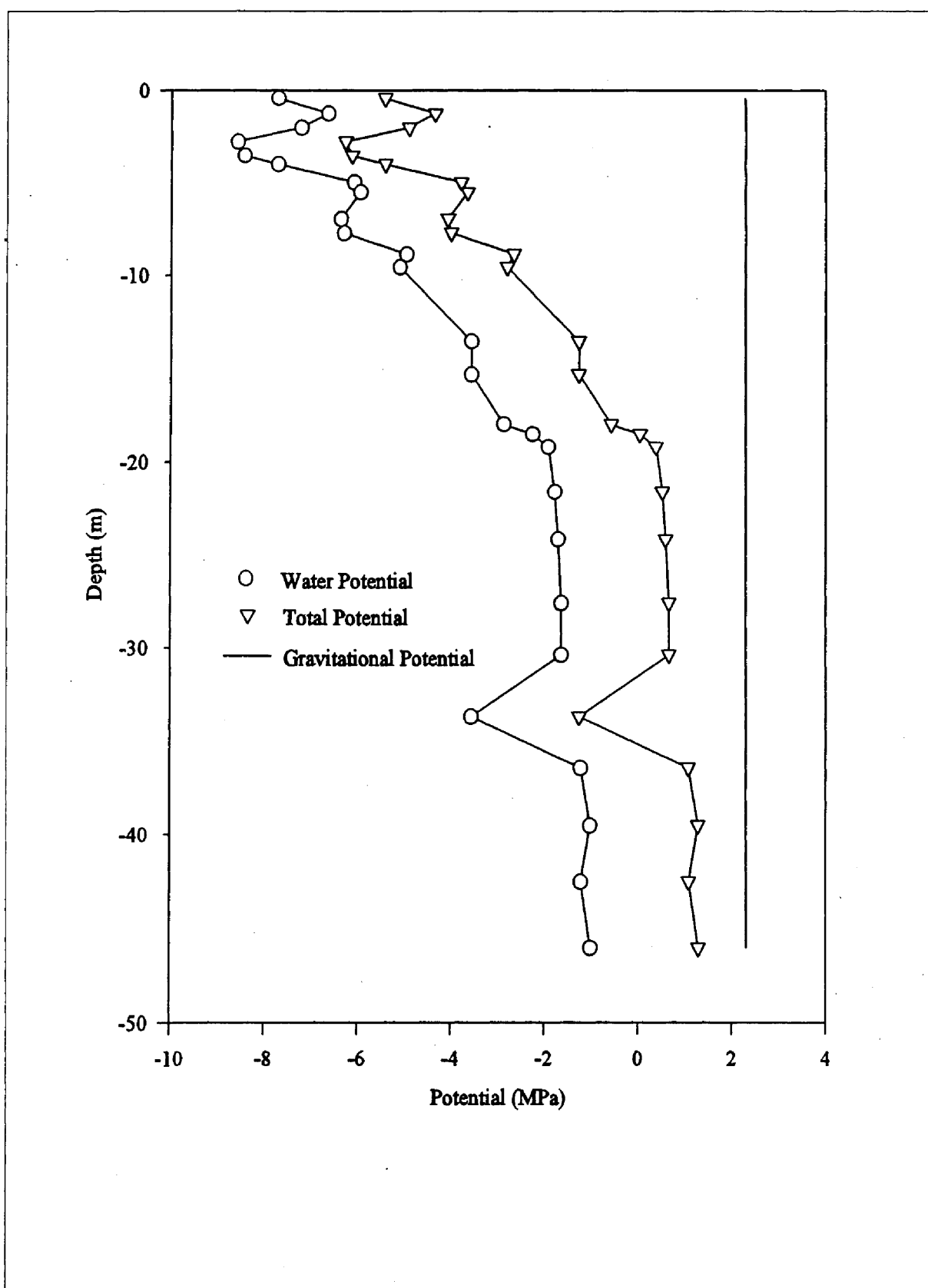


Figure 2.26 Variation of Water Potential With Depth for Borehole RP-2

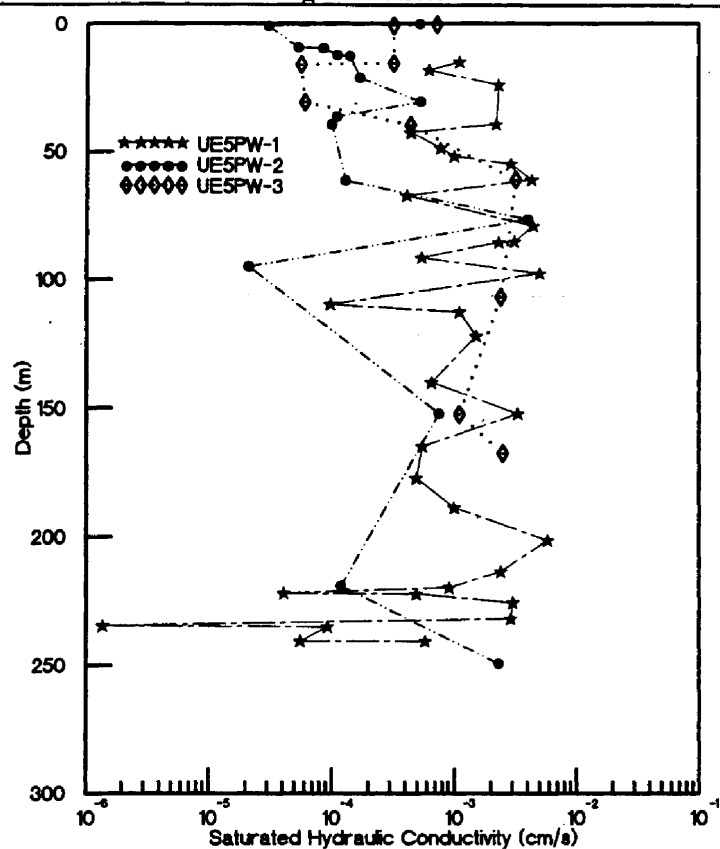
Boreholes AP-1 and AP-2 are located along the eastern boundary of the RWMS and are separated by a distance of 1.5 m (5 ft). The potential profile for AP-1 (*Figure 2.23*) shows some effect on the near-surface matric potentials from precipitation. Below 4 m (13 ft), the total potential gradient indicates evaporative conditions. Conditions are static or nearly static from 20 m to nearly 55 m (66 to 180 ft). Between 55 and 80 m (180 and 262 ft), the gradient indicates evaporative conditions. The low matric potential of the deepest sample is probably an artifact of sampling, as it is not repeated in the AP-2 profile, only 1.5 m (5 ft) distant. The static zone in borehole AP-2 (*Figure 2.24*) begins at about 35 m (115 ft) and extends to the bottom of the borehole at 84 m (276 ft).

Boreholes RP-1 and RP-2 located along the southern boundary of the RWMS are somewhat shallower and are located approximately 11 m (36 ft) apart. The potential profiles for RP-1 (*Figure 2.25*) show a static region beginning at about 28 m (91 ft) and extending to the bottom of the borehole at 46 m (151 ft). The potential profiles for RP-2 (*Figure 2.26*) show a static region beginning at about 20 m (66 ft) and, except for a single data point, extending to the bottom of the borehole at 46 m (151 ft).

Together, these seven boreholes indicate the existence of a static (zero flux) zone which begins between 20 and 40 m (66 and 131 ft) from the surface and has a thickness ranging from 50 to 75 m (164 to 246 ft).

Saturated Hydraulic Conductivity

The saturated hydraulic conductivities (K_{sat}) for 196 undisturbed cores from Pilot Wells UE5PW-1 and UE5PW-2 and five Science Trench Boreholes were determined in the laboratory by REECO (1993b,c) (*Figure 2.27*) using a constant-head permeameter. Analysis of these results showed no trend with depth. Saturated hydraulic conductivity was found to be lognormally distributed. Mean values of log transformed hydraulic conductivities in $\mu\text{m s}^{-1}$ were calculated for three groups of samples representing a range in the spatial scale of



Pilot Wells

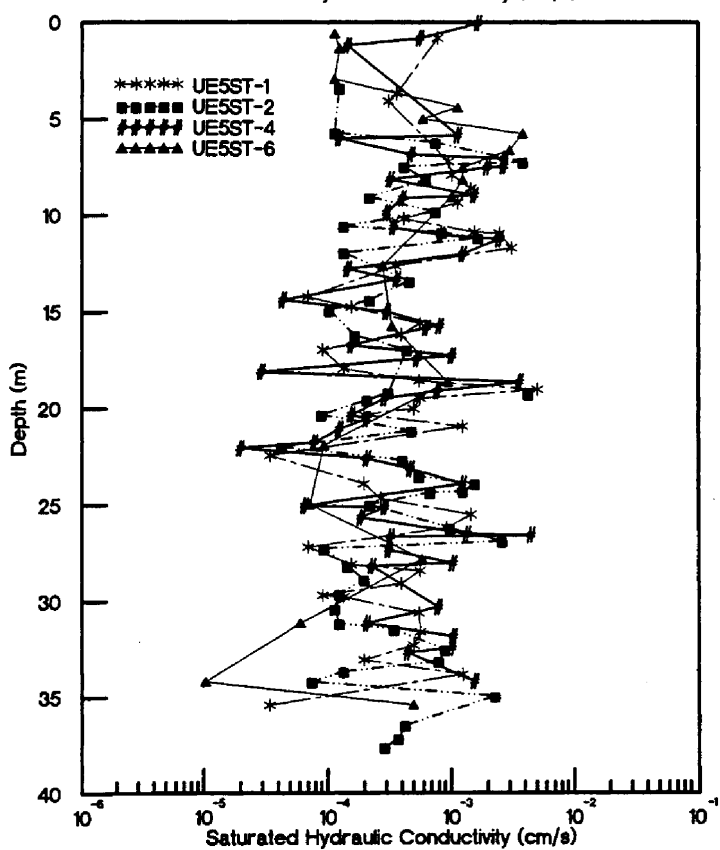
Science Trench
Boreholes

Figure 2.27 Saturated Hydraulic Conductivity Profiles for the Pilot Wells and Science Trench Boreholes Surrounding the Area 5 RWMS

measurements of saturated hydraulic conductivity showed that differences in $\log(K_{sat})$ for vertical and horizontal cores were not significant. Horizontal heterogeneity is not as easily characterized. Because particle size decreases exponentially from the head to the toe within alluvial fans (Friedman and Sanders, 1978), one might expect a decrease in saturated hydraulic conductivity from the north to the south within the confines of the Area 5 RWMS. Nevertheless, this anticipated trend was not observed in any of the sampled trenches. Because the alluvial depositional processes within the vicinity seem to have created relatively uniform bedding in the horizontal direction on the scale of the RWMS site, it is not unreasonable to suspect that the saturated hydraulic conductivity is homogeneous on this scale in the horizontal direction as well.

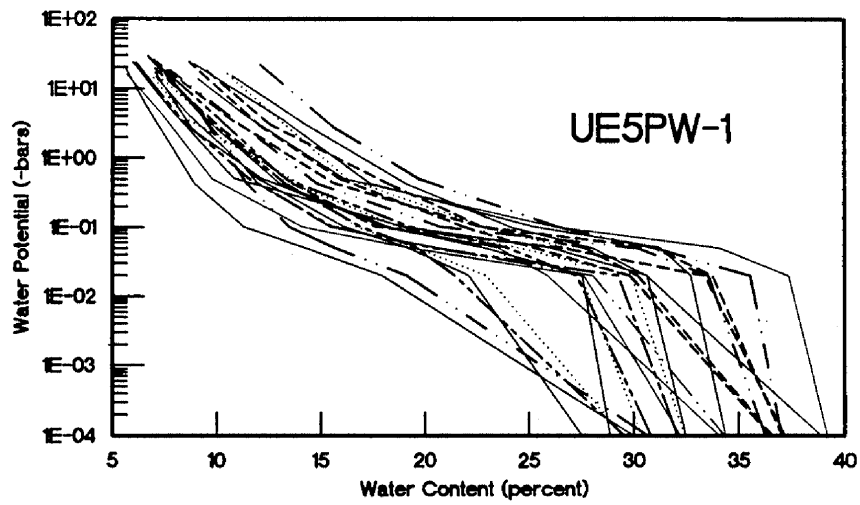
Unsaturated Hydraulic Conductivity – Soil Moisture Retention Relations

Unsaturated hydraulic conductivity, $K(\theta)$, was not measured as a function of water content because of the difficulties of direct measurement at the very low water contents that occur at the RWMS. Instead, hydraulic conductivity was calculated from moisture retention data (drying curve) from the three Pilot Wells, Science Trench Boreholes, existing excavations (REECo, 1993b,c,e), and the saturated hydraulic conductivity data. The moisture-retention function, $\psi(\theta)$, is related to a soil's capacity to retain water at a given energy state or matric potential. The relationship is primarily a function of the texture of a soil (particle-size distribution) and its structure. The character of the moisture retention curves for each Pilot Well are shown in Figure 2.28. Each set of curves for a given Pilot Well reflects the entire sampling depth; i.e., samples taken at different depths are pooled. The general shape of the curves denote a sandy or coarse-grained deposit with a large variation in pore-size distribution (Hillel, 1980). Similar curves, using the cores from the Science Trench Boreholes and existing pit excavations, can be found in REECo (1993c,e). The remarkable similarity between all the curves for the various sampling depths and locations near the Area 5 RWMS lends further support to the hypothesis of gross homogeneity of the hydrologic character of the alluvium.

Moisture retention data (Figure 2.28) was fit to the van Genuchten (1978, 1980) model:

$$\theta_v = \theta_r + (\theta_s - \theta_r) \left[1 + (-\alpha\psi)^n \right]^{-m} \quad (2.1)$$

where θ_v is the volumetric water content ($\text{cm}^3 \text{cm}^{-3}$), θ_s is the saturated volumetric water content ($\text{cm}^3 \text{cm}^{-3}$), θ_r is the residual volumetric water content ($\text{cm}^3 \text{cm}^{-3}$), ψ is the matric potential (cm), and α (cm^{-1}) and n are empirically determined parameters. The parameter m is related to n as $m=1-1/n$.



The van Genuchten parameters and the saturated hydraulic conductivity were used in the Mualem (1976) model for unsaturated hydraulic conductivity to predict the hydraulic conductivity-water content relations. The Mualem model is expressed as:

$$K(\theta) = K_s S^{1/2} \left[1 - \left(1 - S^{1/m} \right)^m \right]^2 \quad (2.2)$$

where K_s is the saturated hydraulic conductivity and S is the effective saturation as defined by:

$$S = \frac{(\theta_v - \theta_r)}{(\theta_s - \theta_r)} \quad (2.3)$$

The unsaturated hydraulic conductivity functions ($K(\theta)$) from Equation 2.2 for the three Pilot Wells are presented in Figure 2.29. At the mean water content for the alluvium (7 to 12 percent), the magnitude of $K(\theta)$ is only about $8.6 \times 10^{-8} \text{ m day}^{-1}$ ($1.0 \times 10^{-10} \text{ cm s}^{-1}$). The magnitude of liquid flow under such low hydraulic conductivities is negligible. Pore water under such circumstances is essentially immobile. These data suggest that liquid flow at the low water contents currently present within the alluvium is highly unlikely.

Insight into the water retention relationship in a native alluvium cap can be obtained from characterization of alluvium backfilled into weighing lysimeters. Water retention relations measured for soil samples obtained from backfilled lysimeters at the RWMS are plotted in Figures 2.30 and 2.31. The water retention model obtained from Area 5 site characterization data is superimposed for comparison. While the model deviates from the measured curves at very low water contents, it is in good agreement between a volumetric water content of 0.10 and near saturation.

Water content monitoring conducted at the RWMS by Levitt *et al.* (1996) indicated no increase of water content below a depth of 1.5 m (4.9 ft) under vegetated conditions for 1995, a year characterized by above-average precipitation. Under bare soil conditions, the water content at a depth of 1.7 m (5.5 ft) has increased from 0.055 to 0.075, while the total storage in the lysimeter has decreased during 1995. The elevated water contents at depth are probably due to irrigation water applied during revegetation of the entire site during 1994.

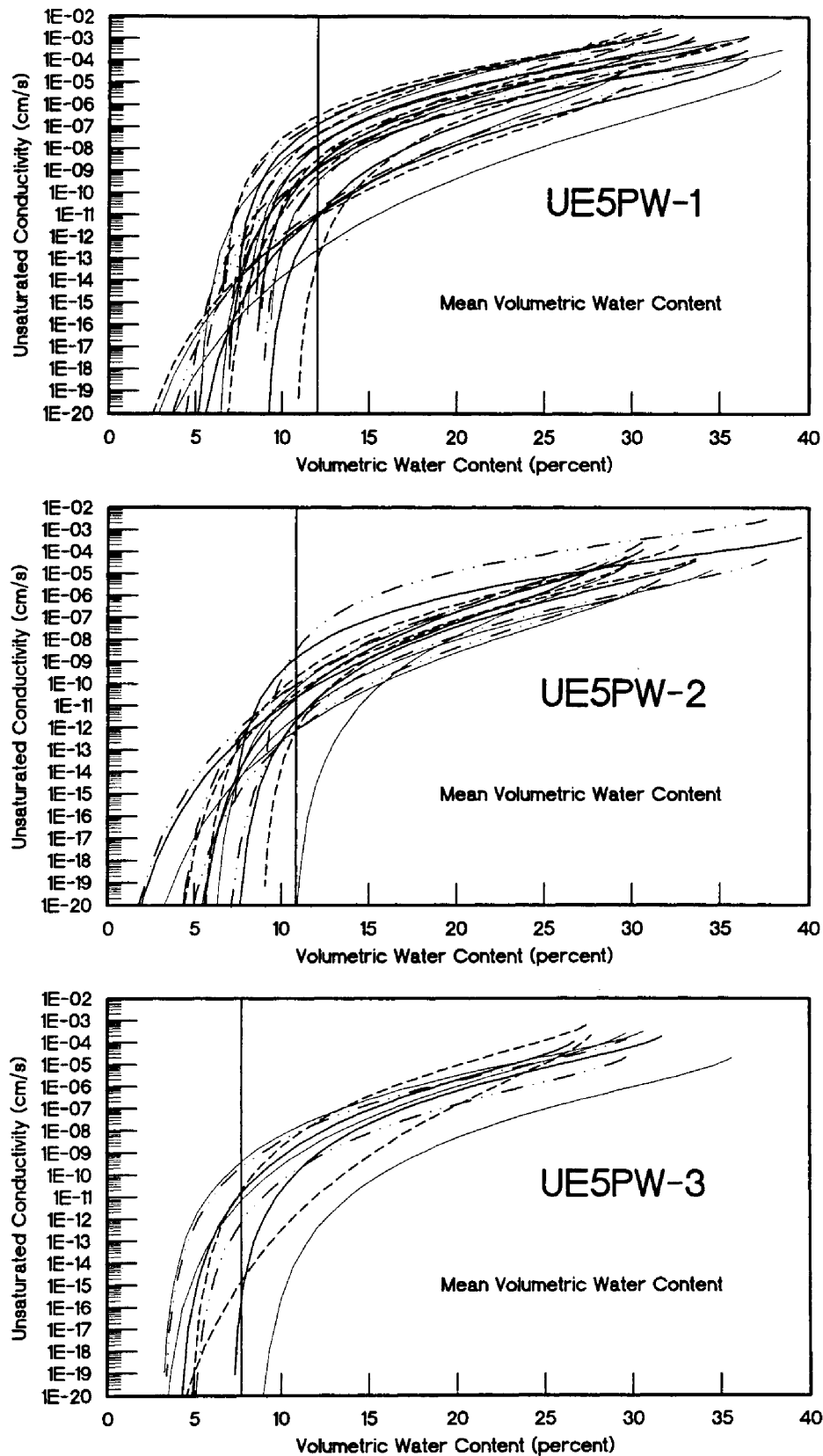


Figure 2.29 Fitted Unsaturated Hydraulic Conductivity Functions From Core Samples in Pilot Wells UE5PW-1, UE5PW-2, and UE5PW-3 (REECo, 1993b)

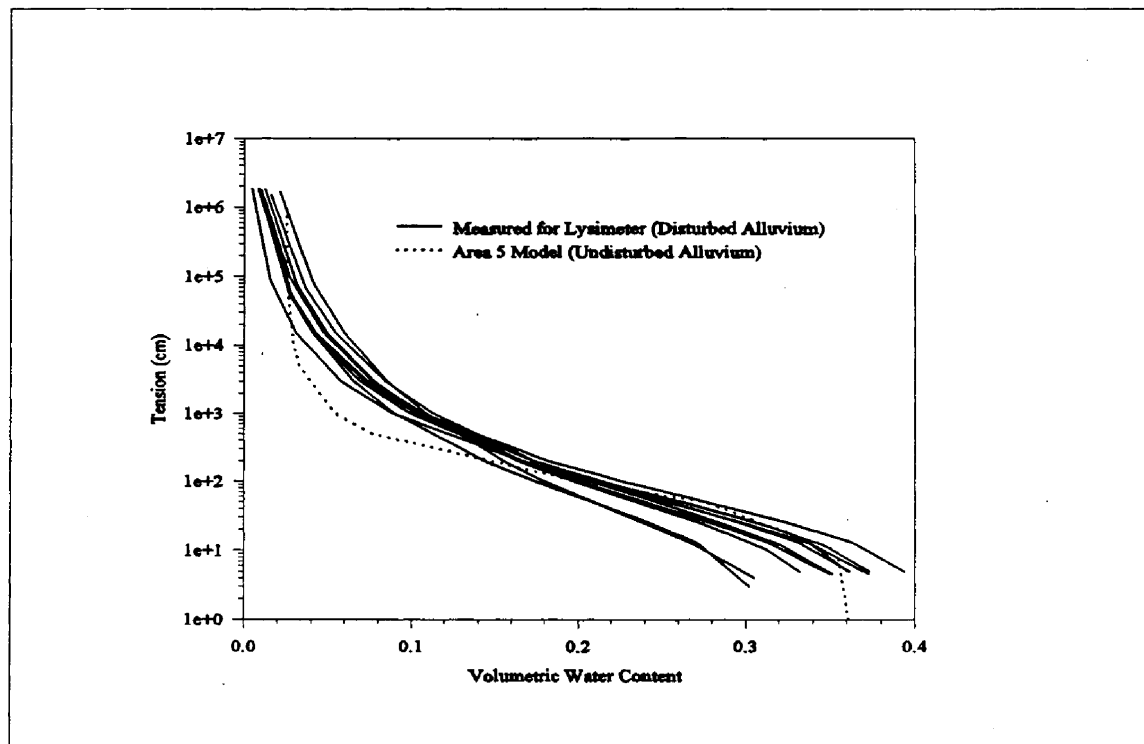
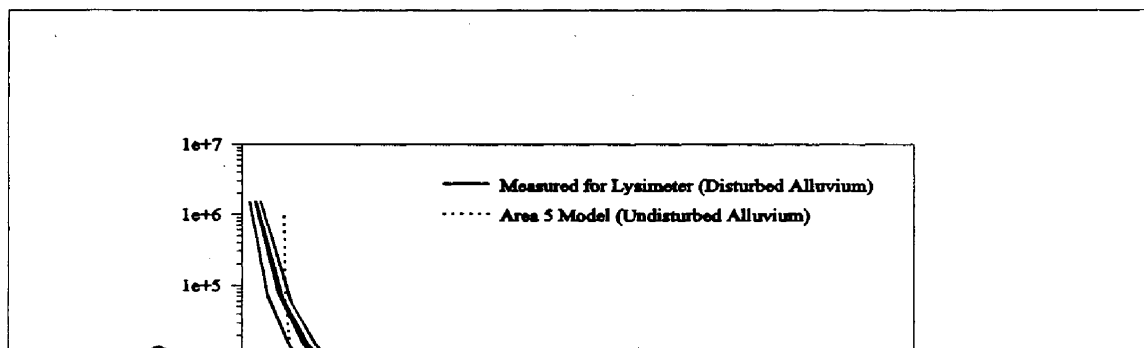


Figure 2.30 Comparison of Water Retention Relations Measured in the North Area 5 Lysimeter With the Model of Water Retention Relations



Unsaturated hydraulic conductivities of repacked alluvium from the Area 5 RWMS obtained from the Mualem (1976) model were compared by Albright (1995). This comparison was made against those based on hydraulic diffusivity obtained from measurements of an evaporating column over the potential range of approximately -20 to -200 Kpa (Rose, 1968). The comparison showed relatively good agreement between the two methods over the range of measurements (see Figure 19 of Albright [1995]).

ENVIRONMENTAL TRACERS IN THE VADOSE ZONE

The concentrations of certain ions, as well as those of stable isotopes of certain elements, can serve as tracers used to estimate vadose zone water movement, travel times, and recharge, independently of a hydraulic analysis. REECo (1993b) measured profiles for chloride (Cl), stable oxygen (^{18}O), and stable deuterium (^2H) in both the Pilot Wells and Science Trench Boreholes surrounding the RWMS. The environmental tracer data support the hypothesis that evaporation is the dominant process governing the rate and direction of water movement within the upper vadose zone under the present arid climate. Downward infiltration to the water table is not indicated under current climatic conditions.

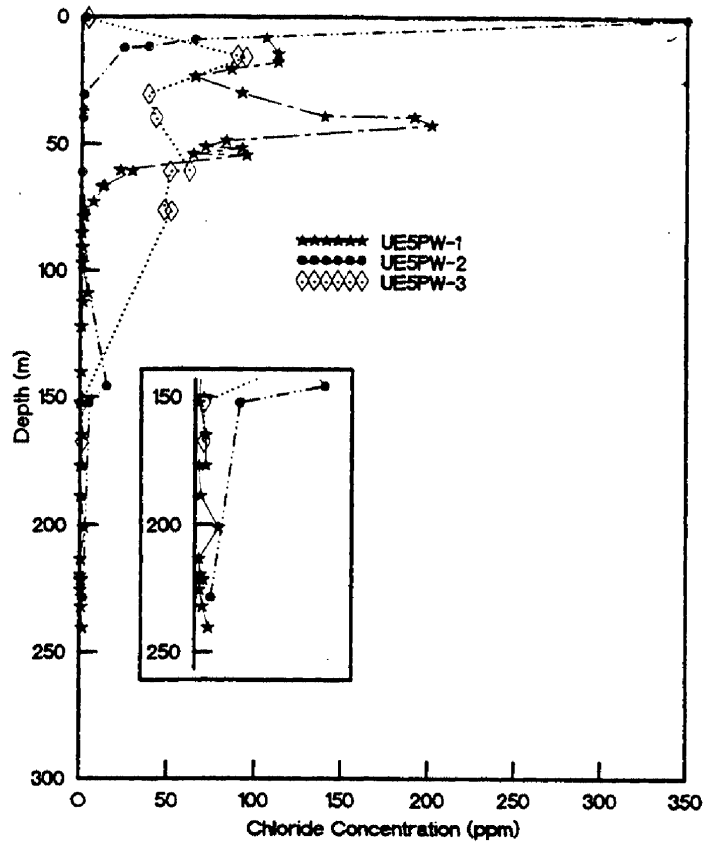
Chloride Profiles

The chloride anion can be viewed as a conservative tracer; it is neither generated nor decomposed within the soil zone. A difference between long-term input and output indicates increasing or decreasing salinity, with which estimates of soil water flux may be derived. This technique is known as the chloride mass balance method (Allison and Hughes, 1983).

Chloride concentrations were reported for both from the Pilot Wells and Science Trench Boreholes (REECo, 1993b,c). These depth profiles, presented in Figure 2.32, show relatively high accumulations of chloride in the shallow subsurface of all the boreholes, suggesting that evaporation rates are high compared to downward movement of water. If downward flow were an important process at the RWMS, chloride concentrations in soil water beneath the root zone would be much lower than those observed in the three Pilot Wells.

Drill cuttings and core samples from Pilot Well UE5PW-2 have a significantly lower chloride accumulation than do the other Pilot Wells (Figure 2.32). Chloride differences, according to Tyler *et al.* (1996), indicate that groundwater recharge was occurring in the vicinity of Pilot Well UE5PW-2 during the last glacial maximum (between 15 and 30 ka). They hypothesize that soil textural and hydraulic property differences and surface geomorphology may explain the differing spatial distribution of recharge in Area 5.

Cores and cuttings from Pilot Well UE5PW-2 have the highest percentage of fines (<200 mesh) (REECo, 1994). The average saturated hydraulic conductivity at Pilot Well UE5PW-2 is the lowest of the three Pilot Wells, which is consistent for a soil with a higher percentage



Pilot Wells

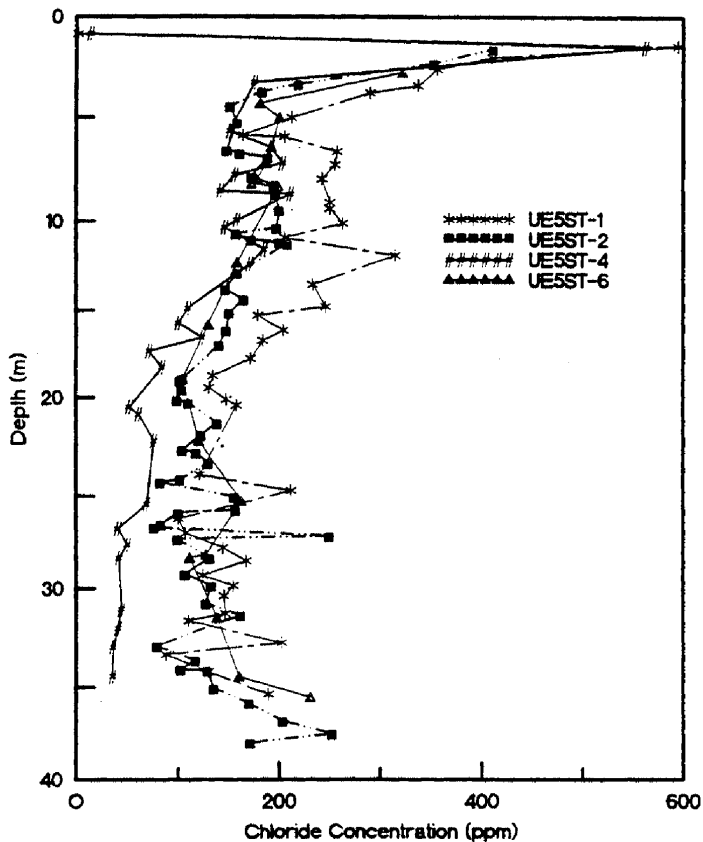
Science Trench
Boreholes

Figure 2.32 Depth Profiles of Dry Chloride Concentrations for Core Samples From the Pilot Wells and Science Trench Boreholes

of fines. Tyler *et al.* (1996) speculates that while the saturated hydraulic conductivity is lower in Pilot Well UE5PW-2 than in Pilot Wells UE5PW-1 and UE5PW-3, the unsaturated hydraulic conductivity may be higher for a corresponding suction. According to Jury *et al.* (1991), coarse-textured soil has a higher conductivity than fine-textured soil at saturation because it contains larger pore spaces. However, coarse-textured soils drain at modest suctions, producing a dramatic decrease in hydraulic conductivity. Fine-textured soils retain a considerably larger amount of water at a given suction and maintain a higher conductivity than coarse-textured soils at lower water contents. Therefore, the fine-textured soils in the vicinity of Pilot Well UE5PW-2 will be more hydraulically conductive in unsaturated conditions than the other Pilot Wells and thereby have a greater ability to recharge the groundwater.

From Allison *et al.* (1994), surface topography has a significant influence on recharge in arid regions. Tyler *et al.* (1996) presents this as another explanation for evidence of historic recharge from Pilot Well UE5PW-2 chloride data. They reference the surficial mapping and aerial photography of the fan surfaces which have revealed the presence of a major lineament crossing the drill site from northeast to southwest at Pilot Well UE5PW-2 (Carr *et al.*, 1967; Miller *et al.*, 1993). This lineament is the product of coalescing alluvial fans which concentrate runoff within a well-defined channelized zone. According to Tyler *et al.* (1996), field evidence suggests that the edge of a sequence of historic fans from the north also defined this feature in the past (Snyder *et al.*, 1994), implying a constancy in converged runoff. Tyler *et al.* (1996) also state that in contrast, no such flow focusing mechanism currently exists at either Pilot Well UE5PW-1 or Pilot Well UE5PW-3. The drill site of Pilot Well UE5PW-1 is located on the more distal portions of the Halfpint alluvial fan and shows no apparent channelization. The drill site of Pilot Well UE5PW-3 lies on coalescing alluvial fans emerging from the Massachusetts Mountains. These fans are smaller than the Halfpint fan and do not supply the same volume of runoff. Channelization is not apparent at Pilot Well UE5PW-3 either. Tyler *et al.* (1996) conclude by stating that during times of elevated runoff, it is likely that this feature would generate more frequent flooding of the area in the vicinity of Pilot Well UE5PW-2, and therefore increase the probability of recharge.

Both Prudic (1994) and Tyler *et al.* (1996) make estimates of recharge rates from chloride profiles for the deeper portion of the vadose zone. Both note that these are paleorecharge rates and not representative of current conditions. Prudic states that downward percolation under current climatic conditions is limited to the upper 10 m (33 ft). The paleorecharge rate was estimated to be 2 mm yr⁻¹ for the Amargosa Desert site and 0.03 to 0.05 mm yr⁻¹ for the Ward Valley site (Prudic, 1994).

Tyler *et al.* (1996) used chloride data from the Pilot Wells to estimate the paleorecharge rate in Area 5. The Science Trench Boreholes (Blout *et al.*, 1995) were excluded from the calculation because they extend only 36 m (118 ft) deep and show chloride accumulation throughout the sampled profile. As noted by Tyler *et al.* (1996), an accumulating profile is

not at steady state and, as such, applying chloride mass balance methods for estimating recharge is not applicable. The following is a summary of the paleorecharge study presented in Tyler *et al.* (1996).

The low and uniform chloride concentrations at depth (< 100 to 150 m [< 328 to 492 ft]) indicate that historically, the vadose zone was in equilibrium and significant recharge must have been occurring to produce the deeper chloride profile. Tyler *et al.* (1996) calculated chloride flux based on an assumed 50 percent increase in precipitation (186 mm yr^{-1}), an estimate of the paleoclimate conditions in Area 5. The estimated paleochloride flux is $105 \text{ mg m}^{-2} \text{ yr}^{-1}$, similar to the estimated chloride paleoflux used by Fouty (1989) and Fabryka-Martin *et al.* (1993). Using this estimate, the calculated paleorecharge rates from deep in the profiles range from 7.6 mm yr^{-1} at Pilot Well UE5PW-1 to 4.4 mm yr^{-1} at Pilot Well UE5PW-2. Recharge of this size, at present, is affiliated with cooler average temperatures and higher annual precipitation. Increased precipitation and cooler temperatures typified glacial climates of the region and imply that conditions at the site during recharging periods were similar to those at higher elevations today.

Prudic (1994) estimated the age of water and the downward percolation rate below a depth of 10 m (33 ft) at a site in the Amargosa Desert south of Beatty, Nevada; and at the Ward Valley site in California. Age estimates were made using chloride concentration profiles. The age of water at a depth of 10 m (33 ft) was estimated by Prudic (1994) to range from 16,000 to 33,000 years ago (ka) for both sites. Chloride ages at a depth of 10 m (33 ft) in Frenchman Flat were estimated by Tyler *et al.* (1996) to be 32 ka for Pilot Well UE5PW-1, 18 ka for Pilot Well UE5PW-2, and 19 ka for Pilot Well UE5PW-3. The chloride profiles demonstrate that recharge is not occurring under the current climate with the most recent cessation of recharge beginning at about 20 to 30 ka.

Stable Isotope Profiles

The stable isotopes of hydrogen and oxygen provide an excellent record of water movement in the subsurface because they are components of the water molecule itself. Three stable isotopes of oxygen (^{16}O , ^{17}O , ^{18}O) and two stable isotopes of hydrogen (^1H , ^2H , or deuterium, denoted D) exist in nature, thus water molecules in precipitation have nine possible isotopic configurations and masses. Each configuration will exhibit a slightly different vapor pressure, as the vapor pressure of any given molecule is inversely proportional to its mass. This implies that fractionation between the heavier molecules and lighter molecules of water can occur during evaporation and precipitation. Isotopic ratios are reported as differences of $^{18}\text{O}/^{16}\text{O}$ and D/H ratios, relative to Standard Mean Ocean Water (SMOW) first defined by Craig (1961a) with reference to a large volume of distilled water distributed by the National Bureau of Standards in the United States. Samples of water are compared by their isotopic compositions of oxygen and hydrogen, expressed as a per mil difference relative to SMOW:

$$\delta^{18}O = \left[\frac{(^{18}O/^{16}O)_{SAMPLE} - (^{18}O/^{16}O)_{SMOW}}{(^{18}O/^{16}O)_{SMOW}} \right] \times 1000 \quad (2.4)$$

Consequently, positive values of ^{18}O and D reflect enrichment in the heavier isotopes of oxygen and hydrogen, and negative values indicate depletion relative to the SMOW standard.

$$\delta D = \left[\frac{(D/H)_{SAMPLE} - (D/H)_{SMOW}}{(D/H)_{SMOW}} \right] \times 1000 \quad (2.5)$$

Once precipitation enters the soil horizon, water in the liquid phase is enriched in ^{18}O and D because evaporation favors the removal of lighter isotopes. Likewise, the liquid phase is enriched in heavy isotopes by condensation of water vapor.

The continuing preferential removal or fractionation of lighter isotopes from the emplaced water caused by both evaporation and condensation should be recorded in pore water as positive (less negative) values compared to the SMOW standard and nearby water at depth. This is exactly what is seen in the stable oxygen/hydrogen profiles for the three Pilot Wells and Science Trench Boreholes shown in Figure 2.33. In general, the ^{18}O and D profiles show greater enrichment of the heavy isotopes in the upper vadose zone (top 30 m [98.4 ft]), suggesting that the shallow vadose-zone water has been subjected to more evaporation/condensation cycles than the deeper water. Using the SMOW reference, a line representing the average ratios of $^{18}O/^{16}O$ and D/H for waters sampled throughout the world, known as the Meteoric Water Line (MWL), has been prepared by Craig (1961a) as shown in Figure 2.34. The MWL shows that the ^{18}O and D values of meteoric water can be represented by the equation:

$$\delta D = 8 \delta^{18}O + 10 \quad (2.6)$$

The importance of the MWL is its use in comparing samples of water as an indication of their origin and climate of formation (Merlivat and Jouzel, 1979; Jouzel and Merlivat, 1984; Jouzel *et al.*, 1991; Stewart, 1975).

Figure 2.34 compares ^{18}O versus D for the three Pilot Wells and the global MWL. The stable isotope lines for the three Pilot Wells lie to the right of the global MWL indicating that the

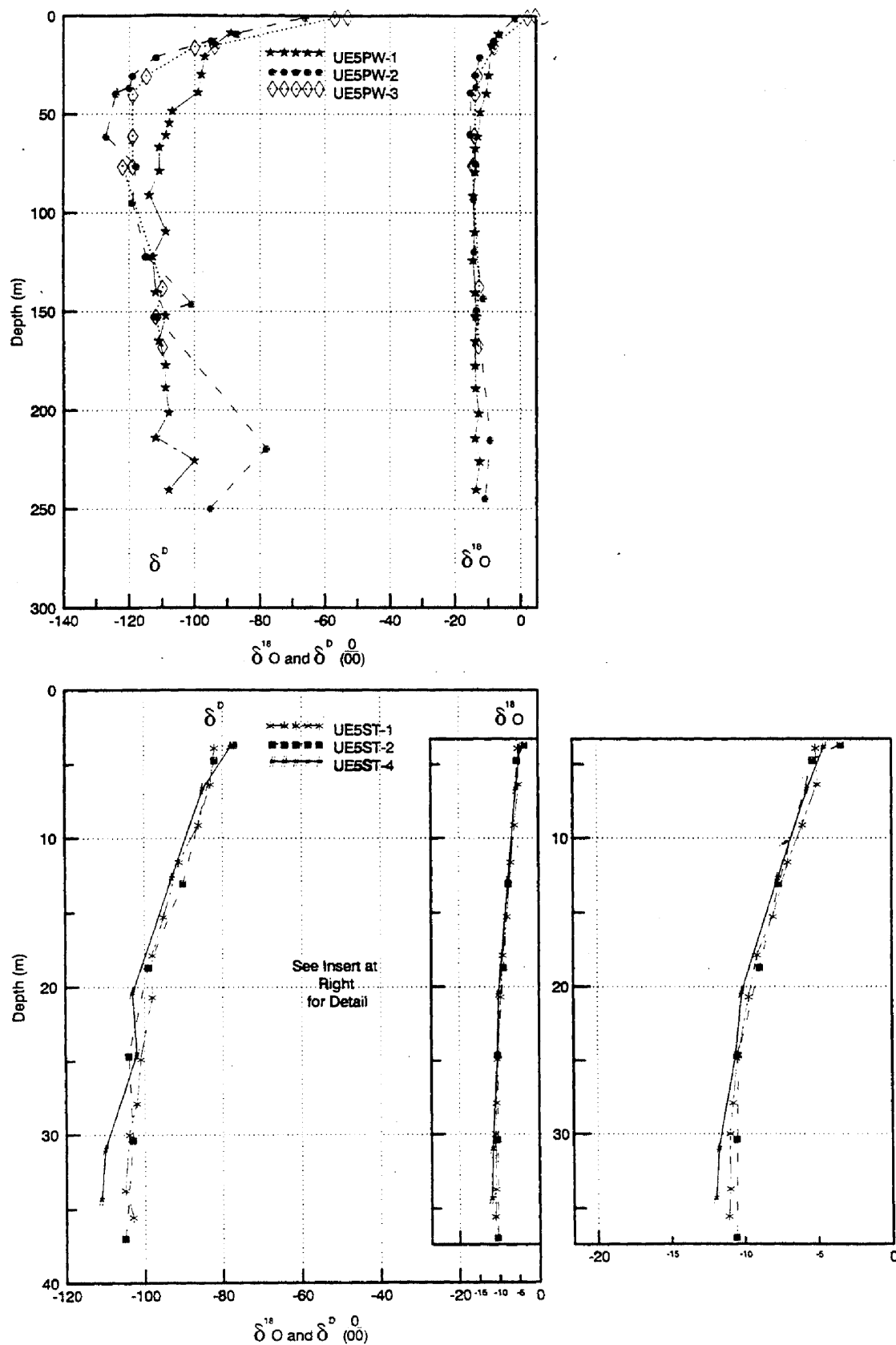


Figure 2.33 Depth Profiles of $\delta^{18}\text{O}$ and δD in Core Samples From the Pilot Wells and Science Trench Boreholes (REECo, 1993c)

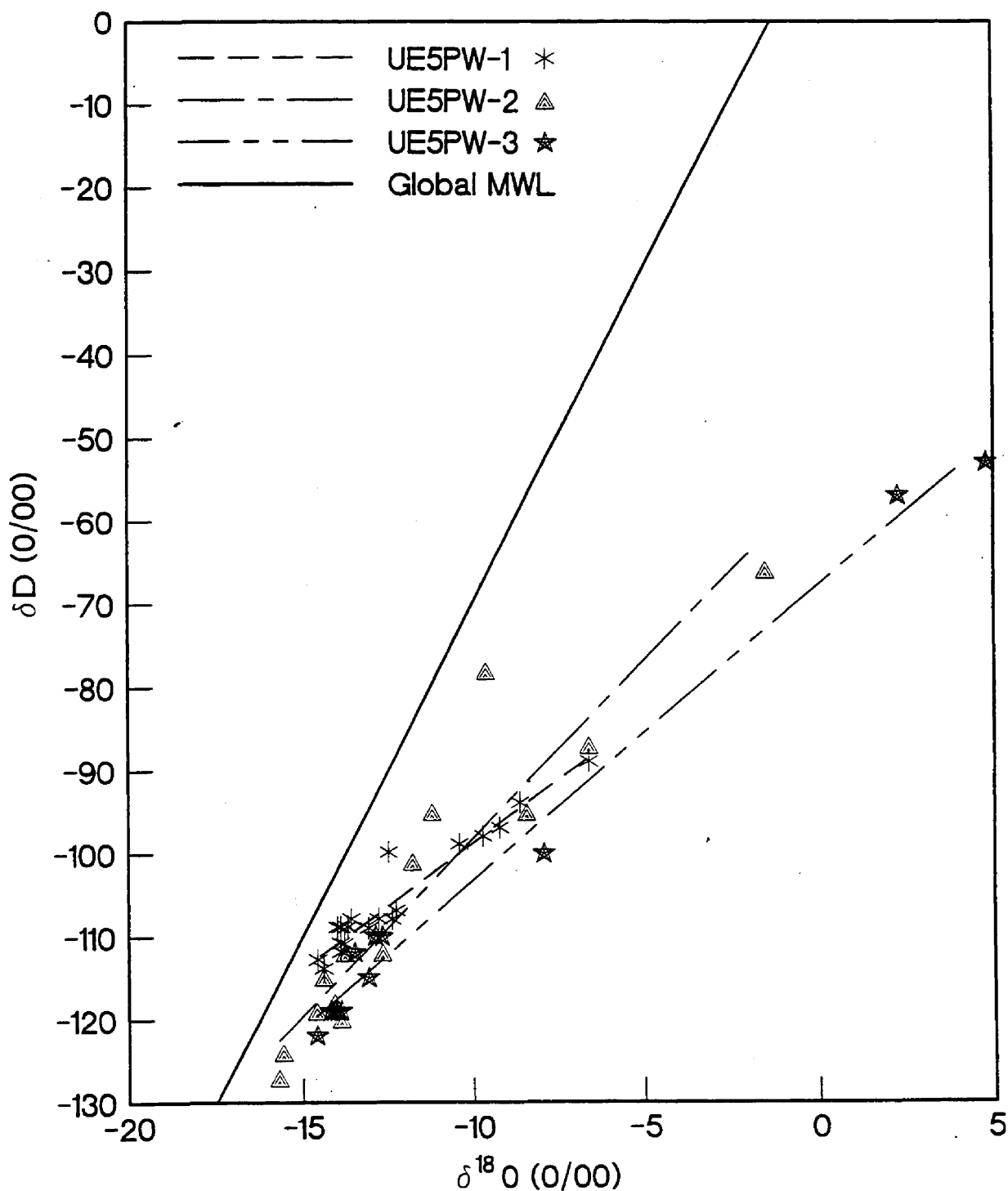


Figure 2.34

Comparison of Stable Isotopes Measured From Core Samples of the Pilot Wells to the Global Meteoric Water Line (MWL) (REECo, 1993b)

waters have been subjected to evaporation over time (Domenico and Schwartz, 1990). These data and figures support the hypothesis that evaporation at the Area 5 RWMS is the dominant hydrologic mechanism in the upper vadose zone compared to downward liquid flow.

Variations Within the Chloride and Stable Isotope Data Sets

The following discussion of chloride and stable isotope data from Area 5 is adapted from Tyler *et al.* (1996). Chloride profiles in the Pilot Wells show similar characteristics in the upper 1 to 2 m (3.3 to 6.6 ft); the chloride concentration is very low, reflecting repeated flushing by precipitation. Below 2 m (6.6 ft), each profile rapidly reaches a maximum concentration of between 250 and 600 mg kg⁻¹ which is typical in arid regions (Phillips, 1994) and indicates either a net infiltration rate which has changed over time, significant nonpiston flow, or both. Below the chloride bulge, chloride concentrations decrease rapidly in Pilot Well UE5PW-2 to a depth of 25 m (82 ft), with low chloride concentrations throughout the rest of the profile; while Pilot Wells UE5PW-1 and UE5PW-3 show a second bulge at 40 and 85 m (131 and 278.8 ft), respectively, before concentrations drop to a range of 0.5 to 2.0 mg kg⁻¹. Total chloride accumulation is much less in Pilot Well UE5PW-2.

The combination of low chloride concentrations at depth, differences in stored chloride between the boreholes, and the appearance of secondary bulges implies a different response to a sequence of recharging events has occurred at each Plot Well site. Recharge was apparently interrupted by a prolonged period of chloride buildup at Pilot Wells UE5PW-1 and UE5PW-2. This was caused by the results of a climatic shift from a warm, arid period

Tyler *et al.* (1996) compares stable isotope data of oxygen and hydrogen in the three Pilot Wells. They identify two distinct populations in the soil-water isotopic compositions: samples collected from the land surface to about 16 m (52 ft) (and to almost 40 m [131 ft] in Pilot Well UE5PW-1) that display evaporative enrichment of ^{18}O relative to ^2H (defined here as shallow soil water), and deeper samples that trend on a line approximately parallel to the Local Meteoric Water Line (LMWL) (defined here as deep soil water). The soil water from both population sets are more depleted than modern precipitation for Area 5 and, in fact, compare favorably with the isotopic signature of the saturated zone. Tyler *et al.* (1996) uses this as evidence that the soil water, as well as groundwater, infiltrated under different climatic conditions, in concurrence with the soil chloride and ^{36}Cl results. The only exception is three samples collected from Pilot Wells UE5PW-2 and UE5PW-3 within 1 m (3.3 ft) of the surface which are isotopically comparable to modern precipitation and therefore provide evidence of current infiltration in the near surface. This theory also is supported by the higher water potentials, ample root distribution, and low chloride concentration observed in the upper 1 to 2 m (3.3 to 6.6 ft) of the soil profile (REEC Co, 1994). Current infiltration was not found below 3 m (9.9 ft). The effect of evaporation on isotopic composition can be detected to a depth of 39 m (128 ft) in Pilot Well UE5PW-1, 8.5 m (27.8 ft) in Pilot Well UE5PW-2, and 16 m (52.4 ft) in Pilot Well UE5PW-3. It is not possible, however, to differentiate between enrichment caused by evaporation and enrichment produced from mixing between shallow, evaporated water and deeper soil water.

Tyler *et al.* (1996) estimates the amount of time required to generate the evaporative profiles from the Pilot Wells, assuming purely diffusional transport from the evaporating front at the land surface through the underlying vadose zone, ignoring advection caused by evaporation. They note that the calculation provides a general time range. Infiltration may occur in response to short-term periods of increased precipitation followed by a return to an evaporative setting which is not necessarily associated with major climate changes. This aborted recharge process would increase the depth of enriched isotopes in the profile. Therefore a calculation based entirely on diffusional transport would serve as an upper limit. Solutions of the diffusion equation for borehole Pilot Well UE5PW-2 range from 10,000 to 15,000 years. This time period agrees reasonably well with the chloride age dates of the soil water, suggesting that the soil profile has not experienced infiltration since the end of the Pleistocene. Calculations for Pilot Well UE5PW-3 yield estimates of up to 30,000 years because of the slightly deeper penetration of the enriched isotopes. Pilot Well UE5PW-1 does not exhibit a diffusion-dominated profile and therefore was not fit with the diffusion model.

Deep soil water infiltration must have occurred under past climate conditions. According to Tyler *et al.* (1996), the similarity of the slopes of the current LMWL and the trend of the deep soil data (depletion in the heavy isotopes as compared to both the weighted mean of current precipitation and the weighted mean of winter-only precipitation) suggests that recharge in the past was from the same source as at present, although at a cooler temperature. From Tyler *et al.* (1996), this coincides with estimates of conditions in the southern Great Basin during the last glacial interval. The source of much of the aquifer recharge may not have been derived from the overlying vadose zone, however, as the chloride concentrations in the

soil water are approximately twice that found in the groundwater. The slight variations in isotopic composition at depth in the Pilot Wells do not deviate from the deep soil water trend, and therefore are not likely a result of evaporation caused by the air used during drilling. Because they do not appear evaporated, their enrichment may represent recharge under a warmer climate or summer-dominated precipitation patterns. The persistence of the deep isotopic variations are surprising, given the estimated ages of the deep soil water. However, these variations support the ages of soil water in the Pilot Wells. Both Pilot Well UE5PW-1 and Pilot Well UE5PW-3 show only moderate variation in the distribution of ^2H and ^{18}O below approximately 100 m (328 ft). The chloride age dates for these deep waters approach 110 ka. In contrast, Pilot Well UE5PW-2 (chloride age of 20 to 35 ka) shows notable departures at depths of 150 m (492 ft) and 225 to 250 m (738 to 820 ft), as well as a more apparent minimum at 50 to 60 m (164 to 197 ft). The persistence of these deviations confirms the chloride data in a relative sense; the soil water in Pilot Well UE5PW-2 may be much younger having less time to diffuse these pulses than Pilot Well UE5PW-1 and Pilot Well UE5PW-3.

EVOLUTION OF VADOSE ZONE CONDITIONS OVER TIME

The near-surface enrichment of stable chloride, bromide, hydrogen, and oxygen also indicates that the present condition of net upward liquid movement through the vadose zone has been relatively long term and that diffuse recharge is essentially negligible. Phillips (1994) suggests that the chloride "bulge" observed in many North American arid soils is the result of dry climatic conditions over at least the last 12,000 years. REECo (1993a) estimates that the downward water soil flux has been very limited for at least the last 10,000 years to allow for the observed accumulation of chloride. An additional estimate for the length of time current vadose-zone conditions have persisted can be obtained from studies within the same climatic and geologic regime at Beatty, Nevada, 80 km (50 mi) west of the Area 5 RWMS (Fouty, 1989). Using the chloride mass balance technique, Fouty (1989) estimated the recharge rate and concluded that drainage below 10 m (33 ft) was minimal or nonexistent for at least the last 6,000 years. The conclusion drawn from the stable isotope data is that the current climatic regime, reflected by the enrichment in the near surface by various stable isotopes, has existed for a very long time and, under this regime, contaminant transport and flow in the liquid phase can be considered minimal.

The soil physical and environmental tracer data obtained from the boreholes in Area 5 point to the conclusion that the system is not at steady state. Instead, the variations in tracers and water potential reveal a history encompassing episodes of recharging and drying over thousands of years driven by changing climatic conditions. Profiles of tracer concentration or water potential must be interpreted with the understanding that these profiles are the result of processes which occur over a range of time scales. Tyler *et al.* (1996) states that because the solute profiles are not at steady state and are accumulating chloride in the upper 125 m (410 ft), it is not appropriate to apply the simple chloride mass balance method to estimate

They are, however, able to use the tracer data from deeper in the profile to estimate the paleorecharge rate (the character of the zero flux surface). The history of water fluxes in Frenchman Flat is presented by Tyler *et al.* (1996) and summarized in the following paragraphs.

The approximate age calculated for the accumulations of chloride found in both Pilot Well UE5PW-1 and Pilot Well UE5PW-3 coincide with maximum lake levels at approximately 120 ka. Prior to this, recharge at all three boreholes was occurring. After this period, chloride begins to accumulate, signaling the end of recharge through the vadose zone at Pilot Wells UE5PW-1 and UE5PW-3. The flux conditions at Pilot Well UE5PW-2 cannot be determined because the profile was completely flushed at some later time.

The secondary bulges at Pilot Well UE5PW-1 and Pilot Well UE5PW-3 have been calculated to be as old as 40 and 50 ka, respectively, based on the chloride ages of the soil water and a simple model of diffusive transport. This marks the beginning of a period of advective transport which transitioned back into a period of chloride accumulation (which continues to this time), indicating an ending to recharge. The timing of the cessation of recharge at Pilot Well UE5PW-2 is later, in the range of 20 to 30 ka. This period is recognized by all of the paleoclimate indicators as a major pluvial period.

Tyler *et al.* (1996) supports the conclusion that recharge in Area 5 has been a function of climate. If a wetter climate developed in the absence of adaptation by the vegetation, fluxes would increase and, in time, as the wetting front moved downward, the vertical extent of the static zones would shrink from the top until the gradient of the total potential was directed downward throughout the entire profile. This condition would support recharge.

The previous discussion did not take into account adaptation of the plant community to utilize additional water. According to the National Research Council in its review of studies of recharge through the vadose zone at Ward Valley (National Research Council, 1995), desert plant communities adapt quickly to changes in annual precipitation. Given the similarities in soil, climate, and vegetation, the Ward Valley findings are equally valid for Frenchman Flat.

SUMMARY OF VADOSE ZONE CHARACTERIZATION DATA

In summary, the following conclusions for the vadose zone can be drawn from the site characterization data:

- The alluvium may be considered homogeneous with respect to particle-size distribution with depth on a gross scale and is characterized as a well-graded, medium sand with gravel and a small amount of fines.
- The hydrologic properties of the alluvium are isotropic. This includes porosity (n), saturated hydraulic conductivity (K_{sat}), moisture retention ($\psi(\theta)$), and unsaturated

hydraulic conductivity ($K(\theta)$) (Sully *et al.*, 1993; Istok *et al.*, 1994). For the purposes of hydrologic modeling, the alluvium penetrated by the Pilot Wells and Science Trench Boreholes can be assumed to be a single homogeneous and isotropic lithological unit.

- Water content of the alluvium is very low near the surface and increases only slightly with depth (from 5 percent at the surface to about 10 percent at a depth of 37 m [121.3 ft]). This indicates that the entire vadose zone is very dry.
- Water potential measurements (H , a measure of the strength of the driving force causing fluid flow) show a large negative gradient in the upper portion of the alluvium (indicating a tendency for water to flow upward to the surface) because of high evapotranspiration at the land surface. The upward potential exists throughout the upper 35 m (115 ft) of alluvium, with the largest upward gradient in the upper 9 m (29.5 ft).
- Very little if any liquid flow is occurring within the upper 35 m (115 ft) of the vadose zone because the unsaturated hydraulic conductivity values ($K(\theta)$) are small due to the low water content in this region.
- Depth profiles show an enrichment near the surface of stable chloride and bromide, as well as the heavier naturally occurring isotopes of hydrogen and oxygen. This provides strong evidence that evaporation is the dominant hydrologic process in the upper vadose zone and that recharge at the Area 5 RWMS is currently negligible. Water that exists deeper in the vadose zone probably entered the system under a much wetter climate.

These data suggest that the small amount of liquid water infiltrating at the surface during infrequent rainfall events (diffuse recharge) does not migrate down to the water table (REECo, 1993a; Ginanni *et al.*, 1993; O'Neill *et al.*, 1993; and Detty *et al.*, 1993), but rather remains close to the surface and is rapidly returned to the atmosphere through evapotranspiration (Fischer, 1992; Scanlon *et al.*, 1991; and Enfield *et al.*, 1973). This finding is consistent with the Gee *et al.* (1994) conclusion that there is no significant drainage within the upper 1.25 m (4.1 ft) of soil at the Beatty site, 80 km (50 mi) west of the RWMS.

CONCEPTUAL MODEL OF UNSATURATED FLOW IN THE VADOSE ZONE

The average magnitude and direction of the total hydraulic potential gradient from point to point within the profile strongly suggests that flow in the vadose zone beneath the Area 5 RWMS is one-dimensional and can be divided into four zones:

- Zone I: An upper zone, approximately 35 m (115 ft) in depth, where a large negative hydraulic potential (driven by evapotranspiration at the surface) creates a potential for upward liquid flow and drying at the near surface.

- Zone II: A static zone where the gradient is negligible. The depth and thickness of the static zone varies with location. In Pilot Well UE5PW-1 (*Figure 2.21*), the static zone occurs from 40 to 90 m (131 to 295 ft).
- Zone III: An intermediate zone immediately below the static zone down to 150 to 220 m (492 to 722 ft), where the hydraulic potential is dominated by gravity drainage causing downward flow. The top of the intermediate zone depends on the depth of the static zone. In Pilot Well UE5PW-1, the top of the intermediate zone is at a depth of about 90 m (295 ft). The high values of water potential and low water content suggest that flow is under a quasi-steady-state condition. This condition presumably was reached a considerable time after the end of a much wetter climatic period when recharge was higher.
- Zone IV: A lower zone, up to a few cm (in) above the water table, where the hydraulic potential is near zero and the water is under a capillary fringe condition with relatively static conditions producing little flow.

The vadose zone conceptual model does not support the existence of a groundwater pathway under existing conditions. Water infiltrating at the Area 5 RWMS is expected to be recycled to the atmosphere rather than recharged to the uppermost aquifer. This model is supported by the water potential profile with depth and the environmental tracer data.

ESTIMATION OF UNSATURATED FLOW RATE AND DIRECTION

In the previous sections, it was shown that infiltrating precipitation at the Area 5 RWMS does not recharge the aquifer but is rapidly recycled to the atmosphere. The thickness and low water content of the vadose zone offers an additional protection against contamination of the uppermost aquifer. In the unlikely event that leachate was able to reach Zone III where

(i.e., groundwater movement was hypothesized to be primarily downward from the alluvium into the underlying aquitards), eventually draining into the lower-carbonate aquifer.

Evidence that recharge through the vadose zone under the present climatic conditions is

extremely small has already been presented, along with additional evidence that the travel

which can be added as vectors to yield the total magnitude and direction of flow within the saturated portions of an isotropic hydrological unit such as the valley-fill aquifer.

Vertical Saturated Flow

There has been no systematic evaluation of the vertical component of the hydraulic gradient in Frenchman Flat. Winograd and Thordarson (1975) concluded that a generalized vertical flow was more likely than a horizontal flow through the uppermost unconfined Cenozoic units. Downward leakage is more likely than horizontal flow because: (1) the water levels in the Cenozoic strata in surrounding valleys were comparable to those observed in Frenchman Flat, indicating an absence of horizontal gradient; (2) water levels in wells tapping the lower-carbonate aquifer, two along the north and east peripheries of the basin and one on the southwestern edge, show a piezometric surface somewhat lower (3 to 10 m [9.8 to 33 ft]) than that in the Cenozoic units, indicating a possible downward vertical gradient; and (3) the lower-carbonate aquifer rises on the edge of the basin (except the west) so that any recharge within the basin, even horizontal, must eventually drain into it. Nevertheless, Winograd and Thordarson also recognized that recharge to the lower-carbonate aquifer from overlying units beneath the valley floors in the NTS seemed improbable under the present climatic conditions (i.e., that vertical seepage through the valley floors was a distant second to recharge from precipitation directly onto the carbonate aquifer, especially in areas of high elevation and rainfall).

The consensus opinion, reached prior to obtaining the vadose zone site characterization data previously presented, was that at least some degree of vertical flow and recharge into the lower units from the Cenozoic units occurred through the valley floors. However, there is no hard evidence for substantial vertical movement in the uppermost aquifer units within the basins of the NTS. Even the minimal vertical flow proposed by Winograd and Thordarson (1975) could, due to mass balance considerations, exist only if vertical recharge first occurs. Evidence that no such recharge occurs has been presented. This is a strong argument against the existence of any significant amount of vertical flow within the Cenozoic units beneath the Frenchman Flat. Also, the existence of vertical flow would imply a declining water table. No evidence of such a decline exists. If vertical flow does indeed occur, it is probably restricted to areas of higher precipitation (e.g., near mountain slopes and peaks surrounding NTS basins where recharge is directly into the Cenozoic units). Some degree of vertical flow also may exist on the margins of the basins, but this is probably minimal within the interior of Frenchman Flat.

The extent of vertical flow beneath the Area 5 RWMS could be ascertained by a comparison of the potentiometric head in the lower units below the RWMS to that found in the saturated Cenozoic aquifer (e.g., to measure the vertical hydraulic gradient). The data required for this comparison are not available. However, a rough approximation of the vertical hydraulic gradient can be estimated from data obtained from existing wells if the following assumptions are made:

- The top of the upper surface of the lower-carbonate unit is approximately 1,340 m (4,396 ft) below the land surface, and the average depth to the water table is about 250 m (820 ft), yielding a saturated thickness above the carbonates of $(1,340-250) = 1,090$ m (3,576 ft). (*Figures 2.9, 2.11, and Table 2.4*).
- The saturated thickness beneath the Area 5 RWMS is composed primarily of the bedded tuff aquitard (*Figures 2.16 and 2.17*).
- For purposes of analysis, the tuff can be considered to be anisotropic but homogeneous (i.e., the vertical hydraulic conductivity is constant in space).
- The maximum difference between potentiometric surfaces for the lower-carbonate aquifer and the upper saturated valley-fill aquifer cited by Winograd and Thordarson (1975) within Frenchman Flat applies beneath the RWMS and is about 10 m (33 ft).

Accordingly, the magnitude of the vertical hydraulic gradient (dH/dz) is $10/1,090 = 0.009174 \text{ m m}^{-1}$. Based on one-dimensional flow theory, Darcy's law can be used to determine the mean pore flow velocity (v) within the bedded tuff aquitard. Given an average water-filled porosity (n_w) of 37.7 percent and the saturated hydraulic conductivity (K_{sat}) of 0.006 m day^{-1} (*Table 2.3*), the estimated vertical mean pore flow velocity is:

$$v = \frac{q}{n} = \frac{K_{sat} dH}{n dz} = \frac{0.006 \text{ m d}^{-1}}{0.377}$$

2.4.2.3 *Water Quality of the Uppermost Aquifer*

Groundwater wells have been developed within Frenchman Flat for drinking water production and as part of investigations supporting underground nuclear testing. Drinking water production wells are sampled routinely for compliance with the Safe Drinking Water Act. Active drinking water wells are located along the western edge of the Frenchman Flat playa approximately 6 km (3.7 mi) south of the Area 5 RWMS. Drinking water wells in Frenchman Flat are completed in the valley-fill aquifer which is the uppermost aquifer beneath the Area 5 RWMS.

Sampling and analysis of the uppermost aquifer in the immediate vicinity of the Area 5 RWMS was initiated in 1993. This corresponded with the completion of the three Pilot Wells (UE5PW-1, UE5PW-2, and UE5PW-3), developed as part of site characterization activities. The analysis of samples from these wells is conducted to comply with the detection monitoring requirements for RCRA interim status treatment, storage, and disposal facilities. Each well is screened over the first 15 m (49 ft) of the uppermost aquifer. The two wells to the east of the site (UE5PW-1 and UE5PW-2) are completed in the valley fill

Table 2.6 Mean Water Quality Parameters for UE5PW-1, UE5PW-2, and UE5PW-3 for 1993

Parameter	UE5PW-1	UE5PW-2	UE5PW-3	Method Detection Limit	Units
pH	8.12	8.26	8.5		
Specific Conductance	0.392	0.384	0.375		mmhos cm ⁻¹
Total Organic Carbon	n.d.†	n.d.	n.d.	1	mg l ⁻¹
Total Organic Halogen	6 - 13	18 - 25	1 - 11	10	µg l ⁻¹
Total As	0.007	0.006	0.001	0.0003	mg l ⁻¹
Dissolved As	0.007	0.006	0.001	0.0003	mg l ⁻¹
Total Ba	0.019	0.015	0.018	0.0005	mg l ⁻¹
Dissolved Ba	0.018	0.015	0.017	0.0005	mg l ⁻¹
Total Cd	-0.0007	4 x 10 ⁻⁵ - 6 x 10 ⁻⁵	4 x 10 ⁻⁵ - 6 x 10 ⁻⁵	3 x 10 ⁻⁵	mg l ⁻¹
Dissolved Cd	0.0009	5 x 10 ⁻⁵ - 7 x 10 ⁻⁵	-0.001	3 x 10 ⁻⁵	mg l ⁻¹
Total Cr	0 - 0.004	0 - 0.005	0 - 0.005	0.005	mg l ⁻¹
Dissolved Cr	0 - 0.004	0 - 0.005	0 - 0.005	0.005	mg l ⁻¹
Total Pb	-0.004	-0.0004	0 - 0.0003	0.0004	mg l ⁻¹
Dissolved Pb	-0.004	-0.0003	0 - 0.0003	0.0004	mg l ⁻¹
Total Se	0.0004 - 0.0009	0.0003 - 0.0008	0 - 0.0006	0.0004	mg l ⁻¹
Dissolved Se	-0.003	0.0002 - 0.0005	0 - 0.0005	0.0004	mg l ⁻¹
Total Ag	0 - 0.007	0 - 0.01	0 - 0.008	0.003	mg l ⁻¹
Dissolved Ag	0 - 0.007	0 - 0.01	0 - 0.008	0.003	mg l ⁻¹
Total Hg	0 - 0.0001	0 - 0.0001	0 - 0.0001	0.0001	mg l ⁻¹
Dissolved Hg	0 - 0.0001	0 - 0.0001	0 - 0.0001	0.0001	mg l ⁻¹
Total Fe	0.028	0.141	0.062	0.003	mg l ⁻¹
Dissolved Fe	0.004 - 0.006	0.088	0.010 - 0.012	0.003	mg l ⁻¹
Total Mn	0.002 - 0.003	0.003 - 0.004	0.011 - 0.012	0.001	mg l ⁻¹
Dissolved Mn	0 - 0.001	0.003 - 0.004	0.011 - 0.012	0.001	mg l ⁻¹
Total Na	54.8	49	51	0.05	mg l ⁻¹
Dissolved Na	53	49.8	51.7	0.05	mg l ⁻¹
Fluoride	2.4	1.1	1.2	0.1	mg l ⁻¹
Nitrate (as NO ₃)	9.7	6.0	14.1	0.04	mg l ⁻¹

Table 2.6 (continued)

Parameter	UE5PW-1	UE5PW-2	UE5PW-3	Method Detection Limit	Units
Chloride	9.3	9.2	8.6	0.1	mg l ⁻¹
Sulfate	35	29.7	31.2	0.1	mg l ⁻¹
Total Dissolved Solids	236	252	218		mg l ⁻¹
Alkalinity (as CaCO ₃)	144	139	129		mg l ⁻¹
Cyanide	0 - 0.0004	0 - 3.33	0 - 0.0004	0.005	mg l ⁻¹
Oil and Grease	0.1 - 0.3	0.3 - 0.5	0.1 - 0.5	0.1	mg l ⁻¹
Volatile Organics	n.d.	n.d.	n.d.		mg l ⁻¹
Semivolatile Organics	n.d.	n.d.	n.d.		mg l ⁻¹
Pesticides	n.d.	n.d.	n.d.		mg l ⁻¹
Herbicides	n.d.	n.d.	n.d.		mg l ⁻¹
Total Gross Alpha	5.1	4.2	5.1	0.7	pCi l ⁻¹
Dissolved Gross Alpha	5.7	3.6	5.6	0.7	pCi l ⁻¹
Total Gross Beta	4.5	4.9	4.6	0.6	pCi l ⁻¹
Dissolved Gross Beta	5	5.4	4.4	0.6	pCi l ⁻¹
³ H	-0.6	10	-0.4	9	pCi l ⁻¹
⁹⁰ Sr	0.09	0.2	0.03	0.09	pCi l ⁻¹
⁹⁹ Tc	0.7	0.5	-0.9	0.7	pCi l ⁻¹
²²⁶ Ra	0.7	0.8	1.5	2	pCi l ⁻¹
²²⁸ Ra	0.04	0.1	0.5	3	pCi l ⁻¹
Total Uranium	0.8	1.8	9.7	5	μg l ⁻¹
²³⁸ Pu	0	0.004	0.001	0.009	pCi l ⁻¹
^{239,240} Pu	0.003	0.003	0.002	0.009	pCi l ⁻¹
Photon Emitters	n.d.	n.d.	n.d.		pCi l ⁻¹

† - n.d. = not detected

2.5 Demography

Population densities in Nevada are among the lowest found in the contiguous 48 states. In 1990, the average population density of Nevada was 4.2 persons per km², much smaller than

the average of 28 per km² for the contiguous 48 states (DOC, 1990). Permanent settlement and development in the arid deserts of southern Nevada has been restricted to areas where surface water, springs, seeps, or shallow groundwater are available or to areas near economically significant mineral resources. Because surface or shallow water resources are rare, the population of Nevada tends to be clustered around a few sites with available water. The intervening land remains largely unpopulated. Recent census data indicate that Nevada's population is overwhelmingly urban and is concentrated in Reno and Las Vegas. A map of Nevada counties, including their 1990 populations, appears in Figure 2.35. At the time of the 1990 census, urban areas with populations greater than 2,500 held 88.3 percent of the population (DOC, 1990) and occupied only 0.9 percent of the land area (Morgan *et al.*, 1993). Most of the remaining population resides in small rural communities with populations less than 2,500. Only 0.3 percent of Nevadans are identified as rural farm residents (DOC, 1990).

Rural lands in Nevada outside the metropolitan areas are undeveloped, uninhabited rangeland, and mountains. The population density of areas classified as rural is only 0.5 per km² (DOC, 1990; Morgan *et al.*, 1993). This is due to both the lack of water resources and the fact that as of 1990, 82.7 percent of Nevada was owned by the U.S. government (Morgan *et al.*, 1993). U.S. government-owned land can be leased to private interests for grazing and mining, but generally is uninhabited except for small transient populations of cowboys, sheep herders, hunters, campers, and prospectors (EPA, 1984). The rural counties surrounding the NTS have extremely low population densities. Nye County has a population density of 0.4 km⁻² and Lincoln County's population density is only 0.1 km⁻².

The Las Vegas metropolitan area is the largest urban center near the NTS, with a 1990 population of approximately 741,000, or 61 percent of the then-residents of Nevada (DOC, 1990). Las Vegas is one of the fastest growing urban areas in the United States and its population has increased significantly since the 1990 census. In recent years, residential and commercial development has increased significantly in other communities in southern Nevada, including Pahrump and Mesquite. Most of the population within an 80-km (50-mi) radius of the RWMS resides within three small rural communities: Indian Springs, Beatty, and the Amargosa/Pahrump Valleys (Figures 2.1 and 2.35). The closest residents to the Area 5 RWMS reside in Indian Springs, population 1,500.

Approximately 950 persons reside in the Amargosa Valley at the Lathrop Wells farming community 50 km (31 mi) southwest of the RWMS (DOE, 1993a). The Pahrump Valley, 80 km (50 mi) to the southwest, has a growing rural population of approximately 15,000 (DOE, 1993a). The next-largest population center in the region is Beatty (population 1,500), located 82 km (51 mi) to the west (DOE, 1993a). There are approximately 18 small settlements, ranches, and mining operations, all with populations of less than 100, within the 80-km (50-mi) radius (EPA, 1984). The Death Valley Monument in California, located to the west of the NTS, can have a transient population ranging from 200 to 12,000 persons (EPA, 1984).

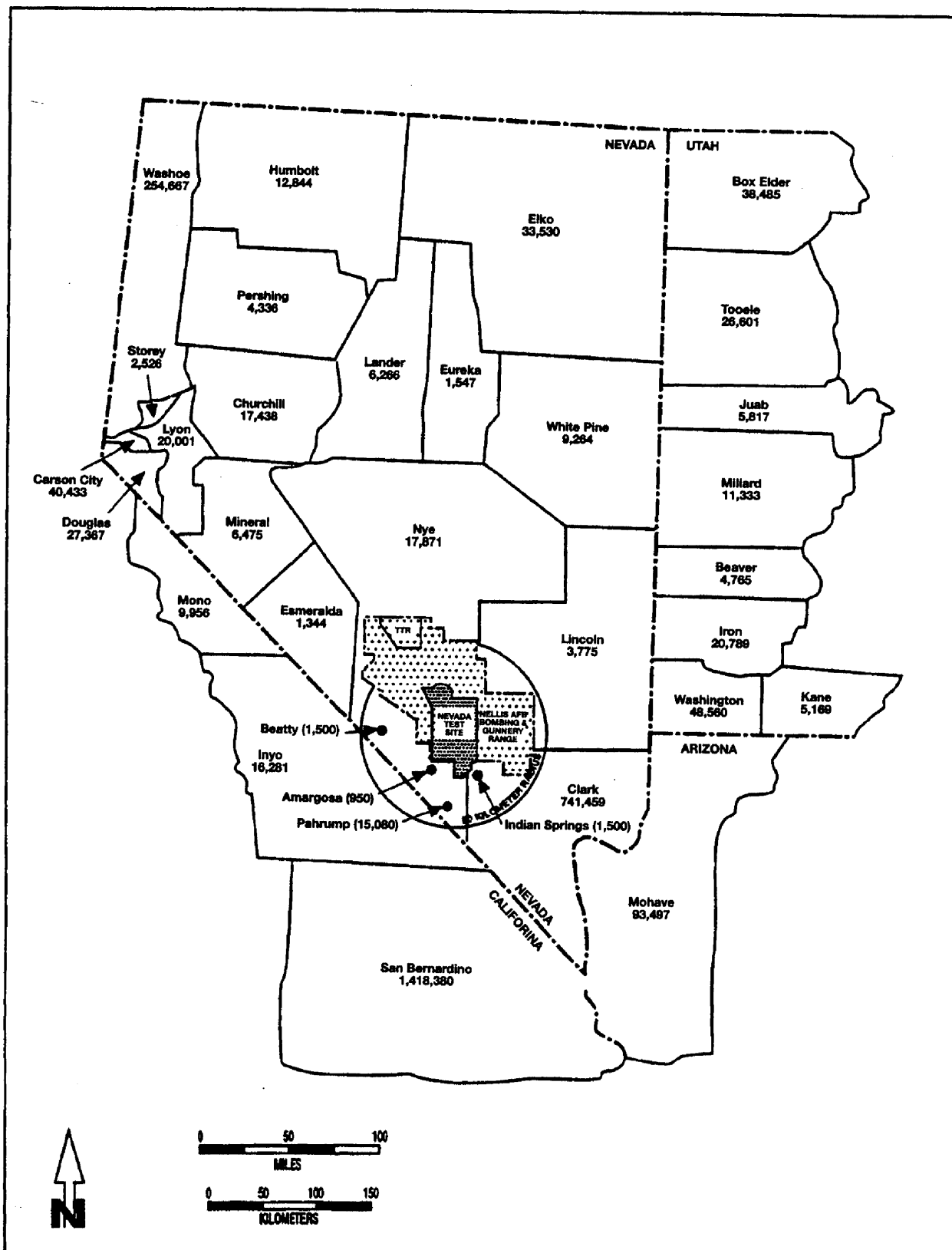


Figure 2.35 Population of Counties in Nevada Based on 1990 Census Estimates (adapted from DOE/NV, 1993a).

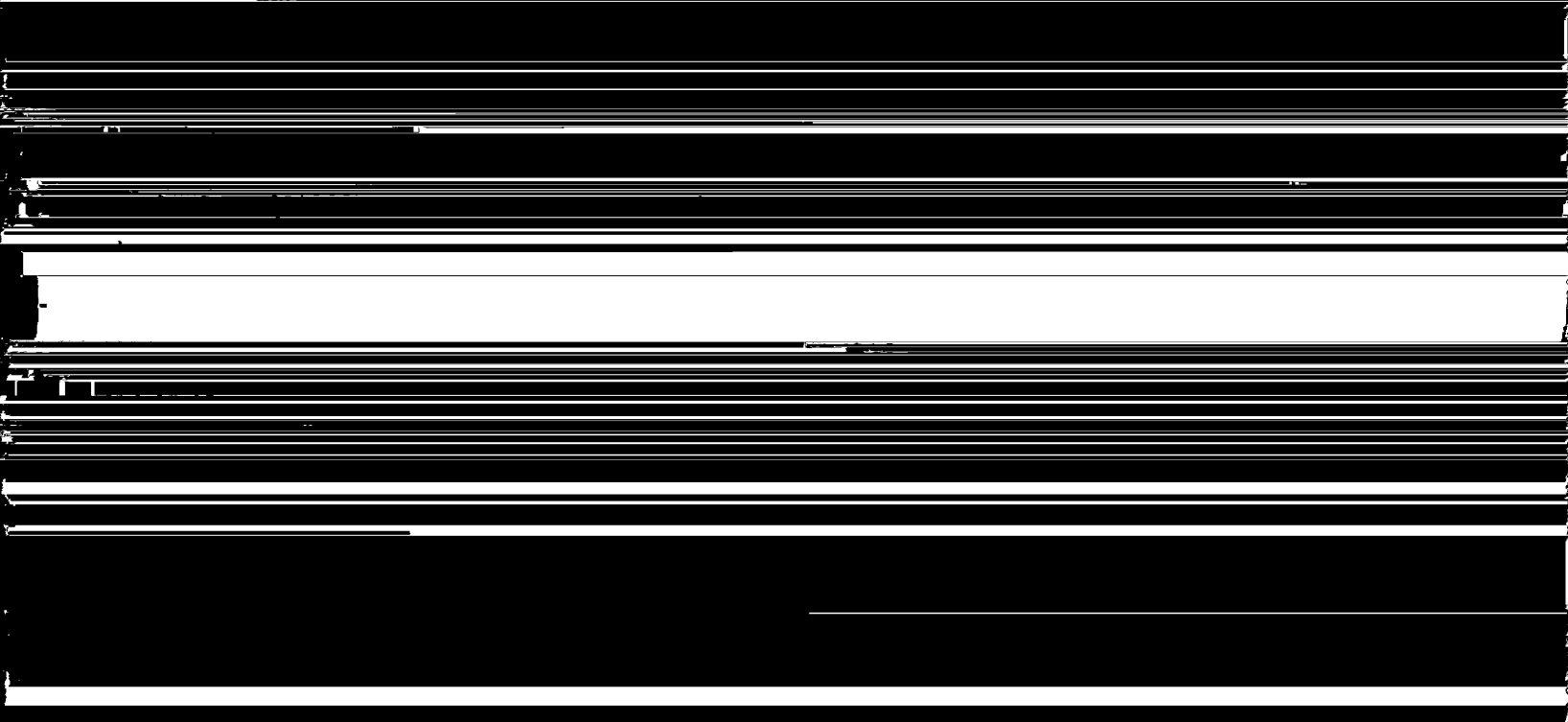
2.6 Land Use

Native Americans were the first to use the lands now within the NTS. The Shoshone lived at local springs and playas over the northern NTS. Springs on the southern NTS have been used by the Southern Paiute tribe. Both groups gathered native plants, including *Oryzopsis hymenoides* (indian rice grass), *Salvia columbaria*, *Elymus cinereus* (wild rye), and pinyon nuts and hunted wild game including rabbits and *Odocoileus hemionus* (mule deer) (Reno and Pippin, 1985). Early settlers established several cattle ranching and wild horse capture operations at local springs, including Cane Spring on the western margin of Frenchman Flat (Reno and Pippin, 1985). Small mining operations have existed on the NTS in the Oak Spring District and the Mine Mountain District (Reno and Pippin, 1985). In 1928, Cane Spring supported 1,500 persons in the mining community of Wahmonie (Allred *et al.*, 1963). Since 1940, the NTS has been a U.S. government-owned, restricted access area used for defense-related activities.

Today, ranching and mining remain as important land use activities in southern Nevada. Recreational activities and irrigation-based agriculture have, in recent years, become important land uses. Favorable economic conditions in Las Vegas have spurred rapid residential development in Clark County.

2.6.1 Geological Resources

Economically significant mining districts have been identified and exploited throughout southern Nevada. Small mining operations have existed on the NTS in the past. However, at this time, no economically significant mineral resources are known to exist within Area 5 (Richard-Haggard, 1983; Gustafson *et al.*, 1993). Most mineral exploration of the NTS was conducted prior to 1940 by unsophisticated operators and little reliable data are available (Richard-Haggard, 1983). The only well-known mineral deposits on the NTS are tungsten deposits in the Oak Spring District, approximately 50 km (31 mi) north of Area 5, which



The only producing oil fields in Nevada are in Railroad Valley, 150 km (93 mi) north of the NTS; and in Eureka County, 193 km (120 mi) to the north (Gustafson *et al.*, 1993). Oil and gas exploration near the NTS has yielded negative results and it is considered unlikely that

Total land area devoted to agriculture in Nevada is low. Overall, only 14.2 percent of Nevada's land area is within farms. In the drier southern counties, only 2.1 percent of the land area is used for agriculture (Table 2.7). Southern Nevada farmland is most likely to be used as pasture, 89.1 percent, followed by cropland, 11.7 percent (Table 2.7). Orchard and woodlands are commercially insignificant. No quantitative data exist for noncommercial agriculture land use, such as household gardens.

Table 2.7 Total Land Area and Farm Land in Southern Nevada for 1987 (from DOC, 1987)

Land Use	Nevada	County		
		Clark	Lincoln	Nye
Land Area (ha)	28,439,700	2,048,900	2,754,400	4,700,100
Farm Land Area (ha)	4,042,254	27,427	18,771	149,903
% Land Area in Farms	14.2	1.3	0.7	3.2
% Farm Land Used as Cropland	8.0	16.8	37.6	7.6 [†]
% Farm Land Used as Orchard	0.005	0.2	0.5	0.02
% Farm Land Used as Woodland	0.09	0.5	‡	‡

[†] - Value Based on 1982 data

[‡] - Single operator reporting

Cropland is predominantly used for the production of livestock feed crops (Table 2.8). Approximately 45.8 percent of southern Nevada cropland is harvested, whereas 30 percent is used directly as pasture (DOC, 1987). Of the harvested cropland, hay is the predominant crop grown, with lesser quantities of barley and silage crops produced (DOC, 1987). Production of legumes, cotton, tobacco, tubers, vegetables, sweet corn, melons, nuts, berries, and fruits is commercially insignificant in southern Nevada (DOC, 1987). However, private production of vegetables does occur on land surrounding the NTS (EPA, 1984).

Richard-Haggard (1983) has reviewed the potential agricultural uses of the NTS and reported that Frenchman Flat contains 4,900 ha (12,108 ac) of irrigable soils. All irrigable soils in

Table 2.8 Cropland in Nevada and Southern Nevada by Use and Crop Grown for 1987 (from DOC, 1987)

Cropland	Nevada	County		
		Clark	Lincoln	Nye†
% Harvested	66.5	53.7	41.1	45.6
% of Cropland that is Harvested and Irrigated	65.3	53.7	41.1	45.6
% Cropland used as Pasture	26.0	30.1	34.1†	‡
% Other Cropland (Idle)	8.5	16.2	16.0†	‡
% Cover Crops Not Harvested or Grazed	0.7	1.3		‡

† - Value based on 1982 data.

‡ - Single operator reporting.

Frenchman Flat have poor water retention characteristics (Richard-Haggard, 1983). Nevertheless, the presence of irrigable soils, adequate groundwater supplies, and 130 to 200 frost-free days per year makes it technically feasible to produce hay crops, such as alfalfa, in the basin (Richard-Haggard, 1983).

Irrigated land is a small fraction, 10.5 percent, of total farm land in southern Nevada (Table 2.9). This reflects the large amount of farm land that is uncultivated open rangeland. However, virtually all harvested crops in southern Nevada are irrigated. Harvested cropland accounts for 48.1 percent of all irrigated land, the rest being used as pasture. Again, most harvested crops are hay crops, intended for consumption by livestock. Richard-Haggard (1983), noting that only 5 percent of irrigable land in Nevada is in use, concluded that current demand for irrigable land is low. The cost of obtaining deep groundwater resources may in part explain this observation. Irrigation of farm land in southern Nevada most commonly occurs where surface water or shallow groundwater is available. These conditions do not occur in Frenchman Flat near the Area 5 RWMS.

Pastureland in southern Nevada is 95.9 percent uncultivated, unirrigated rangeland. Beef cattle are numerically the most common livestock produced, followed by sheep (Table 2.10); hogs and chickens are raised in small numbers (DOC, 1987). With the exception of Clark County, commercial milk production in southern Nevada is insignificant. Several Grade A dairy herds occur in Clark County, but all are greater than 100 km (62 mi) from the NTS (EPA, 1984). In 1984, the EPA reported 83 family dairy cows and 397 family milk goats in Nye, Lincoln, and Clark counties (EPA, 1984).

Table 2.9 Irrigated Land and Irrigated Land by Use in Nevada and Southern Nevada for 1987
(from DOC, 1987)

Irrigated Land	Nevada	County		
		Clark	Lincoln	Nye
% of Farm Land Irrigated	7.8	11.1	30.9	7.9
Irrigated Land by Use				
% Harvested Cropland	67.3†	78.3	50.0	39.5
% Pastureland	32.7	22.1	50.0	60.5

† - Value based on 1982 data.

Table 2.10 Livestock Numbers in Nevada and Southern Nevada in 1987 (from DOC, 1987)

Livestock	Nevada	County		
		Clark	Lincoln	Nye
Cattle, Calves	575,608	15,970	12,237	19,924
Beef Cows	305,018	3,847	6,437	13,403
Milk Cows	17,646	6,432	21	26
Hogs, Pigs	16,505	‡	‡	131
Sheep, Lambs	99,768	2,222	114	6,181
Chickens	18,245	1,221	278	784
Broilers, Meat Chickens	525	§	‡	§

‡ - Single operator reporting

§ - Negligible

Rangeland in southern Nevada has significant limitations. In the Great Basin Desert communities, *Artemisia tridentata* (big sagebrush) can be used as fall and spring pasture and *Atriplex confertifolia* (shadscale) can serve as winter rangeland (Stoddart and Smith, 1955).

Studies of the gut contents of rumen-fistulated steers grazing in Great Basin Desert

communities on the NTS have demonstrated that cattle rumen contents are dramatically

Table 2.11 AUM ha⁻¹ for Various Floral Communities on the NTS (from Richard-Haggard, 1983)

Floral Community	AUM ha ⁻¹
<i>Larrea</i>	0.045
<i>Artemisia</i>	0.024
<i>Coleogyne</i>	0.0086
<i>Larrea - Coleogyne</i>	0.024
<i>Grayia - Lycium</i>	0.033
<i>Atriplex</i>	0.02
<i>Lycium pallidum</i>	0.033
Pinyon - Juniper	0.014

O'Farrell and Emery (1976) report 711 taxa of vascular plants for the NTS and its environs. As many as 70 species per 1,000 m² (3,280 ft²) have been reported (Beatley, 1976).

Historically, the flora of the NTS have been grouped into three major or regional communities: the Mojave Desert community occurring over southern Nevada, the Great Basin Desert community occurring over central Nevada, and a transitional community interspersed between the two (Beatley, 1976; O'Farrell and Emery, 1976). Within each regional community, local communities can be identified via recurring assemblages of numerically dominant and co-dominant perennial shrubs or trees (Beatley, 1976; O'Farrell and Emery, 1976). Local communities grade gradually into one another as edaphic and climatic conditions change, forming a complex patchwork of plant communities. Community composition can be quite complex, with no two locations having the same species composition (Beatley, 1976).

Communities of the Mojave Desert occur over the southern third of the NTS, on the bajadas and mountain ranges at elevations below 1,200 m (3,940 ft). They are limited to areas with mean minimum temperatures greater than -2°C (28°F) and average annual rainfall less than 18.3 cm (7.2 in) (O'Farrell and Emery, 1976). Mojave Desert communities can have highly variable floristic compositions, but all share a shrub clump form dominated by *Larrea tridentata* (creosote bush) and variable co-dominant shrubs (Beatley, 1976). Shrub coverage varies from 7 to 23 percent for Mojave Desert communities found on the NTS (Beatley, 1976). Herbaceous species including perennials and winter annuals can be uniformly interspersed between shrub clumps or only associated with shrub clumps, depending on soil and

climatic conditions (Beatley, 1969; Beatley, 1976). Growth of herbaceous perennials and reproduction and growth of winter annuals is regulated by autumn rains and can vary significantly from year to year with rainfall (Beatley, 1976; Bowers, 1987). Winter annuals in particular undergo mass germinations after heavy autumn rains and reach levels of cover as high as 30 percent (Beatley, 1976). Summer annuals (ephemerals) may appear briefly after late summer rains and reach area coverages up to 8 percent (Beatley, 1976).

Beatley (1976) identified three Mojave Desert bajada communities based on the numerically co-dominant shrub species present. The communities were: the *Larrea tridentata* - *Ambrosia dumosa* (bur sage) community found on loose deep soils; the *Larrea* - *Lycium andersonii* (desert thorn) - *Grayia spinosa* (hop sage) community found at elevations between 1,000 to 1,200 m (3,280 and 3,940 ft); and the *Larrea* - *Atriplex confertifolia* (shadscale) community found on calcareous soils with well-developed pavements and caliche layers (Beatley, 1976). Numerous herbaceous species occur within these communities. See Beatley (1976) for complete descriptions.

Assemblages grouped among transitional desert communities occur under two different situations. Some assemblages occur along elevation gradients between Mojave Desert and Great Basin Desert communities. Others occupy the bottoms of closed basins where cold air accumulates during the night (Beatley, 1976). These communities, although considered transitional, may be completely surrounded by Mojave or Great Basin Desert communities. On the NTS, two transitional communities, *Coleogyne* and *Larrea* - *Grayia* - *Lycium*, occur along elevation gradients between Great Basin and Mojave Desert communities. *Coleogyne ramossima* (blackbush) grows in nearly pure stands on upper elevation bajadas that are beyond the moisture range of Mojave Desert communities (Beatley, 1976). *Larrea* - *Grayia* - *Lycium* assemblages occur on higher bajadas, often below *Coleogyne* communities (Beatley, 1976). Three transitional communities, *Grayia* - *Lycium*, *Lycium pallidum* - *Grayia*, and *Lycium shockleyi* - *Atriplex*, are associated with the lower elevations of closed basins (Beatley, 1974, 1976). Romney *et al.* (1973) report that, in addition to cold nighttime temperatures, soil texture, and salinity are also important in controlling the distributions of these communities. Shrub coverage in transitional communities averages 29 percent (O'Farrell and Emery, 1976).

Great Basin Desert communities occur within basins and on mountains at elevations above 1,500 m (4,920 ft) (O'Farrell and Emery, 1976). These locations are less arid due to lower temperatures and greater precipitation (Beatley, 1976). In comparison to Mojave Desert communities, Great Basin Desert communities tend to have more herbaceous perennials, fewer annuals, and shrub clumps tend to be closer together or absent (Beatley, 1976). These communities are dominated by either *Atriplex* spp. (*A. confertifolia* or *A. canescens* [four-

Undisturbed communities on the NTS are considered climax assemblages (Beatley, 1976). However, steady-state conditions may rarely be observed due to slow vegetative growth and shifting climatic conditions (Hunter, 1992a). A natural succession of plant communities does

become reestablished directly (Beatley, 1976). Some introduced species, however, are associated with disturbed areas and can delay revegetation by native species (O'Farrell and Emery, 1976). These include the winter annual grasses *Brumus rubens* (downy chess) and *B. tectorum* (cheatgrass) and the Russian thistles, *Salsola iberica* and *S. paulsenii* (O'Farrell and Emery, 1976). Populations of these introduced species have apparently been increasing over several decades. Individual plants in Mojave Desert community shrub clumps can be quite old and complete reestablishment of these communities may take centuries (Beatley, 1976). Vasek (1980) reported that *L. tridentata* bushes in the California Mojave Desert had an average age of 32 years and a maximum age of 89 years. On the NTS, individual plants in shrub clumps have been reported to be up to 100 years old and individual clumps have been estimated to persist up to 300 years, based on the rate of accumulation of organic matter (Wallace and Brown, 1979). Mojave Desert *L. tridentata* communities are transitional

[REDACTED]

[REDACTED]

[REDACTED]

[REDACTED]

[REDACTED]

[REDACTED]

[REDACTED]

[REDACTED]

[REDACTED]

Mojave Desert plant communities are characterized by low areal coverage, low standing biomass, low productivity, and high relative biomass turnover (Beatley, 1976; Strojan *et al.*, 1979). Numerous investigators have estimated aboveground plant biomass values for *Larrea* communities, such as those that occur in the vicinity of the Area 5 RWMS (Table 2.12). Estimates of aboveground standing biomass and net annual productivity can be used to estimate the grazing capacity of the land.

Plant biomass is highly correlated with mean annual rainfall (O'Farrell and Emery, 1976), and varies significantly from year to year and with location. Much less is known about belowground biomass, but it has been estimated at approximately 45 percent of aboveground biomass (Wallace *et al.*, 1974).

In absolute terms, net primary productivity is low in these communities, but may be large relative to standing biomass. Romney *et al.* (1977) and Romney and Wallace (1977) have estimated that production is from 1 to 10 percent of standing biomass annually. O'Farrell and Emery (1976) report that most annual production is attributable to winter annuals. Winter annual standing biomass, which represents the production of a single growing season, can vary from 0 to 616 kg ha⁻¹, but a mean value of 90 kg ha⁻¹ has been recorded for the NTS (Beatley, 1969). In contrast, Romney and Wallace (1979) found that perennial shrubs produced the greatest biomass in Rock Valley over a three-year study period. Their estimates of primary productivity as the mean dry weight and one standard deviation were 159 ± 103 kg ha⁻¹ yr⁻¹ for annuals, 407 ± 93 kg ha⁻¹ yr⁻¹ for perennials, and 566 ± 187 kg ha⁻¹ yr⁻¹ total. Over two consecutive years, Bamberg *et al.* (1976) reported aboveground net primary productivity of perennials in Rock Valley to be 125 kg ha⁻¹ and 426 kg ha⁻¹.

Table 2.12 Aboveground Living Dry-Weight Biomass of NTS Plant Communities as Reported By Various Investigators for Frenchman Flat *Larrea* Communities

Source	Community/ Location	Perennials (kg ha ⁻¹)	Annuals (kg ha ⁻¹)	Total (kg ha ⁻¹)
Beatley (1969)	<i>Larrea</i> Frenchman Flat	—	0 - 442 Mean: 66	
Romney <i>et al.</i> (1973)	<i>Larrea</i> Frenchman Flat	113 - 923 Mean: 466	—	
Romney <i>et al.</i> (1977)	<i>Larrea - Ambrosia</i> GMX Site	2,200	—	
Hunter and Medica (1987)	<i>Larrea - Ambrosia</i> Frenchman Flat	2,047 - 4,259 Mean: 3,020	—	
Hunter (1992a)	<i>Larrea - Ambrosia</i> Frenchman Flat	3,491 - 3,527 Mean: 3,509	—	
Hunter (1992b)	<i>Larrea - Ambrosia</i> Frenchman Flat	1,640 - 3,150 Mean: 2,204	—	
Hunter (1992b)	<i>Larrea</i> GMX Site	2,060 - 2,520 Mean: 2,290	—	
EG&G (1982)	<i>Larrea</i> Frenchman Flat	1,375	57	1,432

Larrea tridentata, 64 cm (25 in) for *Ceratoides lanata* (winter fat), 122 cm (48 in) for *Lycium andersonii* (desert thorn), and 97 cm (38 in) for *Grayia spinosa* (Wallace and Romney, 1972). Root systems generally took the form of a large taproot with large secondary roots extending laterally (Wallace and Romney, 1972). Beasley (1960) reported that winter

Vertebrates, although less numerous and diverse, include game and fossorial species. Fish and amphibians are insignificant, due to the lack of permanent surface water. The reptilia include 1 specie of tortoise, 14 species of lizards, and 17 species of snakes (O'Farrell and Emery, 1976). The most abundant species are the lizards *U. stansburiana*, 40 to 80 ha⁻¹; and *C. tigris*, 7 to 25 ha⁻¹ (O'Farrell and Emery, 1976). Overall, reptiles are not believed to be significant to site performance. There are no important game species and only one species is known to burrow, *Gopherus agassizi* (desert tortoise). However, *G. agassizi* occurs only in Mojave Desert environments and is currently very rarely observed.

The avian fauna include at least one fossorial species and many migratory species that may

Table 2.13 Population Density of Rodents and Rabbits in *Larrea* Communities Near the Area 5 RWMS

Species	Population Density (ha ⁻¹)		
	Bradley and Moor, 1975, 1976	Hunter and Medica, 1987	Hunter, 1992a
<i>A. leucurus</i>	0.05 - 0.73	—	—
<i>D. merriami</i>	0 - 1.16	12.6	4.9

Felis concolor (mountain lion), *Lynx rufus* (bobcat), *Odocoileus hemionus* (mule deer), *Antilocapra americana* (pronghorn antelope), and *Ovis canadensis* (desert bighorn sheep). These species are found at the higher elevations of the NTS and are rare transitory visitors to the lower elevations of Frenchman Flat.

Quantitative predictions of the effects of burrowing fauna on site performance are difficult to make due to the lack of relevant data. The quantity of soil transported to the surface is dependent on population density, soil characteristics, and seasonal activity levels. The transport processes are complex. Some species, such as pocket gophers, are reported to selectively transport cobbles and gravels to the surface (Hansen and Morris, 1968; Hankonson *et al.*, 1982). Burrows are frequently reworked and refilled, presumably with both clean and contaminated material, producing a complex mixing of surface soils (Thorne and Andersen, 1990). Burrowing activity is apparently variable in time and with location (Voslamber and Veen, 1985; Thorne and Andersen, 1990).

Burrowing animals may directly affect site performance by burrowing into waste cells and transporting contamination to the surface. Direct intrusion into waste by mammals appears unlikely, as most mammals only burrow to shallow depths. Anderson and Allred (1964) examined 30 kangaroo rat (*Dipodomys microps*) burrows on the NTS. They reported a maximum burrow depth of 61 cm (24 in) and a mean depth of 33 cm (13 in). Burrowing behavior was affected by the texture of the soil (Anderson and Allred, 1964). Winsor and Whicker (1980) found that the pocket gopher (*Thomomys talpoides*) rarely burrows below 30 cm (12 in), and its average burrow depth on their Colorado study site was 13.4 cm (5.3 in). Hankonsen *et al.* (1982) recorded the depths of pocket gopher (*T. bottae*) burrows at a LLW site in northern New Mexico. None of the burrows penetrated below 100 cm (39 in).


Significant numbers of burrowing animals occur within Frenchman Flat and their activities may influence site performance. Direct intrusion into buried waste by vertebrates appears unlikely. Shallow vertebrate burrowing activity may affect site performance by mixing surface soils and by altering cap hydraulic properties and stability. Invertebrate burrowing, although much less studied at the NTS, appears to have the potential for direct intrusion into

sources (NCRP, 1987b). This corresponds to an effective dose equivalent of approximately 300 mrem yr^{-1} , most of which is attributable to inhalation of ^{222}Rn progeny (NCRP, 1987b). Natural sources of radiation exposure include external irradiation from cosmic particles and primordial radionuclides. Exposure to cosmogenic and primordial radionuclides present in air, water, and food are a natural source of internal radiation doses. Man-made sources of radiation are, on average, less important sources of exposure and include, in descending order of importance, medical procedures, consumer products, and industrial sources (NCRP, 1987b). Industrial sources, which include DOE operations among many other sources, and nuclear weapons testing, are estimated to account for approximately 0.8 percent of the average annual effective dose equivalent for United States residents, or approximately 2 mrem (NCRP, 1987b).

The NCRP data presented above is for average United States residents. Current and future residents of the NTS and its environs may be potentially exposed to radionuclides at levels greater than average. Potential sources of exposure in Frenchman Flat, in addition to waste disposal operations, include above- and belowground nuclear weapons tests and safety tests. Between 1951 and 1962, 14 nuclear devices were detonated in the atmosphere over the Frenchman Flat playa. In 1965, three underground nuclear tests were conducted northwest of the playa, approximately 3.5 km (2.2 mi) south of the RWMS (*Figure 2.3*). Two more underground tests were conducted in 1966 and 1968, approximately 2.4 km (1.5 mi) northeast of the RWMS. During 1954 and 1955, several safety tests were conducted at the GMX site, 1.8 km (1.1 mi) southeast of the site. Safety tests involve the destruction of nuclear weapons components and result in the release of radioactive material, most commonly plutonium. In addition, several hundred announced above- and belowground nuclear weapons tests have been conducted in Yucca Flat. Yucca Flat is a north-south trending closed basin, beginning 13 km (7.8 mi) northwest of the RWMS and extending approximately 37 km (23 mi) north. Numerous safety tests have been conducted in Plutonium Valley, a north-south trending valley draining into Yucca Flat. Plutonium Valley lies 11 km (7 mi) north of the RWMS and is separated from Frenchman Flat by French Peak and the Halfpint Range.

Radiological surveys of the surface soils of Frenchman Flat have shown that small localized areas of contamination associated with ground zeros are present on the Frenchman Flat playa and at the GMX site. Most soils of the basin contain concentrations of fallout radionuclides that are consistent with levels expected from global fallout. Barnes *et al.* (1980) surveyed the surface soils of the playa and identified three ground zero areas that were above background: Hamilton, Bfa, and Small Boy. These areas cover approximately 5.7 km^2 (2.2 mi^2) of the Frenchman Flat playa (McArthur, 1991). The radionuclides identified and their maximum contour concentrations, as of 1980, were ^{60}Co (25 pCi g^{-1}), ^{137}Cs (25 pCi g^{-1}), ^{152}Eu (150 pCi g^{-1}), ^{155}Eu (25 pCi g^{-1}), ^{239}Pu (400 pCi g^{-1}), and ^{241}Am (150 pCi g^{-1}) (Barnes *et al.*, 1980). The other area of surface contamination in Frenchman Flat is the GMX site. Gilbert *et al.* (1975) reported $^{239,240}\text{Pu}$ concentrations for soil and vegetation from five regions or strata encompassing 0.12 km^2 (0.046 mi^2) at the GMX ground zero. The mean $^{239,240}\text{Pu}$ concentrations for

soil and vegetation for the highest concentration strata sampled were 7.3 nCi g^{-1} and 0.31 nCi g^{-1} , respectively (Gilbert *et al.*, 1975). McArthur (1991) measured the soil concentration of radionuclides at four sites in Area 5 and estimated the total inventory using *in situ* gamma spectrometry and soil sampling and analysis. The sites (Frenchman Flat playa, GMX, and two underground testing complexes) were chosen based on the results of previous aerial surveys (McArthur, 1991). The Area 5 RWMS and its surrounding soils were not sampled. Inventory results were reported for Frenchman Flat playa and GMX only (Table 2.14). Gilbert's (1975) estimate of the GMX $^{239,240}\text{Pu}$ inventory, 1.5 Ci, is consistent with McArthur's later survey. The inventory of fission products and activation products found at



active RWMS. They reported a mean ^{137}Cs concentration of 0.5 pCi g^{-1} (Atwood and Hertzler, 1989). The results of surface soil surveys indicate that highly localized contamination exists in two regions in Area 5: the GMX site, 1.8 km (1.1 mi) from the RWMS; and Frenchman Flat playa, 3.8 km (2.4 mi) from the RWMS. Surface soils within and adjacent to the RWMS are contaminated at levels expected from global fallout.

Table 2.6 illustrates groundwater monitoring results for the unpermeable aquifer, which

2.9 Area 5 RWMS Facilities Description

The developed portion of the Area 5 RWMS, referred to here as the Low-Level Waste Management Unit (LLWMU), includes 37.2 ha (92 ac) in the southeast corner of the RWMS (Figure 2.37). All waste disposal to date has occurred within the LLWMU. The remaining land, 259 ha (640 ac), remains undeveloped. A mixed waste management unit (MWMU) is planned for the area immediately north of the LLWMU (Figure 2.37). A Mixed Waste Storage Pad (MWSP) is also proposed to be built within the Area 5 RWMS compound at a yet-to-be-selected site.

The LLWMU consists of 17 landfill cells (pits and trenches), 13 GCD boreholes, and a TRU Waste Storage Pad (WSP) (Figure 2.38). A single pit, Pit 3, has received mixed wastes. All other units contain low-level radioactive wastes. Associated with the LLWMU is the Hazardous Waste Storage Unit (HWSU) and several administrative support structures (Figure 2.38). Support buildings include five permanent and nine semipermanent structures (Table 2.15). Three waste storage areas exist within or adjacent to the LLWMU. These are the TRU Waste Storage Pad, the HWSU, and the Mound Strategic Materials Storage Yard (Figure 2.38); however, the waste storage areas are not considered in the performance assessment.

Historically, landfill cells have been described by a four-character code. The first character, either T or P, designates whether the cell is a trench (long, narrow excavation) or a pit (short, broad excavation). The third character is the number assigned to the unit. The final character describes the contents of the cells as unclassified (U) or classified (C).

Low-level radioactive waste disposal was initiated at the Area 5 RWMS in 1961. From 1961 to 1978, LLW generated by NTS operations were disposed at the site by shallow land burial. Eight trenches (T01U, T02U, T04U, T06U, T01C, T03C, T05C, T06C) were filled and closed during this period. Starting in 1978, NTS began accepting LLW generated by off-site DOE facilities. From 1978 until the implementation of DOE Order 5820.2A in 1988, three pits and trenches (P01U, P02U, T07U) were filled and closed.

Ten GCD boreholes were operationally active during this interval (1978 to 1988). Since the implementation of DOE Order 5820.2A on September 26, 1988, six pits and trenches (P03U, P04U, T03U, P06U, T02C, and T04C) and two GCD boreholes have been active. The performance assessment addresses these units only.

Currently, the Area 5 RWMS is open and receiving LLW from the NTS and off-site generators. No mixed waste has been received since 1990, although Pit P03U can accept on-site-generated mixed waste. The Area 5 RWMS does not accept nonradioactive hazardous waste or nonradioactive solid waste for disposal. All hazardous waste generated on site is transferred to an off-site commercial treatment, storage, and disposal facility. Nonradioactive solid wastes are disposed at solid waste landfills not associated with the Area 5 RWMS.

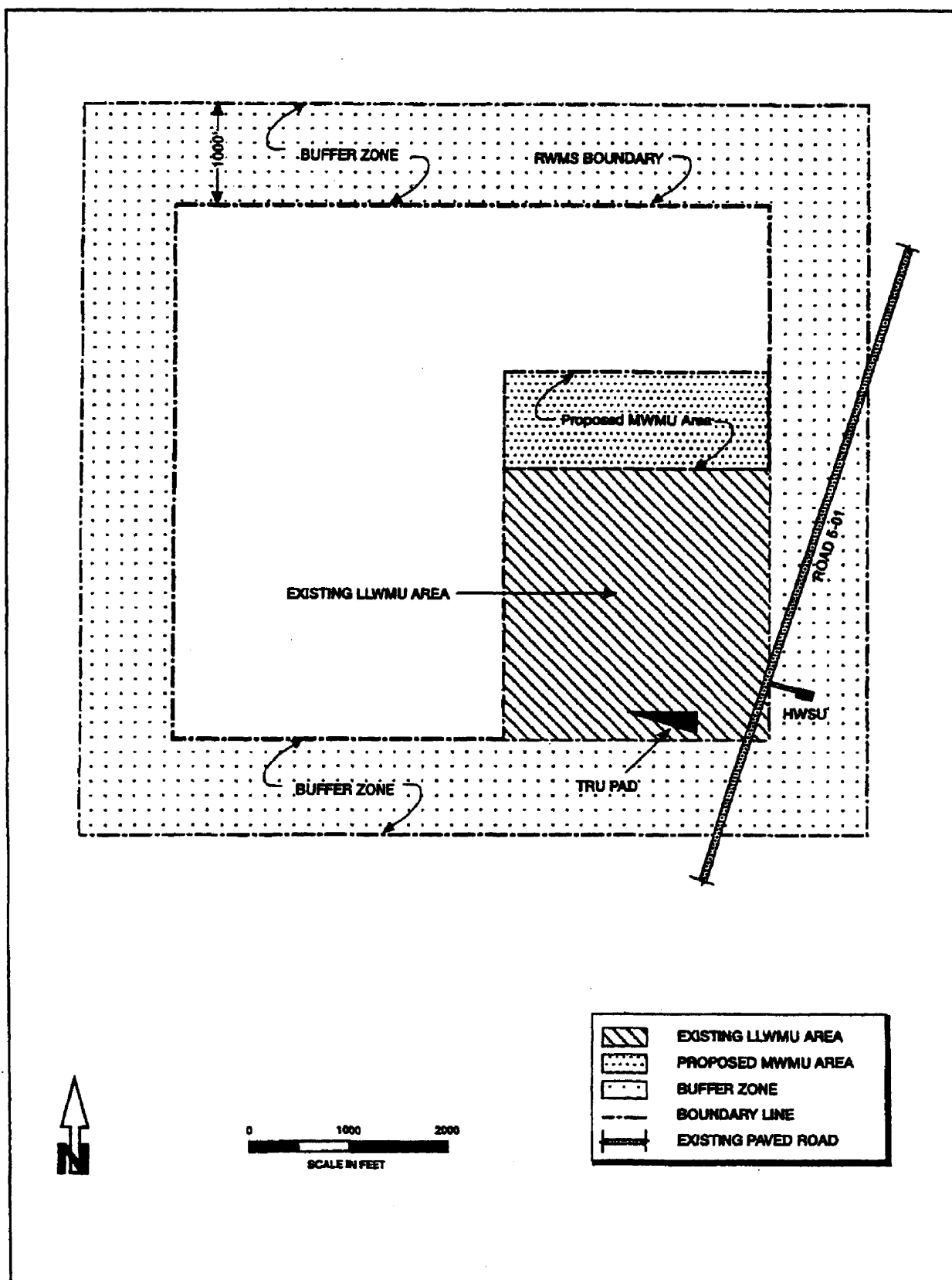


Figure 2.37 Map of the Low-Level Waste Management Unit (LLWMU)

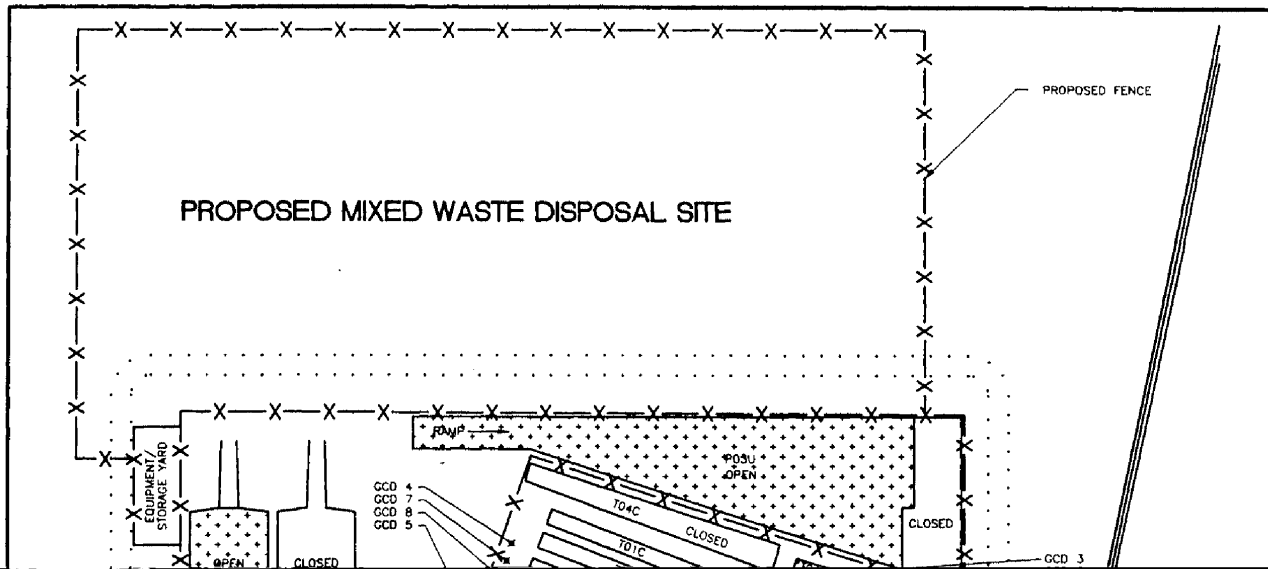


Table 2.15 Existing Support Structures at the Area 5 RWMS and Their Functions

Building No.	Functional Description
5-6	The Special Projects Lab includes the soils test lab, an equipment calibration room, and a core sample storage area.
5-7	Administrative offices.
5-10	Health physics support offices.
5-21	Houses equipment and stores bottled gas and flammable materials (no utilities).
5-19	Part of water system that pumps water to 5-6 and 5-7. System also provides a potable water source for Area 5.
5-18	Used as a craft assembly point and lunch area.
183400	Waiting area for truck drivers (no water or sewer).
178667	Contains sampling pumps and reservoirs for tritium migration tracking by University of California (no water or sewer).
186084	Used to support HWSU operations (no water or sewer).
202616	Contains equipment including an electronic microscope, lab balances, and a sieve shaker (no water or sewer).
202617	Contains scientific equipment (no water or sewer).
183261	Used for storing radiological logistic supplies (no water or sewer).
712240	Provides office space for the HPD supervisor (no water or sewer).
724294	Provides showers and lockers for use by Area 5 RWMS employees.

2.9.1 Shallow Land Burial Operations

LLW is currently landfilled in the Area 5 RWMS in shallow, unlined land disposal trenches and pits. Only two unclassified and two classified pits and trenches have received waste since the implementation of DOE Order 5820.2A (Pit 4 [P04U], Pit 3 [P03U], and Classified Trenches 2 and Trench 4 (T02C and T04C) (*Figure 2.38*). All the pits and trenches active since 1988 remain open and are available to receive waste (Table 2.16). Two cells, Trench 3 (T03U) and Pit 6 (P06U), are open but have not received any waste for permanent disposal. Trench 3 is currently used for storage of special-case thorium waste. This waste will be buried at greater depth to allow attenuation of ^{222}Rn fluxes. Current plans are to place the thorium waste beneath the existing floor of Pit 6 (P06U). Pits and trenches active since 1988 and their approximate volumes are listed in Table 2.17. Pit 4 (P04U) has received the largest volume of waste since 1988 (exclusively LLW). Pit 3 (P03U) has received low volumes of

Table 2.16 **Date of Use and Current Status of Pits and Trenches Receiving Wastes Since the Inception of DOE Order 5820.2A**

Cell Name	Opened	Status
Pit 4 (P04U)	1988	Open, ~80% full
Trench 3 (T03U)	1984	Open, Empty
Pit 6 (P06U)	1990	Open, Empty
Pit 3 (P03U) Trench 2 (T02C)	1987 1988	Open, ~20% Full Closed, Full
Trench 4 (T04C)	1969	Closed, Full

Table 2.17 **Dimensions and Approximate Volume of Pits and Trenches Receiving Waste at the Area 5 RWMS Since the Inception of DOE Order 5820.2A**

Cell Name	Length (m)	Width (m)	Depth (m)	Estimated Total Volume (m ³)
Pit 4 (P04U)	305	61	6.1	9.1×10^4
Trench 3 (T03U)	192	14	4.6	9.1×10^3
Pit 6 (P06U)	192	20	7.4	2.6×10^4

LLW and MW and has been inactive since MW disposal was suspended in 1990. Classified trenches T02C and T04C hold relatively small volumes of LLW and are nearly full at this time. The total area covered by the pits and trenches in the LLWMU is 5.1×10^4 m² or 5.1 ha (12.6 ac) out of the 37.2 ha (92 ac) in the LLWMU. All other pits and trenches indicated in the Area 5 RWMS (*Figure 2.38*) were filled prior to 1988 and are awaiting final closure.

Types of Containers

The waste containers disposed at the site have varied significantly in strength and integrity over time. The available data bases classify the containers as boxes, drums, or nonstandard.

Boxes have been constructed of cardboard, plywood, or steel. The type of box was not differentiated in the records prior to 1992. Between 1978 and 1992, 783,000 boxes were disposed at the site. Cardboard "triwall" boxes were in common use prior to the mid-1980s. These boxes were cardboard containers set on wooden pallets, banded with steel strapping. Contents of these boxes were contained within plastic bags. Cardboard boxes were approximately .6 or 1.2 m (2 or 4 ft) high and were susceptible to crushing if stacked too high. Plywood boxes were delivered in sizes ranging from 2 ft x 4 ft x 8 ft to 4 ft x 8 ft x 8 ft. Wooden pallets or dunnage were used to allow handling with forklifts. Steel boxes are in more general use in the 1990s and are standardized in sizes of 4 ft x 4 ft x 7 ft or 2 ft x 4 ft x 7 ft. Steel feet or forklift slots are typically incorporated into the box design.

Several sizes of drums have been used for disposal at the site, including 55-gallon drums (8 ft³), 83-gallon (13.9 ft³) overpack drums, and large ten-drum overpack containers (jet engine afterburner cases). Between 1978 and 1992, 6 million drums were disposed at the site.

Containers other than standard sized boxes and drums are classified as nonstandard.

Dunnage, blocking, and other packing materials required for delivery and disposal of waste have typically been placed in the excavations with the waste. Typically, both wooden dunnage and blocking and steel strapping material were disposed in the narrow gap between the trench wall and the stacked waste. Any volume above the debris is typically filled with drums, as available.

2.9.1.1 *Mixed Waste Disposal*

Pit 3 is the only shallow land burial unit in the Area 5 RWMS that has received mixed waste. Disposal of low-level (nonhazardous) waste began in Pit 3 in January 1987. Mixed wastes were disposed in Pit 3 for the first time in September 1987, when the state of Nevada granted Pit 3 interim status under RCRA. During its operation as a mixed waste unit, Pit 3 received 4,044 m³ (142,813 ft³) of mixed wastes in a single waste stream. The total volume of waste placed in Pit 3 since 1987 is 26,688 m³ (942,478 ft³). The mixed waste stream placed in Pit 3 was a solid concrete form known as pondcrete generated by the Rocky Flats Plant. At the time of disposal, these wastes were deemed mixed wastes based on the presence of parts per billion (ppb) levels of listed hazardous solvents. The impacts of hazardous constituents in these wastes are not considered in the performance assessment.

DOE is pursuing RCRA permitting of a new mixed waste disposal unit, the Mixed Waste Disposal Unit (MWDU), to be located directly north of the RWMS. The MWDU will be designed and operated to dispose both on-site- and off-site-generated MW. A standard RCRA disposal cell design with liners and leachate collection detection systems has been designed. An alternative design, without liners and utilizing vadose zone monitoring, will be proposed in the revision of the RCRA Part B Permit application. The MWDU was not considered in this performance assessment because of the uncertainty in the final design of the disposal cells. Should mixed waste disposal resume, the planned waste management operations would have to be assessed to determine if this performance assessment is applicable.

2.9.1.2 *Temporary Closure Cap*

Waste containers are typically stacked to about 1.2 m (4 ft) below original grade. Periodically, soil backfill is pushed over the waste in a single lift with a bulldozer. The placed fill layer is approximately 2.4 m (8 ft) thick, which provides a final grade about 1.2 m (4 ft) above original ground elevation. The upper portion of the soil cap is compacted in place. This cover is referred to as a temporary closure cap because the native material is applied routinely over the filled portions of waste disposal cells.

Prior to 1993, general soil fill was placed as backfill. The natural materials at the site contain cobbles up to about 20 cm (8 in) in diameter. Because the spacing between containers is typically much smaller than 20 cm (8 in), bridging of voids is likely. Since 1993, backfill soils have been scalped of material over 5 to 8 cm (2 to 3 in) in diameter to reduce the bridging potential of the soil cover and to promote infilling of the container spacing with soil,

resulting in a reduction of observed subsidence. A bronze plate on top of each corner monument records the cell number, the survey coordinates, and the date the cell was opened and closed. The temporary closure cap will remain until final closure.

Settlement of the temporary closure cap, which is observed periodically, can be attributed to soil infilling the voids between the containers or possible collapse of containers. Photographs from 1982 indicate subsidence is an ongoing process. Observed subsidence has historically varied from shallow depressions, up to 6 m (20 ft) in diameter, to 1.5-m- (5-ft)-deep open cracks. The sources of the depressions have not been specifically identified.

Depressions and cracks, as they form, are filled with soil and regraded by site personnel. The areas or extent of subsidence have not typically been recorded. Presently, areal depressions of about a foot in the soil cover are common over the trench and pit areas.

2.9.2 Greater Confinement Disposal

In 1980, the DOE's National LLW Management Program began reviewing alternatives to shallow land burial of LLW. Although the majority of LLW is routinely and safely disposed using shallow land burial, a portion of the waste was considered unsuitable for shallow land burial because of its high-specific activity or potential for migration into biopathways. In 1981, DOE/NV began a project to demonstrate the feasibility of greater-depth burial in the alluvial sediments of the NTS. The purpose of the project was to investigate the disposal of LLW at a depth sufficient to minimize or to eliminate natural environmental intrusion processes (animal burrowing, rainwater infiltration, plant rooting) into the waste zone. The first unit was experimental and is known as GCD Test or GCDT. The project was also designed to substantially reduce the potential for inadvertent human intrusion.

GCD units are vertical boreholes drilled in the desert alluvium. The boreholes are unlined, except for the upper 3 m (10 ft) which is cased with a corrugated steel culvert. Each is approximately 3 m (10 ft) in diameter, with a total depth of 36 m (118 ft). Waste packages are placed in the bottom of the GCD boreholes to approximately 21 m (70 ft) below the land surface. The holes are then backfilled with native soil. A 1.8-m- (6-ft)-long concrete monument, indicating the location and contents of the borehole, is placed approximately 1.5 m (5 ft) below the surface in each hole. Figure 2.39 shows the design of a GCD borehole. Waste disposed in GCD boreholes includes TRU waste, high-specific activity tritium waste, irradiated fuel rod cladding, and sealed sources. Wastes disposed since the inception of DOE Order 5820.2A contain only ^3H and depleted uranium.

GCD boreholes were used for the disposal of waste from 1983 through 1989. Thirteen GCD boreholes were developed during this period within the LLWMU (*Figure 2.38*). Seven cells have been filled and operationally closed. Three GCD boreholes have received waste and remain open; three GCD cells are empty. Table 2.18 lists the GCD boreholes and their status. GCD boreholes have been designated with sequential numbers and a one-letter code denoting the classification status.

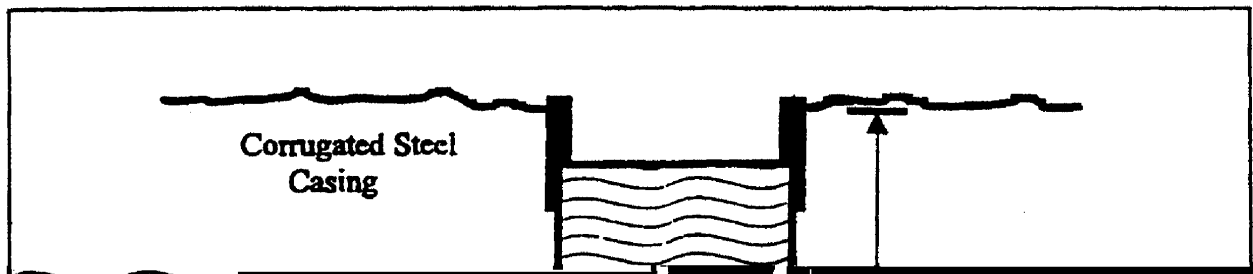


Table 2.18 GCD Boreholes at the Area 5 RWMS

GCD Borehole	Disposal Area	Status
1	Classified	Closed, Full
2	Classified	Closed, Full
3	Classified	Closed, Full
4	Classified	Closed, Full
5	Unclassified	Closed, Full
6	Unclassified	Open, Full
7	Classified	Open, Full
8	Classified	Open, Empty
9	Unclassified	Open, Empty
10	Unclassified	Closed, Full
11	Unclassified	Open, Full
12	Unclassified	Open, Empty
GCDT	Unclassified	Closed, Full

Two GCD boreholes (7C and 10U) have received waste since the implementation of DOE Order 5820.2A. The GCD inventory used in the performance assessment has been limited to those wastes disposed in boreholes 7C and 10U. The GCD program has been inactive since 1989 and is an issue currently being discussed by DOE/NV and the state of Nevada.

2.9.3 Waste Characterization and Certification

Shipment and transfer of LLW to the Area 5 RWMS is controlled by DOE/Headquarters (HQ) and DOE/NV. Generators seeking to dispose waste at the NTS must first obtain written

verification from DOE/HQ that their waste is a defense waste. Approval to ship waste is granted by DOE/NV after the generator documents and implements a waste characterization and waste certification plan that meets the requirements contained in NVO-325 (DOE/NV, 1992). Generator waste characterization plans are designed to physically, chemically, and radiologically characterize waste and to document that waste meets waste acceptance criteria. Waste certification plans are prepared to ensure that waste is identified, segregated, characterized, and packaged in accordance with the requirements of NVO-325, and in a manner that is consistent with the American National Standards Institute/American Society of Mechanical Engineers (ANSI/ASME) NQA-1 requirements (ASME 1990). Successful implementation

technically defensible, and takes into account the different types and forms of previously buried waste and possible future waste. Final cap designs, however, were not available for inclusion in this revision of the performance assessment.

In August 1992, a peer review panel, consisting of experts in cover design and landfill closure, critiqued the Cap Closure Research Program conducted by REEC Co Special Projects Section. As a result of this meeting, a cap closure roadmap was developed by REEC Co, RSN, and MACTEC in December 1992 (RSN *et al.*, 1992). The roadmap served as a basis to develop a program plan outline for integrated closure of the Areas 3 and 5 RWMS waste disposal units.

In June 1993, work was initiated on the Integrated Closure Program. The objectives of this task were to develop site-specific closure designs that use the best available technology, follow relevant regulations, and are commensurate with closure approaches at other DOE facilities. Specifically, the Integrated Closure Program will define closure issues, consider the range of technical closure alternatives, and collect essential technical information to select, design, and construct a site-specific cap at the Areas 3 and 5 RWMSs. The final cap design must be able to function in the arid environment of the NTS and make use of favorable site characteristics such as high evapotranspiration. Closure designs are in preparation at this time.

2.10 Area 5 RWMS Site Inventory

This section describes the radioactive materials inventory for the Area 5 RWMS and the final inventory used for the performance assessment. As noted previously, wastes have been disposed at the NTS Area 5 RWMS since 1961. The inventory described here is limited to those shipments received from FY 1989 to FY 1993. At the time of preparation, FY 1993 was the last year that complete data were available. These data are organized in the database by fiscal year and are also organized throughout this section by fiscal year.

Generators wishing to ship waste to the NTS for disposal must submit an application to DOE/NV for review and approval. Waste generator applications include a description of all required waste streams. Waste stream information submitted in the waste generator appli

site inventory at the time of shipment. These data are transmitted electronically in most instances. Fifteen generators have transferred waste to the Area 5 RWMS since the beginning of FY 1989 (Table 2.19), 11 of which are currently approved (Table 2.20).

~~T.U. 21A C~~

Table 2.21 Summary of Data Fields for Pre-FY 1992 Database Records

Record Indexed by Shipment Number	
Shipment Number	
Generator Identification Code	
Date of Arrival at the RWMS	
Burial Site (Area 3 or 5)	
Site of Generation (NTS, Off Site)	
Operation Type (B-burial, G-generation, R-retrievable)	
External Volume (includes package dimensions)	
Gross Weight (includes weight of package and waste)	
Nuclide	
Nuclide Activity (Ci)	
Waste Code	(Biological Waste, Contaminated Equipment, Decontamination Debris, Dry Solid, Solidified Sludge, Nonclassified)
Nuclide Category	(Transuranic, Uranium/Thorium, Fission Products, Induced Activity, Tritium, Alpha, Other)
Number of Drums in the Shipment	
Number of Boxes in the Shipment	
Number of Nonstandard Boxes in the Shipment	
Record Indexed by Package Number	
Package Identification Code	
Disposal Date	
Container Type (B - box, D - drum, N - nonstandard)	
Disposal Location	
Alpha (identifies the alpha coordinate for the package)	
Numeric (identifies the numeric coordinate for the package)	
Tier (identifies the tier level of disposal)	

After September 30, 1992, a new database, known as the LLW Information System (LLWIS), became operational. Data in the LLWIS are stored in a single record, indexed by package. LLWIS data fields are listed in Table 2.22.

The inventory used in the performance assessment is based on queries of the existing waste management databases. Because important data fields in the pre-FY 1992 database (activity

Table 2.22 Summary of Data Fields for Post-FY 1992 Database Records

Package Identification Code (8 characters, shipment number plus a 6 character package no.)
Waste Stream Identification Code
Arrival Date
Burial Site (Area 5 or Area 3)
Generation Site (NTS, Off Site)
Operation Type (B-burial, G-generation, R-retrievable)
Package Completed Date
Activity Assay Date
Container Code (identifies the type of the waste package)
External Volume (m ³)
Internal Volume (m ³)
Gross Weight (kg)
Net Weight (kg)
Nuclide
Nuclide Activity
Waste Code
Nuclide Category
Disposal Date
Disposal Location

Generator waste characterization methods and reporting methods have caused additional problems with database records. In some instances, generators have used codes for radio-nuclide mixtures. Codes used previously include MFP (mixed fission products), Pu-52 (weapons-grade plutonium), D-238 (depleted uranium), and enriched uranium. Mixture codes found in the database have been replaced with the activities of specific isotopes for the performance assessment. The details of these corrections are described below. In addition, review of the inventory suggests that characterization data are incomplete. For example, the isotope ratios reported by some generators are inconsistent with expected values, suggesting that possibly important isotopes were not reported. These data must be evaluated on a per-generator basis or even a per-waste stream basis because of the many processes represented by NTS generators. These issues and their resolutions are also described below.

2.10.1 Preliminary Inventory

A preliminary inventory was developed based on unrevised database records. This inventory includes all waste disposed from October 1, 1988, through September 30, 1993. It includes

Table 2.23 DOE Facilities Identified as Potential NTS Generators

Kansas City Plant, Kansas City, MO, Allied Signal
 Mound Facility, Miamisburg, OH, EG&G Mound Applied Technologies
 Pinellas Plant, Pinellas Co., FL
 Rocketdyne Division, Canoga Park, CA, Rockwell
 Sandia National Laboratory, Albuquerque, NM
 Battelle Memorial Institute, Columbus, OH
 Idaho National Engineering Laboratory, Idaho Falls, ID
 Johnston Atoll, Defense Nuclear Agency
 Los Alamos National Laboratory, Los Alamos, NM
 Paducah Gaseous Diffusion Plant, Paducah, KY, Martin Marietta Energy Systems
 Portsmouth Gaseous Diffusion Plant, Portsmouth, OH, Martin Marietta Energy Systems
 Oak Ridge Reservation, Oak Ridge, TN
 U.S. Army Defense Consolidation Facility

The total activity of unclassified low-level and mixed wastes disposed by shallow land burial are listed by fiscal year in Table 2.24. The unclassified shallow land burial inventory represents over 60 percent of the total activity and accounts for nearly all of the activity of many radionuclides. The classified shallow land burial inventory is presented in Table 2.25. In comparison, the classified wastes disposed of by shallow land burial account for only 1.2 percent of the site inventory and are limited to ^3H , ^{60}Co , ^{90}Sr and ^{238}U . Classified and unclassified GCD boreholes received waste in FY 1989 and FY 1990. Only two radionuclides were reported, ^3H and ^{238}U . However, the GCD ^3H disposal was a significant fraction (37 percent) of the total site inventory. The GCD inventory is presented in Table 2.26.

Table 2.24 Unrevised Unclassified Shallow Land Burial Radionuclide Inventory in Curies for FY 1989 through FY 1993

Radionuclide	FY89	FY90	FY91	FY92	FY93	Total (Ci)
^{227}Ac	0.018	1.0×10^{-7}				0.018
$^{110\text{m}}\text{Ag}$					1.2×10^{-4}	1.2×10^{-4}
^{241}Am	0.024	0.0064		6.0×10^{-4}	7.5×10^{-4}	0.032
^{243}Am	1.1×10^{-4}	2.0×10^{-8}			1.0×10^{-11}	1.1×10^{-4}
^{133}Ba					5.3×10^{-5}	5.3×10^{-5}
^{140}Ba		2.0×10^{-5}			0.0045	0.0045
^7Be					1.1×10^{-6}	1.1×10^{-6}
^{207}Bi					2.0×10^{-9}	2.0×10^{-9}
^{14}C	0.13	0.0060		0.018	0.22	0.53
^{141}Ce		5.3×10^{-4}			0.014	0.014
^{144}Ce	0.0061	0.0043		0.0010	0.0099	0.022
^{252}Cf	1.1×10^{-5}					1.1×10^{-5}

Table 2.24 (continued)

Radionuclide	FY89	FY90	FY91	FY92	FY93	Total (Ci)
³⁶ Cl					2.0×10^{-8}	2.0×10^{-8}
²⁴² Cm		2.0×10^{-8}				2.0×10^{-8}
²⁴³ Cm	5.0×10^{-4}					5.0×10^{-4}
²⁴⁴ Cm	3.0×10^{-4}	4.3×10^{-7}		0.15	3.8×10^{-4}	0.15
⁵⁷ Co				0.0015	0.0027	0.0043
⁵⁸ Co	1.0×10^{-5}				0.023	0.024
⁶⁰ Co	0.011	0.066			9.0×10^{-4}	0.078
⁵¹ Cr					0.97	0.97
¹³⁴ Cs		0.012		0.15	0.13	0.29
¹³⁶ Cs	2.4×10^{-4}					2.4×10^{-4}
¹³⁷ Cs	0.19	0.19		0.42	0.020	0.82
¹⁵² Eu		2.0×10^{-8}				2.0×10^{-8}
¹⁵⁴ Eu		0.0032				0.0032
¹⁵⁵ Eu		2.3×10^{-10}				2.3×10^{-10}
⁵⁵ Fe	9.0×10^{-6}					9.0×10^{-6}
⁵⁹ Fe		9.5×10^{-6}			0.040	0.040
⁶⁷ Ga				5.0×10^{-5}	2.0×10^{-9}	5.0×10^{-5}
³ H	1.7×10^4	1.7×10^4		1.4	2.8×10^4	6.2×10^4
¹²⁵ I					6.0×10^{-4}	6.0×10^{-4}
¹³¹ I					0.0050	0.0050
¹³³ I					0.0097	0.0097
⁸⁵ Kr		9.0×10^{-5}			0.0081	0.0082
¹⁴⁰ La					0.0045	0.0045
MFP	0.15	0.079				0.23
⁵⁴ Mn		2.1×10^{-4}			0.030	0.030
²² Na	0.050	1.0×10^{-5}			2.8×10^{-6}	0.050
⁹⁵ Nb		7.9×10^{-4}			0.020	0.021
⁵⁹ Ni	3.0×10^{-6}					3.0×10^{-6}
⁶³ Ni	1.8×10^{-4}			0.51	0.038	0.54
²³⁷ Np	0.0010					0.0010
³² P	0.081	0.011			0.0039	0.096
²³¹ Pa		0.0063				0.0063
²¹⁰ Po	1.0×10^{-6}					1.0×10^{-6}
¹⁴⁷ Pm	1.0×10^{-5}			1.0	0.0041	1.0
²¹⁰ Pb	1.0×10^{-6}	2.5×10^{-4}			8.6×10^{-4}	0.0011
²³⁶ Pu					2.0×10^{-12}	2.0×10^{-12}

Table 2.24 (continued)

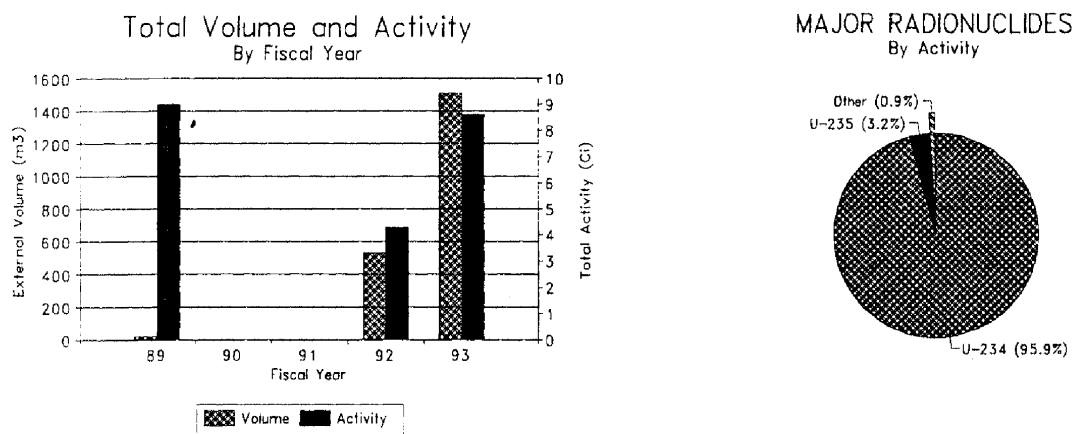
Radionuclide	FY89	FY90	FY91	FY92	FY93	Total (Ci)
²⁴² Pu	1.1×10^{-5}	4.8×10^{-7}		5.7×10^{-7}	2.6×10^{-6}	1.5×10^{-5}
⁵² Pu	33	75				1.1×10^2
²²⁴ Ra					2.4×10^{-6}	2.4×10^{-6}
²²⁶ Ra	0.0099	5.3×10^{-4}			7.0×10^{-4}	0.011
²²⁰ Rn					1.2×10^{-8}	1.2×10^{-8}
²²² Rn					1.0×10^{-9}	1.0×10^{-9}
¹⁰³ Ru		8.7×10^{-4}			0.0079	0.0087
¹⁰⁶ Ru		4.5×10^{-5}			0.0033	0.0034
³⁵ S	0.0034	1.0×10^{-6}			0.13	0.13
¹²⁴ Sb		1.8×10^{-4}				1.8×10^{-4}
¹²⁵ Sb		5.2×10^{-5}				5.2×10^{-5}
⁴⁶ Sc				5.0×10^{-5}	6.4×10^{-5}	1.1×10^{-4}
⁸⁵ Sr				0.11	0.13	0.24
⁹⁰ Sr	0.076	0.27		0.43	0.022	0.80
¹⁸² Ta					0.021	0.021
⁹⁹ Tc					3.4×10^{-8}	3.4×10^{-8}
²²⁸ Th	1.0×10^{-6}	0.0027		31	0.0051	31
²³⁰ Th		0.0016		5.0	0.050	5.1
²³² Th	9.8×10^{-4}	0.011		31	0.19	32
²³² U					0.015	0.015
²³³ U	6.1×10^{-5}	1.0×10^{-4}			2.6×10^{-6}	1.6×10^{-4}
²³⁴ U	2.0×10^{-8}	0.0040	0.0076	0.60	20	21
²³⁵ U	0.54	0.011	9.1×10^{-4}	0.16	1.3	2.0
²³⁸ U	8.4	0.61	0.028	0.63	16	26
⁹⁰ Y	0.0019					0.0019
¹⁶⁹ Yb					0.033	0.033
⁶⁵ Zn	1.0×10^{-5}				0.0033	0.0033
⁹⁵ Zr		5.6×10^{-4}			0.017	0.018
Total	1.7×10^4	1.7×10^4	0.037	77	2.9×10^4	6.2×10^4

Table 2.25 Unrevised Classified Shallow Land Burial Radionuclide Inventory in Curies for FY 1989 through FY 1993

Radionuclide	FY89	FY90	FY91	FY92	FY93	Total
^3H		36		1.0	1.1×10^3	1.1×10^3
^{60}Co		0.060				0.060
^{85}Kr		9.0×10^{-5}			0.0010	0.0011
^{90}Sr		0.12				0.12
^{210}Po					0.0020	0.0020

Generator Profile: General Atomics		
	Total Disposed by Generator FY89 to FY93	Total Disposed as a Percent of Total Site Inventory
Volume (m ³)	2,059	4.4 %
Activity (Ci)	21.9	0.02 %
Major Nuclides in the Generator's Waste Stream		
²³⁴ U	21 Ci	30.6 %
²³⁵ U	0.69 Ci	17.8 %

Figure 2.40 General Atomics Waste Stream Profile for FY 1989 through FY 1993



Generator Profile: Inhalation Toxicology Research Institute		
	Total Disposed by Generator FY89 to FY93	Total Disposed as a Percent of Total Site Inventory
Volume (m ³)	467	0.99 %
Activity (Ci)	2.86	0.003 %
Major Nuclides in the Generator's Waste Stream		
³ H	0.58 Ci	6 × 10 ⁻⁴ %
¹³⁷ Cs	0.56 Ci	56.5 %
⁶³ Ni	0.54 Ci	99.7 %
¹⁴ C	0.53 Ci	99.6 %
⁹⁰ Sr	0.45 Ci	46.9 %
²⁴⁴ Cm	0.15 Ci	99.8 %
Nuclides Contributing Significantly to the Total Site Inventory		
²³² U	0.015 Ci	100 %
²⁴³ Cm	0.0005 Ci	100 %
²⁴³ Am	0.0001 Ci	90.9 %
²²⁶ Ra	0.0068 Ci	61.8 %
³⁶ Cl	2.0 × 10 ⁻⁸ Ci	100 %
²⁰⁷ Pb	2.0 × 10 ⁻⁹ Ci	100 %
¹³³ Ba	5.3 × 10 ⁻⁵ Ci	100 %

Figure 2.41 Inhalation Toxicology Research Institute Waste Stream Profile for FY 1989 through FY 1993



Generator Profile: Lawrence Livermore National Laboratory		
	Total Disposed by Generator FY89 to FY93	Total Disposed as a Percent of Total Site Inventory
Volume (m ³)	951	2.0 %
Activity (Ci)	46,938	46.3 %
Major Nuclides in the Generator's Waste Stream		
³ H	46,933 Ci	46.4 %
Nuclides Contributing Significantly to the Total Site Inventory		
⁵⁹ Ni	3×10 ⁻⁶ Ci	100 %
⁹⁰ Sr	0.21 Ci	22.0 %
⁹³ Zr	4×10 ⁻⁶ Ci	76.8 %
⁹⁹ Tc	5×10 ⁻⁵ Ci	75.5 %
¹⁰⁷ Pd	1×10 ⁻⁶ Ci	74.0 %
¹²⁶ Sn	1×10 ⁻⁶ Ci	76.1 %
¹²⁹ I	3×10 ⁻⁷ Ci	76.7 %
¹³⁵ Cs	5×10 ⁻⁶ Ci	77.7 %

Generator Profile: Pantex		
	Total Disposed by Generator FY89 to FY93	Total Disposed as a Percent of Total Site Inventory

Volume (m³)

469

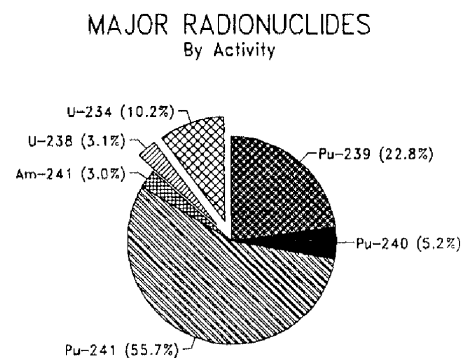
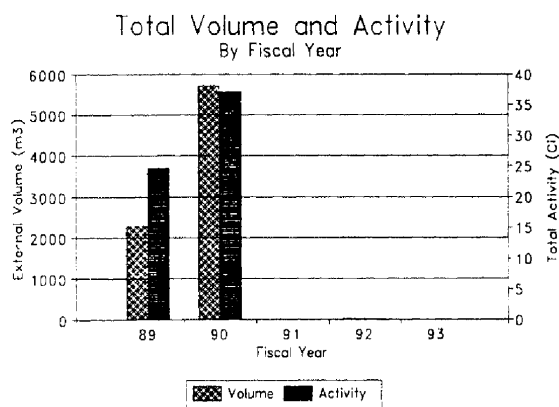
1.0 %

Major Nuclides in the Generator's Waste Stream

Figure 2.43 Pantex Waste Stream Profile for FY 1989 through FY 1993

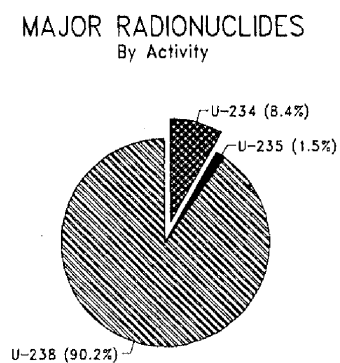
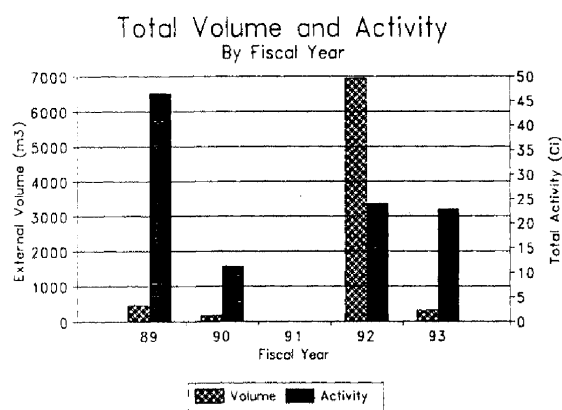
Generator Profile: Rocky Flats Plant		
	Total Disposed by Generator FY89 to FY93	Total Disposed as a Percent of Total Site Inventory
Volume (m ³)	8,018	17.0 %
Activity (Ci)	61.9	0.06 %
Major Nuclides in the Generator's Waste Stream		
²³⁴ U	6.3 Ci	9.1 %
²³⁸ U	1.9 Ci	1.5 %
²³⁹ Pu	14.0 Ci	92.0 %
²⁴⁰ Pu	3.2 Ci	99.6 %
²⁴¹ Pu	34.1 Ci	97.1 %
²⁴¹ Am	1.8 Ci	98.3 %
Nuclides Contributing Significantly to the Total Site Inventory		
²⁴² Pu	3×10 ⁻⁴ Ci	91.7 %

Figure 2.44 Rocky Flats Plant Waste Stream Profile for FY 1989 through FY 1993



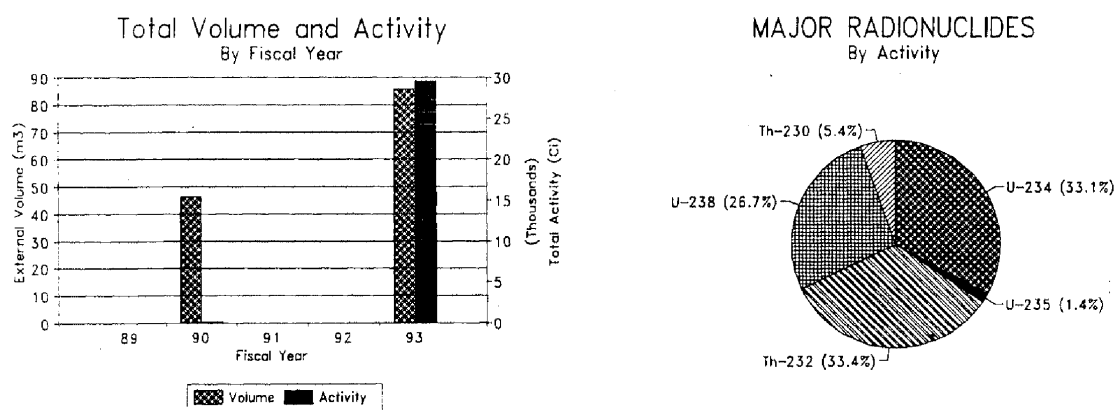
Generator Profile: Aberdeen Proving Grounds		
	Total Disposed by Generator FY89 to FY93	Total Disposed as a Percent of Total Site Inventory
Volume (m ³)	1,266	2.7 %
Activity (Ci)	105	0.1 %
Major Nuclides in the Generator's Waste Stream		
²³⁴ U	8.7 Ci	12.7 %
²³⁵ U	1.5 Ci	39.1 %
²³⁸ U	94 Ci	72.7 %

Figure 2.45 Aberdeen Proving Grounds Waste Stream Profile for FY 1989 through FY 1993



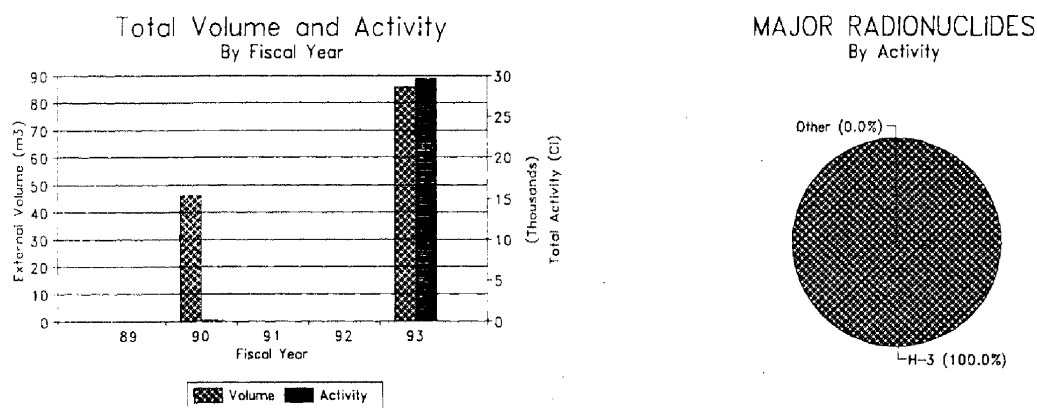
Generator Profile: Fernald Environmental Restoration Management Company		
	Total Disposed by Generator FY89 to FY93	Total Disposed as a Percent of Total Site Inventory
Volume (m ³)	23,393	49.6 %
Activity (Ci)	94	0.09 %
Major Nuclides in the Generator's Waste Stream		
²³⁰ Th	2.8 Ci	99.7 %
²³⁴ U	31 Ci	45.3 %
²³⁵ U	1.3 Ci	33.2 %
²³⁸ U	25 Ci	19.3 %
²³² Th	18 Ci	99.5 %

Figure 2.46 Fernald Environmental Restoration Management Company Waste Stream Profile for FY 1989 through FY 1993



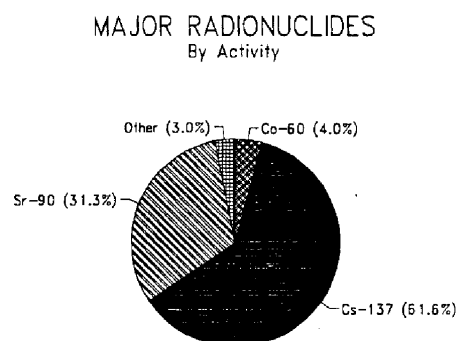
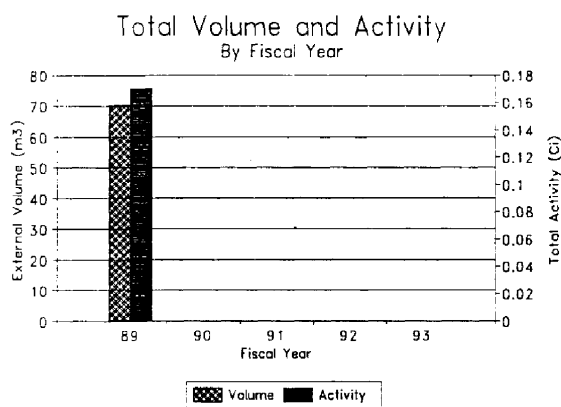
Generator Profile: Sandia National Laboratories, California		
	Total Disposed by Generator FY89 to FY93	Total Disposed as a Percent of Total Site Inventory
Volume (m ³)	132	0.3 %
Activity (Ci)	29,652	29.3 %
Major Nuclides in the Generator's Waste Stream		
³ H	29,650 Ci	29.3 %
Nuclides Contributing Significantly to the Total Site Inventory		
⁶⁰ Co	0.12 Ci	86.7 %
⁹⁰ Sr	0.24 Ci	24.7 %

Figure 2.47 Sandia National Laboratories Waste Stream Profile for FY 1989 through FY 1993



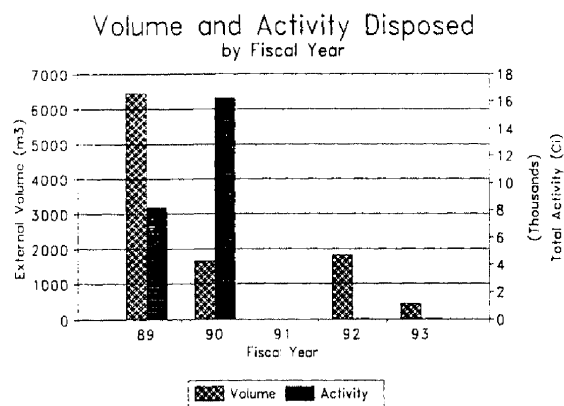
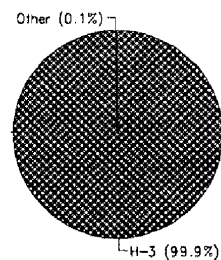
Generator Profile: Rocketdyne Division, Rockwell		
	Total Disposed by Generator FY89 to FY93	Total Disposed as a Percent of Total Site Inventory
Volume (m ³)	70	0.15 %
Activity (Ci)	0.17	2×10 ⁻⁴ %
Major Nuclides in the Generator's Waste Stream		
¹³⁷ Cs	0.10 Ci	10.6 %
⁹⁰ Sr	0.053 Ci	5.5 %
⁶⁰ Co	0.007 Ci	4.9 %

Figure 2.48 Rocketdyne Waste Stream Profile for FY 1989 through FY 1993



Generator Profile: Mound Facility		
	Total Disposed by Generator FY89 to FY93	Total Disposed as a Percent of Total Site Inventory
Volume (m ³)	10271	21.7 %
Activity (Ci)	2.4×10^4	24.1 %
Major Nuclides in the Generator's Waste Stream		
³ H	6.3×10^4 Ci	24.1 %
Nuclides Contributing Significantly to the Total Site Inventory		
²³⁸ Pu	18 Ci	98.0 %
²²⁶ Ra	0.004 Ci	33.4 %
²³³ U	1.6×10^{-4} Ci	61.0 %

Figure 2.49 Mound Waste Stream Profile for FY 1989 through FY 1993

MAJOR RADIONUCLIDES
By Activity

production cycle are represented among NTS generators, with the exception of fuel reprocessing. NTS generators handle a small number of relatively pure isotopes used in nuclear weapons. The predominant nuclides are ^3H and isotopes of uranium, thorium, and plutonium. Waste streams containing actinides are the most important in terms of volume and ^3H waste streams are most important in terms of activity (Table 2.27). Several NTS generators are research laboratories that generate waste streams with numerous radionuclides. These waste streams, however, tend to have radionuclide sources that are well characterized, isotopically pure, and low in activity concentration. Table 2.28 shows a breakdown of the inventory by radionuclide categories as reported by generators. According to generators' reports, only 3×10^{-4} percent of the total activity shipped was associated with mixed fission product waste streams. Based on inventory records, ^{90}Sr and ^{137}Cs account for approximately 0.002 percent of the total activity, or slightly less than 2 Ci. Waste streams containing fission products and activation products originate predominantly from research laboratories at LLNL (Figure 2.42), the Inhalation and Toxicology Research Institute (Figure 2.41), and SNL (Figure 2.47). Fission products and activation products in these waste streams are predominantly from isotopically pure sources. Less than 1 Ci of the total ^{90}Sr and ^{137}Cs activity is suspected to be associated with mixed fission products. Generators producing waste streams with mixed fission products are LLNL-CA, Rocketdyne, and NTS-based generators.

From FY 1989 through FY 1993, the Area 5 RWMS received 47,200 m³ (1,666,852 ft³) of waste. Approximately 93 percent of the volume was associated with actinide-bearing waste streams (Table 2.27). Waste streams received over this period are predominantly (61 percent) heterogeneous mixtures of contaminated debris and equipment (Table 2.28). These waste streams include such materials as laboratory equipment, industrial equipment, building materials, soil, personal protective equipment, furniture, weapons components, and spent radionuclide containers or generators (e.g., gas cylinders, ion exchange resins, adsorption beds).

2.10.2 Inventory Revisions

The raw inventory records, as summarized in Tables 2.24, 2.25, and 2.26, were revised before being used in the performance assessment. First, all nuclides with half-lives less than five years that decay to a stable progeny were deleted from the inventory. These nuclides will decay to negligible levels during the 100-year period of institutional control. The nuclides appearing on the inventory that were deleted for this reason include ^7Be , ^{22}Na , ^{32}P , ^{35}S , ^{46}Sc , ^{51}Cr , ^{54}Mn , ^{55}Fe , ^{57}Co , ^{58}Co , ^{59}Fe , ^{65}Zn , ^{67}Ga , ^{85}Sr , ^{90}Y , ^{95}Nb , ^{95}Zr , ^{103}Ru , ^{106}Ru , $^{110\text{m}}\text{Ag}$, ^{124}Sb , ^{125}Sb , ^{125}I , ^{131}I , ^{133}I , ^{134}Cs , ^{136}Cs , ^{141}Ce , ^{140}Ba , ^{140}La , ^{144}Ce , ^{155}Eu , ^{169}Yb , and ^{182}Ta . Next, any members of a serial decay chain with a half-life less than five years and a supporting parent present with a half-life greater than five years were deleted. These nuclides will reach secular or transient equilibrium during the 100-year period of institutional control. These nuclides included ^{210}Po , ^{224}Ra , ^{220}Rn , ^{222}Rn , and ^{228}Th . Finally, unsupported members of a serial decay chain with a half-life less than five years and with a progeny that has a much longer half-life were converted to the progeny by multiplying with λ_d/λ_p , where λ_p is the parent's decay constant and λ_d is the progeny's decay constant. These nuclides included ^{147}Pm , ^{236}Pu , ^{242}Cm ,

Nuclide Category and Waste Code of Unclassified and Classified LLW Disposed at the Area 5 RWMS

Uranium/ Thorium	Fission Products	Induced Activity	Tritium	Alpha	Other	Total
26,900	143	5.68	2,400	17,100	604	47,200
57.1	0.3	0.012	5.1	36.2	1.3	
234	0.275	0.0815	100,300	749	9.62	101,290
0.2	3×10^{-5}	8×10^{-5}	99	0.7	0.009	

Waste Code of Unclassified and Classified LLW Disposed at the Area 5 RWMS from FY 1989 to

Contaminated Equipment	Decontamination Debris	Dry Solid	Solidified Sludge	Other	Total
3,500	25,000	17,200	796	687	47,200
7.4	53.7	36.5	1.7	0.65	

and ^{252}Cf . Note that the corrections described above were made to develop an isotopic

Table 2.30 Estimated Activity of Plutonium Isotopes and ^{241}Am From An Initial Pu-52 Activity of 107.4 Ci After 20 Years of Decay

Radionuclide	Half-Life (yr)	Pu-52 Weight Fraction† (at t=0)	Specific Activity (Ci g ⁻¹)	Activity from 107.4 Ci of Pu-52 (Ci) (at t=20 yr)	Mean Disposal Rate from FY89 to FY93 (Ci yr ⁻¹)
^{238}Pu	87.75	1.00×10^{-4}	17.1	0.35	0.071
^{239}Pu	24,131	9.38×10^{-1}	6.19×10^{-2}	14	2.8
^{240}Pu	6,569	5.80×10^{-2}	0.227	3.2	0.64
^{241}Pu	14.4	3.60×10^{-3}	103	34	6.8
^{242}Pu	3.76×10^5	3.00×10^{-4}	3.93×10^{-3}	2.8×10^{-4}	5.7×10^{-5}
^{241}Am	432.2	Assumed = 0		1.8	0.36

† - From DOE, 1980

because the majority of processed liquid waste was placed in the evaporation ponds from 1956 to 1985. The final isotopic composition assumed was that of weapons-grade plutonium after 20 years of decay and ingrowth. The activity of plutonium isotopes present in the disposed Pu-52 was calculated as:

$$A_i = \frac{A_{52} f_i SA_i e^{-\lambda_i t}}{SA_{52}} \quad (2.11)$$

where:

- A_i = activity of the ith plutonium isotope,
- A_{52} = activity of Pu-52,
- f_i = Pu-52 weight fraction (at t=0) of the ith plutonium isotope,
- SA_i = specific activity of ith plutonium isotope,
- SA_{52} = specific activity of Pu-52,
- λ_i = decay constant of ith plutonium isotope, and
- t = elapsed time between production and disposal (20 years).

† - The Pu-52 weight fraction was assumed to be 107.4 Ci as reported on the site inventory.

Estimating the ^{241}Am activity is more problematic. Assuming that ^{241}Am follows Pu through the site processes to the evaporation ponds, the ^{241}Am can be estimated by assuming an initial activity of zero and allowing for 20 years of ingrowth. By this method the activity of ^{241}Am is calculated as:

$$A_2 = \frac{A_{52} f SA \lambda_2}{SA_{52} (\lambda_2 - \lambda_1)} (e^{-\lambda_1 t} - e^{-\lambda_2 t}) \quad (2.12)$$

where:

- A_2 = activity of ^{241}Am ,
- A_{52} = activity of Pu-52,
- f = Pu-52 weight fraction of ^{241}Pu at $t=0$,
- SA = specific activity of ^{241}Pu ,
- SA_{52} = specific activity of Pu-52,
- λ_1 = decay constant of ^{241}Pu ,
- λ_2 = decay constant of ^{241}Am , and
- t = elapsed time between last separation and disposal (20 years).

This method yields an ^{241}Am estimate of 1.81 Ci. Overall, the isotopic ratios estimated above for Pu-52 are in reasonable agreement with the ratios reported by the RFP for shipments delivered in FY 1992, the only year that the RFP reported the activities of specific isotopes.

The isotope code MFP was used by three generators in FY 1989 and FY 1990 (Table 2.31). MFP was used to identify mixed fission products. LLNL generated 95.7 percent of the total activity of MFP (0.231 Ci). LLNL reported that the waste stream contained fission products from fast neutron fission of ^{239}Pu during nuclear weapons tests. Although the other two waste streams are minor sources, they too are believed to originate from nuclear testing.

Table 2.31 Generators Using the MFP Code and the Activity Disposed at the Area 5 RWMS

Fiscal Year	Generator	Activity (Ci)
1989	Lawrence Livermore National Laboratory, Livermore, CA	0.14
	EPA Environmental Monitoring Systems Lab, Las Vegas, NV	0.010
1990	Lawrence Livermore National Laboratory, Livermore, CA	0.079
	Reynolds Electrical & Engineering Co., NTS, Mercury, NV	1×10^{-6}

Several simplifying assumptions were made to convert MFP activities to isotopic activities. First, the total MFP activity was assumed to be attributable to a suite of long-lived fission products (Table 2.32). All the precursor fission products in the isobar were assumed to be present as the longest-lived radioactive member of the chain. Decay after the fission event was neglected, given the long half-life of the nuclides considered. Fission yields (the number atoms produced per fission) for fission of ^{239}Pu by unmoderated fission neutrons were taken from Fleming (1967). The cumulative fission yields are summed individual yields beginning with the long-lived member of the chain and including all preceding members. The values used are presented in Table 2.32. The likely presence of activation products was ignored due to the complexities of estimating their activity and the relatively small contribution of MFP activity to the total fission product and activation product inventory. Chemical fractionation was also ignored.

Table 2.32 Estimated Disposal of Fission Products from Waste Streams Using the MFP Code

Radionuclide	Half-life (yr)	Cumulative Yield From Fission of ^{239}Pu	Activity of Fission Products for 0.231 Ci of MFP (Ci)	Mean Annual Disposal Rate (Ci yr ⁻¹)
^{79}Se	6.5×10^4	6.55×10^{-4}	7.5×10^{-7}	1.5×10^{-7}
^{87}Rb	4.7×10^{10}	0.0212	3.3×10^{-11}	6.7×10^{-12}
^{90}Sr	28.6	0.0214	0.055	0.011
^{93}Zr	1.5×10^6	0.0333	1.6×10^{-6}	3.2×10^{-7}
^{99}Tc	2.1×10^5	0.0610	2.1×10^{-5}	4.2×10^{-6}
^{107}Pd	6.5×10^6	0.0395	4.5×10^{-7}	9.0×10^{-8}
^{126}Sn	1.0×10^5	7.51×10^{-4}	5.6×10^{-7}	1.1×10^{-7}
^{129}I	1.6×10^7	0.0298	1.4×10^{-7}	2.8×10^{-8}
^{135}Cs	2.3×10^6	0.0656	2.1×10^{-6}	4.2×10^{-7}
^{137}Cs	30.17	0.0679	0.17	0.034
^{151}Sm	90	0.0088	0.0072	0.0014

The activity of fission products in MFP was calculated as:

$$A_i = A_T \frac{\lambda_i Y_i}{\sum_{j=1}^n \lambda_j Y_j} \quad (2.13)$$

where:

- A_i = activity of the i th fission product,
- A_T = total MFP activity,
- λ_i = radioactive decay constant of i th fission product,
- Y_i = cumulative fission yield of i th fission isobar, and
- n = number of fission chains.

Estimated activities of fission products in MFP shipments received since FY 1988 are presented in *Table 2.32*. In relative terms, the activity from MFP shipments represents a significant fraction of the total fission product inventory. However, the total fission product inventory at the Area 5 RWMS is small and, in absolute terms, the total activity from MFP is insignificant. The significance of the fission product revisions can be assessed by examining the estimated total inventories. The final site fission product inventory can be estimated as the mean disposal rate times the period of operation, 39 years. For two fission products, ^{79}Se and ^{87}Rb , the predicted total inventory is less than the activity that would deliver a CEDE of 25 mrem if the entire inventory were inhaled or ingested by an individual. For this reason, these two nuclides were not added to the inventory. The remaining radionuclides were included in the final inventory and represented minor revisions to the inventory.

It is difficult to measure the quantity of low-specific activity fission products with low-energy radiations such as ^{99}Tc and ^{129}I in heterogeneous wastes. Therefore, it was hypothesized that such nuclides may be present in certain waste streams, but not reported on manifests. The activity of ^{99}Tc reported on the inventory is extremely small and is

Table 2.33 Major Generators of ^{90}Sr and ^{137}Cs and the Source of Radionuclides in Their Waste Streams

Major Generators	^{90}Sr (Ci)	^{137}Cs (Ci)	Fission Product Source
ITRI	0.45	0.56	Isotopically Pure Source
LLNL-CA	0.16	0.15	Not determined
Rocketdyne	0.053	0.10	Irradiated Fuel Decladding
SNL-CA	0.24	0.00021	Isotopically Pure Source
Total from Major Generators	0.90	0.81	
Inventory Total	0.91	0.82	

consists of D&D debris from a hot cell used to separate irradiated fuel from its cladding. The fission product ratios in this waste stream have been altered by differential release from the

Finally, when the inventory was revised, the activities of ^{90}Sr and ^{137}Cs were not altered. As found for the MFP corrections, ^{79}Se and ^{87}Rb corrections were insignificant and were not added to the inventory. The remaining minor fission products listed in Table 2.34 were added to the inventory.

Table 2.34 Estimated Disposal of Minor Fission Products Potentially Present in LLNL-CA and Rocketdyne Waste Streams Containing ^{90}Sr and ^{137}Cs

		Cumulative Yield	Activity of Fission	Mean Annual
	Half-life	From Fission of	Products for 0.463 Ci	Disposal Rate
		of ^{90}Sr and ^{137}Cs		

the activities present are extremely low, generally less than a few microcuries. Those nuclides with potential for any significant impact on site performance have been conservatively added to the inventory.

Inventory records and generator shipping papers suggest that there are problems with the recorded activities of uranium isotopes. Inventory records summarized by generators and by fiscal years show that generators often report only one or two naturally occurring uranium isotopes when at least three are expected (Table 2.35). Descriptions, such as depleted uranium, enriched uranium, and the codes DU and D-238, may have been used in the past. To correct for unreported uranium isotopes, generator applications were reviewed and, in some instances, generators were contacted to determine if a single uranium isotopic mixture could be assumed. In cases where uncertainty existed about uranium isotopic ratios, the final isotopic ratio selected represented the best estimate available. Corrections were performed using the relation:

$$A_E = \frac{A_r f_E SA_E}{f_r SA_r} \quad (2.15)$$

where:

- A_E = estimated activity of the unreported isotope,
- A_r = reported activity of the reference isotope,
- f_E = isotope mass fraction of the unreported isotope,
- f_r = isotope mass fraction of the reference isotope,
- SA_E = specific activity of the unreported isotope, and
- S_r = specific activity of the reference isotope.

No corrections were made when generators reported all three natural isotopes as the records for these shipments were assumed correct.

Three generators (Pantex, SNL, and USAA) have reported only ^{238}U in their waste streams. Review of the generator applications indicated that these waste streams contained depleted uranium only. Additional ^{235}U and ^{234}U were added to the inventory using the reported ^{238}U activity as the reference and an assumed isotopic mixture for depleted uranium (Table 2.35). Five generators reported only ^{238}U and ^{235}U . Among these, three generators (RFP, LLNL, and GA) processed various isotopic mixtures. RFP, LLNL, and GA records were revised assuming that all the ^{238}U reported was depleted uranium and that all the ^{235}U reported was enriched uranium. Actual uranium enrichments used were based on generator applications

Table 2.35 Uranium Isotopes Reported by Generators Each Fiscal Year and Revisions Made to the Inventory

Generator	Recorded Inventory (Ci)			Assumed Isotopic Mixture	Assumed Isotopic Mass Fractions				Estimated Revisions to Uranium Inventory			
	²³⁸ U	²³⁵ U	²³⁴ U		²³⁸ U	²³⁵ U	²³⁴ U	²³⁶ U	²³⁸ U	²³⁵ U	²³⁴ U	²³⁶ U
FY 1989												
Pantex	0.020			Depleted U	0.9975	0.0025	5×10 ⁻⁶			0.00032	0.0019	
RFP	1.9			Depleted U	0.9975	0.0025	5×10 ⁻⁶			0.030	0.18	
RFP		0.20		93% Enriched U	0.0550	0.9315	0.0098	0.0040	0.0018		6.1	0.026
LLNL	0.68	1.0×10 ⁻⁴	2×10 ⁻⁸	Not Revised								
GA	0.014			Depleted U	0.9975	0.0025	5×10 ⁻⁶			0.00023	0.0013	
GA		0.28		93% Enriched U	0.0550	0.9315	0.0098	0.0040	0.0026		8.7	0.037
FERMCO	8.4	0.25		FY91 to FY93 Mean	0.9904	0.0096	7×10 ⁻⁵				10	
USAA	46			Depleted U	0.9975	0.0025	5×10 ⁻⁶			0.75	4.3	
FY 1990												
Mound	0.0035		0.0040	Natural U	0.9927	0.0072	6×10 ⁻⁵			0.00019		
Pantex	1.0			Depleted U	0.9975	0.0025	5×10 ⁻⁶			0.016	0.093	
SNL	0.59			Depleted U	0.9975	0.0025	5×10 ⁻⁶			0.0095	0.055	
LLNL	2.1			Depleted U	0.9975	0.0025	5×10 ⁻⁶			0.034	0.20	
LLNL		1.2×10 ⁻⁶		5% Enriched U	0.9473	0.0520	3×10 ⁻⁴		3×10 ⁻⁶		2×10 ⁻⁵	
FERMCO	0.24	0.011		FY91 to FY93 Mean	0.9904	0.0096	7×10 ⁻⁵				0.30	
USAA	10			Depleted U	0.9975	0.0025	5×10 ⁻⁶			0.16	0.95	

Table 2.35 (continued)

Generator	Recorded Inventory (Ci)		Assumed Isotopic Mixture	Assumed Isotopic Mass Fractions				Estimated Revisions to Uranium Inventory			
	²³⁵ U	²³⁸ U		²³⁵ U	²³⁸ U	²³⁵ U	²³⁸ U	²³⁵ U	²³⁸ U	²³⁵ U	²³⁸ U
FY 1991											
FERMCO	0.028	9.1×10 ⁻⁴	0.0076	Not Revised							
FY 1992											
Pantex	0.0020			Depleted U	0.9975	0.0025	5×10 ⁻⁶			3×10 ⁻⁵	0.00019
GA		0.14		93% Enriched U	0.0550	0.9315	0.0098	0.0040	0.0012		4.1
FERMCO	0.63	0.028	0.60	Not Revised							0.017
USAA	22			Depleted U	0.9975	0.0025	5×10 ⁻⁶			0.35	2.0
FY 1993											
ITRI	2.38×10 ⁻⁵	1.01×10 ⁻⁷		Not Revised							
Pantex	0.00816			Depleted U	0.9975	0.0025	5×10 ⁻⁶			0.00013	0.00076
SNL	0.943			Depleted U	0.9975	0.0025	5×10 ⁻⁶			0.015	0.088
GA		0.271		93% Enriched U	0.0550	0.9315	0.0098	0.0040	0.0025		8.2
FERMCO	15.8	0.998	20.2	Not Revised							0.034
USAA	20.6			Depleted U	0.9975	0.0025	5×10 ⁻⁶			0.33	1.9
Total (Ci)	131	2.18	20.8						0.0082	1.7	48
											0.11

and reports. ITRI records were not modified due to the small activity involved. FERMCO reported ^{238}U and ^{235}U in FY 1989 and FY 1990 and reported all three natural isotopes in subsequent years. Because FERMCO has processed many forms of uranium, the mean isotopic fractions from FY 1991 to FY 1993 and the reported ^{238}U activity were used to estimate the ^{234}U received in FY 1989 and FY 1990. A single generator (Mound) reported ^{238}U and ^{234}U in equal activities. These shipments were assumed to be natural uranium and ^{235}U was added as appropriate. These corrections have a significant effect on the inventory of ^{235}U and ^{234}U . Uranium-235 increases by 78 percent due largely to traces of the isotope in large quantities of isolated uranium. The ^{234}U inventory increases by 221 percent. This is attributable to large

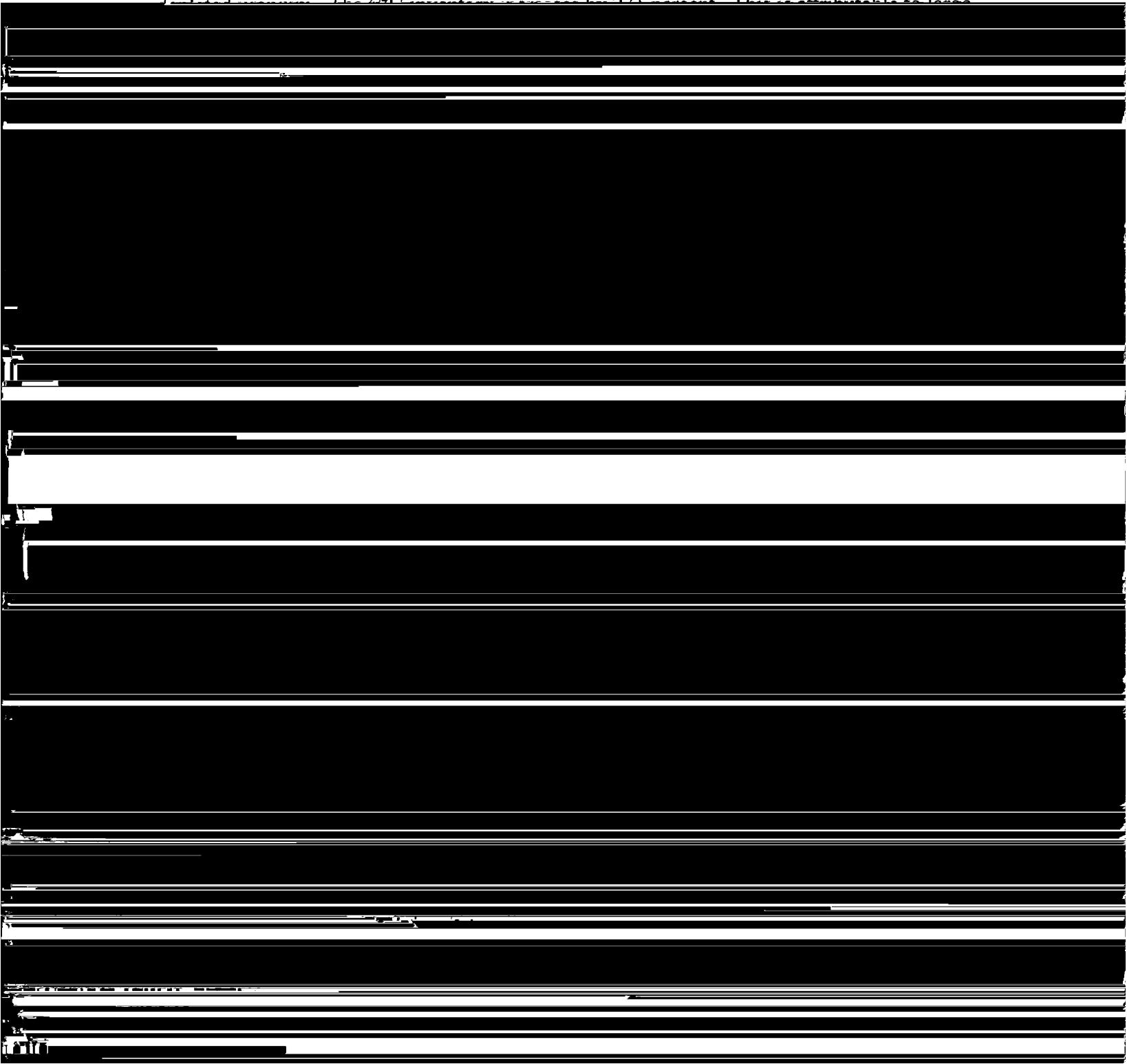


Table 2.36 Unclassified Shallow Land Burial, Classified Shallow Land Burial, and GCD Radionuclide Inventory in Curies. The revised inventory is the summation of Columns 2 through 5.

Radionuclide	Unclassified Shallow Land Burial Inventory FY89 to FY93 (Undecayed Ci)	Classified Shallow Land Burial Inventory FY89 to FY93 (Undecayed Ci)	Unclassified and Classified GCD Inventory FY89 to FY93 (Undecayed Ci)	Revisions to Recorded Inventory (Undecayed Ci)	Revised Inventory (Undecayed Ci)	Mean Annual Input Rate (Ci yr ⁻¹)
³ H	6.2 x 10 ⁴	1.1 x 10 ³	3.8 x 10 ⁴		1.0 x 10 ⁵	2.0 x 10 ⁴
¹⁴ C	0.53				0.53	0.11
³⁶ Cl	2.0 x 10 ⁻⁸				2.0 x 10 ⁻⁸	3.9 x 10 ⁻⁹
⁵⁹ Ni	3.0 x 10 ⁻⁶				3.0 x 10 ⁻⁶	6.0 x 10 ⁻⁷
⁶⁰ Co	0.078	0.060			0.14	0.028
⁶³ Ni	0.54				0.54	0.11
⁸⁵ Kr	0.082	0.0011			0.083	0.017
⁹⁰ Sr	0.80	0.12		0.0055	0.97	0.19
⁹³ Zr				4.8 x 10 ⁻⁶	4.8 x 10 ⁻⁶	9.6 x 10 ⁻⁷
⁹⁹ Tc	3.4 x 10 ⁻⁸			5.2	5.2	0.74
¹⁰⁷ Pd				1.4 x 10 ⁻⁶	1.4 x 10 ⁻⁶	2.8 x 10 ⁻⁷
¹²⁶ Sn				1.7 x 10 ⁻⁶	1.7 x 10 ⁻⁶	3.3 x 10 ⁻⁷
¹²⁹ I				4.2 x 10 ⁻⁷	4.2 x 10 ⁻⁷	8.4 x 10 ⁻⁸
¹³³ Ba	5.3x10 ⁻⁵				5.3 x 10 ⁻⁵	1.1 x 10 ⁻⁵
¹³⁵ Cs				1.2 x 10 ⁻⁵	1.2 x 10 ⁻⁵	2.4 x 10 ⁻⁶
¹³⁷ Cs	0.82			0.17	0.99	0.20

Table 2.36 (continued)

Radionuclide	Unclassified Shallow Land Burial Inventory FY89 to FY93 (Undecayed Ci)	Classified Shallow Land Burial Inventory FY89 to FY93 (Undecayed Ci)	Unclassified and Classified GCD Inventory FY89 to FY93 (Undecayed Ci)	Revisions to Recorded Inventory (Undecayed Ci)	Revised Inventory (Undecayed Ci)	Mean Annual Input Rate (Ci yr ⁻¹)
¹⁵¹ Sm				0.021	0.021	0.0043
¹⁵² Eu	2.1 x 10 ⁻⁸				2.1 x 10 ⁻⁸	4.1 x 10 ⁻⁹
¹⁵⁴ Eu	0.0032				0.0032	6.4 x 10 ⁻⁴
²⁰⁷ Bi	2.0 x 10 ⁻⁹				2.0 x 10 ⁻⁹	4.0 x 10 ⁻¹⁰
²¹⁰ Pb	1.0 x 10 ⁻⁶				1.0 x 10 ⁻⁶	2.0 x 10 ⁻⁷
²²⁶ Ra	0.011				0.011	0.0022
²³⁰ Th	5.1			-5.0	0.066	0.013
²³⁴ U	21			48	69	14
²³⁸ U	26	1.0 x 10 ²	1.9	0.0082	1.3 x 10 ²	26
²³⁸ Pu	19			0.35	19	3.8
²⁴¹ Pu	1.5 x 10 ⁻⁵			2.9 x 10 ⁻⁴	3.0 x 10 ⁻⁴	6.0 x 10 ⁻⁵
²⁴⁴ Cm	0.15				0.15	0.030
²²⁷ Ac	0.018				0.018	0.0036
²³¹ Pa	0.0063				0.0063	0.0013
²³⁵ U	2.0	0.20		1.7	3.9	0.78

Table 2.36 (continued)

	Unclassified Shallow	Classified Shallow	Unclassified and			
--	----------------------	--------------------	------------------	--	--	--

3.0 ANALYSIS OF PERFORMANCE

This chapter describes the development of site-specific scenarios, conceptual models, assumptions, and computer models used in the performance assessment. The first step in the performance assessment process is the development of scenarios. A scenario is defined as the set of features, events, and processes that define the future performance of the burial site. The next step in the performance assessment process is the forming of a detailed schematic model describing the release, transport, and uptake of radionuclides. The development of the schematic model requires that assumptions be made about the magnitude, timing, consequence of the features, events, and processes listed in the scenario. The detailed schematic model is called the conceptual model. Finally, mathematical models are prepared to simulate the conceptual model. This section describes this developmental sequence and the implementation of the final mathematical models.

3.1 Scenario Development and Selection

Uncertainty in performance assessment can be divided into three categories (Bonano and Baca, 1994): (1) uncertainty in the future state of the site (scenario uncertainty), (2) uncertainty in conceptual models, and (3) uncertainty in parameters. Development and analysis of multiple scenarios is one method to account for scenario uncertainty. The approach of this assessment is to analyze a small number of deterministic scenarios representing both reasonable and bounding future states of the site. This section describes the method and rationale of scenario development and selection.

For convenience, two types of scenarios have been developed: the *release scenario* and the *pathway scenario*. The release scenario describes the features, events, and processes that might transport radionuclides to the accessible environment. The pathway scenario represents a reasonable, albeit conservative, view of the pathways in the accessible environment that might transport radionuclides to human receptors. Combined, the two scenarios include all of the features, events, and processes responsible for the transport of radionuclides from the source to humans.

Intruder scenarios were considered as special cases. Inclusion of a separate intruder performance objective in DOE Order 5820.2A was assumed to indicate that intruder analyses were required regardless of the probability of occurrence. Intruder scenarios were not viewed as attempts to realistically predict the future, but rather as hypothetical events that are unlikely to ever occur. The intruder scenarios were analyzed to set conservative concentration limits for waste disposed in the near surface. Developing realistic site-specific intruder scenarios is impossible because predicting human behavior in the future is impossible. The intruder scenarios were assumed to be a systematic method used to set waste concentration limits. Therefore, rather than develop new site-specific intruder scenarios, this analysis has adopted established scenarios. These scenarios were originally presented by the NRC (1981) and further developed by Kennedy and Peloquin (1988). These scenarios have

been used in most LLW performance assessments prepared in the United States. They are reasonable in the sense that they are possible for Frenchman Flat, and conservative because they represent a very restrictive future use of the site. The scenarios have been made site-specific by adjusting parameters or eliminating features as appropriate for a Mojave Desert site.

3.1.1 Release Scenarios

The release scenario is a preliminary list of features, events, and processes that describe the release of radionuclides from the source and surrounding geosphere to the accessible environment. The scenarios were assembled from a screened list of features, events, and processes. This initial screening, based on probability of occurrence, consequence, applicability to the site, and the performance objectives, identified eight broad mechanisms for the release of radionuclides from the disposal site.

In Table 3.1, potential processes releasing radionuclides from a buried LLW source to secondary sources are identified, where secondary sources are defined to be the compartments within the physical environment that may serve as reservoirs of radionuclides for subsequent transport to humans off site. The potential secondary sources identified include shallow soils (including soil detritus), air, vegetation, surface water, and groundwater in the immediate vicinity of the LLW facility.

Table 3.1 Features, Events, and Processes Considered in the Development of the Release Scenarios

Features, Events, and Processes	Secondary Compartment in Accessible Environment
Diffusion of Gases	Atmosphere, Soil
Diffusion of Dissolved Solutes	Soil
Plant Uptake	Soil, Vegetation
Burrowing Animals	Soil
Soil Resuspension	Atmosphere, Vegetation
Advection of Gases	Atmosphere, Soil
Advection of Dissolved Solutes	Groundwater, Soil
Subsidence of the Closure Cap	Atmosphere, Vegetation, Groundwater

Gaseous radionuclides will diffuse through the air-filled pores of the soil cap. Some soils may attenuate gaseous diffusion because entrapped moisture obstructs the pore spaces. The dry condition of the alluvium at the RWMS might more readily allow gaseous diffusion to the surface and into the atmosphere. Thus, transport of volatile or gaseous radionuclides by diffusion was retained in the final release scenario.

In addition to diffusion, transport of gaseous radionuclides could occur through advective flow of gases through the air-filled pores into the atmosphere when the barometric pressure drops rapidly. Because such conditions prevail only during a small fraction of a year, the process is not expected to contribute significantly to the long-term cumulative release. Short-term releases, on the order of hours, that may be caused by decreasing barometric pressure were not considered to be within the scope of the performance assessment. Previous investigations into the long-term cumulative release of radon have concluded that advective transport is quantitatively insignificant (NRC, 1989). Advective transport of gases was retained for scenario development because this is the most conservative assumption.

The Area 5 RWMS lies in a region supporting floral communities characteristic of both the Mojave Desert and the Great Basin Desert. However, the community surrounding the site is usually grouped among Mojave Desert communities (Section 2.6). Plants rooting on the closure cap may transfer buried radioactivity to the surface. Available data for Mojave Desert plants, although sparse, indicate maximum rooting depths of 1 to 2 m (3.2 to 6.6 ft) for shrubs with large tap roots (Section 2.7.1). There are reports of roots visible in trench wells (PSN-1001e) which would suggest rooting depths as great as 6 to 8 m (19.7 to 26.2 ft).

subsequently deposited back on to the soil and plant surfaces. This process was retained for release scenario development.

Two processes, diffusion and advection of solutes in soil pore water, are dependent on the conceptual model of site hydrology. A preliminary screening was conducted to evaluate the potential of these two processes to transport radionuclides from the intact disposal site to the surface soil compartment and the uppermost aquifer. These screening analyses appear in the following section.

The final feature, subsidence, is expected to cause the formation of cracks, fissures, and depressions over the disposal site. Subsidence could potentially lead to the exposure of buried waste containers, enhanced gas transport, cap thinning, and enhanced infiltration. Enhanced infiltration may lead to increased plant growth and transport of contaminants to the uppermost aquifer. Subsidence was retained as a feature for scenario development.

depends on the depth of the static zone. In Pilot Well UE5PW-1, the top of the intermediate zone is at a depth of about 90 m (295 ft).

Zone IV: A lower zone immediately above the water table, where the hydraulic potential is near zero and the water is under a capillary fringe condition, with relatively static conditions producing little flow.

The conceptual model described above suggests several radionuclide transport mechanisms. First, the potential for upward flow in Zone I suggests that upward advection of water may

conductivity is extremely small and predicted travel times are extremely long. Based on these results, transport by the upward advection of liquid water driven by the water potential gradient was eliminated as a potential transport mechanism.

UPWARD ADVECTION UNDER WETTER CONDITIONS RESULTING FROM INFREQUENT RAINFALL

Downward infiltration of water from the soil surface may occur during and after infrequent precipitation events. The depth of infiltration depends upon the hydrologic characteristics of the alluvium, as well as the duration and intensity of precipitation events. The long-term downward extent of the wetting front depends on the atmospheric conditions and plant community which produce evaporation at the soil surface. Wetting of the alluvium to the depth of the waste could allow upward advection to the surface when drying conditions return.

Water content profiles following precipitation events were simulated using a numerical unsaturated flow code (UNSAT2), daily precipitation data for Frenchman Flat, a seasonal evapotranspiration rate estimated using the Penman combination equation (Penman, 1948), and meteorological data from the Area 5 RWMS. This simulation was performed to determine whether moisture from infrequent precipitation could reach buried waste. Complete details of the analysis are presented in Appendix D.

The maximum depth of infiltration predicted by UNSAT2 was about 0.20 to 0.25 m (0.65 to 0.82 ft) (see Figure D.9, Appendix D). The simulated water content profile suggests that evapotranspiration is responsible for reducing the water content in the near surface and is the major factor responsible for preventing water from moving deeper into the profile.

Preliminary data show that the precipitation to evapotranspiration (P/ET) ratio is about 0.07, indicating that rainfall is recycled back into the atmosphere either before it has had the time to infiltrate into the ground surface or soon afterwards. Similar conclusions have been reached at other desert sites in the western United States (Gee *et al.*, 1994; Fouty, 1989; Fischer, 1992; Scanlon, 1994; Scanlon and Milly, 1994; and Scanlon *et al.*, 1991).

The modeling results suggest that infiltrating water is unlikely to reach the depth of the buried waste. Therefore, upward advection under wetter conditions expected after infrequent rainfall was not retained in the final conceptual model for the intact site.

UPWARD DIFFUSION OF DISSOLVED SOLUTES

Because advective transport in near-surface soils at the Area 5 RWMS is believed to be negligible, it may be appropriate to consider the upward diffusion of dissolved solutes. The diffusion of solutes in soil systems has been recognized for many years to be dependent upon the moisture content of the soil as well as the concentration gradient (Heslep and Black, 1954; Stewart and Eck, 1958; Kemper and van Schaik, 1966). These authors' work suggests

that the diffusive flux should be negligible in the extremely dry soils observed at the RWMS where volumetric water content is approximately 0.07.

The upward diffusion of dissolved solutes in the alluvial pore spaces requires a continuous phase of liquid water. The near-surface alluvium is believed to be too dry for such a continuous liquid phase to exist. This conclusion is supported by literature reports of Cl^- diffusion in Ca^{2+} saturated systems (Porter *et al.*, 1960), where zero transmission was observed at water contents ranging from 0.077 to 0.155 in a loam soil. Even using the average background water content of alluvium at the RWMS at depth (approximately 0.10 to 0.12), diffusive transport of radionuclides is not expected to be significant.

3.1.1.2 Summary of Hydrologic Processes and Their Effects on Release and Transport of Radionuclides from the Intact Disposal Site

Based on the hydrologic conceptual model developed from site characterization studies, three potential release and transport mechanisms were evaluated for the intact disposal site. These were upward advection in Zone I under ambient dry conditions, upward diffusion in Zone I, and upward advection in Zone I under wetter conditions resulting from infrequent rainfall. Downward advection in Zone III is not consistent with the conceptual model and was eliminated as a credible transport process. None of the processes evaluated were found to be credible release and transport mechanisms when considered individually. Evaluating these processes simultaneously with other transport processes such as plant uptake is not likely to alter this conclusion. Individually, these hydrologic processes are not expected to transport contamination more than a few centimeters in 10,000 years. Estimates of release by plant uptake or by burrowing animals will not be significantly increased by hydrologic transport on these scales.

3.1.1.3 Summary of the Final Release Scenarios

In Section 3.1.1, eight features, events, and processes leading to release of radionuclides to the accessible environment were introduced. These elements can be combined to create two groups of release scenarios; those representing the intact disposal site and those for the subsided facility. Preliminary screening of the consequences of two of the hydrology-dependent processes, advection and diffusion of dissolved solutes, indicate that they are likely to be of no consequence for the intact site under prevailing climatic conditions. None of the five remaining processes for the intact site (gaseous diffusion, gaseous advection, plant uptake, bioturbation, and resuspension) is mutually exclusive. They can be combined into a single release scenario for the intact site.

Downward advection and diffusion of dissolved solutes is assumed to be possible for the subsided facility because of the greater infiltration. Normally, advection is expected to greatly exceed diffusion, and therefore diffusion can be ignored. The remaining six processes can be retained for a release scenario for the subsided site.

3.1.2 Pathway Scenarios

In Section 3.1.1, the release scenarios for the RWMS facility were described. Analysis of potentially important modes of release from the intact facility to the Area 5 accessible environment suggests that three environmental media may be contaminated: (1) air above the facility, (2) surface soil above the facility, and (3) vegetation above the facility. Release of radionuclides from the subsided facility will lead to contamination of the same media with the addition of the uppermost aquifer. The pathway scenarios described in this section are lists of the transport pathways leading to exposure of the public. The pathways operating at the site after loss of institutional control will be dependent on land use. Future land use was based on the current pattern of use in southern Nevada. Excluding land uses that result in direct intrusion into buried waste, three general classes of land use were hypothesized: (1) transient occupation of the site for recreational or commercial purposes, (2) open rangeland, and (3) permanent domestic residence with ranching.

The transient occupation scenario accounts for most of the land in southern Nevada. This scenario hypothesizes that members of the public will visit but not reside at the site or engage in any agricultural activities. Members of the public were not assumed to be engaged in any specific activity because all of the potential uses involve the same exposure pathways. The likely pathways of exposure are inhalation of suspended soil and external irradiation. This scenario is assumed to begin at the end of institutional control.

The open rangeland scenario assumes that a remotely located ranch uses the site to graze cattle. The site is assumed to be an uncultivated range with the current native flora present. This land use has occurred within Frenchman Flat in the past. Residents at the remote ranch will be exposed directly through consumption of beef and dairy products. Residents at the ranch may also be exposed to suspended soil transported from the site to the residence by atmospheric dispersion. The remote ranch is assumed to be located at the nearest source of water. The community closest to the Area 5 outside the NTS boundary is Indian Springs, 42 km (26 mi) to the southeast. The site closest to the RWMS with water is Cane Spring, located 14.3 km (8.8 mi) to the west on the margin of Frenchman Flat (Section 2.6). Cane Spring is currently within the NTS boundary. This site supported cattle ranching and mining operations prior to U.S. government ownership. During the period of institutional control, residents are exposed through the atmospheric pathway only. After institutional control, residents may consume contaminated meat and dairy products from range-fed cattle grazing

all the pathways described for a transient occupant and an off-site ranch, plus ingestion of contaminated vegetables and soil. A groundwater pathway is not included for the intact disposal site, but is included for the subsided site.

The first two scenarios, transient occupation and open rangeland, are considered the most probable, as they do not require development of water resources at the site. These are the activities currently observed for areas where water resources are lacking, such as Frenchman Flat. In southern Nevada, urban development or cultivation of irrigated crops is tied to the availability of surface water or shallow groundwater. Such resources are not available at the Area 5 RWMS. There are few economic incentives to develop this land because of the limited agricultural potential and great expense of obtaining deep groundwater. Although the resident farming scenario is technically feasible, it is considered highly improbable based on current land use patterns. Resident farming scenarios are commonly analyzed in performance assessments. Although this scenario is highly unlikely for Frenchman Flat, it was analyzed for consistency with other performance assessments. Results for this scenario represent an extreme bounding estimate of site performance.

Three pathway scenarios were developed based on current land-use patterns. Table 3.2 lists the pathways transferring contamination to members of the general public for each scenario adopted. Note that the open rangeland scenario has both an institutional control period and a postinstitutional control period where different pathways operate. The transient occupancy and open rangeland scenarios are not mutually exclusive. Conceptual models developed and assumptions made to quantify these exposures are discussed in Section 3.4.

Table 3.2 Pathways Included in the Transient Occupation, Open Rangeland, and the Resident

Farmer Scenario

Open Rangeland/Resident Farmer

Table 3.2 (continued)

Pathway	Transient Occupation	Open Rangeland/Resident Farmer	
		Institutional Control Period	Postinstitutional Control Period
Ingestion by Humans of Plants Cultivated Off Site		×	×
External Irradiation by Contaminated Cover Soil	×		
External Irradiation by Contaminated Off-Site Soil		×	×
Ingestion of Contaminated Native Flora by Livestock Grazing On Site			×
Ingestion of Contaminated Beef and Milk from Livestock Grazing On Site			×
Ingestion of Contaminated Soil by Humans Off Site		×	×
Ingestion of Contaminated Cover Soil by Grazing Livestock			×
Inhalation of Contaminants in Air by Humans On Site	×		
Inhalation of Contaminants in Air by Humans Off Site		×	×
Resuspension of Contaminated Cover Soil	×		×
Resuspension of Contaminated Off-Site Soil		×	×

3.1.3 Intruder Scenarios

Intruder scenarios have been limited to those previously described for low-level radioactive waste performance assessments (NRC, 1981; Kennedy and Peloquin, 1988). These include both acute and chronic exposure scenarios. Acute exposure scenarios involve exposures of short duration, a few days to years. Acute scenarios previously described include an intruder-construction scenario, a discovery scenario, and a drilling scenario. Previously described chronic intruder scenarios include the intruder-agriculture and postdrilling scenario.

The effects of subsidence have not been considered in the intruder scenarios. Intruder scenarios are not realistic representations of the future state of the site, but rather are a conservative method of setting waste concentration limits. Nevertheless, the massive

subsidence required to significantly alter site performance is likely to preclude chronic



rarely constructed with a basement. This is believed to be due to economic factors. However, excavations can still be prepared during the construction of a slab-on-grade structure. Current construction practices can involve grading or terracing of the site, trenching for utilities, and excavations for septic tanks, swimming pools, or underground storage tanks. Furthermore, soil structure at the Area 5 RWMS does not physically preclude excavation. The intruder-agriculture scenario with basement construction was retained because it is physically possible for this site.

Under the intruder-agriculture scenario, it is assumed that an intruder constructs a residence with a basement on the site and, in the process, exhumes buried waste. The soil and waste from the excavation is spread over an area surrounding the house and mixed homogeneously. The resident is assumed to raise livestock, fruits, and vegetables in the contaminated area. Although the intruder uses groundwater from below the site, there are no groundwater-dependent pathways because contamination of the aquifer is considered physically unreasonable. The intruder is exposed to contamination by:

- Inhalation of resuspended contaminated soil.
- Inhalation of gaseous radionuclides released from the site.
- External irradiation by contaminated soil.
- Ingestion of contaminated soil.
- Ingestion of contaminated beef and milk.
- Ingestion of contaminated fruits and vegetables.

The postdrilling scenario is an extension of the drilling scenario. It assumes that the intruder occupies the site after drilling a water well and grows crops on a mixture of clean soil and contaminated drill cuttings. After exhumation of waste, the exposure pathways are the same as for the intruder-agriculture scenario. The only differences between the two scenarios are the thickness of the contaminated zone and the concentration of radionuclides in the contaminated zone.

In summary, three acute and three chronic intruder scenarios were considered. One acute and two chronic intruder scenarios were retained for analysis. The discovery scenario was eliminated because it was bounded by the intruder-construction scenario. The intruder-construction scenario was eliminated because it is bound by the chronic intruder-agriculture scenario. The acute scenario retained for analysis was the drilling scenario. The chronic scenarios retained were the intruder-agriculture scenario and the postdrilling scenario.

3.1.4 Modeling Cases for Analysis

Modeling cases can be assembled from the hypothesized scenarios, the source terms, and the performance objectives. This assessment considers two source terms at the Area 5 RWMS, a shallow land-burial source term and Pit 6. The shallow land-burial source term includes all of the waste that has been disposed in pits and trenches since the implementation of DOE Order 5820.2A, plus those wastes projected to be disposed by site closure. Pit 6 has been analyzed as a separate source term because it includes a deeper cell prepared for thorium waste. The objective of the Pit 6 analyses is to set a thorium inventory limit for this unit. The all-pathways compliance cases combine the two release scenarios with the transient occupation pathway scenario, the open rangeland, or the resident farmer pathway scenario. Three cases, base case release plus transient occupation, base case release plus open rangeland, and base case release plus the resident farmer, are required to assess compliance of the shallow land burial source term (Table 3.3). Similarly, three cases are generated with the subsided release case. There are no cases required to assess compliance for the thorium waste with the all pathways performance objective because the base case release scenario does not include any features or processes acting at the depth of burial which is 12.2 m (40 ft). Because the subsided release case has the potential to initiate a groundwater pathway for the thorium source term, a case combining subsidence and the resident farmer is required. The resident farmer pathway scenario is the only scenario with on-site water withdrawal. Four cases are required to assess compliance with the radon flux standard (Table 3.3). Three cases, base case release plus transient occupation, base case release plus open rangeland, and base case release plus the resident farmer are required to assess the compliance for release of volatile radionuclides from the shallow land burial source term. No case is required for release of volatile radionuclides from the thorium waste because it does not include ^3H , ^{14}C , or ^{85}Kr source terms. Finally, three cases combining the subsided release case with the three pathway scenarios are required for the volatile radionuclides.

Figure 3.1.4 shows the modeling cases identified for the analysis (Table 3.4). The thorium

Table 3.3 Summary of All-Pathways Modeling Cases Selected for Analysis

Cases for Analysis	Release Scenario	Pathway Scenarios		
		Transient Occupation	Open Rangeland	Resident Farmer
Nonvolatile Nuclides – Shallow Land Burial	Base Case	×	×	×
	Subsided Case	×	×	×
Nonvolatile Nuclides - Thorium Waste (Pit 6)	No Release			
	Subsided Case			×
Radon – Shallow Land Burial	Base Case	No Pathway Scenario		
	Subsided Case	No Pathway Scenario		
Radon – Thorium Waste (Pit 6)	Base Case	No Pathway Scenario		
	Subsided Case	No Pathway Scenario		
Other Volatiles (^3H , ^{14}C , ^{85}Kr) – Shallow Land Burial	Base Case	×	×	×
	Subsided Case	×	×	×

Table 3.4 Summary of Intruder Modeling Cases Selected For Analysis

Cases for Analysis	Acute Intruder Scenarios	Chronic Intruder Scenarios	
	Drilling	Intruder-Agriculture	Postdrilling
Shallow Land Burial	×	×	×
Thorium Waste (Pit 6)	×		×

3.2.1 Source Term

The source term is the contents of the waste disposal cells including the radionuclides available for release to the surrounding environment. Source term conceptual models have been developed that describe the geometry of a shallow land burial pit, the thorium waste cell (Pit 6), and the temporary closure cap. Additional conceptual models describe the performance of the waste containers and waste forms, subsidence, and radionuclide release.

3.2.1.1 *Estimated Shallow Land Burial Inventory at Site Closure*

An estimate of the site inventory at closure has been prepared to estimate long-term site performance. This section describes the projected inventory for shallow land burial and for the thorium waste cell.

The inventory at closure was estimated by assuming that waste received in the future would have the same activity concentration as wastes received from FY 1989 through FY 1993. As the mission of DOE shifts from production to decommissioning and environmental restoration, confidence in this estimate may be reduced. Experience has shown that most of the techniques available to forecast future waste receipts are very unreliable. The analysis

Table 3.5

Serial Radioactive Decay Chains Present in the Area 5 Inventory. Radionuclides determined by BAT6CHN are indicated in italics. All other radionuclides are assumed to be in secular or transient equilibrium with the parent in italics by the end of the institutional control period.

Chain 1	Chain 2	Chain 3	Chain 4	Chain 5	Chain 6	Chain 7	Chain 8
<i>²⁴³Am</i> <i>²³⁹Np</i> <i>²³⁹Pa</i>	<i>²⁴¹Pu</i> <i>²⁴¹Am</i> <i>²³⁷Np</i>	<i>²⁴²Pu</i> <i>²³⁸U</i> <i>²³⁴Th</i>	<i>²³⁸Pu</i> <i>²³⁴U</i> <i>²³⁰Th</i>	<i>²⁴⁴Cm</i> <i>²⁴⁰Pu</i> <i>²³⁶U</i>	<i>²⁴⁸Cm</i> <i>²⁴⁴Pu</i> <i>²⁴⁰U</i>	<i>²⁴³Cm</i> <i>²³⁹Pu</i> <i>²³⁵U</i>	<i>²³²U</i> <i>²²⁸Th</i> <i>²²⁴Ra</i>

Table 3.6 Radionuclide Half-Lives, Branching Fractions, and Equilibrium Factors Used in the Performance Assessment (from Negin and Worku, 1990)

Radionuclide	Half-life (yr)	Branching Fraction	Equilibrium Factor
^3H	12.8	—	—
^{14}C	5730	—	—
^{36}Cl	3.01×10^5	—	—
^{59}Ni	75000	—	—
^{60}Co	5.27	—	—
^{63}Ni	100	—	—
^{79}Se	65000	—	—
^{85}Kr	10.7	—	—
^{90}Sr ^{90}Y	28.6 0.00732	— 1.0	— 1.0
^{93}Zr ^{93}Nb	1.53×10^6 14.6	— 1.0	— 1.0
^{99}Tc	2.13×10^5	—	—
^{107}Pd	6.5×10^6	—	—
^{126}Sn ^{126}Sb	1×10^5 0.034	— 1.0	— 1.0
^{129}I	1.57×10^7	—	—
^{133}Ba	10.5	—	—
^{135}Cs	2.3×10^6	—	—
^{137}Cs $^{137\text{m}}\text{Ba}$	30.17 4.85×10^{-6}	— 0.946	— 1.0
^{151}Sm	90	—	—
^{152}Eu ^{152}Gd	13.6 1.1×10^{14}	— 0.278	— No equilibrium
^{154}Eu	8.8	—	—
^{207}Bi	33.4	—	—
^{232}U ^{228}Th	72 1.913	— 1.0	— 1.0
^{243}Am ^{239}Np	7.38×10^3 6.45×10^{-3}	— 1.0	— 1.0

Table 3.6 (continued)

Radionuclide	Half-life (yr)	Branching Fraction	Equilibrium Factor
^{239}Pu	2.41×10^4	—	—
^{235}U ^{231}Th	7.04×10^8 2.91×10^{-3}	— 1.0	— 1.0
^{231}Pa	3.28×10^4	—	—
^{227}Ac ^{223}Fr ^{227}Th ^{223}Ra ^{219}Rn ^{215}Po ^{211}Pb ^{211}Bi ^{207}Tl ^{211}Po	21.2 4.15×10^{-5} 5.13×10^{-2} 3.93×10^{-2} 1.26×10^{-7} 2.48×10^{-11} 6.87×10^{-5} 4.05×10^{-6} 9.07×10^{-6} 1.64×10^{-8}	— 0.0138 0.9862 1.0 1.0 1.0 1.0 1.0 0.9973 0.0027	1.0 1.0 1.0 1.0 1.0 1.0 1.0 1.0 1.0 1.0
^{241}Pu	14.4	—	—
^{241}Am	432	—	—
^{237}Np ^{233}Pa	2.14×10^6 7.39×10^{-2}	— 1.0	— 1.0
^{233}U	1.59×10^5	—	—
^{229}Th ^{225}Ra ^{225}Ac ^{221}Fr ^{217}At ^{213}Bi ^{209}Tl ^{213}Po ^{209}Pb	7.34×10^3 4.05×10^{-2} 2.74×10^{-2} 9.13×10^{-6} 1.02×10^{-9} 8.68×10^{-5} 4.19×10^{-6} 1.33×10^{-13} 3.71×10^{-4}	— 1.0 1.0 1.0 1.0 1.0 0.0216 0.9784 1.0	— 1.0 1.0 1.0 1.0 1.0 1.0 1.0 1.0
^{242}Pu	3.76×10^5	—	—
^{238}U ^{234}Th $^{234\text{m}}\text{Pa}$ ^{234}Pa	4.47×10^9 6.60×10^{-2} 2.23×10^{-6} 7.65×10^{-4}	— 1.0 1.0 0.0016	— 1.0 1.0 1.0
^{238}Pu	87.8	—	—
^{234}U	2.44×10^5	—	—
^{230}Th	7.7×10^4	—	—

Table 3.6 (continued)

Radionuclide	Half-life (yr)	Branching Fraction	Equilibrium Factor
^{226}Ra	1600	—	—
^{222}Rn	1.05×10^{-2}	1.0	1.0
^{218}Po	5.80×10^{-6}	1.0	1.0
^{214}Pb	5.10×10^{-5}	1.0	1.0
^{214}Bi	3.79×10^{-5}	1.0	1.0
^{214}Po	2.02×10^{-12}	1.0	1.0
^{210}Pb	22.3	—	—
^{210}Bi	6.1×10^{-3}	1.0	1.0
^{210}Po	0.379	1.0	1.018
^{244}Cm	18.1	—	—
^{248}Cm	3.39×10^5	—	—
^{244}Pu	8.26×10^7	—	—
^{240}U	1.60×10^{-3}	1.0	1.0
$^{240\text{m}}\text{Np}$	1.41×10^{-5}	1.0	1.0
^{240}Np	1.23×10^{-4}	0.0011	1.0
^{240}Pu	6540	—	—
^{236}U	3.42×10^6	—	—
^{232}Th	1.40×10^{10}	—	—
^{228}Ra	5.75	—	—
^{228}Ac	7.00×10^{-4}	1.0	1.0
^{228}Th	1.91	—	—
^{224}Ra	9.92×10^{-3}	1.0	1.0
^{220}Rn	1.76×10^{-6}	1.0	1.0
^{216}Po	4.63×10^{-9}	1.0	1.0
^{212}Pb	1.21×10^{-3}	—	1.0
^{212}Bi	1.15×10^{-4}	—	1.0
^{212}Po	9.45×10^{-15}	0.6407	1.0
^{208}Tl	5.81×10^{-6}	0.3593	1.0

Table 3.7 Estimated Activity and Activity Concentration of Wastes Projected to be Disposed by

Radionuclide	Estimated Activity at Closure in 2028 (Ci)	Estimated Mean Activity Concentration at Closure in 2028 (Ci m ⁻³)
³ H	3.18 × 10 ⁵	0.864
¹⁴ C	4.12	1.12 × 10 ⁻⁵
³⁶ Cl	1.54 × 10 ⁻⁷	4.18 × 10 ⁻¹³
⁵⁹ Ni	2.34 × 10 ⁻⁵	6.36 × 10 ⁻¹¹
⁶⁰ Co	0.207	5.68 × 10 ⁻⁷

Table 3.7 (continued)

	Estimated Activity at Closure in	Estimated Mean Activity Concentration at Closure in 2028
--	----------------------------------	---

Table 3.7 (continued)

Radionuclide	Estimated Activity at Closure in 2028 (Ci)	Estimated Mean Activity Concentration at Closure in 2028 (Ci m ⁻³)
²³⁰ Th	0.606	1.65 × 10 ⁻⁶
²²⁶ Ra	0.0906	2.46 × 10 ⁻⁷
²²² Rn	0.0906	2.46 × 10 ⁻⁷
²¹⁸ Po	0.0906	2.46 × 10 ⁻⁷
²¹⁴ Pb	0.0906	2.46 × 10 ⁻⁷
²¹⁴ Bi	0.0906	2.46 × 10 ⁻⁷
²¹⁴ Po	0.0906	2.46 × 10 ⁻⁷
²¹⁰ Pb	0.0368	1.00 × 10 ⁻⁷
²¹⁰ Bi	0.0368	1.00 × 10 ⁻⁷
²¹⁰ Po	0.0375	1.02 × 10 ⁻⁷
²⁴⁴ Cm	0.623	1.69 × 10 ⁻⁶
²⁴⁸ Cm	6.74 × 10 ⁻¹⁰	1.83 × 10 ⁻¹⁵
²⁴⁴ Pu ²⁴⁰ U ^{240m} Np ²⁴⁰ Np	negligible	negligible
²⁴⁰ Pu	24.7	6.72 × 10 ⁻⁵
²³⁶ U	0.858	2.33 × 10 ⁻⁶
²³² Th	1.89	5.13 × 10 ⁻⁶
²²⁸ Ra	1.46	3.98 × 10 ⁻⁶
²²⁸ Ac	1.46	3.98 × 10 ⁻⁶
²²⁸ Th	1.42	3.86 × 10 ⁻⁶
²²⁴ Ra	1.42	3.86 × 10 ⁻⁶
²²⁰ Rn	1.42	3.86 × 10 ⁻⁶
²¹⁶ Po	1.42	3.86 × 10 ⁻⁶
²¹² Pb	1.42	3.86 × 10 ⁻⁶
²¹² Bi	1.42	3.86 × 10 ⁻⁶
²¹² Po	0.910	2.47 × 10 ⁻⁶
²⁰⁸ Tl	0.510	1.39 × 10 ⁻⁶

negligible - less than 1 × 10⁻¹² Ci

3.2.1.2 Estimated Thorium Waste Inventory at Closure

Pit 6 (P06U) has been selected for the disposal of thorium source material generated by the Fernald Environmental Management Project (FEMP). The FEMP thorium source material

will be managed as a separate case because it is unsuitable for disposal by shallow land burial as routinely conducted at the RWMS. The thorium source material was to be used as fertile fuel in ^{233}U breeder reactors. Since the termination of U.S. breeder programs, all the thorium source material at the FEMP has been declared waste and is being transferred to the NTS for disposal. On a mass basis, these wastes are predominantly thorium metal, ThO_2 , and

$\text{Th}(\text{OH})_4$ with lesser amounts of thorium oxalate and $\text{Th}(\text{Cl})_4$. On a nuclide basis, the wastes are predominantly ^{232}Th and its progeny. Small amounts of ^{230}Th present in the original ore were carried through the refining process and are present in the waste. The ^{230}Th will generate ^{222}Rn gas as ^{226}Ra is produced by radioactive decay. The peak ^{226}Ra concentration will occur in 9,000 to 10,000 years.

The FEMP shipped 368 m^3 ($12,995.8\text{ ft}^3$) of thorium waste to the NTS in FY 1992. An inventory at closure can be estimated assuming that the lower cell of Pit 6 will be filled with waste having the same activity concentration as waste received in FY 1992. Because the thorium source material received is nearly pure thorium, it is unlikely that the final inventory could be greater than this estimate. The thorium waste will be disposed in the bottom of Pit 6 (P06U) in a 3.6-m- (11.8-ft)-thick layer. The volume available for disposal is $5,600\text{ m}^3$ ($197,762\text{ ft}^3$). The total activity of ^{232}Th , ^{228}Th , and ^{230}Th was calculated as the product of the activity concentration of FY 1992 waste and the volume of the lower cell of Pit 6.

Based on generator-supplied information, the members of the ^{232}Th decay were assumed to be in secular equilibrium at the time of disposal. This suggests that at least 30 years of ingrowth had occurred by 1992. Assuming that the trench is filled and closed by 2028, approximately 66 years of decay and ingrowth will have occurred by closure. The activity at closure was calculated assuming an initially pure source of ^{232}Th , ^{228}Th , and ^{230}Th and 66 years of decay (Table 3.8).

3.2.1.3 *Shallow Land Burial Waste Cell Conceptual Model*

Low-level radioactive wastes and mixed wastes have been managed at the Area 5 RWMS by burial in shallow unlined pits and trenches and by burial in GCD boreholes. The dimensions of pits and trenches at the RWMS is variable. The dimensions have been selected to fit within the boundaries of the site and existing excavations, so that land allocated to waste disposal is fully utilized. In contrast, GCD dimensions have remained constant. This section describes a conceptual model of a trench used in performance-assessment modeling. A single generic waste disposal cell was used in the analyses to avoid performing analyses for each pit and trench. It is not believed that performing separate analyses for each pit and trench, with its unique dimensions, will add any greater confidence to the results of the performance assessment. The dimensions likely to have the greatest impact on model results are the thickness of the cap and the thickness of the waste due to the one-dimensional nature of the analyses. The cap thickness is constant for all waste cells and the thickness of the waste is the least variable of the waste cell dimensions (see Table 2.17). Most waste cells have been excavated to approximately 6 m (19.6 ft), allowing placement of foundations of

Table 3.8 Preliminary Estimate of the Inventory of Thorium Waste That Could Be Disposed in the Lower Cell of Pit 6 (P06U)

	Estimated Activity at Closure in	Estimated Mean Activity Concentration at Closure in 2028
--	----------------------------------	---

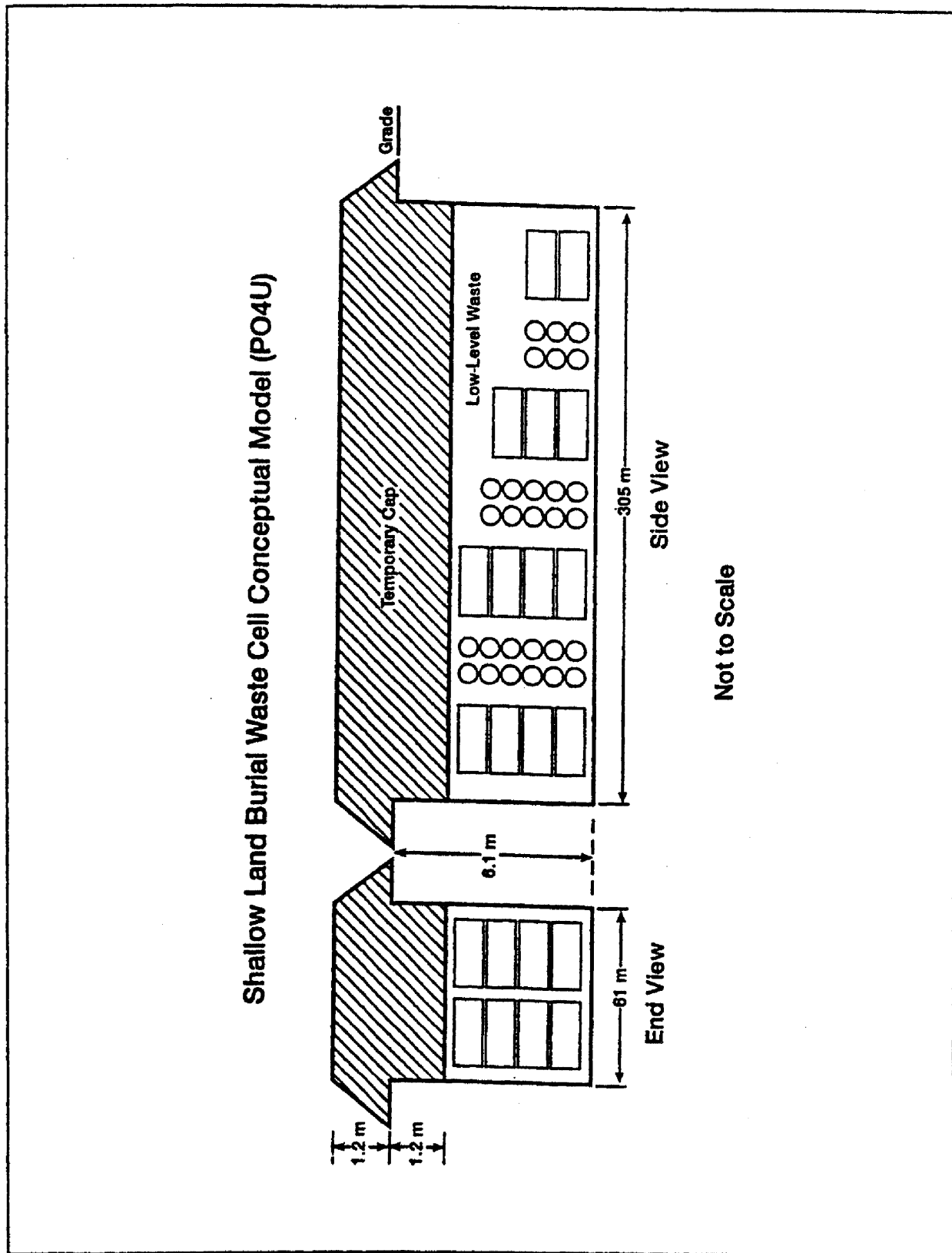


Figure 3.1 Conceptual Model of Shallow Land Burial Pits and Trenches

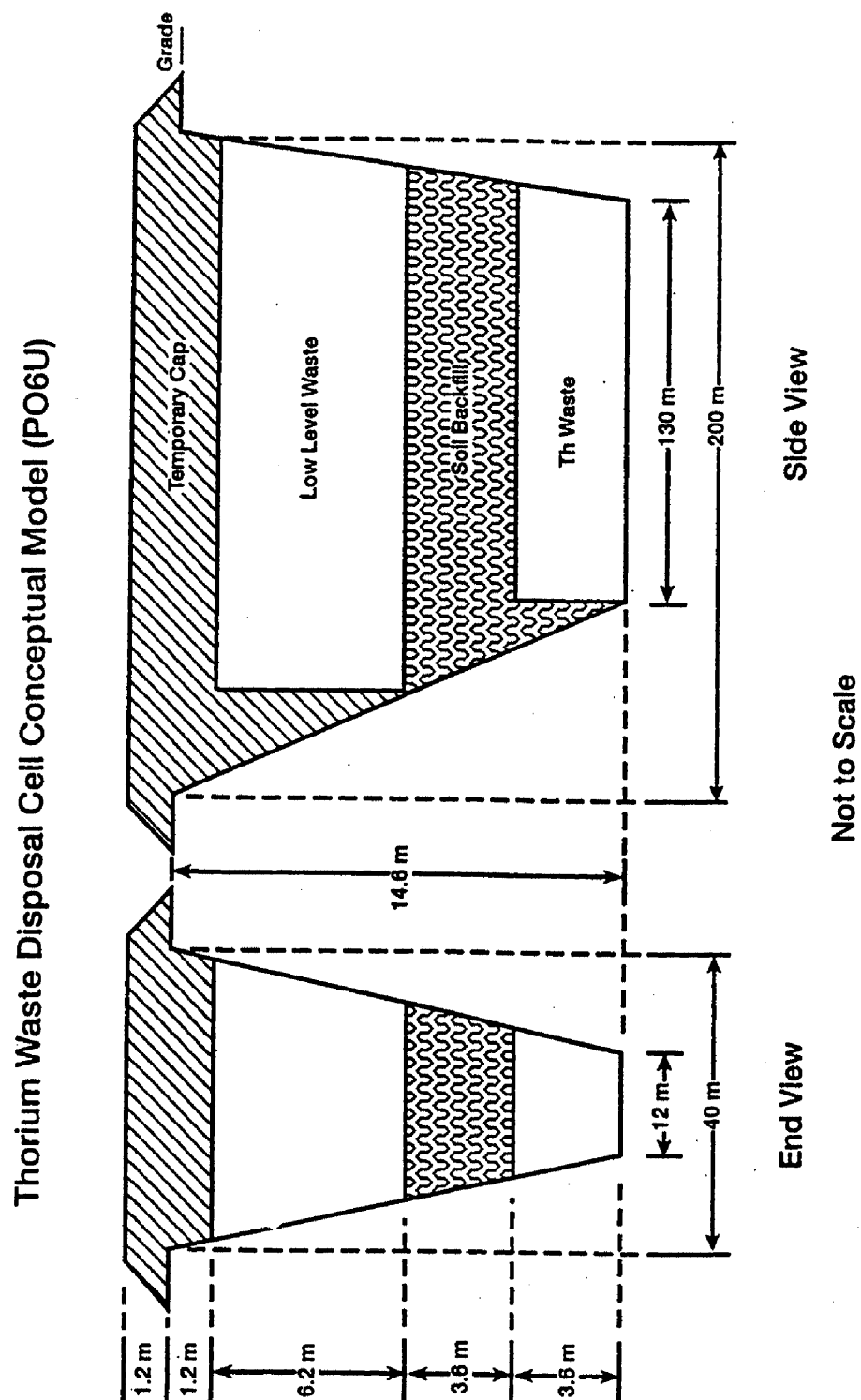


Figure 3.2 Conceptual Model of Pit 6 (P06U) and Placement of Thorium Waste

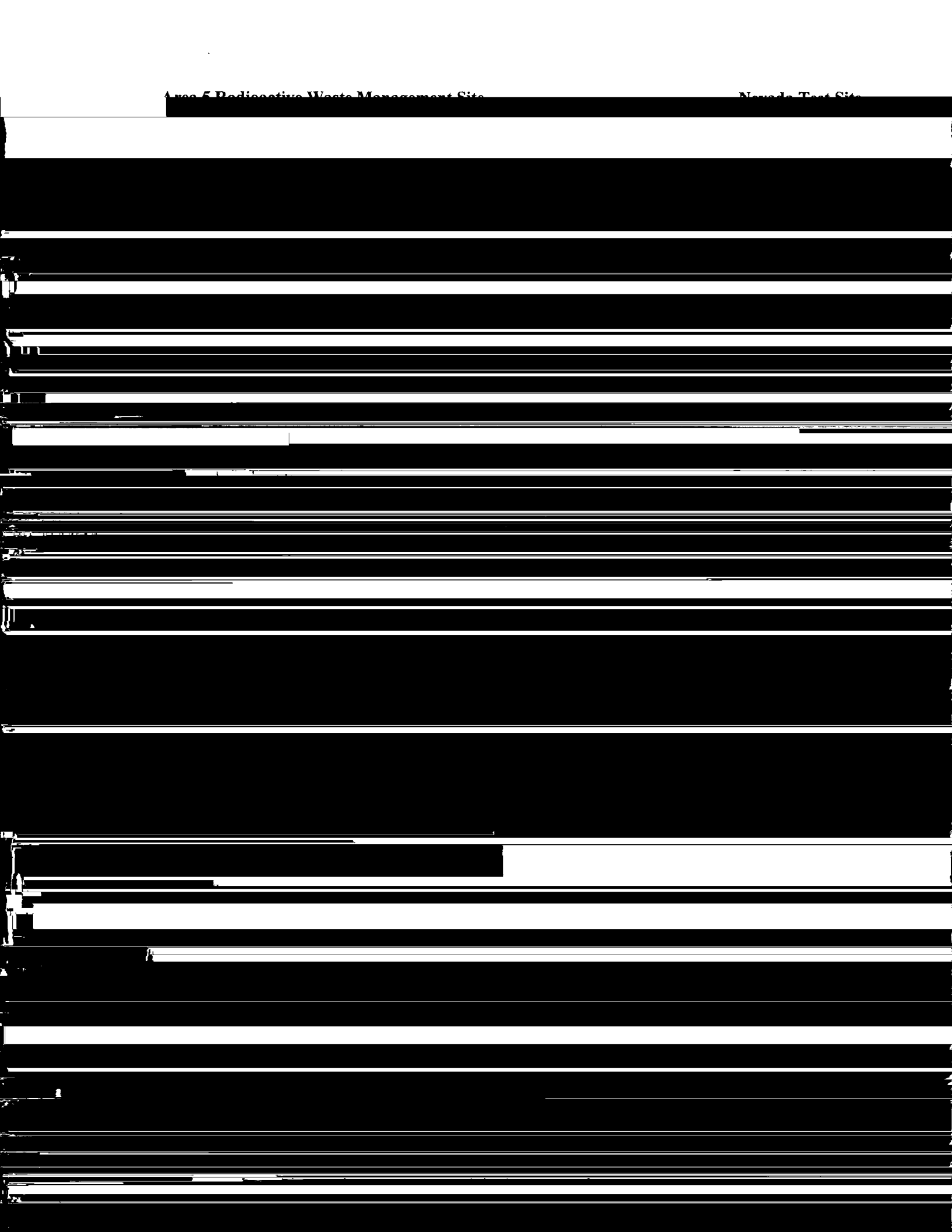


Table 3.9 Parameter Values Assumed for the Universal Soil Loss Equation

Universal Soil Loss Equation: $A = R K L S C P$ (3.3)	
Parameter	Assumed Value
R - Rainfall Erosivity	20.0
K - Soil Erodibility Index	0.10
LS - Length Slope Factor	0.25
C - Crop Management Factor	0.18
P - Erosion Control Practice Factor	1.0
ρ - Soil Bulk Density	1.65 g cm ⁻³
$A = 0.09 \text{ ton acre}^{-1} \text{ yr}^{-1} \text{ (} 1 \times 10^{-5} \text{ m yr}^{-1} \text{ for } \rho = 1.65 \text{ g cm}^{-3} \text{)}$	

The conceptual model of cap performance for the base case release scenario is that a 2.4-m (7.8-ft) alluvium cover will be present for 10,000 years. This is an unrealistic model adopted in lieu of a final closure cap design. It is believed to be a conservative model based on the following conclusions. First, it is certain that a cap of at least 2.4 m (7.8 ft) will be present because 2.4-m (7.8-ft) caps are currently in place. Second, erosion estimates suggest that cap thickness will change little over the next 10,000 years. Finally, it is very likely that the final closure cap will be much thicker than 2.4 m (7.8 ft). Preliminary conceptual designs call for a cap 5.4 m (17.7 ft) thick (Johnejack and Elletson, 1994). The estimated erosion rates are not great enough to reduce this thickness to 2.4 m (7.8 ft). Therefore, assuming that a 2.4-m (7.8-ft)-thick cap is present over the next 10,000 years appears to be a conservative assumption for an intact cap.

3.2.1.6 Waste Form Conceptual Model

The chemical and physical form of the waste and the integrity of the containers can have an impact on radionuclide release calculations, especially in an arid environment. Wastes disposed at the Area 5 RWMS are packaged predominantly in metal drums, metal boxes, and wooden boxes. Little is known about the degradation of these containers under the conditions prevalent at the NTS. No information about the chemical or physical form of the waste can be obtained from the site database.

Based on the lack of information about the waste form and containers, it was necessary to adopt a very conservative model. For the base case release scenario, waste packages were assumed to completely degrade by the end of institutional control. No credit was taken for the ability of the waste forms to resist release and dispersion. The waste was assumed to have degraded to a material indistinguishable from soil by the end of institutional control.

Under the arid conditions of the NTS, most metal and wood containers and many waste forms are likely to survive intact for a considerable time. However, in the absence of reliable data, it was conservatively assumed for the base case release scenario that all radionuclides were immediately available for uptake and release at closure.

3.2.1.7 *Subsidence Assumptions and Conceptual Model*

Subsidence or settlement of waste and the closure cap may occur from:

- Deformation and crushing of the containers under load (self weight and soil cover).
- Decomposition of the containers and associated collapse caused by:
 - Voids within the container.
 - Decomposition of the waste within the container.
 - Compression of the waste material.
 - Infilling of the initial and subsequently created voids with soil cover material, which is both hastened and exacerbated by:
 - ❖ Earthquake ground shaking.
 - ❖ Induced ground shaking (testing and construction).
 - ❖ Flow of water through the soil.

Factors influencing the magnitude of subsidence of the soil cover over the pits and trenches include:

- Decay rate of the various containers.
- Change in bulk density of the containers upon collapse.
- Initial void space between the containers and extent of initial infilling of these voids with cover soil.
- Depth of the waste within the pit/trench.
- Relative density of the cover soil over the waste.

Representative values for each factor was assigned as described below. These values were used to estimate surface subsidence at 100 and 10,000 years after closure.

In the following discussions, the collapsible void space is the presently open void space that is expected to be ultimately filled under the anticipated time and load conditions, expressed as a percentage of the initial height. This value does not include the voids in the waste and soil infill which will inherently always be present.

RATE OF DECAY OF CONTAINERS

Only cardboard “triwall” containers are assumed to decompose within the institutional control period, 100 years after closure. Many of these containers may already be crushed to near their final volume by the load of the overlying containers and the cover soil.

The structural life of the metal drums, wooden debris, wood pallets, and plywood boxes could be less than 100 years. However, in the arid climate of the NTS, many of the containers are expected to maintain integrity during this period. The assumption that these materials maintain integrity beyond the institutional control period does not affect the amount of predicted subsidence, but does shift occurrence until after the end of institutional control.

The time during which steel boxes are expected to maintain structural integrity is difficult to quantify. Steel boxes were assumed to maintain integrity for over 100 years. Table 3.10 summarizes assumed container longevity.

Table 3.10 Assumed Integrity Life of Containers

Container	Type	Decay Period
Drums	Metal	Greater than 100 years
Boxes	Metal	Greater than 100 years
	Plywood	Greater than 100 years
	Cardboard	Less than 100 years
Debris/Dunnage and Pallets	Wood	Greater than 100 years

CHANGE IN BULK DENSITY UPON CONTAINER COLLAPSE

Waste containers received at the Area 5 RWMS are thought to contain significant void space. Reasons containers might contain void space include:

- The container weight limit is exceeded prior to complete filling.
- Settling of contents during shipping.
- Other constraints during filling operations (ease, safety, etc.).

To estimate the collapsible void space within each container and the compressibility of the waste (under the weight of the overlying waste, soil cover, and cap), bulk densities of waste shipments were calculated for selected years. Bulk density is defined as the weight of the

waste and container, divided by the exterior volume of the container, which typically includes dunnage and box feet.

For this analysis, drummed waste and boxed waste were not differentiated, due to sparsity of data to support differentiation. Boxes and drums were assumed to be packed to a relatively uniform bulk density in any given year. The calculated bulk densities for selected years are presented in Table 3.11.

Table 3.11 Bulk Densities of All Waste Containers in Selected Years

Year	Bulk Density		Notes
	kg m ⁻³	lbs ft ⁻³	
1980	482	30	
1983	757	47	Large number shipments containing many drums
1985	532	33	
1988	638	40	Large quantity of waste received, including over 2 million drums
1990	480	30	
1995	875	55	Primarily metal boxes received; supercompaction in use by generators

A final bulk density must be determined or assumed from a bulk density (and compressibility) assigned to the waste following decay of the container and compression of the waste. This value is directly related to the waste itself.

To determine the type of waste typically received, available data for the waste streams from the three largest generators (EG&G Mound Applied Technologies; EG&G Rocky Flats; and FEMP) were evaluated, as defined by weight and number of containers. These generators, and the general type of waste shipped, are described in Table 3.12.

For waste disposed between 1980 and 1990, containerized bulk densities ranged from 482 to 775 kg m⁻³ (30 to 47 lb ft⁻³), with an average bulk density of 578 kg m⁻³ (36 lb ft⁻³) (Table 3.11). Final bulk densities were estimated based on the loosely defined waste stream form. Assuming average long-term compressed density of 1,607 kg m⁻³ (100 lb ft⁻³), including biodegradation, the average compressible void space is 64 percent. Waste disposed in 1995, which was assumed to be representative of post-1990 waste, had an average bulk density of 875 kg m⁻³ (55 lb ft⁻³). This yields a compressible void space of 45 percent.

Table 3.12 Descriptions of Typical Waste From Three Largest Generators

Generator Code	Generator	Type of Waste
AMDM	EG&G Mound Applied Technologies (description from 1990 application)	Cement-solidified tritium, cement-solidified sludge, sewage sludge with fly ash, laboratory waste (trash), equipment, oil in absorbent, soil, decontaminating and decommissioning debris. Assume an average compressed density of $1.6 \times 10^3 \text{ kg m}^{-3}$ (100 lbs ft ⁻³)
ARIR	EG&G Rocky Flats	No applications for disposal prior to 1992 were available for review, but Rocky Flats shipments typically consisted of soil- and cement-stabilized sludge.

The collapse potential of the dumped debris adjacent to the pit walls is not readily quantifiable. Because debris depths vary from nil to full waste height, a collapse potential of 80 percent is assumed as a conservative estimate.

DEPTH OF THE WASTE WITHIN THE PITS AND TRENCHES

The depth of waste in each trench and pit equals the depth of the trench/pit, minus 1.2 m (4 ft). The as-built depths of each of the trenches and pits are given in Figure 3.3.

COMPRESSIBILITY OF THE COVER SOIL OVER THE WASTE

Historically, the cover soil placed over the waste has been dozed into place in a single layer. This practice typically causes future settlement. However, the cover soil will be capped during closure. It is assumed that the cover soil will be compacted during closure cap construction, thereby minimizing subsequent settlement of the cover soil. Therefore, compression of the layer of cover soil is not considered.

Densification of the loosely dumped soil in the deep slots between the trench wall and the waste containers is likely. In these locations, where debris or drums have not been used as infill, a compressibility of 18 percent is expected. This was calculated assuming a densification from 70 to 85 percent relative compaction.

EXPECTED SUBSIDENCE

Expected long-term subsidence for various conditions within a trench or pit has been evaluated. *Figure 3.3* reports the compressibility due to the average void-space within each container; the void space between containers, where appropriate; and other void spaces, as noted, for a variety of container types and configurations. These scenarios only approximate actual conditions, as waste placement methods have varied both over time and between pits.

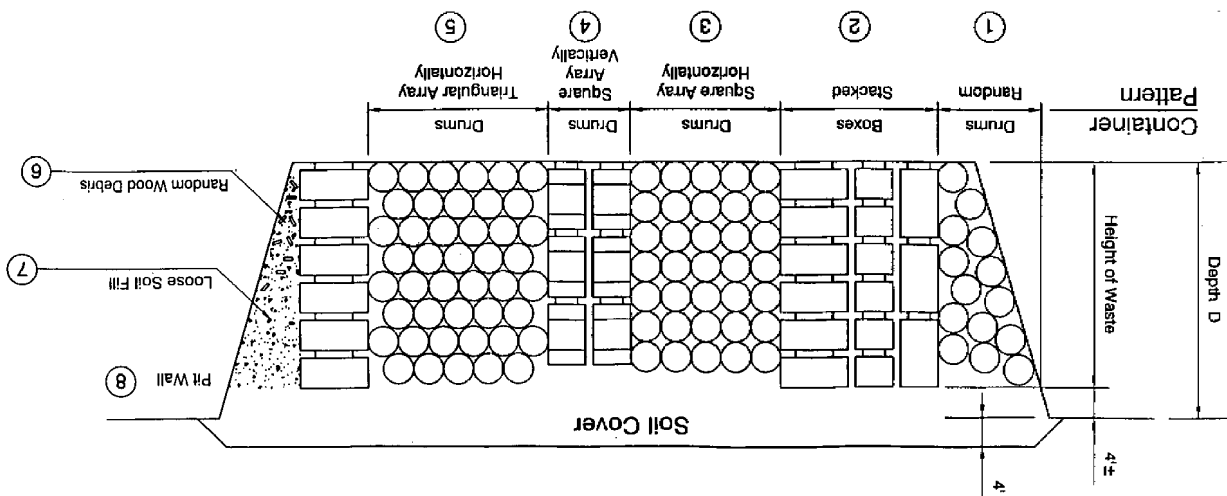
The lower portion of *Figure 3.3* presents the potential subsidence for each container arrangement. In addition, the maximum expected settlement adjacent to the trench wall for debris or soil infilling is given. In general, this is the location where the highest differential settlement is expected, where differential settlement is the difference in settlement between two points divided by the horizontal distance between the points. No settlement is anticipated in the original ground at the trench edge.

Figure 3.3 could be misinterpreted to indicate that subsidence will occur uniformly within a given region of a trench. In reality, subsidence will vary with each waste stream and container type within each trench. Waste will contain “hard spots,” which will settle substantially less than average, and “soft spots,” which will settle substantially more. Variations from predicted subsidence of 20 percent or more should be expected.

This Page Intentionally Left Blank

Figure 3.3 Table of Expected Subsidence

Compressibility of Container	Pre-1990				Post-1990			
	①	②	③	④	⑤	⑥	⑦	⑧
Pre-1990	64%	64%	64%	64%	64%	N/A	N/A	0
Post-1990	45%	45%	45%	45%	45%	N/A	N/A	0
Void Space								
Pallet	N/A	Included	N/A	13%	N/A	80%	18%	0
Other	9%-30%	—	22%	22%	9%	80%	80%	0
Total Void Space (rounded)								
Pre-1990	70%	65%	70%	75%	65%	80%	20%	0
Post-1990	55%	45%	55%	65%	50%	80%	80%	0



Pit/Trench No.	Operation Dates	Depth	Height of	①	②	③	④	⑤	⑥	⑦	⑧
P01U	1978-1983	28'	24'	17'	16'	17'	18'	19'	5'	0	0
P02U	1985-1987	25'	21'	15'	14'	15'	16'	17'	4'	0	0
P03U	1987-Present	30'	26'	14'-18'	12'-17'	14'-18'	17'-19'	13'-17'	21'	5'	0
P04U	1988-1995	20'	16'	9'-11'	7'-10'	9'-11'	10'-12'	8'-10'	13'	3'	0
P05U	1995-Present	22'	18'	10'	8'	10'	12'	9'	14'	4'	0
P06U	1994-Present	48'	44'	24'	20'	24'	N/A*	22'	N/A**	9'	0
T01U	1961-1965	15'	11'	7'	7'	7'	8'	7'	9'	2'	0
T02U	1972-1978	15'	11'	7'	7'	7'	8'	7'	9'	2'	0
T03U	1992-Present	15'	11'	6'	5'	6'	7'	5'	9'	2'	0
T04U	1970-1978	15'	11'	7'	7'	7'	8'	7'	9'	2'	0
T06U	1965-1970	15'	11'	7'	7'	7'	8'	7'	9'	2'	0
T07U	1978-1979	15'	11'	7'	7'	7'	8'	7'	9'	2'	0
T08U	New	24'	7'								
T09C	1960-1969	15'	11'	7'	7'	7'	8'	7'	9'	2'	0
T09C	1960-1969	15'	11'	7'	7'	7'	8'	7'	9'	2'	0
T09C	1995-Present	15'	11'	6'	5'	6'	7'	5'	9'	2'	0
T09C	1995-Present	15'	11'	6'	5'	6'	7'	5'	9'	2'	0
T09C	1995-Present	15'	11'	6'	5'	6'	7'	5'	9'	2'	0

*This stacking arrangement will not be used in this pit.
 **Wall slope flattened; debris will not be stacked to full height.

$$Q_j = D_{ej} \times \left(\frac{C_{0j}}{z} \right) \times A \quad (3.3)$$

where:

- D_{ej} = effective diffusion coefficient of radionuclide j, in pore spaces, $\text{m}^2 \text{yr}^{-1}$;
 C_{0j} = initial air concentration of radionuclide j in the pores of the waste zone, Ci m^{-3} ;
 z = mean diffusion length, m; and
 A = area of the disposal unit, m^2 .

The expression above represents a maximum release rate because it assumes that the initial inventory is immediately available for release and that it is not significantly depleted over a year of release. Realistically, depletion due to volatilization may greatly alter the concentration in the waste during a period of one year.

To estimate C_{0j} for ^3H and ^{14}C , the chemical form of these radionuclides in the waste form must be taken into account. Tritium released to the pores of the waste form is assumed to be water vapor (i.e., HTO). This assumption is conservative because the dose conversion factor for inhalation of HTO is many orders of magnitude greater than that for HT. A significant fraction of the source term is HTO, and much of the HT released will be oxidized to HTO in the soil pore water before reaching the atmosphere. Therefore, this assumption is believed to be conservative. Carbon-14 is assumed to be solely associated with gaseous CO_2 in the air-filled pores. This is a conservative assumption because numerous carbon compounds are expected to exist in the waste and subsurface environment, all of which would compete with CO_2 for the available ^{14}C . The ^{14}C inventory received to date originates from research laboratories (*Figure 2.41*) and is believed to be in a relatively labile form (i.e., not activated metal).

To estimate the air concentration of HTO at the source, $C_{0,\text{H-3}}$, the concentration of ^3H in the pore water is assumed to equal its concentration in water vapor. The amount of water vapor, and thus HTO vapor, in the pores is a function of temperature and relative humidity. At 100 percent relative humidity, which can be assumed for the pores due to the presence of residual water, the concentration of water vapor, $C_{\text{v,H}_2\text{O}}$ in g m^{-3} , was estimated from:

$$C_{\text{v,H}_2\text{O}} = 10^3 \frac{P_v}{RT} \times MW \quad (3.4)$$

where:

- 10^3 = unit conversion factor, L m⁻³;
- P_v = vapor pressure at given temperature, atm;
- R = gas constant (0.082 L-atm/mol-°K);
- T = temperature, °K ; and
- MW = molecular weight of water, 18 g mol⁻¹.

Assuming a subsurface temperature of about 283 °K (10 °C [50 °F]), corresponding to a vapor pressure of water of 1.2×10^{-2} atm (9.21 mm Hg), the concentration of water vapor in the voids is approximately 0.2 g m⁻³.

diffusivity in soils to the unhindered diffusivity in air. The diffusion coefficient of water vapor in air is approximately $754 \text{ m}^2 \text{ yr}^{-1}$ (CRC, 1981); thus, the effective diffusion coefficient for water vapor in soil is approximately $136 \text{ m}^2 \text{ yr}^{-1}$.

Using a pore gas ^3H concentration of $9.4 \times 10^{-5} \text{ Ci m}^{-3}$ in Equation 3.3, an average diffusion path length of 4.9 m (16.1 ft) (the 2.4-m [7.8-ft] soil cover plus one-half of the total waste compartment depth of 4.9 m [16.1 ft]), a total disposal area of $7.5 \times 10^4 \text{ m}^2$, and a diffusion coefficient for water vapor in soil of $136 \text{ m}^2 \text{ yr}^{-1}$, the maximum release rate of HTO to the atmosphere at closure is estimated to be 200 Ci yr^{-1} . This is an extremely conservative value due to the simplified computational approach not accounting for the first-order dependence of the release rate on the pore water concentration and the assumption that HTO diffuses

Table 3.13 Summary of Parameters Used to Estimate Release Rates of Volatile Radionuclides

Module	Parameter Description	Value Assumed	Source of Value Selected
Diffusion	D_{aj} , Diffusion Coefficient in Air, $m^2 yr^{-1}$	3H 754 ^{14}C 440	CRC, 1981 CRC, 1981
	ϵ , Porosity of Upper Vadose Zone Soils, Dimensionless	0.36	REECo, 1993c
	θ_v , Volumetric Water Content of Upper Vadose Zone Soils, Dimensionless	0.086	REECo, 1993c

Subsidence is expected to cause the temporary formation of cracks and fissures in the closure cap. Gaseous diffusion of HTO in cracks was accounted for by assigning a free-air diffusion coefficient. Ten percent of the cap was assumed to be cracks at any given time. Any subsidence occurring during the period of active institutional control was assumed to be remediated. Therefore, increased gaseous 3H releases are not expected to occur before 100 years after closure.

Depressions formed by sudden collapse of the cap and slumping of surrounding materials into the depression could potentially thin the closure cap. Soil settling into voids between packages could also cause cap thinning. These processes are not expected to occur uniformly over the cap. However, the fraction of the cap that will be affected is unknown. It was conservatively assumed that 25 percent of the cap would collapse and that the thinning would be proportional.

Adopting the assumptions above, the diffusion length becomes 4.2 m (14 ft) over the entire cap and the diffusion coefficient becomes $754 m^2 yr^{-1}$ over 10 percent of the cap. With the assumptions above, the 3H release rate is unchanged at closure, but increases from 0.89 to 1.0 Ci yr^{-1} at the end of active institutional control.

3.2.2.3 Base Case Conceptual Model for Radon Transport

Radon is a noble gas produced by the radioactive decay of radium. Three isotopes of radon (^{219}Rn , ^{220}Rn , and ^{222}Rn) can be generated by LLW. Radon produced in buried LLW may be transported to the atmosphere by diffusion through the soil pore space and by advection of soil pore gas to the atmosphere. This section describes the conceptual model for radon transport.

Radon transport is assumed to occur within uniform regions representing the cap, buried waste, and the alluvium below the waste cell. These regions are assumed homogeneous and isotropic with respect to all properties. Natural soils are a three-phase, porous medium

consisting of air-filled pores, water-filled pores, and the solid soil matrix. Radon is transported to the atmosphere by molecular diffusion in the air-filled pore space and advective flow of the soil pore gas to the atmosphere (Nazaroff, 1992; Rogers and Nielson, 1991a). Processes that may retard or reduce radon transport are adsorption onto solid surfaces, adsorption into the liquid phase, and radioactive decay (Nazaroff, 1992; Rogers and Nielson, 1991a).

The conceptual model assumes that the fate of radon within any representative elementary volume is governed by molecular diffusion, advection, and radioactive decay in the gas phase only. Diffusion and advection of radon will be retarded in the water-filled pore space relative to the air-filled pores. Transport will be retarded further by adsorption of radon onto the solid soil matrix. Therefore, it is conservative to assume that radon transport is limited to the gas phase (Rogers and Nielson, 1991a). Molecular diffusion of radon within the air-filled pore space can be represented by Fick's Law:

$$J_D = -D \frac{\partial C(x,t)}{\partial x} \quad (3.7)$$

where:

- J_D = mass flux of radon transported by diffusion, $\text{kg m}^{-2} \text{s}^{-1}$;
- D = diffusion coefficient of radon in soil, $\text{m}^2 \text{s}^{-1}$; and
- $C(x,t)$ = mass concentration of radon per volume of pore space, kg m^{-3} .

The flux of radon due to advection can be described by:

$$J_A = \frac{q_{air}}{\epsilon} C(x,t) \quad (3.8)$$

where:

- J_A = mass flux of radon transported by advection, $\text{kg m}^{-2} \text{s}^{-1}$;
- q_{air} = specific discharge of soil pore gas, $\text{m}^3 \text{m}^{-2} \text{s}^{-1}$; and
- ϵ = porosity, dimensionless.

Combining the expressions for the diffusive and advective flux with production and radioactive decay gives the one-dimensional equation of continuity for radon in pore spaces:

$$\frac{\partial C(x,t)}{\partial t} = D \frac{\partial^2 C(x,t)}{\partial x^2} + S_o(x) + S_{sx}(x) - \frac{1}{\epsilon} \frac{\partial (q_{air} C(x,t))}{\partial x} - \lambda_1 C(x,t) \quad (3.9)$$

where:

- $S_o(x)$ = radon production rate per unit volume in air-filled pores of native alluvium, $\text{kg m}^{-3} \text{ s}^{-1}$;
 $S_{sx}(x)$ = radon production rate per unit volume in air-filled pores of waste, $\text{kg m}^{-3} \text{ s}^{-1}$;
 and
 λ_1 = radon radioactive decay constant s^{-1} .

Advection varies in space and time with atmospheric pressure. Pressure-induced changes in the specific discharge velocity can be obtained from Darcy's law:

$$q_{air} = - \frac{\kappa}{\eta} \left(\frac{\partial P}{\partial x} - \rho_{air} g \right) \quad (3.10)$$

where:

- κ = air permeability, m^2 ;
 η = air viscosity, Pascal s¹;
 P = air pressure, Pascal s;
 ρ_{air} = air density, kg m^{-3} ; and
 g = gravitational acceleration, m s^{-2} .

Darcy's law, the relation that $q_{air} = \epsilon V$, where V is the advective velocity, and the ideal gas law can be combined in the mass balance expression:

$$\frac{\partial (\epsilon \rho_{air})}{\partial t} + \frac{\partial (\rho_{air} q_{air})}{\partial x} = 0 \quad (3.11)$$

to obtain an expression for $\partial q_{air} / \partial x$ (see Lindstrom *et al.*, 1992b).

The radon production rate in air-filled pores of native alluvium was determined from field measurements of radon activity concentrations at sufficient depths where advective and

diffusive losses are negligible. Under these conditions, production of radon in the pore space from decay of radium is equal to the radon decay rate. The measured radon activity concentration is converted to a mass production rate as:

$$S_o(x) = Q_o(\infty, t) \frac{M_1}{A} \quad (3.12)$$

where:

$$\begin{aligned} Q_o(\infty, t) &= \text{measured radon activity concentration at depth in soil pore volume,} \\ &\quad \text{m}^{-3} \text{ s}^{-1}; \\ M_1 &= \text{atomic mass of radon, kg; and} \\ A &= \text{Avogadro's number } (6.022 \times 10^{23}) \end{aligned}$$

The radon production rate in air-filled pores of waste is given by:

$$S_{sx}(x) = \frac{(1 - \epsilon)}{\epsilon} \frac{M_1}{M_0} \lambda_0 C_{sx}(x) \quad (3.13)$$

where:

$$\begin{aligned} M_0 &= \text{atomic mass of radium, kg;} \\ \lambda_0 &= \text{radium radioactive decay constant, s}^{-1}; \text{ and} \\ C_{sx}(x) &= \text{radium mass concentration in waste, kg m}^{-3}. \end{aligned}$$

Although the conceptual model does not explicitly include an emanation coefficient, the equation for the waste source term (Equation 3.13) implies that the emanation coefficient is numerically equivalent to $(1 - \epsilon)$.

The radon conceptual model is implemented in the CASCADR9 computer code (Lindstrom *et al.*, 1992b; Cawfield *et al.*, 1993b). Briefly, continuity is assumed at the soil-atmosphere and waste-soil interfaces for radionuclide flux, radionuclide concentration, advective velocity, and barometric pressure. A 0.1-m (0.32-ft) atmospheric mixing layer is assumed to be present at the soil-air interface (Lindstrom *et al.*, 1993a). The eddy diffusivity of the atmospheric mixing layer varies within a 24-hour period. At the soil atmosphere boundary,

pressure data sets have shown that radon flux reaches a nearly steady-state condition after 10 to 20 days depending on the depth of burial. This can be confirmed by observing that the cumulative radon flux becomes approximately linear in 10 to 20 days. Therefore, model runs were performed with 40 days of barometric pressure data collected from Julian day 110 to 150. This period included the greatest pressure fluctuations in the data set. The average annual flux is taken as the average flux observed on day 39. The average flux is calculated as the difference in cumulative flux (pCi m^{-2}) between the end and the beginning of the 24-hour period divided by the number of seconds in 24 hours. Soil and waste radon source terms are assumed to be constant during the 40-day simulation. The model output is used to obtain a ratio between waste cell concentration and flux at the air-soil interface. Because the flux is a linear function of the waste-cell concentration, flux can be predicted based on the waste-cell concentration. Parameter values used for the radon model appear in Table 3.14. The porosity and air permeability of soil are best estimate values from near-surface site characterization studies (REECo, 1993c). The diffusion coefficient in soil is empirically derived from soil porosity. The porosity and air permeability of the waste are unknown and conservative values were selected.

Table 3.14 Parameters Used in the Radon Transport Model CASCADR9

Layer	Domain	Porosity ϵ ($\text{m}^3 \text{m}^{-3}$)	Diffusion Coefficient D ($\text{m}^2 \text{s}^{-1}$)	Air Permeability κ (10^{-12}m)
Shallow Land Burial Cell				
Cap	0 to -2.4 m	0.36	2.2×10^{-6}	1
Waste	-2.4 to -7.3 m	0.67	5.5×10^{-6}	200
Thorium Waste Cell (P06U)				
Cap	0 to -2.4 m	0.36	2.2×10^{-6}	1
Waste	-2.4 to -8.6 m	0.67	5.5×10^{-6}	200
Soil Layer	-8.6 to -12.2 m	0.36	2.2×10^{-6}	1
Th Waste	-12.2 to -15.8 m	0.67	5.5×10^{-6}	200

SCREENING OF RADON ISOTOPES

There are potentially three isotopes of radon produced by radioactive wastes. Two isotopes, ^{219}Rn and ^{220}Rn , have half-lives less than 1 minute and can be eliminated by simple screening calculations. The NRC has published a gaseous diffusion model for predicting radon attenuation in soil caps in Regulatory Guide 3.64 (NRC, 1989). For the case where the source term

layer is thick relative to the cap and radon flux attenuation is greater than 10 times in the cap, it can be shown that:

$$\frac{J_c}{J_w} = \frac{2e^{(-x\sqrt{\lambda/D_c})}}{1 + \sqrt{a_w/a_c}} \quad (3.14)$$

where:

- J_c = radon flux from the soil cap, pCi m⁻² s⁻¹;
- J_w = radon flux from the bare waste, pCi m⁻² s⁻¹;
- x = cap thickness, m;
- λ = radon decay constant, s⁻¹;
- D_c = radon diffusion coefficient for cap soil, m² s⁻¹;
- a_w = waste interface constant, m⁻² s⁻¹; and
- a_c = cap interface constant, m⁻² s⁻¹.

The general formula for the interface constants is:

$$a = \epsilon^2 D [1 - (1 - k)m]^2 \quad (3.15)$$

where:

- ϵ = porosity, dimensionless;
- D = diffusion coefficient, m² s⁻¹;
- k = partition coefficient for radon gas in water, dimensionless; and
- m = moisture saturation fraction, dimensionless.

Assuming parameter values as given in *Table 3.14* for soil and waste, a partition coefficient of 0.26 (NRC, 1989), and a saturation fraction of 0.24 (REECo, 1993c), the radon attenuation (J_c/J_w) can be calculated for several cap thicknesses (*Table 3.15*).

Based on these results, it can be concluded that ²¹⁹Rn and ²²⁰Rn can be neglected for all cases where a soil cap or building foundation is present between the source and the receptor.

Table 3.15 Approximate Attenuation of ^{219}Rn and ^{220}Rn Fluxes in Soil Caps

Cap Thickness	Radon Flux Attenuation (J_c/J_w)	
	^{219}Rn	^{220}Rn
0.03 m	0.0001	0.07
0.1 m	3×10^{-13}	0.001
1 m	2×10^{-123}	9×10^{-28}

3.2.2.4 Subsided Case Conceptual Model for Radon Transport

The conceptual model for radon was modified by assuming a free air diffusion coefficient for cracks occurring over 10 percent of the closure cap. Cracks were assumed to be present over the period when subsidence was active. This period was assumed to be 100 to 1,000 years. The free-air diffusion coefficient was assumed to be $1.1 \times 10^{-5} \text{ m}^2 \text{ s}^{-1}$ (Rogers and Nielson, 1991b). Cap thinning was assumed to occur over the entire interval evaluated.

3.2.2.5 Base Case Parameters for Nonvolatile Radionuclides

The release scenario includes three processes affecting nonvolatile radionuclides: plant uptake, bioturbation, and resuspension of surface soil. This section summarizes the parameter estimation for these processes.

ROOT UPTAKE RATE COEFFICIENT

In Section 2.7, the natural flora of the NTS was described. The plant community surrounding the Area 5 RWMS is a *Larrea - Ambrosia* community characteristic of the Mojave Desert. The root uptake module incorporates parameters characteristic of this plant community when site-specific data were available.

The maximum rooting depth of native plants at the Area 5 RWMS remains uncertain. All

averaging between 1 to 4 m (3.2 to 13.1 ft). Some of the species noted in this later study also exist at the NTS. Thus, it was assumed that some fraction of the roots of the plants inhabiting Area 5 in the future may penetrate the waste. The fraction assumed (later referred to as F_{rw}) was 5 percent based on the data assembled in a literature review by Foxx *et al.* (1984),

The depth of the subsurface soil compartment illustrated in *Figure 3.5* is assumed to be 1.4 m (4.6 ft) which is the remaining depth of soil from the base of the shallow soils compartment to the top of the waste compartment. As with the shallow soils compartment, this compartment is assumed to be well mixed as a result of uptake by, and decay of, plant roots in the subsurface soil and by the action of burrowing animals.

The effective depth of the waste compartment is the depth of penetration of plant roots into the waste layer. The maximum credible rooting depth for plants occurring at Area 5 was assumed to be 4 m (13.1 ft), based on the best available data (Foxy *et al.*, 1984). A 4-m- (13.1-ft)-deep plant root would allow access to a 1.6-m (5.2-ft) layer of waste and 2.4 m (7.9 ft) of cover material (*Figure 3.5*). The effective depth of the waste compartment was rounded up to 2 m (6.6 ft), giving a maximum rooting depth of 4.4 m (14.4 ft).

The rate coefficients, $K_{r1,j}$, $K_{r2,j}$, and $K_{r3,j}$, quantify the rate of plant-mediated transfer of radionuclides from the waste to the overlying soils (*Figure 3.5*). These coefficients represent the fraction of radionuclides in the waste compartment that are transferred to either the shallow soils or subsurface soil compartment annually and thus represent fractional release rates. Estimates of these release rates were obtained by assuming that the uptake rate is

directly proportional to the measured concentration ratios between plants and soils and to annual biomass production rates. Radionuclides taken up by plants each year are assumed released back to the shallow and subsurface soils compartment as a result of biomass decay.

The rate coefficient describing root transport of radionuclides from the waste compartment to

Baes *et al.* (1984) and Ng *et al.* (1982) were the primary sources for the plant-soil concentration ratios, B_{jv} , defined as the ratio of the concentration per dry mass of plant roots, shoots, and leaves ($C_i \text{ g}^{-1}$) to the concentration per dry mass of soil ($C_i \text{ g}^{-1}$). For elements with mean B_{jv} values for nonreproductive portions of crops reported by both references, the higher of the two values was adopted. The values assumed are listed in Table E.1 of Appendix E. Site-specific values were used when available, as was the case for a few radionuclides. However, most of the NTS data were collected without distinguishing between the contribution of root uptake and atmospheric deposition on plant surfaces. The later route, atmospheric deposition, is reported to be extremely important at the NTS due to easy resuspension of the exposed dry soils and xeriphytic plant adaptations (resins, hair) that effectively trap soil particulates (Gilbert *et al.*, 1988; Romney *et al.*, 1981). Therefore, the site-specific values assumed were selected from greenhouse studies rather than field studies, when available. Deposition of radionuclides on plants was described in a separate module described below.

The value of B_p , defined as the yearly aboveground production of plants, was assumed to be 40 g m^{-2} . This is an approximate mean value for net primary productivity for perennial shrubs in the vicinity of Area 5 and is discussed in Section 2.7.1.

The ratio of aboveground to belowground productivity, B_{ab} , was estimated from biomass distribution between roots and shoots. Root productivity data were not available for the shrub communities of interest. Using the root-to-shoot biomass ratios requires the assumption that biomass ratios are similar to productivity ratios for above- and belowground biomass. While quite variable between species, time of year, and age of plants, the biomass ratio between roots and shoots varies between about 0.6 and 2.3 for vegetation native to the Mojave Desert (Wallace *et al.*, 1974). A representative mid-range value of 1.0 was assumed for B_{ab} .

The fraction of vegetation with roots which penetrate into the waste compartment, F_{rw} , and the maximum depth of the waste compartment that may be penetrated by roots, H_w , were discussed earlier and were assigned respective values of 0.05 and 2 m (0.16 and 6.5 ft). The dry bulk density assumed for soil and waste is $1.6 \times 10^6 \text{ g m}^{-3}$ based on data collected in the Science Trench Borehole Study (REECo, 1993c).

Plant roots not penetrating the waste compartment were assumed to be uniformly distributed in the cap. This assumption is made in lieu of site-specific data for vertical distribution of root biomass of native or introduced species at the NTS. Therefore, the fraction of perennial shrub roots assumed present in the shallow soils compartment, F_{rs} , is 0.42. The value of 0.42 is based on the assumed 1-m (3.3-ft) depth of the shallow soils compartment relative to the total 2.4-m (7.87-ft) depth of the overlying soil column.

The coefficient K_{r2} represents the transfer of radionuclides from the waste compartment to the subsurface soil compartment. This coefficient is estimated from:

$$K_{r2j} = B_{jv} \times \frac{B_p}{B_{ab}} \times F_{ru} \times F_{rw} \times \frac{1}{H_w} \times \frac{1}{\rho_b} \quad (3.17)$$

where F_{ru} is the fraction of deep-rooted shrub roots in the subsurface soils compartment. The

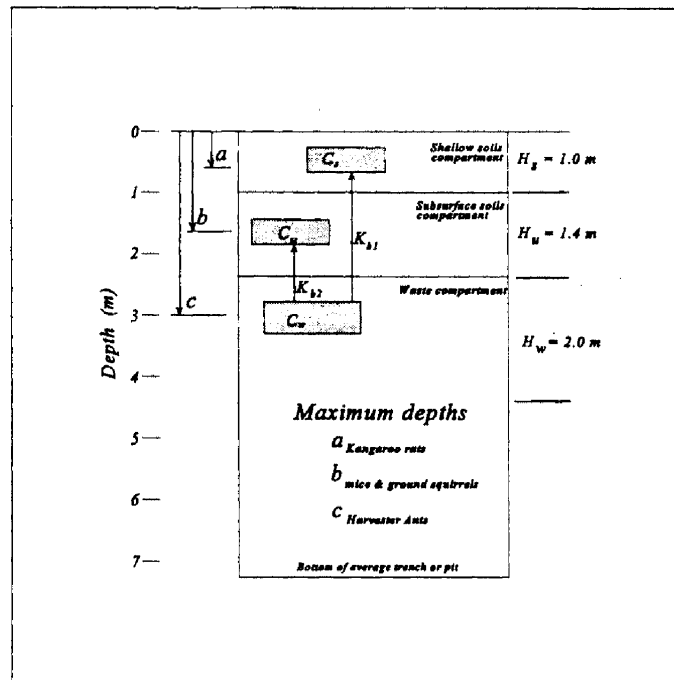


Figure 3.6 Conceptual Model of Burrowing Animal Transport

1979; Blom *et al.*, 1991a). Harvester ants occur on the NTS, but there is no data specific to the NTS. Although other burrowers (predominantly rodents) exist in Area 5 (Section 2.7.2), the burrows tend to be shallow relative to those of ants and to the depth of the waste form. As indicated in Table 2.13, the rodent population near the Area 5 RWMS is reported to include kangaroo rats, a few species of mice, and ground squirrels with densities ranging from 5×10^{-6} to 3×10^{-3} individuals m^{-2} . Anderson and Allred (1964) report that kangaroo rats burrow no deeper than 0.6 m (1.9 ft) at the NTS and burrow depths for kangaroo rats, mice, and ground squirrels at the INEL are reported to be less than 1.4 m (4.6 ft) (Reynolds and Laundré, 1988; DOE, 1983). Thus, the actions of burrowers other than ants are assumed to redistribute the soil within compartments and are not considered explicitly in the conceptual model for burrowing animals. Soil movement between the shallow and subsurface soil compartments was not considered.

The rate coefficient K_{b1} represents the transfer of radionuclides from the waste to the shallow soil compartment through the actions of burrowing ants. The amount of excavated soil transferred to the shallow surface soil compartment is assumed to be proportional to the depth of the shallow soil compartment relative to the depth of the cover. The value of K_{b1} can be calculated from:

$$K_{bi} = \frac{1}{\rho_b} \times A_b \times D_d \times \frac{1}{H_w} \times \frac{H_s}{H_u + H_s} \quad (3.20)$$

where:

- A_b = amount of soil excavated by each ant colony in the waste zone, g yr⁻¹;
- D_d = density of burrower (ant colony) that burrows as deep as the waste zone, colonies m⁻², and
- H_s = average depth of the shallow soils compartment, m.

The values of ρ_b , H_w , and H_u are the same as were used in the derivation of transfer coefficients for root uptake.

According to Fitzner *et al.* (1979), the amount of soil excavated by an individual harvester ant colony at the Hanford site ranged from 7.1×10^{-4} to 3.1×10^{-3} m³ over the life of the colony. Assuming a bulk soil density of 1.6×10^6 g m⁻³, this corresponds to a range of 1.1×10^3 to 5.0×10^3 g soil moved. Fitzner *et al.* (1979) also reports an average of 3.8×10^3 g of soil was excavated by harvester ants in eastern Colorado over the life of the colony. With this information, a value of A_b can be estimated if an estimate of the life of the colony can be obtained. Blom *et al.* (1991b) reports that harvester ant species may persist for 17 to 50 years based on data from other locations in the Midwest. Because this value is likely to vary considerably from location to location, a conservative value of 10 years was assumed to obtain a conservative estimate of A_b from the Fitzner *et al.* (1979) data. Assuming the maximum soil movement per colony observed by Fitzner *et al.* (1979) (5.0×10^3 g per lifetime) and a 10-year lifetime, an estimate of A_b of 5.0×10^2 g yr⁻¹ is obtained. Before finalizing the estimate for A_b , the fraction of ant burrows occurring in the waste zone must be considered. Fitzner *et al.* (1979) estimates that 11 percent of soil excavated by ants comes from depths greater than 1.5 m (4.9 ft), although the source of data supporting this estimate is unclear. The value of A_b used in the assessment, 100 g yr⁻¹ excavated per colony, assumes that 20 percent of the soil excavated by a colony comes from a depth greater than 2.4 m (7.8 ft).

Harvester ant colony density, D_d , has been reported by Fitzner *et al.* (1979) at the Hanford site, and Blom *et al.* (1991a) at INEL, to range from 0 to 1.6×10^{-2} colonies m⁻².

An average density of 1×10^{-2} colonies m⁻² was assumed for this assessment. In the equation for K_{bi} , the ratio of the depth of the shallow soils compartment (H_s) to the total depth of the soil column above the waste ($H_u + H_s$) partitions the amount of excavated contaminated soil equally between the two soil compartments on a per-volume basis, as was noted earlier.

The parameter K_{b2} represents the transfer of radionuclides from the waste to the subsurface soils as a result of ant burrows constructed in the waste. Again, in the equation for K_{b2} below, the ratio of the depth of the subsurface soils compartment (H_u) to the total depth of the soil column above the waste ($H_u + H_s$) allows partitioning of the amount of excavated contaminated soil equally between the two soil compartments on a per-volume basis. The transfer rate coefficient K_{b2} was calculated as:

$$K_{b2} = \frac{1}{\rho_b} \times A_b \times D_d \times \frac{1}{H_w} \times \frac{H_u}{H_u + H_s} \quad (3.21)$$

The calculated value of K_{b1} , estimating the fractional annual release rate of any radionuclide, from the waste to the shallow soils compartment, is $1.3 \times 10^{-7} \text{ yr}^{-1}$. The calculated value of K_{b2} , estimating the fractional annual release rate of any radionuclide from the waste compartment to the subsurface soils compartment, is $1.8 \times 10^{-7} \text{ yr}^{-1}$.

RESUSPENSION COEFFICIENT

Contamination of air above the RWMS facility may occur as volatile radionuclides are released, as discussed in the previous section, or when contaminated shallow surface soils are suspended and resuspended by the wind. The rate constant for the resuspension module, representing the fractional average annual loss of radionuclides from the shallow soils compartment, is estimated from a review by Layton *et al.* (1993) of calculated resuspension rates for the NTS based on $^{239,240}\text{Pu}$ data. The assumed value of the resuspension rate for this module is $1 \times 10^{-4} \text{ yr}^{-1}$, selected from a range of 3.15×10^{-5} to $3.15 \times 10^{-4} \text{ yr}^{-1}$.

3.2.2.6 Subsided Case Parameters for Nonvolatile Radionuclides

The nonvolatile radionuclide release parameters were modified for the subsided case by assuming the cap thickness was reduced by 25 percent and that annual aboveground perennial shrub biomass productivity increases. Cap thinning was assumed to reduce the cap thickness to 1.8 m (5.9 ft). The shallow soils compartment was assumed to remain 1 m (3.3 ft) thick. Subsurface soil compartment depth decreases to 0.8 m (2.6 ft) and the rooting depth in the waste increases to 2.2 m (7.2 ft). The fraction of roots reaching the waste was assumed to

3.2.2.7 Summary of Parameters for the Base Case and Subsided Case Conceptual Model for Nonvolatile Radionuclides

The previous sections describe the development of rate coefficients for the base case and subsided case conceptual model of nonvolatile radionuclide release. The parameters, assumed values, and sources are summarized in Table 3.16.

Table 3.16 Parameters Used to Estimate Transfer Rate Coefficients for Nonvolatile Radionuclides

Module	Parameter Description	Base Case	Subsided Case	Source
Root Uptake	B_{ab} , Ratio of Above- to Below-ground Productivity for Shrubs, g yr^{-1} above per g yr^{-1} below	1	1	Wallace <i>et al.</i> , 1974
	B_{jv} , Radionuclide-Specific Plant-Soil Concentration Ratio	Table E.1	Table E.1	see Table E.1
	B_p , Annual Perennial Shrub Biomass Productivity (aboveground) $\text{g dry wt m}^{-2} \text{yr}^{-1}$	40	70	Romney and Wallace, 1979; Bamberg <i>et al.</i> , 1976; Strojan <i>et al.</i> , 1979; Hunter <i>et al.</i> , 1980
	F_{rs} , Fraction of Perennial Shrub Roots in the Shallow Soils Compartment	0.42	0.55	Based on Assumption that Root Mass Evenly Distributed in Cap
	F_{rw} , Fraction of Perennial Shrub Roots in the Subsurface Soils Compartment	0.53	0.35	Based on Assumption that Root Mass Evenly Distributed in Cap
	F_{rw} , Fraction of Perennial Shrubs with Roots in Waste	0.05	0.10	Foxx <i>et al.</i> , 1984
	H_s , Depth of the Shallow Soils	1	1	Depth Chosen to Represent Maximum Rooting Depth of

Table 3.16 (continued)

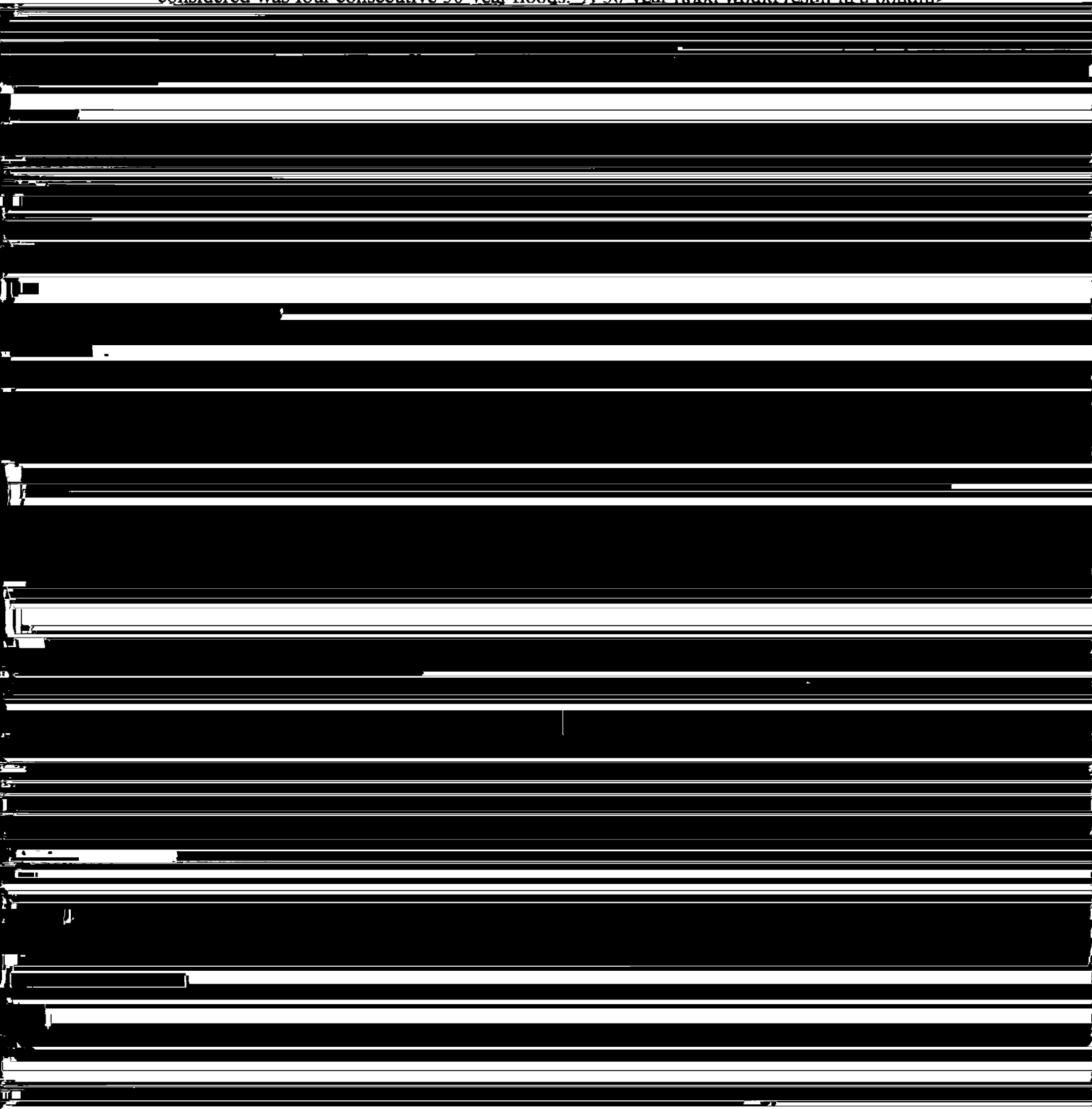
Module	Parameter Description	Base Case	Subsided Case	Source
Root Uptake (Continued)	H_w , Depth of the Waste Accessible to Roots and Burrowing Animals, m	2	2.2	Foxx <i>et al.</i> , 1984
	ρ_b , Bulk Density of Soil, g m ⁻³	1.6×10^6	1.6×10^6	REEC Co, 1993c
Burrowing Animals	A_b , Amount of Soil Excavated by Each Ant Colony in the Waste Zone, g yr ⁻¹	100	100	Fitzner <i>et al.</i> , 1979
	D_a , Density of Ant Colonies, colonies m ⁻²	0.01	0.01	Blom <i>et al.</i> , 1991a; Fitzner <i>et al.</i> , 1979

- A_{uj} = activity of radionuclide j in subsurface soil, C_i ;
- A_{wj} = activity of radionuclide j in waste accessible to biointruders, C_i ;
- B_j = branching ratio from parent to radionuclide j , dimensionless;
- K_{r1j} = fractional root uptake rate for radionuclide j from the waste compartment to the shallow soils, yr^{-1} ;
- K_{r3j} = fractional root uptake rate for radionuclide j from the subsurface soil compartment to the shallow soils, yr^{-1} ;
- K_{bl} = fractional transfer rate for radionuclides from the waste compartment to the shallow soils, based on burrowing animal activity (radionuclide-independent), yr^{-1} ;
- λ_{rj} = radioactive decay constant for radionuclide j , yr^{-1} ; and
- K_s = resuspension rate, yr^{-1} .

The concentration of radionuclide j in the shallow soils compartment, C_{sj} , is estimated by dividing that compartment's total activity by the product of its volume and the soil density. The volume of the shallow soils compartment, V_s , is the surface area of all trenches and pits

where $A_{w,j-1}$ is the activity of the parent of radionuclide j in the waste compartment. The initial activity in the accessible waste compartment is the total inventory which is accessible

In addition to the occurrence of three consecutive 200-year floods, a more frequent, but less intense, event with the same probability of occurrence was also considered. The event considered was four consecutive 50-year floods. A 50-year flood would result in a ponding



A flood assessment was performed at the Area 5 RWMS to determine the 2-, 10-, and 100-year peak discharges (Schmeltzer *et al.* 1992). The hydrographs from these events were

Values of parameters describing the weather conditions (i.e., temperature, relative humidity, effective eddy diffusivity at the boundary layer) were chosen to represent typical values that were held constant throughout the simulation. Although these parameters exhibit diurnal, as well as seasonal variations, it was not necessary to model these. The movement of the wetting front is largely governed by the magnitude and frequency of the ponding and, as long as the weather parameters reasonably represent the average conditions, they do not greatly affect its movement.

The measured matric potentials in the analyzed soil column were used for the initial condition with zero pressure at the water table.

Variations in saturation or pressure versus depth over time identify the wetting front as it advances downward. The wetting front has a transition zone, ending where the initial conditions remain unaffected. For consistency, a point of maximum saturation at the beginning of the front was chosen to define the location of the front at any time.

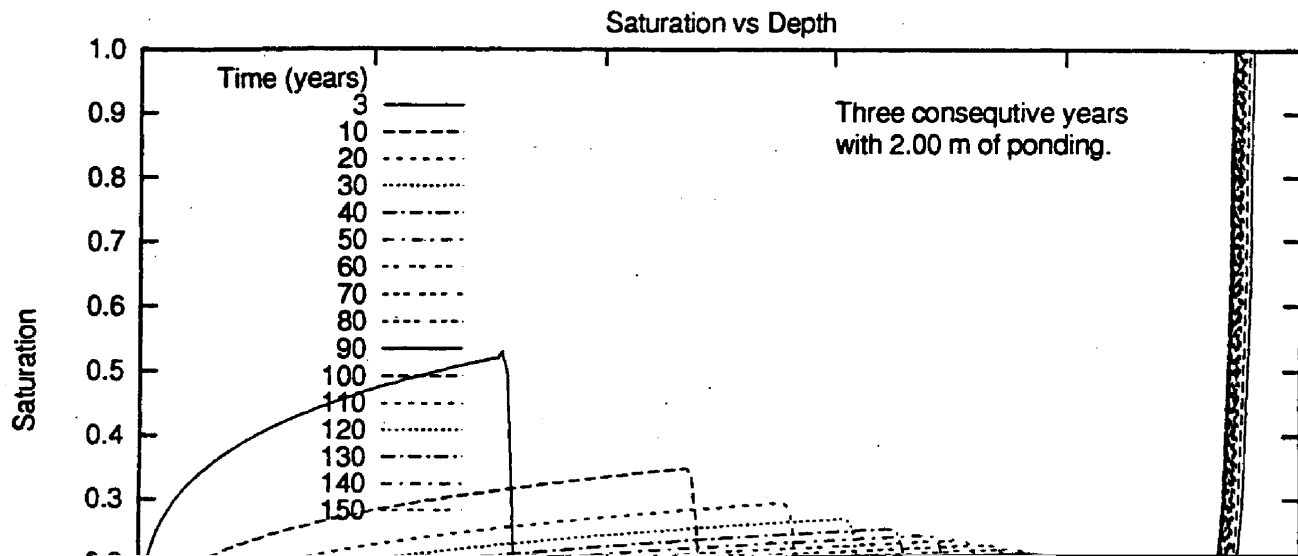
For the case of three consecutive years with 2 m (6.6 ft) of hypothesized ponding, the wetting front would reach the water table in about 140 years and would recharge the water table at an initial rate of about 1.9 cm (0.75 in) per year. The movement of the wetting front is shown in Figure 3.7. Recharge would continually decline thereafter, unless another sequence of significant ponding occurs.

In the case of four consecutive years with 1.07 m (3.5 ft) of hypothesized ponding, the wetting front was found to advance more slowly, and to recharge the water table at a slower rate than in the preceding case. The movement of the wetting front is shown in Figure 3.7.

The case with 2 m (6.6 ft) of ponding was chosen for groundwater pathway analysis because it leads to greater recharge. The recharge to the water table for this case is shown in Figure 3.8.

3.2.2.10 Saturated-Zone-Flow and Capture-Zone Analysis

Groundwater flow was simulated under the assumption that a groundwater extraction well, located at 100 m (320 ft) from the site was pumping $48.1 \text{ m}^3 \text{ day}^{-1}$ ($1700 \text{ ft}^3 \text{ day}^{-1}$ or 8.8



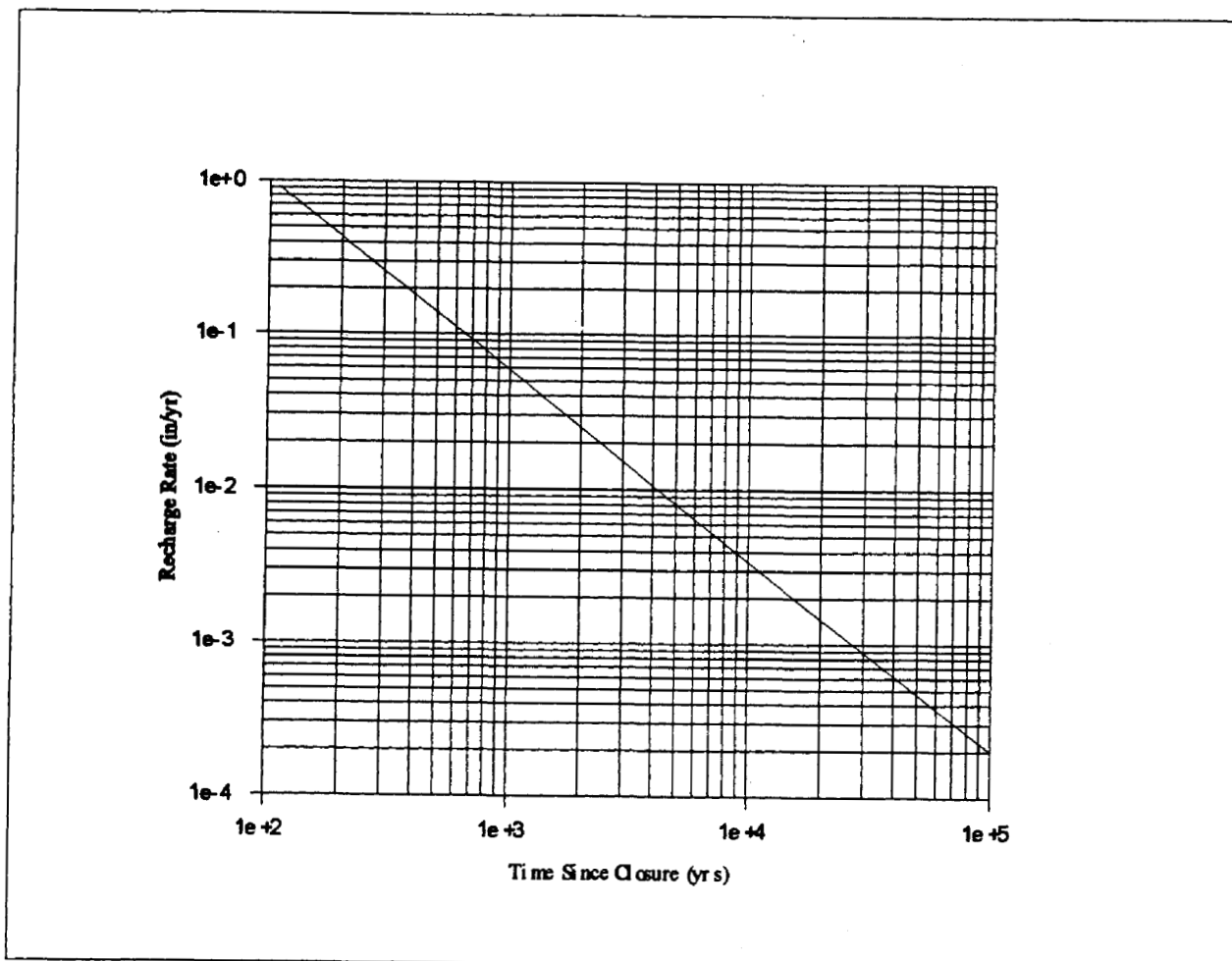


Figure 3.8 Recharge of the Uppermost Aquifer Over Time After Four Consecutive 1.07-m-Deep Ponding Events in a Subsidence Feature

Table 3.18 Assumed Alluvial Aquifer Parameters

Thickness	~183 m	600 ft
Hydraulic conductivity	$10^{-3} \text{ cm s}^{-1}$	2.8 ft day^{-1}
Specific yield	0.27	
Porosity	0.4	

From the onset of recharge to the water table to any given time, which is taken as the time of travel in the saturated zone, varying fractions of the area representing the area of recharge (footprint of the cap) would be captured by the pumping well. The capture zone at any time within the recharge area was delineated using MODPATH, and its area was used to calculate the dilution ratio as follows. For any given time, the average recharge from the onset of

recharge to the given time was first estimated from *Figure 3.8*. The average recharge rate was then multiplied by the area of the capture zone within the recharge area, and the resulting quantity was divided into the pumping rate to yield the average dilution ratio for that time. If a radionuclide moves with water ($K_d=0$), this is the dilution it would experience because the contaminated area at any time represents a fraction of the total area affected by pumping. For radionuclides with non-zero K_d , the procedure is the same except that the times used in the previous calculation are to be interpreted as retarded times obtained by multiplying the unretarded times by the respective retardation factor for the radionuclide in question. The estimated dilution ratios at selected times are presented in Table 3.19. Note that the "Total Travel Time" is the sum of the travel time in the vadose zone (about 140 years for $K_d=0$) and the time of travel in the saturated zone.

Table 3.19 Dilution Ratios and Recharge Over Time for Several K_d Values

Total Travel Time (yrs)	Percent of Disposal Area Captured	Average Recharge (in yr ⁻¹)	Dilution Ratio
$K_d = 0 \text{ ml g}^{-1}$			
277	2.15	0.49	183.0
414	4.68	0.25	165.0
961	13.80	0.19	74.6
1.51×10^3	33.30	0.14	42.6
2.88×10^3	53.30	0.07	49.3
4.25×10^3	70.00	0.05	53.1
8.36×10^3	85.00	0.03	77.4
5.01×10^4	100.00	0.01	239.0
$K_d = 1 \text{ ml g}^{-1}$			
1.92×10^3	2.15	0.07	1.28×10^3
2.87×10^3	4.68	0.05	822
6.67×10^3	13.80	0.03	466
1.05×10^4	33.30	0.01	577
2.00×10^4	53.30	0.01	361
2.95×10^4	70.00	0.01	275
5.80×10^4	85.00	0.01	226
3.48×10^5	100.00	0.01	1.66×10^3
$K_d = 10 \text{ ml g}^{-1}$			
1.67×10^4	2.15	0.0025	3.58×10^4

2.50×10^4	4.68	0.0025	1.64×10^4
5.81×10^4	13.80	0.0025	5.59×10^3

Table 3.19 (continued)

Total Travel Time (yrs)	Percent of Disposal Area Captured	Average Recharge (in yr ⁻¹)	Dilution Ratio
2.57×10^5	70.00	0.0025	1.10×10^3
5.05×10^5	85.00	0.0025	905
3.03×10^6	100	0.0025	769
$K_d = 100 \text{ ml g}^{-1}$			
1.65×10^5	2.15	0.001	8.94×10^4
2.46×10^5	4.68	0.001	4.11×10^4
5.72×10^5	13.8	0.001	1.40×10^4
8.98×10^5	33.3	0.001	5.77×10^3
1.71×10^6	53.3	0.001	3.61×10^3
2.53×10^6	70.0	0.001	2.75×10^3
4.98×10^6	85.0	0.001	2.26×10^3

RADIONUCLIDE SCREENING ANALYSIS

Radionuclides evaluated in the groundwater pathway were selected based on a screening analysis. The concentration of the leachate, C_{lj} , was conservatively estimated as:

$$C_{lj} = \frac{C_{wj}}{\theta + \rho K_d} \quad (3.25)$$

where:

- C_{wj} = waste activity concentration of nuclide j, Ci m⁻³;
- C_{lj} = leachate activity concentration of nuclide j, Ci m⁻³;
- θ = volumetric water content, dimensionless;
- ρ = bulk density of waste, g cm⁻³; and
- K_d = distribution coefficient, ml g⁻¹.

Because subsidence is most likely to be a near-term process, radionuclides were screened based on the waste activity concentration, C_w , at the time of loss of institutional control. The volumetric water content was assumed to be 0.36. A compacted waste bulk density of 1.6 g cm⁻³ was assumed. Nuclides were assigned conservative K_d values (Table 3.20).

Table 3.20 Assumed Kd Values

K _d (ml g ⁻¹)	Elements
0	H, C, Cl, Tc, I, U
1	Co, Sr, Cs, Ba, Pa
10	Pd, Eu, Pb, Ac, Ra, Np
100	Ni, Zr, Sn, Sm, Bi, Th, Pu, Am, Cm

The concentration of some radionuclides in leachate may be controlled by solubility rather than adsorption. The concentration of radionuclides limited by solubility were estimated by:

$$C_{i,j} = \frac{C_{w,j} S_L}{\sum_{k=1}^n C_{w,k} / Q_k} \quad (3.26)$$

where:

- S_L = solubility limit of the element, g m⁻³;
 $C_{w,k}$ = activity concentration of isotope k in waste, Ci m⁻³; and
 Q_k = specific activity of isotope k, Ci g⁻¹.

The solubility limited concentration was estimated for Ra, Th, U, Pu, and Am using the solubility limits reported by Price *et al.* (1993) for Frenchman Flat groundwater (Table 3.21). Using Equation 3.26, two elements, Th and U, were found to be limited by solubility.

Table 3.21 Solubility Limits of Elements in Frenchman Flat Groundwater

Element	Controlling Phase	Solubility Limit (g m ⁻³)
Ra	RaSO ₄	0.023
Th	Th(OH) ₄	0.14
U	(UO ₂) ₂ SiO ₄ ·2H ₂ O (Soddyite)	0.017
Pu	Pu(OH) ₄	29.4
Am	AmOHCO ₃	0.003

The leachate concentrations obtained were screened based on the dose received by consumption of 730 L yr⁻¹ of leachate. Nuclides causing a dose greater than 1 mrem yr⁻¹ or having progeny that could cause a dose greater than 1 mrem yr⁻¹ were retained. Radionuclides retained for the shallow land burial inventory were ³H, ¹⁴C, ⁹⁰Sr, ¹³⁷Cs, ²³⁸Pu, ²¹⁰Pb, ²²⁶Ra, ²³⁰Th, ²³⁴U, ²³⁸U, ²²⁷Ac, ²³¹Pa, ²³⁵U, ²³⁹Pu, ²³⁷Np, ²⁴¹Pu, ²⁴¹Am, ²⁴⁰Pu, and ²³²Th. A single radionuclide (²³²Th) was retained for the Pit 6 Th inventory.

The remaining radionuclides were screened based on travel times. The travel time in the unsaturated zone, ignoring dispersion, is given by:

$$t_R = t \left(1 + \frac{\rho K_d}{\theta} \right) \quad (3.27)$$

where:

- t_R = retarded travel time in the unsaturated zone, yr; and
- t = travel time, yr.

The travel time was the time for the wetting front to reach the uppermost aquifer, obtained from infiltration modeling (140 years). Nuclides with retarded travel times greater than six half-lives were eliminated. This removed seven nuclides: ³H, ⁹⁰Sr, ¹³⁷Cs, ²¹⁰Pb, ²²⁷Ac, ²⁴¹Am, and ²⁴¹Pu. Nuclides with travel times greater than 10,000 years were also eliminated. The nuclides remaining for groundwater pathway analysis of the shallow land burial inventory are

The concentration of the leachate, $C_1(t)$, was the initial leachate concentration at 100 years decayed over the elapsed travel time. For radionuclides with radioactive progeny, the Bateman equations were solved numerically with the BAT6CHN program (Lindstrom *et al.*, 1990). The dilution ratio is element-specific. For radioactive progeny, dilution factors were selected for the parent if the parent had a lower K_d value, except for Pa. For ^{231}Pa , the activity initially present in the leachate was assumed to have the K_d of Pa. All Pa produced by radioactive decay during travel through the vadose zone was assumed to have the K_d of uranium.

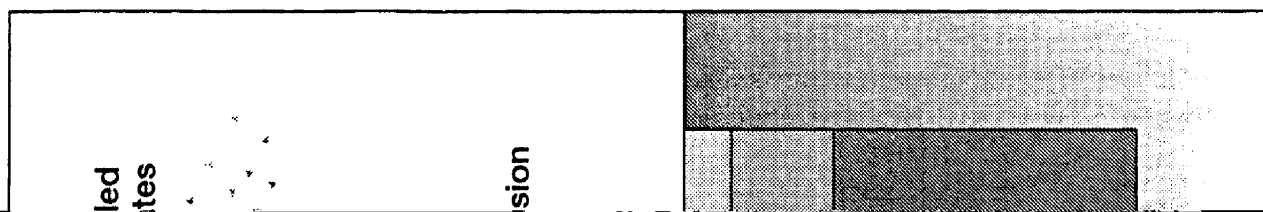
3.2.3 Pathway Scenario Assumptions and Conceptual Models

This section describes the conceptual models and assumptions for the pathway scenarios. The pathway scenarios describe the pathways in the accessible environment which could transfer radionuclides to members of the public. Specifically, these models estimate the concentration of radionuclides in environmental media and the potential doses to humans for the two scenarios considered. Justification of important assumptions are provided.

3.2.3.1 Transient Occupation Scenario

The transient occupation scenario describes potential human exposures to radionuclides released from the RWMS to the accessible environment immediately above the facility. This scenario does not begin until 100 years after closure because it is assumed that active institutional control will exclude members of the public for at least 100 years.

The transient occupation scenario assumes that members of the public may be present at the site, but do not permanently reside at the site or engage in agricultural activities. Review of land-use patterns in southern Nevada indicates that many areas have no permanent residents, but are used on a short-term basis for recreational activities (hunting, camping, prospecting, off-road vehicle use, wildlife observation) and commercial activities (livestock herding, mineral exploration). The transient occupation scenario was developed to account for the possibility that members of the public might use the site for purposes other than agriculture or as a permanent residence. These latter two uses are extremely unlikely for a site without easily obtainable water resources. No specific land-use activity was assumed for the scenario. All the reasonable transient land-use options were assumed to have the same pathways for exposure and therefore were considered to be approximately equivalent. The pathways were assumed to be limited to direct external exposure and inhalation (*Table 3.2*). The pathways operating in the base case release scenario and the transient occupancy scenario are summarized in Figure 3.9. Tritium and ^{14}C can be present in gaseous and nonvolatile forms. Because the partitioning between the two physical states is unknown, doses were calculated assuming that all the activity was present in both forms. The activity concentration of volatile radionuclides (HTO , $^{14}\text{CO}_2$, and ^{85}Kr) in air were calculated



assuming the maximum release rate was released into a 2-m- (6.6 ft-)-high mixing zone over the waste site. The steady state concentration was:

$$C_{g,j} = \frac{Q_j}{H_{mix} U \sqrt{A}} \quad (3.29)$$

where:

- $C_{g,j}$ = activity concentration of gaseous radionuclide j, Ci m⁻³;
- Q_j = activity release rate, Ci yr⁻¹;
- H_{mix} = mixing zone height, m;
- U = mean wind speed, m yr⁻¹; and
- A = area of release, m².

The mean wind speed was assumed to be 2 m s⁻¹ and the area of release was the area of the pits and trenches, 7.5 × 10⁴ m². The mixing height was conservatively assumed to be 2 m (6.6 ft). Calculation of the release rate was described in Section 3.2.2.1.

Methods for calculating the activity concentration of nonvolatile radionuclides in soil were described in the previous section. The concentration of particulate radionuclides in air were

The enrichment factor, E_f , is used to correct for nonuniform concentration among various soil particle size groups. An enrichment factor greater than one indicates that the radionuclides are more concentrated on the resuspendible size fractions (i.e., the concentration of radionuclides on suspended soil is greater than the average concentration over all particle sizes), while a factor less than one indicates that enrichment occurs among less mobile fractions. According to Layton *et al.* (1993), enrichment factors for plutonium aerosols at two locations on the NTS, one of which was in Area 5, were almost unity (0.87 to 1.04). The enrichment factor was assumed to be unity for the estimates of resuspension calculated here.

In addition to the conservative mass loading factor of 10^{-4} g m^{-3} , an additional source of conservatism in the mass loading model is the absence of a correction for area size. The model described by the equation for mass loading does not consider the dilution of the resuspended radionuclides by uncontaminated dust upwind of the Area 5 RWMS. Rather, the model assumes that the source area is sufficiently large to negate such dilution effects. The amount of conservatism added by this assumption is a function of the ratio of the particle

conversion factors for exposure to soil contaminated to various depths. The values selected assume that the contamination is distributed to infinite depth (see Table E.3). Because the shallow soil compartment is 1 m (3.3 ft) deep in this model, assuming an infinite depth of contamination is conservative. Radioactive progeny that could be assumed to be in equilibrium with the parent were accounted for by adding the dose conversion factor of the progeny to that of the parent.

Maximum inhalation doses from particulate radionuclides were calculated from:

$$D_{j,\max}^{inh} = 1920 \times DCF_j^{inh} \times C_{a,j} \quad (3.32)$$

where DCF_j^{inh} is the CEDE conversion factor for inhalation of radionuclide j (DOE, 1988c) and the number 1,920 represents the annual volumetric intake of air by inhalation, in $\text{m}^3 \text{yr}^{-1}$, for a transient occupant assumed to be at the Area 5 RWMS for 2,000 hours per year.

For gaseous radionuclides, the dose was calculated as:

$$D_{j,\max}^{gas} = 1920 \times DCF_j^{inh} \times C_{g,j} \quad (3.33)$$

The dose equivalent from radionuclides listed in *Table 3.5* in italics were calculated using Equation 3.31 and 3.32. The dose conversion factor, DCF_j^{inh} , includes the dose from all progeny produced within the body. A few of the italicized radionuclides in *Table 3.5* have progeny with sufficiently long half-lives and retention times that the dose from inhalation of the progeny is a significant fraction of the dose from the parent. In these cases, the progeny were assumed in equilibrium with the parent and the DCF_j^{inh} of the progeny were added to the value for the parent. Radionuclide dose conversion factors corrected in this fashion were those for ^{93}Zr , ^{126}Sn , ^{210}Pb , ^{227}Ac , ^{229}Th , and ^{237}Np . The ^3H dose conversion factor was multiplied by a factor of 1.5 to account for dermal absorption. Values of dose conversion factors used are listed in Table E.3.

The bounding dose calculations for the transient occupant scenario, based on maximum soil concentrations, indicated that nine radionuclides (^{226}Ra , ^{227}Ac , ^{228}Th , ^{230}Th , ^{231}Pa , ^{234}U , ^{235}U , ^{238}U , and ^{239}Pu) contributed greater than $0.025 \text{ mrem yr}^{-1}$ each to a transient occupant. Only these radionuclides were considered in subsequent dose estimates. For these more significant radionuclides, doses were calculated based on the time-dependant soil and air concentrations generated by solution of Equations 3.22 through 3.24, 3.29 and 3.30. The results of the calculations performed, in terms of peak dose and 10,000-year dose (if the peak occurs after 10,000 years), for each radionuclide are provided in Section 4.1.

3.2.3.2 Open Rangeland Scenario

The open rangeland scenario assumes that a ranch is or will be established at an off-site location with available water after closure of the RWMS. The locations nearest the RWMS with available water are Indian Springs, which is outside the current NTS boundary, approximately 42 km (26 mi) to the southeast; and Cane Spring, which is within the current NTS boundary, approximately 14.3 km (8.9 mi) to the southwest.

Exposure pathways for off-site members of the public include atmospheric transport of volatile or suspended radionuclides from the RWMS, deposition of atmospheric radionuclides on soil and crops at the residence location, and transfer of radionuclides from native vegetation and soil at the RWMS to milk and beef from cattle grazing on site. During the period of institutional control, pathways involving the grazing of cattle over the facility are not considered.

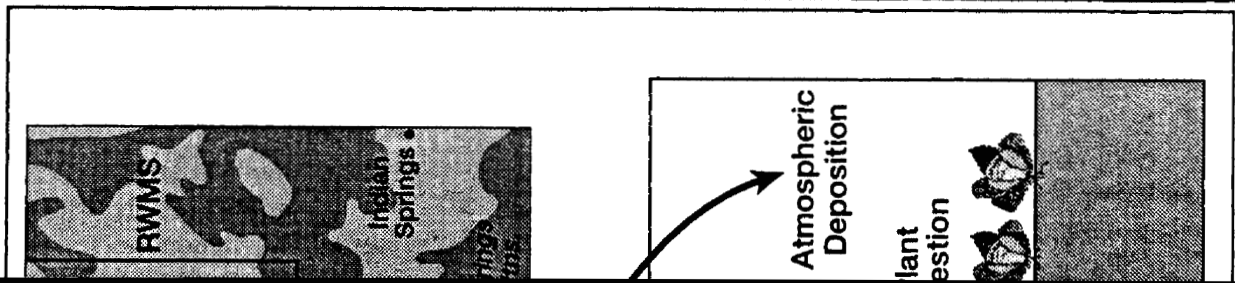
A complete list of the pathways in the conceptual model for the open rangeland scenario is provided in *Table 3.2* and *Figure 3.10*. All of these pathways, with the exception of those for volatile emissions of ^3H , ^{14}C , and ^{85}Kr , are tied to the estimated shallow soil activity, A_{sj} (Equation 3.22). Using these estimated soil activities, the concentration of radionuclides in vegetation and grazing animals at Area 5, and the source of suspended radionuclides to the atmosphere are calculated as described below.

Radionuclide concentrations in native vegetation grown in the cover surface soil compartment of the RWMS are estimated by considering uptake of radionuclides by roots and deposition of suspended soil which is contaminated with radionuclides on plant surfaces. Internal contamination of plants, resulting from root uptake, is expressed as:

$$C_{vj}^{int} = B_{jv} \times \frac{A_{sj}}{V_s} \times \frac{1}{\rho_b} \quad (3.34)$$

where:

- C_{vj}^{int} = internal concentration of radionuclide j in vegetation, Ci g^{-1} ;
- B_{jv} = plant-soil concentration ratio for radionuclide j , Ci g^{-1} dry plant per Ci g^{-1} dry soil;
- A_{sj} = activity of radionuclide j in shallow soil compartment, Ci ;
- V_s = volume of the shallow soils compartment, m^3 ; and
- ρ_b = dry bulk density of soil, g m^{-3} .



Values for B_{jv} are listed in Table E.1. The dry bulk density of soil for Area 5 shallow soils is $1.6 \times 10^6 \text{ g m}^{-3}$ (REECo, 1993c). The soil activity, A_{sj} , is assumed to be that estimated for the shallow soils compartment, according to Equation 3.22. Annual grasses, which are the preferred food of grazing animals in southern Nevada (Section 2.6), are unlikely to have roots exceeding the 1-m (3-ft) depth of the shallow soil compartment. The volume of the shallow soils compartment is assumed to be $7.5 \times 10^4 \text{ m}^3$.

The external contamination of vegetation from deposition of suspended radionuclides on the stems and leaves of plants is estimated from:

$$C_{vj}^{ext} = \frac{V_d \times F_v}{\lambda_w} \times C_{aj} \quad (3.35)$$

where:

- C_{vj}^{ext} = external concentration of radionuclide j on vegetation, Ci g⁻¹;
- V_d = deposition velocity, m yr⁻¹;
- F_v = foliar interception factor, m² g⁻¹ dry vegetation;
- λ_w = weathering constant, yr⁻¹; and
- C_{aj} = suspended air concentration of radionuclide j over the cover soil, Ci m⁻³.

Equations 3.34 and 3.35 are similar to equations used in the NRC Regulatory Guide 1.109 (NRC, 1977) and by Martin and Bloom (1980) for predicting contamination of vegetation, but assume that plant growth and radioactive decay do not decrease the radionuclide concentration in the vegetation.

The deposition velocity in Equation 3.35, V_d , is assumed to be $6.3 \times 10^4 \text{ m yr}^{-1}$ (0.2 cm s^{-1}). This value strongly depends on wind speed and particle size (Martin and Bloom, 1980). Baes *et al.* (1984) assume a value of $3.2 \times 10^4 \text{ m yr}^{-1}$ for coarse suspended matter, citing data by Sehmel (1980).

The foliar interception fraction, F_v , is assumed to be $10^{-3} \text{ m}^2 \text{ g}^{-1}$, a conservative value based on a review of data by Martin and Bloom (1980) specific to the NTS, indicating a mean of about $4 \times 10^{-4} \text{ m}^2 \text{ g}^{-1}$, with a maximum value of $1.1 \times 10^{-3} \text{ m}^2 \text{ g}^{-1}$. The weathering rate, representing the effective rate of loss of radionuclides deposited on plant surfaces, λ_w , is assumed to be 18 yr^{-1} . This is the default value used in the NRC Regulatory Guide 1.109. The value of 18 yr^{-1} corresponds to a weathering half-time of 14 days. Martin and Bloom (1980) suggest that the weathering half-time increases as a function of time, beginning at a value of around one day and increasing to a value more than two orders of magnitude higher

for remaining surficial contamination. However, this type of weathering model was considered too complex to be supported by the data available; thus, the default value of 14 days was adopted.

The concentration in air above the cover soil, C_{aj} , was calculated according to Equation 3.30, using the mass loading approach. Values of A_{sj} were calculated as in Equation 3.22, above.

The open rangeland scenario requires an estimate of radionuclide concentrations in beef and milk from cattle grazing over the Area 5 RWMS. These concentrations were calculated in a manner similar to that used in the NRC Regulatory Guide 1.109. However, radioactive decay occurring between ingestion of forage and consumption of milk or beef was neglected because the radionuclides in *Table 3.7* are long-lived relative to holdup times.

The small area of the RWMS and low productivity of Mojave Desert rangeland combine to limit the grazing potential. In Section 2.6, the number of animal unit months (AUM) per hectare for cattle grazing on native vegetation on Frenchman Flat was estimated to be 0.07 based on considerations of standing biomass and generic forage ingestion rates. Assuming a total contaminated area of $7.5 \times 10^4 \text{ m}^2$, the site represents about 1 AUM. That is, one cow could be sustained by natural forage on the site for one month. Rather than account for the potentially nonsteady-state conditions that would arise for livestock grazing for one or two months on the site, it was assumed that contaminated beef and milk were available year round to the off-site residents. The radionuclide concentration in the beef and milk represents the steady-state concentration for livestock grazing continuously on contaminated areas. It should be emphasized that this is an extremely conservative assumption made to simplify computations.

For milk, the concentration of radionuclide j , C_{mj} in Ci kg^{-1} , is estimated from:

$$C_{mj} = F_{mj} \times \left(I_v \times C_{vj} + I_s \times \frac{A_{sj}}{V_s \times \rho_b} \right) \quad (3.36)$$

where:

- F_{mj} = fraction of daily ingested radionuclide j found in milk, day kg^{-1} milk;
- I_v = contaminated forage ingestion rate of cattle, $\text{g dry plant day}^{-1}$;
- C_{vj} = concentration of radionuclide j in forage vegetation, Ci g^{-1} dry plant;
- I_s = contaminated soil ingestion rate of cattle, $\text{g dry soil day}^{-1}$;
- A_{sj} = activity of radionuclide j in shallow soil compartment, Ci ;

The concentration in vegetation, $C_{v,j}$ is the sum of $C_{v,j}^{ext}$ and $C_{v,j}^{int}$ from Equations 3.34 and 3.35. Values of $F_{m,j}$ (Table E.1) were adopted from a compilation of these values by Baes *et al.* (1980) for all radionuclides except ^3H and ^{14}C , which were not available in that document. Values of $F_{m,j}$ for ^3H and ^{14}C were obtained from the NRC Regulatory Guide 1.109, Revision 1 (NRC, 1977), which provided values based on specific activity considerations for these radionuclides.

The assumed forage consumption rate of cattle grazing on native flora at the Area 5 RWMS, I_v , was 8 kg dry vegetation day^{-1} , based on a review of site-specific and desert forage consumption studies for cattle by Martin and Bloom (1980). The assumed soil consumption

External doses were calculated from Equation 3.31 which was modified to represent exposure over the entire year rather than for 2,000 hours yr^{-1} . Doses from inhalation of suspended radionuclides in air above the facility, $D_{j,\text{max}}^{\text{inh}}$, were calculated from Equation 3.32, which was modified to consider continuous exposure throughout the year.

Equations 3.34 through 3.37 were used to evaluate the radionuclide activity concentration in vegetation, beef, and milk concentrations at the Area 5 RWMS. The CEDE from ingestion of contaminated vegetation, milk, soil, and beef (D_j^{ing}) was calculated from:

$$D_j^{\text{ing}} = DCF_j^{\text{ing}} \times \left[U_v (C_{vj}^{\text{int}} + C_{vj}^{\text{ext}}) + U_s \frac{A_{sj}}{V_s \rho_b} + U_m C_{mj} + U_b C_{bj} \right] \quad (3.38)$$

where U_v , U_s , U_m , and U_b are intake rates of vegetation (g dry yr^{-1}), soil (g yr^{-1}), milk (kg yr^{-1}), and beef (kg yr^{-1}), respectively. The DCF_j^{ing} is the CEDE conversion factor for ingestion of

important in ingestion pathways (^{237}Np and ^{241}Am). The final list of radionuclides for the open rangeland scenario with the off-site resident consists of: ^3H , ^{14}C , ^{85}Kr , ^{210}Pb , ^{226}Ra , ^{227}Ac , ^{228}Ra , ^{228}Th , ^{230}Th , ^{231}Pa , ^{234}U , ^{235}U , ^{237}Np , ^{238}U , ^{239}Pu , and ^{241}Am .

3.2.3.4 Full Pathway Analysis for the Open Rangeland Scenario

The nuclides retained from the screening analysis were carried through a full pathway analysis with atmospheric dispersion to the location of the off-site resident. For volatile ^3H , ^{14}C , and ^{85}Kr , atmospheric transport calculations were performed to estimate air, soil, and vegetation concentrations at the ranch location. Release rates estimated for ^3H , ^{14}C , and ^{85}Kr in Section 3.2.2.1 provided source terms for atmospheric transport. Off-site air concentrations, $C_{ax,j}$, were estimated for these source terms using CAP88-PC (EPA, 1992), an EPA-sanctioned code developed for estimating TEDE to members of the public resulting from radionuclide emissions to air. Site-specific atmospheric conditions available for Frenchman Flat were used for the computations, and the source was assumed to be an area source of $7.5 \times 10^4 \text{ m}^2$. Air concentrations at Indian Springs (42 km [26 mi] southeast of Area 5) were calculated. Volatilization is assumed to occur immediately after facility closure during the period of institutional control. Because Cane Springs (14.3 km [8.9 mi] south-southwest of Area 5) is within the NTS boundary, air concentrations of volatile forms of ^3H , ^{14}C , and ^{85}Kr are not calculated at this location for the period of institutional control.

Concentrations of ^3H and ^{14}C in soil at the off-site location ($C_{sx,j}$ in Ci m^{-3}) were calculated using the deposition velocity, V_d , introduced in Equation 3.35. Krypton-85, a noble gas, causes an air-immersion dose only; thus, soil and vegetation concentrations of ^{85}Kr are immaterial. The equation describing the relationship of $C_{sx,j}$ to $C_{ax,j}$, the air concentration at the residence location is:

$$C_{sx,j} = \frac{V_d C_{ax,j}}{1.0 K_s} \times \frac{1}{\rho_b} \quad (3.39)$$

Equation 3.39 assumes that equilibrium exists between deposition and resuspension and that the amount deposited becomes mixed to the depth of the shallow soils compartment, represented by the factor of 1.0 in the equation. Concentrations of ^3H and ^{14}C in vegetation were calculated according to Equations 3.34 and 3.35, replacing $A_{s,j}$ with $C_{sx,j}$ and $C_{a,j}$ with $C_{ax,j}$. That is:

$$C_{vx,j}^{int} = B_{jv} \times \frac{C_{sx,j}}{V_s} \times \frac{1}{\rho_b} \quad (3.40)$$

and

$$C_{vx,j}^{ext} = \frac{V_d \times F_v}{\lambda_w} \times C_{ax,j} \quad (3.41)$$

where $C_{vx,j}^{int}$ and $C_{vx,j}^{ext}$ are the vegetation concentrations at the off-site location. The total vegetation concentration, $C_{vx,j}$, is the sum of $C_{vx,j}^{int}$ and $C_{vx,j}^{ext}$.

Concentrations of ^3H and ^{14}C in milk and beef from direct inhalation of volatile forms of these radionuclides were neglected. Livestock intake of these radionuclides was calculated for the nonvolatile forms only.

The CEDE from inhalation of ^3H and ^{14}C was calculated from:

$$D_j^{inh} = C_{ax,j} \times DCF_j^{inh} \times 8400 \quad (3.42)$$

where $C_{ax,j}$ is the CAP88-determined air concentration at the off-site location in Ci m^{-3} . The dose conversion factor for ^3H was corrected for dermal adsorption by multiplying by 1.5. For ^{85}Kr , the air-immersion dose factor, in mrem yr^{-1} per Ci m^{-3} , obtained from Eckerman and Ryman (1993), was multiplied by the CAP88-determined air concentration for this radionuclide to calculate dose. Doses resulting from ingestion of vegetation and inadvertent ingestion of soil contaminated with ^3H and ^{14}C at the location of residence were calculated according to:

$$D_j^{ing} = DCF_j^{ing} \times \left[U_v (C_{vj}^{int} + C_{vj}^{ext}) + U_s \frac{A_{sj}}{V_s \rho_b} + U_m C_{mj} + U_b C_{bj} \right] \quad (3.43)$$

setting the concentration in milk, C_{mj} , and the concentration in beef, C_{bj} , to zero.

For nonvolatile forms of ^3H , ^{14}C , and the other 13 nonvolatile radionuclides, full pathway analysis was performed. Air, soil, and vegetation concentrations at Indian Springs and at Cane Springs were calculated, after the 100-year institutional control period. As with the volatile radionuclides, the CAP88-PC methodology was applied to estimate off-site concentrations. The time-dependent source term from the Area 5 RWMS to the atmosphere, $S_{aj}(t)$ in Ci yr^{-1} , arises from the suspension of contaminated soil in air and was calculated

$$S_{aj}(t) = A_{sj}(t) \times K_s \quad (3.44)$$

where $A_{sj}(t)$ is the activity of radionuclide j in the shallow soils compartment above the facility. The value of $A_{sj}(t)$ is calculated as a function of time from Equation 3.22. The assumed value of the resuspension rate, K_s , is 10^{-4} yr^{-1} . Maximum and 10,000-year air concentrations at the two locations are presented in Table E.5. Concentrations in soil ($C_{sx,j}$) and vegetation ($C_{vx,j}$) at both residence locations were calculated according to Equations 3.39, 3.40, and 3.41. Concentrations in beef and milk were calculated assuming cattle grazed over

Radionuclides released to the surface soils above the Area 5 RWMS could be transported to an off-site ranch at 100 m (330 ft) by atmospheric dispersion, by sediment transport, and by biological transport. Modeling these transport processes would be complex. Because of the close proximity to the site (100 m [330 ft]), the concentration would probably vary significantly over the dimensions of a ranch large enough to support a subsistence farmer. The activities of animals and transport in ephemeral channels might also lead to nonuniform

concentrations. The concentration of radionuclides in soil at 100 m (330 ft) is 11

Table 3.23 Parameters Used in the Release and Pathways Conceptual Model to Estimate Environmental Concentrations and TEDE

Parameter Description	Pathway Assumed	Value Assumed	Source of Value Selected
B_{pv} , Plant-Soil Concentration Ratio (Ci g^{-1} dry plant: Ci g^{-1} dry soil)	Internal Contamination of Vegetation	Table E.1	see Table E.1
$\text{DCF}_j^{\text{ext}}$, External Effective Dose Equivalent Conversion Factor (mrem yr^{-1} per Ci m^{-3} soil)	Exposure to Contaminated Soil	Table E.3	Eckerman and Ryman, 1993
$\text{DCF}_j^{\text{ing}}$, Ingestion CEDE Conversion Factor ($\text{rem per } \mu\text{Ci}$)	Exposure to Contaminated Vegetation, Beef, or Milk	Table E.3	DOE, 1988b
$\text{DCF}_j^{\text{inh}}$, Inhalation Dose Conversion Factor ($\text{rem per } \mu\text{Ci}$)	Exposure to Contaminated Air	Table E.3	DOE, 1988b
E_t , Enrichment Factor	Suspension of Contaminated Soil into Air	1	Layton <i>et al.</i> 1993
F_b , Fraction of a Cow's Daily Ingestion of Radionuclide j that is in Each kg of Beef (day kg^{-1})	Contamination of Beef	Table E.1	see Table E.1
F_m , Fraction of a Cow's Daily Ingestion of Radionuclide j that is in Each kg of Milk (day kg^{-1})	Contamination of Milk	Table E.1	see Table E.1
F_v , Foliar Interception Factor ($\text{m}^2 \text{g}^{-1}$)	External Contamination of Vegetation	10^{-3}	Martin and Bloom, 1980
I_s , Soil Ingestion Rate for Cattle (kg day^{-1})	Contamination of Beef and Milk	0.5	Martin and Bloom, 1980; Smith, 1977
I_v , Native Forage Consumption Rate for Cattle, (kg dry day^{-1})	Contamination of Beef and Milk	8	Martin and Bloom, 1980
K_{b1} , Fractional Transfer Rate from Waste to Shallow Soils by Burrowing Animals (yr^{-1})	Contamination of Shallow Soils	1.3×10^{-7}	see Section 3.2.2
K_{b2} , Fractional Transfer Rate from Waste to Subsurface Soils by Burrowing Animals (yr^{-1})	Contamination of Subsurface Soils	1.8×10^{-7}	see Section 3.2.2
K_{r1j} , Root Uptake Rate from Waste to Shallow Soils (yr^{-1})	Contamination of Shallow Soils	Table E.2	see Section 3.2.2
K_{r2j} , Root Uptake Rate from Waste to Subsurface Soils (yr^{-1})	Contamination of Subsurface Soils	Table E.2	see Section 3.2.2

Table 3.23 (continued)

Parameter Description	Pathway Assumed	Value Assumed	Source of Value Selected
$K_{r,j}$, Root Uptake Rate from Subsurface Soils to Shallow Soils (yr^{-1})	Contamination of Shallow Soils	Table E.2	see Section 3.2.2
K_s , Soil Resuspension Rate (yr^{-1})	Source Term for Atmospheric Transport Off Site	10^{-4}	see Section 3.2.2
M_s , Mass Loading Factor (g m^{-3})	Contamination of Air Above Facility	10^{-4}	EPA, 1990
U_b , Average Intake Rate of Beef (kg wet yr^{-1})	Exposure to Contaminated Beef	30	Rupp, 1990
U_m , Average Intake Rate of Milk (kg wet yr^{-1})	Exposure to Contaminated Milk	220	Rupp, 1990
U_s , Inadvertent Intake Rate of Soil (g yr^{-1})	Exposure (internal) to Contaminated Soil	40	EPA 1989
U_v , Average Intake Rate of Vegetables and Fruit (g dry yr^{-1})	Exposure to Contaminated Vegetation	32000	Rupp, 1990
V_d , Deposition Velocity (m yr^{-1})	External Contamination of Vegetation and Off-Site Soil	3.3×10^4	Baes <i>et al.</i> , 1984; EPA, 1992
V_s , Volume of the Shallow Soils Compartment (m^3)	Contamination of Shallow Soils	7.5×10^4	see Section 2.9
$\lambda_{r,j}$, Radioactive Decay Constant, yr^{-1}	Contamination of Air and Soils	Table E.3	Kocher, 1981
λ_w , Weathering Constant for External Contamination of Vegetation, yr^{-1}	External Contamination of Vegetation	18	NRC, 1977
ρ_b , Dry Bulk Density of Soil (g m^{-3})	Contamination of Shallow Soils	1.6×10^6	REECo, 1993c

intruder scenarios is a method to ensure that the site is preserved for very restrictive future uses, thereby ensuring that the site is not a legacy. This is accomplished by determining the maximum waste concentration that meets the performance objective. This section describes the conceptual models and assumptions used to analyze the intruder scenarios. The conceptual models were implemented with the RESRAD computer code (Yu *et al.*, 1993). The

RESRAD results presented are all for zero elapsed time, thereby eliminating the time-dependant processes (erosion, leaching, and radioactive decay) incorporated in the RESRAD code. Erosion and leaching of the contaminated zone are not believed to be important processes at the NTS over the short duration of an intruder scenario. Radioactive decay of the source term was performed with the RadDecay computer code (Negin and Worku, 1991).

3.3.1 Acute Intruder Scenarios

Three acute intruder scenarios were considered: the discovery scenario, intruder-construction scenario, and intruder-drilling scenario. Intrusion was assumed to be possible from the end of the 100-year institutional control period to the end of the 10,000-year compliance interval. Two of the scenarios, the discovery and the intruder-construction scenario, were not analyzed because the expected doses are bounded by chronic intruder scenarios. The discovery scenario and intruder-construction scenario are very similar except that the discovery scenario can occur earlier, before waste forms have decomposed. Because no credit for waste form is taken in this assessment and all waste forms are assumed to have decayed to a soil-like material by the end of the institutional control period, the discovery and construction scenarios are assumed equivalent.

The intruder-construction scenario describes the exposure of an intruder building a residence over the site. It is an acute scenario which precedes the chronic intruder-agriculture scenario. Based on previously described scenarios (NRC, 1981), the intruder is assumed to excavate 600 m^3 ($21,000 \text{ ft}^3$) from a 10- by 20-m (32.8- by 65.6-ft) foundation that is 3 m (9.9 ft) deep. Because the assumed cap thickness is 2.4 m (7.9 ft), 120 m^3 ($4,000 \text{ ft}^3$) of waste is excavated.

3.3.1.1 Conceptual Models and Assumptions for the Acute Drilling Scenario

The drilling intruder scenario is a short-term, or acute scenario involving exposure to drill cuttings from a borehole penetrating a trench or pit. Again, because no credit is taken for the waste form integrity, this scenario is assumed to be possible at any time after the 100-year institutional control period. The site inventory is assumed to remain totally isolated until the time of intrusion. The models for radionuclide release from the undisturbed site, described in Section 3.2.2, predict that less than 5 percent of the inventory of the most mobile particulate radionuclides will be released from the facility in 10,000 years. Therefore, it is reasonable and conservative to assume that radioactive decay is the only process changing the source term prior to intrusion.

The drillers are assumed to be exposed to contaminated cuttings while drilling a 0.3-m- (0.99-ft)-diameter borehole to the uppermost aquifer. The time required to complete the drilling is assumed to be 100 hours. During the event, the drillers are assumed to be exposed by external irradiation, inhalation, and inadvertent ingestion of soil. The drillers are assumed to be in the center of a 1,000-m² (10,763-ft²) area contaminated with cuttings for the 100-hour exposure period. Drill cuttings are usually held in a mud pit adjacent to the drill rig. The drillers were assumed to be in the mud pit to simplify the geometry of external irradiation. This is a conservative assumption made to simplify the analysis. The activity concentration of radionuclides in the cuttings is:

$$C = 1 \times 10^{12} \times C_w \times \frac{t_w f_d}{D_b \rho} \quad (3.45)$$

where:

- $C_{s,j}$ = soil activity concentration of radionuclide j, pCi g⁻¹;
- $C_{w,j}$ = waste activity concentration of radionuclide j at the time of intrusion, Ci m⁻³;
- t_w = thickness of the waste zone, m;
- f_d = facility design factor, dimensionless,
- D_b = total depth of the borehole, m; and
- ρ = bulk density of the alluvium, g m⁻³.

The waste activity concentrations at the time of intrusion were determined using RadDecay (Negin and Worku, 1991). The facility design factor is a dilution factor that accounts for clean soil that fills void spaces between waste packages. The design factor was assumed to be 0.75. The depth of the borehole was assumed to be 235 m (770.9 ft) and the bulk density was assumed to be 1.6 × 10⁶ g m⁻³. The waste cell thicknesses were 4.9 m (16 ft) for the

shallow land burial trenches, 6.2 m (20.3 ft) for the upper cell of Pit 6, and 3.6 m (11.8 ft) for the lower cell. The volume of soil excavated, 17 m³ (600 ft³), when spread over a 1,000-m² (10,763-ft²) area, creates a final contaminated zone approximately 0.02 m (0.8 in) thick.

The CEDE to the drillers from the inadvertent ingestion of soil is given by:

$$D_{soil,j} = C_{s,j} \times DCF_{ing} \times FSI \times FA \times FCD_s \times FO_s \quad (3.46)$$

where:

- $D_{soil,j}$ = CEDE from ingestion of radionuclide j in soil, mrem yr⁻¹;
- DCF_{ing} = ingestion CEDE conversion factor, mrem pCi⁻¹;
- FSI = annual intake of soil, g yr⁻¹;
- FA = area factor, dimensionless;
- FCD_s = soil ingestion cover and depth factor, dimensionless; and
- FO_s = soil ingestion occupancy factor, dimensionless.

The dose conversion factors used are the default values in RESRAD. These are the most conservative values in DOE (1988b, 1988c). This approach is reasonable because no information on chemical or physical form of the waste constituents is available. The annual soil ingestion rate was assumed to be 40 g yr⁻¹. The area factor for a 1,000-m² (10,763-ft²) area was assumed to be 1.0. The cover and depth factor was assumed also to be 1.0. The soil ingestion occupancy factor is the fraction of the time in a year spent on site or 0.011 for 100 hours.

The CEDE from inhalation of suspended cuttings was calculated from:

$$D_{inh,j} = C_{s,j} \times DCF_{inh} \times ASR \times FA_{inh} \times FCD_{inh} \times FO_{inh} \times FI \quad (3.47)$$

where:

- $D_{inh,j}$ = CEDE from inhalation of radionuclide j, mrem yr⁻¹;
- DCF_{inh} = inhalation CEDE conversion factor, mrem pCi⁻¹;
- ASR = soil mass loading in air, g m⁻³;
- FA_{inh} = area factor for inhalation pathway, dimensionless;
- FCD_{inh} = inhalation cover and depth factor, dimensionless;
- FO_{inh} = occupancy factor for inhalation pathway, dimensionless; and
- FI = annual intake of air, m³ yr⁻¹.

An intermediate soil mass loading value of $1.5 \times 10^{-4} \text{ g m}^{-3}$ was assumed based on the assumption that the drill cuttings would be wet and not as easily resuspended as dry cuttings. The cover and depth factor and occupancy factor were the same as in the soil ingestion pathway. The annual intake of air was assumed to be $8,400 \text{ m}^3 \text{ yr}^{-1}$. The cover and depth factor was calculated as:

$$FA_{inh} = \frac{\sqrt{A}}{\sqrt{A} + DL} \quad (3.48)$$

where:

A = area of contaminated zone, m^2 ; and
DL = dilution length, m.

The area of the contaminated zone was $1,000 \text{ m}^2$ ($10,763 \text{ ft}^2$) and the assumed dilution length is 3 m (9.9 ft).

The dose from inhalation of ^3H was calculated assuming HTO was the only form present. The CEDE from inhalation and dermal absorption of HTO was calculated from:

$$D_{inh,H-3} = 1.5 \times DCF_{inh} \times FO_{inh} \times FI \times C_{a,H-3} \quad (3.49)$$

where:

$D_{inh,H-3}$ = CEDE from inhalation and absorption of HTO, mrem yr^{-1} ; and
 $C_{a,H-3}$ = activity concentration of HTO in air, pCi m^{-3} .

The concentration of HTO in air is calculated assuming that all of the HTO is in the soil pore water. The flux from the surface is the product of the soil pore water ^3H concentration and annual evapotranspiration. This flux is assumed to be mixed into a 2-m (6.6-ft) mixing zone. The concentration of HTO in air is given by:

$$C_{a,H-3} = \frac{3.17 \times 10^{-8} \times 0.5 \times \frac{\rho C_s}{\theta_v} \times E_t \times \sqrt{A}}{H_{mix} \times U} \quad (3.50)$$

where:

θ_v = volumetric water content, dimensionless;

E_t = evapotranspiration rate, m yr^{-1} ;

L = height of atmospheric mixing zone, m;

The volumetric water content of the cuttings was assumed to be the same as the near-surface alluvium, 0.086. The evapotranspiration factor is the annual quantity of water evaporated from the surface, which was assumed to be equal to the annual rainfall of about 0.1 m yr^{-1} . The mixing height and mean wind speed assumed were 2 m (6.6 ft) and 2 m s^{-1} , respectively.

The dose from inhalation of ^{14}C is calculated in a similar fashion. All airborne ^{14}C is assumed to be $^{14}\text{CO}_2$. The CEDE from inhalation of $^{14}\text{CO}_2$ is calculated as:

$$D_{inh, C-14} = DCF_{inh} \times FO_{inh} \times FI \times C_{a, C-14} \quad (3.51)$$

where:

$D_{inh, C-14}$ = CEDE from inhalation of $^{14}\text{CO}_2$, mrem yr^{-1} ; and

C = activity concentration of $^{14}\text{CO}_2$ in air, Ci m^{-3} .

$$EVS_N = 1 \times 10^6 \times C_{s,C-14} \times E \times \rho \times d_{ref} \quad (3.53)$$

where:

E = carbon evasion rate constant, yr^{-1} ; and
 d_{ref} = reference soil depth, m.

The carbon evasion rate constant was assumed to be 22 yr^{-1} which is a RESRAD default value based on empirical measurements (Yu *et al.*, 1993). The soil layer releasing $^{14}\text{CO}_2$ was assumed to be equal to the depth of the contaminated zone, 0.02 m (0.8 in).

The effective dose equivalent from external irradiation was calculated from:

$$D_{ext,j} = C_{s,j} \times DCF_{ext} \times \rho \times FO_{ext} \times FS \times FA \times FD \times FC \quad (3.54)$$

where:

$D_{ext,j}$ = effective dose equivalent from external exposure, mrem yr^{-1} ;
 DCF_{ext} = external dose conversion factor, mrem yr^{-1} per pCi m^{-3} ;
 FS = shape factor, dimensionless;
 FD = depth factor, dimensionless;
 FC = cover factor, dimensionless; and
 FO_{ext} = occupancy factor for external irradiation, dimensionless.

The shape factor, area factor, and cover factor were assumed to be 1.0. The depth factor corrects the external dose conversion factor for an infinitely deep contaminated zone to a value appropriate for the actual depth of the contaminated zone. The depth factor is determined within RESRAD for each radionuclide by interpolation between tabulated values (Yu *et al.*, 1993). The occupancy factor for external irradiation is the fraction of time spent at the site annually or 0.011. Parameters used in the acute drilling scenario are summarized in Table 3.24.

The acute drilling scenario was analyzed for the shallow land burial inventory and for Pit 6

Table 3.24 Summary of Parameters Used in the Drilling Intruder Scenario

Parameter	Acute Intruder Scenarios
	Drilling
Area of Contaminated Zone (m^2)	1,000
Thickness of Contaminated Zone (m)	0.016
Bulk Density of Contaminated Zone (g m^{-3})	1.6×10^6
Occupancy Factors	
Soil Ingestion	0.011
Inhalation	0.011
External	0.011
Mass Loading (g m^{-3})	1×10^{-4}
Soil Ingestion Rate (g yr^{-1})	40
Annual Intake of Air ($\text{m}^3 \text{yr}^{-1}$)	8,400
Annual Evapotranspiration Factor, E_t (m yr^{-1})	0.099
Atmospheric Mixing Height, H_{mix} (m)	2
Annual Average Wind Speed, U (m s^{-1})	2
Carbon Evasion Rate, E (yr^{-1})	22
Carbon Release Depth, d_{ref} (m)	0.016

3.3.2 Chronic Intruder Scenarios

Two chronic or long-term intruder scenarios were considered in Section 3.1.3: the intruder-agriculture scenario and the postdrilling scenario. This section describes the conceptual models and assumption used for the chronic intruder scenarios.

3.3.2.1 Conceptual Model and Assumptions for the Intruder-Agriculture Scenario

The intruder-agriculture scenario follows the intruder-construction scenario and assumes that the intruder lives in a residence built upon a mixture of exhumed waste and soil. It is assumed that the waste has degraded to the point where it is indistinguishable from soil. This is a very conservative assumption for most waste forms, but is reasonable for soil waste streams. Because this assessment does not specify the waste form, assuming the waste was equivalent to soil at the end of institutional control was the only justified assumption. The intruder is assumed to engage in agricultural activities at the site. The agricultural pathways

were selected based on the most common agricultural activities currently observed in southern Nevada. The scenario represents a commercial cattle ranching operation that produces a forage crop. In addition to commercial activities, small quantities of fruit, vegetables, and milk are assumed to be produced for private purposes. Because contamination of the aquifer has been eliminated, the scenario includes no pathways involving contaminated water. The intruder is exposed through the following pathways:

- External irradiation from radionuclides in surface soil.
- Inhalation of particulate radionuclides resuspended from surface soils and inhalation of gaseous radionuclides release from surface soil.
- Inhalation of gaseous radionuclides released from buried waste.
- Ingestion of contaminated soil.
- Ingestion of contaminated beef and dairy products produced at the site.
- Ingestion of contaminated fruits and vegetables produced at the site (Figure 3.11).

The intruder is assumed to construct a 200-m² (2,152.7-ft²) house with a 2.5-m- (8.2-ft)-deep

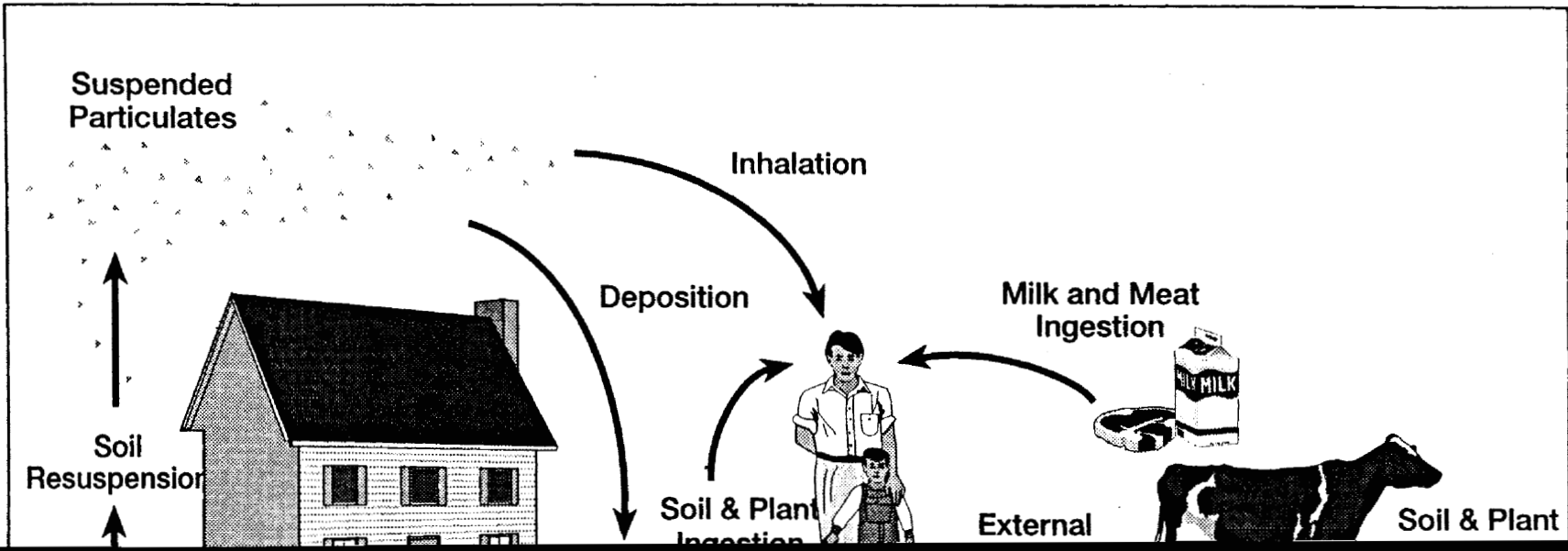


Figure 3.11 Pathways Leading to Exposure Scenario

clide j , pCi g^{-1} ;
clide j at the time of intrusion, Ci m^{-3} ;
and

and the bulk density of the contaminated

ing Equation 3.46. The occupancy factor for
r the acute scenario. The intruder is
tdoors 20 percent of the time, and off site for
n occupancy factor of 0.7.

ulate radionuclides from the contaminated
48. The inhalation occupancy factor
r outdoor levels (Alzona *et al.*, 1975). This

$^{14}\text{CO}_2$ released from the surface
as 3.49 through 3.53. All parameters were
to be equal to the depth of the contaminated
pn of ^{222}Rn and its short-term progeny
s calculated using RESRAD models.

released from the waste zone was performed
was performed for the 100-year time interval
d be completely released by 10,000 years.
s calculated using Equations 3.29 and 3.33.
was the time spent outdoors, 1,752 hours,
were used to estimate the CEDE from ^{222}Rn
ite. These models include estimates for

r while indoors was calculated separately
concentration was calculated by converting
ssuming a steady-state concentration in the
-state gas concentration in the residence,

$$F = \frac{J_f A_f}{k V} \quad (3.56)$$

into residence, $\text{pCi m}^{-2} \text{ yr}^{-1}$;
 above the ground surface, m^2 ;
 rate, yr^{-1} ; and
 residence, m^3 .

From the site of 4.12 Ci yr^{-1} gives a flux of $5.5 \times 10^7 \text{ pCi m}^{-2} \text{ yr}^{-1}$. These fluxes assume that the entire site is exposed to the atmosphere. The HTO release rate of 200 Ci yr^{-1} gives a flux of $5.5 \times 10^7 \text{ pCi m}^{-2} \text{ yr}^{-1}$. The area of the foundation, including the walls, is 350 m^2 . The residence is $1,000 \text{ m}^3$ ($35,314.6 \text{ ft}^3$). The assumed ventilation rate from HTO and $^{14}\text{CO}_2$ is calculated as in Equation 3.33, ranging from $1,920 \text{ m}^3$ to $1,680 \text{ m}^3$ ($67,804 \text{ ft}^3$ to $59,328 \text{ ft}^3$) per hour. The ^{85}Kr dose was calculated using an effective time for immersion.

The irradiation from the contaminated zone was calculated using the occupancy factor in this case includes a very conservative value of 0.7 (NRC, 1977).

For ingestion of contaminated fruits, vegetables, beef, and poultry, the food ingestion rates were the same as used in the pathway analysis. The amount of food that can be grown in the contaminated zone of $26,909 \text{ ft}^2$ area, RESRAD estimates that 50 percent of a pound of beef and dairy products can be produced on site. Reduced downward to 25 percent, given the difficulties of garden-to-market animal product fraction was adjusted upward to 25 percent more likely. Comparison of these estimates with agricultural data indicate that they are physically possible. The radionuclide resulting CEDE assume plant uptake by the roots and foliar at ingestion is then:

Nevada Test Site

(3.57)

cm yr^{-1} ;
dimensionless;

g^{-1} soil;
dimensionless;

on a wet mass
in the pathway
annual intake
rock. Calculations
ates. For root
ness divided by the
uation 3.48. The

(3.58)

Site

n
/o

9)

is

3-99

$$D_{b,j} = C_{s,j} \times FD \times B_b \times DCF_{ing} \times DF_b \times (DF_f(B_{jv} \times FCD_{veg} + FA \times ASR \times FAR)) \quad (3.60)$$

where:

- D_b = CEDE from radionuclide j from ingestion of milk, mrem yr⁻¹;
- B_b = beef transfer coefficient, day kg⁻¹;
- Df_b = annual intake of beef, kg yr⁻¹;
- Df_f = intake of fodder by livestock, g day⁻¹; and
- Df_s = intake of soil by livestock, g day⁻¹.

The fodder-to-meat transfer coefficients are the same as were used in the pathway scenarios (see E.1). The intake rates assumed are specified in Table 3.25.

Table 3.25 Summary of Parameters Used in the Intruder-Agriculture and Postdrilling Intruder Scenarios

Parameter	Chronic Intruder Scenarios	
	Intruder-Agriculture	Postdrilling
Area of Contaminated Zone (m ²)	2,500	2,500
Thickness of Contaminated Zone (m)	0.24	0.15
Bulk Density of Contaminated Zone (g m ⁻³)	1.6 × 10 ⁶	1.6 × 10 ⁶
Occupancy Factor		
Soil Ingestion	0.7	0.7
Inhalation	0.4	0.4
External	0.55	0.55
Mass Loading (g m ⁻³)	1 × 10 ⁻⁴	1 × 10 ⁻⁴
Soil Ingestion Rate (g yr ⁻¹)	40	40
Annual Intake of Air (m ⁻³ yr ⁻¹)	8,400	8,400
Annual Intake of Fruit and Vegetable (kg yr ⁻¹)	160 (wet), 32 (dry)	160 (wet), 32 (dry)
Annual Intake of Meat Products (kg yr ⁻¹)	30	30

Table 3.25 (continued)

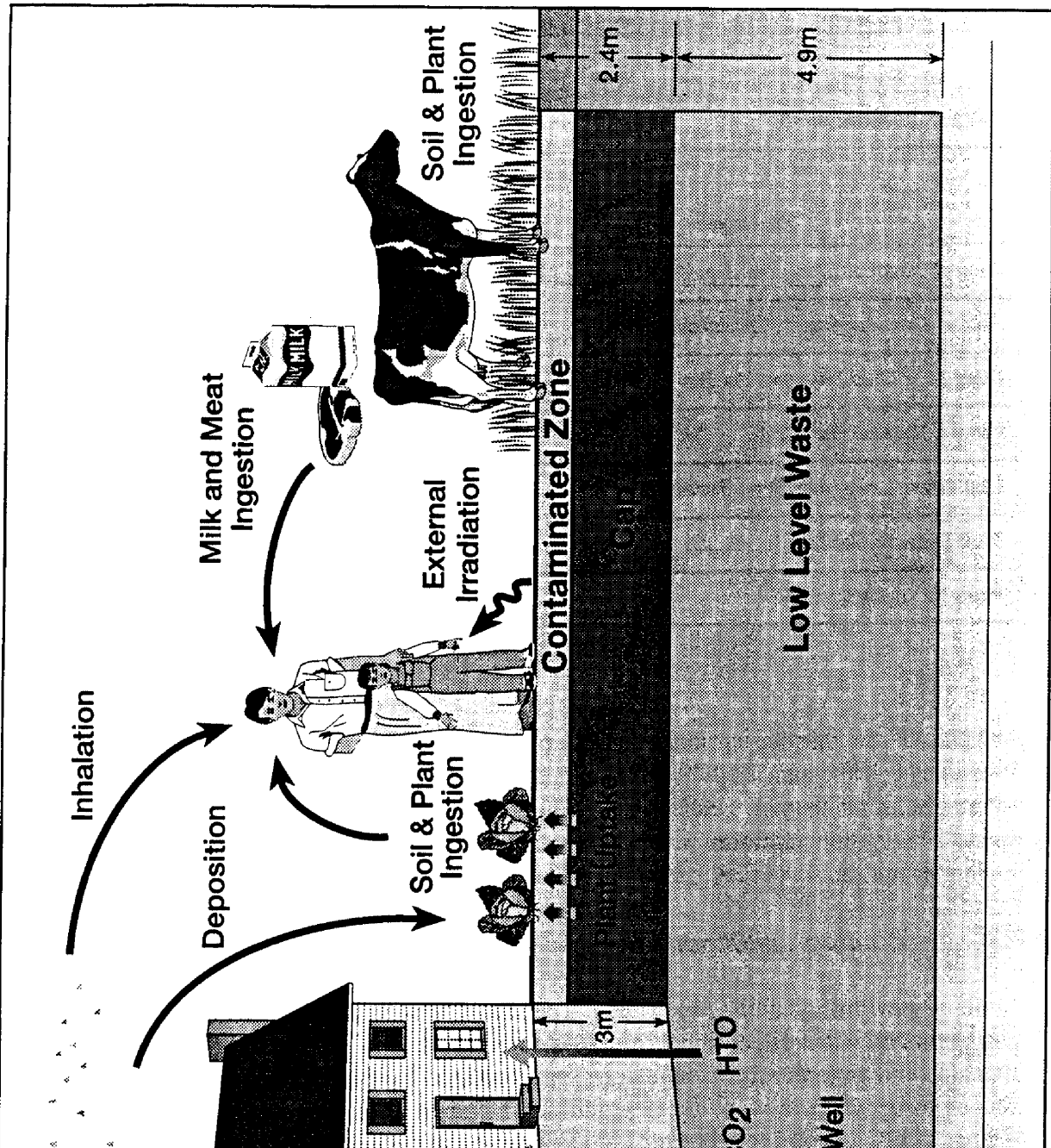
Parameter	Chronic Intruder Scenarios	
	Intruder-Agriculture	Postdrilling
Annual Intake of Dairy Products (kg yr^{-1})	220	220
Fodder Consumption by Livestock (kg d^{-1})	50 (wet), 10 (dry)	50 (wet), 10 (dry)
Fraction of Diet Produced On Site	0.25	0.25
Carbon Release Depth (m)	0.24	0.15
Vegetation Cover and Depth Factor, FCD_v	0.27	0.17
Food Transfer Factors, B_{jv} , B_m , B_b	See Table E.1	See Table E.1
Humidity in Air (g m^{-3})	4.7	4.7

Analysis of the intruder-agriculture scenario was performed for the shallow land burial inventory at 100 years, 10,000 years, and at the time of maximum activity for radionuclides with maximums beyond 10,000 years. This scenario is not required for Pit 6 because the waste activity concentration in the upper cell is the same as that for the shallow land burial inventory and the lower cell is too deep for this scenario to be credible.

3.3.2.2 Conceptual Model and Assumptions for the Postdrilling Scenario

In the postdrilling scenario, an intruder is assumed to construct a residence on a site contaminated with drill cuttings from a waste disposal cell. The intruder is assumed to raise livestock and cultivate fruit, vegetables, and fodder as in the intruder-agriculture scenario. The exposure pathways are identical to those included in the intruder-agriculture scenario (Figure 3.12). Overall, the postdrilling scenario is the same as the intruder-agriculture scenario with three exceptions. First, the volume of waste exhumed is less; consequently, the thickness and the activity concentration of the contaminated zone is less. Second, the inventory of waste that can be exhumed is expanded because the borehole passes through the entire trench to the uppermost aquifer. Third, the postdrilling intrusion scenario does not include the excavation of a basement in the waste site.

The borehole is assumed to be a 0.3-m- (0.98-ft)-diameter water production well extending at least 235 m (770.9 ft) to the uppermost aquifer. Again, the waste is assumed to have decomposed to the point that it is indistinguishable from soil by the end of the 100-year institutional control period. The drilling equipment is assumed to be capable of penetrating all waste forms at this time. The total volume of cuttings from the hypothetical borehole will be 17 m^3 (600 ft^3). The intruder is assumed to spread this material over $2,500 \text{ m}^2$ ($26,909 \text{ ft}^2$), creating



a 0.007-m- (0.3 in)-thick contaminated zone. During development of the site, the intruder is assumed to mix this contaminated layer to a final depth of 0.15 m (0.48 ft). This depth represents a depth of mixing for common agricultural implements. The activity concentration of radionuclides in the contaminated zone is calculated as:

$$C_{s,j} = 1 \times 10^{12} \times C_{w,j} \times \frac{\pi r^2 t_w f_d}{A_c D_c \rho} \quad (3.61)$$

where:

- $C_{s,j}$ = soil activity concentration of radionuclide j, pCi g⁻¹;
- r = radius of the borehole, m;
- t_w = thickness of the waste zone, m;
- f_d = facility design factor, dimensionless;
- A_c = area of the contaminated zone, m²;
- D_c = final depth of the contaminated zone, m; and
- ρ = bulk density of the alluvium, g m⁻³.

The pathway models described in the previous sections were used to estimate the TEDE to the postdrilling intruder. Again, the only differences between features included in the two scenarios are the inventory available, the activity concentration of the contaminated zone, the thickness of the contaminated zone, and the presence of a basement. The parameters used are the same except those that are tied to the contaminated zone thickness. These parameters are the soil reference depth in the carbon evasion model (Equation 3.53), the depth factor in the external exposure model (Equation 3.54), and the cover and depth factor in the plant ingestion model (Equation 3.57). Parameters used in both chronic scenarios are summarized in Table 3.25.

3.4 Computer Software

This section describes the computer software used to prepare the performance assessment, including quality assurance activities. All of the software used is well known within the radiological assessment community except for three codes, BAT6CHN, CASCADR9, and ODIRE developed by Lindstrom *et al.* (1990, 1992b).

3.4.1 TIME-ZERO Computer Code

The TIME-ZERO computer code was used to solve the system of linear differential equations developed to describe the conceptual model of nonvolatile radionuclide release. TIME-ZERO (Kirchner, 1990) is an integrated set of software tools which simplifies the process of

writing simulation models. One of the tools is an interactive code generator which simplifies the construction of computer models. The linear differential equations are written in TIME-ZERO, which then automatically produces the FORTRAN source code.

The differential equations describing the release of nonvolatile radionuclides (Equations 3.22 through 3.24) were solved using the TIME-ZERO computer code (Kirchner, 1990). The equations were solved using a fourth-order Runge-Kutta numerical solution. Analytical solutions to the equations describing the plant uptake and burrowing animal system were developed and used for verification of the results. However, the TIME-ZERO model was needed for solution of radionuclide decay chains because analytical solutions are not easily obtainable. Two models were developed in TIME-ZERO, a model for handling single radionuclides referred to as MODELNTS and a model to handle decay chains with up to seven members referred to as NTSCHAIN.

The analytical solution giving the activity in the waste compartment was:

$$A_{w,j}(t) = A_{w,j}(t=0) e^{-(K_{eff,j} t)} \quad (3.62)$$

where:

- $A_{w,j}$ = activity of radionuclide j in waste compartment, Ci;
- $K_{eff,j}$ = $\lambda_{r,j} + K_{b1} + K_{b2} + K_{r1,j} + K_{r2,j}$, yr^{-1} ;
- $\lambda_{r,j}$ = decay rate constant for radionuclide j , yr^{-1} ;
- K_{b1} = rate constant for radionuclides transferred to surface soil from ant burrows in waste, yr^{-1} ;
- K_{b2} = rate constant for radionuclides transferred to subsurface soil from ant burrows in waste, yr^{-1} ;
- $K_{r1,j}$ = rate constant for radionuclide j transferred to surface soil from plant roots in waste, yr^{-1} ;
- $K_{r2,j}$ = rate constant for radionuclide j transferred to subsurface soil from plant roots in waste, yr^{-1} ; and
- t = time, yr.

The analytical solution giving the activity in the subsurface soil compartment was:

$$A_{u,j}(t) = A_{w,j}(t=0) \times (K_{b2} + K_{r2,j}) \times \frac{e^{-(K_{eff,j} t)} - e^{-((\lambda_{r,j} + K_{r3,j}) t)}}{(\lambda_{r,j} + K_{r3,j} - K_{eff,j})} \quad (3.63)$$

where:

- $A_{u,j}$ = activity of radionuclide j in subsurface soil compartment, Ci; and
 $K_{r3,j}$ = rate constant for radionuclide j transport to surface soil from plant roots in subsurface soil, yr^{-1} .

The analytical solution for the activity in the surface soil compartment was:

$$\begin{aligned}
 A_s(t) = & \frac{(K_{b1} + K_{r1}) \times A_w(t=0) \times (e^{-(K_{eff} t)} - e^{-(\lambda_r + K_s - K_{eff}) t})}{(\lambda_r + K_s - K_{eff})} \\
 & + \frac{(K_{b2} + K_{r2}) \times A_w(t=0) \times K_{r3} \times (e^{-(K_{eff} t)} - e^{-(\lambda_r + K_{r3} - K_{eff}) t})}{(\lambda_r + K_{r3} - K_{eff})(\lambda_r + K_s - K_{eff})} \\
 & + \frac{(K_{b2} + K_{r2}) \times A_w(t=0) \times K_{r3} \times (e^{-(K_s + \lambda_r) t} - e^{-(\lambda_r + K_{r3} - K_{eff}) t})}{(\lambda_r + K_{r3} - K_{eff})(K_s - K_{r3})}
 \end{aligned} \quad (3.64)$$

where:

- A_s = activity in surface soil compartment, Ci; and
 K_s = rate constant for resuspension, yr^{-1} .

In addition, mass balance checks were made for each simulation based upon the conservation of atoms. This was accomplished by converting the activity in each compartment at any time t to the number of atoms according to:

$$N_j(I) = \frac{C_j(I) \times CF}{\lambda_r(I)} \quad (3.65)$$

where:

- $N_j(I)$ = number of atoms of radionuclide I in compartment, j ;
 $C_j(I)$ = activity of radionuclide I in compartment j , Ci;
 $\lambda_r(I)$ = decay rate constant of radionuclide I , yr^{-1} ; and
 CF = conversion factor, disintegrations yr^{-1} per Ci (1.1668×10^{18}).

An air compartment was added to the TIME-ZERO models to ensure that atoms were not lost from the system. The air compartment was a sink for atoms being transferred from the surface soil compartment to the air by the resuspension rate constant.

The percent difference in the initial number of atoms and the number of atoms at any time t was then calculated as:

$$PD = \frac{(N_t - N_i)}{N_i} \times 100 \quad (3.66)$$

where:

- PD = percent difference in the number of atoms,
- N_i = initial number of atoms,
- N_t = number of atoms at time t during the simulation, and
- 100 = conversion factor to percent.

The analytical solutions and conservation of atoms were sufficient checks to ensure that the numerical solution was accurate for single radionuclides. However, radionuclide chains were more difficult to assess. Radionuclide chain solutions were checked for accuracy by three methods: (1) the first radionuclide in the chain was checked against the analytical solution to ensure that the root uptake and burrowing animal models were accurate, (2) the overall conservation of atoms was tracked to ensure that atoms were neither lost nor gained in the system, and (3) the ingrowth of a given progeny was verified by summing all of the model compartments (i.e., waste compartment, subsurface soil compartment, surface soil compartment, and the air compartment) and comparing the number of progeny atoms from TIME-ZERO to the result from the Bateman ingrowth equations. The solution of radionuclide chains in a numerical model requires simplification of the chains. The simplification is required to prevent the development of a stiff differential equation. The simplification involves modeling only those members of the decay chain with half-lives equal to or greater than one year. Assumptions for the remaining radionuclides with half-lives less than one year can be made assuming equilibrium and factoring in the branching fractions.

All of the model runs were found to have less than 1 percent error in the mass balance of atoms. This was considered acceptable for a numerical solution to the linear differential equations.

3.4.2 The CASCADR9 Computer Code

The CASCADR9 computer code was used to estimate radon fluxes from waste disposal cells. CASCADR9 was developed to model the transport of radon in porous media. It considers

the effects of molecular diffusion, advection, and radioactive decay of radon in the air-filled pores. Various versions of the CASCADR code have been documented in seven publications (Lindstrom *et al.*, 1992b,c; Cawfield *et al.*, 1993a,b; Lindstrom *et al.*, 1993a,b; Lindstrom *et al.*, 1994). A sensitivity analysis of CASCADR9 has been conducted and is described in Lindstrom *et al.* (1994).

Verification of the diffusion and radioactive decay portion of the CASCADR9 code has been documented in Cawfield *et al.* (1993a) and Lindstrom *et al.* (1994). These verifications were performed by obtaining CASCADR9 results for cases with constant air pressure, and therefore, zero advective transport. The CASCADR9 output was then compared to results obtained from analytical solutions to the diffusion equation. These verification tests demonstrated that the diffusive transport model in CASCADR9 is essentially equivalent to the analytical solutions.

A benchmark test was performed by comparing CASCADR9 results to NRC Regulatory Guide 3.64 (NRC, 1989) results. Regulatory Guide 3.64 was developed to determine the attenuation of radon fluxes by earthen covers on uranium mill tailings. The two models do not consider the same transport mechanisms, but Regulatory Guide 3.64 represents the standard method for design of caps for radon attenuation and a comparison of the two models is useful. The Regulatory Guide 3.64 method considers radon diffusion, radioactive decay, and the effects of soil-water content. CASCADR9 considers radon diffusion, radioactive decay, and advection, and does not consider the effects of water content. The first test evaluated was the two-layer (cap and waste) shallow land burial problem described in Section 3.2.2.3. Each model was parameterized using equivalent values for the shallow land burial case. Equivalent results were obtained from each model (Table 3.26). The conceptual differences between the two models suggest that CASCADR9 would predict greater transport because it includes an additional transport process (advection) and neglects the effects of water-filled pores. The observation that the two methods give equivalent results for the shallow land burial problem suggest that the effects of advection and water-filled pore spaces are negligible for this case. The second test evaluated was the four-layer problem describing Pit 6. Again, each model was run with identical parameters, and the differences noted. The K factors (flux per activity concentration, m s^{-1}) for the upper cells are nearly identical (Table 3.26). However, for the lower cell test case, the CASCADR9 K factor is slightly

Table 3.26 Results of Benchmark Tests Between CASCADR9 and NRC Regulatory Guide 3.64

Test Cases	K Factors	
	CASCADR9	NRC Reg. Guide 3.64
Shallow Land Burial (K_{SLB})	$5.6 \times 10^{-8} \text{ m s}^{-1}$	$5.5 \times 10^{-8} \text{ m s}^{-1}$
Pit 6 Upper Cell (K_{P6U})	$5.3 \times 10^{-8} \text{ m s}^{-1}$	$5.5 \times 10^{-8} \text{ m s}^{-1}$
Pit 6 Lower Cell (K_{P6L})	$3.3 \times 10^{-11} \text{ m s}^{-1}$	$2.7 \times 10^{-11} \text{ m s}^{-1}$

The RESRAD code has the capability to predict the concentration of radionuclides over time by including radioactive decay and redistribution effects such as erosion and leaching. The results used in this assessment are the results provided for the case where the elapsed time is zero. This eliminates all time-dependant effects from the model. The dose equivalents are then linearly proportional to the soil concentration as described in Section 3.3.

A verification of the RESRAD pathway analyses was performed by spreadsheet calculations using the parameters and equations described in Section 3.3. The difference between the verification results and the RESRAD results were generally less than 1 percent. The only exception was the doses from ^3H and ^{14}C in the ingestion pathways. In these cases, results were within an order of magnitude of those obtained from RESRAD, with RESRAD results

models described in Regulatory Guide 1.109 (NRC, 1977). The code is widely used in radiological assessments. The CAP88-PC code was used in this assessment to estimate the concentrations of airborne radionuclides at the off-site residences in the all pathways analyses.

3.4.5 Radioactive Decay Computer Codes

Two computer codes were used to solve serial radioactive decay chains. These were RADDECAY (Negin and Worku, 1991) and BAT6CHN (Lindstrom *et al.*, 1990). RADDECAY is a commercially available software product that is used widely in radiological assessments. BAT6CHN was developed specifically for NTS performance assessment activities. Numerous test cases were run with each code and compared. The two codes were found to produce results that were essentially equivalent. Each code used the same nuclear decay data.

3.4.6 The ODIRE Computer Code

The infiltration of water ponded in a subsided cap was modeled with the ODIRE computer code. ODIRE has been tested and partially verified by its authors. Lindstrom *et al.* (1995) cross-checked the output of ODIRE with that of UNSAT-H, Version 2.0 (Fayer and Jones, 1990). The scenario used was a pulsed infiltration study. The two models were in excellent agreement. Unpublished comparisons between ODIRE and other codes are:

- ODIRE was compared with both UNSAT-H (Version 2.0) and with UNSAT2. The scenario used was taken directly from the UNSAT2 Manual, Section 7, which described the results of a laboratory column infiltration experiment (Skaggs *et al.*, 1970). In the case studied, ODIRE and UNSAT-H gave identical results; UNSAT2 failed when the sand column was dry.
- ODIRE was compared with HYDRUS (Kool and van Genuchten, 1989). The scenario used was taken directly from the HYDRUS Manual, Section 4-1, Example 1. The results were in excellent agreement.

3.5 Quality Assurance

Preparation of the performance assessment has been subject to the quality assurance requirements described in the REECo Quality Management Plan (QMP). The QMP implements the requirements in DOE Order 5700.6C.

The QMP provides broad direction for planning and accomplishment of activities affecting quality under suitably controlled conditions, including training and indoctrination of personnel, documentation of conditions found during surveillance and audits, testing, special processes, and use of computer codes and equipment to ensure the accomplishment of the performance objectives.

3.5.1 Site Characterization and Monitoring Quality Assurance

Procedures ERW-501, "Sample Control"; and L-F11.003, "Engineering Analysis Calculations," describe the quality-affecting work done for site characterization. The Engineering Department is responsible for maintaining this procedure.

Procedure ERW-501 identifies key environmental site characterization process controls to be implemented when sample collection is required. Sample control typically includes initial planing, collection, transport, storage, testing, and/or disposal. Procedure L-F11.003 describes the methodology and responsibilities used to establish the process for developing and controlling engineering analysis, and outlines the required steps and documentation to complete design calculations.

3.5.2 Software Quality Assurance

Modeling tasks supporting the performance assessment were performed by personnel at BN and Oak Ridge National Laboratory/Grand Junction. Each organization was responsible for developing and maintaining software quality assurance procedures.

Each investigator performing modeling analyses followed written quality assurance procedures implementing the requirements of NQA-1 (ASME, 1989) and DOE/LLW-102 (Seitz *et al.*, 1990).

Software was selected based on its applicability to the conceptual model of the system and level of documentation. Preference was given to software developed and sanctioned by U.S. government agencies for use in radiological assessments or to codes with documented histories of quality assurance testing and verification. Two codes were developed by REEC_o, CASCADR9 and BAT6CHN. These codes were developed under BN Procedure WOD-B09, "Mathematical Modeling and Model Building." Software analysis (the process of evaluating software quality by conducting analyses of variable usage, complexity analysis, or coverage analysis) was not performed for commercial or U.S. government-sanctioned software.

Each investigator performing modeling analyses was responsible for maintaining control of installed software, verification testing, and documentation of model results. Verification testing, the process of evaluating the implementation of the mathematical model, and the accuracy of numerical solutions was performed for all software. Verification testing consisted of comparison of model results with known solutions for specific problems and by benchmark testing against established software.

This chapter describes the results of the performance assessment and discusses parameter sensitivity and the uncertainty of the performance assessment results. The performance assessment has considered two classes of scenarios. The first class of scenarios, the release and pathway scenarios described in Sections 3.1.1 and 3.1.2, were analyzed to estimate the TEDE to members of the general public. The relevant performance objectives for these analyses are 25 mrem yr⁻¹ from all pathways, 10 mrem yr⁻¹ from atmospheric pathways, an annual average radon flux rate less than 20 pCi m⁻² s⁻¹, and a requirement to protect groundwater resources.

The second class of scenarios analyzed, described in Section 3.1.3, are the intruder scenarios. These assume future residents at the site have inadvertently exhumed buried waste and are exposed to the contamination while residing at the site. Intruder scenario analyses are

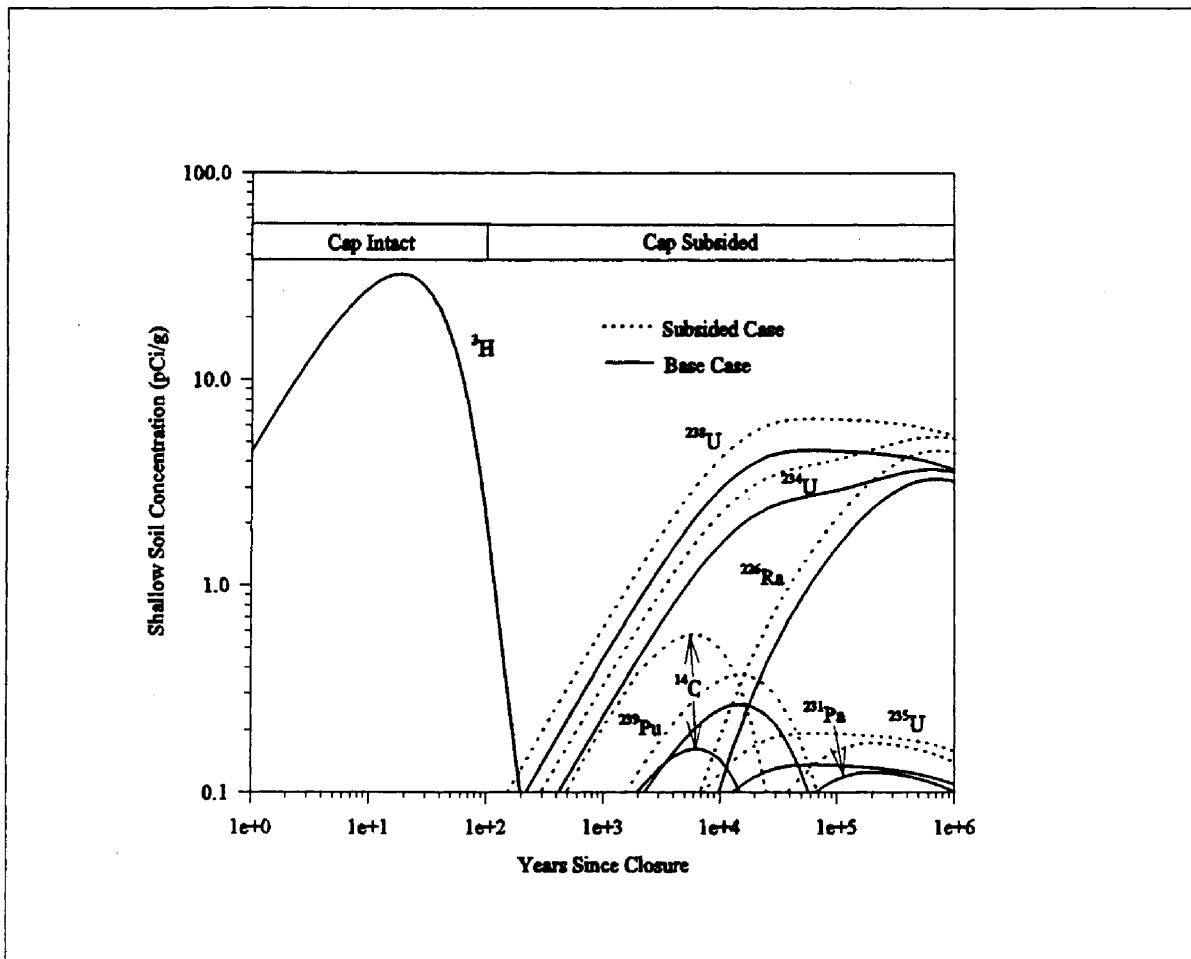


Figure 4.1 Estimated Surface Soil Concentration for the Base Case and Subsided Case. The base case assumes no subsidence. The subsided case assumes complete subsidence at 100 years.

evaluated as if the inventory was both gaseous and nonvolatile. This causes a conservative double counting of ^3H and ^{14}C that was considered acceptable given the low doses expected. Gaseous radionuclides were evaluated for each pathway scenario.

4.1.1.1 Results for the Transient Occupancy Scenario

The transient occupancy scenario estimates the dose to members of the public visiting the site for up to 2,000 hours per year. Exposure is assumed to occur through inhalation and external exposure only. Nine nonvolatile radionuclides were found to meet the screening criterion. All reach their peak concentration after the 10,000-year compliance interval. Therefore, the maximum dose in the 10,000-year compliance interval is the dose at 10,000 years.

The all-pathways TEDE estimated for members of the general public resulting from transient occupancy above the Area 5 RWMS appear in Table 4.1. The dose from short-lived radioactive progeny in equilibrium with their parents were added to the dose from the parent. Parent nuclides that include the dose from short-lived progeny are denoted in Table 4.1 as "+D."

Table 4.1 Estimated 10,000-Year and Maximum All-Pathway TEDE for Members of the General Public Exposed to Nonvolatile Radionuclides in the Transient Occupancy Scenario

Radionuclide	TEDE at 10,000 Years (mrem yr ⁻¹)	Maximum TEDE	
		Time of Max. (yr)	Max. TEDE (mrem yr ⁻¹)
²³⁹ Pu	0.025	15,000	0.027
²³⁵ U+D	0.018	60,000	0.027
²³¹ Pa	0.005	200,000	0.038
²²⁷ Ac+D	0.028	200,000	0.22
²³⁸ U+D	0.16	61,000	0.25
²³⁴ U	0.041	670,000	0.099
²³⁰ Th	0.0085	711,000	0.21
²²⁶ Ra+D	0.27	710,000	8.8
²²⁸ Th+D	0.031	56,000	0.049
Total	0.59	700,000	9.0

In the first 10,000 years after closure, the total dose from all nonvolatile radionuclides is expected to be less than 1 mrem yr⁻¹ for a person spending up to 2,000 hours per year at the Area 5 RWMS (Figure 4.2). The dose is mostly due to external exposure from ²²⁶Ra+D and inhalation of ²³⁸U+D. Because estimated doses will scale linearly with time of occupancy, it is possible to estimate the dose per hour spent at the site. The model predicts that individuals

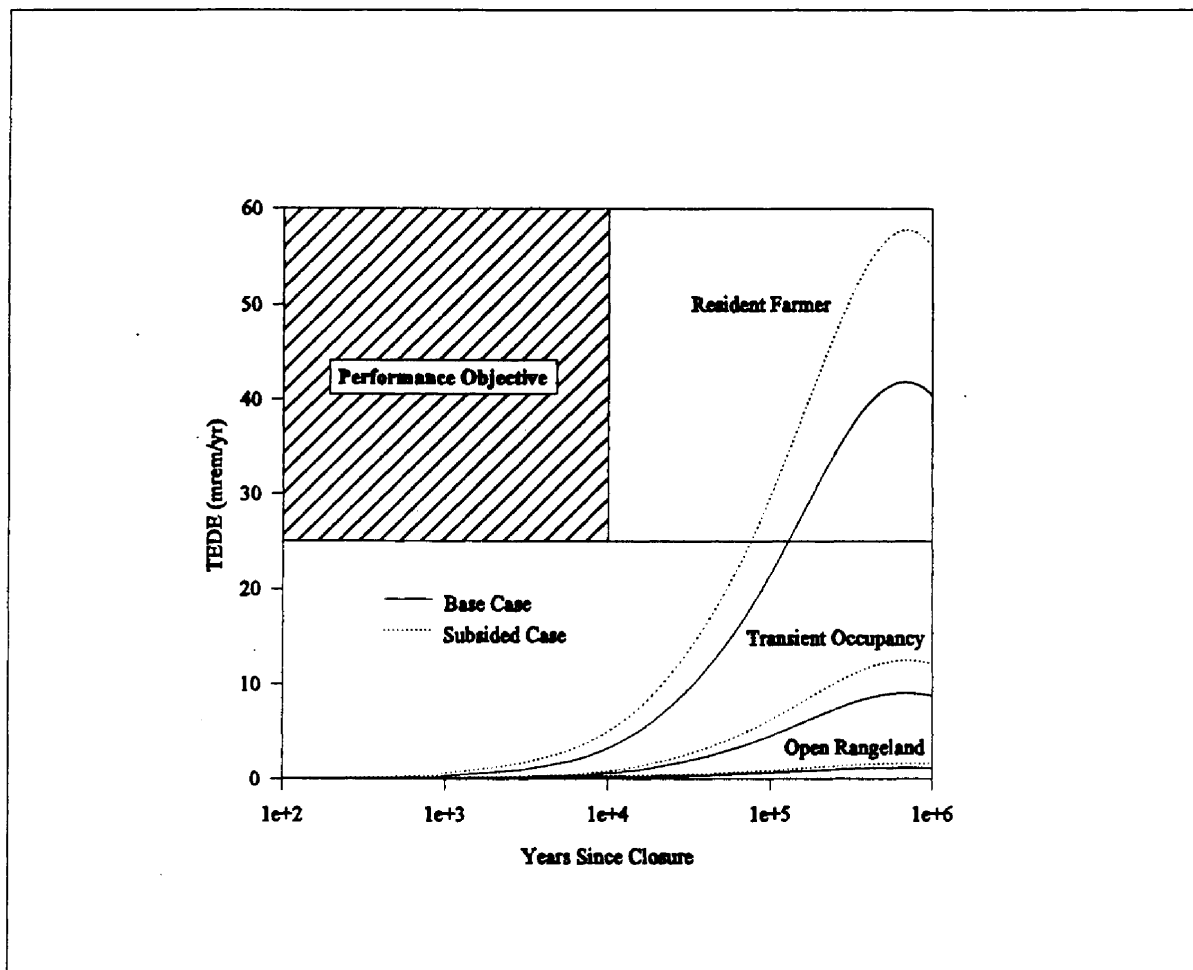


Figure 4.2. All-Pathways TEDE for Nonvolatile Radionuclides Released Under the Base Case and Subsidized Case Release Scenarios

highly conservative. The additional depth of burial will significantly reduce the dose by reducing or eliminating upward release pathways.

Intermediate results for the analyses above are presented in Appendix E. Soil activities and concentrations, calculated from the model described in Section 3.2.2.8, appear in Table E.4. Doses from inhalation and external exposure are listed in Tables E.6 and E.7.

4.1.1.2 Results for the Open Rangeland Scenario

The open rangeland scenario with an off-site ranch was described in Section 3.2.3.2. This scenario estimates the dose to members of the public residing off site and using the RWMS to graze livestock. Doses have been evaluated at two off-site locations with sufficient water to support permanent residents. The closest off-site residents are assumed to be at Indian

Springs during the 100-year institutional control period. Cane Springs, which is currently within the NTS boundary, is assumed to be available for development when institutional control ceases. During institutional control, exposure occurs through the atmospheric dispersion of contaminated soil and gaseous radionuclides. This is assumed to lead to contamination of air and soil at the off-site residence. The residents receive dose from external radiation from soils, inhalation of airborne radioactivity, and ingestion of foodstuffs grown at the off-site location. After institutional control ceases, the off-site resident continues to be exposed by all the pathways operating at the off-site location plus an additional pathway, ingestion of contaminated beef and milk from cattle grazing at the Area 5 RWMS.

As in the transient occupancy scenario, radionuclides in the inventory were screened and a limited number of nuclides were carried through the full pathway analysis. The maximum TEDE, corresponding to the time of peak soil concentration and the 10,000-year doses for nonvolatile radionuclides, are given for Indian Springs and Cane Springs in Table 4.2. The only difference between the two off-site locations, other than distances from the Area 5 RWMS, is that Cane Springs is not accessible until the end of the 100-year institutional control period. The same pathways are operating at both locations after the loss of institutional control. The ^3H and ^{14}C doses in Table 4.2 are based on calculations assuming that these nuclides are released only in a nonvolatile form.

Table 4.2 Estimated 10,000-Year and Maximum TEDE From Nonvolatile Radionuclides in the Open Rangeland Scenario

Radionuclide	TEDE at 10,000 years		Time of Maximum (years)	Maximum TEDE	
	Indian Springs	Cane Springs		Indian Springs	Cane Springs
	(mrem yr ⁻¹)			(mrem yr ⁻¹)	
³ H	†	†	100	9.2 × 10 ⁻³	9.2 × 10 ⁻³
¹⁴ C	0.051	0.051	6,300	0.058	0.058
²³⁹ Pu	2.4 × 10 ⁻⁵	7.3 × 10 ⁻⁵	15,000	2.6 × 10 ⁻⁵	8.5 × 10 ⁻⁵
²³⁵ U+D	1.7 × 10 ⁻³	1.7 × 10 ⁻³	60,000	2.6 × 10 ⁻³	2.6 × 10 ⁻³
²³¹ Pa	1.3 × 10 ⁻⁴	1.4 × 10 ⁻⁴	200,000	1.0 × 10 ⁻³	1.1 × 10 ⁻³
²²⁷ Ac+D	6.6 × 10 ⁻⁴	7.0 × 10 ⁻⁴	200,000	5.1 × 10 ⁻³	5.4 × 10 ⁻³
²³⁸ U+D	0.051	0.051	61,000	0.081	0.081
²³⁴ U	0.031	0.031	670,000	0.075	0.076
²³⁰ Th	4.7 × 10 ⁻⁵	6.4 × 10 ⁻⁵	710,000	1.2 × 10 ⁻³	1.6 × 10 ⁻³
²²⁶ Ra+D	6.5 × 10 ⁻³	6.5 × 10 ⁻³	710,000	0.21	0.21
²¹⁰ Pb+D	0.027	0.027	710,000	0.85	0.85
²²⁸ Ra+D	3.6 × 10 ⁻⁴	3.6 × 10 ⁻⁴	56,000	5.6 × 10 ⁻⁴	5.6 × 10 ⁻⁴

Table 4.2 (continued)

Radionuclide	TEDE at 10,000 years		Maximum TEDE		
	Indian Springs	Cane Springs	Time of Maximum (years)	Indian Springs	Cane Springs
	(mrem yr ⁻¹)			(mrem yr ⁻¹)	
²²⁸ Th+D	1.5 × 10 ⁻⁶	4.4 × 10 ⁻⁶	56,000	2.3 × 10 ⁻⁶	6.9 × 10 ⁻⁶
²⁴¹ Am	†	†	1,000	9.9 × 10 ⁻⁵	1.0 × 10 ⁻⁴
²³⁷ Np+D	9.0 × 10 ⁻⁵	9.0 × 10 ⁻⁵	53,000	1.6 × 10 ⁻⁴	1.6 × 10 ⁻⁴
Total	0.17	0.17	700,000	1.2	1.3

† - Maximum occurred before 10,000 years and dose at 10,000 years is negligible.

The maximum estimated TEDE within the 10,000-year compliance period is approximately 0.2 mrem yr⁻¹ and occurs at the end of the interval. The doses at the two off-site locations are approximately equal because most of the dose is from ingestion of beef and milk produced at the RWMS. The nuclides with maximum doses before 10,000 years are ³H, ¹⁴C, and ²⁴¹Am. Approximately 85 percent of the dose at 10,000 years is from ingestion of ²³⁸U+D, ²³⁴U, and ²¹⁰Pb+D in milk.

Most radionuclides reach a maximum soil concentration after the 10,000-year compliance interval because they are produced by radioactive decay of long-lived parents such as ²³⁸U and ²³⁵U (*Figure 4.1*). The maximum TEDE occurs about 700,000 years after closure and is slightly greater than 1 mrem yr⁻¹ (*Figure 4.2*). Again, the doses are from ingestion of ²³⁸U+D (6 percent), ²³⁴U+D (6 percent), ²²⁶Ra+D (15 percent), and ²¹⁰Pb+D (56 percent) in milk produced at the Area 5 RWMS.

Intermediate results for the open rangeland scenario can be found in Appendix E. Off-site air concentrations at Indian Springs and Cane Springs appear in Table E.5. Doses by exposure pathway are given in Tables E.8 and E.9 of Appendix E.

4.1.1.3 Results for the Resident Farmer Scenario

The resident farmer scenario is equivalent to the open rangeland scenario with the off-site ranch located at the edge of the 100-m (330-ft) buffer zone. This scenario was analyzed to provide consistency with other performance assessments. It is extremely unlikely that a resident will permanently occupy this site and engage in intensive agriculture. Therefore, the results for this scenario represent an extreme or bounding estimate of site performance.

The earliest the ranch was assumed to be present was at the time of closure. Because institutional controls are assumed to be present for 100 years after closure, direct access to the site was assumed to be impossible for this period. Soil at the off-site ranch was assumed

to have the same concentration as soil directly over the site (*Figure 4.1*). The concentration of most nonvolatile radionuclides in shallow soils increases slowly. Most do not reach a maximum for several thousand years, with the exception of ^3H . Therefore, the exposure during the institutional control period would potentially be dominated by the release of volatile radionuclides and nonvolatile ^3H . The estimated dose from nonvolatile ^3H is estimated to be only 0.5 mrem yr^{-1} (Table 4.3). Active institutional controls are likely to eliminate the potential of exposure to nonvolatile ^3H for at least the first 100 years after closure. By the end of the 100-year active institutional control period, the ^{14}C and ^{85}Kr sources are assumed to completely released and the nonvolatile ^3H dose will decrease to $0.002 \text{ mrem yr}^{-1}$ by radioactive decay alone.

Table 4.3 Estimated All-Pathways TEDE from Nonvolatile Radionuclides at 10,000 Years and at the Time of the Maximum Dose for a Resident Farmer Located 100 m (330 ft) From the Area 5 RWMS

Radionuclide	TEDE at 10,000 Years (mrem yr ⁻¹)	Maximum TEDE	
		Time of Max. (Years after Closure)	Maximum TEDE (mrem yr ⁻¹)
^3H	†	17	0.48
^{14}C	0.11	6,300	0.11
^{239}Pu	0.24	15,000	0.24
$^{235}\text{U}+\text{D}$	0.084	60,000	0.13
^{231}Pa	0.032	200,000	0.26
$^{227}\text{Ac}+\text{D}$	0.14	200,000	1.1
$^{238}\text{U}+\text{D}$	0.89	61,000	1.4
^{234}U	0.29	670,000	0.69
^{230}Th	0.042	710,000	1.0
$^{226}\text{Ra}+\text{D}$	1.2	710,000	39
$^{210}\text{Pb}+\text{D}$	0.028	710,000	8.7
^{240}Pu	0.023	7,000	0.025
$^{228}\text{Ra}+\text{D}$	0.034	56,000	0.053
$^{228}\text{Th}+\text{D}$	0.14	56,000	0.22
^{241}Am	5.4×10^{-8}	1,000	0.016
$^{237}\text{Np}+\text{D}$	0.13	53,000	0.22
Total	3.4	700,000	42

† - Source term is assumed to be completely depleted at 10,000 years by decay and release.

After ^3H is depleted, the concentration of other nonvolatile radionuclides in shallow soils is expected to increase gradually. By 10,000 years, the TEDE is estimated to increase to 4 mrem yr^{-1} (Table 4.3). Uranium-238+D and $^{226}\text{Ra}+\text{D}$ are the two greatest contributors to the dose. The pathways in decreasing order of significance were external irradiation (51 percent), inhalation (21 percent), plant ingestion (18 percent), milk ingestion (4 percent), soil ingestion (4 percent), and beef ingestion (0.6 percent). The dose is predominantly caused by external irradiation by $^{226}\text{Ra}+\text{D}$ (33 percent); inhalation of $^{238}\text{U}+\text{D}$, ^{234}U , and ^{239}Pu (16 percent); and ingestion of $^{210}\text{Pb}+\text{D}$ (7 percent).

After 10,000 years, the TEDE will increase gradually, reaching a peak when the concentration of ^{238}U progeny reach their peak concentration at 700,000 years. The peak TEDE at 700,000 years is estimated to be approximately 42 mrem yr^{-1} . The major contributors are external exposure from $^{226}\text{Ra}+\text{D}$ (72 percent) and ingestion of $^{210}\text{Pb}+\text{D}$ (16 percent).

The results for the resident farmer scenario should be interpreted considering the low probability of occurrence of the scenario and the conservative nature of the models. These models are simple screening calculations performed to provide reasonable assurance of compliance. This analysis was performed for comparison with other performance assessments. Even with the extremely conservative assumptions, the doses within the 10,000-year compliance interval are below the performance objective of 25 mrem yr^{-1} .

4.1.2 All-Pathways Analysis – Subsided Case Release Scenario

The concentration of nonvolatile radionuclides in shallow surface soil increases slightly for the subsided case release scenario for all radionuclides (Figure 4.1). The increase for most radionuclides is approximately 20 to 40 percent. At 10,000 years, $^{238}\text{U}+\text{D}$ and $^{226}\text{Ra}+\text{D}$ are major contributors to the dose in all scenarios. Under the subsided case, the ^{238}U shallow surface soil concentration increases from 2.9 to 4.1 pCi g^{-1} and the ^{226}Ra concentration increases from 0.10 to 0.14 pCi g^{-1} . The nonvolatile ^3H release remains largely unchanged because most of the release occurs prior to subsidence. The largest increase was found for ^{14}C . This increase is caused by the high plant-soil concentration ratio and deeper rooting of plants in the waste zone.

Subsidence also has the potential to initiate a groundwater pathway. The transient visitor scenario and the open rangeland scenario do not include an on-site resident. The only scenario that includes groundwater withdrawal at the site is the resident farmer. Therefore groundwater doses were evaluated for this scenario only.

Radionuclides were screened in the groundwater pathway based on their doses and potential to reach the aquifer in 10,000 years. The hydrologic analysis of transport suggests that seven long-lived nuclides and their progeny in the shallow land burial inventory have the potential

The average pit subsidence anticipated within the period of institutional control (100 years) is much smaller than that reported in *Figure 3.3*. At the end of institutional control, subsidence should be expected to vary from the full predicted subsidence (for areas with cardboard containers stacked full height) to essentially no subsidence (for areas with steel boxes stacked full height). The maximum subsidence is expected at some time after 100 years.

Analysis of the potential for subsidence at the Area 5 RWMS suggests that settling from 2 to 7 m (7 to 24 ft) is possible, depending on the waste containers, stacking configuration, and waste thickness. The greatest subsidence, 6 to 7 m (21 to 24 ft), is predicted for the waste cells with the greatest waste thicknesses, P06U and P03U. The maximum subsidence estimated for more typical trenches, with 3 to 5 m (11 to 16 ft) of waste, is 1.5 to 4 m (5 to 13 ft).

Subsidence could alter cap performance in several ways. In a worst-case early subsidence scenario, an abrupt collapse would form a depression with vertical walls. If the depression were greater than 2.4 m (7.8 ft), the depth of the temporary closure cover, waste containers might be exposed in the walls of the depression. Waste in the surrounding walls might

~~continually tumble into the depression. The effect of such a collapse might be thinning of the~~

- Increased transport of nonvolatile radionuclides by plants due to increased primary productivity from enhanced infiltration, and
- Downward advection of dissolved solutes to the uppermost aquifer caused by infiltration of run-on during major flood events.

The release scenario describes the processes of transporting volatile and nonvolatile radionuclides from the waste to soil, air, and vegetation. A conceptual model describing the base case release scenario is presented in Figure 3.4. The conceptual model and corresponding mathematical models based on Figure 3.4 have been subdivided into three models: one for volatile radionuclides, excluding radon; one for radon; and one for nonvolatile radionuclides.

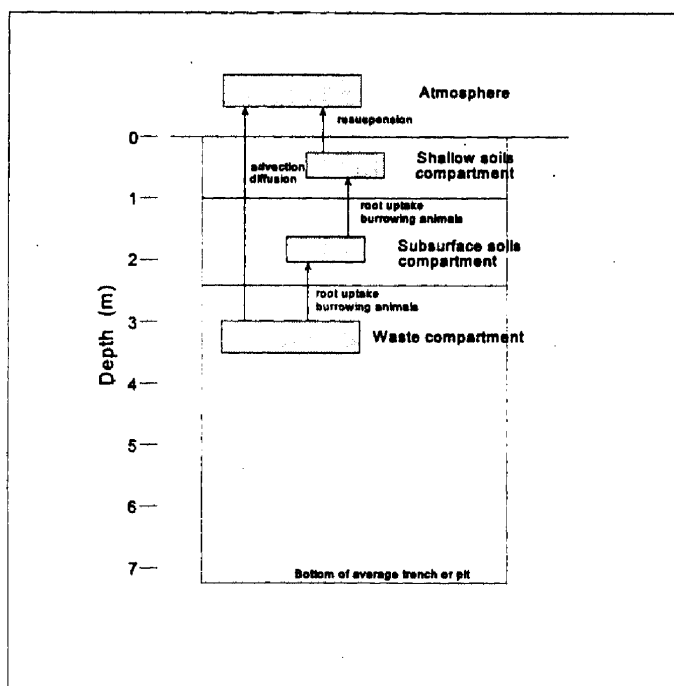


Figure 3.4 Conceptual Model of Radionuclide Release

3.2.2.1 Base Case Conceptual Model for Volatile Radionuclides Excluding Radon

The release of gaseous species of ^3H , ^{14}C , and ^{85}Kr to the air above the RWMS facility was assumed to be controlled by gaseous diffusion in the air-filled pore space. Assuming that the concentration gradient is constant over time, a conservative release rate, Q_i in Ci yr^{-1} , can be estimated from a modified one-dimensional flux equation of the form:

to reach the aquifer in 10,000 years (Table 4.4). These nuclides are either parent radionu-

clides with low K_d values or long-lived progeny assumed to migrate with a parent. The amount of radioactive ingrowth in 10,000 years is small for most long-lived members of uranium decay chains. Therefore, the maximum concentrations are controlled more by dilution effects than by ingrowth or decay. Nuclides in the Pit 6 thorium inventory are not expected to reach the aquifer in 10,000 years.

Table 4.4 Maximum Concentration of Long-lived Nuclides Expected to Reach the Aquifer in 10,000 Years Under the Subsided Case Release Scenario With Infiltration of Run-on

Radionuclide	Assumed K_d (ml g ⁻¹)	Time of Maximum Concentration (yrs)	Maximum Concentration (pCi L ⁻¹)
¹⁴ C	0	1,500	600
²³⁸ U	0	1,500	0.1
²³⁴ U	0	1,500	0.07
²³⁰ Th	Uranium Parent: 0	1,500	0.2
²²⁶ Ra	Uranium Parent: 0	1,500	0.3
²¹⁰ Pb	Uranium Parent: 0	1,500	0.3

Table 4.5 Comparison of All-Pathway TEDE From Nonvolatile Radionuclides Under the Base Case Release and Subsided Case Release Scenario

Pathway Scenario	TEDE at 10,000 years (mrem yr ⁻¹)		TEDE at Maximum (mrem yr ⁻¹)	
	Base Case	Subsided Case	Base Case	Subsided Case
Transient Occupancy	0.59	0.79	9.0	12
Open Rangeland - Indian Springs	0.17	0.34	1.2	1.6
Open Rangeland - Cane Springs	0.17	0.34	1.3	1.6
Resident Farmer	3.4	17	42	70

Subsidence combined with ponding of run-on has the potential to initiate a groundwater pathway in the resident farmer scenario. The groundwater dose was calculated assuming that the resident consumes 2 L day⁻¹ of drinking water. The estimated maximum CEDE is 12 mrem yr⁻¹ (Table 4.6). Because most of the dose is from ²³¹Pa and ²²⁷Ac+D, the maximum is expected to occur at approximately 6,600 years. This dose is considered an extreme bounding value because it assumes a release scenario with a very conservative upper limit of infiltration and a very conservative pathway scenario. The additional dose from the groundwater pathway increases the all-pathways TEDE in the resident farmer scenario to approximately 17 mrem yr⁻¹ at 10,000 years.

Table 4.6 Maximum CEDE to a Resident Farmer at 100 m From Ingestion of 2 L day⁻¹ of Groundwater

Nuclide	Time of Maximum (yrs)	CEDE (mrem yr ⁻¹)
¹⁴ C	1,500	0.9
²³⁸ U+D	1,500	0.02
²³⁴ U	1,500	0.01
²³⁰ Th	1,500	0.08
²²⁶ Ra+D	1,500	0.2
²¹⁰ Pb+D	1,500	2

²³⁵ U+D	1,500	7 × 10 ⁻⁴
²³¹ Pa	6,600	4
²²⁷ Ac+D	6,600	5
Total		12

4.1.3 Atmospheric Pathway – Base Case Release Scenario

Exposure to gaseous radionuclides through the atmospheric pathway was evaluated separately. These calculations assume that gaseous radionuclides were released at a maximum rate, based on diffusion in the air-filled pores.

4.1.3.1 *Results for the Transient Occupancy Scenario*

In the transient occupancy scenario, gaseous radionuclides were assumed to be diluted into a 2-m (6.6-ft) atmospheric mixing zone. Under the conceptual model for release of gaseous radionuclides, the release rate decreases over time as nuclides decay. Therefore, the maximum doses within the compliance interval would occur at the end of institutional control. The total dose from volatile ^3H , ^{14}C , and ^{85}Kr combined was estimated to be 0.01 mrem at 100 years. Tritium and ^{85}Kr decay to negligible levels during the period of

Table 4.7 shows that the estimated TEDE is much less than $0.001 \text{ mrem yr}^{-1}$. The distance to the nearest resident allows for significant dilution. Doses from ingestion of nonvolatile ^3H and ^{14}C incorporated into milk and beef produced at the site are much greater than the dose from inhalation of volatile forms.

The dose from resuspended soil particulates deposited at the off-site ranch reaches a maximum value in the compliance period at 10,000 years. The maximum dose occurs at Cane Springs because it is closer to the RWMS. The 10,000-year dose at Cane Springs is $4 \times 10^{-4} \text{ mrem yr}^{-1}$.

4.1.3.3 Results for the Resident Farmer Scenario

In the resident farmer scenario, gaseous radionuclides were dispersed over a 100-m (330-ft) distance to the assumed location of the off-site residence. The maximum volatile radionuclide release rate is expected at closure and will decrease thereafter as the source is depleted by release and radioactive decay. The maximum expected TEDE during the institutional control period is approximately 6 mrem yr^{-1} from inhalation and dermal absorption of ^3H (Table 4.8). It is unlikely that a ranch will be developed at the site boundary during institutional control. If the scenario is delayed to 100 years after closure, the TEDE from ^3H declines to $0.03 \text{ mrem yr}^{-1}$.

Table 4.8 Estimated TEDE for Exposure of a Resident Farmer to Volatile Radionuclides at the 100-m Buffer Boundary. The TEDE is the maximum value, which is expected to occur at closure.

Nuclide	Concentration at 100 m (Ci m^{-3})	TEDE (mrem yr^{-1})
^3H	8.0×10^{-9}	6.4
^{14}C	1.7×10^{-10}	0.034
^{85}Kr	1.1×10^{-12}	1.5×10^{-5}

The TEDE from inhalation of resuspended soil particulates increases throughout the compliance period. The maximum dose from inhalation of soil particulates is $0.77 \text{ mrem yr}^{-1}$ at 10,000 years.

4.1.4 Atmospheric Pathway – Subsided Release Case

The release of gaseous radionuclides in the subsided case release scenario was described in Section 3.2.2.2. Subsidence was assumed to occur at 100 years, when active institutional control ends. Therefore, the release of ^3H was estimated to remain unchanged at 200 Ci yr^{-1}

at closure. After active institutional control when subsidence occurs, the ^3H release rate was estimated to be 1.0 Ci yr^{-1} . All other gaseous radionuclides were assumed to be completely released in the first year and were not affected by subsidence.

For the subsided case, the TEDE from release of gaseous radionuclides in the transient occupancy scenario remains unchanged at $0.01 \text{ mrem yr}^{-1}$ at 100 years after closure. The dose in the open rangeland scenario remains unchanged at closure for Indian Springs. The doses are less than $3 \times 10^{-6} \text{ mrem yr}^{-1}$ at 100 years. The dose to a resident farmer at 100 m (330 ft) remains unchanged at 6 mrem yr^{-1} at closure. At 100 years when subsidence occurs, the TEDE from ^3H is estimated to be $0.03 \text{ mrem yr}^{-1}$.

Subsidence has no significant effect on the release of gaseous radionuclides. Subsidence has no significant effect on the release of ^{14}C and ^{85}Kr because the entire inventory is assumed to be released for both release scenarios. Subsidence increases ^3H releases, but ^3H undergoes significant radioactive decay during the period of active institutional control, before unremediated subsidence begins.

4.1.5 Radon Flux from Shallow Land Burial Trenches and Pits

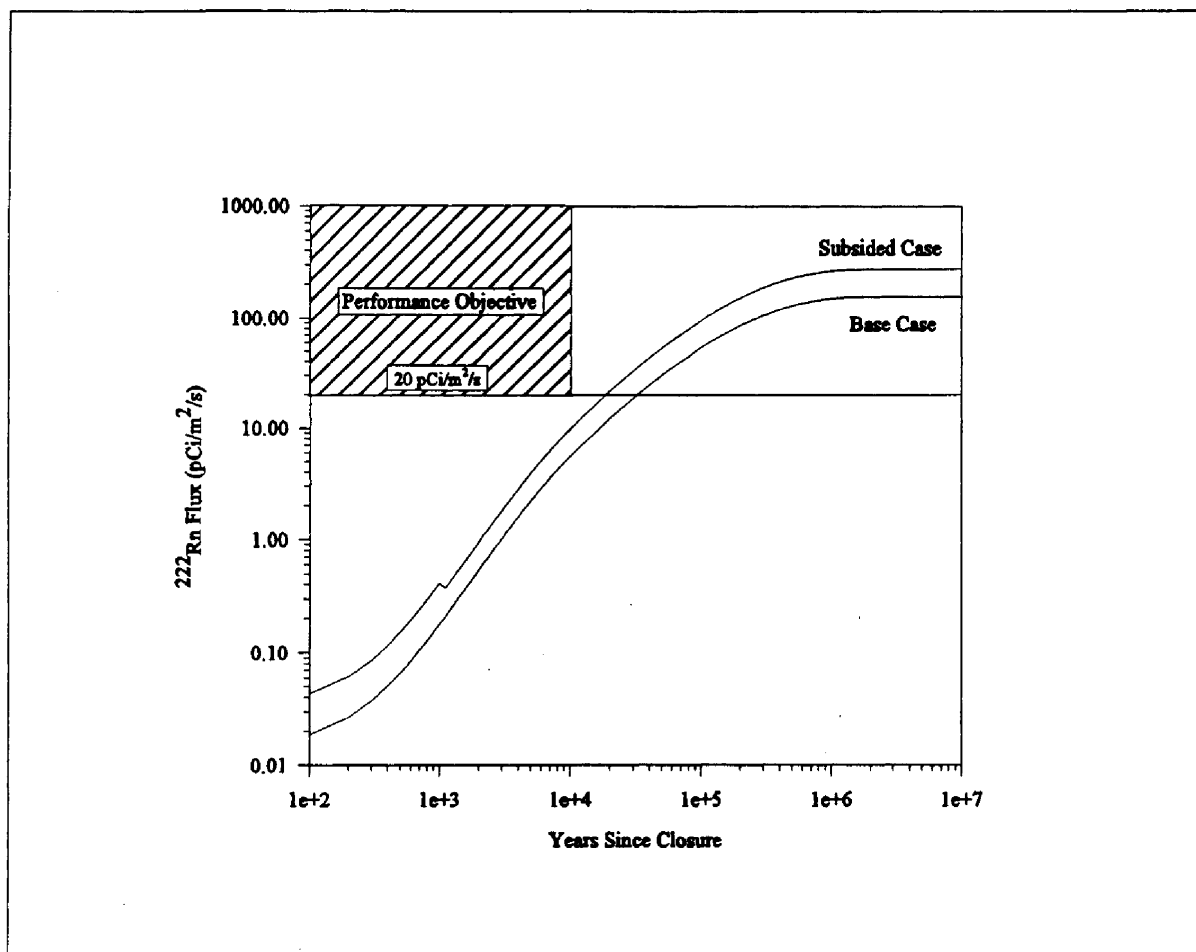
The CASCADR9 computer code has been used to estimate K_{SLB} , the ratio between ^{222}Rn surface flux and ^{226}Ra activity concentration for the shallow land burial geometry. The flux from shallow land burial trenches and pits (J_{SLB}) at any given time is:

$$J_{\text{SLB}} = 1 \times 10^{-12} K_{\text{SLB}} C_{\text{SLB}}(t) \quad (\text{pCi m}^{-2} \text{ s}^{-1}) \quad (4.1)$$

where C_{SLB} is the shallow land burial ^{226}Ra activity concentration in units of Ci m^{-3} . The activity concentration of ^{226}Ra will increase very slowly over the next 10,000 years, not reaching a peak for several million years. The predicted radon fluxes for the base case and subsided case are presented in Table 4.9 and Figure 4.3. The flux remains below the performance objective of $20 \text{ pCi m}^{-2} \text{ s}^{-1}$ throughout the 10,000-year compliance period for both cases. As shown in Figure 4.3, the base case flux exceeds the performance objective in approximately 30,000 years and reaches a peak of $156 \text{ pCi m}^{-2} \text{ s}^{-1}$ in 3.5×10^6 years. The flux results beyond 30,000 years are considered very conservative because they assume that cap thickness remains constant. In reality, closure caps should eventually be buried by accumulating sediments. It is likely that much more than 2.4 m (7.9 ft) of sediment will cover the site in 3.5×10^6 years and that the actual peak fluxes will be much smaller than those predicted here for a 2.4-m (7.9-ft) cover. Approximately 4.5 m (14.8 ft) of cover would be required to attenuate the peak flux occurring at 3.5×10^6 years to $20 \text{ pCi m}^{-2} \text{ s}^{-1}$. Subsidence is conservatively estimated to increase the average annual fluxes by approximately a factor of two. The performance objective is exceeded at approximately 20,000 years for the subsided case.

Table 4.9 Estimated Radon Flux From Shallow Land Burial Trenches and Pits

Years Since Closure	^{226}Ra Activity Concentration (Ci m^{-3})	Base Case $K_{\text{SLB}} = 5.6 \times 10^{-8} \text{ m s}^{-1}$	Subsided Case 0 - 1000 yrs: $K_{\text{SLB}} = 1.3 \times 10^{-7} \text{ m s}^{-1}$ 1000+ yrs: $K_{\text{SLB}} = 1.0 \times 10^{-7} \text{ m s}^{-1}$
		^{222}Rn Flux ($\text{pCi m}^{-2} \text{ s}^{-1}$)	^{222}Rn Flux ($\text{pCi m}^{-2} \text{ s}^{-1}$)
100	3.3×10^{-7}	0.018	0.043
10,000	1.0×10^{-4}	5.6	10
3.5×10^6	2.8×10^{-3}	156	280

Figure 4.3 Estimated ^{222}Rn Flux From a Shallow Land Burial Waste Cell for the Base Case and Subsided Case Release Scenarios

4.1.6 Estimated Radon Flux from Pit 6 (P06U)

Pit 6 has been modified to accept a thorium waste stream containing ^{230}Th . CASCADR9 was used to develop a ratio between surface flux and activity concentration (K-factor) for each waste cell. The waste cells can be considered independently and the results summed to obtain the total flux. The peak ^{226}Ra activity concentrations occur at different times for the two waste cells. This is because of differing initial concentrations of long-lived parent nuclides. When the thorium waste reaches its peak ^{226}Ra concentration in 9,000 years, the concentration of LLW in the upper cell is two orders of magnitude lower. The LLW in the upper cell will not reach its maximum concentration for several million years, when ^{230}Th in the lower cell will have decayed to background. Assuming the independent K factors for each cell, the total flux is:

$$J_{P6} = 1 \times 10^{12} (K_{P6U} C_{SLB}(t) + K_{P6L} C_{P6L}(t)) \quad (\text{pCi m}^{-2} \text{s}^{-1}) \quad (4.2)$$

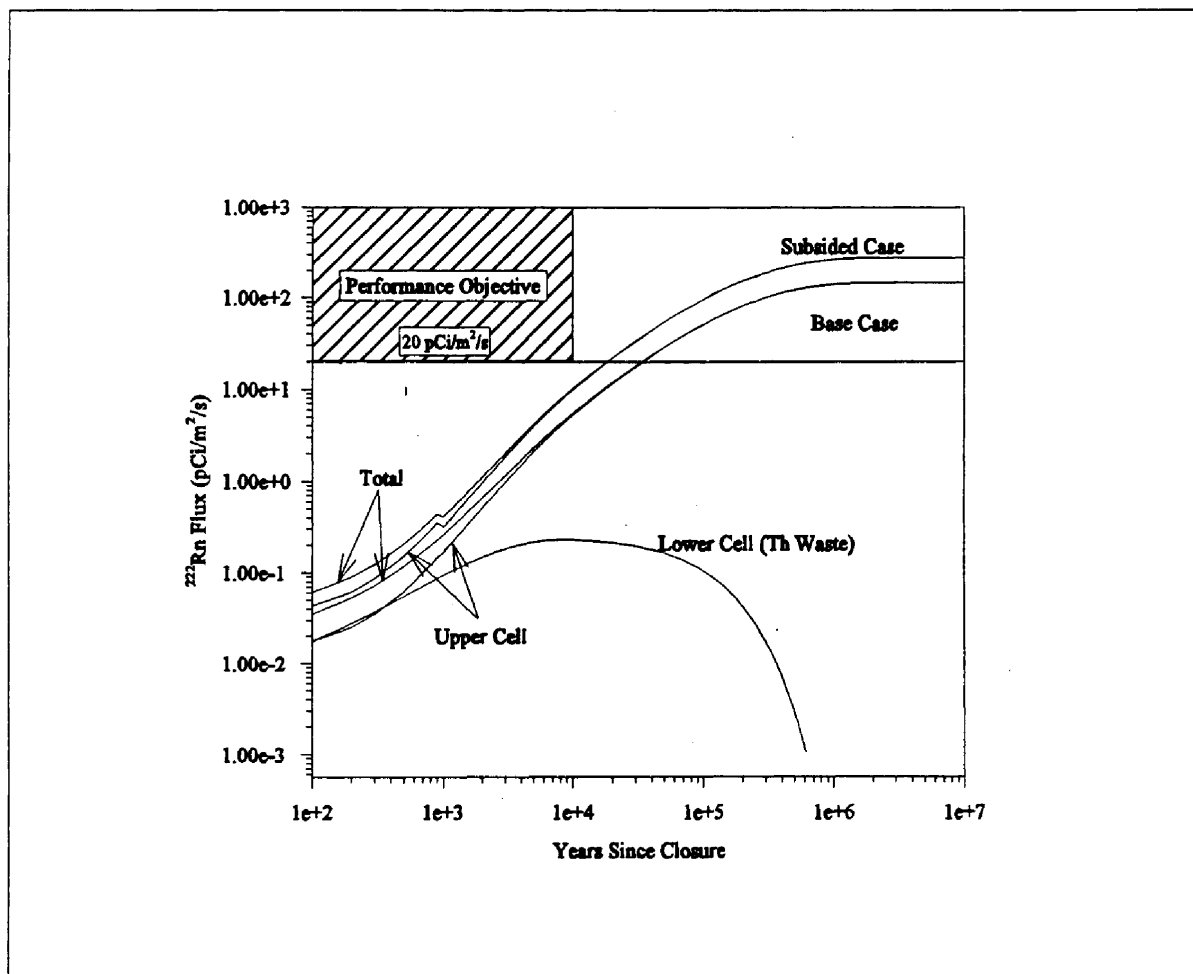
where:

- J_{P6} = surface ^{222}Rn flux from Pit 6 ($\text{pCi m}^{-2} \text{s}^{-1}$),
- K_{P6U} = ratio of surface flux to ^{226}Ra activity concentration in the upper cell of Pit 6 (m s^{-1}),
- K_{P6L} = ratio of surface flux to ^{226}Ra activity concentration in the lower cell of Pit 6 (m s^{-1}), and
- $C_{P6L}(t)$ = activity concentration ^{226}Ra in the lower cell of Pit 6 (Ci m^{-3}).

Total radon flux from Pit 6 is presented in Table 4.10 and in Figure 4.4. The total flux remains below the performance objective limit of $20 \text{ pCi m}^{-2} \text{s}^{-1}$ during the entire 10,000-year compliance interval for the base case and subsided case. Subsidence approximately doubles the flux. For the first 700 years, the flux from each cell is approximately equal. After this time, the ^{222}Rn flux from the upper cell begins to exceed the flux from the Th waste and the predictions are very similar to those for the shallow land burial case. Although the ^{226}Ra source term in the Th waste is greater, the upper cell produces a greater flux because the burial is more shallow. By 10,000 years, the total flux for the base case reaches $5.5 \text{ pCi m}^{-2} \text{s}^{-1}$, approximately equal to the flux predicted for the shallow land burial case. The total flux for the base case exceeds the $20 \text{ pCi m}^{-2} \text{s}^{-1}$ limit in approximately 30,000 years and reaches a peak in 3.5×10^6 years. Total fluxes beyond 30,000 years are likely to be less than estimated here because alluvial sediment accumulating at the site is likely to increase the overburden. The flux limit is exceeded in approximately 20,000 years for the subsided case.

Table 4.10 Estimated Total ^{222}Rn Flux From Pit 6 (P06U)

Years Since Closure	$K_{\text{P6U}} = 5.3 \times 10^{-8} \text{ m s}^{-1}$ $K_{\text{P6L}} = 3.3 \times 10^{-11} \text{ m s}^{-1}$	0-1000 yrs: $K_{\text{P6U}} = 1.3 \times 10^{-7} \text{ m s}^{-1}$ 1000+ yrs: $K_{\text{P6U}} = 1.0 \times 10^{-7} \text{ m s}^{-1}$ $K_{\text{P6L}} = 3.3 \times 10^{-11} \text{ m s}^{-1}$
	Pit 6 Total ^{222}Rn Flux ($\text{pCi m}^{-2} \text{ s}^{-1}$)	Pit 6 Total ^{222}Rn Flux ($\text{pCi m}^{-2} \text{ s}^{-1}$)
100	0.035	0.061
9,000	4.9	9.0
10,000	5.6	10
3.5×10^6	147	280

Figure 4.4 Estimated ^{222}Rn Flux From Pit 6 (P06U) for the Base Case and Subsidized Case Release Scenarios

4.1.7 Protection of Groundwater Resources

Under the base case scenario, infiltration and recharge of the aquifer at the Area 5 RWMS does not occur and protection of groundwater resources is assured. Subsidence, however, has the potential to initiate recharge if large amounts of run-on pond in a subsidence feature. Even under these extreme conditions, model results suggest that the uppermost aquifer would still be suitable as a source of drinking water.

The first standard for groundwater protection is that the combined concentration of ^{226}Ra and ^{228}Ra not exceed 5 pCi L^{-1} . There were no credible conditions causing ^{228}Ra to reach the aquifer in 10,000 years. Its long-lived parent, ^{232}Th , has a travel time greater than 160,000 years. The estimated ^{226}Ra concentration migrating with its uranium parents is well below the 5 pCi L^{-1} limit throughout the 10,000-year compliance period (Table 4.11). Background ^{226}Ra and ^{228}Ra in the alluvial aquifer is less than the detection limit, so the man-made plus natural total radium is expected to remain below 5 pCi L^{-1} .

Table 4.11 Estimated Total Radium Activity Concentrations at the Time of the Peak Uranium Concentration and at 10,000 Years

Standard	Total Ra at 1,500 Years	Total Ra at 10,000 years
$^{226}\text{Ra} + ^{228}\text{Ra} < 5 \text{ pCi L}^{-1}$	0.3 pCi L^{-1}	0.1 pCi L^{-1}

The second standard for groundwater protection is for the gross alpha concentration,

Table 4.12 (continued)

Nuclide	Assumed Kd (ml g ⁻¹)	Time of Maximum (yr)	Maximum Gross Alpha (pCi L ⁻¹)
²³¹ Pa	Mixed	6,600	0.5
²²⁷ Ac+D [†]	Mixed	6,600	1.5
Total			2.8

[†] ²²⁷Ac+D = ²²⁷Ac, ²²⁷Th, ²²³Ra

The third standard is that the dose equivalent to the total body or any organ from beta particle and photon radioactivity does not exceed 4 mrem yr⁻¹. The only nuclide meeting the definition of man-made beta particle and photon radioactivity is ¹⁴C. The sum of the fractions for ¹⁴C is

$$\frac{600 \text{ pCi L}^{-1}}{2,000 \text{ pCi L}^{-1}} = 0.3 \quad (4.3)$$

Because the sum of fractions is less than 1.0, the performance objective is not exceeded. The dose equivalent using the dosimetry system described would be approximately 1 mrem yr⁻¹ to body fat. Man-made beta particle and photon radioactivity has not been detected in the uppermost aquifer beneath the Area 5 RWMS.

The final criterion, evaluated for information only, was that the total uranium concentration be less than 20 µg L⁻¹. Because the assumed solubility limit of uranium in Frenchman Flat groundwater was 17 µg L⁻¹, compliance with this criterion is assured. The maximum concentration of waste-derived uranium is estimated to be 0.3 µg L⁻¹. The highest naturally occurring uranium value measured for Area 5 in UE5PW-3 is 9.7 µg L⁻¹. Therefore, the total uranium concentration is expected to be approximately 10 µg L⁻¹.

4.2 Analysis Results for Intruder Scenarios

This section describes the results of intruder analyses. Intruder scenarios are hypothetical events analyzed to estimate the risk to persons intruding into buried waste after loss of institutional control. Intruder analyses are performed to determine the activity concentration of waste suitable for disposal in the near surface. Three intruder analyses, one acute and two chronic, were analyzed: the drilling scenario (acute), the intruder-agriculture scenario

(chronic), and postdrilling scenario (chronic). Two source terms were analyzed in the performance assessment, the inventory for shallow land burial pits and trenches and the inventory for Pit 6.

4.2.1 Analysis Results for the Acute Intruder Drilling Scenario

The intruder drilling scenario is a short-term exposure scenario that assumes an intruder is exposed to contaminated drill cuttings. Complete details of the scenario, conceptual models and assumptions, are provided in Section 3.3.1. The intruders are assumed to be exposed via inhalation of resuspended drill cuttings, inadvertent ingestion of cuttings, and external irradiation from the drilling fluids. The time of exposure is assumed to be 100 hours, approximately two weeks. The acute drilling scenario was analyzed for the shallow land burial inventory and for Pit 6. Results are presented for 100 years, 10,000 years and, if

Table 4.13 Soil Activity Concentrations and TEDE for the Acute Drilling Scenario With the Shallow Land Burial Inventory. Soil activity concentration is the estimated concentration of the drill cuttings created by the intruder.

Radionuclide	At 100 years		At 10,000 years		At Time of Maximum Dose		
	Soil Conc. (pCi g ⁻¹)	TEDE (mrem)	Soil Conc. (pCi g ⁻¹)	TEDE (mrem)	Time (years)	Soil Conc. (pCi g ⁻¹)	TEDE (mrem)
³ H	30	3.9×10^{-4}			100	30	3.9×10^{-4}
¹⁴ C	0.11	2.7×10^{-4}	0.033	8.1×10^{-5}	100	0.11	2.7×10^{-4}
³⁶ Cl	4.1×10^{-9}	1.7×10^{-14}	4.0×10^{-9}	1.6×10^{-14}	100	4.1×10^{-9}	1.7×10^{-14}
⁵⁹ Ni	6.2×10^{-7}	9.5×10^{-14}	5.7×10^{-7}	8.7×10^{-14}	100	6.2×10^{-7}	9.5×10^{-14}
⁶⁰ Co	1.1×10^{-8}	4.4×10^{-10}			100	1.1×10^{-8}	4.4×10^{-10}
⁶³ Ni	0.049	1.6×10^{-8}			100	0.049	1.6×10^{-8}
⁹⁰ Sr+D	0.011	9.4×10^{-7}			100	0.011	9.4×10^{-7}
⁹³ Zr+D	1.0×10^{-6}	6.2×10^{-12}	1.0×10^{-6}	6.2×10^{-12}	100	1.0×10^{-6}	6.2×10^{-12}
⁹⁹ Tc	0.75	5.5×10^{-7}	0.75	5.3×10^{-7}	100	0.75	5.5×10^{-7}
¹⁰⁷ Pd	2.9×10^{-7}	6.9×10^{-14}	2.9×10^{-7}	6.9×10^{-14}	100	2.9×10^{-7}	6.9×10^{-14}
¹²⁶ Sn+D	3.4×10^{-7}	4.3×10^{-8}	3.2×10^{-7}	4.0×10^{-8}	100	3.4×10^{-7}	4.3×10^{-8}
¹²⁹ I	8.7×10^{-8}	2.5×10^{-11}	8.7×10^{-8}	2.5×10^{-11}	100	8.7×10^{-8}	2.5×10^{-11}
¹³³ Ba	5.3×10^{-9}	4.7×10^{-11}			100	5.3×10^{-9}	4.7×10^{-11}
¹³⁵ Cs	2.4×10^{-6}	8.3×10^{-12}	2.4×10^{-6}	8.1×10^{-12}	100	2.4×10^{-6}	8.3×10^{-12}
¹³⁷ Cs+D	0.013	1.4×10^{-4}			100	0.013	1.4×10^{-4}
¹⁵¹ Sm	1.7×10^{-3}	9.5×10^{-10}			100	1.7×10^{-3}	9.5×10^{-10}
¹⁵² Eu	1.1×10^{-11}	2.0×10^{-13}			100	1.1×10^{-11}	2.0×10^{-13}
¹⁵⁴ Eu	7.8×10^{-8}	1.6×10^{-9}			100	7.8×10^{-8}	1.6×10^{-9}
²⁰⁷ Pb	3.6×10^{-11}	7.5×10^{-13}			100	3.6×10^{-11}	7.5×10^{-13}

Table 4.13 (continued)

Radionuclide	At 100 years		At 10,000 years		At Time of Maximum Dose		
	Soil Conc. (pCi g ⁻¹)	TEDE (mrem)	Soil Conc. (pCi g ⁻¹)	TEDE (mrem)	Time (years)	Soil Conc. (pCi g ⁻¹)	TEDE (mrem)
²³² U	1.0 × 10 ⁻³	9.6 × 10 ⁻⁶			100	1.0 × 10 ⁻³	9.6 × 10 ⁻⁶
²³² Am+D	2.3 × 10 ⁻⁵	2.8 × 10 ⁻⁷	9.0 × 10 ⁻⁶	1.1 × 10 ⁻⁷	100	2.3 × 10 ⁻⁵	2.8 × 10 ⁻⁷
²³⁹ Pu	3.1	0.028	2.3	0.021	100	3.1	0.028
²³⁸ U+D	0.80	3.8 × 10 ⁻³	0.81	3.8 × 10 ⁻³	450,000	0.80	3.8 × 10 ⁻³
²³¹ Pa	3.3 × 10 ⁻³	7.6 × 10 ⁻⁵	0.15	3.6 × 10 ⁻³	450,000	0.80	0.018
²²⁷ Ac+D	2.8 × 10 ⁻³	2.9 × 10 ⁻⁴	0.15	0.016	450,000	0.80	0.083
²⁴¹ Pu	0.027	4.8 × 10 ⁻⁶			100	0.027	4.8 × 10 ⁻⁶
²⁴¹ Am	0.52	4.8 × 10 ⁻³			100	0.52	4.8 × 10 ⁻³
²³⁷ Np+D	2.3 × 10 ⁻⁴	2.8 × 10 ⁻⁶	3.1 × 10 ⁻⁴	3.8 × 10 ⁻⁶	4,600	3.3 × 10 ⁻⁴	4.1 × 10 ⁻⁶
²³² U	3.4 × 10 ⁻⁵	6.4 × 10 ⁻⁸	4.6 × 10 ⁻⁵	8.6 × 10 ⁻⁸	640,000	2.6 × 10 ⁻⁴	4.8 × 10 ⁻⁷
²²⁹ Th+D	3.8 × 10 ⁻⁷	1.2 × 10 ⁻⁸	2.5 × 10 ⁻⁵	8.2 × 10 ⁻⁷	640,000	2.6 × 10 ⁻⁴	8.4 × 10 ⁻⁶
²⁴¹ Pu	6.2 × 10 ⁻⁵	5.2 × 10 ⁻⁷	6.1 × 10 ⁻⁵	5.1 × 10 ⁻⁷	100	6.2 × 10 ⁻⁵	5.2 × 10 ⁻⁷
²³⁸ U+D	27	0.054	27	0.054	3,500,000	27	0.054
²³⁹ Pu	1.5	0.012			100	1.5	0.012
²³⁴ U	14	0.027	14	0.027	3,500,000	27	0.051
²³⁰ Th	0.029	1.3 × 10 ⁻⁴	1.2	5.7 × 10 ⁻³	3,500,000	27	0.12

Table 4.13 (continued)

Radionuclide	At 100 years		At 10,000 years		At Time of Maximum Dose		
	Soil Conc. (pCi g ⁻¹)	TEDE (mrem)	Soil Conc. (pCi g ⁻¹)	TEDE (mrem)	Time (years)	Soil Conc. (pCi g ⁻¹)	TEDE (mrem)
²²⁶ Ra+D	3.3×10^{-3}	8.9×10^{-5}	0.97	0.026	3,500,000	27	0.73
²¹⁰ Pb+D	2.9×10^{-3}	9.7×10^{-6}	0.97	3.3×10^{-3}	3,500,000	27	0.091
²⁴⁴ Cm	3.6×10^{-4}	1.7×10^{-6}			100	3.6×10^{-4}	1.7×10^{-6}
²⁴⁸ Cm	1.8×10^{-11}	5.9×10^{-13}	1.7×10^{-11}	5.7×10^{-13}	100	1.8×10^{-11}	5.9×10^{-13}
²⁴⁰ Pu	0.65	5.7×10^{-3}	0.23	2.0×10^{-3}	100	0.65	5.7×10^{-3}
²³⁶ U	0.023	4.0×10^{-5}	0.023	4.0×10^{-5}	32,000	0.023	4.0×10^{-5}
²³² Th	0.051	1.2×10^{-3}	0.050	1.1×10^{-3}	100	0.051	1.2×10^{-3}
²²⁸ Ra+D	0.051	7.7×10^{-4}	0.050	7.6×10^{-4}	100	0.051	7.7×10^{-4}
²²⁸ Th+D	0.051	1.2×10^{-3}	0.050	1.2×10^{-3}	100	0.051	1.2×10^{-3}
Total		0.15		0.17			

Table 4.14 Soil Activity Concentrations and TEDE for the Acute Drilling Scenario for Pit 6 (P06U) at 100 Years. Soil activity concentration is the estimated concentration of the drill cuttings created by the intruder.

--	--	--	--

Table 4.14 (continued)

Radionuclide	Upper Cell		Lower Cell		Total TEDE (mrem)
	Soil Conc. (pCi g ⁻¹)	TEDE (mrem)	Soil Conc. (pCi g ⁻¹)	TEDE (mrem)	
²⁴¹ Pu	0.034	6.1 × 10 ⁻⁶			6.1 × 10 ⁻⁶
²⁴¹ Am	0.66	6.1 × 10 ⁻³			6.1 × 10 ⁻³
²³⁷ Np+D	2.9 × 10 ⁻⁴	3.5 × 10 ⁻⁶			3.5 × 10 ⁻⁶
²³³ U	4.3 × 10 ⁻⁵	8.1 × 10 ⁻⁸			8.1 × 10 ⁻⁸
²²⁹ Th+D	4.8 × 10 ⁻⁷	1.5 × 10 ⁻⁸			1.5 × 10 ⁻⁸
²⁴² Pu	7.8 × 10 ⁻⁵	6.6 × 10 ⁻⁷			6.6 × 10 ⁻⁷
²³⁸ U+D	34	0.068			0.068
²³⁸ Pu	1.9	0.015			0.015
²³⁴ U	18	0.034			0.034
²³⁰ Th	0.037	1.6 × 10 ⁻⁴	55	0.25	0.25
²²⁶ Ra+D	4.2 × 10 ⁻³	1.1 × 10 ⁻⁴	3.8	0.10	0.10
²¹⁰ Pb+D	3.7 × 10 ⁻³	1.2 × 10 ⁻⁵	3.1	0.010	0.010
²⁴⁴ Cm	4.6 × 10 ⁻⁴	2.1 × 10 ⁻⁶			2.1 × 10 ⁻⁶
²⁴⁸ Cm	2.3 × 10 ⁻¹¹	7.5 × 10 ⁻¹³			7.5 × 10 ⁻¹³
²⁴⁰ Pu	0.82	7.2 × 10 ⁻³			7.2 × 10 ⁻³
²³⁶ U	0.029	5.1 × 10 ⁻⁵			5.1 × 10 ⁻⁷
²³² Th	0.064	1.5 × 10 ⁻³	355	8.1	8.1
²²⁸ Ra+D	0.064	9.7 × 10 ⁻⁴	355	5.4	5.4
²²⁸ Th+D	0.064	1.5 × 10 ⁻³	355	8.2	8.2
Total		0.18		22	22

Table 4.15 Soil Activity Concentrations and TEDE for the Acute Drilling Scenario for Pit 6 (P06U) at 10,000 Years. Results for the lower cell are for 9,000 years, when the activity concentration of ^{226}Ra reaches its peak. Soil activity concentration is the estimated concentration of the drill cuttings created by the intruder.

Radionuclide	Upper Cell		Lower Cell		Total TEDE (mrem)
	Soil Conc. (pCi g ⁻¹)	TEDE (mrem)	Soil Conc. (pCi g ⁻¹)	TEDE (mrem)	
^{14}C	0.042	8.1×10^{-5}			8.1×10^{-5}
^{36}Cl	5.1×10^{-9}	2.0×10^{-14}			2.0×10^{-14}
^{59}Ni	7.2×10^{-7}	1.1×10^{-13}			1.1×10^{-13}
$^{93}\text{Zr}+\text{D}$	1.3×10^{-6}	7.8×10^{-12}			7.8×10^{-12}
^{99}Tc	0.93	7.0×10^{-7}			7.0×10^{-7}
^{107}Pd	3.7×10^{-7}	8.7×10^{-14}			8.7×10^{-14}
$^{126}\text{Sn}+\text{D}$	4.0×10^{-7}	5.1×10^{-8}			5.1×10^{-8}
^{129}I	1.1×10^{-7}	3.2×10^{-11}			3.2×10^{-11}
^{135}Cs	2.9×10^{-6}	1.0×10^{-11}			1.0×10^{-11}
$^{243}\text{Am}+\text{D}$	1.1×10^{-5}	1.4×10^{-7}			1.4×10^{-7}
^{239}Pu	2.9	0.027			0.027
$^{235}\text{U}+\text{D}$	1.0	4.8×10^{-3}			4.8×10^{-3}
^{231}Pa	0.19	4.5×10^{-3}			4.5×10^{-3}
$^{227}\text{Ac}+\text{D}$	0.19	0.020			0.020
$^{237}\text{Np}+\text{D}$	3.9×10^{-4}	4.8×10^{-6}			4.8×10^{-6}
^{233}U	5.8×10^{-5}	1.1×10^{-7}			1.1×10^{-7}
$^{229}\text{Th}+\text{D}$	3.2×10^{-5}	1.0×10^{-6}			1.0×10^{-6}
^{242}Pu	7.7×10^{-5}	6.4×10^{-7}			6.4×10^{-7}
$^{238}\text{U}+\text{D}$	34	0.068			0.068
^{234}U	18	0.034			0.034
^{230}Th	1.5	7.2×10^{-3}	51	0.22	0.24

Table 4.15 (continued)

Radionuclide	Upper Cell		Lower Cell		Total TEDE (mrem)
	Soil Conc. (pCi g ⁻¹)	TEDE (mrem)	Soil Conc. (pCi g ⁻¹)	TEDE (mrem)	
²⁴⁰ Pu	0.29	2.5×10^{-3}			2.5×10^{-3}
²³⁶ U	0.029	5.1×10^{-5}			5.1×10^{-5}
²³² Th	0.063	1.4×10^{-3}	355	8.1	8.1
²²⁸ Ra+D	0.063	9.6×10^{-4}	355	5.4	5.4
²²⁸ Th+D	0.063	1.5×10^{-3}	355	8.1	8.1
Total		0.21		23	23

contribute equally to the dose. The external dose is predominantly from ²²⁸Ra+D and ²²⁸Th+D. The inhalation doses are from ²³²Th+D. At 10,000 years, the estimated TEDE increases slightly to 23 mrem as ²²⁶Ra and ²¹⁰Pb are produced by radioactive decay.

4.2.2 Analysis Results for the Chronic Intruder-Agriculture Scenario

The intruder-agriculture scenario is a chronic exposure scenario that assumes an intruder constructs a residence over the site. A 2,500-m² (26,909-ft²) contaminated zone is created from waste exhumed from construction excavations. The waste is assumed to be indistinguishable from soil at the time of intrusion. The intruder then lives within the contaminated zone and produces fruit, vegetables, meat, and milk. Twenty-five percent of the intruder's diet is assumed produced in the contaminated zone. Complete details of the exposure pathways and assumptions are provided in Section 3.3.2.1. This scenario was analyzed for the shallow land burial inventory only, because the lower cell of Pit 6 is too deep to be penetrated by an excavation for a basement and the upper cell has the same activity concentration as the shallow land burial inventory. It was assumed that this scenario could occur any time after the end of institutional control. This scenario is used to determine the concentration of wastes that can be disposed at a 2.4 m (7.9 ft) depth.

The TEDE received by the intruder at 100 years was estimated to be 84 mrem yr⁻¹ (Table 4.16). Inhalation and external irradiation are the most important pathways, contributing 81 percent of the dose. The remaining dose is due to soil ingestion (12 percent) and food ingestion (7 percent). The most important nuclides, in decreasing order of importance, were ²³⁸U+D, ²³⁹Pu, ²³⁴U, ²³⁸Pu, ²³⁵U+D, and ²⁴¹Am. One hundred years after closure, external irradiation doses are contributed mostly by ²³⁸U+D and ²³⁵U+D. Inhalation doses are due to ²³⁸U+D, ²³⁴U, and ²³⁹Pu. The nuclides contributing most of the dose in the

Table 4.16 Soil Activity Concentrations and TEDE for the Intruder-Agriculture Scenario With the Shallow Land Burial Inventory. Soil activity concentration is the estimated concentration of the surface contaminated zone created by the intruder.

Radionuclide	At 100 years		At 10,000 years		At Time of Maximum Dose		
	Soil Conc. (pCi g ⁻¹)	TEDE (mrem yr ⁻¹)	Soil Conc. (pCi g ⁻¹)	TEDE (mrem yr ⁻¹)	Time (years)	Soil Conc. (pCi g ⁻¹)	TEDE (mrem yr ⁻¹)
³ H	286	2.4			100	286	2.4
¹⁴ C	1.0	0.40	0.31	0.072	100	1.0	0.40
³⁶ Cl	3.9×10^{-8}	4.9×10^{-8}	3.8×10^{-8}	4.8×10^{-8}	100	3.9×10^{-8}	4.9×10^{-8}
⁵⁹ Ni	6.0×10^{-6}	3.3×10^{-10}	5.4×10^{-6}	3.0×10^{-10}	100	6.0×10^{-6}	3.3×10^{-10}
⁶⁰ Co	1.0×10^{-7}	1.2×10^{-6}			100	1.0×10^{-7}	1.2×10^{-6}
⁶³ Ni	0.47	6.7×10^{-5}			100	0.47	6.7×10^{-5}
⁹⁰ Sr+D	0.11	0.13			100	0.11	0.13
⁹³ Zr+D	9.6×10^{-6}	7.0×10^{-9}	9.6×10^{-6}	7.1×10^{-9}	100	9.6×10^{-6}	7.0×10^{-9}
⁹⁹ Tc	7.5	0.057	7.0	0.056	100	7.0	0.056
¹⁰⁷ Pd	2.8×10^{-6}	2.0×10^{-10}	2.8×10^{-6}	2.0×10^{-10}	100	2.8×10^{-6}	2.0×10^{-10}
¹²⁶ Sn+D	3.3×10^{-6}	4.9×10^{-5}	3.1×10^{-6}	4.6×10^{-5}	100	3.3×10^{-6}	4.9×10^{-5}
¹²⁹ I	8.3×10^{-7}	3.6×10^{-7}	8.3×10^{-7}	3.6×10^{-7}	100	8.3×10^{-7}	3.6×10^{-7}
¹³³ Ba	5.1×10^{-8}	5.4×10^{-8}			100	5.1×10^{-8}	5.4×10^{-8}
¹³⁵ Cs	2.4×10^{-5}	8.7×10^{-8}	2.4×10^{-5}	8.7×10^{-8}	100	2.4×10^{-5}	8.7×10^{-8}
¹³⁷ Cs+D	0.13	0.36			100	0.13	0.36

Table 4.16 (continued)

Radionuclide	At 100 years		At 10,000 years		At Time of Maximum Dose		
	Soil Conc. (pCi g ⁻¹)	TEDE (mrem yr ⁻¹)	Soil Conc. (pCi g ⁻¹)	TEDE (mrem yr ⁻¹)	Time (years)	Soil Conc. (pCi g ⁻¹)	TEDE (mrem yr ⁻¹)
¹⁵¹ Sm	0.017	5.6×10^{-7}			100	0.017	5.6×10^{-7}
¹⁵² Eu	1.1×10^{-10}	5.6×10^{-10}			100	1.1×10^{-10}	5.6×10^{-10}
¹⁵⁴ Eu	7.5×10^{-7}	4.3×10^{-6}			100	7.5×10^{-7}	4.3×10^{-6}
²⁰⁷ Bi	3.4×10^{-10}	1.8×10^{-9}			100	3.4×10^{-10}	1.8×10^{-9}
²³² U	9.6×10^{-3}	3.8×10^{-3}			100	9.6×10^{-3}	3.8×10^{-3}
²⁴³ Am+D	2.2×10^{-4}	3.0×10^{-4}	8.5×10^{-5}	1.2×10^{-4}	100	2.2×10^{-4}	3.0×10^{-4}
²³⁹ Pu	30	12	23	8.8	100	30	12
²³⁵ U+D	7.7	4.4	7.7	4.4	450,000	7.7	4.4
²³¹ Pa	0.032	0.034	1.5	1.6	450,000	7.7	8.2
²²⁷ Ac+D	0.027	0.14	1.5	7.7	450,000	7.7	40
²⁴¹ Pu	0.26	1.9×10^{-3}			100	0.26	1.9×10^{-3}
²⁴¹ Am	5.0	4.0			100	5.0	4.0
²³⁷ Np+D	2.2×10^{-3}	0.037	3.0×10^{-3}	0.051	4,600	3.2×10^{-3}	0.054
²³³ U	3.3×10^{-4}	2.6×10^{-5}	4.4×10^{-4}	3.4×10^{-5}	640,000	2.5×10^{-3}	1.9×10^{-4}
²²⁹ Th+D	3.6×10^{-6}	8.2×10^{-6}	2.4×10^{-4}	5.4×10^{-4}	640,000	2.5×10^{-3}	5.5×10^{-3}
²⁴² Pu	5.9×10^{-4}	2.2×10^{-4}	5.8×10^{-4}	2.1×10^{-4}	100	5.9×10^{-4}	2.2×10^{-4}

Table 4.16 (continued)

Radionuclide	At 100 years		At 10,000 years		At Time of Maximum Dose		
	Soil Conc. (pCi g ⁻¹)	TEDE (mrem yr ⁻¹)	Soil Conc. (pCi g ⁻¹)	TEDE (mrem yr ⁻¹)	Time (years)	Soil Conc. (pCi g ⁻¹)	TEDE (mrem yr ⁻¹)
²³⁸ U+D	259	36	259	36	3,500,000	259	36
²³⁸ Pu	15	5.1			100	15	5.1
²³⁴ U	136	11	139	11	3,500,000	259	20
²³⁰ Th	0.28	0.048	12	2.1	3,500,000	259	45
²²⁶ Ra+D	0.031	0.25	9.3	76	3,500,000	259	2.1 × 10 ³
²¹⁰ Pb+D	0.028	0.011	9.3	3.6	3,500,000	259	100
²⁴⁴ Cm	3.4 × 10 ⁻³	6.9 × 10 ⁻⁴			100	3.4 × 10 ⁻³	6.9 × 10 ⁻⁴
²⁴⁸ Cm	1.7 × 10 ⁻¹⁰	2.4 × 10 ⁻¹⁰	1.7 × 10 ⁻¹⁰	2.4 × 10 ⁻¹⁰	100	1.7 × 10 ⁻¹⁰	2.4 × 10 ⁻¹⁰
²⁴⁰ Pu	6.2	2.4	2.2	0.85	100	6.2	2.2
²³⁶ U	0.22	0.016	0.22	0.016	32,000	0.22	0.016
²³² Th	0.49	0.42	0.48	0.41	100	0.49	0.42

ingestion pathways are $^{238}\text{U}+\text{D}$, ^{234}U , ^{239}Pu , and ^{241}Am . By 10,000 years, the estimated TEDE increases to 157 mrem yr^{-1} as the activity concentration of progeny of ^{238}U and ^{235}U increases. The increase in dose is due largely to external irradiation from $^{226}\text{Ra}+\text{D}$.

4.2.3 Analysis Results for the Chronic Postdrilling Scenario

The intruder postdrilling scenario assumes that an intruder builds a residence on an area contaminated with drill cuttings from the disposal site. As in the intruder-agriculture scenario, the intruder produces meat, milk, fruit, and vegetables within the contaminated zone. A complete description of the models and assumptions for the postdrilling scenario are presented in Section 3.3.2.2. The postdrilling scenario is the same as the intruder-agriculture scenario except for differences in the activity concentration and thickness of the contaminated zone. The postdrilling scenario applies to a greater source term because a borehole may penetrate any waste cell between the surface and the aquifer. Therefore, the scenario was analyzed for a shallow land burial trench and Pit 6. The scenario was assumed to occur between 100 years and 10,000 years. The waste is assumed to be indistinguishable from soil at this time. Results from the postdrilling scenario were used to develop concentration limits for wastes disposed below 4 m (13.1 ft). Common construction excavations are unlikely to extend below 4 m (13.1 ft).

The estimated TEDE at 100 years was $0.70 \text{ mrem yr}^{-1}$ for a postdrilling intruder penetrating a shallow land burial trench (Table 4.17). Approximately 49 percent of the dose is due to inhalation of ^3H and ^{14}C released from the buried waste. The remainder of the dose is from exposure to the waste exhumed by the intruder. The contribution of the pathways was 25 percent from inhalation of resuspended activity, 16 percent from external irradiation, 6 percent from soil ingestion, and 2 percent from ingestion of agricultural products. The important nuclides and pathways for the exhumed waste are essentially the same as for the intruder-agriculture scenario because the source term and pathway parameters are equivalent. The postdrilling scenario differs from the intruder-agriculture scenario in the greater relative contribution of volatile ^3H and ^{14}C released from the waste. At 10,000 years, the dose increases slightly to $0.71 \text{ mrem yr}^{-1}$. By 10,000 years, the dose from the release of volatile ^3H and ^{14}C is negligible. However, this decrease is offset by increasing external irradiation

Table 4.17 Soil Activity Concentrations and TEDE for the Postdrilling Scenario With the Shallow Land Burial Inventory. Soil activity concentration is the estimated concentration of the surface contaminated zone created by the intruder.

Radionuclide	At 100 years		At 10,000 years		At Time of Maximum Dose		
	Soil Conc. (pCi g ⁻¹)	TEDE (mrem yr ⁻¹)	Soil Conc. (pCi g ⁻¹)	TEDE (mrem yr ⁻¹)	Time (years)	Soil Conc. (pCi g ⁻¹)	TEDE (mrem yr ⁻¹)
¹ H	1.3	0.16			100	1.3	0.16
¹⁴ C	4.8 × 10 ⁻³	0.18	1.4 × 10 ⁻³	5.4 × 10 ⁻²	100	4.8 × 10 ⁻³	0.18
³⁶ Cl	1.8 × 10 ⁻¹⁰	1.4 × 10 ⁻¹⁰	1.8 × 10 ⁻¹⁰	1.4 × 10 ⁻¹⁰	100	1.8 × 10 ⁻¹⁰	1.4 × 10 ⁻¹⁰
⁵⁹ Ni	2.7 × 10 ⁻⁸	1.2 × 10 ⁻¹²	2.5 × 10 ⁻⁸	1.1 × 10 ⁻¹²	100	2.7 × 10 ⁻⁸	1.2 × 10 ⁻¹²
⁶⁰ Co	4.8 × 10 ⁻¹⁰	5.0 × 10 ⁻⁹			100	4.8 × 10 ⁻¹⁰	5.0 × 10 ⁻⁹
⁶³ Ni	2.2 × 10 ⁻³	2.3 × 10 ⁻⁷			100	2.2 × 10 ⁻³	2.3 × 10 ⁻⁷
⁹⁰ Sr+D	5.1 × 10 ⁻⁴	3.7 × 10 ⁻⁴			100	5.1 × 10 ⁻⁴	3.7 × 10 ⁻⁴
⁹³ Zr+D	4.8 × 10 ⁻⁸	2.6 × 10 ⁻¹¹	4.8 × 10 ⁻⁸	2.6 × 10 ⁻¹¹	100	4.8 × 10 ⁻⁸	2.6 × 10 ⁻¹¹
⁹⁹ Tc	0.034	1.7 × 10 ⁻⁴	0.033	1.7 × 10 ⁻⁴	100	0.034	1.7 × 10 ⁻⁴
¹⁰⁷ Pd	1.3 × 10 ⁻⁸	8.2 × 10 ⁻¹³	1.3 × 10 ⁻⁸	8.2 × 10 ⁻¹³	100	1.3 × 10 ⁻⁸	8.2 × 10 ⁻¹³
¹²⁶ Sn+D	1.5 × 10 ⁻⁸	2.2 × 10 ⁻⁷	1.4 × 10 ⁻⁸	2.1 × 10 ⁻⁷	100	1.5 × 10 ⁻⁸	2.2 × 10 ⁻⁷
¹²⁹ I	3.9 × 10 ⁻⁹	1.2 × 10 ⁻⁹	3.9 × 10 ⁻⁹	1.2 × 10 ⁻⁹	100	3.9 × 10 ⁻⁹	1.2 × 10 ⁻⁹
¹³³ Ba	2.3 × 10 ⁻¹⁰	2.5 × 10 ⁻¹⁰			100	2.3 × 10 ⁻¹⁰	2.5 × 10 ⁻¹⁰
¹³⁵ Cs	1.1 × 10 ⁻⁷	3.3 × 10 ⁻¹⁰	1.1 × 10 ⁻⁸	3.3 × 10 ⁻¹⁰	100	1.1 × 10 ⁻⁸	3.3 × 10 ⁻¹⁰
¹³⁷ Cs+D	6.0 × 10 ⁻⁴	1.5 × 10 ⁻³			100	6.0 × 10 ⁻⁴	1.5 × 10 ⁻³
¹⁵¹ Sm	7.7 × 10 ⁻⁵	2.5 × 10 ⁻⁹			100	7.7 × 10 ⁻⁵	2.5 × 10 ⁻⁹
¹⁵² Eu	5.0 × 10 ⁻¹³	2.3 × 10 ⁻¹²			100	5.0 × 10 ⁻¹³	2.3 × 10 ⁻¹²
¹⁵⁴ Eu	3.4 × 10 ⁻⁹	1.7 × 10 ⁻⁸			100	3.4 × 10 ⁻⁹	1.7 × 10 ⁻⁸

Table 4.17 (continued)

Radionuclide	At 100 years		At 10,000 years		At Time of Maximum Dose		
	Soil Conc. (pCi g ⁻¹)	TEDE (mrem yr ⁻¹)	Soil Conc. (pCi g ⁻¹)	TEDE (mrem yr ⁻¹)	Time (years)	Soil Conc. (pCi g ⁻¹)	TEDE (mrem yr ⁻¹)
²⁰⁷ Bi	1.6×10^{-12}	7.6×10^{-12}			100	1.6×10^{-12}	7.6×10^{-12}
²³² U	4.4×10^{-5}	1.7×10^{-5}			100	4.4×10^{-5}	1.7×10^{-5}

Table 4.17 (continued)

Radionuclide	At 100 years		At 10,000 years		At Time of Maximum Dose		
	Soil Conc. (pCi g ⁻¹)	TEDE (mrem yr ⁻¹)	Soil Conc. (pCi g ⁻¹)	TEDE (mrem yr ⁻¹)	Time (years)	Soil Conc. (pCi g ⁻¹)	TEDE (mrem yr ⁻¹)
²³⁴ U	0.63	0.049	0.64	0.050	3,500,000	1.2	0.093
²³⁰ Th	1.3×10^{-3}	2.2×10^{-4}	0.055	1.9×10^{-3}	3,500,000	1.2	0.21
²²⁶ Ra+D	1.4×10^{-4}	1.0×10^{-3}	0.043	0.30	3,500,000	1.2	8.4
²¹⁰ Pb+D	1.3×10^{-4}	4.3×10^{-5}	0.043	0.014	3,500,000	1.2	0.40
²⁴⁴ Cm	1.6×10^{-5}	3.2×10^{-6}			100	1.6×10^{-5}	3.2×10^{-6}
²⁴⁸ Cm	7.9×10^{-13}	1.1×10^{-12}	7.7×10^{-13}	1.1×10^{-12}	100	7.9×10^{-13}	1.1×10^{-12}
²⁴⁰ Pu	0.029	0.011	0.010	3.9×10^{-3}	100	0.029	0.011
²³⁵ U	1.0×10^{-3}	7.3×10^{-5}	1.0×10^{-3}	7.3×10^{-5}	32,000	1.0×10^{-3}	7.3×10^{-5}
²³² Th	2.3×10^{-3}	1.9×10^{-3}	2.2×10^{-3}	1.9×10^{-3}	100	2.3×10^{-3}	2.2×10^{-3}
²²⁸ Ra+D	2.3×10^{-3}	8.5×10^{-3}	2.2×10^{-3}	8.4×10^{-3}	100	2.3×10^{-3}	8.5×10^{-3}
²²⁸ Th+D	2.3×10^{-3}	0.013	2.2×10^{-3}	0.012	100	2.3×10^{-3}	0.013
Total		0.70		0.71			

Table 4.18 Soil Activity Concentrations and TEDE for the Postdrilling Scenario for Pit 6 (P06U) at 100 Years. Soil activity concentration is the estimated concentration of the surface contaminated zone created by the intruder.

Radionuclide	Upper Cell		Lower Cell		Total TEDE (mrem yr ⁻¹)
	Soil Conc. (pCi g ⁻¹)	TEDE (mrem yr ⁻¹)	Soil Conc. (pCi g ⁻¹)	TEDE (mrem yr ⁻¹)	
³ H	1.6	0.16			0.16
¹⁴ C	6.1 × 10 ⁻³	0.18			0.18
³⁶ Cl	2.3 × 10 ⁻¹⁰	1.8 × 10 ⁻¹⁰			1.8 × 10 ⁻¹⁰
⁵⁹ Ni	3.4 × 10 ⁻⁸	1.5 × 10 ⁻¹²			1.5 × 10 ⁻¹²
⁶⁰ Co	6.1 × 10 ⁻¹⁰	6.3 × 10 ⁻⁹			6.3 × 10 ⁻⁹
⁶³ Ni	2.8 × 10 ⁻³	2.9 × 10 ⁻⁷			2.9 × 10 ⁻⁷
⁹⁰ Sr+D	6.4 × 10 ⁻⁴	4.7 × 10 ⁻⁴			4.7 × 10 ⁻⁴
⁹³ Zr+D	6.1 × 10 ⁻⁸	3.3 × 10 ⁻¹¹			3.3 × 10 ⁻¹¹
⁹⁹ Tc	0.044	2.2 × 10 ⁻⁴			2.2 × 10 ⁻⁴
¹⁰⁷ Pd	1.6 × 10 ⁻⁸	1.0 × 10 ⁻¹²			1.0 × 10 ⁻¹²
¹²⁶ Sn+D	1.9 × 10 ⁻⁸	2.8 × 10 ⁻⁷			2.8 × 10 ⁻⁷
¹²⁹ I	4.9 × 10 ⁻⁹	1.5 × 10 ⁻⁹			1.5 × 10 ⁻⁹
¹³³ Ba	2.9 × 10 ⁻¹⁰	3.2 × 10 ⁻¹⁰			3.2 × 10 ⁻¹⁰
¹³⁵ Cs	1.4 × 10 ⁻⁸	4.2 × 10 ⁻¹⁰			4.2 × 10 ⁻¹⁰
¹³⁷ Cs+D	7.6 × 10 ⁻⁴	1.9 × 10 ⁻³			1.9 × 10 ⁻³
¹⁵¹ Sm	9.7 × 10 ⁻⁵	3.2 × 10 ⁻⁹			3.2 × 10 ⁻⁹
¹⁵² Eu	6.3 × 10 ⁻¹³	2.9 × 10 ⁻¹²			2.9 × 10 ⁻¹²
¹⁵⁴ Eu	4.3 × 10 ⁻⁹	2.1 × 10 ⁻⁸			2.1 × 10 ⁻⁸
²⁰⁷ Pb	2.0 × 10 ⁻¹²	9.6 × 10 ⁻¹²			9.6 × 10 ⁻¹²
²³² U	5.6 × 10 ⁻⁵	2.3 × 10 ⁻⁵			2.3 × 10 ⁻⁵
²⁴³ Am+D	1.3 × 10 ⁻⁶	1.5 × 10 ⁻⁶			1.5 × 10 ⁻⁶
²³⁹ Pu	0.18	0.067			0.067
²³⁵ U+D	0.045	0.025			0.025
²³¹ Pa	1.9 × 10 ⁻⁴	2.0 × 10 ⁻⁴			2.0 × 10 ⁻⁴
²²⁷ Ac+D	1.5 × 10 ⁻⁴	8.2 × 10 ⁻⁴			8.2 × 10 ⁻⁴

Table 4.18 (continued)

Radionuclide	Upper Cell		Lower Cell		Total TEDE (mrem yr ⁻¹)
	Soil Conc. (pCi g ⁻¹)	TEDE (mrem yr ⁻¹)	Soil Conc. (pCi g ⁻¹)	TEDE (mrem yr ⁻¹)	
²⁴¹ Pu	1.5 × 10 ⁻³	1.1 × 10 ⁻⁵			1.1 × 10 ⁻⁵
²⁴¹ Am	0.029	0.019			0.019
²³⁷ Np+D	1.2 × 10 ⁻⁵	1.5 × 10 ⁻⁴			1.5 × 10 ⁻⁴
²³³ U	1.9 × 10 ⁻⁶	1.5 × 10 ⁻⁷			1.5 × 10 ⁻⁷
²²⁹ Th+D	2.1 × 10 ⁻⁸	4.5 × 10 ⁻⁸			4.5 × 10 ⁻⁸
²⁴² Pu	3.4 × 10 ⁻⁶	1.4 × 10 ⁻⁶			1.4 × 10 ⁻⁶
²³⁸ U+D	1.5	0.20			0.20
²³⁸ Pu	0.086	0.029			0.029
²³⁴ U	0.78	0.062			0.062
²³⁰ Th	1.6 × 10 ⁻³	2.8 × 10 ⁻⁴	2.4	0.42	0.42
²²⁶ Ra+D	1.8 × 10 ⁻⁴	1.3 × 10 ⁻³	0.17	1.2	1.2
²¹⁰ Pb+D	1.6 × 10 ⁻⁴	5.4 × 10 ⁻⁵	0.14	0.046	0.046
²⁴⁴ Cm	2.0 × 10 ⁻⁵	4.0 × 10 ⁻⁶			4.0 × 10 ⁻⁶
²⁴⁸ Cm	1.0 × 10 ⁻¹²	1.4 × 10 ⁻¹²			1.4 × 10 ⁻¹²
²⁴⁰ Pu	0.037	0.014			0.014
²³⁶ U	1.3 × 10 ⁻³	9.2 × 10 ⁻⁵			9.2 × 10 ⁻⁷
²³² Th	2.9 × 10 ⁻³	2.4 × 10 ⁻³	16	14	14
²²⁸ Ra+D	2.9 × 10 ⁻³	0011	16	59	59
²²⁸ Th+D	2.9 × 10 ⁻³	0.016	16	87	87
Total		0.80		162	163

Table 4.19 Soil Activity Concentrations and TEDE for the Postdrilling Scenario for Pit 6 (P06U) at 10,000 Years. Soil activity concentration is the estimated concentration of the surface contaminated zone created by the intruder.

Radionuclide	Upper Cell		Lower Cell		Total TEDE (mrem yr ⁻¹)
	Soil Conc. (pCi g ⁻¹)	TEDE (mrem yr ⁻¹)	Soil Conc. (pCi g ⁻¹)	TEDE (mrem yr ⁻¹)	
¹⁴ C	1.8 × 10 ⁻³	0.068			0.068
³⁶ Cl	2.3 × 10 ⁻¹⁰	1.8 × 10 ⁻¹⁰			1.8 × 10 ⁻¹⁰
⁵⁹ Ni	3.2 × 10 ⁻⁸	1.4 × 10 ⁻¹²			1.4 × 10 ⁻¹²
⁹³ Zr+D	6.1 × 10 ⁻⁸	3.3 × 10 ⁻¹¹			3.3 × 10 ⁻¹¹
⁹⁹ Tc	0.042	2.1 × 10 ⁻⁴			2.1 × 10 ⁻⁴
¹⁰⁷ Pd	1.6 × 10 ⁻⁸	1.0 × 10 ⁻¹²			1.0 × 10 ⁻¹²
¹²⁶ Sn+D	1.8 × 10 ⁻⁸	2.7 × 10 ⁻⁷			2.7 × 10 ⁻⁷
¹²⁹ I	4.9 × 10 ⁻⁹	1.5 × 10 ⁻⁹			1.5 × 10 ⁻⁹
¹³⁵ Cs	7.6 × 10 ⁻⁸	2.3 × 10 ⁻¹⁰			2.3 × 10 ⁻¹⁰
²⁴³ Am+D	4.9 × 10 ⁻⁷	6.1 × 10 ⁻⁷			6.1 × 10 ⁻⁷
²³⁹ Pu	0.13	0.051			0.051
²³⁵ U+D	0.045	0.025			0.025
²³¹ Pa	8.6 × 10 ⁻³	9.3 × 10 ⁻³			9.3 × 10 ⁻³
²²⁷ Ac+D	8.6 × 10 ⁻³	0.044			0.044
²³⁷ Np+D	1.8 × 10 ⁻⁵	1.9 × 10 ⁻⁴			1.9 × 10 ⁻⁴
²³³ U	2.5 × 10 ⁻⁶	2.0 × 10 ⁻⁷			2.0 × 10 ⁻⁷
²²⁹ Th+D	1.4 × 10 ⁻⁶	2.9 × 10 ⁻⁶			2.9 × 10 ⁻⁶
²⁴² Pu	3.4 × 10 ⁻⁶	1.2 × 10 ⁻⁶			1.2 × 10 ⁻⁶
²³⁸ U+D	1.5	0.20			0.20
²³⁴ U	0.81	0.063			0.063
²³⁰ Th	0.069	2.4 × 10 ⁻³	2.2	0.39	0.39
²²⁶ Ra+D	0.054	0.38	2.2	16	16
²¹⁰ Pb+D	0.054	0.018	2.2	0.75	0.77

Table 4.19 (continued)

	Unner Cell	Lower Cell	
--	------------	------------	--

Table 4.20 Estimated Radon-222 Dose Results for Intruders Residing Over a Shallow Land Burial Trench

Cap Thickness	Foundation	CEDE (mrem yr ⁻¹)		
		100 years	10,000 years	3.5 × 10 ⁶ years
2.4 m	Slab	1.7	510	1.4 × 10 ⁴
2.4 m	2.8-m Basement	17	5.1 × 10 ³	1.5 × 10 ⁵
4.0 m	Slab	0.36	107	2.9 × 10 ³
4.0 m	2.8-m Basement	5.3	1.6 × 10 ³	4.4 × 10 ⁴
4.5 m	Slab	0.22	65	1.8 × 10 ³
4.5 m	2.8-m Basement	3.3	975	2.7 × 10 ⁴

become available for subsequent transport to humans, are plant-uptake rates, soil excavation rates by burrowing insects, and radioactive ingrowth. Large uncertainties are associated with the two biological processes, especially with respect to the subsurface distribution of root biomass, insect colony density, and soil movement by insects.

A simplified sensitivity analysis was carried out for the purpose of evaluating the effect of release rates on surface soil concentration. Sensitivity to radioactive decay constants was not examined because these were assumed subject to minimal uncertainty. Each of the remaining rates identified in Section 3.2.2, including the resuspension rate, K_s ; the root-uptake rates, K_{r1} , K_{r2} , and K_{r3} ; and release rates attributable to burrowing ants, K_{b1} and K_{b2} , were varied to evaluate the sensitivity of the activity of ²²⁶Ra and ¹⁴C in the surface soil compartment to changes in these rates. Radium-226 was chosen for this analysis because it is one of the most important sources of dose to the general public, according to *Tables 4.1* and *4.2*, and has a relatively small plant-soil concentration factor. Carbon-14 was selected because it has a high plant-soil concentration factor.

The results of the sensitivity analysis for ²²⁶Ra are presented in *Table 4.21*. This table lists release rate parameters and results, in terms of activity released, for various sensitivity cases. The base case value represents the soil concentration resulting from values of K_s , K_{r1} , K_{r2} , K_{r3} , K_{b1} , and K_{b2} used in the performance assessment for the intact site (*Table 3.16*).

The results presented for ²²⁶Ra in *Table 4.21* indicate that the activity released is fairly insensitive to parameters in the root uptake model and most sensitive to the burrowing animal transfer rate, K_{b1} . This parameter represents the movement of radionuclides from the waste to the shallow soil. The model for ²²⁶Ra was also found to be sensitive to the resuspension rate, K_s , representing fractional loss from the soil compartment. Root-uptake parameters are

Table 4.21 Results of the Sensitivity Analysis for ^{226}Ra in the Base-Case Release Model

Parameter	Parameter Value (yr^{-1})	Maximum ^{226}Ra Shallow Soil Activity [†] (Ci)
Base Case	—	1.0×10^{-4}
K_s	$1.0 \times 10^{-5} \text{ §}$	1.1×10^{-4}
K_s	$1.0 \times 10^{-3} \ddagger$	5.7×10^{-5}
K_{b1}	$1.3 \times 10^{-6} \ddagger$	1.0×10^{-3}
K_{b1}	$1.3 \times 10^{-8} \text{ §}$	1.1×10^{-5}
K_{b2}	$1.8 \times 10^{-6} \ddagger$	1.0×10^{-4}
K_{b2}	$1.8 \times 10^{-8} \text{ §}$	1.0×10^{-4}
K_{r1}	$1.3 \times 10^{-8} \ddagger$	1.1×10^{-4}
K_{r1}	$1.3 \times 10^{-10} \text{ §}$	1.0×10^{-4}
K_{r2}	$5.4 \times 10^{-9} \ddagger$	1.0×10^{-4}
K_{r2}	$5.4 \times 10^{-11} \text{ §}$	1.0×10^{-4}
K_{r3}	$3.8 \times 10^{-7} \ddagger$	1.0×10^{-4}
K_{r3}	$3.8 \times 10^{-9} \text{ §}$	1.0×10^{-4}

[†] Per unit activity (Ci) in waste.

[‡] Value is a factor of ten higher than the base case; all other parameters the same as the base case.

[§] Value is a factor of ten lower than the base case; all other parameters the same as the base case.

less important for ^{226}Ra because the parameters defining K_{r1} , which include the radionuclide-specific parameter B_{jv} , are relatively low for this radionuclide. Table 4.21 suggests that, for ^{226}Ra , the soil activity is linearly related to K_{b1} which, according to Equation 3.20, is linearly related to the amount of soil excavated by ants in the waste zone and the burrower colony density, both of which are highly uncertain. Sensitivity of ^{226}Ra to the resuspension rate is

Table 4.22 Results of Sensitivity Analysis for Nonvolatile ^{14}C in the Base Case Release Model

Parameter	Parameter Value (yr^{-1})	Maximum ^{14}C Surface Soil Activity [†] (Ci)
Base Case	—	4.7×10^{-3}
K_s	$1.0 \times 10^{-5} §$	6.3×10^{-3}
K_s	$1.0 \times 10^{-3} ‡$	1.4×10^{-3}
K_{b1}	$1.3 \times 10^{-6} ‡$	5.7×10^{-3}
K_{b1}	$1.3 \times 10^{-8} §$	4.6×10^{-3}
K_{b2}	$1.8 \times 10^{-6} ‡$	5.0×10^{-3}
K_{b2}	$1.8 \times 10^{-8} §$	4.6×10^{-3}
K_{r1}	$4.9 \times 10^{-5} ‡$	3.7×10^{-2}
K_{r1}	$4.9 \times 10^{-7} §$	9.8×10^{-4}
K_{r2}	$1.8 \times 10^{-5} ‡$	7.7×10^{-3}
K_{r2}	$1.8 \times 10^{-7} §$	4.4×10^{-3}
K_{r3}	$7.4 \times 10^{-4} ‡$	5.7×10^{-3}
K_{r3}	$7.4 \times 10^{-6} §$	4.3×10^{-3}

† Per unit activity (Ci) in waste.

‡ Value is a factor of ten higher than the base case; all other parameters the same as the base case.

§ Value is a factor of ten lower than the base case; all other parameters the same as the base case.

is approximately proportional to K_{r1} , the root transfer factor from the waste to the surface soil. From Equation 3.16, it can be seen that K_{r1} is the product of the plant-soil concentration factor and several poorly-known biological factors, such as plant productivity and rooting depth. As expected, the sensitivity to the resuspension factor is greater for ^{14}C than ^{226}Ra because of the greater half-life.

4.3.2 Inventory Sensitivity and Uncertainty

Sensitivity and uncertainty analyses of waste activity concentration was conducted under four cases. Only the base case release scenario, the transient occupancy scenario, and the open rangeland scenario were evaluated. Only nuclides shown to be significant in screening calculations were considered. Results from a Monte Carlo analysis show that it is highly unlikely that uncertainty in inventory could cause the maximum TEDE to members of the general public to exceed 25 mrem yr^{-1} within 10,000 years.

The four cases evaluated were:

- Case (1): Concentration of all nuclides vary independently. Dose is calculated for the transient occupancy scenario.
- Case (2): The concentrations of members of serial decay chains vary together. Within each decay chain, simulated concentration divided by reported concentration is a random constant. The concentration of all other nuclides varies independently. Dose is calculated for the transient occupancy scenario.
- Case (3): Concentration of all nuclides vary independently. Dose is calculated for the open rangeland scenario.
- Case (4): The concentrations of members of serial decay chains vary together. Within each chain, simulated concentration divided by reported concentration is a random constant. The concentration of all other nuclides varies independently. Dose is calculated for the open rangeland scenario.

The two methods of representing uncertainty about concentration, independent variation of all nuclides (Cases [1] and [3]), and having all members of a chain vary together (Cases [2] and [4]) are extreme models; the true state of uncertainty, which is difficult to quantify, lies between these extremes.

4.3.2.1 *Converting Waste Activity Concentration into TEDE*

For the two scenarios analyzed, the TEDE is proportional to the activity concentration of the waste. For each scenario, TEDE was calculated as:

$$D = \sum_{j=1}^n C_j \times DCF_j \quad (4.4)$$

where n is the number of nuclides and, for each nuclide, C_j is the waste activity concentration at time zero and DCF_j is the scenario dose conversion factor. This analysis investigated the uncertainty and sensitivity of C_j , the waste-activity concentration. The scenario dose conversion factors were derived as the ratio of the TEDE at 10,000 years to the activity concentration at closure. For nuclides that decay to other radioactive species, the TEDE used to calculate the dose conversion factors included the dose from all the progeny produced in 10,000 years. A list of the nuclides and scenario dose conversion factors for the transient occupancy scenario (Cases [1] and [2]) appears in Table 4.23. A similar list for the open rangeland scenario (Cases [3] and [4]) appears in Table 4.24.

Table 4.23 Dose Conversion Factors for the Transient Occupancy Scenario (Cases [1] and [2])

Nuclide	Decay Chain	DCF _i (mrem yr ⁻¹ per Ci m ⁻³)
²³⁹ Pu	1	78
²³⁵ U+D	2	6.2×10^2
²³¹ Pa	2	1.7×10^3
²²⁷ Ac+D	2	9.8×10^{-136}
²³⁸ U+D	3	61
²³⁴ U	3	2.1×10^2
²³⁰ Th	3	2.6×10^3
²²⁶ Ra+D	3	36
²³² Th	4	6.0×10^3
²²⁸ Ra+D	4	0.00
²²⁸ Th+D	4	0.00

Table 4.24 Dose Conversion Factors for the Open Rangeland Scenario (Cases [3] and [4])

Nuclide	Decay Chain	DCF _i (mrem yr ⁻¹ per Ci m ⁻³)
³ H	1	0.011
¹⁴ C	2	5.2×10^2
²⁴⁰ Pu	3	0.12
²⁴¹ Am	4	2.0
²³⁷ Np+D	5	4.2×10^3
²³⁹ Pu	6	0.23
²³⁵ U+D	7	31
²³¹ Pa	7	43
²²⁷ Ac+D	7	2.4×10^{-137}
²³⁸ U+D	8	19
²³⁴ U	8	43
²³⁰ Th	8	3.1×10^2

Table 4.24 (continued)

Nuclide	Decay Chain	DCF _i (mrem yr ⁻¹ per Ci m ⁻³)
²²⁶ Ra+D	8	4.4
²³² Th	9	71
²²⁸ Ra+D	9	0.00
²²⁸ Th+D	9	0.00

4.3.2.2 Assigning Probability Distributions for Waste Activity Concentrations

Data for assignment of probability distributions for waste activity

concentrations simply do not exist. Hence, distributions were assigned via judgment. The lognormal distribution has a central role in environmental statistics. Many physical and chemical processes tend to produce results that follow a lognormal distribution (Hattis and Burmaster, 1994). Quantities that are the product or sum of many independent terms tend to approximately have a lognormal distribution (Benjamin and Cornell, 1970). Hence, in the absence of contrary evidence, concentrations were assumed lognormally distributed.

Waste generators are not required to report uncertainty in waste activity concentration. Therefore, data required to estimate uncertainty are not available at the NTS. Rather than attempting to reconstruct an estimate of uncertainty in waste activity concentration, a

realizations did the TEDE exceed 25 mrem yr^{-1} (Table 4.25). In Case (2), the TEDE exceeded 25 mrem yr^{-1} in 8 of the 3,000 realizations. In Cases (3) and (4), the TEDE did not exceed 25 mrem yr^{-1} in any of the 3,000 realizations.

Table 4.25 Descriptive Statistics for Monte Carlo Uncertainty Analysis of Waste Activity Concentration

Case	Minimum (mrem yr ⁻¹)	25th Percentile (mrem yr ⁻¹)	Median (mrem yr ⁻¹)	75th Percentile (mrem yr ⁻¹)	Maximum (mrem yr ⁻¹)	Fraction of Realizations Exceeding 25 mrem yr ⁻¹
1	0.12	0.56	0.99	1.7	48	0.001
2	0.03	0.41	0.79	1.6	44	0.003
3	0.03	0.18	0.32	0.56	12	0.000
4	0.02	0.15	0.28	0.50	11	0.000

Responses between Cases (1) and (2) are similar, as are those of Cases (3) and (4). In both instances, assuming independence tends to give slightly larger doses. In this analysis, statistical independence is a conservative assumption, if dose is measured by mean, median, or any but the most extreme percentiles. It is not known if this is true in general.

Cumulative distribution functions (value on y-axis equals proportion of realizations of dose not exceeding the corresponding value on the x-axis) of the 3,000 realizations under Cases (1), (2), (3), and (4) appear in Figures 4.5, 4.6, 4.7, and 4.8, respectively. This is an estimate of the probability that the uncertain dose, uncertain because of inventory uncertainty, will not exceed a given value. Note that, to improve readability, the x-axis is on a logarithmic scale.

These analyses show that, under certain untested (and untestable) but reasonable assumptions, inventory uncertainty is not large enough to cause the site to fail to meet the performance objectives.

4.3.2.4 Analysis of Monte Carlo Results for Sensitivity

The method of sensitivity analysis used here is the one advocated by Iman and Conover (1979) in which inputs and outputs are converted to ranks and the Pearson correlation coefficients of the ranks are calculated. Large absolute values of the correlation indicate that the dose is sensitive to the concentration of the corresponding nuclide; values near zero

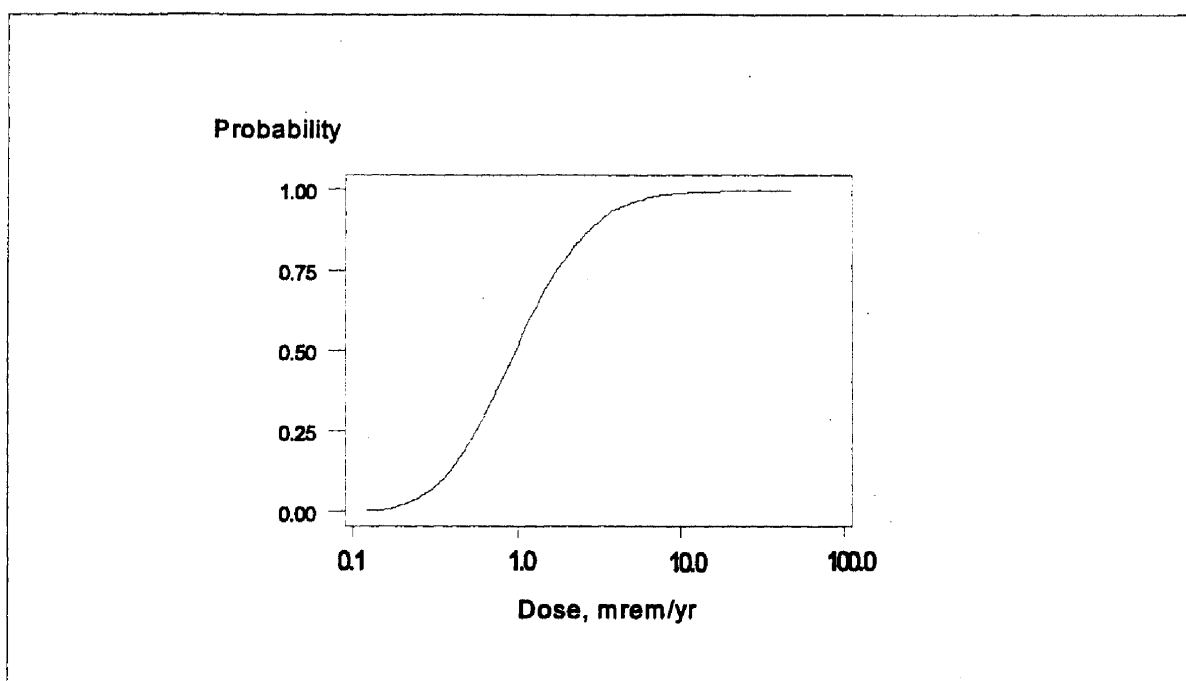


Figure 4.5 Cumulative Distribution Function of Monte Carlo Realizations of TEDE Under Case (1)

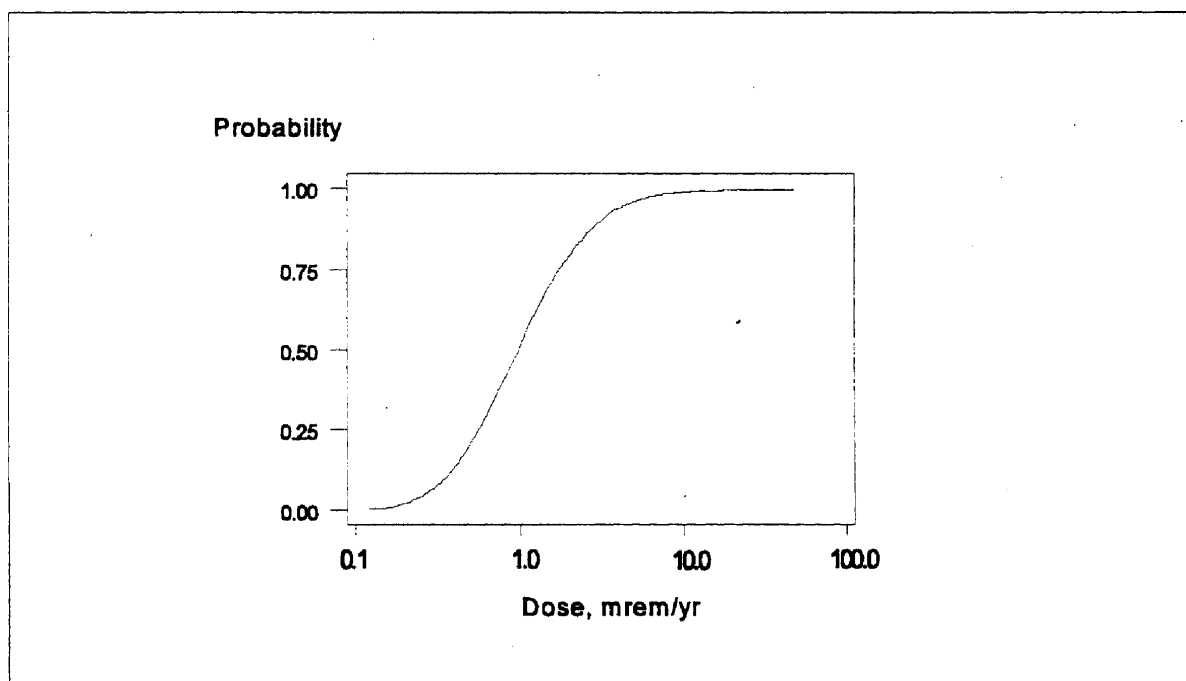


Figure 4.6 Cumulative Distribution Function of Monte Carlo Realizations of TEDE Under Case (2)

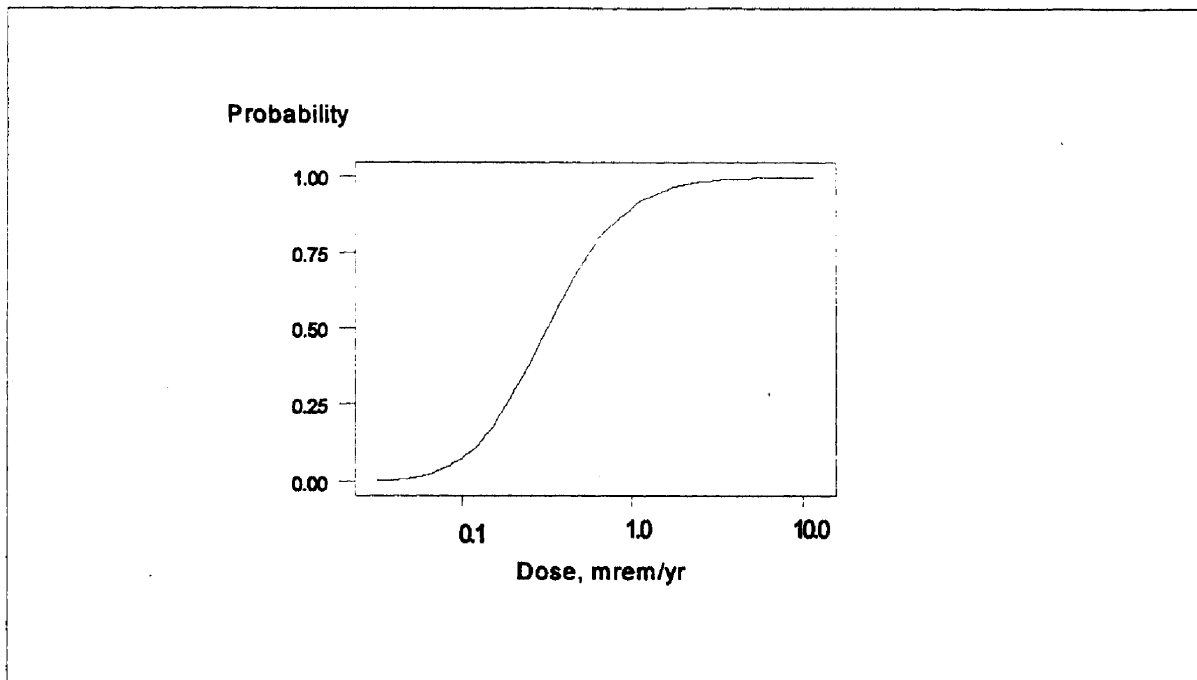


Figure 4.7 Cumulative Distribution Function of Monte Carlo Realizations of TEDE Under Case (3)

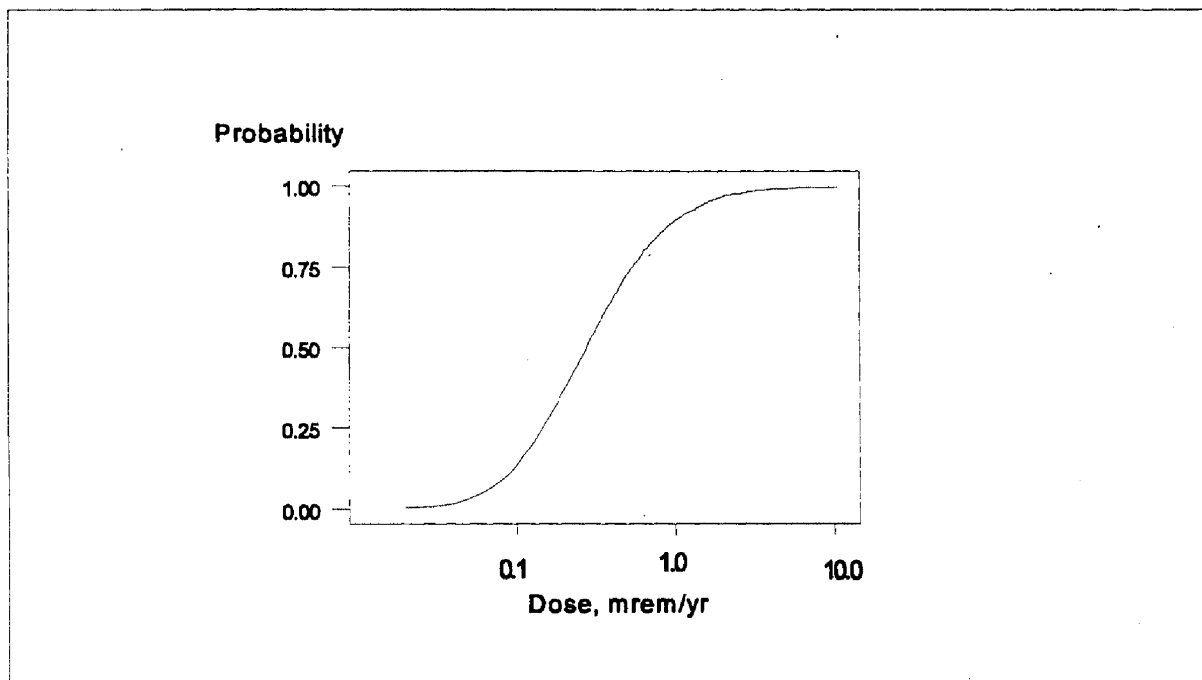


Figure 4.8 Cumulative Distribution Function of Monte Carlo Realizations of TEDE Under Case (4)

indicate little sensitivity. This method was chosen because there was no compelling reason to choose any other and, using this method, sensitivity can be readily evaluated from the Monte Carlo results.

In Case (1), TEDEs are most sensitive to the concentrations of ^{234}U and $^{238}\text{U}+\text{D}$ (Table 3.7). Doses in these scenarios do not include the contribution from radon. The contributions of the other nuclides to dose are relatively minor. In Case (2), where concentrations of a chain vary together, TEDE is sensitive to the concentrations of the members of the ^{238}U chain (Table 4.26). As expected, all members of a given chain show the same correlation; this is because, in Case (2), the concentrations of all members of a chain vary together. The contributions of the concentrations of other nuclides to dose are relatively minor. In Case (3), doses are most sensitive to the concentrations of ^{234}U , $^{238}\text{U}+\text{D}$, and ^{14}C (Table 4.27). The contributions of the other nuclides to dose are relatively minor. In Case (4), where concentrations of a chain vary together, TEDE is sensitive to the concentrations of members of the ^{238}U chain and to the concentration of ^{14}C (Table 4.27). The contributions of the concentrations of other nuclides to dose are relatively minor. Hence, as in the uncertainty analysis, the differences in conclusions between Cases (1) and (2) and between Cases (3) and (4) are minor, indicating that the assumption of statistical independence has little impact.

Table 4.26 Rank Correlations under Cases (1) and (2)

Nuclide	Rank Correlation	
	Case (1)	Case (2)
^{239}Pu	0.073	0.128
$^{235}\text{U}+\text{D}$	0.153	0.213
^{231}Pa	0.003	0.213
$^{227}\text{Ac}+\text{D}$	0.009	0.213
$^{238}\text{U}+\text{D}$	0.434	0.897
^{234}U	0.699	0.897
^{230}Th	0.041	0.897
$^{226}\text{Ra}+\text{D}$	-0.012	0.897
^{232}Th	0.147	0.124
$^{228}\text{Ra}+\text{D}$	-0.011	0.124
$^{228}\text{Th}+\text{D}$	-0.016	0.124

Table 4.27 Rank Correlations Under Case (3) and Case (4)

Nuclide	Rank Correlation	
	Case (3)	Case (4)
^3H	0.122	0.102
^{14}C	0.475	0.466
^{240}Pu	-0.008	0.004
^{241}Am	0.005	0.010
$^{237}\text{Np}+\text{D}$	0.006	-0.013
^{239}Pu	-0.011	0.040
$^{235}\text{U}+\text{D}$	0.059	0.037
^{231}Pa	-0.017	0.037
$^{227}\text{Ac}+\text{D}$	-0.006	0.037
$^{238}\text{U}+\text{D}$	0.433	0.748
^{234}U	0.501	0.748
^{230}Th	0.040	0.748
$^{226}\text{Ra}+\text{D}$	-0.026	0.748
^{232}Th	-0.002	-0.014
$^{228}\text{Ra}+\text{D}$	-0.019	-0.014
$^{228}\text{Th}+\text{D}$	-0.005	-0.014

4.3.3 Radon Flux Sensitivity and Uncertainty Analysis

Lindstrom *et al.* (1994) performed a sensitivity analysis of CASCADR9 that considered source term concentration, background radon concentration, half-life, porosity, period and amplitude of the atmospheric pressure wave, and eddy diffusivity of the atmosphere soil mixing layer. The most important parameters for cases where the source term was larger than the background concentration, in decreasing order of significance, were porosity, half-life, and source term concentration. The uncertainty in radiological half-life was assumed to be negligible and its effect was not examined. Uncertainty in radon flux results was assessed by setting the porosity and ^{226}Ra source term to bounding values and examining the effect on flux. In addition, because thickness of the waste layer was not considered by Lindstrom *et al.* (1994), a bounding case with maximum waste thickness for the Area 5 RWMS (P03U) was considered to assess the importance of thicker waste layers.

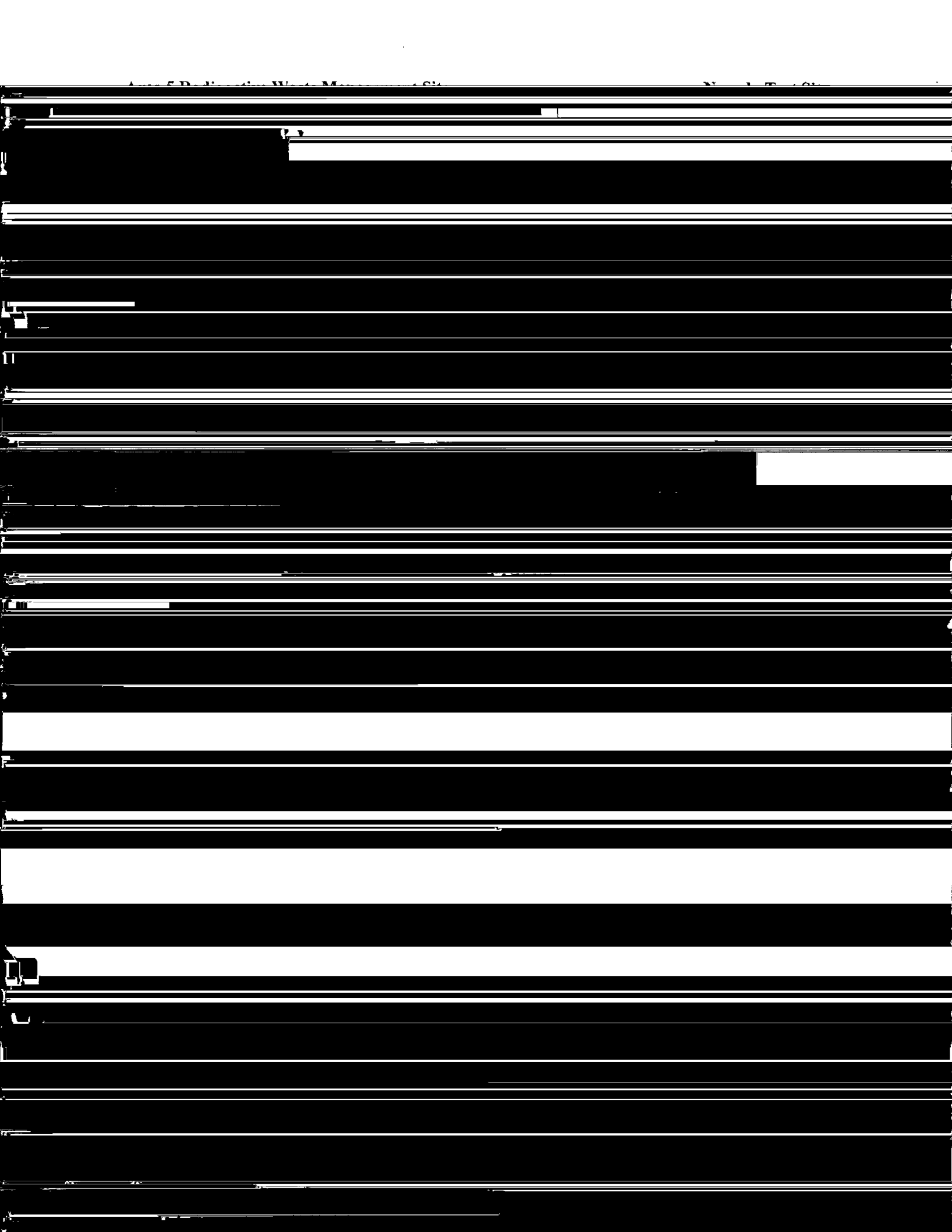
Uncertainty in the radon results for the shallow land burial waste cells was assessed by varying waste cell thickness, waste porosity, soil porosity, and radium inventory. Waste cell thickness is not constant for all pits and trenches at the Area 5 RWMS. A single case (Case [1]) was run to assess the importance of waste cell thickness. The thickness used, 7.9 m (25.9 ft), corresponds to the thickest cell constructed at the RWMS, Pit 3 (P03U). The results indicate that the K_{SLB} factor decreases slightly with the increase in thickness from 4.9 to 7.9 m (16.07 to 25.9 ft) (Table 4.28). It was concluded that waste cell thickness over the range of values observed at the RWMS has a negligible effect on radon flux uncertainty. Three cases were run to assess the significance of uncertainty in porosity (Table 4.28). The porosity values selected represent the bounding values for both soil and waste. The maximum porosity observed for shallow alluvium is approximately 0.50 (REECo, 1993c). For the waste, lower porosity will increase the flux by increasing the concentration of the gas source term. The lowest reasonable porosity value for waste was assumed to be the same as that of the alluvium, 0.36. Because radon flux will scale linearly with the radium concentration, specific modeling cases were not analyzed.

Table 4.28 Uncertainty Cases and Results for the Radon K-Factors for Shallow Land Burial. Varied parameters are listed. All other parameters are as in the base case (see Table 3.11).

Uncertainty Case	Waste Cell Thickness (m)	Cap Porosity	Waste Porosity	K_{SLB} Factor ($m\ s^{-1}$)
Base Case	4.9	0.36	0.67	5.6×10^{-8}
Case 1	7.9	0.36	0.67	5.3×10^{-8}
Case 2a	4.9	0.50	0.67	1.2×10^{-7}
Case 2b	4.9	0.36	0.36	1.4×10^{-7}
Case 2c	4.9	0.50	0.36	2.3×10^{-7}

The uncertainty in radon flux from Pit 6 was assessed in a similar fashion (Table 4.29). The porosity of similar material was always assumed to be the same; that is, the cap and backfill soil porosities are always the same, and the upper and lower cell waste porosities are always the same. The selected combinations represent bounding values.

Radon fluxes for two bounding cases for the shallow land burial cells are presented in Table 4.30. Case 2b, representing a combination of the best estimate alluvium porosity and worst-case waste porosity, meets the flux standard. Case 2c, which includes the worst-case



4.4 Interpretation of Analysis Results

4.4.1 Interpretation of Doses to Members of the General Public

To interpret the results presented in Section 4.1.1 for members of the general public, it is necessary to consider the conservative assumptions inherent in the underlying calculations and the sensitivities and uncertainties associated with these calculations. The following discussion reviews the conservative assumptions in the estimated release rates to the accessible environment and in the calculations of subsequent transport, exposure, and dose. The results are then interpreted in light of these conservative assumptions and the model sensitivities discussed above.

In Section 3.2.2, the models and equations describing the assumptions made to estimate the release rate of radionuclides from the waste to the near-field environment were presented. Four main pathways of release were identified in the conceptual model: (1) diffusion of volatile radionuclides through the soil cap, (2) root uptake of radionuclides from the waste to overlying soil, (3) transport of radionuclides as a result of soil excavation by burrowing animals, and (4) resuspension of radionuclides to the air from contaminated surface soil. Whenever possible, reasonable parameter values, representative of the NTS, were selected. Nevertheless, because of the lack of data or poor quality of some data, conservative values (values which tend to maximize the estimated doses) were selected for many parameters. Conservative assumptions inherent in estimates of release rates characterizing these pathways are listed below.

- To evaluate the release of potentially volatile radionuclides, the entire inventories of ^3H and ^{14}C are assumed to be immediately available for diffusion, as HTO and $^{14}\text{CO}_2$ (Section 3.2.2.1).
- Diffusive flux is assumed proportional to the initial concentration of the volatile radionuclide, until the entire inventory is depleted. In reality, the driving force or concentration gradient would decline as diffusion occurs.
- Exchange of ^3H or ^{14}C with hydrogen or carbon in the vadose zone during diffusion to the surface is neglected.
- To evaluate the release of nonvolatile forms of ^3H and ^{14}C , the entire inventory of these radionuclides is assumed nonvolatile.
- Five percent of the root biomass is assumed to penetrate to depths below 2.4 m (7.9 ft). This is highly conservative, as evidence to date indicates most roots are within 1.5 m (4.9 ft) of the surface (Section 3.2.2.5).

- The annual amount of soil excavated by insects is maximized by conservatively assuming a 10-year colony lifetime and selecting an upper-limit value for the percentage of soil excavated from depths greater than 1.5 m (4.9 ft).

Conservative assumptions inherent in estimates of dose from the release of radionuclides from the undisturbed site include the following:

- Transient visitors are assumed to spend up to 2,000 hours per year at the site.
- The neglect of shielding by structures in the transient occupancy scenario.
- The assumption that inhalation of suspended soils occurs continuously during the time of occupation (i.e., no indoor residency occurs).
- The use of a conservative estimate of the annual average mass loading parameter, M_s , of 10^{-4} g soil per m^{-3} of air.
- The lack of a correction for source area size in the mass loading equation, so the facility is assumed to have an infinite area.
- The use of conservative values for deposition velocity and foliar interception fraction.
- The open rangeland and resident farmer scenario assumes that the entire vegetable intake is produced at the off-site residence and that all milk and meat products consumed are produced in contaminated areas at the RWMS.

It is extremely conservative to assume that all the beef and milk consumed is produced at the

Area 5 RWMS. As much as 91 percent of the dose in the open rangeland scenario is due to

conservative because it assumes 5 percent of the plant roots penetrate to a depth of 4.4 m (14.4 ft). Site-specific data suggest that perennials native to the area rarely root below 2 m (6.6 ft). The Area 5 RWMS inventory does not currently contain high-activity concentrations of nuclides concentrated by plants such as ^{14}C , ^{99}Tc , and ^{129}I . Therefore, the current models suggest that sensitivity to plant uptake does not appear to be as important as sensitivity to burrowing animal transport.

The results presented in Section 4.1.1 indicate that TEDE to members of the general public from the Area 5 RWMS facility through all pathways and through the atmospheric pathway are less than 10 mrem yr^{-1} at any time, and less than 1 mrem yr^{-1} during the first 10,000 years after closure for the two most probable scenarios, transient occupancy and open rangeland. The TEDE estimated for a resident farmer at the site boundary was slightly higher. The peak dose during the compliance period occurs at closure and is 6 mrem yr^{-1} from the release of ^3H . Doses decreased to approximately 4 mrem yr^{-1} at the end of 10,000 years. An uncertainty analysis of inventory and release rate constants suggests that it is unlikely that the performance objective will be exceeded.

Subsidence was found to have three potential impacts. If subsidence causes cap thinning, the release of nonvolatile radionuclides increases. The increase is largest for radionuclides with high plant-soil concentration factors. This may cause doses to increase significantly if the land is used for agriculture. Subsidence also has the potential to initiate a groundwater pathway if accompanied by ponding and infiltration of run-on. Subsidence potentially may increase the release of volatile radionuclides. However, the timing of subsidence and radioactive decay of the inventory tends to minimize the impact of increased release of gaseous radionuclides. All performance objectives were met when subsidence was included in the conceptual model of radionuclide release.

4.4.2 Interpretation of Radon Flux Results

The flux of ^{222}Rn from waste disposal cells at the Area 5 RWMS has been estimated considering its diffusive and advective transport in the air-filled pore space. The radon flux was estimated to be approximately $6 \text{ pCi m}^{-2} \text{ s}^{-1}$ at 10,000 years for both shallow land burial trenches and Pit 6 using best estimate parameters in the base case release scenario. The flux increases to $10 \text{ pCi m}^{-2} \text{ s}^{-1}$ at 10,000 years for a subsided cap. These results were shown to be most sensitive to waste porosity and waste ^{226}Ra activity concentration. Bounding values for waste porosity and ^{226}Ra activity concentration were not sufficient to generate cases that exceed the $20 \text{ pCi m}^{-2} \text{ s}^{-1}$ flux limit at 10,000 years. These results suggest that although waste streams currently being received at the Area 5 RWMS and disposed at a depth of 2.4 m (7.9 ft) are very close to the flux limit at 10,000 years, it is unlikely that the standard will be exceeded. Because the final closure cap is very likely to be thicker than 2.4 m (7.9 ft), the fluxes can be expected to be attenuated to below $20 \text{ pCi m}^{-2} \text{ s}^{-1}$.

4.4.3 Interpretation of Doses to Inadvertent Intruders

Three intruder scenarios were evaluated for the Area 5 RWMS. The intruder scenarios have been analyzed primarily to set conservative waste concentration limits for various waste disposal options. The intruder performance objective is the limiting criterion in the near-term because natural release processes from the undisturbed site operate very slowly. Over thousands of years, the models of undisturbed site performance suggest that natural transport processes can cause certain long-lived radionuclides to accumulate in the shallow soils. However, soil concentrations and doses in the intruder-agriculture scenario still bound the results for the members of the public for the inventory below 2.4 m (7.9 ft). For deeper source terms, natural release processes are expected to be reduced, and the postdrilling scenario is expected to be the bounding scenario.


Intruder scenarios represent an extremely conservative method of setting waste concentration limits. It is unlikely that these events will ever occur or that the projected doses will ever be realized. In addition, very conservative assumptions have been made, including:

- The assumption that intrusion and chronic exposure can begin within 100 years after site closure. The arid conditions at the Area 5 RWMS will probably ensure that many of the waste forms present will remain intact and identifiable as refuse for many hundreds, if not thousands, of years. It is unlikely that an intruder would disperse refuse over an area that

- The assumptions that the intruder spends 70 percent of their time on site, respire at the rate of $8,400 \text{ m}^3 \text{ yr}^{-1}$, and is exposed to a dusting loading of $1.5 \times 10^{-4} \text{ g m}^{-3}$. These are conservative values that contribute to the inhalation dose, which is a major route of exposure. The high occupancy factor also contributes to the external doses, which is the other major exposure pathway. The intruder's residence is assumed to transmit 70 percent of incident photons.
- The assumption that 25 percent of the intruder's entire diet consists of food produced in the contaminated zone. Although this is physically possible, it is unlikely that an individual would consume such a small area this intensively. Furthermore, the extreme climate

The drilling scenario involves exposure to soil with a significantly greater activity concentration than occurs in the subsequent chronic postdrilling scenario. Therefore, the drilling scenario was evaluated for comparison with the performance objectives. The total effective dose equivalent was estimated to be 0.15 mrem at 100 years and 0.17 mrem at 10,000 years for a driller penetrating a shallow land burial trench. The results for Pit 6 were 22 mrem at 100 years and 23 mrem at 10,000 years. The doses are significantly less than the 500 mrem limit and provide reasonable assurance of compliance.

Two chronic intruder scenarios were considered in the performance assessment. The intruder-agriculture scenario describes the exposure of an on-site resident to soil contaminated with waste from a construction excavation. This scenario was evaluated to determine



This leads to a total inventory limit for the lower cell of Pit 6 of 174 Ci of ^{232}Th . Preliminary estimates of the total ^{232}Th inventory at FEMP indicate the inventory is significantly less than the 174 Ci limit and that this inventory can be placed in Pit 6. Compliance with the performance objectives for Pit 6 can be assured by implementing a ^{232}Th inventory limit for the lower cell.

The dose to an intruder from inhalation of short-lived progeny of radon was estimated in Section 4.2.4. These analyses showed that the dose from radon released from the buried waste zone far surpasses the dose from the contaminated zone on the surface. Therefore, a single analysis is applicable to all intruder scenarios. The results of the analyses indicate that reasonable protection is provided out to 10,000 years, when at least 4 m (13.1 ft) of cap is present for attenuation of the fluxes. The NCRP has estimated that an average individual receives approximately 200 mrem yr^{-1} from background exposure to radon (NCRP, 1987). With a 4-m (13.1-ft) cap present, the highest CEDE from buried waste was 107 mrem yr^{-1} , approximately one-fourth of the annual background exposure.

5.0 PERFORMANCE EVALUATION

A performance assessment is the systematic analysis of the risks posed by a waste-management system to the general public and the environment and a comparison of those risks to the performance objectives. This section summarizes the results of the performance assessment presented in the previous sections and compares those results with the performance objectives. Additionally, the implications of the performance assessment for site characterization, site monitoring, waste operations, and future performance assessments are discussed.

5.1 Comparison of Performance Assessment Results With the Performance Objectives

This performance assessment assesses the risk to two populations. The risk to the general public has been assessed through the analysis of several scenarios of varying probability. The base case and subsided case scenarios represent reasonably probable scenarios for the release of radionuclides from differing waste forms to the accessible environment. Estimates of upward release of volatile and nonvolatile radionuclides were greater for the subsided case. The differences are small, however, compared to the overall uncertainty in the analysis. The most significant difference between the two release scenarios was their potential for downward release to the aquifer. Downward transport is not credible for the base case scenario. Subsidence, combined with extreme bounding estimates of run-on and infiltration, can potentially cause downward transport to the aquifer. This scenario is considered an extreme bounding case due to the conservative estimates of subsidence, infiltration, and

Table 5.1 Maximum Performance Assessment Results for Members of the General Public in the Transient Occupancy and Open Rangeland Scenarios

Performance Objective	Performance Assessment Result		Conclusion
	Base Case	Subsided Case	
25 mrem yr ⁻¹ from All Pathways	0.6 mrem yr ⁻¹	0.8 mrem yr ⁻¹	Complies
10 mrem yr ⁻¹ from Airborne Emissions Excluding Radon	0.2 mrem yr ⁻¹	0.2 mrem yr ⁻¹	Complies
Average Annual ²²² Rn Flux Less Than 20 pCi m ⁻² s ⁻¹	6 pCi m ⁻² s ⁻¹	10 pCi m ⁻² s ⁻¹	Complies
Protect Groundwater Resources			
²²⁶ Ra + ²²⁸ Ra < 5 pCi L ⁻¹	Not Detected [†]	0.3 pCi L ⁻¹	Complies
Gross Alpha < 15 pCi L ⁻¹	6 pCi L ⁻¹ [†]	9 pCi L ⁻¹	Complies
Dose from Man-made Beta-Gamma Emitters < 4 mrem yr ⁻¹	Zero Release to Aquifer in 10,000 Years	1 mrem yr ⁻¹	Complies

[†] - Indicates natural background level.

The much less likely resident farmer scenario combined with the base case and the subsided case release scenarios yields greater doses. However, even for these extreme bounding scenarios, the performance objectives were met.

Several characteristics of the Area 5 RWMS contribute to the low dose estimates. The high potential evapotranspiration, low rainfall, and thick vadose zone prevent radionuclides from being leached from the waste to the aquifer. The extremely low water content of the near-surface alluvium minimizes the potential for upward advection and diffusion of dissolved solutes. The potential for release by plant uptake is reduced by the low productivity and shallow rooting depth of native floral communities. These characteristics combine to minimize the release of radionuclides from the intact waste disposal units.

The impact of radionuclides released from the facility is minimized by the low population density and limited land use options near the site. The probability of residential or urban development at the site is low because of the lack of surface water or shallow groundwater. Agricultural development is rendered unlikely by the lack of water, poor soils, and extreme temperatures.

Exposures through airborne pathways (gases and suspended particulates) were also extremely low. The greatest TEDE in the transient occupancy and open rangeland scenarios from exposure to airborne radioactivity, excluding radon, was 0.2 mrem yr⁻¹. Radon emissions

were estimated to remain below $6 \text{ pCi m}^{-2} \text{ s}^{-1}$ for 10,000 years after closure for the base case and to increase to $10 \text{ pCi m}^{-2} \text{ s}^{-1}$ for the subsided case. The highest atmospheric dose, 6 mrem yr^{-1} , was estimated for a resident farmer at the site boundary at closure. However, it is unlikely that a resident farmer would reside at the site boundary during active institutional control. If this scenario is delayed for 100 years, the atmospheric dose decreased to $0.03 \text{ mrem yr}^{-1}$.

Protection of groundwater resources are ensured by the natural properties of the disposal site rather than the performance of engineered barriers or stabilized waste forms. Site characterization studies have demonstrated that the vadose zone is approximately 235 m (770.9 ft) thick and that the water potential gradient is upward in the upper 35 m (114.8 ft). Water in the upper 35 m (114.8 ft) of the alluvium tends to move upward rather than downward to the aquifer. Although there is a potential for upward migration, upward advection and diffusion are rendered negligible by the extremely dry conditions. A modeling study of transient conditions in the vadose zone suggests that infiltrating precipitation does not affect the water content and water potential profile below a depth of about 0.25 m (0.82 ft). Therefore, the

Table 5.2 Performance Assessment Results for Intruder Scenarios. Results are based on current waste management practices. Conclusions regarding compliance are based on implementation of trench activity limits and installation of a final closure cap.

Performance Objective	Performance Assessment Result		Conclusion
	Shallow Land Burial	Pit 6 (P06U)	
500 mrem Acute Scenario Drilling	0.2 mrem	23 mrem	Complies/Complies
100 mrem Chronic Scenario Agriculture	157 mrem yr ⁻¹	Not Applicable	Complies [†]

- X = cost of radiation protection, and
 Y = cost of the health detriment.

The gross benefit of each disposal option is likely equivalent if the same waste inventory is disposed. If the gross benefit can be assumed to be constant for each disposal option, the optimum solution corresponds to the minimum value of $(P + X + Y)$ or the total cost. The cost of the project is expected to be mostly due to the cost of disposal operations (construction and filling of disposal cells), the cost of final closure of the site, and any maintenance costs incurred during institutional control. The cost of radiation protection in the future after institutional control can be assumed to be effectively zero. The cost of the health detriment can be estimated in its simplest form as:

$$Y = \alpha S_E^C \quad (5.2)$$

where:

- α = monetary cost assigned to unit of collective dose, and
 S_E^C = collective dose commitment.

The collective dose commitment can be estimated as:

$$S_E^C = \int_a^b \int_0^\infty H_E(t) N(H_E, t) dH_E dt \quad (5.3)$$

where:

- $H_E(t)$ = total effective dose equivalent,
 $N(H_E, t)$ = population frequency distribution of TEDE
 a = start of compliance period, and
 b = end of compliance period.

Considering the disposal option evaluated in the performance assessment, the collective dose commitment can be estimated after several assumptions. Assume that for the transient occupancy and open rangeland scenarios, a single family unit of five persons is exposed throughout the compliance period and that each person receives the TEDE estimated in the performance assessment. The compliance period is assumed to begin at closure and end at

rangeland scenarios combined with the base case release scenario are 13 and 6 person-rems, respectively. The collective doses for the subeided case increased to 18 and 12 person-rems

The results of the performance assessment can be used to set waste concentration limits. These limits should be developed and justified as a performance assessment maintenance activity.

The sensitivity analysis of the radionuclide release model indicated that the model was most sensitive to the quantity of buried waste excavated by invertebrates for nuclides with low plant-soil concentration factors. For nuclides with high plant-soil concentration ratios, model results were found to be most sensitive to uptake by plants with roots in the buried waste. Relatively little site-specific data are available concerning the ability of insects or plants to transport materials to the surface from the depth of burial. Uncertainty could be reduced with additional data on the occurrence, population densities, excavation rates, and the depth distribution of invertebrate burrows in Frenchman Flat. No site-specific data were identified concerning invertebrate burrowing. Reliable data on the rooting depth of native perennial plants in Frenchman Flat should be collected. Site-specific studies reported to date are, in all cases, anecdotal. More rigorous investigations of native and introduced plant rooting depth are worthy of consideration. Productivity of native floral communities has been studied and reported for many years at several plots within Frenchman Flat and Rock Valley. Plant productivity and biomass are comparatively well known. Plant-soil concentration ratios have been well studied and site-specific values are available for Pu and Am. Plant-soil concentration ratios show a high degree of variability due to the difficulties of controlling chemical and biological conditions during uptake experiments. It is doubtful that additional site-specific measurement will significantly reduce variability in this parameter. A great deal of plant-soil concentration data would be required to significantly reduce uncertainty in this parameter.

The performance assessment results support current site-monitoring efforts. Few release mechanisms were identified that would lead to detectable radioactivity in environmental samples during the operational period. Site-monitoring results are consistent with this conclusion. The only release pathway expected in the near term is diffusion of gases. The only gaseous nuclide with an inventory sufficient to be detected in environmental samples is ^3H . Site-monitoring results have detected ^3H in soil, vegetation, and air only. The absence of nonvolatile radionuclides in surface soils and vegetation suggests that containers remain intact or that few roots reach the buried waste. Sampling of cap soil and vegetation for nonvolatile radionuclides may provide an early indication of container failure.

In view of the lack of movement of water to the water table, it is extremely unlikely that radionuclides from the disposal site will ever be detected in the groundwater. Groundwater monitoring could be reduced in frequency and limited to screening analyses such as ^3H , gross beta, and gross alpha. Vadose zone monitoring offers an earlier indication of release and is preferred to groundwater monitoring.

The performance assessment results indicate the importance of depth of burial at the Area 5 RWMS. This analysis suggests that there are wastes being received at the Area 5 RWMS that require a depth of burial of up to 4 to 5 m (13.1 to 16.4 ft). Depth of burial is a design

feature that can be controlled by the site operator. Future performance assessments should continue to evaluate the adequacy of the depth of burial and closure cap design. Future performance assessment models could be significantly improved with the completion of a closure cap design and development of conceptual models of long-term cap performance.

6.0 PREPARERS

6.1 Principal Investigators

Gregory J. Shott

M.S. Health Physics, Georgia Institute of Technology – 1996
M.S. Ocean and Fishery Science, University of Washington – 1984
B.S. Biology, University of New Hampshire – 1981

Gregory J. Shott is a Certified Health Physicist (CHP) with ten years of experience in environmental monitoring and waste management. Gregory Shott acted as the project manager, prepared the intruder pathway analysis, and assisted in the preparation of all radiological analyses.

Lawrence E. Barker

Ph.D. Statistics, Florida State University – 1979
M.S. Statistics, Florida State University – 1976
B.S. Mathematics, University of Kentucky – 1975

Lawrence Barker has been with Bechtel Nevada since 1989, where his statistical expertise has contributed to the solutions of many problems in waste management, environmental monitoring, and site characterization. He was on the faculty of the Department of Mathematics at the University of Tennessee for five years. His work has recently appeared in *Soil Science Society American Journal*, as well as numerous DOE publications. Lawrence Barker prepared the Monte Carlo uncertainty analyses and acted as an editor for the performance assessment.

Stuart E. Rawlinson

Ph.D. Geology, University of Alaska – 1990
M.S. Geology, University of Alaska – 1979
B.S. Geology, California State University, Long Beach – 1974
A.A. Liberal Arts, Los Angeles Harbor College – 1972

Dr. Stuart Rawlinson is a Certified Geologist with the American Institute of Professional Geologists, a Certified Geologist in Alaska, and a Certified Environmental Manager in Nevada. He has 20 years' experience in development, management, and implementation of geological and related technical studies for site characterization, performance assessment; and assessments of natural resources and natural hazards. Dr. Rawlinson has been with Bechtel Nevada and predecessor contractors since 1988, using his expertise in support of the DOE/NV Office of Environmental Management. He previously worked for the State of Alaska Division of Geological and Geophysical

Surveys, and for the Outer Continental Shelf Environmental Assessment Program through the University of Alaska. Dr. Rawlinson contributed primarily to the introductory and summary sections, and served as editor of the document.

Michael J. Sully

Ph.D. Soil Science, University of California, Davis – 1984.
M.S. Atmospheric Science, University of California, Davis – 1979.
B.A. Physics, University of Montana, Missoula – 1976.

Michael Sully is the principal hydrologist in charge of the site characterization of flow, transport properties, and field investigation of soil-plant-water interactions. He has served as an assistant professor at the Department of Hydrology and Water Resources at the University of Arizona, and as an experimental scientist at CSIRO Division of Environmental Mechanics in Canberra, Australia. He has submitted numerous research articles for both national and international publications.

Beth A. Moore

M.S. Hydrology, University of Idaho – 1983
B.S. Geology and Marine Sciences, Pennsylvania State University – 1978
A.A. Computer Programming, Midland College, Texas – 1993

Beth More is a hydrogeologist with over 16 years' experience in waste site characterization and hydrogeology. Ms. Moore has been with the U.S. DOE/NV since 1995 as Project Manager for Low-Level Waste Performance Assessments and Site Characterization in the Waste Management Program. She previously worked as a consultant and contractor to the U.S. DOE and U.S. EPA.

6.2 Contributors

David E. Cawlfeld, Bechtel Nevada
Camilla W. Deckert, Bechtel Nevada
Lane W. Elletson, Bechtel Nevada
Angelos N. Findikakis, Bechtel San Francisco
Thomas M. Fitzmaurice, Bechtel Nevada
Frederick T. Lindstrom, Bechtel Nevada
Deron G. Linkenheil, Bechtel Nevada
Ann Moylan, Bechtel Nevada
Laura McDowell-Boyer, Oak Ridge National Laboratory, Grand Junction, Colorado
Subhash C. Mehrotra, Bechtel Oak Ridge
Curtis J. Muller, Bechtel Nevada
Shannon M. Parsons, Bechtel Nevada

Frederick T. Lindstrom, Bechtel Nevada
Deron G. Linkenheil, Bechtel Nevada
Ann Moylan, Bechtel Nevada

This Page Intentionally Left Blank

7.0 REFERENCES

- Albright, W., 1995. Physical and Hydraulic Characteristics of Bentonite-Amended Soil from Area 5, Nevada Test Site. Report No. DOE/NV11508-XX, U.S. Department of Energy, Nevada Operations Office, Las Vegas, Nevada.
- Allison, G. B., and M.W. Hughes, 1983. The Use of Natural Tracers As Indicators of Soil-Water Movement in a Temperate Semiarid Region. J. of Hydr., 60:157-173.
- Allmendinger, R.W., T. A. Hauge, E. C. Hauser, C. J. Potter, S. L. Klemper, K. D. Nelson, P. Knuepfer, and J. Oliver, 1987. Overview of the COCORP 40° N Transect.

- Baca, R. G., and S. O. Magnuson, 1992. FLASH – Finite Element Computer Code for Variably Saturated Flow. EGG-GEO-10274. EG&G Idaho Inc., Idaho Falls, Idaho.
- Baes III, C. F., R. D. Sharp, A. L. Sjoreen, and R. W. Shor, 1984. A Review and Analysis of Parameters for Assessing Transport of Environmentally Released Radionuclides Through Agriculture. DE85-000 287. ORNL-5786. Oak Ridge National Laboratory, Oak Ridge, Tennessee.
- Bamberg, S. A., A. T. Volmer, G. E. Kleinkopf, and T. L. Ackerman, 1976. A Comparison of Seasonal Primary Production of Mojave Desert Shrubs During Wet and Dry Years. Amer. Midland Naturalist 95(2):398-405.
- Barnes, J. J., R. T. Giacomini, R. T. Reiman, and B. Elliot, 1980. NTS Radiological Assessment Project: Results for Frenchman Lake Region on Area 5. DOE/DP/01253-17. Water Resources Center, Desert Research Institute, University of Nevada, Las Vegas, Nevada.
- Battis, J. D., 1978. Geophysical Studies for Missile Basin: Seismic Risk Studies in the Western United States. TI-ALEX(02)-FSR-78-01. Texas Instruments Inc., Houston, Texas.
- Bear, J., 1972. Dynamics of Fluids in Porous Media. Dover Publications Inc., New York, New York.
- Beatley, J. C., 1976. Vascular Plants of the Nevada Test Site and Central-Southern Nevada: Ecologic and Geographic Distributions. TID-26881. U.S. Department of Commerce, Springfield, Virginia.
- , 1974. Effects of Rainfall and Temperature on the Distribution and Behavior of *Larrea tridentata* (Creosote Bush) in the Mojave Desert of Nevada. Ecology 55:245-261.
- , 1969. Biomass of Desert Winter Annual Plant Populations in Southern Nevada. Oikos 20:261-273.
- Bellin, A., P. Salandin, and A. Rinaldo, 1992. Simulation in Heterogeneous Porous Formations: Statistics, First-Order Theories, Convergence of Computations. Water Res. Research 28(9):2211-2227.
- Benjamin, J. R., and C. A. Cornell, 1970. Probability, Statistics, and Decisions for Civil Engineers. McGraw Hill, New York, New York.

Benz, H. M., R. B. Smith, and W. D. Mooney, 1990. Crustal Structure of the Northwestern Basin and Range Province From the 1986 Program for Array Seismic Studies of the Continental Lithospheric Seismic Experiment. J. Geophy. Res. 95:21823-21842.

Biggar, J. W., and D. R. Nielsen, 1967. Miscible Displacement and Leaching Phenomenon in Irrigation of Agricultural Lands. Amer. Soc. Agrn. 254-274.

Black, S. C., and D. D. Smith, 1984. Nevada Test Site Environmental Report Summary.

1075. Ecological Studies of Small Vertebrates in Plutonium Contaminated Study

h

- Cameron, D. R., and A. Klute, 1977. Convective-Dispersive Solute Transport With a Combined Equilibrium and Kinetic Adsorption Model. *Water Res. Research* 13(1):183-188.
- Campbell, K. W., 1980. Seismic Hazard Analysis for the NTS Spent Reactor Fuel Test Site. UCRL-15620. Lawrence Livermore National Laboratory, Livermore, California.
- Carr, W. J., 1984. Regional Structural Setting of Yucca Mountain, Southwestern Nevada, and Late Cenozoic Rates of Tectonic Activity in Part of the Southwestern Great Basin, Nevada and California. USGS Open-File Report 84-854. U.S. Geological Survey, U.S. Government Printing Office, Washington, DC.
- , 1974. Summary of Tectonic and Structural Evidence for Stress Orientation at the Nevada Test Site. USGS Open-File Report 74-176. U.S. Geological Survey, U.S. Government Printing Office, Washington, DC.
- Carr, W. J., G. D. Bath, D. L. Healey, and R. M. Hazelwood, 1975. Geology of Northern Frenchman Flat, Nevada Test Site. USGS Report 474-216. U.S. Geological Survey, U.S. Government Printing Office, Washington, DC.
- , 1967. Geology of Northern Frenchman Flat, Nevada Test Site. NTS-188. U.S. Geological Survey Technical Letter. U.S. Geological Survey, U.S. Government Printing Office, Washington, DC.
- Case, C., J. Davis, R. French, and S. Raker, 1984. Site Characterization in Connection With the Low-Level Defense Waste Management Site in Area 5 of the Nevada Test Site, Nye County, Nevada, Final Report. Publication No. 45034. Water Resources Center, Desert Research Institute, University of Nevada, Las Vegas, Nevada.
- Case, M. J., and M. D. Otis, 1988. Guidelines for Radiological Performance Assessment of DOE Low-Level Radioactive Waste Disposal Sites. DOE/LLW-62T. U.S. Department of Energy, Idaho Operations Office, Idaho Falls, Idaho.
- Catchings, R. D., and W. D. Mooney, 1991. Basin and Range Crustal and Upper Mantle Structure, Northwest to Central Nevada. *J. Geophys. Res.* 96:6247-6267.
- Cawfield, D. E., K. B. Been, D. F. Emer, F. T. Lindstrom, and G. J. Shott, 1993a. CASCADR: An m-chain gas phase radionuclide transport and fate model. Volume 2 - User's Manual for CASCADR8. DOE/NV/10630-57. Reynolds Electrical & Engineering Co., Inc., Las Vegas, Nevada.

- Cawlfeld, D. E., D. F. Emer, F. T. Lindstrom, and G. J. Shott, 1993b. CASCADR: An m-chain gas phase radionuclide transport and fate model. Volume 4 - User's Manual for CASCADR9. DOE/NV/10630-63. Reynolds Electrical & Engineering Co., Inc., Las Vegas, Nevada.
- Chapman, J. B., 1993. Groundwater Investigations Near the RWMS. Letter Report, Desert Research Institute, Las Vegas, Nevada.
- Chapman, J. B., and B. F. Lyles, 1993. Groundwater Chemistry at the Nevada Test Site: Data and Preliminary Interpretations. Publication No. 45100. Water Resources Center, Desert Research Institute, University of Nevada, Las Vegas, Nevada.
- Christiansen, R. L., and P. W. Lipman, 1972. Cenozoic Volcanism and Plate Tectonic Evolution of the Western United States, II, Late Cenozoic. Trans. of the Royal Soc. London. Ser. A. Vol. 271:249-284.
- Christiansen, R. L., P. W. Lipman, W. J. Carr, F. M. Byers, P. P. Orkild, and K. A. Sargent, 1977. Timber Mountain-Oasis Valley Caldera Complex of Southern Nevada. Geol. Soc. Am. Bull. 88:943-956.
- Craig, H., 1961a. Standard for Reporting Concentrations of Deuterium and Oxygen-18 in Natural Waters. Science 133:1833-1934.
- , 1961b. Isotopic Variations in Meteoric Waters. Science 133:1702-1703.
- CRC Press, Inc., 1981. CRC Handbook of Chemistry and Physics. Robert C. Weast and Melvin J. Astle (eds.), Boca Raton, Florida.
- Crowe, B. M., 1990. Basaltic Volcanism Episodes of the Yucca Mountain Region. p. 65-73. In: High-Level Radioactive Waste Management. Proceedings of the international topic meeting sponsored by the American Society of Civil Engineers for the American Nuclear Society. Co-sponsored by the American Chemical Society . . . [et al.]. Hosted by the University of Nevada, Las Vegas, Nevada; American Nuclear Society, Inc., La Grange Par., Illinois; and American Society of Civil Engineers. New York. April 8-12, 1990.
- Crowe, B. M., K. H. Wohletz, D. T. Vaniman, E. Gladney, and N. Bower, 1986. Status of Volcanic Hazards Studies for the Nevada Nuclear Waste Storage Investigations. Los Alamos National Laboratory Report LA-9325-MS. Los Alamos, New Mexico.
- Crowe, B. M., and W. J. Carr, 1980. Preliminary Assessment of the Risk of Volcanism at a Proposed Nuclear Waste Repository in the Southern Great Basin. USGS Open File Report 80-357. U.S. Geological Survey, U.S. Government Printing Office, Washington, DC.

Crowe, B. M., S. Self, D. Vaniman, R. Amos, and F. Perry, 1983. Aspects of Potential Magmatic Disruption of a High-Level Radioactive Waste Repository in Southern Nevada. J. of Geology 91:259-276.

Cvetkovic, V., A. M. Shapiro, and G. Dagan, 1992. A Solute Flux Approach to Transport in Heterogeneous Formations, 2) uncertainty analysis. Water Res. Research, 28(6): 1277-1289.

- Dodge, R. L., W. R. Hansen, W. E. Kennedy, D. W. Layton, D. W. Lee, S. T. Maheras, S. M. Neuder, E. L. Wilhite, R. U. Curl, K. F. Grahn, B. A. Heath, and K. H. Turner, 1991. Performance Assessment Review Guide for DOE Low-Level Radioactive Waste Disposal Facilities. DOE/LLW-93. Idaho National Engineering Laboratory, Idaho Falls, Idaho.
- Domenico, P. A., and F. W. Schwartz, 1990. Physical and Chemical Hydrogeology. John Wiley and Sons, Inc., New York, New York.
- Donahue, R. L., R. W. Miller, and J. C. Shickluna, 1983. An Introduction to Soils and Plant Growth. Prentice-Hall, Englewood, New Jersey.
- Dozier, B. L., and S. E. Rawlinson, 1991. Conceptual Model for the Geology in Area 5, the Nevada Test Site. Reynolds Electrical & Engineering Co., Inc., Las Vegas, Nevada.
- Duke, H. R., 1973. Drainage Design Based Upon Aeration Hydrology. Paper No. 61. Colorado State University, Fort Collins, Colorado.
- Eckerman, K. F., and J. C. Ryman, 1993. External Exposure to Radionuclides in Air, Water, and Soil. Federal Guidance Report No. 12. U.S. Environmental Protection Agency, Washington, DC.
- EG&G, 1982. Description of Major Vegetation Associations and Their Potential Contribution to Range Fires Generated by LNG Combustion Tests on Frenchman Flat – Nevada Test Site, Nye County, Nevada. EGG 1183-2444. EG&G, Goleta, California.
- Energy Research and Development Administration, 1977. Nevada Test Site Final Environmental Impact Statement. ERDA-155. U.S. Government Printing Office, Washington, DC.
- Enfield, C. G., J. J. C. Hsieh, and A.W. Warrick, 1973. Evaluation of Water Flux Above a Deep Water Table Using Thermocouple Psychrometers. Soil Sci. Soc. Amer. Proc. 27:968-970.
- Fayer, M. J., and T. L. Jones, 1990. UNSAT-H, Version 2.0: Unsaturated Soil Water and Heat Flow Model. PNL-6779, Pacific Northwest Laboratory, Richland, Washington.
- Feddes, R. A., E. Bresler, and S. P. Neuman, 1974. Field Test of a Modified Numerical Model for Water Uptake by Root Systems. Water Res. Research 10(6):1199-1206.
- Fiero, G. W. and G. B. Maxey, 1970. Hydrogeology of the Devil's Hole Area, Ash Meadows, Nevada. Center for Water Resources Research, Desert Research Institute, University of Nevada, Reno, Nevada.

- Fischer, J. M., 1992. Sediment Properties and Water Movement Through Shallow Unsaturated Alluvium at an Arid Site for Disposal of Low-Level Radioactive Waste Near Beatty, Nye County, Nevada. U.S. Geological Survey Water Resources Investigation Report 92-4032. U.S. Geological Survey, U.S. Government Printing Office, Washington, DC.
- Fitzner, R. E., K. A. Gano, W. H. Rickard, and L. E. Rogers, 1979. Characterization of the Hanford 300 Area Burial Grounds: Task IV - Biological transport. PNL-2774. Pacific Northwest Laboratory, Richland, Washington.
- Fleck, R. J., 1970. Tectonic Style, Magnitude, and Age of Deformation in the Sevier Orogenic Belt in Southern Nevada and Eastern California. Geol. Soc. Amer. Bull. 81:1705-1720.
- Fleming, E. H., 1969. The Fission Product Decay Chains (^{239}Pu with fission spectrum neutrons). UCRL-50243 (Vol. 1). Lawrence Radiation Laboratory, University of California, Livermore, California.
- Fouty, S. C., 1989. Chloride Mass Balance as a Method for Determining Long-Term Groundwater Recharge Rates and Geomorphic Surface Stability in Arid and Semiarid Regions, Whiskey Flat and Beatty, Nevada. M.S. thesis. University of Arizona, Tucson, Arizona.
- Foxx, T. S., G. D. Tierney, and J. M. Williams, 1984. Rooting Depths of Plants on Low-Level Waste Disposal Sites. LA-10253-MS. Los Alamos National Laboratory, Los Alamos, New Mexico.
- Freeze, R. A., and J. A. Cherry, 1979. Groundwater. Prentice-Hall, Inc., Englewood Cliffs, New Jersey.
- French, R. H., 1993. Letter Report on FY1993 Evaporation Studies at ER 6-1 Ponds to Stephen J. Lawrence. DOE Environmental Restoration and Waste Management. Desert Research Institute/Water Resources Center. September 29, 1993.
- , 1985. A Preliminary Analysis of Precipitation in Southern Nevada. Pub. No. 45042. Desert Research Institute, University of Nevada, Reno, Nevada.
- Frère, M., and G. F. Popov, 1979. Agrometeorological Crop Monitoring and Forecasting. FAO Plant Production and Protection Paper 17. FAO, Rome, Italy.
- Fried, J. J., 1981. Groundwater Pollution Mathematical Modeling: Improvement or Stagnation? The Science of the Total Environment 21:283-298.

- Friedman, I., J. Gleason, and A. Warden, 1993. Ancient Climate From Deuterium Content of Water in Volcanic Glass, Climate Change in Continental Records. Geophysical Monograph 78:309-319.
- Friedman, G. M., and J. E. Sanders, 1978. Principles of Sedimentology. John Wiley and Sons, Inc., New York, New York.
- Frizzell, V. L., Jr., and J. Shulters, 1990. Geologic Map of the Nevada Test Site, Southern Nevada. USGS Map 1-2046. Miscellaneous Investigation Series. U.S. Geological Survey, U.S. Government Printing Office, Washington, DC.
- Gardner, W., and J. Chatelain, 1947. Thermodynamic Potential and Soil Moisture. Soil Sci. Soc., Am. Proc., 11:100-102.
- Gardner, W. R., 1958. Some Steady-State Solutions of the Unsaturated Moisture Flow Equation With Application to Evaporation From a Water Table. Soil Sci. 85:228-232.
- Gee, G. W., P. J. Wierenga, B. J. Andraski, M. H. Young, M. J. Fayer, and M. L. Rockhold, 1994. Variations in Water Balance and Recharge Potential at Three Western Desert Sites. Soil Sci. Soc. Am. J. 58(1):63-72.
- Gilbert, R. O., 1977. Revised Total Amounts of $^{239,240}\text{Pu}$ in Surface Soil at Safety-Shot Sites. p. 423-430. In: M. G. White, P. B. Dunaway, and D. L. Wireman (eds.), NVO-181. Transuranics in Desert Ecosystems. Nevada Applied Ecology Group, U.S. Department of Energy, Nevada Operations Office, Las Vegas, Nevada.
- Gilbert, R. O., L. L. Eberhardt, E. B. Fowler, E. M. Romney, E. H. Essington, and J. E. Kinnear, 1975. Statistical Analysis of $^{239,240}\text{Pu}$ and ^{241}Am Contamination of Soil and Vegetation on the NAEG Study Sites. p. 43-88. In: M. G. White and P. B. Dunaway (eds.), NVO-153, The Radioecology of Plutonium and Other Transuranics in Desert Environments. ERDA, Nevada Operations Office, Las Vegas, Nevada.
- Gilbert, R. O., J. H. Shinn, E. H. Essington, T. Tamura, E. M. Romney, K. S. Moor, and T. P. O'Farrell, 1988. Radionuclide Transport From Soil to Native Vegetation, Kangaroo Rats, and Grazing Cattle on the Nevada Test Site. Health Phys. 55(5):869-874.
- Ginanni, J. M., L. J. O'Neill, D. P. Hammermeister, D. O. Blout, B. L. Dozier, M. J. Sully, K. R. Johnejack, D. F. Emer, and S. W. Tyler, 1993. Hydrogeologic Characterization of an Arid Zone Radioactive Waste Management Site. 15th Annual USDOE Low-Level Radioactive Waste Management Conference, Phoenix, Arizona. December 1-3, 1993.

Green, C. R., and W. D. Sellers (eds.). 1964. Arizona Climate. The University of Arizona

- Hantush, M. S., 1964. Hydraulics of Wells. In: V.T. Chow (ed.), *Advances in Hydrosiences*, Vol. 1. Academic Press, New York, New York.
- Harris, H. D., 1959. Late Mesozoic Positive Area in Western Utah. *Am. Assoc. Pet. Geol. Bull.* Vol. 43(11):2636-2652.
- Hattis, D. B., and D. E. Burmaster, 1994. Assessment of Variability and Uncertainty Distributions for Practical Risk Assessments. *Risk Analysis* 14:713-730.
- Hedstrom, W. E., A. T. Corey, and H. R. Duke, 1971. *Models for Subsurface Drainage*. Hydrology Paper No. 48. Colorado State University, Fort Collins, Colorado.
- Hem, J. D., 1985. *Study and Interpretation of the Chemical Characteristics of Natural Water*. 3rd ed., U.S. Geological Survey Water-Supply Paper 2254. U.S. Geological Survey, U.S. Government Printing Office, Washington, DC.
- Heslep, J. M., and C. A. Black, 1954. Diffusion of Fertilizer Phosphorus in Soils. *Soil Sci.* 78:389-401.
- Hillel, D., 1980. *Fundamentals of Soil Physics*. Academic Press, New York, New York.
- Holbrook, W. S., R. D. Catchings, and C. M. Jarchow, 1991. Origin of Deep Crustal Reflections: Implications of Coincident Seismic Refraction and Reflection Data in Nevada. *Geology* 19:175-179.
- Hoover, D. L., 1968. Genesis of Zeolites, Nevada Test Site. p. 275-284. In: E. B. Eckel (ed.), *Nevada Test Site*. Geol. Soc. Am. Mem. (110).
- Hudson, M. H., 1992. Paleomagnetic Data Bearing on the Origin of Arcuate Structures in the French Peak–Massachusetts Mountain Area of Southern Nevada. *Geol. Soc. Amer. Bull.* 104:581-594.
- Hunt, C. B., T. W. Robinson, W. A. Bowles, and A. L. Washburn, 1966. *Hydrologic Basin, Death Valley California*. U.S. Geological Survey Prof. Paper 494-B. U.S. Geological Survey, U.S. Government Printing Office, Washington, DC.
- Hunter, P. H., D. H. Card, and K. Horton, 1982. *Safety Assessment for Area 5 Radioactive Waste Management Site*. DOE/NV/00410-54. Ford, Bacon and Davis Utah Inc., and Reynolds Electrical & Engineering Co., Inc., Las Vegas, Nevada.
- Hunter, R. B., 1992a. *Status of the Flora and Fauna on the Nevada Test Site*. DOE/NV/10630-29. Reynolds Electrical & Engineering Co., Inc., Las Vegas, Nevada.

- , 1992b. Trends in Perennial Plant Populations on the Nevada Test Site, 1989-1991. Unpublished manuscript.
- Hunter, R. B., M. B. Saethre, P. A. Medica, P. D. Greger, and E. M. Romney, 1991. Biological Studies in the Impact Zone of the Liquefied Gaseous Fuels Spill Test Facility in the Frenchman Flat, Nevada. DOE/NV/10630-15. Reynolds Electrical & Engineering Co., Inc., Las Vegas, Nevada.
- Hunter, R. B., and P. A. Medica, 1987. Status of the Flora and Fauna on the Nevada Test Site in 1987. Publ. 6873. NTIS, Springfield, Virginia
- Hunter, R. B., E. M. Romney, A. Wallace, and J. E. Kinnear, 1980. Residual Effects of Supplemental Moisture on the Plant Populations of Plots in the Northern Mojave Desert. Great Basin Nat. Mem. 4:24-27.
- Huyakorn, P. S., and S. Panday, 1990. VAM3d-CG – Variably Saturated Analysis Model in Three Dimensions With Preconditioned Conjugate Gradient Matrix Solvers; documentation and user's guide, Version 2.1. HGL/89-02. Hydrogeologic, Inc., Herndon, Virginia.
- Iman, R. L., and W. J. Conover, 1979. The Use of the Rank Transformation in Regression. *Technometrics* 21:499-509.
- International Commission on Radiological Protection, 1990. 1990 Recommendations of the International Commission on Radiological Protection. ICRP Publication 60. Pergamon Press, New York, New York.
- , 1982. Cost-Benefit Analysis in the Optimization of Radiation Protection. ICRP Publication 37. Pergamon Press, New York, NY.
- , 1979. Limits for Intakes of Radionuclides by Workers, Part 1. ICRP Publication 30, Pergamon Press, New York, New York.
- , 1977. Recommendations of the ICRP. ICRP Publication 26. Pergamon Press, New York, New York.
- Istok, J. D., D. O. Blout, L. Barker, K. R. Johnejack, and D. P. Hammermeister, 1994. Spatial Variability in Alluvium Properties at a Low-Level Nuclear Waste Site. *Soil Sci. Soc. Am. J.* 58(4):1040-1051.

- Izett, G., 1988. The Bishop Ash Bed (Middle Pleistocene) and Some Older (Pliocene and Pleistocene) Chemically and Mineralogically Similar Ash Beds in California, Nevada, and Utah. U.S. Geological Survey Bulletin 1675. U.S. Geological Survey, U.S. Government Printing Office, Washington, DC.
- Jackson, R. D., B. A. Kimball, R. J. Reginato, and F. S. Nakayama, 1973. Diurnal Soil-Water Evaporation: Time-Depth-Flux Patterns. Soil Sci. Soc. Am. Proc., 37:505-509.
- Jensen, M. E., R. D. Burman, and R. G. Allen (eds.), 1990. Evapotranspiration and Irrigation Water Requirements. No. 70, Manuals and Reports on Engineering Practice. American Society of Civil Engineers, New York, New York.
- Johnejack, K. R., and L. W. Elletson, 1994. Alternative Evaluation Study: Generic Cells for Arid Areas and Covers for the U3AX/BL Disposal Unit. Reynolds Electrical & Engineering Co., Inc., Las Vegas, Nevada.
- Johnson, R. B., and J. R. Ege, 1964. Geology of the Pluto Site, Area 401, Nevada Test Site, Nye County, Nevada. USGS Open File Report TEI-841. U.S. Geological Survey, U.S. Government Printing Office, Washington, DC.
- Jouzel, J., and L. Merlivat, 1984. Deuterium and Oxygen-18 in Precipitation: Modeling of the Isotopic Effects During Snow Formation. J. Geophys. Res. 89(D7):11749-11757.
- Jouzel, J., R. D. Koster, R. D. Suozzo, G. L. Russell, J. W. While, and W. J. Broecker, 1991. Simulations of the HDO and H₂¹⁸O Atmospheric Cycles Using the NASA General Circulation Model (GCM): Sensitivity Experiments for Present-Day Conditions. J. Geophys. Res. 96(D4):7495-7507.
- Judson, S., K. S. Deffeyes, and R. B. Hargraves, 1976. Physical Geology. Prentice-Hall, Inc., Englewood Cliffs, New Jersey.
- Jurwitz, L. R., 1953. Arizona's Two-Season Rainfall Pattern. Weatherwise 6(4):96-99.
- Jury, W. A., W. R. Gardner, and W. H. Gardner, 1991. Soil Physics. John Wiley and Sons, Inc., New York, New York.
- Jury, W. A., D. Russo, G. Sposito, and H. Elabd, 1987. The Spatial Variability of Water and Solute Transport Properties in Unsaturated Soil. Hilgardia 55:1-56.
- Kemper, W. D., and J. C. Van Schaik, 1966. Diffusion of Salts in Clay-Water Systems. Soil Sci. Soc. Amer. Proc. 30:534-540.

Kennedy, W. E. Jr., and R. A. Peloquin, 1988. Intruder Scenarios for Site-Specific Low-Level Radioactive Waste Classification. DOE/LLW-71T. U.S. Department of Energy, Idaho Operations Office, Idaho Falls, Idaho.

Kennedy, W. E., and D. L. Strenge, 1992. Residual Radioactive Contamination From



corporating Equilibrium and Rate-
el conceptualizations and analytic

ume, 1993. Risk Assessment of
tal Sites Located on the Nevada Test
awrence Livermore National

ty of U in the Kidney: A

nanni, 1996. An Arid Zone
nd Closure Investigations at the
ruary 26-29, 1996, Tucson, Arizona.

A Dynamic One-Dimensional
Water Vapor Flow Model.
Engineering Co., Inc., Las Vegas,

Mathematical Model of Plant
he Model. J. Env. Qual. 20:129-

ffern, B. L. Dozier, D. F. Emer, and
e Under the Radioactive Waste
ite: The Dupuit-Forcheimer
(eds.), Interdisciplinary Approaches
tute of Hydrology.

t, and M. E. Donahue, 1992b.
ransport and fate model, Volume 1.
neering Co., Inc., Las Vegas,

Emer, and G. J. Shott, 1992c. A
20 Derived From Thorium-232 Low-
lioactive Waste Management Site in
-38/UC-721. Reynolds Electrical &

Cawlfeld, D. F. Emer, and G. J. Shott, 1993a. A Modeling Study of Depth of Burial of Depleted Uranium and Thorium on Radon Gas Flux Alluvium Soil Radioactive Waste Management Site. DOE/NV/Reynolds Electrical & Engineering Co., Inc., Las Vegas, Nevada.

Cawlfeld, M. E. Donahue, D. E. Emer, and G. J. Shott, 1993b. A Model of the Transport and Fate of Radon-222 Derived From Thorium-230 Low-Flow in the Near-Surface Zone of the Radioactive Waste Management Site in Nevada Test Site. DOE/NV/10630-58. Reynolds Electrical & Engineering Co., Inc., Las Vegas, Nevada.

Cawlfeld, and L. E. Barker, 1994. Sensitivity Analysis of the Noble Gas Transport and Fate Model: CASCADR9. DOE/NV/11432-129. Reynolds Electrical & Engineering Co., Inc., Las Vegas, Nevada.

Chemical Comparison of Glassy and Crystalline Volcanic Rocks. Survey Bulletin 1201-D. U.S. Geological Survey, U.S. Government Printing Office, Washington, DC.

Condon, and H. L. Beck, 1964. Field Spectrometric Investigations of Radiation in the U.S.A. In: J. A. S. Adams and W. M. Lowder (eds.), Radiation Environment. University of Chicago Press, Chicago, Illinois.

Roberts, and J. A. Cherry, 1985. Transport of Organic Contaminants in Groundwater. Environ. Sci. Technol., 19(5):384-392.

Maheras, H. D. Nguyen, A. S. Rood, J. I. Sipos, M. J. Case, M. A. Emer, and M. E. Donahue, 1992. Radiological Performance Assessment of the Radioactive Waste Management Site at the Nevada Test Site, Idaho National Engineering Laboratory, Idaho Falls, Idaho.

F. Bloom, 1980. Nevada Applied Ecology Group Model for Uranium Transport and Dose to Man. p. 459-513. In: W. C. Hanson (ed.), Radioactive Elements in the Environment. DOE/TIC-22800. U.S. Department of Energy, Washington, DC.

Radionuclides in Surface Soil at the Nevada Test Site. Pub. 45077. 1975-02. Water Resources Center, Desert Research Institute, University of Nevada, Las Vegas, Nevada.

A. W. Harbaugh, 1988. A Modular Three-Dimensional Finite-Difference Groundwater Flow Model. Techniques of Water Resources Investigations, Report 9-A3. U.S. Geological Survey, Washington, DC.

1 Climate Interpretation of the Deuterium-Oxygen-18
Geophys. Res. 84(C8):5029-5038.

view and Summary of the Potential for Tectonic,
at the Nevada Test Site Defense Waste Disposal Site.
rces Center, Desert Research Institute, University of

Gravity Interpretation of Frenchman Flat and
Geological Survey Technical Letter NTS-93. U.S.
ment Printing Office, Washington, DC.

eters for Environmental Radiological Assessments.
rmation Center, Office of Scientific and Technical

Snyder, 1993. Lineaments Identified in Northern
nd Clark Counties, Nevada. Map Scale 1:24,000.
Vegas, Nevada.

chmeltzer, 1994. A Multiple-Method Approach to
el Radioactive Waste Management Site,
nty, Nevada. Proceedings of Waste Management

d J. F. Keely, 1987. Performance and Analysis of
cations for Contaminant Modeling – A Project
337-341.

e, 1983. An Examination of Scale-Dependent
lwater 21(6):715-725.

90. Principles of Environmental Physics – 2nd
ondon, England.

, and R. A. Young, 1963. Groundwater Test Well 2,
Nevada. USGS Open File Report TEI-808. U.S.
ment Printing Office, Washington, DC.

est Holes, and Springs in the Nevada Test Site Area.
lements Investigations Report 781, 22 p.

io, 1993. Nevada in Perspective. Morgan Quitno

- Mualem, Y., 1976. A New Model for Predicting the Hydraulic Conductivity of Unsaturated Porous Media. *Water Res. Research* 12:513-522.
- Murray, F. W., 1967. On the Computation of Saturation Vapor Pressure. *J. Applied. Meteor.* 6:203-204.
- Naft, R. L., 1990. On the Nature of the Dispersive Flux in Saturated Heterogeneous Porous Media. *Water Res. Research* 26(5):1013-1026.
- National Bureau of Standards, 1963. Maximum Permissible Body Burdens and Maximum Permissible Concentrations of Radionuclides in Air and in Water for Occupational Exposure. U.S. Department of Commerce, National Bureau of Standards, Gaithersburg, Maryland.
- National Council on Radiation Protection and Measurements, 1987a. Exposure of the Population in the United States and Canada From Natural and Background Radiation. NCRP Report No. 94. NCRP, Bethesda, Maryland.
- , 1987b. Ionizing Radiation Exposure of the Population of the United States. NCRP Report No. 93. NCRP, Bethesda, Maryland.
- , 1975. Natural Background Radiation in the United States. NCRP Report No. 45. NCRP, Bethesda, Maryland.
- National Research Council, 1995. Ward Valley, An Examination of Seven Issues in Earth Sciences and Ecology. National Academy Press, Washington, DC.
- Nations, D., and E. Stump, 1981. *Geology of Arizona*. Kendall Hunt Publishers, Dubuque, Iowa.
- Nazaroff, W. W., 1992. Radon Transport From Soil to Air. *Reviews of Geophysics* 30(2):137-160.
- Negin, C. A., and G. Worku, 1992. *Microshield, Version 4, User's Manual*. Grove Engineering, Rockville, Maryland.
- , 1991. *Raddecay, Radioactive Nuclide Library and Decay Software. Version 4 user's manual*. Grove 91-1, Grove Engineering, Inc., Rockville, Maryland.
- Neuman, S. P., R. A. Feddes, and E. Bresler, 1974. Finite Element Simulation of Flow in Saturated-Unsaturated Soils Considering Water Uptake by Plants, Development of Methods, Tools and Solutions for Unsaturated Flow. Third Annual Report. Technion, Haifa, Israel.

Ng, Y. C., C. S. Colsher, and S. E. Thompson, 1982. Soil-to-Plant Concentration Factors for Radiological Assessments. NUREG/CR-2975. UCID-19463. Lawrence Livermore National Laboratory, Livermore, California.

Nuclear Regulatory Commission, 1989. Calculation of Radon Flux Attenuation by Earthen Uranium Mill Tailings Covers. Regulatory Guide 3.64. U.S. Nuclear Regulatory Commission, Washington, DC.

———, 1984. A Revised Modeling Strategy Document for High-Level Waste Performance Assessment. U.S. Nuclear Regulatory Commission, Washington, DC.

———, 1981. Draft Environmental Impact Statement on 10 CFR Part 61, "Licensing Requirements for Land Disposal of Radioactive Waste." Appendices G-Q. NUREG-0782. Vol 4. U.S. Nuclear Regulatory Commission, Washington, DC.

———, 1977. Calculation of Annual Doses to Man From Routine Releases of Reactor Effluents for the Purpose of Evaluating With 10 CFR Part 50. Appendix I.

- Oster, C. A., J. C. Sonnichsen, and R. T. Jaske, 1970. Numerical Solution to the Convective Diffusion Equation. *Water Res. Research* 6(6):1746-1752.
- Parsons, R. W., 1966. Permeability of Idealized Fractured Rock. *Soc. Pet. Eng. Jour.* 6(2):126-136.
- Parzen, E., 1960. *Modern Probability Theory and Its Applications*. John Wiley & Sons, Inc., New York, New York.
- Passioura, J. B., and D. A. Rose, 1971. Hydrodynamic Dispersion in Aggregated Media, 2) effects of velocity and aggregate size. *Soil Sci.* 111(6):345-351.
- Penman, H. L., 1948. Natural Evaporation From Open Water, Bare Soil and Grass. *Proceedings of Royal Society of London* A193:120-146.
- Phillips, F. M., 1994. Environmental Tracers for Water Movement in Desert Soils: A Regional Assessment for the American Southwest. *Soil Sci. Soc. Am. J.* 58:15-24.
- Pinder, G. F., and W. G. Gray, 1977. *Finite Element Simulation in Surface and Subsurface Hydrology*. Academic Press, New York, New York.
- Pollock, D. W., 1989. Documentation of Computer Programs to Complete and Display Pathlines Using Results from the U.S. Geological Survey Modular Three-Dimensional Finite-Difference Groundwater Model, U.S. Geological Survey, Open File Report 89-381, Washington, DC.
- Porter, L. K., W. D. Kemper, R. D. Jackson, and B. A. Stewart, 1960. Chloride Diffusion in Soils as Influenced by Moisture Content. *Soil Sci. Soc. Amer. Proc.* 24:460-463.
- Price C. E., and W. Thordarson, 1961. Groundwater Test Well A, Nevada Test Site, Nye County, Nevada: A Summary of Lithologic Data, Aquifer Tests, and Construction. USGS Open File Report TEI-800. U.S. Geological Survey, U.S. Government Printing Office, Washington, DC.
- Price, L. L., D. A. Zimmerman, N. E. Olague, S. H. Conrad, and C. P. Harlan, 1993. Preliminary Performance Assessment of the Greater Confinement Disposal Facility at the Nevada Test Site, Vol. 3: Supporting details. SAND91-0047, UC-721, Sandia National Laboratories, Albuquerque, New Mexico.
- Prudic, D. E., 1994. Estimates of Percolation Rates and Ages of Water in Unsaturated Sediments at Two Mojave Desert Sites, California-Nevada. U.S. Geological Survey ~~Water Resources Investigative Report 94-4160, Denver, Colorado.~~

Quiring, R. F., 1968. Climatological Data, Nevada Test Site and Nuclear Rocket
Development Station. ERL TM APL 7. Environmental Sciences Administration.

- REEC Co., 1995. U3ax/bl Demonstration Cover Conceptual Design Analysis – Integrated Closure Program for the Area 3 and Area 5 Radioactive Waste Management Sites, Nevada Test Site. Reynolds Electrical and Engineering Co., Inc., Las Vegas, Nevada.
- , 1993a. Draft Section E Report – Evidence and Arguments Supporting A Waiver From Groundwater Monitoring and Exemption From Requirements for Liners and Leachate Collection Systems at the Area 5 RWMS on the Nevada Test Site, Nye County, Nevada. Special Projects Section, Environmental Restoration & Technology Development Department, Environmental Management Division, Reynolds Electrical & Engineering Co., Inc., Las Vegas, Nevada.
- , 1993b. Site Characterization and Monitoring Data From Area 5 Pilot Wells, Nevada Test Site, Nye County, Nevada. Reynolds Electrical & Engineering Co. Inc., Las Vegas, Nevada.
- , 1993c. Hydrogeologic Data for Science Trench Boreholes at the Area 5 Radioactive Waste Management Site, Nevada Test Site, Nye County Nevada. Special Projects Section, Environmental Restoration & Technology Development Department, Environmental Management Division, Reynolds Electrical & Engineering Co., Inc., Las Vegas, Nevada.
- , 1993d. Area 5 Groundwater Monitoring Task, FY 1993 Annual Report, Nevada Test Site, Nye, County, Nevada. Reynolds Electrical & Engineering Co. Inc., Las Vegas, Nevada.
- , 1993e. Hydrogeologic Data for Existing Excavations at the Area 5 Radioactive Waste Management Site, Nevada Test Site, Nye County Nevada. Special Projects Section, Environmental Restoration & Technology Development Department, Environmental Management Division, Reynolds Electrical & Engineering Co., Inc., Las Vegas, Nevada.
- , 1992. Air Emissions Annual Report. Reynolds Electrical and Engineering Co. Inc., Las Vegas, Nevada.
- , 1985. U3ax/bl Demonstration Cover Conceptual Design Analysis – Integrated Closure Program for the Area 3 and Area 5 Radioactive Waste Management Sites, Nevada Test Site. Reynolds Electrical and Engineering Co., Inc., Las Vegas, Nevada.
- Richard-Haggard, K., 1983. Economic Potential of Alternative Land and Natural Resource Uses at the Nevada Test Site. Pub. 45030. Water Resources Center, Desert Research Institute, University of Nevada, Reno, Nevada.
- Richens, V. B., 1966. Notes on the Digging Activity of a Northern Pocket Gopher. J. of Mammology 47(3):531-533.

- Robinson, B. P., and W. A. Beetem, 1965. Chemical Data on Water From Supply Wells, Nevada Test Site. U.S. Geological Survey Technical Letter NTS-104. U.S. Geological Survey, U.S. Government Printing Office, Washington, DC.
- Rogers, A. M., D. M. Perkins, and F. A. McKeon, 1977. A Preliminary Assessment of the Seismic Hazard of the Nevada Test Site Region. *Bull. Seismol. Soc. Amer.* 67:1587-1606.
- Rogers, V. C., and K. K. Nielson, 1991a. Multiphase Radon Generation and Transport in Porous Materials. *Health Physics* 60(6):807-815.
- , 1991b. Correlations for Predicting Air Permabilities and ^{222}Rn Diffusion Coefficients of Soils. *Health Physics* 61(2):225-230.
- Romney, E. M., V. Q. Hale, A. Wallace, O. R. Lint, J. D. Childress, H. Kaaz, G. V. Alexander, J. E. Kinnear, and T. Ackerman, 1973. Some Characteristics of Soil and Perennial Vegetation in a Northern Mojave Desert Area of the Nevada Test Site. UCLA Publication 122-916. NTIS, Department of Commerce, Springfield, Virginia.
- Romney, E. M., A. Wallace, J. Kinnear, and R. O. Gilbert, 1977. Estimated Inventory of Plutonium and Uranium Radionuclides for Vegetation in Aged Fallout Areas. p. 35-52. In: M. G. White, P. B. Dunaway, and W. A. Howard (eds.), NVO-171, Environmental Plutonium on the Nevada Test Site and Environs. USERDA, Las Vegas, Nevada.
- Romney, E. M., A. Wallace, R. K. Schulz, and P. B. Dunaway, 1981. Plant Root Uptake of $^{239,240}\text{Pu}$ and ^{241}Am From Soils Containing Aged Fallout Materials. IAEA-SM-257/83, International Symposium on Migration in the Terrestrial Environment of Long-Lived Radionuclides From the Nuclear Fuel Cycle, Knoxville, Tennessee, July 27-31, 1981.
- Romney, E. M., and A. Wallace, 1977. Plutonium Contamination of Vegetation in Dusty Field Environments. p.287-302. In: M. G. White and P. B. Dunaway (eds.), NVO-178, Transuranics in Natural Environments. Nevada Applied Ecology Group, Las Vegas, Nevada.
- Rose, D. A., 1968. Water Movement in Porous Materials. III. Evaporation of Water From Soil. *Br. J. Appl. Physics*, 1:1779-1791.
- Ross, B. J., and C. M. Koplik, 1979. A New Numerical Method for Solving the Solute Transport Equation. *Water Res. Research* 15(4):949-955.

- Ross, C. S., and R. L. Smith, 1961. Ash-Flow Tuffs – Their Origin, Geologic Relations, and Identification. USGS Professional Paper 366. U.S. Geological Survey, U.S. Government Printing Office, Washington, DC.
- Rothermich, N. E., and A. T. Vollmer, 1986. Analysis of Soils From the Area 5 Radioactive Waste Management Site: A Comparison of 1979 and 1984 Data. RWM-8. Reynolds Electrical & Engineering Co. Inc., Las Vegas, Nevada.
- Rubin, J. R., and R. V. James, 1973. Dispersion-Affected Transport of Reacting Solutes in Saturated Porous Media: Galerkin Method Applied to Equilibrium-Controlled Exchange in Unidirectional Steady Water Flow. Water Res. Research 9(5):1332-1356.
- Rubin, Y., and G. Dagan, 1992. Conditional Estimation of Solute Travel Time in Heterogeneous Formations: Impact of Transmissivity Measurements. Water Res. Research 28(4):1033-1040.
- Rubenstein, R. Y., 1981. Simulation and the Monte Carlo Method. John Wiley & Sons, New York, New York.
- Runchal, A. K., and B. Sagar, 1992. PORFLOW: A Model for Fluid Flow Heat and Mass Transport in Multifluid, Multiphase Fractured or Porous Media. Users manual, Version 2.4. ACRI/016/Rev. G. Analytic and Computational Research Inc., Los Angeles, California.
- , 1989. PORFLO-3: A Mathematical Mode for Fluid Flow, Heat and Mass Transport in Variably Saturated Geologic Media. Users manual, Version 1.0. WHC-EP-0042. Westinghouse Hanford Operations, Richland, Washington.
- Rupp, E. M., 1990. Age-Dependent Values of Dietary Intake for Assessing Human Exposure to Environmental Pollutants. Health Phys. 20:151-162.

- Scanlon, B. R., 1994. Water Fluxes and Heat in Desert Soils, 1) Field studies. *Water Res. Research* 30(3):709-719.
- Scanlon, B. R., and P. C. D. Milly, 1994. Water and Heat Fluxes in Desert Soils, 2) Numerical simulations. *Water Res. Research* 30(3):721-733.
- Scanlon, B. R., F. P. Wang, and B. C. Richter, 1991. Field Studies and Numerical Modeling of Unsaturated Flow in the Chihuahuan Desert. Texas Rep. Invest, 1999. Bureau of Econ. Geology, University of Texas, Austin, Texas.
- Schanz, R. W., and A. Salhotra, 1992. Evaluation of the Rackwitz-Fiessler Uncertainty Analysis Method for Environmental Fate and Transport Models. *Water Res. Research* 28(4):1071-1079.
- Scheidegger, A., 1954. Statistical Hydrodynamics in Porous Media. *J. Applied Physics* 25:994-1001.
- Scheidegger, A. E., 1974. The Physics of Flow Through Porous Media. 3rd ed., University of Toronto Press, Toronto.
- Schmeltzer, J. S., J. J. Miller, and D. L. Gustafson, 1993. Flood Assessment at the Area 5 Radioactive Waste Management Site and the Proposed Hazardous Waste Storage Unit, DOE/Nevada Test Site, Nye County, Nevada. Raytheon Services Nevada (paginated by section), Las Vegas, Nevada.
- Schoff, S. L., and J. E. Moore, 1964. Chemistry and Movement of Groundwater, Nevada Test Site. U.S. Geological Survey Open-File Report TEI-838. U.S. Geological Survey, U.S. Government Printing Office, Washington, DC..
- Secor, D. T., 1962. Geology of the Central Spring Mountains, Nevada. Ph.D. dissertation, Stanford University, Palo Alto, California.
- Sehmel, G. A., 1980. Particle and Gas Dry Deposition: A Review. *Atmos. Environ.* 14:983-1011.
- Seitz, R. R., S. D. Mathews, and K. M. Kostelnik, 1990. Guidelines for Acquisition, Installation, and Testing of Performance Assessment Software. DOE/LLW-102. Idaho National Engineering Laboratory, Idaho Falls, Idaho.
- Shippers, L. R., 1989. Background Information for the Development of a Low-Level Waste Performance Assessment Methodology: Identification of Potential Exposure Pathways. NUREG/CR-5453. Vol. 1., SAND89-2509. Sandia National Laboratories, Albuquerque, New Mexico.

- Shippers, L. R., and C. P. Harlan, 1989. Background Information for the Development of a Low-Level Waste Performance Assessment Methodology: Assessment of Relative Significance of Migration and Exposure Pathways. NUREG/CR-5453. Vol. 2., SAND89-2509. Sandia National Laboratories, Albuquerque, New Mexico.
- Skaggs, R. W., E. J. Monke, and L. F. Huggins, 1970. An Approximate Method for Determining the Hydraulic Conductivity Function of an Unsaturated Flow. Technical Report No. 11. Water Resources Research Center, Purdue University, Lafayette, Indiana.
- Smith, D. D., 1977. Grazing Studies on a Contaminated Range of the Nevada Test Site, pp. 139-150. In: M. G. White, P. B. Dunaway and W. A. Howard (eds.), NVO-171, Environmental Plutonium on the Nevada Test Site. NVO-171. Nevada Applied Ecology Group, Energy Research and Development Administration, Las Vegas, Nevada.
- Smith, D. D., K. W. Brown, R. A. Brechbill, K. R. Giles, and A. L. Lesperance, 1972. The Radionuclide and Botanical Composition of the Diet of Cattle Grazing the Area 18 Range of the Nevada Test Site. SWRHL-110. Western Environmental Research Laboratory, U.S. Environmental Protection Agency, NTIS, Springfield, Virginia.
- Smith, R. L., 1960. Zones and Zonal Variations in Welded Ash Flows. USGS Professional Paper 354-F. U.S. Geological Survey, U.S. Government Printing Office, Washington, DC.
- Snyder, K. E., D. L. Gustafson, H. E. Huckins-Gang, J. J. Miller, and S. E. Rawlinson, 1995. Surficial Geology and Performance Assessment for A Radioactive Waste Management Facility at the Nevada Test Site. U.S. Department of Energy Report DOE/NV/10833-25, UC721, 5 pp.
- Snyder, K. E., D. L. Gustafson, J. J. Miller, and S. E. Rawlinson, 1994a. Geologic Components of Site Characterization and Performance Assessment for a Radioactive Waste Management Facility at the Nevada Test Site. U.S. Department of Energy Report USDOE/NV/10833-20, UC-721. Raytheon Services Nevada, Las Vegas, Nevada.
- Snyder, K. E., and D. L. Gustafson, 1994b. Interim Report of Trench Mapping Near the Area 5 Radioactive Waste Management Site, DOE/Nevada Test Site, Nye County, Nevada. Raytheon Services Nevada, Las Vegas Nevada.
- Snyder, K. E., S. M. Parsons, and D. L. Gustafson, 1993. Field Results of Subsurface Geologic Mapping at the Area 5 Radioactive Waste Management Site, DOE/Nevada Test Site, Nye County, Nevada. Raytheon Services Nevada, Las Vegas, Nevada.

State of Nevada, 1993. Water controls; air pollution. Nevada Administrative Code. Chapter 445. State of Nevada, Carson City, Nevada.

———, 1990. Underground water and wells. Nevada Administrative Code. Chapter 534. State of Nevada, Carson City, Nevada.

Stephens, D. B., 1994. A Perspective on Diffuse Natural Recharge Mechanisms in Areas of Low Precipitation. Soil Sci. Soc. Am. J. 58:40-48.

Stewart, B. A., and H. V. Eck, 1958. The Movement of Surface-Applied Nitrates Into Soils at Five Moisture Levels. Soil Sci. Soc. Amer. Proc. 22:260-262.

Stewart, J. H., 1971. Basin and Range Structure: A System of Horsts and Grabens Produced by Down-Sloped Extension. Geol. Soc. Amer. Bull. 82:1010-1044.

Thorne, D. H., and D. C. Andersen, 1990. Long-Term Soil Disturbance Pattern by a Pocket Gopher, *Geomys bursarius*. J. of Mammology 71(1):84-89.

Travis, B., 1985. TRACR3D: A Model of Flow and Transport in Porous Media. LA-9667-MS. Los Alamos National Laboratory, Los Alamos, New Mexico.

Trinosky, P., 1989. Safety Analysis Report for Defense Waste Management Department. Kaiser Engineers, Oakland, California.

Twiss, R. J., and E. M. Moores, 1992. Structural Geology. W. H. Freeman and Company, New York, New York.

Tolson, S. W., J. R. Gorman, S. H. Conrad, D. R. Hays, J. A. D. R. B. and J. L. Miller

- , 1980. Final Environmental Impact Statement Rocky Flats Plant Site. DOE/EIS-0064. U.S. Department of Energy, Washington, DC.
- U.S. Department of Energy/Nevada Operations Office, 1995. Position Paper on Radioactive Waste Performance Assessment Methodologies for the Nevada Test Site (in preparation).
- , 1993a. Annual Site Environmental Report–1992. DOE/NV/10630-66. NTIS, Springfield, Virginia.
- , 1993b. Groundwater Protection Management Program Plan for the DOE Nevada Field Office. U.S. Department of Energy, Nevada Field Office, Las Vegas, Nevada.
- , 1992. Nevada Test Site Defense Waste Acceptance Criteria, Certification, and Transfer Requirements. NVO-325. NTIS, Springfield, Virginia.
- U.S. Department of Interior, 1985. Public Land Use Statistics, Vol. 170. U.S. Government Printing Office, Washington, DC.
- U.S. Ecology, 1995. Central Interstate Compact Low-Level Waste Disposal Facility, Safety Analysis Report, Rev. 8. Butte, Nebraska.
- U.S. Environmental Protection Agency, 1996. National Primary Drinking Water Regulations. Code of Federal Regulations, 40 CFR 141. U.S. Government Printing Office, Washington, DC.
- , 1992. CAP88-PC, Version 1.00, Clean Air Act Assessment Package – 1988. U.S. Environmental Protection Agency, Washington, DC.
- , 1991. National Primary Drinking Water Regulations. Proposed Rules. FR33050.
- , 1990. Transuranium Elements, Vol. 2, Technical Basis for Remedial Actions. EPA 520/1-90-016. U.S. Environmental Protection Agency, Washington, DC.
- , 1989. Risk Assessment Guidance for Superfund, Vol. I, Human Health Evaluation Manual (Part A). EPA/540/1-89/002. U.S. Environmental Protection Agency, Washington, DC.
- , 1985. Nationwide Occurrence of Radon and Other Natural Radioactivity in Public Water Supplies. EPA 520/5-85-008. Eastern Environmental Radiation Facility, Montgomery, Alabama.
- , 1984. Population Distribution Around the Nevada Test Site 1984. EPA-600/4-84-067. Environmental Monitoring Systems Laboratory, Las Vegas, Nevada.

- , 1981. Preliminary Grazing Studies With Rumen-Fistulated Steers at Selected Nuclear Sites. EPA-600/3-81-004. Environmental Monitoring Systems Laboratory, Las Vegas, Nevada.
- . Health and Environmental Protection Standards for Uranium and Thorium Mill Tailings. Code of Federal Regulations, 40 CFR Part 192. U.S. Government Printing Office, Washington DC.
- . Environmental Protection Standards for Management and Disposal of Spent Nuclear Fuel, High-level and Transuranic Wastes. Code of Federal Regulations, 40 CFR Part 191. U.S. Government Printing Office, Washington DC.
- . National Interim Primary Drinking Water Standards. Code of Federal Regulations, 40 CFR Part 141. U.S. Government Printing Office, Washington DC.
- . National Emission Standards for Hazardous Air Pollutants. Code of Federal Regulations, 40 CFR Part 61. U.S. Government Printing Office, Washington DC.
- U.S. Nuclear Regulatory Commission, 1989. Calculation of Radon Flux Attenuation by Earthen Uranium Mill Tailings Covers. Regulatory Guide 3.64. U.S. Nuclear Regulatory Commission, Washington, DC.
- , 1984. A Revised Modeling Strategy Document for High-level Waste Performance Assessment. U.S. Nuclear Regulatory Commission, Washington, DC.
- , 1981. Draft Environmental Impact Statement on 10 CFR Part 6, "Licensing Requirements for Land Disposal of Radioactive Waste." Appendices G-Q. NUREG-0782. Vol 4. USNRC, Washington, DC.
- , 1977. Calculation of Annual Doses to Man From Routine Releases of Reactor Effluents for the Purpose of Evaluating Compliance with 10 CFR Part 50, Appendix I. Regulatory Guide 1.109. U.S. Nuclear Regulatory Commission, Washington, DC.
- van Genuchten, M. T., and R. J. Wagenet, 1989. Two-Site/Two-Region Models for Pesticide Transport and Degradation: Theoretical Development and Analytical Solutions. Soil Sci. Amer. Jour. 153:1303-1309.
- van Genuchten, M. T., 1980. A Closed-Form Equation for Predicting the Hydraulic Conductivity of Unsaturated Soils. Soil Sci. Soc. Am. J. 45:892-898.
- , 1978. Calculating the Unsaturated Hydraulic Conductivity with a New Closed-Form Analytical Model. Ph.D. dissertation, Princeton University, Princeton, New Jersey.

- Vasek, F. C., 1980. Creosote Bush: Long-Lived Clones of the Mojave Desert. *Amer. J. Bot.* 67(2):246-255.
- Voslamber, B., and A. W. L. Veen, 1985. Digging by Badgers and Rabbits on Some Wooded Slopes in Belgium. *Earth Surface Processes and Landforms* 10:79-82.
- Voss, C. I., 1984. A Finite-Element Simulation Model for Saturated-Unsaturated Fluid-Density-Dependent Groundwater Flow and Energy Transport or Chemically-Reactive Single-Species Solute Transport. U.S. Geological Survey, Reston, Virginia.
- Waddel, R. K., 1984. Hydrology of Yucca Mountain and Vicinity, Nevada-California Investigative Results Through Mid-1983. U.S. Geological Survey Investigative Report 84-4267. U.S. Geological Survey, U.S. Government Printing Office, Washington, DC.
- Walker, G. E., and T. E. Eakin, 1963. Geology and Groundwater of Amargosa Desert, Nevada-California. Groundwater Resources – Reconnaissance Survey Report 14. Nevada Department of Conservation and Natural Resources, Carson City, Nevada.
- Wallace, A., and E. M. Romney, 1972. Radioecology and Ecophysiology of Desert Plants at the Nevada Test Site. TID-25954. NTIS, Department of Commerce, Springfield, Virginia.
- Wallace, A., S. A. Bamberg, and J. W. Cha, 1974. Quantitative Studies of Roots of Perennial Plants in the Mojave Desert. *Ecology* 55:1160-1162.
- Warren, J. E., and H. S. Price, 1961. Flow in Heterogeneous Porous Media. *Am. Inst. Mining Metallurgy Petrol. Eng. Trans.* 222:153-169.
- Warrick, A. W., 1971. Simultaneous Solute and Water Transport for an Unsaturated Soil. *Water Res. Research* 7(5):1216-1225.
- Wells, S. G., L. D. McFadden, C. E. Renault, and B. M. Crowe, 1990. Geomorphic Assessment of Late Quaternary Volcanism in the Yucca Mountain Area, Southern Nevada: Implications for the Proposed High-Level Radioactive Waste Repository. *Geology* 18:549-553.
- Wei, C. Y., and W. Y. J. Shieh, 1979. Transient Seepage Analysis of Guri Dam. *Jour. Tech. Coun. ASCE*, 105(TCI):135-147.
- Wernicke, B., J. E. Spencer, B. C. Burchfiel, and P. L. Guth, 1982. Magnitude of Crustal Extension in the Southern Great Basin. *Geology* 10:499-502.

- Winograd, I. J. and W. Thordarson, 1975. Hydrologic and Hydrochemical Framework, South-Central Great Basin, Nevada-California, With Special Reference to the Nevada Test Site. U.S. Geological Professional Paper 712-C. U.S. Government Printing Office, Washington, DC.
- Winograd, I. J., and A. C. Riggs, 1984. Recharge to the Spring Mountains, Nevada: Isotopic Evidence. *Geo. Soc. Amer. Abs. Prog.* 16:698.
- Winsor, T. F., and F. W. Whicker, 1980. Pocket Gophers and Redistribution of Plutonium in Soil. *Health Physics* 39:257-262.
- Wood, D. E., R. U. Curl, D. R. Armstrong, J. R. Cook, M. R. Dolenc, D. C. Kocher, K. W. Owens, E. P. Regnier, G. W. Roles, R. R. Seitz, and M. I. Wood, 1994. Performance Assessment Task Team Progress Report. DOE/LLW-157. Idaho National Engineering Laboratory. Idaho Falls, Idaho.
- Yates, S. R., and C. G. Enfield, 1989. Transport of Dissolved Substances with Second-Order Reaction. *Water Res. Research* 25(7):1757-1762.
- Yeh, G. T., T. C. Jim, and R. Srivastava, 1991. Analytical Solutions for One-Dimensional, Transient Infiltration Toward the Water Table in Homogeneous and Layered Soils. *Water Res. Research* 27(5):753-762.
- Yeh, G. T., 1987. FEMWATER: A Finite-Element Model of Water Flow Through Saturated-Unsaturated Porous Media – First Revision. ORNL-5567/R1. Oak Ridge National Laboratory, Oak Ridge, Tennessee.
- Yeh, G. T., and D. S. Ward, 1981. FEMWASTE: A Finite-Element Model of Waste Transport Through Saturated-Unsaturated Porous Media. ORNL-5601. Oak Ridge National Laboratory, Oak Ridge, Tennessee.
- , 1979. FEMWATER: A Finite-Element Model of Water Flow Through Saturated-Unsaturated Porous Media. ORNL-5567. Oak Ridge National Laboratory, Oak Ridge, Tennessee.
- Young, R. A., 1965. Records of Well and Test Holes Drilled at the Nevada Test Site and Vicinity Since 1960. U.S. Geological Survey Technical Letter NTS-117. U.S. Geological Survey, U.S. Government Printing Office, Washington, DC.
- Yu, C., A. J. Zielen, J. J. Cheng, Y. C. Yuan, L. G. Jones, D. J. LePore, Y. Y. Wang, C. O. Loureiro, E. Gnanapragasm, E. Faillace, A. Wallo III, W. A. Williams, and H. Peterson, 1993. Manual for Implementing Residual Radioactive Material Guidelines Using RESRAD, Version 5.0. Argonne National Laboratory, Argonne, Illinois.

Zaslavsky, D., and G. Sinai, 1981. Subsurface Hydrology: V. In-surface transient flow. Jour. Hydr. Div. Am. Soc. Civil Eng., 107 (HYI):65-93.

Zoback, M. L., and M. D. Zoback, 1980. Faulting Patterns in North-Central Nevada and Strength of the Crust. J. Geophys. Res. 85(B1):275-284.

Zoback, M. L., and G. A. Thompson, 1978. Basin and Range Rifting in Northern Nevada: Clues From a Mid-Miocene Rift and its Sequent Offsets. Geology 6:111-116.

Zonge Engineering, 1990. Final Report: Vector CSAMT survey of the Frenchman Flat project, Nevada Test Site, Nevada. Zonge Engineering and Research Org. Inc., Tucson, Arizona.

APPENDIX A

NEVADA TEST SITE

WASTE ACCEPTANCE CRITERIA STATEMENTS

5.5 Waste Acceptance Criteria Statements

Address each of the following waste acceptance criteria (WAC). Provide a brief statement of the NVO-325 criteria objective. State the regulatory or other reference(s) as provided in the WAC and provide a brief discussion of how each waste stream will comply with the individual criteria. In addition, where compliance is procedurally controlled, reference the applicable procedure(s). For example:

- 1) **Closure:** The package closure shall be sturdy enough that it will not be breached under normal handling conditions and will not serve as a weak point for package failure (per NVO-325, 5.5.1.3.A).

Compliance Method: Waste containers shall be closed with metal clips and banding, per procedure XXXX, to prevent breaching under normal

Waste Stream Information

types of wastes and are intended to facilitate handling and provide health and safety protection of personnel at the disposal site.

5.5.1.1 General Waste Form Criteria

These waste form criteria are based on current DOE LLW management policies and practices per DOE Order 5820.2A guidelines. Any waste streams not meeting these basic requirements must be evaluated on a case-by-case basis and must not compromise the performance objectives for the disposal site or violate any permit requirements.

A. Transuranics: LLW must have a transuranic nuclide concentration less than 100 nCi/g. The mass of the waste container, including shielding, shall not be used in calculating the specific activity of the waste.

B. Hazardous Waste Components: LLW offered for disposal at NTS waste management sites shall not exhibit any characteristics of, or be listed as, hazardous waste as identified in Title 40 CFR 261, "Identification and Listing of Hazardous Waste" or state-of-generation

C. Free Liquids: Free liquids mean liquids which readily separate from the solid portion of a waste under ambient temperature and pressure conditions.

LLW disposed at the NTS waste management sites shall contain as little free liquids as is reasonably achievable, but in no case shall the liquid equal or exceed 0.5 percent by volume of the external waste container and shall meet the following criteria:

Waste Stream Information

- If absorbent materials are added to a waste for control of free liquids, the generator must calculate the volume of liquid in the waste and use a quantity of sorbent material sufficient to absorb a minimum of twice the calculated volume of the liquid. Please note when significant differences of temperature exist between the generating site and the disposing site, provisions for additional absorbent materials must be made for affected waste forms.
- To demonstrate compliance with the free liquids requirement, the generator may be required to use Method 9095 (Paint Filter Test) as described in "Test Methods For Evaluating Solid Wastes, Physical/Chemical Methods." (EPA Publication No. SW-846) The Paint Filter Test may not be applicable to certain waste forms; e.g., concrete. If the generator determines that the waste form is not conducive to the Paint Filter Test, documentation must be provided to substantiate the claim.

D. Particulates: Fine particulate wastes shall be immobilized so that the waste package contains no more than 1 weight percent of less-than-10-micrometer-diameter particles, or 15 weight percent of less-than-200-micrometer-diameter particles. Waste that is known to be in a particulate form or in a form that could mechanically or chemically be transformed to a particulate during handling and interim storage shall be immobilized.

When immobilization is impractical, other acceptable waste packaging shall be used, such as the following:

- Overpacking (i.e., 55-gallon drum inside 83- or 85-gallon drum);
- steel box with no liner;
- wooden box with a minimum of 6-mil sealed plastic liner;
- steel drum with a minimum of 6-mil sealed plastic liner.

E. Gases: LLW gases shall be stabilized or absorbed so that pressure in the waste package does not exceed 1.5 atmospheres at 20° C.

Waste Stream Information

Compressed gases as defined by Title 49, CFR 173.300, including unpunctured aerosol cans, will not be accepted for storage or disposal. Aerosol cans will have puncture disfigurements recognizable by (RTR). Expended gas cylinders must have the valve mechanism removed.

- F. Stabilization:** Where practical, waste shall be treated to reduce volume, promote waste minimization, and provide a more structurally and chemically stable waste form.

Structural stability can be accomplished by crushing, shredding, and placing a smaller piece inside an opening of a larger piece, such as nesting pipes.

Chemical stability must be documented to show that significant



J. Explosives and Pyrophorics: LLW containing explosive and/or pyrophoric material in a form that may spontaneously explode or combust, if the container is breached, will not be accepted.

The NTS waste package criteria include regulatory criteria to meet applicable DOE, EPA, and DOT requirements and criteria established to meet site-specific requirements at NTS waste management sites. Defense waste shipped to NTS waste management sites for disposal or storage must be packaged in accordance with all DOE and DOT regulations. These include the requirements of DOE Order 1540.1, "Materials Transportation and Traffic Management"; Titles 49, CFR 173.448, "General Transportation Requirements"; 49 CFR 173.474, "Quality Control for Construction of Packaging," and 49 CFR 173.475, "Quality Control Requirements Prior to Each Shipment of Radioactive Materials."

A. Design: Type A packaging shall be designed to meet Title 49 CFR 173.411, "General Design Requirements," and Title 49 CFR 173.412, "Additional Design Requirements for Type A Packages." Type A packages must have been evaluated under the DOE Type A package Certification Program (see MLM-3245, "DOT 7A Type A Certification Document" or succeeding DOE publication). Type B packaging must meet the applicable requirements of Title 10 CFR 71. Strong, tight packaging used for shipping limited quantities and low specific activity LLW excepted by Titles 49 CFR 173.421 and 173.425, respectively, must be constructed so that it will not leak during normal transportation and handling conditions.

B. Nuclear Safety: The quantity of fissile radioactive materials shall be limited so that an infinite array of such packages will remain subcritical. This quantity shall be determined on the basis of a specific nuclear

Waste Stream Information

- C. Nuclear Heating:** The quantity of radioactive materials shall be limited for each waste matrix and package type so that the effects of nuclear decay heat will not adversely affect the physical or chemical stability of the contents or package integrity. See Title 49 CFR 173.442, "Thermal Limitations," for temperature limits of accessible external package surfaces.
- D. Radiation Levels:** The external radiation levels for packages shall not exceed 200 millirem per hour on contact during handling, shipment, and disposal unless specifically excepted by DOT regulations. See Title 49 CFR 173.441, "Radiation Level Limitations." Type B containers that will be unloaded by remote procedures will be addressed on a case-by-case basis.
- E. External Contamination:** Packages shall be within DOT contamination limits upon receipt at NTS. See Title 49 CFR 173.443, "Contamination Control." On-site generators refer to current NTS external contamination limits.
- F. Activity Limits:** The activity limits listed in Title 49 CFR 173.431, "Activity Limits for Type A and Type B Packages," shall be met. Where applicable, the activity limits of Titles 49 CFR 173.421, "Limited Quantities of Radioactive Materials," and 49 CFR 173.425, "Transport Requirements for Low-Specific Activity Radioactive Materials," shall be met for strong, tight packages. See Section 5.5.5.2 for additional requirements for activity limits outside of this range.
- G. Multiple Hazards:** Waste containing multiple hazards shall be packaged according to the level of hazard as defined in Title 49 CFR 173.2, "Classification of Material Having More than One Hazard."

5.5.1.3 NTS Specific Package Criteria

The use of properly designed packaging reduces the chance of radiological or occupational safety occurrences during transportation, handling, and disposal operations. In addition, preplanning the size and load of each package is

Waste Stream Information

- C. Nuclear Heating:** The quantity of radioactive materials shall be limited for each waste matrix and package type so that the effects of nuclear decay heat will not adversely affect the physical or chemical stability of the contents or package integrity. See Title 49 CFR 173.442, "Thermal Limitations," for temperature limits of accessible external package surfaces.
- D. Radiation Levels:** The external radiation levels for packages shall not exceed 200 millirem per hour on contact during handling, shipment, and disposal unless specifically excepted by DOT regulations. See Title 49 CFR 173.441, "Radiation Level Limitations." Type B containers that will be unloaded by remote procedures will be addressed on a case-by-case basis.
- E. External Contamination:** Packages shall be within DOT contamination limits upon receipt at NTS. See Title 49 CFR 173.443, "Contamination Control." On-site generators refer to current NTS external contamination limits.
- F. Activity Limits:** The activity limits listed in Title 49 CFR 173.431, "Activity Limits for Type A and Type B Packages," shall be met. Where applicable, the activity limits of Titles 49 CFR 173.421, "Limited Quantities of Radioactive Materials," and 49 CFR 173.425, "Transport Requirements for Low-Specific Activity Radioactive Materials," shall be met for strong, tight packages. See Section 5.5.5.2 for additional requirements for activity limits outside of this range.
- G. Multiple Hazards:** Waste containing multiple hazards shall be packaged according to the level of hazard as defined in Title 49 CFR 173.2, "Classification of Material Having More than One Hazard."

5.5.1.3 NTS Specific Package Criteria

The use of properly designed packaging reduces the chance of radiological or occupational safety occurrences during transportation, handling, and disposal operations. In addition, preplanning the size and load of each package is

Waste Stream Information

- E. Weight:** In addition to the weight limits set for specific packaging designs, NTS imposes limits of 4,082 kg (9,000 pounds) per box and 544 kg (1,200 pounds) per 208-liter (55-gallon) drum. Packages exceeding 4,082 kg (9,000 pounds) require crane or large forklift removal and must be approved by REECo/WMD prior to shipment. Shipments of this type must be in a removable-top or removable-side trailer.
- F. Loading:** Waste packages shall be loaded to ensure that the interior volume is as efficiently and compactly loaded as practical. High density loading will allow efficient RWMS space utilization and provide a more stable waste form that will reduce subsidence and enhance the long-term performance of the disposal site.
- G. Nonstandard Type A Packaging:** Use of DOT Type A packages not previously evaluated under the DOE Type A Package Certification Program (see MLM- 3245, etc.) will not be permitted.
- H. Package Protection:** The generator shall take the following precautions to protect the waste package after closure.
1. The preshipment storage environment shall be controlled to avoid adverse influence from weather or other factors on the containment capability of the waste packaging during handling, storage, and transport. The generator preparing waste for preshipment storage shall take all reasonable precautions to preclude the accumulation of moisture on or in packages prior to their arrival at the NTS.
 2. A form of Tamper Indicating Device (TID) shall be applied to each waste container, once certification actions have been completed.
 3. Each waste package shall be prepared for shipment so as to minimize damage during transit. Minor damage incurred during transit, not attributable to poor packaging, will be repaired at the RWMS without charge to the waste generator. Costs for repairs of damage caused by waste generator or carrier negligence as well as any necessary decontamination to meet DOE Order 5480.11 will be charged to the waste generator.

Waste Stream Information

I. Marking and Labeling: Each waste package shall have the following information:

1. Marking and labeling as required in Title 49 CFR 172, subparts D and E.
2. Signed NV-211 "Packaging Certification" label (revision date January 27, 1989) (see Figure 8, page 76). If the waste is unpackaged bulk, a signed NV-211 label must accompany the shipment papers. These labels can be obtained from REECo/WMD.

2. Shipping label in the following sequence: Two alpha character

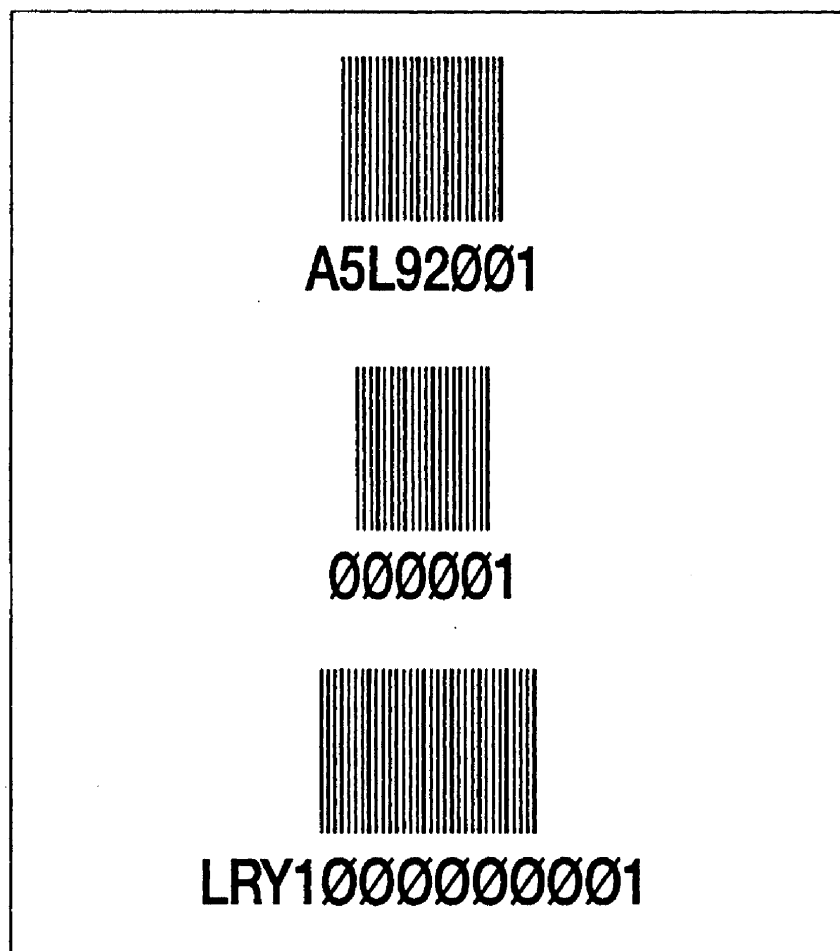
3. 1.0" high barcode.
4. Human readable interpretation (HRI) 0.50" high printed below the barcode.
5. Spacing between barcode and HRI will be 0.10".
6. Minimum left and right margin (quiet zones) will be at least 0.25".
7. All barcodes and HRI will be stacked with a minimum separation of 0.50" and in the following order: shipment number, container number, and waste stream identification number. (See Figures 6A and 6B.)

Note: Waste Stream ID number will not have the dash barcoded.
EXAMPLE: LRY5-000000001 would be barcoded as
LRY5000000001.

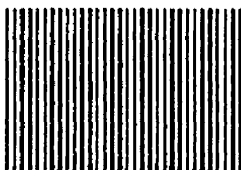
8. A total of two barcode labels shall be placed on each box or nonstandard package near the top and on opposite sides. Drums will have a total of two barcode labels, one on top of the drum lid and one on the side near the top.
9. A sample barcode must be submitted to WMD prior to the first shipment to ensure that WMD equipment can be used to read the barcode. WMD will provide barcodes if you are a low-volume

Waste Stream Information

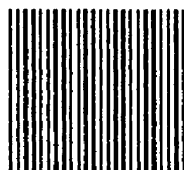
Figure 6A Barcode Label



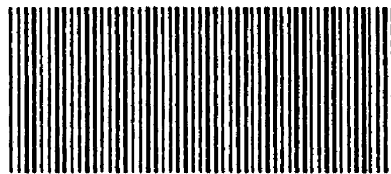
MINIMUM REQUIREMENTS FOR HIGH DENSITY BARCODE LABEL



A5L92001



000001



LRY1000000001

Waste Stream Information

5.5.2 Additional Criteria for Mixed Waste

In addition to meeting all of the LLW WAC, MW offered for disposal at the Area 5 RWMS Mixed Waste Management Unit (MWMU) must meet the criteria described below.

Note: MW will not be accepted for bulk disposal in the Area 3 RWMS. MW containing asbestos will be handled on a case-by-case basis. State-of-generation requirements for identifying, treatment, and disposal will also apply.

A. Free Liquids: MW disposed at the NTS shall contain no free liquids.

- Residual liquids in well-drained containers shall be mixed with absorbent or solidified so that free liquids are no longer observed.
- If absorbent materials are added to a waste for control of free liquids, the generator must calculate the volume of liquid in the waste and use a quantity of sorbent material sufficient to absorb a minimum of twice the calculated volume of the liquid. Please note when significant differences of temperature exist between the generating site and the disposing site, provisions for additional absorbent materials must be made for affected waste forms.
- To demonstrate the absence of free liquids, the generator may be required to use Method 9095 (Paint Filter Test) as described in "Test Methods For Evaluating Solid Wastes, Physical/Chemical Methods." (EPA Publication No. SW-846) The Paint Filter Test may not be applicable to certain waste forms; e.g., concrete. If the generator determines that the waste form is not conducive to the Paint Filter Test, documentation must be provided to substantiate the claim.

Waste Stream Information

- B. Treatment:** All MW accepted for disposal at the MWMU must comply with land disposal restrictions for the hazardous component(s) as specified under Title 40 CFR 268, "Land Disposal Restrictions" unless treated as specified under Title 40 CFR 268, Subpart D, "Treatment Standards."
- C. Reactive Wastes:** All reactive wastes must be treated in accordance with Title 40 CFR 268, Subpart D, "Treatment Standards."
- D. Potentially Incompatible Wastes:** Wastes must be identified by the most appropriate compatibility group listed in Title 40 CFR 264, Appendix V, "Examples of Potentially Incompatible Waste," to ensure that incompatible wastes are not shipped or disposed together. Incompatible MW shall be packaged in accordance with Title 40 CFR 264.177, "Special Requirements for Incompatible Wastes."
- E. Marking and Labeling:** MW packages of 110 gallons or less must be marked in accordance with Title 40 CFR 262.32(b). Intrasite shipments shall be marked and labeled in accordance with the above requirements as well as NV 54XG.1A, "DOE/NV Radiological Safety Manual." Marking and labeling of the waste packages shall be for the hazardous component in addition to the radioactive component. Limited quantity MW must be classified according to the requirements for hazardous components as defined by Title 49 CFR 173.2.
- F. Package Protection:** The requirements of Title 40 CFR 264, Subpart I, "Use and Management of Containers," shall be met for MW packages.

5.5.3 Additional Criteria for Transuranic/Transuranic Mixed Waste

Requests for storage of all TRU waste will be considered on a case-by-case basis.

TRU waste must meet all the LLW WAC including DOE/HQ designation, application to DOE/NV, and participation in the waste generator approval process. TRU waste is only accepted at the NTS for interim storage prior to shipment to the Waste Isolation Pilot Plant (WIPP). In addition, the generator

Waste Stream Information

will be required to provide documentation with their application that the waste



5.5.4 Additional Criteria for Bulk Waste

Bulk waste is disposed of in Area 3. It generally exists in a form not suited to the conventional packaging requirements of Area 5. In addition to meeting the LLW WAC, bulk LLW must meet the requirements of Title 49 CFR 173.425(c). NTS-generated bulk waste must be transported in accordance with NV 54XG.1A, "DOE/NV Radiological Safety Manual," and applicable DOT requirements.

Bulk waste containers must be approved by DOE/NV. Bulk waste containers may be returned to the generator after decontamination to meet NV 54XG.1A, "DOE/NV Radiological Safety Manual," off-site release limits. Decontamination and return of bulk waste containers will incur additional operational costs for the generator.

Note: MW will not be accepted for bulk disposal.

5.5.5 Additional Criteria for Case-by-Case Waste

In addition to meeting LLW WAC, the following case-by-case waste types offered for disposal at the NTS must meet the criteria described below.

5.5.5.1 Weight

Waste Stream Information

5.5.5.3 Radioactively Contaminated Asbestos

All regulated asbestos that is friable or otherwise capable of giving off friable asbestos dust must be wetted with a water and surfactant mix and stored in two plastic bags whose combined thickness equals at least 6 mil. The plastic bags must be overpacked in a leak-resistant wood or metal container that meets applicable shipping requirements for the radioactive content of the package involved. Sharp edges and corners within the package shall be padded or otherwise protected to prevent damage to the plastic inner wrap during handling, shipping, and disposal. Because the asbestos must be wetted during abatement activities, an absorbent must be added to ensure compliance with the free liquid requirement for LLW, see Section 5.5.1.1.C.

For further reference on regulated asbestos, see 40 CFR 61.140-61.157 and state-of-generation regulations. All LLW containing regulated asbestos shall be packaged, marked, and labeled in accordance with the requirements of 40 CFR 61.150.

Note: Any regulated asbestos waste must be segregated into a separate waste stream.

SEALAND® containers are accepted on a case-by-case basis.

5.5.5.4 DOE Comparable Greater-Than-Class-C as Defined in 10 CFR 61.55

Disposal systems for such waste must be justified by a site-specific performance assessment through the National Environment Policy Act (NEPA) process and with the concurrence of EM-32 for all EM-1 disposal facilities and of NE-20 for those disposal facilities under the cognizance of NE-1.

Disposition of waste designated as greater-than-class-C, as defined in Title 10 CFR 61.55, will be handled as special case waste. Greater-than-class-C waste will be considered for disposal on a case-by-case basis depending on existing site-specific waste classification limits or limits that may be developed based on performance assessments.

APPENDIX B
SUPPLEMENTAL GEOLOGICAL INFORMATION

General Stratigraphy Beneath the NTS

The stratigraphy beneath the NTS can be broadly classified, based on a hydrologic framework, into eight primary units with associated lithologic character as diagramed in Figure B.1 (Winograd and Thordarson, 1975). *Figure B.1* is a highly idealized conceptual perspective of a very complex region. Because of erosion and structural deformation, the complete stratigraphic section does not exist everywhere within the NTS, as seen on a surficial geological map of the area.

The stratigraphic units were deposited over long periods of geologic time under varying depositional environments. The lithologies range from older sedimentary rocks overlain by younger volcanic deposits of ash-fall and ash-flow tuff, and minor basalts. The topmost unit on which the Area 5 RWMS is located consists of unconsolidated valley fill alluvium. These units are described below from bottom to top, oldest to youngest.

Lower Clastic Rocks

The lowermost strata, which rests on Precambrian crystalline basement rock, are Precambrian sedimentary deposits. These deposits represent some of the first sediment deposited in the Cordilleran miogeosyncline, a gently subsiding, marine, depositional basin that was located off the western edge of North America. The Cordilleran miogeosyncline was a depositional basin from the Precambrian through Devonian period. The earliest deposits in the Cordilleran miogeosyncline were predominantly sandstones, siltstones, and shales derived from sediment eroded from the craton. These deposits have been classified into four formations (Burchfiel, 1964): the Zabriskie Quartzite, Wood Canyon Formation, Stirling Quartzite, and the Johnnie Formation. The lower half of the Carrara Formation is also commonly included in the lower clastic rocks. These units are predominantly composed of quartzite and shale-siltstone layers, with a total thickness estimated at over 3,000 m (9,840 ft).

The clastic rock units are highly fractured, although fractures are commonly completely sealed by quartz, calcite, and mica-chlorite ingrowths. The only major outcrop in the NTS region is on the northeast side of the Halfpint Range (Frizzell and Shulters, 1990). Elsewhere within the NTS, the unit is believed to be buried deep beneath overlying units of Paleozoic limestone and Tertiary volcanic rocks.

Lower Carbonate Rocks

The lower clastic rocks are directly overlain by a succession of carbonate rocks. These carbonate rocks consist of limestone and dolomite deposited when clastic deposition originating from the craton decreased, providing a clear, calm-water environment suitable for

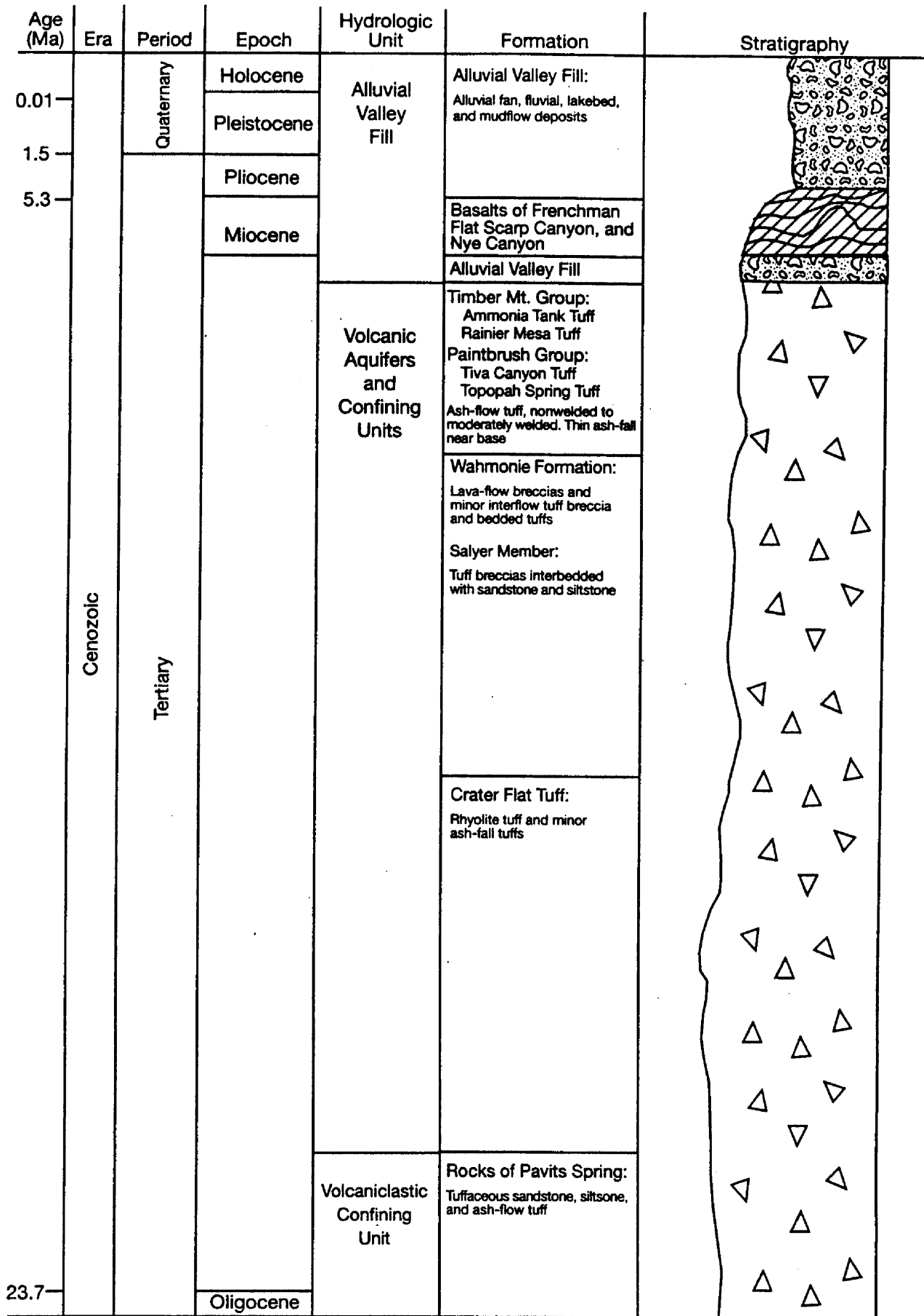
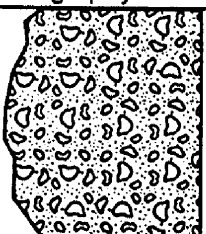
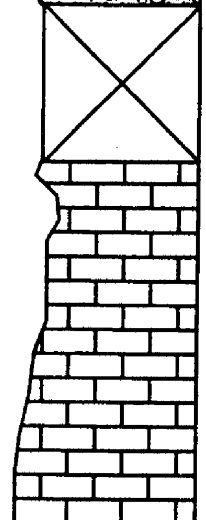
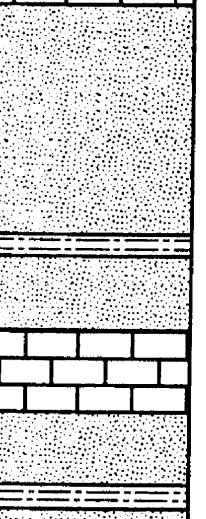
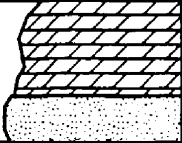


Figure B.1 General Stratigraphy and Time Sequence at the NTS

Age (Ma)	Era	Period	Epoch	Hydrologic Unit	Formation	Stratigraphy
	Cenozoic	Tertiary	Oligocene	Tertiary Seditments	Horse Spring Formation: Fresh-water limestone, siltstone, sandstone, conglomerate, and tuff	
36.6			Eocene			
66.4			Paleocene			
	Mesozoic			Granitic Stock	No exposure in the vicinity of Frenchman Flat	
245		Permian		Upper Carbonate Aquifer	Bird Spring Formation: Limestone	
286		Pennsylvanian				
320					Undivided Carbonate: Limestone, siltstone, and shale	
		Mississippian		Upper Clastic Confining Unit	Chainman Shale and/or Eleana Formation: Argillite, siltstone, sandstone, and minor limestone and conglomerate	
360						

Age (Ma)	Era	Period	Epoch	Hydrologic Unit	Formation	Stratigraphy
			Late	Lower Carbonate Aquifer	Ely Springs Dolomite: Dolomite	
		UN			Eureka Quartzite: Quartzite	

carbonate-producing organisms. Occasional influxes of sediment from the craton are recorded as minor sandstone, siltstone, and shale deposits interbedded with the carbonate rocks. This lower carbonate succession contains the Carrara Formation, Bonanza King Formation, Nopah Formation, Pogonip Formation, Eureka Quartzite, Ely Springs Dolomite, Laketown Dolomite, Sevy Dolomite, Simonson Dolomite, and the Guilmetted Formation. The Carrara Formation at the base of this succession contains sandstone and siltstone which are considered transitional with the underlying lower clastic rocks. These thick carbonate units are collectively more than 4,570 m (14,990 ft) thick.

The carbonates are highly fractured and locally brecciated near fault traces. Most outcrops exhibit three or more sets of joints and high-angle fractures (Winograd and Thordarson, 1975). According to core logs, the fracture fill consists of breccia and clay gouge, calcite, and dolomite. Although clay gouge fill provides strong evidence for the existence of fault planes, the most common fill materials are calcite and dolomite, followed by quartz and iron-manganese oxides.

Upper Clastic Rocks

During the late Devonian Period (360 Ma), an island arc collided into the North American craton. The resulting Antler Orogeny resulted in uplift and deformation of the deposits of the Cordilleran miogeosyncline. Evidence of the collision is seen in the Roberts Mountains in central Nevada, where deep marine facies were thrust as far as 160 km (100 mi) over thinner platform deposits. The Antler Orogeny initiated a long period of alternating depositional environments. Influx of immature clastic sediments, due to turbidity and debris flows shed off the craton during periods of uplift during the Mississippian Period (330 Ma), probably formed the Eleana and Chainman Shale Formations. The Eleana Formation consists of a thick section of fine-grained sandstone to quartz-pebble conglomerate and comprises the upper clastic rocks unit, whereas the Chainman Shale is primarily finer grained shale. Near Yucca Flat, the unit is upwards of 1,210 m (4,000 ft) thick; however, outcrops are limited in the vicinity of Frenchman Flat to CP Basin.

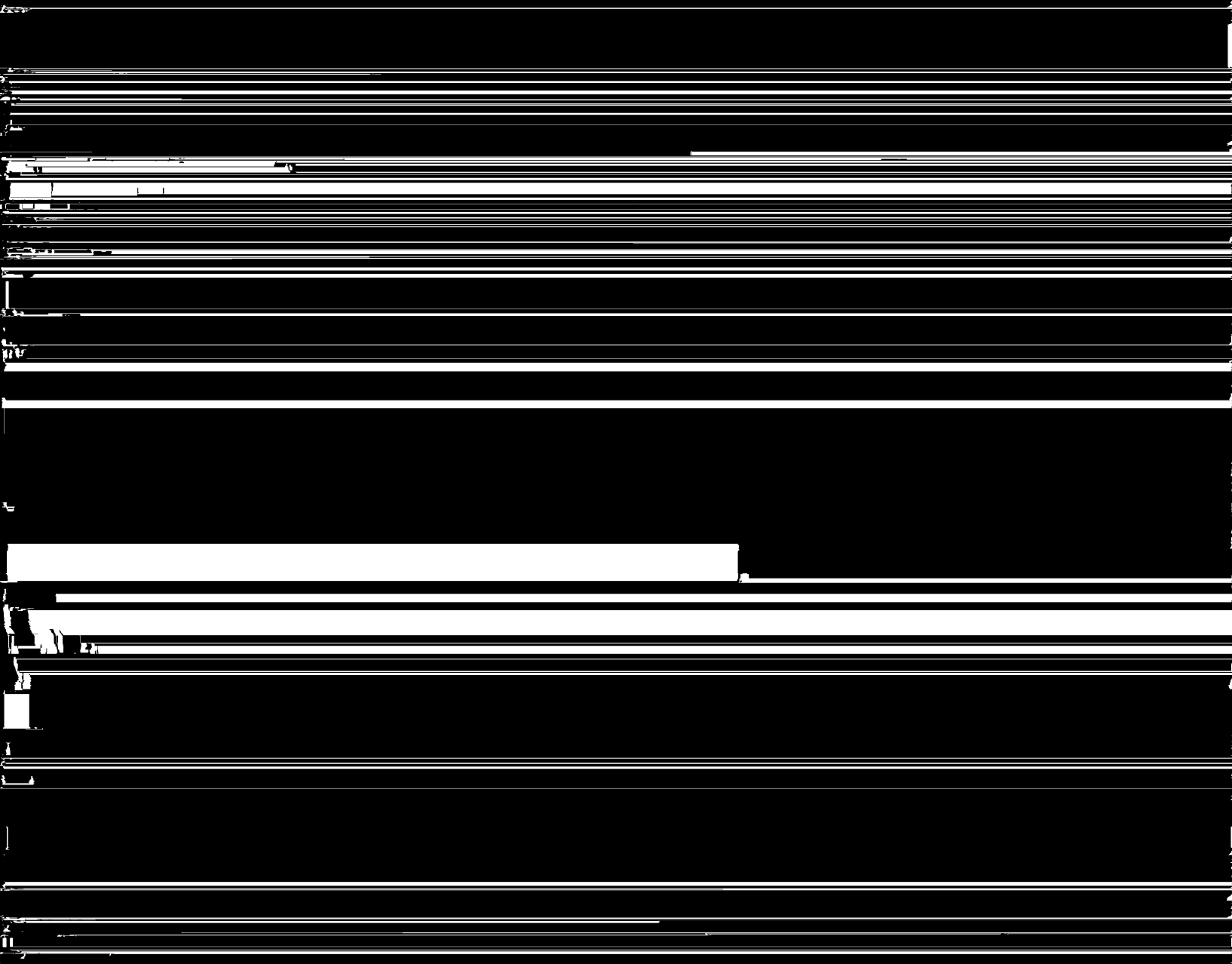
Upper Carbonate Rocks

During the late Mississippian to Permian Period (330 to 240 Ma), when the basin experienced more stable, shallow-marine conditions, the 1,300-m (4,265 ft)-thick upper carbonate unit was deposited. This unit is composed of the limestones of an undivided

Granitic Stocks

The Mesozoic and early Cenozoic periods were dominated by granitic intrusions and thrust faulting. In the vicinity of Frenchman Flat, no intrusive bodies are present. The only significant occurrence of intrusive bodies on the NTS is in the extreme northern and north-western portions of Yucca Flat. Here, coarse porphyritic monzonite-granite and quartz-monzonite magmas were extruded into limestone of the Pogonip group (Frizzell and Shulters, 1991).

During the Nevadan Orogeny, granitic intrusions were emplaced throughout the western United States. During the slightly younger Sevier Orogeny, the great compressional strain in

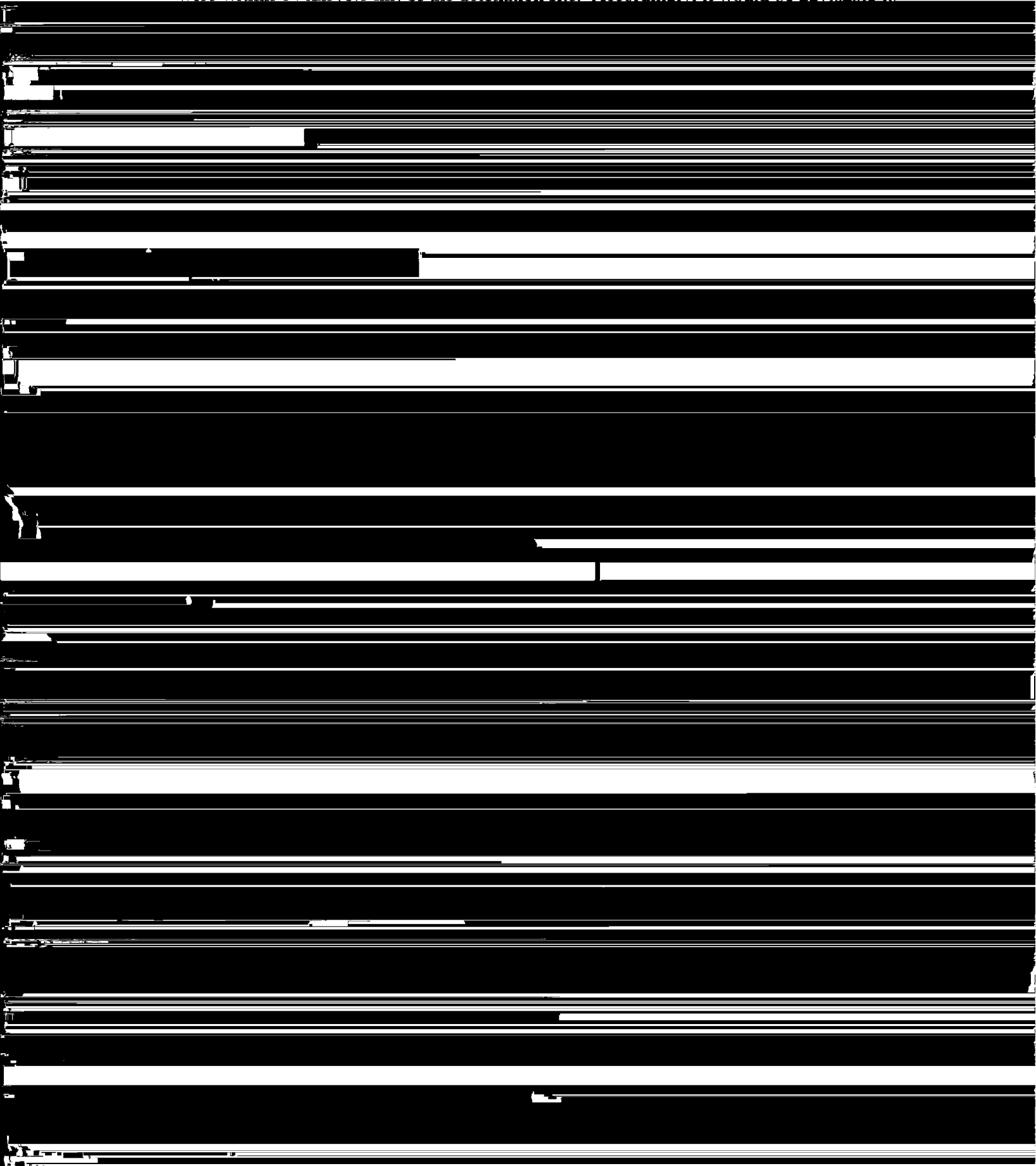


younger strata. Better-known thrust faults from this event are the Lee Canyon, Wheeler, and Keystone thrusts. These strike roughly north and northeast along the Spring Mountains, 55 to 95 km (34 to 60 mi) to the southeast of the NTS (Fleck, 1970; Burchfiel, 1974). Sedimentation was sparse throughout the area during this time, as shown by the unconformity on

Ash-flow tuffs, however, are consolidated rock formed by catastrophic explosions of hot pyroclastic material (volcanic ash and gases). The resulting deposits exhibit neither bedding nor sorting and could have taken years to cool after emplacement. During cooling, they experience much compaction and internal welding of particles. The degree of welding is generally greater in the center of the unit, resulting in a dense zone of little porosity sandwiched between zones of partial welding. Subsequent cooling of these units produces marked jointing and foliation patterns (Ross and Smith, 1961; Smith, 1960). Such distinctions are important because the structure and mode of emplacement between ash-flow and

Although the western margin of the NTS lies within an area believed to have a high risk for potential seismicity, activity has historically been low to moderate. The most recent earthquake of significance was of magnitude 5.6, occurring on June 29, 1992. Its epicenter was approximately 15 km (9 mi) to the southwest of the Area 5 RWMS near Skull Mountain, at a depth of 10 km (6 mi). The Area 5 RWMS was unaffected. In August 1971, an earthquake of magnitude 4.3 occurred along the Cane Spring Fault zone, approximately 7.2 km (4.5 mi) north of the Area 5 RWMS. An earthquake of 4.5 magnitude occurred in February 1972 along

were within 14 km (8.6 mi) of the detonation site. Accordingly, it would be advisable to



where:

$$\binom{n}{x} = \frac{n!}{x! (n-x)!} \text{ for } x = 0, 1, 2, \dots, n. \quad (\text{B.2})$$

Because the probability of a success (earthquake of magnitude 6.8 or greater) is assumed to be a constant $7.87 \times 10^{-5} \text{ yr}^{-1}$ (1/12,700 yr), and because the probability that there are 0, 1, 2, . . . , 10,000 earthquakes sums to one, the probability there are one or more earthquakes of magnitude 6.8 or greater is:

$$\begin{aligned} \text{Risk} &= \\ 1 - P(\text{no successes}) &= \\ 1 - \binom{10000}{0} (7.87 \times 10^{-5})^0 (1 - 7.87 \times 10^{-5})^{10000} & \quad (\text{B.3}) \end{aligned}$$

These calculations suggest there is a 54.5 percent chance of one or more earthquakes greater than 6.8 in the next 10,000 years. Note that if the calculations are repeated with the less conservative return time of 15,000 years, the probability of an earthquake falls to 0.486.

Despite the moderate risk of seismic damage, the limited use of engineered structures at Area 5 RWMS makes the site intrinsically less prone to significant earthquake damage than an aboveground facility or a facility using engineered belowground vaults. Unless a major earthquake centered on the Area 5 RWMS occurred, at worst only limited compaction, caused by the consolidation of alluvium, might be expected. Given the large return times associated with the largest events, coupled with the small likelihood that an event would be centered upon the Area 5 RWMS, it is unlikely that the integrity of the RWMS would be compromised.

VOLCANIC RISK ANALYSIS

Data concerning the hazards of future volcanism in the NTS region have been acquired from ongoing assessments of the volcanic hazard at Yucca Mountain, located approximately 45 km (28 mi) west of the RWMS. The close proximity of Yucca Mountain to the RWMS suggests that the volcanic hazard associated at the RWMS can be garnered from the data gathered at Yucca Mountain.

Crowe *et al.* (1983) concluded that further silicic volcanism was not realistic, given the age evidence by Christiansen *et al.* (1977) and Byers *et al.* (1976) for the ash-flow and ash-fall tuffs in nearby caldera systems. The most recent volcanism, associated with the Death

Valley-Pancake Range Volcanic Belt (Wells *et al.*, 1990), has been basaltic. The Death Valley-Pancake Range Volcanic Belt, a 50-km- (31-mi)-wide swath of activity that transects the NTS trending north-south throughout southern Nevada, is characterized by cinder cones

3t Site

45'

15'

halt
of
age
Ma

00'

asalt
of
Nye
chyon
4 Ma

45'

tion

ement

Volcanism would be much more localized
position would be restricted to the
within 2 to 10 km (1.2 to 6.2 mi) of the
(B.4). K-Ar dating methods, coupled with
nearby volcanic regions, indicate that
activity of the Area 5 RWMS in the near

The NTS area has been given by Wells
activity (the Lathrop Wells Cone) near
B.4, based on a comparison to a similar
however, neglects the K-Ar data that dates
B.4a (RSN, 1994). Even in view of this
that the estimated hazard from renewed
for a 10,000-year postclosure period for
hazard was provided by Crowe and Carr
for a high-level waste repository disruption
of 10^{-9} per year for an area within a 25- to

Yucca Mountain by Crowe and Carr
hundred million that volcanism will
occur, the risk is given by:

(B.4)

that chance (one percent of one percent),
within the next 10,000 years. Renewal
likely.

This Page Intentionally Left Blank

APPENDIX C

**Response to the DOE Peer Review Panel
Request for Additional Information on the
Area 5 Performance Assessment (Revision 2.0)
Received October 31, 1995**

Response to Request for Additional Information on the Area 5 Performance Assessment (Revision 2.0), Received October-31, 1995

1. **Request 1.a.(2)(a):** Provide a discussion of how the Zero Flux Plane (ZFP) formed over the past thousands of years and how it might evolve over the next several thousand years.

Response: One possible explanation of the development and formation of the Zero Flux Plane (or Zone) has been provided in Section 2.4.2.2 "Subsurface Hydrology," under the section entitled "Evolution of Vadose Zone Conditions over Time."

Turning to the second part of the request, future evolution of the zero flux zone, prediction of the flux distribution in the alluvium of Frenchman Flat depends on knowledge of the hydraulic properties of the alluvium and the nature of the boundary conditions. If we assume that the hydraulic properties of the alluvium do not change, prediction of the nature of the zero flux zone over the "next several thousand years" requires a prediction of climate change and corresponding vegetation change over that

Response: One possible explanation of the lower chloride levels in UE5PW-2 is presented in Section 2.4.2.2, "Subsurface Hydrology," under the section entitled "Chloride Profiles."

3. **Request 1.a.(2)(c):** Explain how a disturbed soil/sediment profile can be expected to perform as well as the natural profile over the performance period.

Response: Disturbed profiles analogous to native alluvium covers are currently being monitored in two weighing lysimeters located in Frenchman Flat near the Area 5 RWMS (Levitt *et al.*, 1996). Water retention relations measured for soil samples obtained from both lysimeters are plotted in *Figures 2.31* and *2.32*. The water retention model used for the Area 5 Performance Assessment (Revision 2.0) is superimposed for comparison. While the model deviates from the measured curves at very low water contents, it is in good agreement between a volumetric water content of 0.10 and near saturation. The calculations of water flux under unit gradient conditions were made using a volumetric water content of 0.10.

Water content monitoring conducted by Levitt *et al.* (1996) indicated no increase of water content below a depth of 1.5 m (5 ft) under vegetated conditions for 1995, a year characterized by above average precipitation. Under bare soil conditions, the water content at a depth of 1.7 m (5.6 ft) increased from 0.055 to 0.075, while the total storage in the lysimeter has decreased during 1995. The elevated water contents at depth are probably due to irrigation water applied during revegetation of the entire site during 1994.

4. **Request 1.a.(2)(d):** Estimate downward percolation rates from the chloride and stable isotope data from the pilot wells and the science trench boreholes.

Response: A response cannot be provided for the second part of this request. Stable isotope ratios of deuterium and oxygen-18 are used to indicate the occurrence of processes which change the isotopic composition of water (Domenico and Schwartz, 1990). Processes commonly observed through analysis of stable isotope ratios are evaporation, CO₂ exchange, and exchange with rock minerals. Stable isotope ratios are not used to estimate the magnitude of water fluxes.

The Science Trench Boreholes extend only as deep as 36 m (119 ft) and show chloride accumulation throughout the profile sampled. As noted by Tyler *et al.* (1996), an accumulating profile is not at steady state and, as such, it is inappropriate to apply chloride mass balance methods for estimating current recharge.

Chloride data from deeper in the profile can be used to estimate the paleorecharge rate. Estimates of paleorecharge are provided in Section 2.4.2.2, "Subsurface Hydrology," under the section entitled "Chloride Profiles."

5. **Request 1.a.(2)(e):** Compare the chloride and stable isotope data from the RWMS with Prudic's data and analyses.

Response: A response cannot be provided for the second part of this request. Stable isotope ratios of deuterium and oxygen-18 are used to indicate the occurrence of processes which change the isotopic composition of water (Domenico and Schwartz, 1990). Processes commonly observed through analysis of stable isotope ratios are evaporation, CO₂ exchange, and exchange with rock minerals. Stable isotope ratios are not used to estimate the magnitude of water fluxes. Furthermore, Prudic (1994) did not

analyze stable isotope data.

Prudic (1994) estimated the age of water and the downward percolation rate below a depth of 10 m (33 ft) at a site in the Amargosa Desert south of Beatty, Nevada; and at the Ward Valley site in California. Age estimates were made using chloride concentration profiles. Prudic's results are discussed and compared with data for the Area 5 RWMS in Section 2.4.2.2, "Subsurface Hydrology," under the section entitled "Chloride Profiles."

6. **Request 1.a.(2)(f):** Discuss whether consideration of the topography of the RWMS could help explain the observed differences in the chloride profiles.

Response: Before addressing the above issue specifically, it is important to note that despite variations in the recharge history observed for each borehole, the chloride profiles demonstrate that recharge is not occurring under the current climate with the most recent cessation of recharge beginning at about 20 to 30 ka. The influences of topography are discussed in Section 2.4.2.2, "Subsurface Hydrology," under the section entitled "Chloride Profiles."

7. **Request 1.a.(2)(g):** Discuss variations within the chloride and stable isotope data sets.

Response: Additional discussion has been provided in Section 2.4.2.2, "Subsurface Hydrology," under in the section entitled "Water Content."

10. **Request 1.b.(2):** Please provide confirmation of the unsaturated hydraulic conductivity value derived from the van Genuchten and Mualem methods.

Response: Additional discussion of the applicability of unsaturated hydraulic conductivity values has been included in the Section 2.4.2.2, "Subsurface Hydrology," under the section entitled "Unsaturated Hydraulic Conductivity – Soil Moisture Retention Relations."

11. **Request 1.c.(2)(a):** Please discuss the sensitivity of the conceptual model for unsaturated zone flow and transport to the assumed residual water content.

Response: The conceptual model of the hydrology for the Area 5 Performance Assessment (Revision 2.0) was developed from the Pilot Well and Science Trench Boreholes site characterization data. These data show a net upward driving force for liquid water from the zero flux zone, some 35 m (115 ft) deep, to the surface (Zone I), and a net downward tendency for flow through Zone III. These data also include tracer measurements indicating that infiltrating water has been removed by evaporation from the upper vadose zone for thousands of years. Based on the site characterization data, it was also concluded that conditions were too dry for significant upward advection and diffusion to occur.

Although it is true that an estimate of the residual moisture content in the alluvium was retrieved from the characterization data, the value of residual moisture content alone did not determine a hydrological conceptual model. The residual moisture content is a modeling parameter. In this particular case, it was used to define the van Genuchten relationship of unsaturated hydraulic conductivity with water content. While it is true that higher parameter values of residual water content may yield higher values of unsaturated hydraulic conductivity at a given water content, this will affect modeling predictions rather than the conclusions made from the site characterization data.

The site characterization data does not define the dynamic conditions in the very near surface where conditions may be periodically altered by atmospheric conditions. The purpose of the UNSAT2 14-year infiltration scenario was to investigate, on a preliminary basis, dynamic conditions in the very near surface. The UNSAT2 simulation, may have shown a greater depth of water penetration into the top meter of alluvium if a more conservative parameter set (including a lower residual water content) had been used. This in turn may have affected our conclusions about the magnitude of upward advection and diffusion. However, given the shallow burial of this source term and the assumption that plants and animals penetrate directly into the waste, it is unlikely that upward advection or diffusion would be significant relative to transport by plants and animals.

We view site characterization data to be superior to modeling results. Our long-term goal is to use site characterization data from the Area 5 lysimeters and micrometeorological station to calibrate a model such as UNSAT-H. This model will then be available to estimate performance of the system under conditions that cannot be observed directly.

12. **Request 1.c.(2)(b):** Please discuss the sensitivity of the vadose zone travel time to unsaturated hydraulic conductivity values.

Response: A Monte Carlo analysis of unretarded travel time has been included in Appendix D.

13. **Request 1.c.(2)(c):** Please discuss the sensitivity of the depth of the Zero Flux Plane to climate.

Response: A qualitative discussion of the effects of a wetter climate are discussed in Section 2.4.2.2, "Subsurface Hydrology," under the section entitled "Evolution of Vadose Zone Conditions over Time."

14. **Request 1.e.(2):** Please discuss the significance of the above-mentioned statement (page D-12) in light of the conceptual model for water movement in Zone I.

Response: The statement referenced on page D-12, "... it is not reasonable to consider vapor flow as an important mechanism for water movement in the vadose zone," is incorrect. Vapor flow is important for water movement. The statement has been clarified to state that, "... it is not reasonable to consider vapor flow as an important mechanism for radionuclide migration in the vadose zone." Tritium is the only radionuclide that could migrate by this mechanism. Tritium has been handled separately using very a conservative model.

15. **Request 2.b.(1):** Please provide a description of actions taken by waste operations in response to the recommendations in Sections 5.2 and 5.3 of the performance assessment. Please include any plans, schedules, and actions that will be taken in response to recommendations, as well as those actions already taken.

Response: Many of the recommendations made in the PA have to do with waste acceptance criteria and waste acceptance procedures. As such, these issues are most appropriately addressed by the Radioactive Waste Acceptance Program (RWAP) maintained by DOE/NV. Current waste acceptance criteria are defined in NVO-325 (Rev. 1), *Nevada Test Site Defense Waste Acceptance Criteria, Certification, and Transfer*. This document was being revised during preparation of the Area 5 Performance Assessment. Performance assessment requirements will be implemented in the waste acceptance criteria.

16. **Request 3.b.(1):** Please discuss the potential for trench cap subsidence and its effect on the long-term site behavior in meeting the performance objectives. Include in this discussion the long-term effects of cap erosion following subsidence, localized infiltration, and the subsequent migration of solutes. The discussion should include both downward migration and upward migration.

Response: Subsidence was evaluated by adding an additional release scenario for a subsided trench. Additional sections have been added to Chapters 2, 3, and 4 describing the potential for subsidence, its consequences for release and its consequences for each pathway scenario.

17. **Request 3.b.(2):** Please describe plans, if any, for closure cap studies.

Response: In FY 1996, the Integrated Closure Program has three primary tasks being conducted by BN staff: Integrated Closure, U3axbl Closure, and Closure Engineering (activities are listed with the U3axbl Closure task). Some activities conducted as part of the Integrated Closure Program in the past have been transferred to the Low-Level Waste Performance Assessment task:

- Gas Generation. Qualitatively evaluate the potential for disposed wastes to generate gases and vapors, and model movement of such products within the waste and cover.
- Subsidence Monitoring. Develop a subsidence monitoring plan. Install stations and monitor subsidence on existing interim closure covers. Information to optimize final cover design.
- Hydrology Monitoring. Install psychrometers and monitor moisture within existing interim closure caps. Information to optimize final cover design.

The above activities and others (e.g., flood hazard assessment) being conducted under the Low-level Waste Performance Assessment task provide data required in general for the Integrated Closure Program, but also specifically will provide initial information requested by the Peer Review Panel; results of this work will be available at the end of FY 1996. The hydrology monitoring work above, work being conducted by Desert Research Institute in FY 1996, and work proposed by BN for FY 1996 are now being redefined to be complimentary and avoid duplication. Activities being conducted by Desert Research Institute in FY 1996 are:

- Closure Studies. Determine impacts of subsidence on transport of radioactive waste from Area 5 trenches and Greater Confinement Disposal. Numerical simulation of subsidence rates and surface water drainage.
- Closure Working Group Support. Model the current cover design to determine hydrologic performance. Include subsidence and increased precipitation.

An activity proposed by BN for FY 1996 is:

- Waste Cell Flow Regime. Simulate the flow regime in a waste cell below a subsidence induced depression in the surface of a cover. Includes transport through backfill/impermeable containers and calibration and verification of flow and transport models.

The U3axbl Closure task being conducted by BN in FY 1996 will provide data required in general for the Integrated Closure Program and for closure of U3axbl, but specifically BN will provide initial information requested by the Peer Review Panel. Activities of the U3axbl Closure are listed below.

- Conceptual Design Support. Provide consultation specifically for the U3axbl conceptual design report and subtasks for closure engineering, including meetings, writing, and review.
- Title I and II Design. Provide Title I and II designs of a closure cover for U3axbl.
- Value Engineering Study. Provide a value engineering study of the closure cover for U3axbl.
- Alternative Evaluation Study
 - At-grade Cover. Develop an at-grade demonstration cover.
 - Subsidence Mitigation. Evaluate methods to minimize subsidence.
 - Waste Form Optimization. Determine waste forms that will minimize subsidence.

Physical Properties. Determine the physical properties of cover materials.

- Groundwater Monitoring Waiver. Develop a request for waiver of groundwater monitoring for U3axbl. Provide support to revision of the Area 5 groundwater monitoring waiver.

Annual review and update of the Integrated Closure Program provides for inclusion of activities that address known or newly identified gaps in data. The FY 1996 review and update is anticipated to considerably modify the Program, primarily by establishing dates for permanent closure of specific waste cells and identifying activities that have to be accomplished to reach those goals. Although the cover is designed to accommodate increased infiltration (as resulting from ponding in surface depressions caused by subsidence), and withstand erosion for long periods of time, tasks will be conducted in FY 1996 and outyears to increase understanding of processes or events that potentially compromise performance of the cover.

18. **Request 4.b:** Please provide the results of an analysis of the resident farmer scenario.

Response: The performance assessment has been revised to include a resident farmer scenario for consistency. Analysis methods appear in Section 3.2.4.5 and results are presented in Section 4.1.1.3.

19. **Request 5.b.(a):** Please update the inventory to include these radionuclides and discuss the impact of the radionuclides on the projected doses.

Response: The inventory has been modified to include ^{99}Tc estimated to be present in Fernald enriched uranium waste streams. The inventory was not revised to include additional ^{239}Pu in Mound ^{238}Pu waste streams because this quantity was estimated to be small relative to the existing inventory. Overall results were unaffected by these additions.

20. **Request 5.b.(b):** Please provide a sensitivity and uncertainty analysis on the influence of the inventory uncertainties. What is the uncertainty in the inventory and what effect would overestimates and underestimates have on the projected radiation doses estimates for Area 5? Discuss the possibility that the inventory estimates could be uncertain enough to cause the site to exceed the performance objectives.

Response: A Monte Carlo analysis of inventory uncertainty has been included in Section 4.3.2. "Inventory Sensitivity and Uncertainty."

21. **Request 6.a.(2):** Please provide justification for the selection of dust loading of $5.65 \times 10^{-4} \text{ g m}^{-3}$ (intruder-construction scenario) and $1.54 \times 10^{-4} \text{ g m}^{-3}$ (intruder-agriculture scenario). Why are these values given to three significant figures? Did the EIS describe the source of these mass loadings? What is the basis of the text on page 3-232 indicating that a mass loading of $1.54 \times 10^{-4} \text{ g m}^{-3}$ is low because of the wetness of the drill cuttings?

Response: References and justification for these parameters have been added to the revised text in Section 3.3.

22. **Request 6.b.(2):** Please provide the source or justification for the value of the shielding factor.

Response: References for the shielding factor has been added to the revised text in Section 3.3.

23. **Request 6.c.(2):** Please provide the basis for the [National Council on Radiation Protection] NCRP estimate of 0.6 pCi/g.

Response: The NCRP data cited in the performance assessment was derived from the work of Lowder *et al.* (1964).

24. **Request 6.d.(2):** Please provide the basis or justification for this value [of the indoor fractional mass loading].

Response: A reference for the indoor fractional mass loading has been added to the text in Section 3.3.

25. **Request 6.e.(2):** Does the DCF for ^{238}U reflect the yield-weighted contribution from ^{234}Pa ? If not, please provide revised dose estimates including ^{234}Pa .

Response: The external dose conversion factor for $^{238}\text{U}+\text{D}$ appearing in Table E.3 of the Performance Assessment (Revision 2.0) did not include the contribution of ^{234}Pa . The dose conversion factor has been revised and all results updated. Overall, this correction had a negligible impact on the results.

26. **Request 6.f.(2):** Do the concentrations of radionuclides on plant surfaces include the contribution from rain splash? If not, please give the rational for excluding this process.

Response: The performance assessment does not explicitly model rain splash. Our decision not to include rain splash is based on the low and infrequent precipitation at the NTS, minor contribution of ingestion pathways to the doses estimated in this assessment, and compensating addition of soil ingestion. The soil ingestion rates used in the performance assessment include soil intakes from ingestion of soil on vegetation. This was believed to compensate for the processes of rain splash, which is only one of several processes leading to contamination of plant surfaces with soil particulates.

Response: Cane Spring is approximately 14 km (8 mi) southwest of the Area 5 RWMS. It discharges between 8 and 11 liters per minute from volcanic tuff of the Oak Spring Formation (Moore, 1961). The water-bearing formation is likely perched and localized (Moore, 1961) and fed by recharge in the surrounding mountains. Transmission of water is through fractures (Moore, 1961), but likely includes inherent porosity.

Cane Spring is approximately 1,280 m (4,225 ft) above mean sea level. The elevation at the Area 5 RWMS is approximately 975 m (3,217 m) above mean sea level. The Area 5 RWMS is underlain by alluvium approximately 400 m (1,320 ft) thick, which is underlain by volcanic rocks approximately 900 m (2,970 ft) thick, which is underlain by carbonate rocks. The water table is within the alluvium, approximately 235 m (775 ft)

APPENDIX D

HYDROLOGIC CONCEPTUAL MODEL DEVELOPMENT

D.1 Hydrologic Conceptual Model Development

This appendix describes the development of the hydrologic conceptual model for the Area 5 RWMS. The hydrologic conceptual model describes the processes controlling the movement of water within the vadose zone. The model has been interpreted to identify processes that could lead to the release of radionuclides from the source.

Hydrologic and climatic characterization data are available for the NTS (Winograd and Thordarson, 1975; Schoff and Moore, 1964), and for the Area 5 RWMS (REECo, 1993a,b,c; French, 1993; Snyder *et al.*, 1993; RSN, 1991a,b; Sully *et al.*, 1995; Lindstrom *et al.*, 1992; and Detty *et al.*, 1993). Additional studies have been performed to determine the hydrologic behavior of other sites with similar environments (Gee *et al.*, 1994; Fouty, 1989; Fischer, 1992; Scanlon, 1994; Scanlon and Milly, 1994; Scanlon *et al.*, 1991). These may be applied, by analogy, to the performance assessment of the Area 5 RWMS.

A preliminary hydrologic conceptual model has been developed from site-specific hydrologic data (Section 2.4.2.2). This model proposes that the movement of moisture in the vadose zone beneath the Area 5 RWMS can be delineated into four regions of liquid movement:

- Zone I: An upper zone, approximately 35 m (115 ft) in depth, where a high evapotranspiration rate at the surface creates a large negative hydraulic potential for upward liquid flow and drying at the near-surface.
- Zone II: A static zone where the gradient is negligible. The depth and thickness of the static zone varies with location. At Pilot Well UE5PW-1 the static zone occurs from 40 to 90 m (131 to 295 ft).
- Zone III: An intermediate zone below the static zone and extending down 150 to 220 m (492 to 722 ft), dominated by gravity drainage or vertical downward flow. The top of the intermediate zone occurs at 90 m (295 ft) in Pilot Well UE5PW-1. The high water potentials and low water contents in this zone suggest that flow is under a quasi-steady-state condition. This condition was reached a considerable time after the end of a much wetter climatic period when recharge was higher.
- Zone IV: A lower zone, immediately above the water table, where the hydraulic potential is near zero and the water is under a capillary fringe condition with relatively static conditions producing little flow.

Additionally, site characterization data indicate that the alluvium can be considered as a homogenous, isotropic medium (Sully *et al.*, 1993; Istok *et al.*, 1994). This appendix

focuses on the processes controlling the movement of water in Zone I and their implications for radionuclide transport. The upper 35 m (115 ft) of the alluvium (Zone I) is emphasized because all disposal units are within this zone.

Five hydrologic processes have the potential to affect water movement within Zone I (Figure D.1). These processes are:

- Transient precipitation-infiltration events.
- Variable seasonal evapotranspiration.
- Vapor flow driven by thermal gradient.
- Upward and/or downward advective liquid flow.
- Upward diffusion of nuclides within liquid phase driven by concentration gradient.

The timing and magnitude of precipitation and evapotranspiration are major factors controlling water movement in the vadose zone. The sole source of water in the system is precipitation. High evapotranspiration removes much of the precipitation entering the system before it can infiltrate to significant depths. The dry conditions that prevail most of the time in the near surface lead to extremely low unsaturated hydraulic conductivities and little movement of moisture. The natural hydrologic conditions at the Area 5 RWMS act to reduce the potential for radionuclide release and transport.

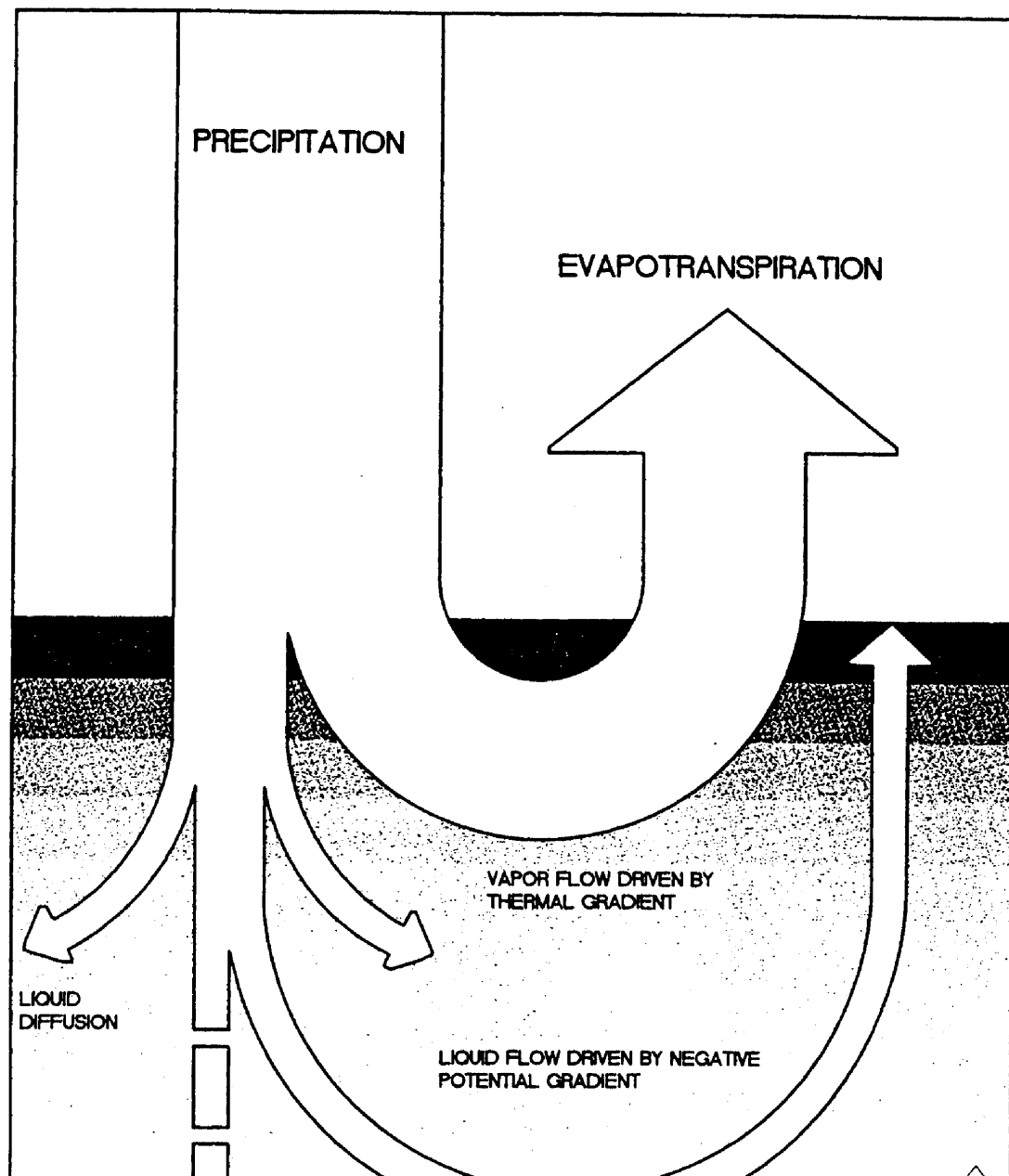
D.1.1 Screening of Hydrologic Processes

This section describes the results of a preliminary evaluation of the significance of hydrologic processes. It is based on site characterization data and results from analogous desert sites.

D.1.1.1 Precipitation

Precipitation is the sole source of water entering the vadose zone. The duration and intensity of precipitation is highly variable in Frenchman Flat, ranging from short, intense isolated thunderstorms in the summer to longer, lower-intensity events in the winter.

The longest record of daily rainfall near the Area 5 RWMS (as of 1995) covers a 31-year period, from 1963 to 1994, recorded by the National Oceanographic and Atmospheric Administration (NOAA) at Well 5B (Table D.1), of which the most recent 14-year period is available on electronic media. Over this period, the mean annual rainfall was 12.55 cm (4.9 in). The annual total was highly variable ranging from a minimum of 2.90 cm (1.1 in) to a maximum of 23.42 cm (9.2 in). Figure D.2 shows the 14-year period used in hydrologic modeling in Section 2.4.



Monthly Precipitation (cm) for the Period From January 1963 to December 1993 at Frenchman Flat (Well 5B)

	FEB	MAR	APR	MAY	JUN	JUL	AUG	SEP	OCT	NOV	DEC	YEAR
6	1.803	0.381	0.356	0.610	0.660	—	0.889	5.486	0.508	1.676	0.051	12.497
6	—	0.838	1.270	0.229	0.686	0.305	1.676	—	0.178	0.356	—	5.893
7	—	0.991	4.216	0.533	0.686	0.762	1.829	0.025	0.025	3.531	5.791	18.847
5	0.787	0.178	0.178	0.406	0.076	0.015	0.253	0.533	—	1.676	5.69	5.539
3	—	0.635	1.803	0.381	0.559	0.635	0.787	1.803	—	2.896	0.584	12.497
9	1.245	0.076	0.559	—	0.432	2.184	0.102	—	0.711	0.356	0.203	6.096
3	7.087	1.118	0.279	0.406	2.235	0.559	—	1.016	1.041	0.533	0.076	18.974
	2.540	0.711	0.762	—	0.051	0.178	1.372	—	—	1.626	0.737	7.976
	0.305	0.203	0.076	2.108	—	0.152	2.159	0.076	0.025	—	3/378	8.484
	—	—	0.178	0.076	1.524	—	0.991	1.524	1.854	3.454	—	9.601
1	3.251	6.096	0.305	1.448	0.127	0.025	0.076	0.051	0.356	1.372	1.270	16.027
3	0.051	0.229	—	—	—	4.140	—	—	1.930	0.203	3.302	13.208
8	0.330	1.448	1.473	0.457	—	0.381	0.102	1.270	0.610	—	0.051	6.299
	3.327	0.102	0.660	1.041	—	1.753	—	2.565	2.870	—	0.025	12.344
5	—	—	—	2.616	0.559	0.203	3.835	1.702	0.076	—	1.194	11.760
2	5.639	4.902	1.270	0.127	—	—	—	0.051	0.533	3.226	1.499	22.149
8	0.762	2.210	—	0.279	—	1.905	1.981	—	0.025	0.025	1.118	10.744
9	2.794	3.658	3.381	0.584	0.152	2.159	—	0.483	0.051	—	—	13.961
4	0.229	2.286	0.889	0.864	—	—	0.406	3.277	0.051	0.813	—	9.398

Performance

Table D.1 (continued)

Area 5 Radi

YR	JAN	FEB	MAR	APR	MAY	JUN	JUL	AUG	SEP	OCT	NOV	DEC	YEAR
82	0.787	1.016	4.293	0.965	2.057	0.305	1.676	2.134	2.565	0.533	1.575	0.787	18.694

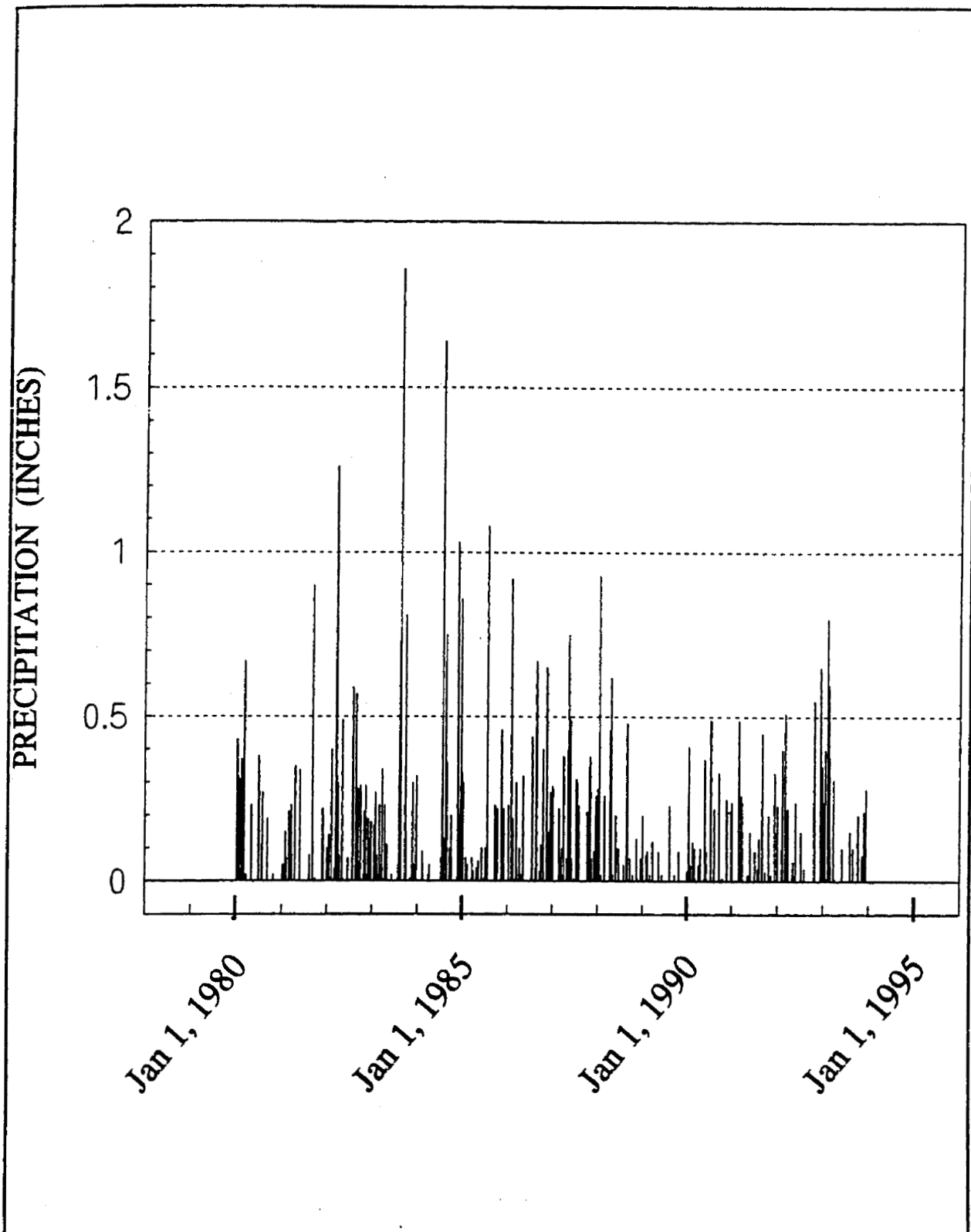


Figure D.2 Daily Precipitation Data Collected for Well 5B at Frenchman Flat From 1980 to 1994 (NOAA)

D.1.1.2 *Evapotranspiration*

Evapotranspiration (ET) includes evaporation from bare soil, due to solar radiation and transpiration of water from the subsurface into the atmosphere via vegetation. Evapotranspiration varies widely, depending upon the species of vegetation, soil structure, temperature, and supply of water. Evapotranspiration can refer to either potential evapotranspiration (ET_{POT}) or actual evapotranspiration (ET_{ACT}). ET_{POT} is that amount of evaporation that would arise from a soil if enough water were always available to meet the evaporative demand. As soil dries, it becomes increasingly difficult to transmit water from the wetter areas within the soil profile to the surface, where evaporation takes place. This inhibits the evaporative process, making the actual evapotranspiration, ET_{ACT} , considerably less than ET_{POT} . Evapotranspiration may be determined either from an energy balance analysis, by empirical calculation, or by pan evaporation measurements (Monteith *et al.*

atmospheric pressure, and wind speed. The micrometeorology station at the Area 5 RWMS records these variables. A modified form of the Penman equation (Jensen *et al.*, 1990) is:

$$\lambda E_{to} = \frac{\Delta}{\Delta + \gamma} (R_n - G) + \frac{\gamma}{\Delta + \gamma} 6.43 W_f (e_z^0 - e_z) \quad (D.1)$$

where:

- E_{to} = potential evapotranspiration;
- λ = latent heat of vaporization (kJ kg^{-1});
- Δ = slope of saturation vapor pressure curve $(4098 e^0)/(T+237.3)^2$, ($\text{kPa } ^\circ\text{C}^{-1}$); Tetens (1930) and Murray (1967);
- T = dry bulb temperature ($^\circ\text{C}$);
- e^0 = saturation vapor pressure (kPa);
- γ = psychrometric constant $(C_p P)/(0.622 \lambda)$ ($\text{kPa } ^\circ\text{C}^{-1}$), ($\text{kPa } ^\circ\text{C}^{-1}$);
- C_p = specific heat of moist air at constant pressure ($1.013 \text{ kJ kg}^{-1} ^\circ\text{C}$);
- P = atmospheric pressure (kPa);
- R_n = net radiation ($\text{MJ m}^{-2} \text{ d}^{-1}$);
- G = average daily sensible heat flux to the soil ($\text{MJ m}^{-2} \text{ d}^{-1}$);
- $(R_n - G)$ = difference between incoming solar radiation and outgoing long-wave radiation from the soil surface;
- W_f = linear wind coefficient or function;
- e_z^0 = saturation vapor pressure over water (kPa);
- e_z = actual vapor pressure at z level above ground surface (kPa); and
- $(e_z^0 - e_z)$ = vapor saturation deficit.

The linear wind coefficient or wind function is given by:

$$W_f = (a_w + b_w u_2) \quad (D.2)$$

- where:
- $R_n > 0$ $a_w = 0.27$ and $b_w = 0.526$
 - $R_n \leq 0$ $a_w = 1.14$ and $b_w = 0.401$ (Frère and Popov, 1979), and
 - u_2 = wind speed at 2 m above ground surface (km d^{-1}).

The potential ET at the Area 5 RWMS was estimated using the modified Penman equation above and data collected at the micrometeorology station. Because the micrometeorology data set available at the time of analysis was limited to 211 days (from January 1, 1993, through July 30, 1993), the ET_{POT} was calculated for roughly half a year through the summer solstice on June 21. The data show a consistent rise in the evaporative demand from the winter months into the summer. A fourth-order polynomial was fit to the data to smooth the scatter within the individual data points and provide a smooth curve relating the evaporative demand to the time of year (Figure D.3). The fitted curve for the first 6 months of the year, where the independent variable x denotes day of the year (January 1 = 1, January 2 = 2, etc.), was:

$$ET_{pot} = -2.287E-8x^4 + 7.580E-6x^3 - 6.430E-4x^2 + 0.0450x + 0.978. \quad (D.3)$$

The coefficient of determination (r^2) for this model was 0.84. The ET_{POT} for the rest of the cycle, from the summer solstice through the end of December, was approximated by reflecting the curve (mirror image) about the summer solstice, which yielded a plausible set of values for the entire year.

D.1.1.3 Vapor Flow Driven by Thermal Gradient

Water transport by vapor flow at the Area 5 RWMS involves vertical diffusive fluxes driven by vapor pressure gradients. These vapor pressure gradients may be caused by (1) spatial variations of water content, which are associated with the matric potential gradient, which influences the vapor pressure driving force; and (2) surficial warming of the soil due to incident solar radiation, which can produce a thermal gradient. These two vapor flow mechanisms are termed isothermal and nonisothermal (thermal), respectively.

Isothermal vapor flow is generally neglected in transport analyses because the effects only occur extremely close to the surface, and are otherwise very small in magnitude. Scanlon and Milly (1994) found that upward isothermal vapor flow at a Chihuahuan Desert site was significant only within the top 5 cm (1.9 in) of the soil profile. Based on these data, there is no reason to believe that upward isothermal vapor flow in the Mojave Desert has any significant impact on radionuclide transport at the RWMS.

Thermal vapor flow plays a larger role in the subsurface. Thermal gradients lead to vapor pressure gradients because the vapor pressure of water is strongly dependent on temperature. The direction of vapor flow due to thermal gradients varies seasonally and daily. In the upper 10 to 20 cm (3.9 to 7.8 in) of alluvium, the solar radiation at the surface causes a negative thermal gradient which quickly fades with increasing depth, driving water vapor within the pore spaces of the alluvium downward below the surface. In the winter, the

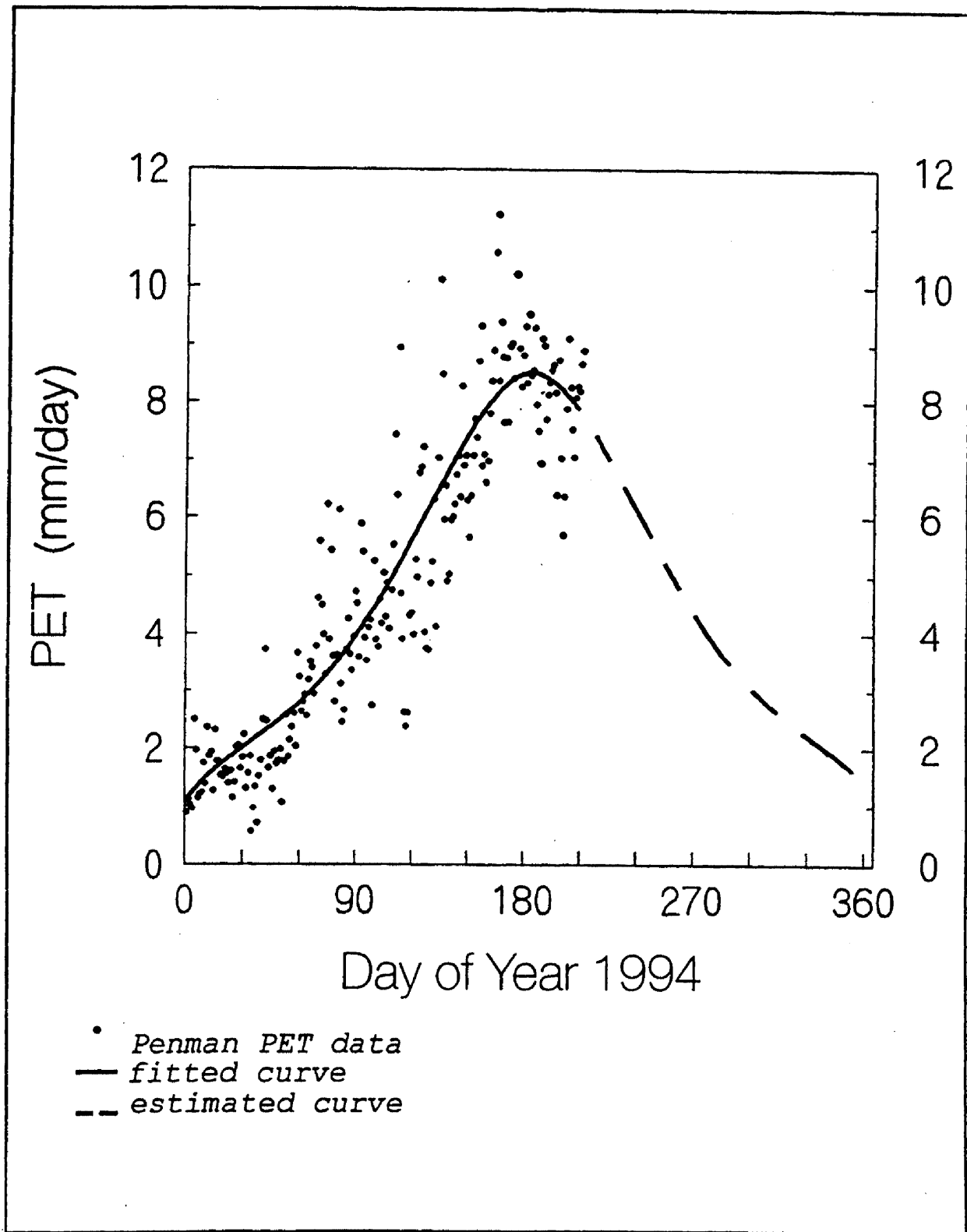


Figure D.3 Potential Evapotranspiration Calculated With a Modified Form of the Penman Equation (Jenson *et al.*, 1991) Using Micrometeorological Data Collected at the Area 5 RWMS.

thermal gradient is upward, and the tendency for vapor movement is up and out of the soil into the atmosphere. This cyclical behavior also occurs on a daily basis as well. This conceptual model of vapor movement is supported by Scanlon and Milly (1994). They showed that although both thermal and isothermal vapor fluxes are small below 30 cm (11.8 in), water movement in the Chihuahuan Desert was dominated by the thermal vapor flux. The magnitude of thermal vapor flux in the subsurface was extremely small, and ranged from 1.5 mm yr^{-1} , at a depth of 0.5 m (1.6 ft), to 0.17 mm yr^{-1} , at a depth of 5 m (16.4 ft). The high degree of climate-induced surface heating tended to cause downward movement of soil water vapor from the surface after each rainfall. The vapor flow quickly died away once the water content was removed from the near surface.

Because Frenchman Flat and the Chihuahuan Desert have similar climates, one would expect Scanlon and Milly's findings to hold at the Area 5 RWMS as well. Although thermal vapor

Frenchman Flat is an important process for water movement, it is not believed to play an

METHOD OF ANALYSIS

The mean travel time for upward advection was determined by discretizing the smoothed water potential profile and using a step-wise constant approximation for $d\psi/dz$. Isotropic conditions can be assumed (REECo, 1993c; Istok *et al.*, 1994; Sully *et al.*, 1993).

Darcy's law for isotropic vertical unsaturated flow,

$$q_z = -K(\theta) \left[\frac{d\psi}{dz} + 1 \right] \quad (D.4)$$

may be used to calculate the velocity (v) of the pore fluid ($v=q_z/n$, where n is the water-filled porosity). Because upward flow occurs only within the top 30 to 35 m (99 to 115 ft) of alluvium, data from the Science Trench Boreholes (REECo, 1993c) was used rather than from the Pilot Wells (REECo, 1993b). Using a mean smoothed matric potential profile of the top portion over all of the Science Trench Boreholes (Figure D.4), the slope of the profile $d\psi/dz$ was discretized into segments (Figure D.5). A step-wise approximation of the Darcian flux along the profile was generated by assuming that the value for $d\psi/dz$ is constant within each segment.

The unsaturated hydraulic conductivity was estimated using the geometric mean soil-water characteristic data obtained from the Science Trench Boreholes (Figures D.6 and D.7, and Table D.2). A relation between water content and matric potential was obtained by fitting water retention data to a model by van Genuchten (1978; 1980) of the form:

$$\theta_v = \theta_r + (\theta_s - \theta_r) \left[1 + (-\alpha \psi)^n \right]^{-m} \quad (D.5)$$

where θ_v is the volumetric water content ($\text{cm}^3 \text{cm}^{-3}$), θ_s is the saturated volumetric water content, θ_r is the residual volumetric water content, ψ is the matric potential (cm), and α , (cm^{-1}), and n are fit parameters. The parameter m is related to n as $m=1-1/n$. The unsaturated hydraulic conductivity function $K(\theta)$ was obtained by substitution of the van Genuchten model parameters into the Mualem (1976) model for unsaturated hydraulic conductivity. Doing this we obtain:

$$K(\theta) = K_s S^{1/2} \left[1 - \left(1 - S^{1/m} \right)^m \right]^2 \quad (D.6)$$

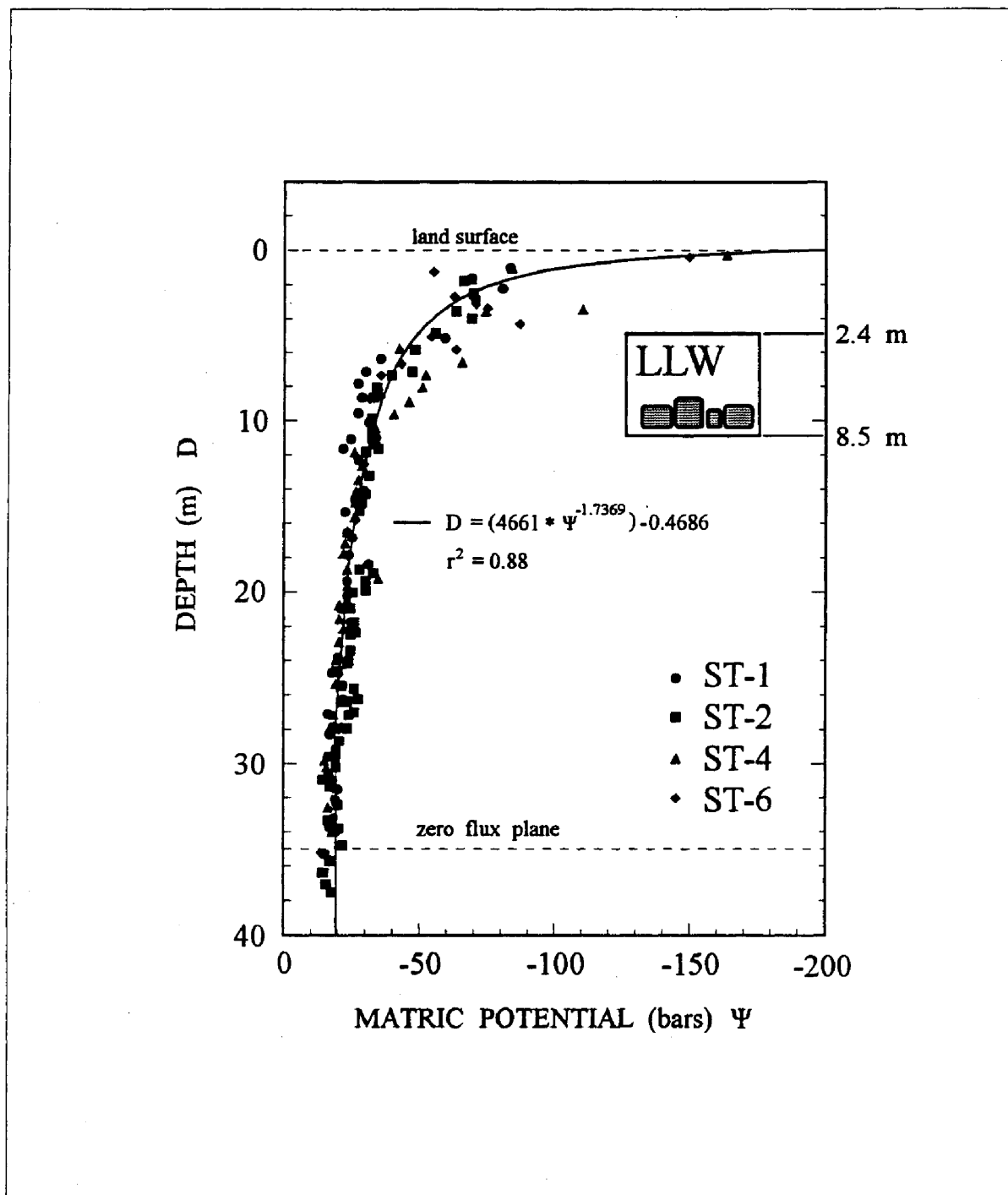
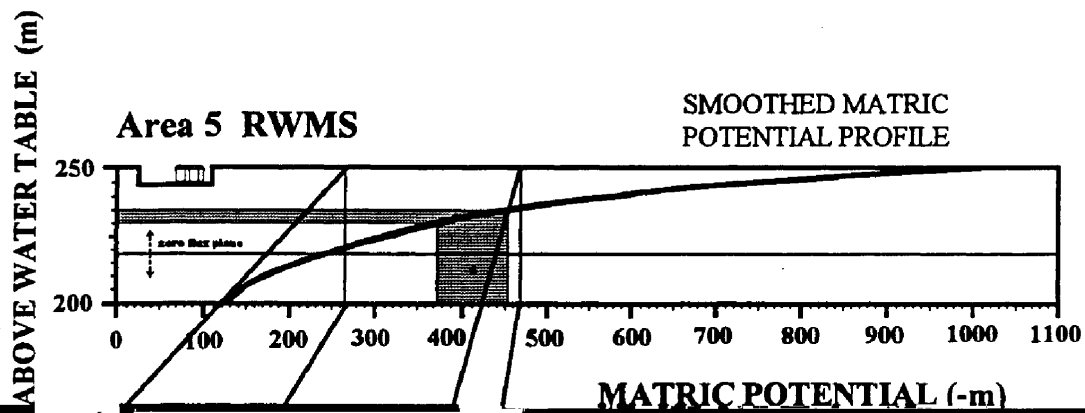


Figure D.4 Smoothed Average Depth Profile (modified power function) Calculated From Near-Surface Matric Potential Data. Surface data was collected for alluvium from the Science Trench Boreholes (REECo, 1993c). Diagram of a shallow land burial low-level waste cell at the Area 5 RWMS is included to indicate the average vertical dimensions of a generic waste cell with respect to the land surface (including a temporary 2.4-m cap of native alluvium).



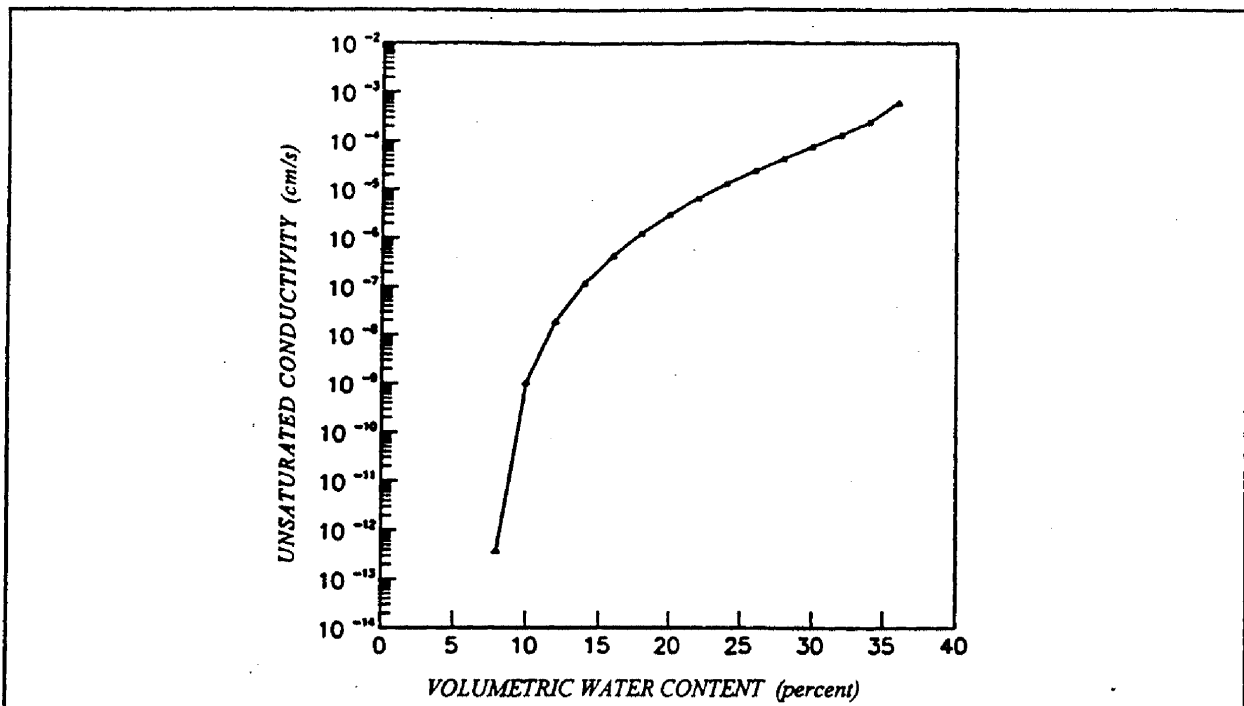


Figure D.6 Mean Soil Moisture Characteristic Curve for Alluvium From the Science Trench Boreholes

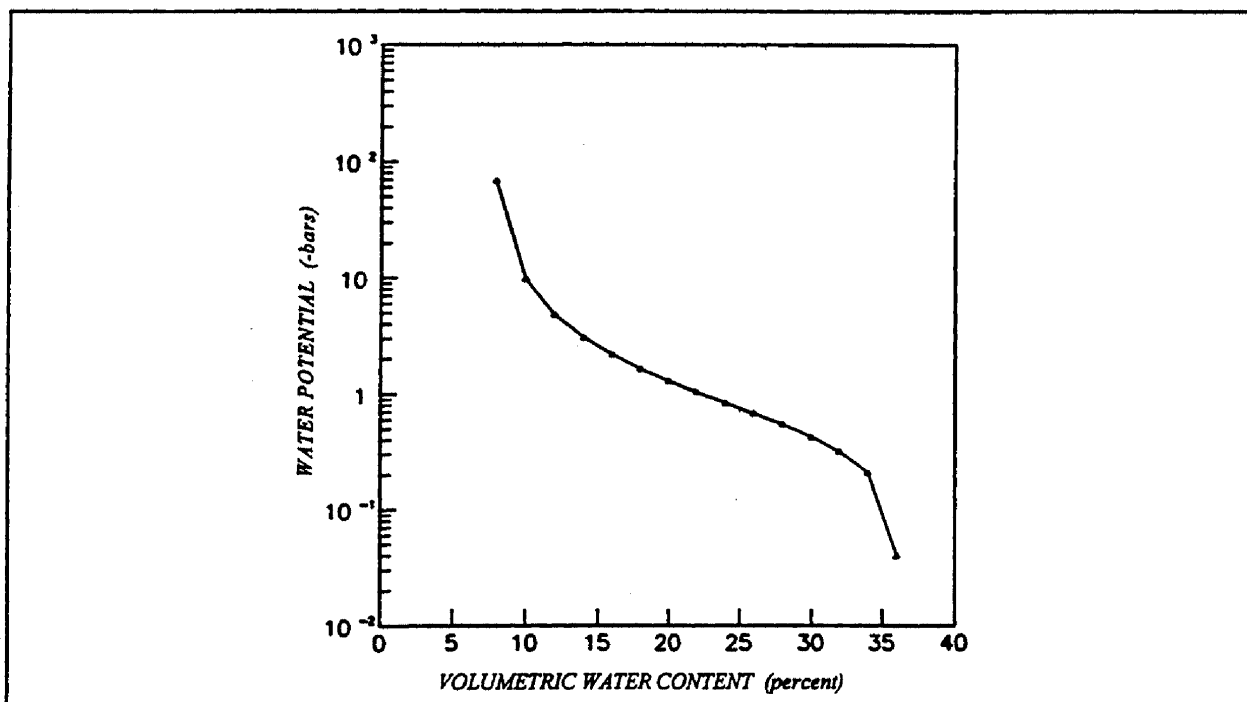


Figure D.7 Mean Soil Moisture Characteristic Curve for Alluvium From the Science Trench Boreholes

Table D.2 Descriptive Statistics for Hydraulic Properties (fitted van Genuchten parameters) From All Science Trench Borehole Core Samples (UeST-1, ST-2A, ST-2, ST-4, ST-5, ST-6, ST-7). "Min" and "max" are minimum and maximum; "mean" and "s" are, respectively, the geometric mean and arithmetic standard deviation (REECo, 1993c).

Statistic	θ_r (cm ³ cm ⁻³)	θ_s (cm ³ cm ⁻³)	α (cm ⁻¹)	n	K_{sat} (cm s ⁻¹)
-----------	---	---	------------------------------	-----	---------------------------------

RESULTS FOR UPWARD ADVECTIVE LIQUID FLOW

The calculations described above suggest that the total time for liquid water to travel 2.4 m (8 ft) up from the top of the emplaced waste to the land surface (based on matric potential as the only driving force) is about 5×10^8 years ($0.000048 \text{ mm yr}^{-1}$). The distance traveled in 10,000 years is estimated to be less than 1 cm (0.16 in). This extremely long travel time is the result of the very low water content in the alluvium. Based on these calculations, upward advection of contaminants is not expected to be a concern under the dry ambient conditions

D.1.1.6 *Summary of Screening Analysis*

A preliminary screening analysis of hydrologic processes affecting water movement in the vadose zone has been performed. The implications of these processes for radionuclide transport has been evaluated. Although thermal vapor fluxes at analog sites have been found to be significant, this process is not a viable mechanism for radionuclide transport. While a potential for upward advective flow exists, the prevailing dry conditions of the alluvium

~~and its hydraulic conductivity to such low levels that most radionuclides will decay before~~



algebraic equations which are eventually solved for matric potential at all nodes at any given time, using a Gaussian elimination scheme specifically tailored for symmetric positive-definite banded-type matrices.

Acceptable boundary conditions include prescribed head, prescribed flux, and various atmospheric limited conditions such as seepage faces and infiltration/evaporation. Transient conditions are allowed for by changing both the type and/or value of boundary conditions by a restart feature.

D.2.1.2 Theoretical Framework

The governing equation solved in the UNSAT2 code is Darcy's Law for variably saturated flow or Richard's equation. Combined with the mass continuity equation in vertical one-dimensional form for homogeneous isotropic media, the equation is:

$$\frac{\partial}{\partial z} \cdot \left(K(\psi) \cdot \left(\frac{\partial \psi}{\partial z} + 1 \right) \right) = (C(\psi) + \beta S_s) \frac{\partial \psi}{\partial t} \pm S \quad (D.9)$$

where:

$K(\psi)$	=	hydraulic conductivity,
ψ	=	water potential,
t	=	time,
z	=	depth dimension,
$C(\psi)$	=	specific moisture capacity = $\partial\theta/\partial\psi$,
θ	=	volumetric water content,
S	=	source/sink term,
S_s	=	specific storage, and
β	=	0 in unsaturated zone, 1 in saturated zone.

Equation D.9 states that the amount of liquid advection and/or drainage into or out of a discrete elementary volume of porous material due to a matric gradient, is equal to the change in storage within the volume, plus or minus additional outside sources or sinks. The specific storage is assumed constant in time in saturated regions, and zero in unsaturated flow regions, because only in saturated systems is storage affected to any degree by compressibility effects. Hysteresis in either the moisture characteristic curve, $\theta(\psi)$, or the specific moisture capacity, $C(\psi)$, is not considered in the code.

D.2.1.3 Code Requirements

UNSAT2 was originally developed for use on an IBM system, and was documented for a CDC 6600/7600 mainframe system. The program has been written in standard FORTRAN-77. Computer memory and peripheral disk storage requirements are a function of the size of the problem (i.e., number of defining nodes and/or elements). Because of the implementation of the finite element method, large amounts of core memory are not normally required for successful simulations.

Initial testing revealed that a 7,000-node 2-D simulation is possible on an IBM 80486-66 MHz PC with 16 Mb memory utilizing a 32-bit FORTRAN compiler operating under the WINDOWS[®] 3.1/DOS operating system. Because the performance assessment simulations were one-dimensional, the PC provided more than enough resources to accomplish the modeling task.

The input data required by UNSAT2 include the simulation title, output control, general simulation control data (number of nodal points, maximum number of iterations, simulation time, step size, etc.), porous material properties (porosity, hydraulic properties), and nodal point and element information (type of boundary conditions, etc.).

Initial conditions are satisfied by providing the matric potential at every node within the domain. Hydraulic properties must be specified for each material if the simulation involves a heterogenous system. These include saturated hydraulic conductivity, specific storage, porosity, relative conductivity as a function of moisture content, and matric potential as a function of water content. Functional relationships supplied as a user option within the program include the van Genuchten model, the Gardner model, the Garner-Russo model, or a user-defined formulation.

D.2.1.4 Output Options

The current version of UNSAT2 provides an output file containing the x, y, z coordinates, matric potential, nodal number, and total head values at the end of the simulation. The plotting program used, TECPLOT[®], needed input in a different format. Thus, several modifications were added to the code to provide input for TECPLOT[®]. In particular, a new subroutine called UNPLOT was added to provide a real-time visual interface to UNSAT2 when one-dimensional simulations were performed. UNPLOT allows the user to observe the evolving matric potential and water content profiles and iteration process during the simulation. Additional segments of code were added to the main program and to the subroutines MOIST and FEM to allow the user to output matric potential and moisture content versus the nodal coordinate system into an output file, suitable for use as an input file for the plotting program TECPLOT[®].

D.2.1.5 Numerical Code Verification

Verification and Validation

Code verification refers to the degree to which a computer code can accurately reproduce or reflect the mathematics used to describe the natural phenomena being simulated. Generally, a mathematical model is considered verified when the results from a model can be shown to be accurate approximations to exact analytical solutions, even if the exact analytical solution does not reproduce the natural phenomena itself. Thus, verification is simply a test to determine if the mathematical representation within the model is sound and error-free. Validation, on the other hand, has been defined by various authors as either (1) "assurance that a model, as embodied in a computer code, is a correct representation of the process or system for which it is intended" (NRC, 1984); or as (2) "a process whose objective is to ascertain that the code or model indeed reflects the behavior of the real world" (DOE, 1986).

To verify that the numerical code in UNSAT2 could accurately reproduce the underlying mathematics of Richard's equation (Equation D.9), a comparison of the solution obtained

from UNSAT2 for a transient problem was compared to the exact solution obtained from

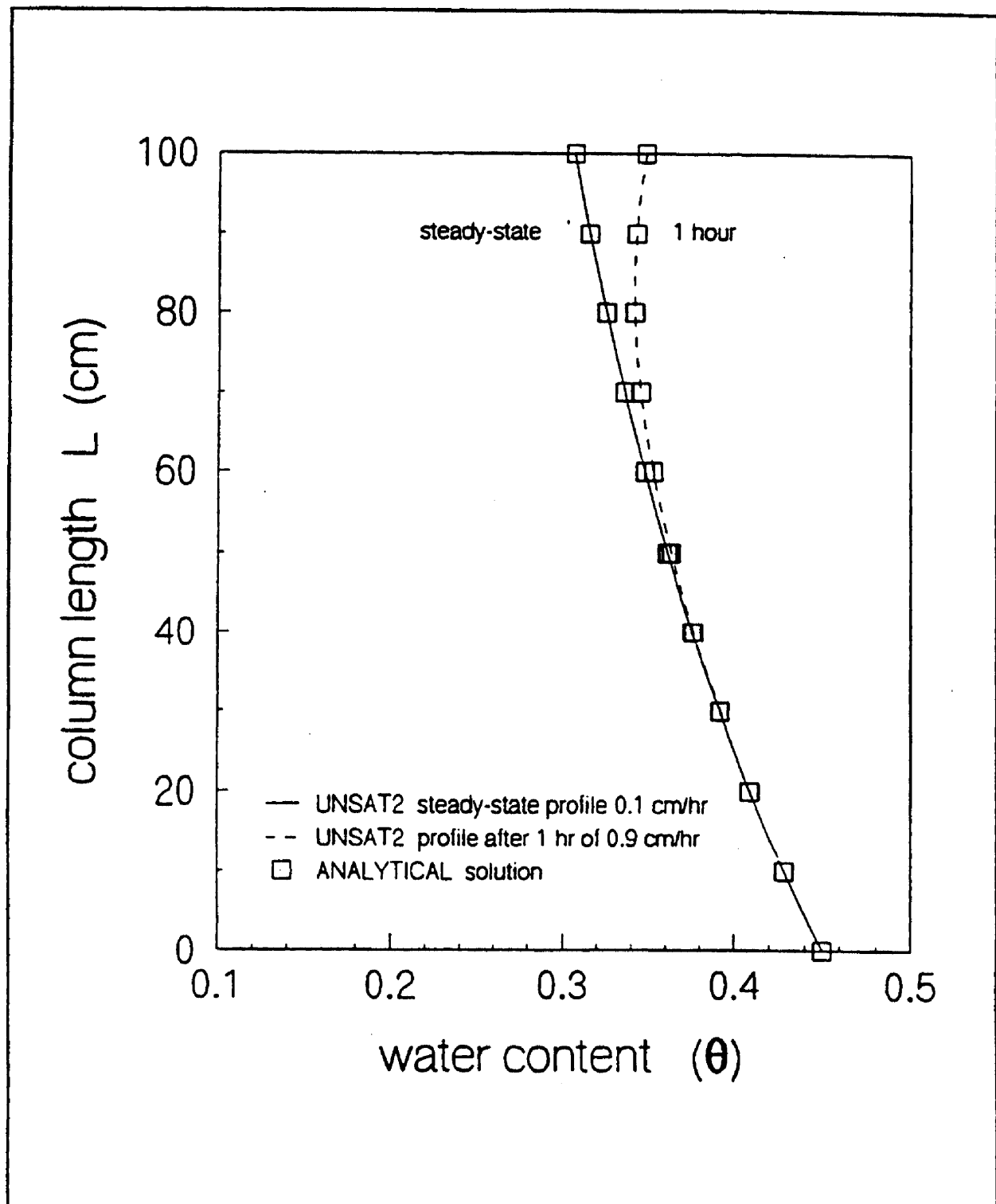



Figure D.8 UNSAT2 Solution (solid lines) versus the Analytical Solution of Yeh and Srivastava (1991) (boxes) for Wetting Profile Simulation for a 100-cm-long Soil Column with a Water Table at the Bottom. (102 nodal points, 50 elements, 100 max iterations, 0.25 initial time interval, 0.05 min time interval, 1.1 multiplier, 0.1 max iteration error.)

Only through site characterization and monitoring over an extended period of time can sufficient confidence be gained that the model reflects the real site over a broad range of conditions. Because of the site-specific nature of this process, validation of the UNSAT2 code is not yet possible due to unavailability of relevant data. When enough data become available for the environmental conditions at the RWMS, it will be possible to validate the code against a range of conditions.

However, the code has been validated numerous times at other locations. The reader is referred to the UNSAT2 manual (Davis and Neuman, 1983) for specific instances in which the UNSAT2 simulation results were compared to laboratory and field data. In particular, the code was validated for two laboratory experiments involving drainage from a one-dimensional column experiment, and a two-dimensional flume test (Skaggs *et al.*, 1970; Duke, 1973; and Hedstrom *et al.*, 1971), and one two-dimensional field-scale study (Neuman *et al.*



D.2.2.2 Model Boundary Conditions

The simulation was performed using the longest record of tabulated daily precipitation data available for the Area 5 RWMS, a 14-year record collected within Frenchman Flat at Well 5B (*Table D.1*). Daily variation in evapotranspiration was estimated in Section D.1.1.2 from a modified form of the Penman equation (Jensen *et al.*, 1990).

Because the simulation was one-dimensional in the vertical direction, the boundary conditions both at the soil surface and at depth were specified. The soil surface boundary condition was variable; i.e., the upper boundary condition was changed every 24 hours. The magnitude of either evaporation or infiltration occurring at the nodes along the soil surface was a function of the water content history in the soil and the weather conditions each day during the 14-year simulation. Daily data were used because the actual rate of evaporation each day may be limited by the ability of the soil to transmit water upward to the surface. Conversely, the actual rate of infiltration may be limited by the infiltration capacity of the soil.

The simulation began with daily rainfall data from January 1, 1980, and ended with daily data from December 31, 1993. Rainfall over each 24-hour period was treated as a positive flux. On days in which there was no precipitation, the evapotranspiration rate, as calculated from the Penman equation, was averaged over each 24-hour period and applied as a negative flux at the surface nodes.

The bottom boundary condition was set at the water table as a prescribed head condition ($\psi=0$).

D.2.2.3 Initial Conditions

The initial conditions assumed for the simulation include the water potential profile or water content distribution in the alluvium with depth. This condition was set equal to the smoothed average water potential profile shown in *Figure D.4* from the Science Trench Borehole data (REECo, 1993c).

D.2.2.4 Model Domain Discretization

The one-dimensional domain was modeled with a 281-rectangular-element grid network of 564 nodes. The domain discretization was very fine, both at the soil surface (0.01 m [0.39 in]) and at the water table, and expands to 2 m (6.6 ft) in the center of the domain.

D.2.2.5 Parameter Selection

The hydrologic parameters used in the simulation were derived from data in the Science Trench Borehole Report (REECo, 1993c). These included the geometric mean for saturated hydraulic conductivity, residual and saturated water content, and the van Genuchten fitting

parameters alpha (α) and (n) for the average water characteristic curve. These values are summarized in Table D.4 and *Figures D.6* and *D.7*. Because the alluvium can be treated hydrologically as an isotropic homogeneous medium (Sully *et al.*, 1993; Istok *et al.*, 1994), no layering was incorporated into the model.

Table D.4 Parameter Values Used for the Transient Infiltration Model Using the UNSAT2 Flow Code

Parameter Description	Symbol	Value for Simulation
Saturated hydraulic conductivity	K_s	0.6390 m-dy ⁻¹
Rainfall infiltration rate	—	variable - daily
Evapotranspiration rate		variable - daily

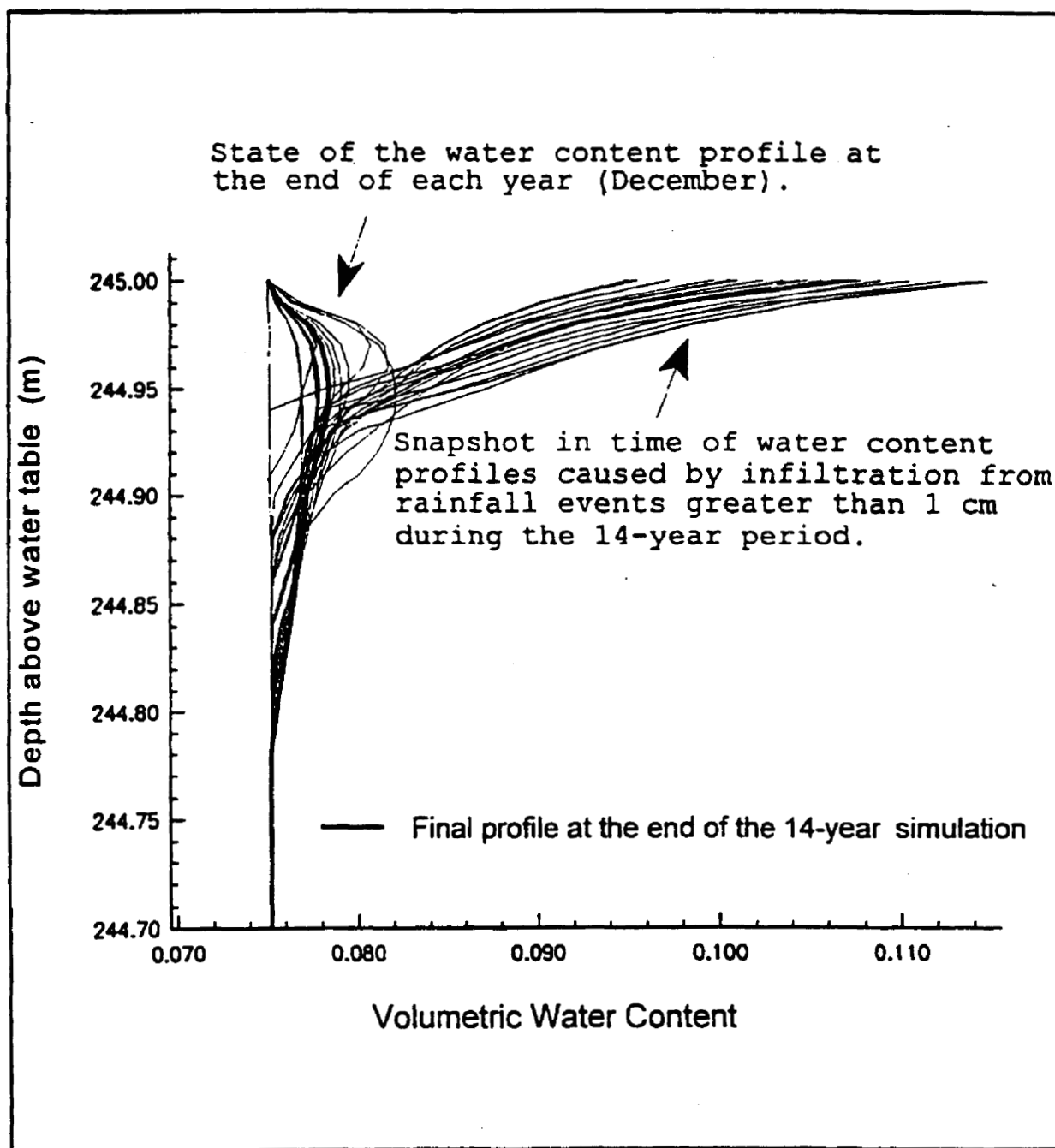


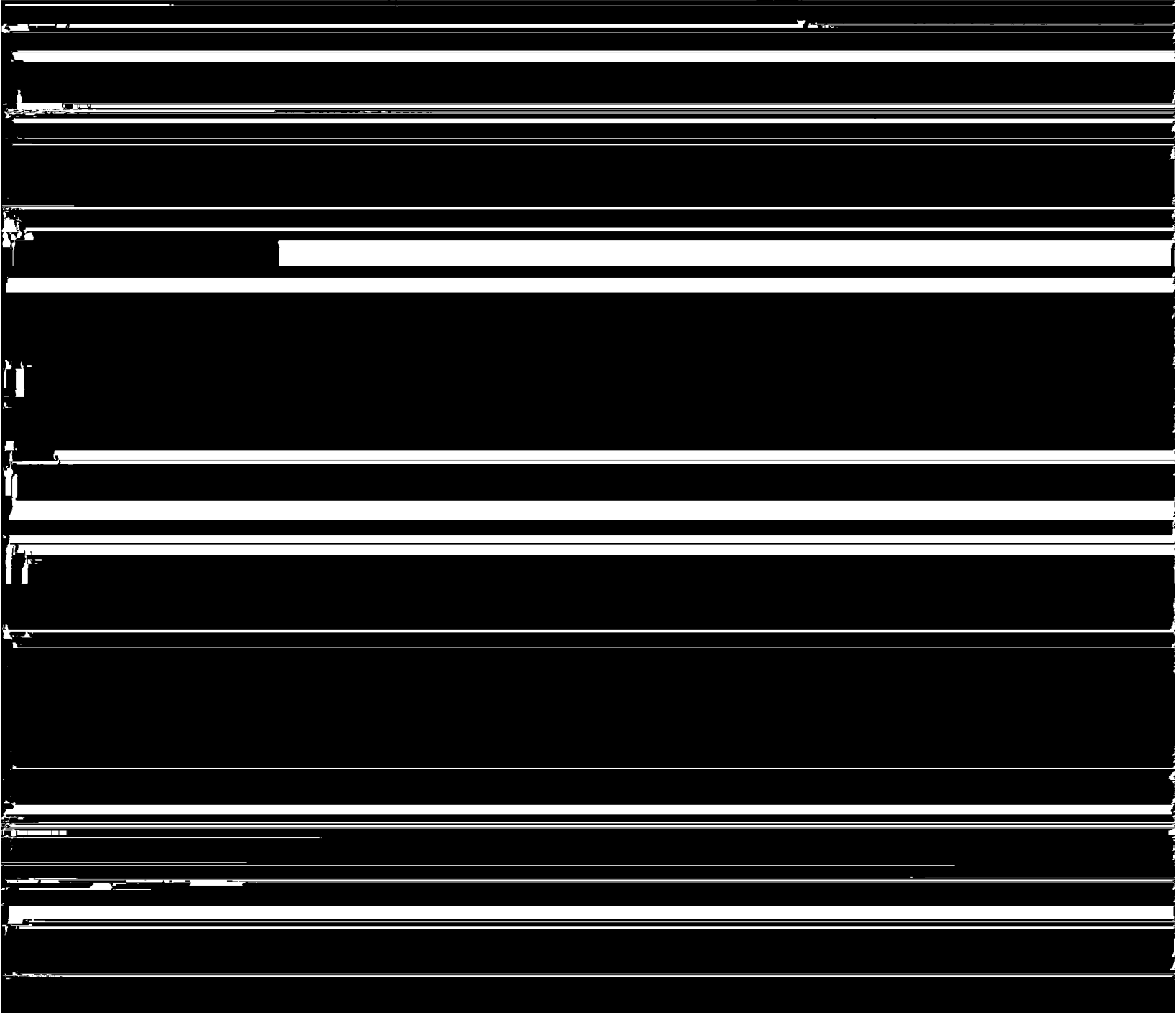
Figure D.9 Transient Modeling Case Showing the Evolution of the Water Content Profile According to the UNSAT2 Flow Code for a 14-Year Simulation of the Area 5 RWMS Using Actual Daily Precipitation Data and Estimated Potential Evapotranspiration Calculated With the Penman Equation

The simulated results show that under the conditions modeled (indicative of the current arid climate regime), most of the precipitation available for recharge is recycled back to the atmosphere because of the large daily evaporative demand at the surface. Even though the simulation was for a limited period of time (14 years), these results are a strong indication

METHOD

The travel time for water to flow from the bottom of the static zone to the capillary fringe region (i.e. Zone III) was simulated by calculating the individual travel times through individual layers, and summing them over the entire thickness of the unsaturated zone. Because the hydrologic parameter values used in the simulation varied according to pdf's taken from core data, a range of simulated travel times was obtained for which statistical significance was assigned.

Two separate sets of 7,500 simulations were performed, one in which the individual thickness of each alluvial layer was assumed to be a constant 1.6 m (5.2 ft) thick (an average value taken from the range of 0.6 to 2.6 m [1.9 to 8.5 ft] found by Snyder and Gustafson



number of times the simulated travel time was less than that specified value). Point estimates of the travel time were obtained from the mean or median of all the realizations.

ASSIGNMENT OF SITE-SPECIFIC PDF'S FOR THE HYDROGEOLOGIC PROPERTIES AT THE AREA 5 RWMS

The hydrogeologic properties according to the specified pdf's were chosen for each horizon down to the water table, using data from REEC Co (1993a,b). Sully *et al.* (1993) and Istok *et al.* (1994) studied variograms of hydrogeologic properties of soil at depth near the Area 5 RWMS. They found no evidence for vertical heterogeneity and showed that variograms of soil characteristics either have short correlation lengths or exhibit a pure nugget effect.

Hence, hydrogeologic properties can be modeled as statistically independent among horizons.

The individual hydrogeologic parameters varied via Monte Carlo analysis within each layer were:

- θ_r , or residual moisture content (percent),
- θ_s , or saturated moisture content (percent),
- α and n , the van Genuchten (1980) curve fitting parameters (α - cm^{-1} , n - dimensionless),
- K_s , saturated hydraulic conductivity (cm sec^{-1}),
- ψ , matric potential (cm of water).

As hydrogeologic parameters within a given horizon are often strongly dependent, conditional pdf's were determined (pdf's for the above parameters were determined sequentially, and were allowed to depend on hydrogeologic conditions previously chosen).

RESIDUAL MOISTURE CONTENT, θ_r , (PERCENT)

Ten percent of the observed values of θ_r equal 0.00; the nonzero values occur over a

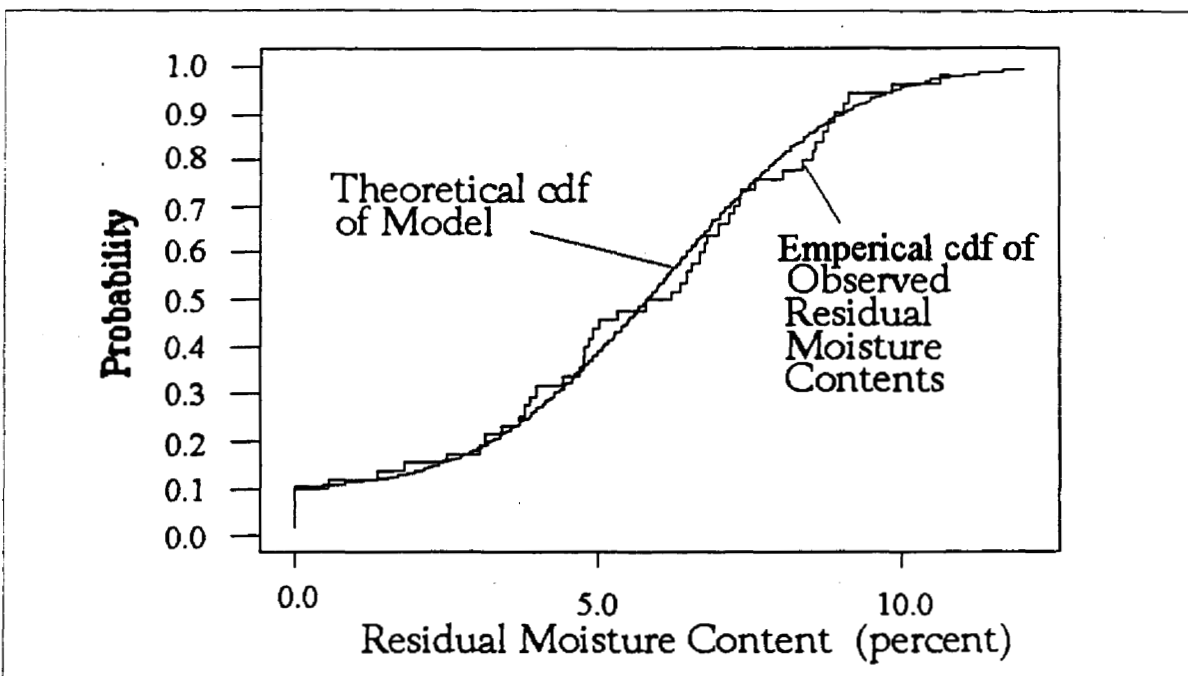


Figure D.10 Comparison of Empirical and Fitted cdf's for Residual Moisture Content

SATURATED MOISTURE CONTENT, θ_s , (PERCENT)

An examination of the data shows that larger values of θ_s are often associated with larger values of θ_r . A regression analysis ($r^2 = .184$, p value of F-test = 0.002) indicates that the model

$$\theta_s \text{ (percent)} = 29.80 + 0.502 \theta_r \text{ (percent)} + \epsilon_1,$$

where ϵ_1 is normally distributed with mean 0.00 and standard deviation 3.13, fit the data reasonably well. A plot of the observed values, together with the fitted line, appears in Figure D.11.

THE VAN GENUCHTEN (1980) CURVE FITTING PARAMETER, α , (1/LENGTH)

A sensitivity analysis, not reported here in detail, showed that travel time depends more strongly on α than on the other parameters in the van Genuchten (1980) equation. Accordingly, great care was taken in fitting a distribution to α .

An examination of the data showed that α varied with n in a nonlinear fashion. Indeed, the relationship between α and n is nonmonotone, with larger values of α associated with both very large and very small values of n . An exploratory data analysis, in which many

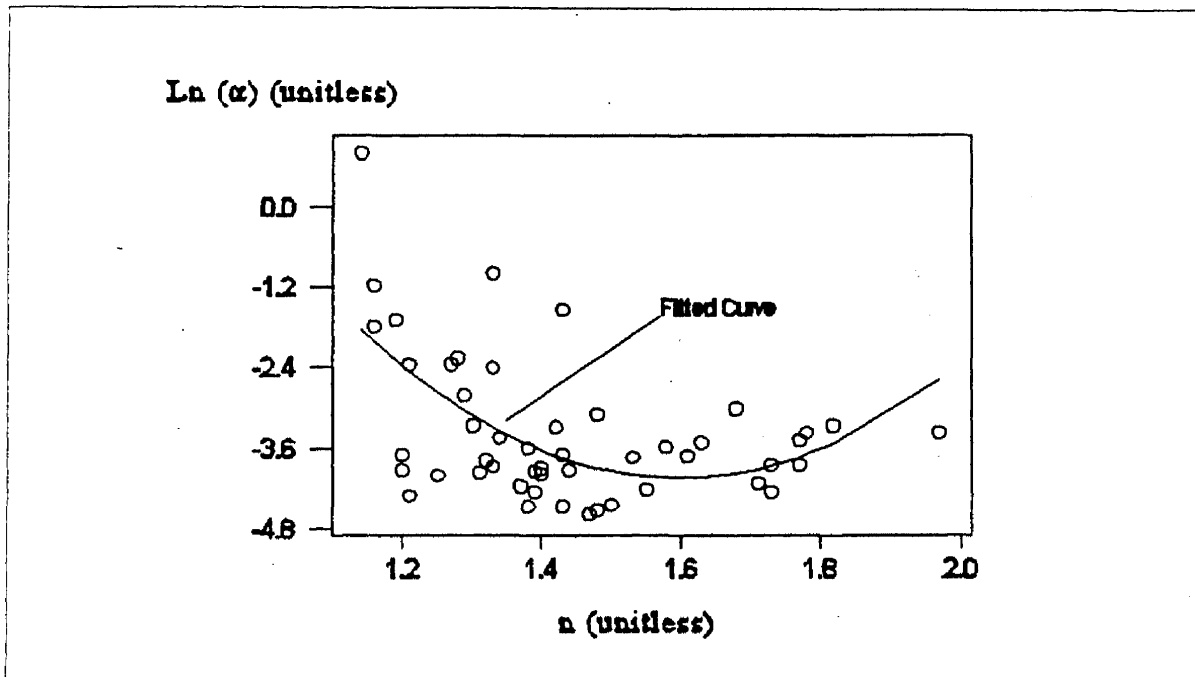


Figure D.12 Plot of $\ln(\alpha)$, Unitless, versus n , Unitless, Along With Fitted Curve

THE VAN GENUCHTEN (1980) CURVE FITTING PARAMETER, n , (UNITLESS)

The parameter m is defined as $1 - 1/n$; hence, if m can be modeled, n can be calculated. An examination of the data shows that larger values of m are often associated with larger values of θ_r . A regression analysis ($r^2 = .628$, p value of F-test less than 0.001) indicates that the model

$$\ln(1 - 1/n) \text{ (unitless)} = -1.80 + 0.0931\theta_r \text{ (percent)} + \epsilon_3,$$

where ϵ_3 is normally distributed with mean 0.00 and standard deviation 0.210, fit the data

reasonably well. A plot of the observed values, together with the fitted line,

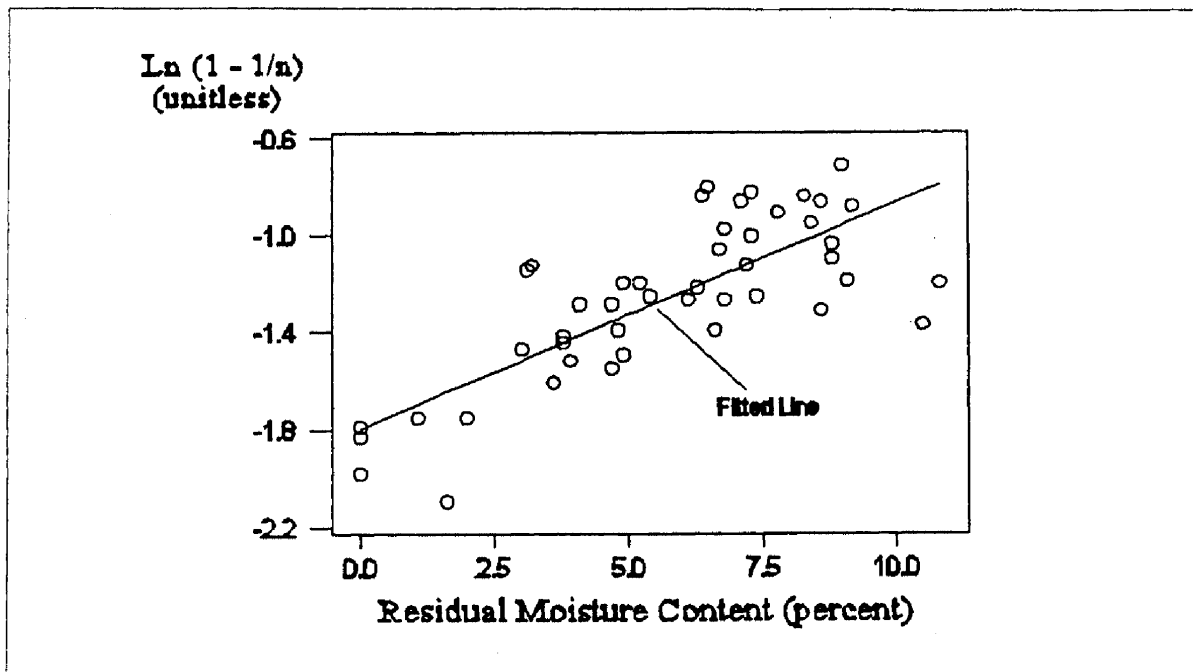


Figure D.13 Plot of $\ln(1 - 1/n) = m$ (Unitless) versus Residual Moisture Content (Percent), Along With Fitted Line

MATRIC POTENTIAL, ψ , (CM OF WATER)

Travel time depends both on $\psi(z)$, matric potential as a function of depth, and $d\psi(z)/dz$, the derivative of $\psi(z)$ with respect to depth. Matric potential, $\psi(z)$, is modeled here by regressing the natural logarithm of observed depths on the natural logarithm of the negative of observed values of ψ in Zone III, with the resulting model:

$$\ln(z) \text{ (meters)} = 8.404 - 1.723 \ln(-\psi) \text{ (bars)} + \epsilon_4,$$

where ϵ_4 is normally distributed with mean 0.0 and standard deviation 0.305 ($r^2 = 0.874$, p-value of F-test less than 0.001). As the regression of $\ln(-\psi)$ on $\ln(z)$ gives a very similar curve, the issue of which variable to treat as dependent and which to treat as independent is of little concern. In the simulations, uncertainty in ψ was accounted for via the term ϵ_4 . A sensitivity analysis showed that $d\psi/dz$ had little impact on travel time. Therefore, this factor was treated deterministically.

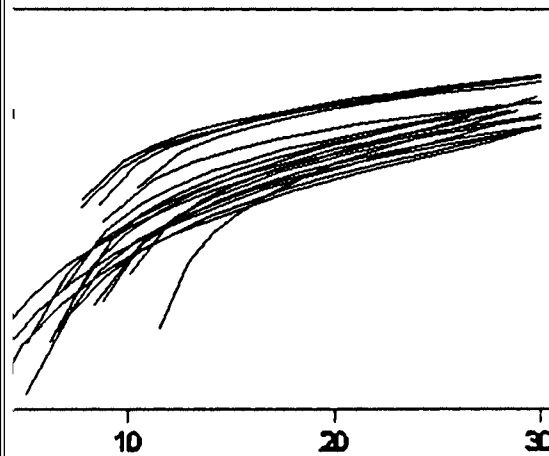
PERFORMANCE OF THE HYDROLOGIC PARAMETER MODEL

The adequacy of the fitted pdf's is best demonstrated by a comparison of the $K(\theta)$ curves observed from empirical data (REECo, 1993a,b) and the simulated $K(\theta)$ curves. This is

5. Figure D.14 shows all 20 observed $K(\theta)$ curves, taken from Figure D.15 shows 20 simulated $K(\theta)$ curves, derived from the same parameters. While no formal goodness-of-fit test is used, it is seen that the observed and simulated $K(\theta)$ curves behave in a similar manner.

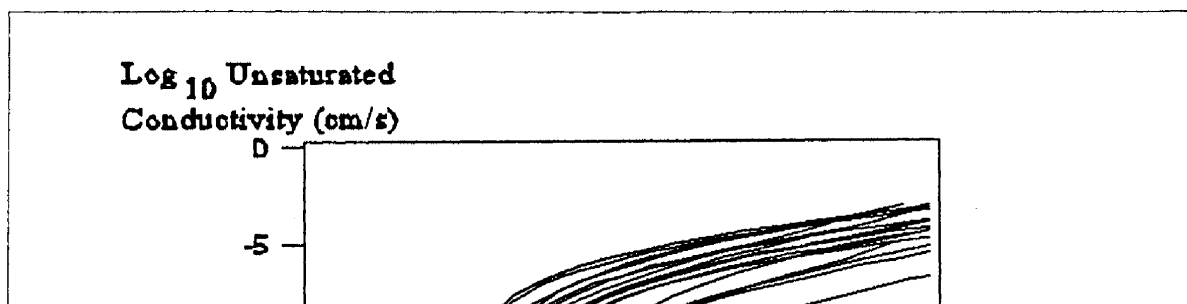
is

For a given thickness, 7,500 realizations were generated. The number of realizations per thickness was chosen so that the standard error of the mean was less than one-half of one percent. The descriptive statistics for these two sets of realizations appear in Table D.1.



Volumetric Water Content (percent)

Log($K(\theta)$)



The cumulative distribution function (cdf) for the constant horizon thickness case appears in Figure D.16. The cdf for the variable horizon thickness case appears in Figure D.17. In both figures, the horizontal axis, marked in logarithmic scale, gives the number of years required for infiltrating water to travel to the water table. The vertical axis gives the probability that the water will have traveled to the water table within that time. It can be readily seen that the two cdf's differ little. Differences occur primarily at the very large travel times (more than 200,000 years).

The following conclusions can be derived from *Table D.5* and *Figures D.16* and *D.17*:

- Travel time is relatively insensitive to assumptions concerning horizon thickness, as long as horizon thickness remains within the range of what was reported in Snyder and Gustafson (1994). Hence, the inaccuracy introduced by assuming constant thickness horizons is small.
- Mean and median travel times from the simulations are less (approximately 15 to 20 percent) than what was estimated in previous deterministic analyses. However, predicted unretarded travel times are still quite large, on the order of tens of thousands of years.
- The Monte Carlo realizations indicate that the probability of infiltrating water traveling to the water table in less than 30,000 years is very small. In both sets of realizations, ninety-nine realizations out of a hundred (probability 0.99) resulted in a travel time of greater than 29,600 years.
- In all realizations, unretarded travel time was more than 19,000 years. As there were 7,500 realizations under each model, the probability of travel time being less than 10,000 years is vanishingly small.

Unretarded travel time estimates are provided here as an additional supporting argument for ignoring the groundwater pathway under current conditions. In the extremely unlikely event that transport to the aquifer were to occur (or is occurring now), the probability of contaminants reaching the aquifer in 10,000 years is negligible. If retardation is considered, travel times become sufficiently long to allow most radionuclides to decay to negligible concentra-

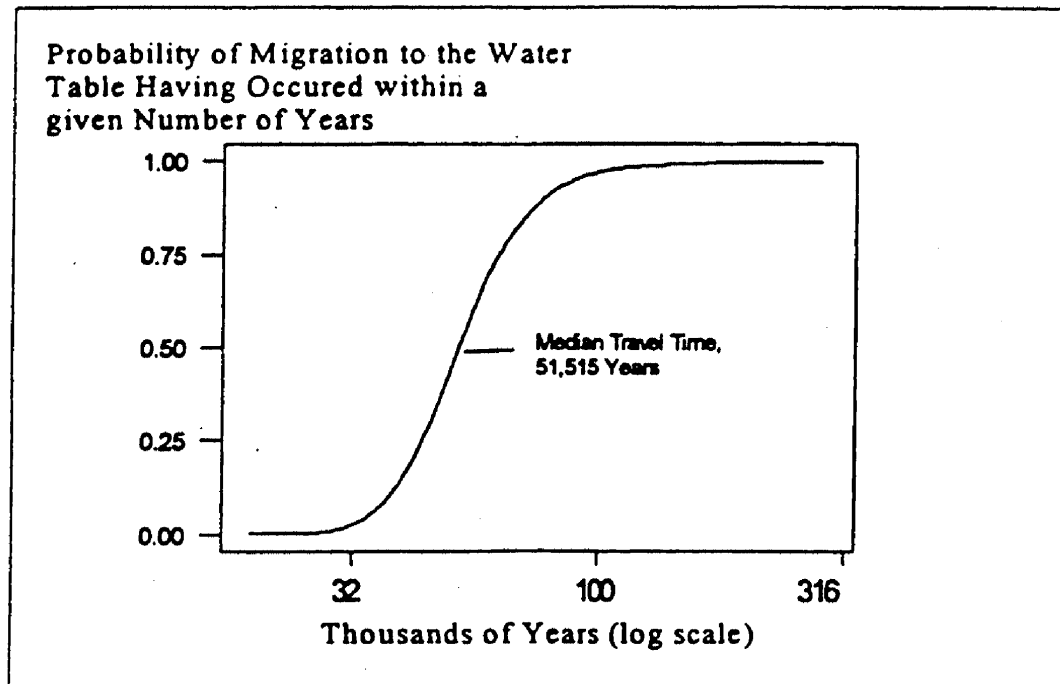


Figure D.16 Cumulative Distribution Function of 7,500 Monte Carlo Realizations of the Base Ten Logarithm of the Time Required for Water to Travel to the Water Table. Horizon thickness is uniformly distributed between 0.6 and 2.6 meters.

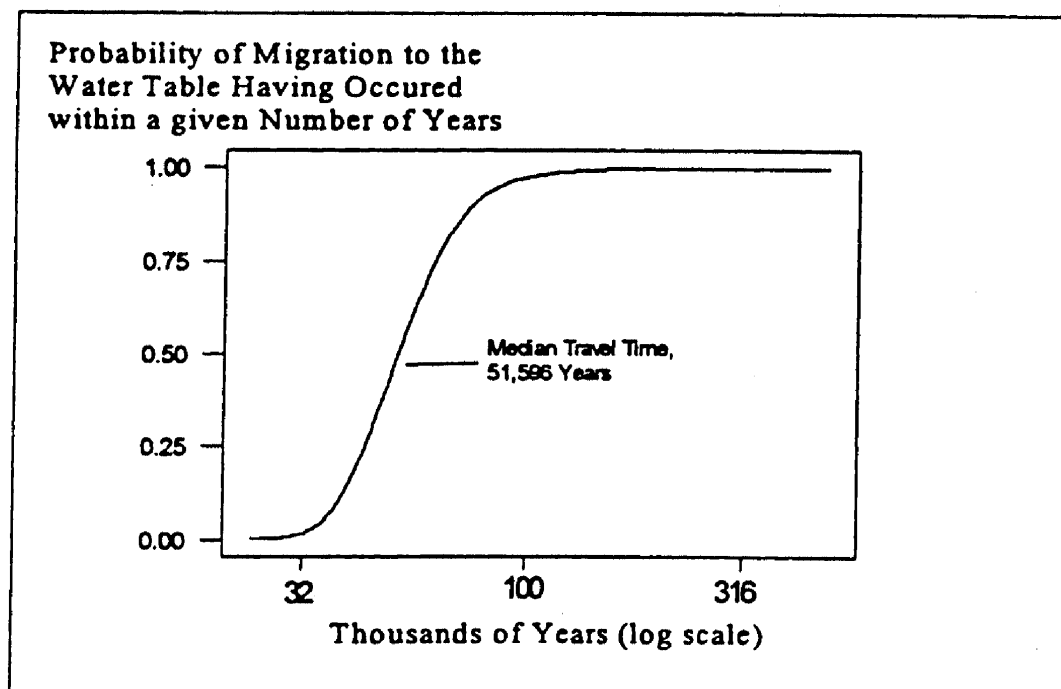


Figure D.17 Cumulative Distribution of 7,500 Monte Carlo Realizations of the Base Ten Logarithm of the Time Required for Water to Travel to the Water Table. Horizon thickness is constant at 1.6 m.

Area 5 RWMS are located in Zone I, a 35-m- (115-ft)-thick surface zone where the potential for water movement is upward. Under the usual ambient conditions, the alluvium in Zone I is so dry that upward liquid advection occurs at negligible rates. The potential for diffusion of solutes is also eliminated in Zone I by the extremely dry conditions. Monte Carlo estimates of travel time suggest that if recharge were to occur, the travel time would greatly

APPENDIX E

PARAMETERS AND INTERMEDIATE RESULTS FOR THE RELEASE AND PATHWAY SCENARIOS

Table E.1 Radionuclide-Specific, Soil-Plant Dry Mass Concentration Factors and Transfer Parameters for Milk and Beef.

Element	B_{jv}	B_{jv} Reference	F_m^a (day kg ⁻¹)	F_b^a (day kg ⁻¹)
Ac	3.5e-004	Bv from Baes <i>et al.</i> , 1984	2.0e-005	2.5e-005
Am	4.0e-002	Romney <i>et al.</i> , 1981	4.0e-007	3.5e-004
Ba	5.1e-002	CR from Ng <i>et al.</i> , 1982	3.5e-004	1.5e-004
Bi	5.0e-003	Bv from Baes <i>et al.</i> , 1984	5.0e-004	4.0e-004
C	5.5e+000	NRC, 1977	1.2e-002	3.1e-002
Cl	7.0e+001	Bv from Baes <i>et al.</i> , 1984	1.5e-002	8.0e-002
Cm	1.5e-005	Bv from Baes <i>et al.</i> , 1984	2.0e-005	3.5e-004
Co	2.4e-001	CR from Ng <i>et al.</i> , 1982	2.0e-003	2.0e-002
Cs	6.0e-002	Gilbert <i>et al.</i> , 1988	7.0e-003	2.0e-002
Eu	4.0e-003	Bv from Baes <i>et al.</i> , 1984	2.0e-005	5.0e-003
H	4.8e+000	NRC, 1977	1.0e-002	1.2e-002
I	3.1e-001	CR from Ng <i>et al.</i> , 1982	1.0e-002	7.0e-003
Ni	7.4e-002	CR from Ng <i>et al.</i> , 1982	1.0e-003	6.0e-003
Np	1.9e+000	CR from Ng <i>et al.</i> , 1982	5.0e-006	5.5e-005
Pa	2.5e-004	Bv from Baes <i>et al.</i> , 1984	5.0e-006	1.0e-005
Pb	9.0e-003	Bv from Baes <i>et al.</i> , 1984	2.5e-004	3.0e-004
Pd	4.0e-002	Bv from Baes <i>et al.</i> , 1984	1.0e-002	4.0e-003
Pu	2.0e-003	Romney <i>et al.</i> , 1981	1.0e-007	5.0e-007

Table E.1 (continued)

Element	B_{iv}	B_{iv} Reference	F_m^a (day kg ⁻¹)	F_b^a (day kg ⁻¹)
Ra	1.5e-003	Bv from Baes <i>et al.</i> , 1984	4.5e-004	2.5e-004
Sm	4.0e-003	Bv from Baes <i>et al.</i> , 1984	2.0e-005	5.0e-003
Sn	6.0e-003	Bv from Baes <i>et al.</i> , 1984	1.0e-003	8.0e-002
Sr	3.5e+000	CR from Ng <i>et al.</i> , 1982	1.5e-003	3.0e-004
Tc	1.5e+000	Bv from Baes <i>et al.</i> , 1984	1.0e-002	8.5e-003
Th	8.5e-005	Bv from Baes <i>et al.</i> , 1984	5.0e-006	6.0e-006
U	4.0e-003	Bv from Baes <i>et al.</i> , 1984	6.0e-004	2.0e-004
Zr	8.1e-002	CR from Ng <i>et al.</i> , 1982	3.0e-005	5.5e-003

^a From Baes *et al.*, 1984, except for H-3 and C-14, from NRC, 1977.

Table E.2 Fractional Release Rates for Root-Uptake Module.

Element	Base Case			Subsided Case		
	K_{r1}, yr^{-1} (waste to shallow soils)	K_{r2}, yr^{-1} (waste to subsurface soils)	K_{r3}, yr^{-1} (subsurface soils to shallow soils)	K_{r1}, yr^{-1} (waste to shallow soils)	K_{r2}, yr^{-1} (waste to subsurface soils)	K_{r3}, yr^{-1} (subsurface soils to shallow soils)
H	4.26e-6	1.59e-6	6.45e-5	1.46e-5	3.31e-6	1.42e-4
C	4.88e-6	1.82e-6	7.39e-5	1.68e-5	3.79e-6	1.63e-4
Cl	6.21e-5	2.32e-5	9.41e-4	2.14e-4	4.82e-5	2.08e-3
Ni	6.57e-8	2.45e-8	9.95e-7	2.26e-7	5.10e-8	2.19e-6
Co	2.13e-7	7.95e-8	3.23e-6	7.32e-7	1.65e-7	7.12e-6
Kr	0.00e+000	0.00e+000	0.00e+000	0.00e+000	0.000e+000	0.000e+000
Sr	3.11e-6	1.16e-6	4.70e-5	1.07e-5	2.41e-6	1.04e-4
Zr	7.19e-8	2.68e-8	1.09e-6	2.47e-7	5.58e-8	2.40e-6
Tc	1.33e-6	4.97e-7	2.02e-5	4.58e-6	1.03e-6	4.45e-5
Pd	3.55e-8	1.33e-8	5.38e-7	1.22e-7	2.76e-8	1.19e-6
Sn	5.33e-9	1.99e-9	8.06e-8	1.83e-8	4.13e-9	1.78e-7
I	2.75e-7	1.03e-7	4.17e-6	9.46e-7	2.14e-7	9.20e-6
Ba	4.53e-8	1.69e-8	6.85e-7	1.56e-7	3.51e-8	1.51e-6
Cs	5.33e-8	1.99e-8	8.06e-7	1.83e-7	4.13e-8	1.78e-6
Sm	3.55e-9	1.33e-9	5.38e-8	1.22e-8	2.76e-9	1.19e-7
Eu	3.55e-9	1.33e-9	5.38e-8	1.22e-8	2.76e-9	1.19e-7
Bi	4.44e-9	1.66e-9	6.72e-8	1.53e-8	3.44e-9	1.48e-7
Pb	7.99e-9	2.98e-9	1.21e-7	2.75e-8	6.20e-9	2.67e-7
Ra	1.33e-9	4.97e-010	2.02e-8	4.58e-9	1.03e-9	4.45e-8
Ac	3.11e-010	1.16e-010	4.70e-9	1.07e-9	2.41e-10	1.04e-8

Table E.2 (continued)

Element	K_{r1}, yr^{-1} (waste to shallow soils)	K_{r2}, yr^{-1} (waste to subsurface soils)	K_{r3}, yr^{-1} (subsurface soils to shallow soils)	K_{r1}, yr^{-1} (waste to shallow soils)	K_{r2}, yr^{-1} (waste to subsurface soils)	K_{r3}, yr^{-1} (subsurface soils to shallow soils)
Th	7.54e-11	2.82e-11	1.14e-9	2.59e-10	5.86e-11	2.52e-9
Pa	2.22e-10	8.28e-11	3.36e-9	7.63e-10	1.72e-10	7.42e-9
U	3.55e-9	1.33e-9	5.38e-8	1.22e-8	2.76e-11	1.19e-7
Np	1.69e-6	6.29e-7	2.55e-5	5.80e-6	1.31e-6	5.64e-5
Pu	1.78e-9	6.63e-10	2.69e-8	6.10e-9	1.38e-9	5.93e-8
Am	3.55e-8	1.33e-8	5.38e-7	1.22e-8	2.76e-9	1.19e-7
Cm	1.33e-11	4.97e-12	2.02e-10	4.58e-11	1.03e-11	4.45e-10

Table E.3 Radionuclide Half-Lives and Dose-Conversion Factors.

Radionuclide ^a	Half-life (years)	DCF _{ing} (rem μCi^{-1}) ^b	DCF _{inh} (rem μCi^{-1}) ^b	DCF _{ext} (mrem yr ⁻¹ per $\mu\text{Ci m}^{-3}$ soil) ^c
Ac-227	2.18e+001	1.50e+001	6.70e+003	1.10e+000
Th-227				
Ra-223				
Rn-219				
Po-215				
Pb-211				
Bi-211				
Tl-207				
Po-211				
Am-241	4.32e+002	4.50e+000	5.20e+002	2.70e-002
Am-243	7.38e+003	4.50e+000	5.20e+002	5.60e-001
Np-239				
Ba-133	1.05e+001	3.20e-003	6.90e-003	1.20e+000
Bi-207	3.34e+001	4.90e-003	1.40e-002	5.90e+000
C-14	5.73e+003	2.10e-003	2.40e-005	8.40e-006
Cl-36	3.01e+005	3.00e-003	2.00e-002	1.50e-003
Cm-243	2.85e+001	2.90e+000	3.50e+002	3.60e-001
Cm-244	1.81e+001	2.30e+000	2.70e+002	9.80e-005
Cm-248	3.39e+005	1.60e+001	1.90e+003	5.50e-005
Co-60	5.27e+000	2.60e-002	1.50e-001	1.00e+001
Cs-135	2.30e+006	7.10e-003	4.50e-003	2.40e-005
Cs-137	3.02e+001	5.00e-002	3.20e-002	2.30e+000
Ba-137m				
Eu-152	1.36e+001	6.00e-003	2.20e-001	4.40e+000
Eu-154	8.80e+000	9.10e-003	2.60e-001	4.80e+000
H-3	1.23e+001	6.30e-005	9.50e-005 ^d	0.00e+000
I-129	1.57e+007	2.80e-001	1.80e-001	8.10e-003
Kr-85	1.07e+001	0.00e+000	0.00e+000	1.40e+001 ^e
Ni-59	7.50e+004	2.00e-004	1.30e-003	0.00e+000
Ni-63	1.00e+002	5.40e-004	3.00e-003	0.00e+000
Np-237	2.14e+006	3.90e+000	4.90e+002	6.90e-001
Pa-233				
Pa-231	3.28e+004	1.10e+001	1.30e+003	1.20e-001
Pb-210	2.23e+001	6.70e+000	2.10e+001	3.80e-003
Bi-210				
Po-210				
Pd-107	6.50e+006	1.40e-004	1.30e-002	0.00e+000
Pu-238	8.78e+001	3.80e+000	4.60e+002	9.50e-005
Pu-239	2.41e+004	4.30e+000	5.10e+002	1.80e-004
Pu-240	6.57e+003	4.30e+000	5.10e+002	9.20e-005
Pu-241	1.44e+001	8.60e-002	1.00e+001	3.70e-006
Pu-242	3.76e+005	4.10e+000	4.80e+002	8.00e-005
Pu-244	8.26e+007	4.00e+000	4.80e+002	1.30e+000
U-240				
Np-240m				
Ra-226	1.60e+003	1.10e+000	7.90e+000	7.00e+000
Rn-222				
Po-218				
Pb-214				

Table E.3 (continued)

Radionuclide ^a	Half-life (years)	DCF _{ing} (rem μCi^{-1}) ^b	DCF _{inh} (rem μCi^{-1}) ^b	DCF _{ext} (mrem yr ⁻¹ per μCm^{-3} i soil) ^c
Bi-214				
Po-214				
Ra-228	5.75e+000	1.20e+000	4.20e+000	3.70e+000
Ac-228				
Sm-151	9.00e+001	3.40e-004	2.90e-002	6.20e-007
Sn-126	1.00e+005	2.70e-002	9.60e-002	1.70e+001
Sb-126m				
Sb-126				
Sr-90	2.86e+001	1.30e-001	1.30e+000	1.50e-002
Y-90				
Tc-99	2.13e+005	1.30e-003	7.50e-003	7.80e-005
Th-228	1.91e+000	3.80e-001	3.10e+002	1.56e+001
Ra-224				
Po-216				
Pb-212				
Bi-212				
Po-212				
Th-229	7.34e+003	3.90e+000	2.00e+003	8.90e+000
Ra-225				
Ac-225				
Fr-221				
At-217				
Bi-213				
Tl-209				
Po-213				
Pb-209				
Th-230	7.70e+004	5.30e-001	3.20e+002	7.60e-004
Th-232	1.40e+010	2.80e+000	1.60e+003	3.30e-004
U-232	7.20e+001	1.30e+000	6.70e+002	4.60e-004
U-233	1.59e+005	2.70e-001	1.30e+002	8.70e-004
U-234	2.44e+005	2.60e-001	1.30e+002	2.50e-004
U-235	7.04e+008	2.50e-001	1.20e+002	4.70e-001
Th-231				
U-236	2.34e+007	2.50e-001	1.20e+002	1.30e-004

Table E.4 Maximum Activity and Activity Concentration in the Surface Soil Compartment for the Base-Case Release Scenario.

Radionuclide	Maximum Concentration (Ci m ⁻³)	Maximum Activity (Ci)	Activity at 10,000 yr (Ci)
Ac-227	2.1e-007	1.6e-002	2.0e-003
Am-241	4.0e-009	3.0e-004	1.0e-009
Am-243	2.1e-012	1.6e-007	a
Ba-133	8.4e-016	6.3e-011	a
Bi-207	1.3e-019	9.6e-015	a
C-14	2.5e-007	1.9e-002	1.9e-002
Cl-36	2.7e-013	2.0e-008	2.1e-008
Cm-243	1.3e-014	9.5e-010	a
Cm-244	4.4e-012	3.3e-007	a
Cm-248	4.4e-018	3.3e-013	2.3e-013
Co-60	1.1e-012	8.3e-008	a
Cs-135	6.0e-013	4.5e-008	2.4e-008
Cs-137	8.3e-011	6.2e-006	a
Eu-152	3.6e-019	2.7e-014	a
Eu-154	2.7e-014	2.0e-009	a
H-3	4.8e-005	3.6e+000	a,b
H-3	2.3e-006	1.8e-001	a,c
I-129	1.0e-013	7.5e-009	3.5e-009
Ni-59	1.9e-013	1.4e-008	1.1e-008
Ni-63	2.1e-010	1.5e-005	a

Table E.4 (continued)

Radionuclide	Maximum Concentration (Ci m ⁻³)	Maximum Activity (Ci)	Activity at 10,000 yr (Ci)
Pu-240	4.4e-008	3.3e-003	3.0e-003
Pu-241	7.1e-010	5.3e-005	a
Pu-242	1.6e-011	1.2e-006	8.0e-017
Pu-244	1.5e-020	1.1e-015	2.1e-017
Ra-226	5.5e-006	4.1e-001	1.3e-002
Ra-228	1.4e-008	1.0e-003	6.6e-004
Sm-151	5.0e-013	3.8e-008	a
Sn-126	7.6e-014	5.7e-009	4.3e-009
Sr-90	1.3e-009	9.8e-005	a
Tc-99	3.9e-011	2.9e-006	2.0e-006
Th-228	1.4e-008	1.0e-003	6.6e-004
Th-229	6.3e-011	4.7e-006	5.6e-007
Th-230	5.5e-006	4.1e-001	1.7e-002
Th-232	1.4e-008	1.0e-003	6.6e-004
U-232	3.0e-012	2.2e-007	a
U-233	9.2e-011	6.9e-006	1.6e-006
U-234	6.3e-006	4.7e-001	2.0e-001
U-235	2.2e-007	1.7e-002	1.1e-002
U-236	6.4e-009	4.8e-004	3.0e-004
U-238	7.6e-006	5.7e-001	3.6e-001
Zr-93	4.8e-013	3.6e-008	2.0e-008

^a Peak occurs before 10,000 years; therefore, 10,000-year value is not used in dose calculations.

^b Values shown are for the H-3 peak during institutional control at 17 years; used to calculate maximum off-site inhalation, external, and crop-ingestion doses.

^c Values shown are the H-3 values at 100 years; used to calculate maximum off-site milk and beef ingestion doses (cattle are not assumed to be grazed on site before 100 years).

Table E.5 Calculated Off-Site Air Concentrations for Nonvolatile Radionuclides at 10,000 Years and at the Maximum for the Base Case Release Scenario.

Radionuclide	Time of Maximum	Max. Air Conc. (Ci m ⁻³)		10,000 yr Air Conc. (Ci m ⁻³)	
		Cane Springs	Indian Springs	Cane Springs	Indian Springs
C-14	6498	3.7e-21	2.9e-20	3.3e-21	2.6e-20
H-3	17	6.5e-19	na ^a	0.0	0.0
H-3 ^b	100	3.2e-20	2.5e-19	0.0	0.0
U-238	61,000	1.0e-20	2.2e-19	6.5e-21	1.4e-19
U-234	665,000	8.5e-21	1.8e-19	3.5e-21	7.4e-20
Th-230	711,000	7.4e-21	1.6e-19	3.0e-22	6.3e-21
Ra-226	713,000	7.4e-21	1.6e-19	2.3e-22	4.9e-21
Pb-210	713,000	7.4e-21	1.6e-19	2.3e-22	4.9e-21
Pu-240	7,000	5.9e-23	1.2e-21	5.4e-23	1.1e-21
Th-232	56,000	1.8e-23	3.9e-22	1.2e-23	2.5e-22
Ra-228	56,000	1.8e-23	3.9e-22	1.2e-23	2.5e-22
Th-228	56,000	1.8e-23	3.9e-22	1.2e-23	2.5e-22
Am-241	1,000	5.5e-24	1.2e-22	1.8e-29	3.9e-28
Pu-239	15,000	6.0e-22	1.3e-20	5.6e-22	1.2e-20
U-235	60,000	3.0e-22	6.4e-21	1.9e-22	4.1e-21
Pa-231	199,000	2.8e-22	5.9e-21	3.7e-23	7.7e-22
Ac-227	199,000	2.8e-22	5.9e-21	3.6e-23	7.7e-22
Np-237	53,000	2.1e-24	4.4e-23	1.1e-24	2.4e-23

^a Air concentration at Cane Springs of no consequence before 100 years postclosure; location is on site during institutional control period.

^b Air concentrations for H-3 at 100 years used to calculate maximum dose, at which time grazing is first assumed to occur over facility.

Table E.6 Maximum Doses for the Combined Base Case Release and Transient Occupancy Scenario.

Radionuclide	Time of Maximum	Inhalation CEDE (mrem yr ⁻¹)	External EDE (mrem yr ⁻¹)	TEDE (mrem yr ⁻¹)
Ra-226	713,000	5.2e-03	8.8	8.8
Ac-227	199,000	1.7e-01	5.2e-02	2.2e-01
Th-228	56,000	5.1e-04	4.8e-02	4.9e-02
Th-230	711,000	2.1e-01	9.5e-04	2.1e-01
Pa-231	199,000	3.2e-02	5.7e-03	3.8e-02
U-234	665,000	9.8e-02	3.6e-04	9.9e-02
U-235	60,000	3.2e-03	2.4e-02	2.7e-02
U-238	61,000	1.1e-01	1.4e-01	2.5e-01
Pu-239	15,000	2.7e-02	1.8e-05	2.7e-02
Sum				9.7

Table E.7 Doses for the Combined Base Case and Transient Occupancy Scenario at 10,000 Years.

Radionuclide	Inhalation CEDE (mrem yr ⁻¹)	External EDE (mrem yr ⁻¹)	TEDE (mrem yr ⁻¹)
Ra-226	1.6e-04	2.7e-01	2.7e-01
Ac-227	2.2e-02	6.8e-03	2.8e-02
Th-228	3.3e-04	3.1e-02	3.1e-02
Th-230	8.5e-03	3.8e-05	8.5e-03
Pa-231	4.2e-03	7.4e-04	5.0e-03
U-234	4.1e-02	1.4e-04	4.1e-02
U-235	2.1e-03	1.5e-02	1.8e-02
U-238	7.0e-02	9.1e-02	1.6e-01
Pu-239	2.5e-02	1.7e-05	2.5e-02
Sum			5.9e-01

Table E.8 Maximum Doses for Nonvolatile Radionuclides in the Base Case and Open Rangeland Scenario.

Radionuclide	Time of Maximum	Inhalation CEDE (mrem yr ⁻¹)		Crop Ingestion CEDE (mrem yr ⁻¹)		Milk Ingestion CEDE (mrem yr ⁻¹)	Beef ingestion CEDE (mrem yr ⁻¹)	External EDE (mrem yr ⁻¹)	
		Indian Springs	Cane Springs	Indian Springs	Cane Springs			Indian Springs	Cane Springs
H-3 ^a	100	1.7e-11	1.3e-10	1.7e-07	9.4e-07	7.9e-03	1.3e-03	0.0	0.0
C-14	6,830	7.5e-13	5.8e-12	5.4e-07	4.2e-06	4.3e-02	1.5e-02	2.0e-11	1.5e-10
Pb-210	713,000	1.3e-06	2.8e-05	1.1e-05	2.4e-04	7.3e-01	1.2e-01	1.8e-08	3.8e-07
Ra-226	713,000	4.9e-07	1.0e-05	1.1e-06	2.3e-05	1.9e-01	1.5e-02	3.3e-05	6.9e-04

Ra-228

56,000

6.5e-10

1.4e-08

2.9e-09

6.1e-08

5.2e-04

3.9e-05

4.3e-08

9.0e-07

Table E.9 Doses at 10,000 Years for Nonvolatile Radionuclides in the Base Case and Open Rangeland Scenario.

Radionuclide	Inhalation CEDE (mrem yr ⁻¹)		Crop Ingestion CEDE (mrem yr ⁻¹)		Milk Ingestion CEDE (mrem yr ⁻¹)	Beef ingestion CEDE (mrem yr ⁻¹)	External EDE (mrem yr ⁻¹)	
	Indian Springs	Cane Springs	Indian Springs	Cane Springs			Indian Springs	Cane Springs
H-3*	0.0	0.0	0.0	0.0	0.0	0.0	0.0	0.0
C-14	6.7e-13	5.2e-12	4.9e-07	3.8e-06	3.8e-02	1.3e-02	1.8e-11	1.4e-10
Pb-210	4.1e-08	8.6e-07	3.5e-07	7.4e-06	2.3e-02	3.7e-03	5.6e-10	1.2e-08
Ra-226	1.5e-08	3.2e-07	3.3e-08	7.0e-07	6.0e-03	4.6e-04	1.0e-06	2.2e-05
Ac-227	2.1e-06	4.3e-05	6.4e-08	1.3e-06	5.6e-04	9.6e-05	2.5e-08	5.3e-07
Ra-228	4.2e-10	8.8e-09	1.9e-09	3.9e-08	3.3e-04	2.5e-05	2.8e-08	5.8e-07
Th-228	3.1e-08	6.5e-07	5.1e-10	1.1e-08	1.2e-06	1.9e-07	1.2e-07	2.4e-06
Th-230	8.0e-07	1.7e-05	1.8e-08	3.8e-07	4.0e-05	6.6e-06	1.4e-10	3.0e-09
Pa-231	4.0e-07	8.4e-06	4.6e-08	9.8e-07	1.0e-04	2.8e-05	2.8e-09	5.8e-08
Th-232	1.6e-07	3.3e-06	3.7e-09	7.9e-08	8.5e-06	1.4e-06	2.5e-12	5.2e-11
U-234	3.8e-06	8.1e-05	1.5e-07	3.1e-06	3.0e-02	1.4e-03	5.5e-10	1.2e-08
U-235	2.0e-07	4.1e-06	7.9e-09	1.7e-07	1.6e-03	7.2e-05	5.7e-08	1.2e-06
Np-237	4.7e-09	1.0e-07	1.1e-07	2.3e-06	3.6e-05	5.4e-05	5.0e-10	1.1e-08
U-238	6.6e-06	1.4e-04	2.4e-07	5.1e-06	4.9e-02	2.2e-03	3.4e-07	7.2e-06
Pu-239	2.4e-06	5.1e-05	3.3e-07	7.0e-06	1.3e-05	8.7e-06	6.4e-11	1.3e-09
Pu-240	2.3e-07	4.9e-06	3.2e-08	6.7e-07	1.2e-06	8.4e-07	3.1e-12	6.6e-11
Am-241	8.0e-14	1.7e-12	5.1e-14	1.1e-12	2.8e-12	3.3e-10	3.1e-16	6.6e-15
Sum	1.7e-05	3.5e-04	1.9e-06	3.3e-05	1.5e-01	2.1e-02	1.6e-06	3.4e-05